Doctoral Thesis

University of Granada

Doctoral Programme in Fundamental and Systems Biology

Analysis and functional characterization of two tomato genes involved in the mycorrhization process

Tania Ho Plágaro

2018

Tesis Doctoral

Universidad de Granada

Programa de Doctorado en Biología Fundamental y de Sistemas

Análisis y caracterización funcional de dos genes de tomate implicados en el proceso de micorrización

Tania Ho Plágaro

2018

Editor: Universidad de Granada. Tesis Doctorales
Autor: Tania Ho Plágaro
ISBN: 978-84-9163-932-9
URI: http://hdl.handle.net/10481/52451

Universidad de Granada

Facultad de Ciencias

Programa de Doctorado en Biología Fundamental y de Sistemas

Consejo Superior de Investigaciones Científicas (CSIC)

Estación Experimental del Zaidín (EEZ)

Departamento Microbiología del Suelo y Sistemas Simbióticos

Memoria presentada por Dña. Tania Ho Plágaro, licenciada en Biología,

para optar al grado de Doctor en Ciencias Biológicas

por la universidad de Granada con mención internacional.

Memory presented to aspire to Doctor in Biology

(with mention "International Doctor")

Fdo: **Tania Ho Plágaro**

Vº Bº del director de la Tesis Doctoral/ *Thesis supervisor*

Fdo: **José Manuel García Garrido**
Investigador Científico del CSIC

Granada, 2018

Esta Tesis Doctoral ha sido realizada en el Departamento de Microbiología del Suelo y Sistemas Simbióticos (Grupo de investigación "Microorganismos Rizosféricos Promotores del Crecimiento Vegetal"), de la Estación Experimental del Zaidín (EEZ) del Consejo Superior de Investigaciones Científicas (CSIC).

Para la realización del presente trabajo, la licenciada Tania Ho Plágaro fue financiada por el proyecto de investigación AGL2011-25930 concedido por el Ministerio de Economía y Competitividad, así como con las siguientes ayudas asociadas al mismo:

- Beca de Formación de Personal Investigador (Ref. ayuda FPI: : BES-2012-052057) desde el 1 de marzo de 2013 al 28 de febrero del 2017 (4 años).

- Estancia Breve en el *Structural Biology Laboratory, Graduate School of Biological Sciences, Nara Institute of Science and Technology (NAIST)* en Nara, Japón, bajo la supervisión del Dr. Toshio Hakoshima (Ref. EEBB-I-14-07870) del 21 de agosto de 2014 hasta 18 de diciembre de 2014 (4 meses).

- Estancia Breve la *Plant Biology Division* de la *Samuel Roberts Noble Foundation* en Ardmore, Oklahoma, EEUU, bajo la supervisión de Michael Udvardi (Ref. EEBB-I-16- 11379), desde el día 31 de marzo de 2016 hasta el día 28 de julio de 2016 (4 meses).

Parte de los resultados presentados en esta memoria de Tesis Doctoral han sido publicados en las siguientes revistas internacionales o están en vías de publicación:

Ho-Plágaro, T., Huertas, R., Tamayo-Navarrete, M. I., Ocampo, J. A., & García-Garrido, J. M. (2018). An improved method for *Agrobacterium rhizogenes*-mediated transformation of tomato suitable for the study of arbuscular mycorrhizal symbiosis. *Plant methods*, *14*(1), 34. https://doi.org/10.1186/s13007-018-0304-9

Ho-Plágaro, T., Huertas, R., Tamayo-Navarrete, M. I., Ocampo, J. A., & García-Garrido, J. M. (2018). *Tsb* of *Solanum lycopersicum*, a gene that encodes a putative MAP protein, modulates arbuscule activity in Arbuscular Mycorrhiza symbiosis. *Physiologia plantarum*. (Under review)

Ho-Plágaro, T., Huertas, R., Tamayo-Navarrete, M. I., Ocampo, J. A., & García-Garrido, J. M. Involvement of a strigolactone like receptor in the regulation of hormone balance during arbuscular mycorrhiza formation in tomato. *Frontiers in Plant Sciences*, as part of the Research Topic *The Role of Plant Hormones in Plant-Microbe Symbioses.* (In preparation).

Ho-Plágaro, T., Huertas, R., Tamayo-Navarrete, M. I., Ocampo, J. A., & García-Garrido, J. M. (2018). *SlDLK2*, a Novel Upregulated gene in Tomato Roots Colonized by AM fungi, encoding an α, β-hydrolase that acts as a negative regulator of arbuscule branching. (In preparation)

Ho-Plágaro, T, Molinero-Rosales, N, I., Ocampo, J. A. & García-Garrido, J. M. GRAS transcription factors during mycorrhizal development in tomato. (In preparation).

Asimismo, parte de los resultados obtenidos durante esta Tesis Doctoral han sido presentados en los siguientes congresos y reuniones científicas:

- XXI Reunión de la Sociedad Española de Fisiología Vegetal y XIV Congreso Hispano-Luso de Fisiología Vegetal. Toledo (14/6/15-17/6/15). Póster: Characterization and functional analysis of a tomato *α,β-hydrolase* gene responsive to mycorrhization

- The 2nd International Molecular Mycorrhiza Meeting. Cambridge (3/9/15-4/9/15). Póster: Characterization and functional analysis of a tomato *α,β-hydrolase* gene responsive to mycorrhization

El doctorado/*The doctoral candidate* Tania Ho Plágaro y el director de tesis/*and the thesis supervisor* José Manuel García Garrido

Garantizamos, al firmar esta tesis doctoral, que el trabajo ha sido realizado por el doctorando bajo la dirección del director de tesis y, hasta nuestro conocimiento alcanza, en la realización del trabajo se han respetado los derechos de otros autores a ser citados, cuando se han utilizado sus resultados o publicaciones.

/

Guarantee, by signing this doctoral thesis, that the work has been done by the doctoral candidate under the direction of the thesis supervisor and, as far as our knowledge reaches, in the performance of the work, the rights of other authors to be cited (when their results or publications have been used) have been respected.

Lugar y fecha/*Place and date*:

Director de la Tesis/ *Thesis supervisor*;

Firma/Signed

José Manuel García Garrido

Doctorando/*Doctoral candidate*:

Firma/Signed

Tania Ho Plágaro

Índice

Summary/Resumen

Summary

Arbuscular mycorrhizal (AM) fungi are microscopic fungi that live in symbiosis with the roots of most plants. Among the benefits provided to the plants by this interaction we must highlight a better nutrition and a higher resistance to biotic and abiotic stresses. As both symbionts have coevolved for a long time, probably from the beginning of plant adaptation to the land environment, it is expected that the mechanisms for regulation of mycorrhizal development have also coevolved with plants. In this manner, the development and establishment of the AM symbiosis are fine-tuned regulated by environmental factors including nutritional conditions, as well as by molecular dialog and signaling mechanisms, and by a complex network of transcription factors and cofactors. The understanding of the symbiotic process and the key components for its regulation is essential in order to elucidate by what mechanisms the plant is benefited from the interaction with the AM fungi, and to develop strategies to improve the management of the mycorrhizal associations in order to use them as an alternative to the chemical fertilizers and pesticides. Our team work is focused in the analysis of the molecular processes underlying the AM symbiosis using the tomato plant, which constitutes a model plant for physiological and genetic studies and, in addition, it is a worldwide important crop.

In this work, two AM-induced genes from tomato, *tsb* and *SlDLK2*, are subjected to their functional characterization and analysis, due to their possible role in the mycorrhization process. Particularly, *tsb* was chosen because of its possible function in cytoskeleton rearrangements during mycorrhization; while *SlDLK2*, encoding for a protein from the α,β-hydrolase family, because of its possible role as a relevant hormonal receptor involved in signaling during the mycorrhizal process.

First of all, in order to quickly and easily screen the functionality of these genes during mycorrhization, a method for obtaining composite tomato plants using *Agrobacterium rhizogenes*-mediated transformation was implemented. The resulting plants were composed of a transformed root system and a wild type aerial part. An optimized protocol was successfully set up for the transformation and

generation of composite seedlings for mycorrhizal studies, with high success rates and that allows to undoubtedly identifying and selecting tomato cotransformed roots from the beginning until the harvesting time through visual selection using the fluorophore marker DsRed, without the requirement of antibiotics. Three different binary vectors were tested for silencing, overexpressing and promoter-GUS expression studies, that have allowed us to successfully perform a functional analysis of the candidate genes. This method, which have been recently published (Ho-Plágaro et al. 2018), is presented in **Chapter 1** of this doctoral dissertation.

The research carried out regarding the *tsb* gene is shown in **Chapter 2**. *Tsb* encodes a putative MAP (Microtubule Associated Protein) that belongs to a family of MAPs unique from Solanaceae plants. Some of the members of this MAP family have been previously described as pollen specific and with a function in cytoskeleton rearrangements and the formation of the pollen tube (Zhao et al. 2006; Huang et al. 2007; Liu et al. 2013). Here, through the analysis of *tsb*-silenced and *tsb*-overexpressing composite plants, a decreased expression was observed for genes related to arbuscule functionality in the AM *tsb*-silenced roots compared to the wildtype AM roots. In agreement with this result, *tsb*-overexpressing roots showed an induction all genes used as markers of arbuscule and fungal activities. Moreover, the cortical microtubule array seems to be perturbed in *tsb*-overexpressing roots. Microtubules and microfilaments are not only known to determine the structure of the cell and its organelles, but also to be involved in the intracellular transportation mechanisms, because they act as "tracks" for the clathrin vesicle trafficking, the main means of transport of the cell, consequently determining the endocytosis and exocytotic pathways. The results obtained in this work point to a role of *tsb* in restructuring the microtubule cytoskeleton in the cortical cells of the roots during mycorrhization and indicate that the action of *tsb* is related to the specific exocytosis processes for the delivery of proteins and compounds to the periarbuscular membrane and the symbiotic interface to allow arbuscule functionality and activity.

The second gene studied in this work is a gene that encodes for a protein belonging to the α.β-hydrolase family, particularly to the DLK2 group. For this reason, it was named as *SlDLK2*. Curiously, the DLK2 protein group is phylogenetically very close to the strigolactone receptors (D14) and the karrikin receptors (KAI2).

Strigolactones are plant hormones that play an important role in presymbiotic signaling during mycorrhization. In addition, the karrikin receptor KAI2 has been recently shown to be essential for the AM symbiosis (Gutjahr et al. 2015). However, DLK2 α.β-hydrolases are little characterized, and no relation has yet been found between DLK2 and the mycorrhization process. In **Chapter 3** is presented our research work performed to elucidate if SlDLK2 is a signaling receptor important during MA symbiosis. Composite plants with transformed roots were obtained, and we observed that *SlDLK2* silencing showed a significant increase of AM fungal development in the host roots and an induction of mycorrhizal functionality (determined in terms of transcriptional levels). However, *SlDLK2* overexpression gives place to an anomalous arbuscule development, with lack of branching, what suggest that SlDLK2 has a clear role in the development and branching of the arbuscules. Additionally, SlDLK2 has a conserved catalytic triad, responsible of the hydrolytic activity described for the strigolactone and karrikin receptors, and here we have actually probed that SlDLK2 retains some ability to interact and hydrolyze synthetic strigolactones. Although our research have not allowed us to elucidate the chemical structure of the specific ligand for SlDLK2, the results obtained so far point to the C13 α-ionols derivatives as the possible ligands.

Finally, in **Chapter 4**, in order to clarify the possible signaling role of the SlDLK2 receptor during mycorrhization, transcriptomic alterations and the predicted changes in metabolic pathways in *SlDLK2*-silenced plants are shown, and the causes and consequences of these changes are discussed. Biggest changes observed were associated to a nutrient starvation and induced defense signature in the *SlDLK2*-RNAi mycorrhizal roots, probably as a consequence of the higher AM development and/or activity in these plants. However, examination of many other differentially expressed genes supports the idea of SlDLK2 as a negative regulator of mycorrhization, and that SlDLK2 might be important to activate GA signaling, restrict hexose production and carbohydrate supply to the AM fungus, and induce a number of resistance mechanisms, in order to control AM fungal development.

Resumen

Los hongos micorrícico arbusculares (MA) son hongos microscópicos que viven en simbiosis con las raíces de la mayoría de las plantas. Entre los beneficios que aporta la formación de MA para las plantas caben destacar desde una mejor nutrición, hasta una mayor defensa ante estreses tanto bióticos como abióticos. Como consecuencia de la larga coevolución en simbiosis, dado que posiblemente esta asociación se formó desde el inicio de la adaptación de las plantas al medio terrestre, los mecanismos de regulación y control del desarrollo de la simbiosis han ido evolucionando a la par que la propia evolución de las plantas. Así, el desarrollo y establecimiento de la simbiosis MA están regulados muy finamente, tanto por condicionantes medioambientales incluyendo aspectos nutricionales, como por mecanismos de diálogo y señalización molecular, así como por una compleja red de factores y cofactores transcripcionales. La comprensión del proceso simbiótico y de los elementos clave en su regulación es esencial a la hora de averiguar los mecanismos por los que la planta es beneficiada en su interacción con los hongos MA, y desarrollar estrategias que permitan una mejor gestión de dicha asociación y de su aprovechamiento como alternativa al uso de fertilizantes químicos y plaguicidas. Nuestro equipo de trabajo está focalizado en desgranar los procesos moleculares que ocurren en la simbiosis MA, tomando como modelo la planta de tomate, ya que, además de suponer uno de los cultivos más importantes a escala mundial, es una planta muy adecuada para el estudio de la micorrización, entre otras razones por ser una planta modelo de estudios fisiológicos y genéticos.

En este trabajo se ha realizado la caracterización y el análisis funcional de dos genes de tomate inducidos por micorrización, y denominados *tsb* y *SlDLK2*, candidatos a jugar un papel relevante en la simbiosis MA. Concretamente, uno de ellos, el *tsb*, se eligió por ser posiblemente importante para la reorganización del citosqueleto de las células de la raíz durante la micorrización, y el segundo de ellos, *SlDLK2*, por codificar para una proteína de la familia α/β-hidrolasa que podría ser un posible receptor hormonal relevante en la señalización del proceso micorrícico.

Como primer paso y para evaluar de manera rápida y eficaz la funcionalidad de estos genes en la simbiosis MA, se ha implementado un método para la obtención de

plantas "compuestas" de tomate, es decir, plantas con un sistema radical transformado pero con la parte aérea silvestre, generadas mediante transformación por *Agrobacterium rhizogenes*. Se ha conseguido un protocolo optimizado para la transformación y generación de plántulas compuestas para experimentos de micorrización con una gran tasa de éxito, y que además permite la identificación inequívoca de aquellas raíces transformadas desde el inicio hasta el momento de su cosecha mediante una selección visual, usando el fluoróforo DsRed, y sin necesidad de antibióticos. Se dispone de una colección de vectores binarios de transformación, tanto para experimentos de silenciamiento, sobrexpresión, o análisis de la actividad de promotores, que nos ha permitido realizar un análisis funcional de los genes objeto de estudio. Este método, que actualmente constituye una herramienta base en nuestro laboratorio, ha sido publicado recientemente (Ho-Plágaro et al. 2018) y es presentado en el **Capítulo 1** de esta memoria de Tesis.

La investigación desarrollada en torno al gen *tsb* se expone en el **Capítulo 2**. El gen *tsb* codifica para una putativa MAP (Proteína Asociada a Microtúbulos), perteneciente a una familia de MAPs exclusiva de Solanáceas, dentro de la cual algunos miembros han sido anteriormente descritos como específicos del polen y con una función en la restructuración del citosqueleto y en la formación del tubo polínico (Zhao et al. 2006; Huang et al. 2007; Liu et al. 2013). Aquí, a través del análisis de plantas compuestas silenciadas y sobreexpresadas para tal gen, se han obtenido resultados que muestran que, comparativamente con las raíces silvestres, en las raíces silenciadas se observa una disminución de la expresión de genes relacionados con la funcionalidad del arbúsculo. En consonancia, en las raíces con sobreexpresión del *tsb* se incrementa la inducción de todos los genes marcadores de la actividad arbuscular, así como de la actividad fúngica. Además, la organización de los microtúbulos corticales parece verse alterada en las células sobreexpresadas para el gen *tsb*. Los microtúbulos y microfilamentos no sólo se conocen por su papel en determinar la estructura de la célula y sus orgánulos, sino también por su implicación en los mecanismos de transporte intracelular, ya que actúan como las "vías de circulación" para el tráfico de las vesículas de clatrina, el principal medio de transporte en las células, y por lo tanto determinan las rutas de endocitosis y exocitosis. Los resultados de este trabajo apuntan a que el gen *tsb* está implicado en

la restructuración del citosqueleto de microtúbulos (MT) en las células del córtex durante la micorrización y que su acción quizás sea especialmente importante en los procesos de exocitosis específicos para la liberación de proteínas y compuestos a la membrana periarbuscular y a la interfase simbiótica que permiten la correcta funcionalidad y actividad del arbúsculo.

El segundo gen estudiado en este trabajo ha sido el gen que codifica para una proteína perteneciente a la familia α,β-hidrolasa, concretamente al grupo DLK2, de ahí que haya sido nombrada como SlDLK2. Curiosamente, el grupo de proteínas DLK2 está muy cercano filogenéticamente a los receptores de estrigolactonas (receptores D14) y de karrikinas (receptores KAI2). Las estrigolactonas son hormonas vegetales que tras ser exudadas por las raíces de las plantas juegan un papel importante en la señalización presimbiótica durante la micorrización. Por otra parte, recientemente se ha descubierto que el receptor de karrikinas, KAI2, parece ser esencial para la micorrización (Gutjahr et al. 2015). Sin embargo, las α,β-hidrolasas de tipo DLK2 están poco caracterizadas, y no existe en la literatura ninguna mención de su posible relación con la micorrización. En el **Capítulo 3** se presenta la investigación realizada tratando de dilucidar si SlDLK2 es un receptor importante en la señalización durante la simbiosis MA. Los resultados con plantas compuestas con raíces transformadas mostraron que el silenciamiento de *SlDLK2* provoca un incremento leve pero significativo tanto del desarrollo del hongo MA en la raíz hospedadora, como de la funcionalidad de la micorrización (determinada a nivel transcripcional), mientras que la sobreexpresión de *SlDLK2* da lugar a una reducción de la colonización micorrícica y de su funcionalidad, así como a un desarrollo anómalo de los arbúsculos, carentes de ramificación, lo cual indica un papel claro de SlDLK2 en el desarrollo y ramificación de los arbúsculos. Además, SlDLK2 tiene conservada la tríada catalítica responsable de la actividad hidrolítica descrita para los receptores de estrigolactonas y karrikinas, y aquí hemos comprobado que efectivamente SlDLK2 tiene cierta capacidad de interaccionar e hidrolizar estrigolactonas sintéticas. No obstante, la investigación realizada hasta el momento no nos ha permitido aún elucidar la naturaleza química del ligando específico de SlDLK2, si bien los resultados apuntan a que quizás se trate de moléculas derivadas de los C13 α-ionoles.

Finalmente, en el **Capítulo 4**, y con el objetivo de esclarecer la posible señalización mediada por el receptor SlDLK2 durante la micorrización, se presentan los resultados del análisis de las alteraciones transcriptómicas que sufren las plantas micorrizadas al ser silenciadas para *SlDLK2*, así como se discuten las causas y/o consecuencias de dichos cambios en función de las rutas metabólicas afectadas. Los cambios más destacables que presentaron las raíces *SlDLK2* RNAi micorrizadas parecen estar relacionados con una situación de deficiencia nutricional y con la activación de mecanismos de defensa, lo cual podría ser interpretado como una consecuencia del mayor desarrollo y/o actividad micorrícica en dichas plantas. Sin embargo, al examinar en detalle otros genes diferencialmente expresados, los resultados apoyan la idea de que SlDLK2 actúe como un regulador negativo de la micorrización, pudiendo jugar un papel importante en la activación de la señalización mediada por giberelinas, restringiendo la producción de hexosas y el aporte de hidrocarburos al hongo, así como induciendo una serie de mecanismos de resistencia a fin de controlar el desarrollo fúngico.

Introducción (Introduction)

1. La simbiosis Micorrícico-Arbuscular (MA)

La simbiosis micorrícico-arbuscular (MA) es la simbiosis que más predomina y la que está más extendida en el reino vegetal (Smith and Read 2008). Esta asociación mutualista microorganismo-planta se establece entre los hongos endosimbióticos MA (hongos microscópicos del suelo que conforman el filum Glomeromycota) (Smith and Read 2008) y plantas superiores, incluyendo la mayoría de las especies de interés agrícola y forestal. En las células corticales de la raíz, los hongos MA desarrollan estructuras intraradicales muy ramificadas y especializadas, denominadas arbúsculos, en los que ocurre el intercambio bidireccional de nutrientes entre la planta y el hongo (Bonfante and Requena 2011; Gutjahr and Parniske 2013). El hongo MA incrementa la capacidad exploradora de la planta a través de una extensa red de hifas externas en la rizosfera, que son capaces de tomar de forma muy eficiente agua y nutrientes, principalmente fosfato inorgánico, de zonas del suelo inaccesibles a las raíces (Smith and Read 2008), y estos nutrientes son transportados hasta los arbúsculos, donde son transferidos a la planta. A cambio, el hongo obtiene el carbono que requiere de la planta en forma de productos de la fotosíntesis (Javot et al. 2007b; Harrison 1999; Govindarajulu et al. 2005; Smith and Read 2008) o de lípidos (Wewer et al. 2014; Jiang et al. 2017). Durante el establecimiento de la simbiosis MA, las células de la planta sufren grandes cambios morfológicos y funcionales, lo que sugiere que existe un alto grado de interacción entre ambos organismos simbiontes a nivel celular, molecular y genético.

2. Filogenia, evolución y clasificación de hongos MA

Hace 475 millones de años (Ma), a mediados del Ordovícico, comienza el registro fósil de las plantas terrestres (Wellman et al. 2003); mientras que las primeras esporas e hifas fosilizadas han sido detectadas en sustratos de hace 460 Ma, y se asemejan tremendamente a los hongos micorrícico-arbusculares actuales (Redecker et al. 2000), pertenecientes al filum Glomeromycota (o Mucuromycota).

Debido a que los primeros fósiles encontrados correspondientes tanto a plantas terrestres como a estructuras similares a los hongos MA, datan de fechas muy parecidas, se cree de que las asociaciones MA se pudieron originar en las primeras plantas terrestres hace 450 Ma (Taylor and Osborn 1996; Brundrett 2002). Sin embargo, realmente el primer fósil bien preservado de la interacción simbiótica MA es un rizoma micorrícico que data de hace 407 Ma en el yacimiento del Devónico de Rhynie Chert (Taylor and Osborn 1996; Krings et al. 2007).

Los estudios genómicos muestran que algunos genes simbióticos vegetales preceden a las plantas terrestres (Delaux et al. 2015; Martin et al. 2017). Además, la simbiosis MA y la simbiosis *Rhizobium*-leguminosa comparten muchos mecanismos de señalización y de regulación, y se da una pérdida común de genes simbióticos en los linajes de plantas no micorrícicas (Delaux et al. 2015; Bravo et al. 2016; Kamel et al. 2017a). Por último, la simbiosis MA está ampliamente distribuida en las actuales familias del reino vegetal, y se encuentra en muchas plantas terrestres tempranas que carecen de un sistema radical verdadero, incluyendo hepáticas, antoceros, licófitas y helechos. De este modo, las evidencias fósiles, así como los datos moleculares, y el hecho de que la simbiosis MA está actualmente presente en las familias de plantas con más antigüedad, apoyan la idea de que los hongos MA puedan tener un origen temprano único común y que aparecieron junto con las primeras plantas terrestres carentes aún de sistemas radiculares verdaderos (Brundrett 2002; Bravo et al. 2016; Field et al. 2012), en lugar de aparecer tarde en el Silúrico cuando la complejidad vegetal incrementó rápidamente.

A la expansión generalizada de la micorrización por hongos MA en las primeras plantas terrestres, le siguieron dos olas evolutivas más de simbiosis micorrícicas, asociadas a los cambios climáticos y a un incremento de la complejidad en los hábitats y en los suelos (Brundrett and Tedersoo 2018). En particular, en el Cretácico, además de aparecer linajes de plantas no micorrícicas, también surgieron los grupos fúngicos Ascomycota y Basidiomycota relacionados con nuevos tipos de micorrizas: las ericoides, las orquioides y múltiples familias de ectomicorrizas. Finalmente, en la actualidad está teniendo lugar una tercera ola de diversificación de las micorrizas, asociada a la rápida diversificación del mundo vegetal en los puntos calientes de biodiversidad y a la presencia de raíces cada vez más complejas.

Hoy en día, la diversidad micorrícica en las plantas terrestres se estima como sigue: 72% micorrizas arbusculares, 2.0% ectomicorrizas, 1.5% micorrizas ericoides, 10% micorrizas orquioides, un 7% con un patrón inconsistente, ya que a veces muestran asociaciones MA y otras veces no están micorrizadas, y el 8% son totalmente no micorrícicas. Este último grupo incluye especialistas nutricionales, como plantas carnívoras y parásitas, o especialistas en hábitats, como los epífitos (Brundrett and Tedersoo 2018).

En el año 2001, los estudios filogenéticos de hongos micocrrícicos llevados a cabo por Schüβler et al. (2001), basados en las secuencias rRNA de la subunidad pequeña ribosomal (Fig. 1), y teniendo en cuenta caracteres morfológicos y ecológicos, demostraron que los hongos micorrícicos arbusculares (junto con el hongo *Gosiphon pyriformis* endosimbionte de cianobacterias) constituían un grupo monofilético. Por dicha razón, los hongos MA fueron eliminados del grupo polifilético Zygomycota, y recolocados en un nuevo Phylum de pequeño tamaño que fue denominado Glomeromycota (Schüβler et al. 2001).

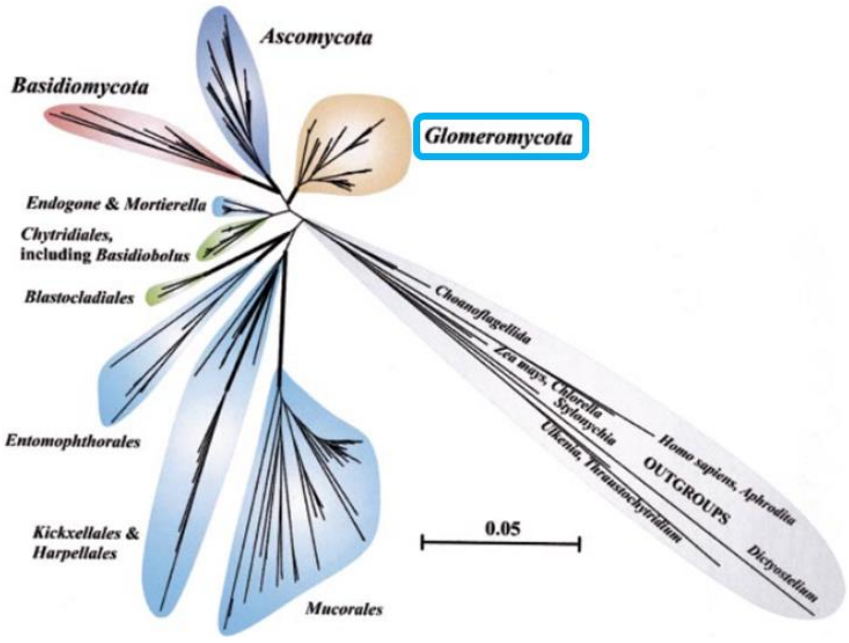

Figura 1. Filogenia de los hongos basada en secuencias rRNA de la subunidad pequeña ribosomal. Imagen tomada de Schüβler et al. (2001). El Phylum Glomeromycota, el cual está constituido por los hongos micorrícico-arbusculares, está señalado en un recuadro azul.

Aunque la sistemática de los taxones del Phylum Glomeromycota tradicionalmente se ha basado en la morfología de las esporas, la insuficiencia de caracteres morfológicos detectables ha hecho que hoy en día la filogenia y clasificación de este grupo se apoye en gran medida en datos filogenéticos de naturaleza molecular. Tras sufrir numerosos cambios y revisiones sistemáticas durante la primera década desde su creación, actualmente el Phylum Glomeromycota cuenta con 4 órdenes, 11 familias, 22 géneros y 230 especies descritas (Schüßler and Walker 2010) (Figure 2).

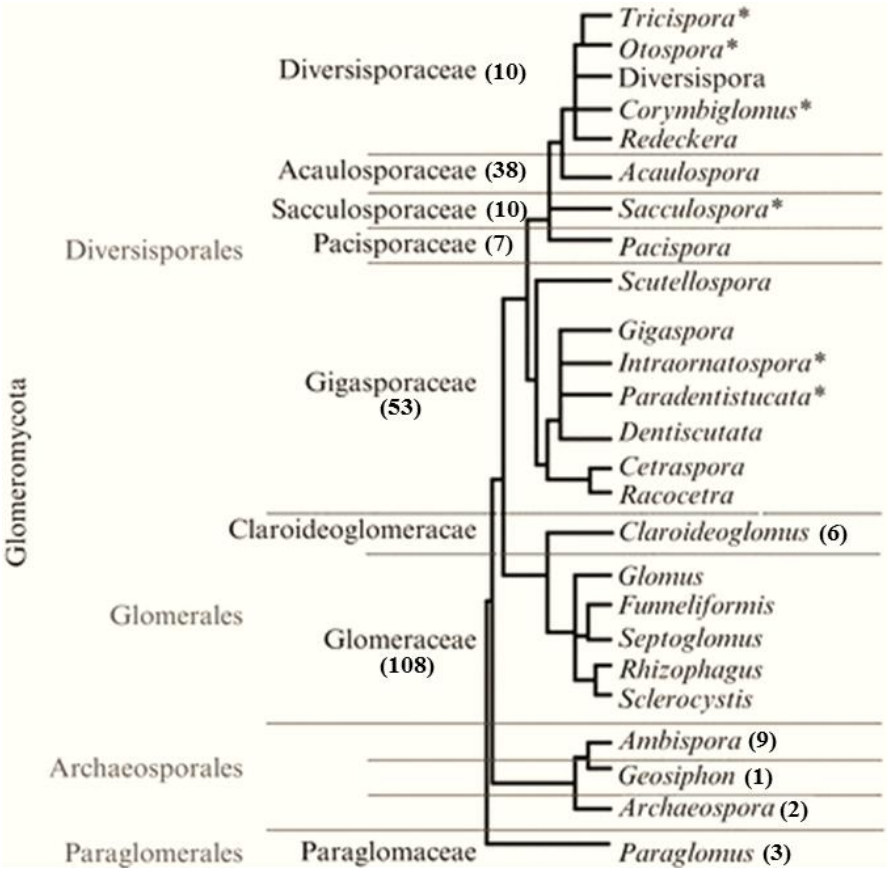

Figure 2. Taxonomía de los hongos micorrícico arbusculares propuesta por Redecker et al. (2013), Krüger et al. (2012), y Oehl et al. (2011). Imagen tomada de Souza (2015). El número de especies descritas para los diferentes taxones está indicada entre paréntesis. *Evidencias insuficientes, pero grupos aún mantenidos.

Aunque los datos moleculares reflejan mejor las relaciones filogenéticas de los hongos formadores de micorrizas arbusculares, aún se siguen empleando de forma rutinaria clasificaciones de carácter anatómico. Cabe destacar los dos tipos principales de micorrizas arbusculares reconocidos actualmente en función de las características morfológicas del proceso de colonización: el tipo Arum y el tipo Paris (Dickson 2004) (Fig. 3). El tipo Paris se caracteriza por un crecimiento intracelular de las hifas, a lo largo de las cuales se forman "enrollados hifales" o "arbúsculos enrollados" también intracelulares. En cambio, el tipo Arum forma hifas que crecen intercelularmente y penetran en las células corticales formando los típicos arbúsculos. En ambos tipos se puede dar la formación de vesículas intracelulares. Ambos tipos morfológicos dependen de la combinación entre la especie fúngica y vegetal (Dickson 2004). Aunque se cree que el tipo Paris es el más frecuente en la naturaleza, la mayoría de los genes simbióticos vegetales han sido caracterizados micorrizas tipo Arum (Dickson 2004; Cosme et al. 2018), el cual es el comúnmente encontrado en sistemas radiculares de crecimiento rápido característicos de las plantas de cultivo. En el caso del tomate (y del pepino), se ha observado que es posible la coexistencia de ambos tipos morfológicos de micorrizas arbusculares (Kubota et al. 2005).

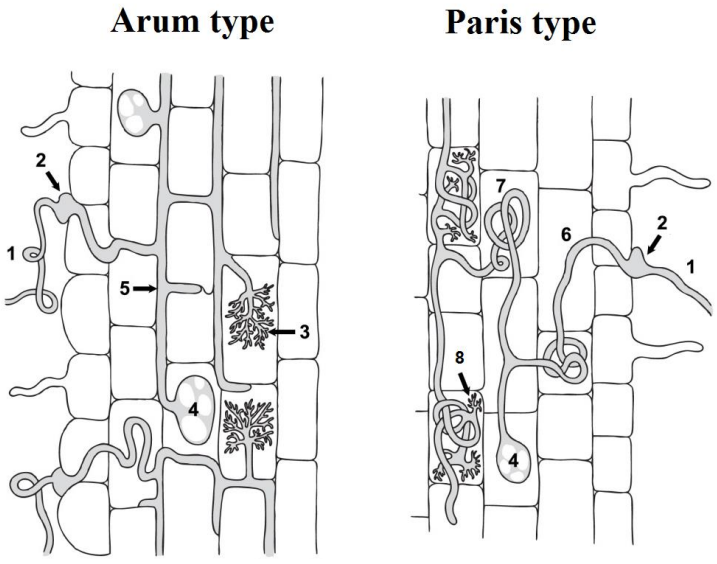

Figura 3. Características de los dos tipos morfológicos de micorrizas arbusculares: tipo Arum y tipo Paris. **1. Micelio extrarradical; 2 hipopodio; 3 arbúsculos típicos; ; 4 vesícula; 5 hifas intercelulares; 6 hifas intracelulares; 7 enrollados hifales; 8 arbúsculos enrollados. Modificación de la ilustración elaborada por** Gávor M. Kovács (Eötvös Loránd University, Department of Plant Anatomy).

Aunque existen numerosos tipos de interacciones micorrícico arbusculares dependiendo de la especie fúngica y de la planta hospedadora, la mayoría de los estudios se restringen al uso de unas pocas especies modelo. Los hongos MA mayoritariamente utilizados son *Rhizophagus irregularis*, *Funneliformis mosseae*, *Gigaspora rosea* y *Gigaspora margarita*; mientras que las plantas hospedadoras más frecuentemente usadas como modelo para los estudios de interacción MA son *Medicago truncatula*, *Lotus japonicus*, arroz (*Oryza sativa*), o algunas solanáceas como la patata (*Solanum tuberosum*) y el tomate (*Solanum lycopersicum*), este último utilizado como modelo en nuestro grupo de investigación.

Rhizophagus irregularis DAOM 197198

Rhizophagus irregularis es uno de los hongos MA más extendidos y comunes en los suelos agrícolas y naturales. El modelo de hongo *R. irregularis* es el que más se usa en investigación porque fue la primera especie de hongo MA que se consiguió establecer en cultivo de órganos radiculares "in vitro", siendo inicialmente determinado como *Glomus intraradices* (Chabot et al. 1992). Los aislados descendientes de este cultivo de raíces establecido en Canadá, frecuentemente referido como DAOM 197198, han sido usados extensamente. Se ha empleado como inóculo para biofertilizantes comerciales desde los años 90 debido a su alta infectividad, y se ha publicado su genoma, tanto nuclear como mitocondrial (Tisserant et al. 2013; Nadimi et al. 2012).

En cuanto a su nombre científico, tal y como explican Malbreil et al. (2014) y Young (2015), irónicamente, el hongo MA mejor estudiado ha sido sujeto a la más compleja secuencia de nombres. La cepa DAOM197198, inicialmente denominada *Glomus intraradices*, pasó a llamarse *Glomus irregulare* cuando una comparación de secuencias de rRNA mostró que había una alta similitud entre ambas especies (Stockinger et al. 2009; Sokolski et al. 2010), a pesar de que DAOM197198 carecía de las esporas irregulares originalmente consideradas como una característica diagnóstica de *Glomus irregulare*. Más tarde, la filogenia de los hongos MA propuesta por Schüßler and Walker (2010) y Krüger et al. (2012), dio lugar a varios géneros nuevos. Como consecuencia *Glomus irregulare* pasó a ser *Rhizophagus irregularis*. El término *Rhizophagus* fue recuperado a partir del primer nombre de género

atribuido históricamente a *Glomus* por Dangeard (1896), quien describió a este organismo como un posible patógeno de raíces causante de la enfermedad del álamo (Rhizo/phagus, etimológicamente "comedor de raíces"). Sin embargo, recientemente se ha discutido que el hongo MA moderno no casa demasiado con la descripción hecha por Dangeard (1896), por lo que el nuevo nombre *Rhizoglomus irregulare* ha sido propuesto para DAOM 197198 (Sieverding et al. 2015). Sin embargo, como *Rhizophagus irregularis* es y sigue siendo el nombre científico más empleado durante los últimos años para designar a DAOM 197198, hemos decidido usar dicho nombre científico en el presente trabajo.

R. irregularis se caracteriza por formar esporas redondeadas (40-190 micras de diámetro) y vesículas en el interior de la raíz de la planta hospedadora. La pared es de tipo amorfo, presentando una capa externa evanescente y una o dos capas internas laminadas de color más oscuro. El grosor de la pared varía entre 3 y 15 micras y se extiende hacia el pedúnculo de la espora en forma de tubo. El color de la espora puede variar desde amarillo hasta marrón claro. Las esporas y las vesículas se forman en el interior de la raíz de la planta hospedadora, sin embargo, también pueden encontrarse libremente en el suelo, provenientes de restos de otras raíces colonizadas (Schenck y Smith, 1982). Como todos los hongos micorrícicos, *R. irregularis* es un hongo asexual, cuyas esporas e hifas son multinucleadas, pudiendo presentar una sola espora miles de núcleos. Este hecho hace imposible la obtención de mutantes estables con las metodologías que se conocen actualmente. Pese a ello, se han llevado a cabo proyectos de expresión transitoria de genes marcadores mediante biobalística (Harrier and Millam 2001; Helber and Requena 2008), así como de silenciamiento inducido por el hospedador (HIGS) (Tsuzuki et al. 2016; Helber et al. 2011).

3. El ciclo simbiótico

El ciclo simbiótico se inicia en la rizosfera, con la comunicación química entre el hongo micorrícico arbuscular (MA) y las raíces de la planta hospedadora. Antes del contacto físico entre ambos simbiontes, los dos organismos liberan señales para

inducirse respuestas preparativas mutuamente (Buee et al. 2000; Chabaud et al. 2011). Las raíces de la planta exudan estrigolactonas (SLs) y las liberan a la rizosfera, sobre todo en respuesta a condiciones de falta de fosfato en el medio. Una vez en la rizosfera, las SLs inducen la germinación de esporas del hongo MA, así como el crecimiento y ramificación de sus hifas hacia la raíz hospedadora (Waters et al. 2017). Por otra parte, el hongo MA libera los llamados factores Myc (Myc-LCOs y Myc-COs), los cuales son reconocidos por receptores de la planta (De Mita et al. 2014; Den Camp et al. 2011; Miyata et al. 2014; Zhang et al. 2015a) y desencadenan una ruta de señalización conocida como "common symbiosis signaling pathway" (CSSP) debido a que es común a los dos tipos de simbiosis planta-rhizosfera más estudiados: la simbiosis MA y la simbiosis *Rhizobium*-leguminosa (Oldroyd 2013). Un esquema general del CSSP se muestra en la Figura 4.

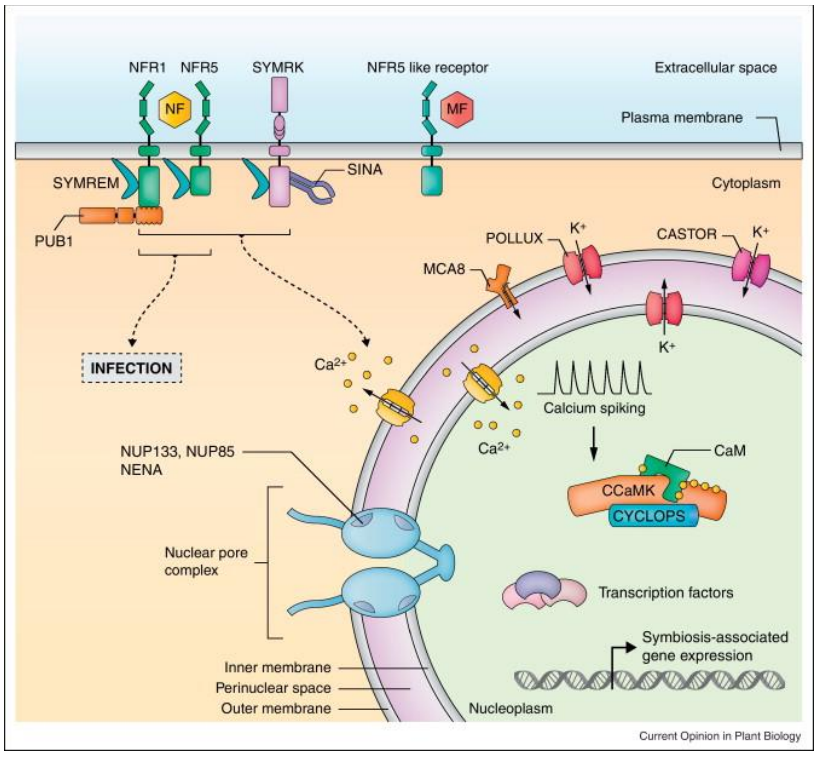

Figura 4. Ruta común de señalización simbiótica (CSSP; Common Symbiosis Signalling Pathway) en la simbiosis micorrícico-arbuscular y en la simbiosis raíz-nódulo. La percepción de las señales derivadas de hongos MA (MF; Myc Factors) o de Rhizobium (NF; Nod Factors) por mediación de kinasas receptoras tipo LysM, desencadenan la transducción temprana de la señal simbiótica. Los factores Myc y Nod inducen picos de calcio dentro y alrededor del núcleo de la célula vegetal (kosuta et al., 2008). En concreto, los picos de calcio perinucleares se dan gracias a la liberación de calcio por parte de algún compartimento de reserva (muy probablemente la envoltura nuclear) a través de canales de calcio todavía no identificados. Los canales permeables a potasio CASTOR y POLLUX pueden compensar el

desbalance de cargas iónicas. Las nucleoporinas NUP85 y NUP133 son necesarias para que se produzcan los picos de calcio, aunque su modo de acción aún se desconoce. La proteína kinasa dependiente de calcio-calmodulina (CCaMK) forma un complejo con el factor de transcripción CYCLOPS, que se fosforila y activa desencadenando una gran parte de las respuestas simbióticas. Figura tomada de Singh and Parniske (2012). La nomenclatura empleada para las proteínas es la correspondiente a *Lotus japonicus*.

El CSSP, muy probablemente junto con otras rutas de señalización independientes del CSSP (Madsen et al. 2010; Hayashi et al. 2010), desencadena una serie de mecanismos que preparan a la raíz para la interacción simbiótica.

En el desarrollo del hongo dentro de la raíz se distinguen distintas etapas (Fig. 5). Cuando la hifa en crecimiento contacta con la superficie de la raíz, se forma una estructura fúngica llamada hifopodio o apresorio. A continuación, las células epidérmicas de la raíz sufren una serie de eventos de reorganización para formar el aparato de prepenetración (PPA) que guía y permite el paso de la hifa a través de la célula vegetal (Genre et al. 2005; Genre et al. 2008). Después de atravesar la epidermis, la hifa crece y se ramifica intercelularmente hasta alcanzar las células del córtex, en las cuales penetra y forma estructuras intracelulares altamente ramificadas denominadas arbúsculos. Además, eventualmente se forman en el apoplasto de las células corticales unas estructuras denominadas vesículas, las cuales se cree que funcionan como órganos de reserva para el hongo MA. En el micelio extraradical se suelen formar nuevas esporas al final de las hifas.

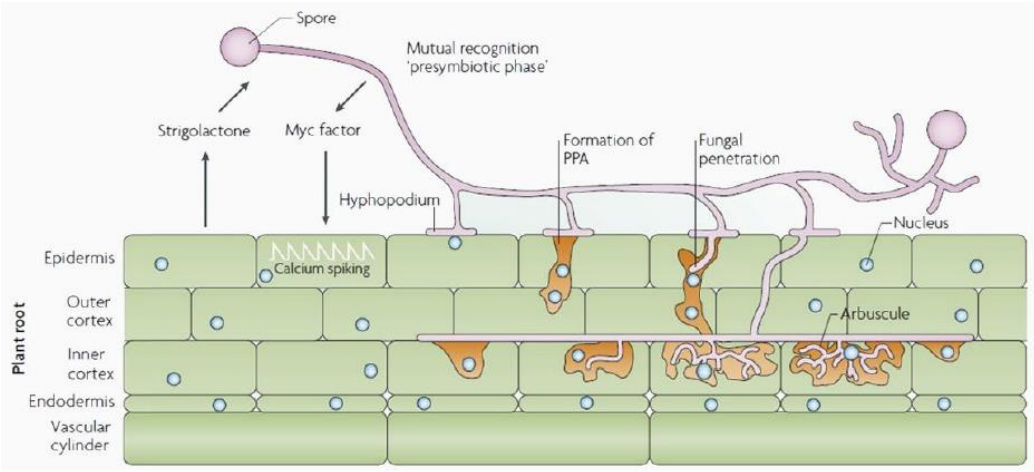

Figura 5. Etapas en el desarrollo de las micorrizas arbusculares. Ilustración modificada de Parniske (2008).

Los arbúsculos (Fig. 6) están delimitados por una membrana vegetal denominada membrana periarbuscular, que separa al arbúsculo del citoplasma vegetal (Parniske 2008) y que posee una composición única en proteínas de transporte específicas para permitir el intercambio de nutrientes con el simbionte fúngico (Harrison et al. 2002; Javot et al. 2007a; Kobae and Hata 2010; Yang et al. 2012; Krajinski et al. 2014; Wang et al. 2014a).

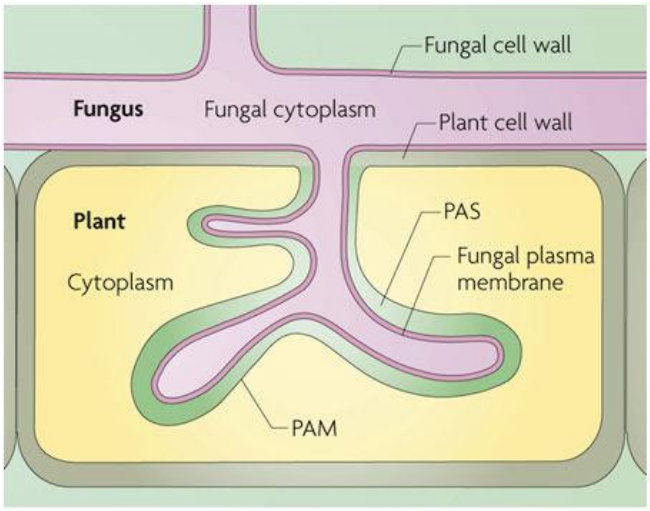

Figura 6. Representación esquemática del arbúsculo. Las ramificaciones fúngicas que penetran las células vegetales están rodeadas por una membrana derivada de la célula vegetal ("membrana periarbuscular") que forma un continuo con la membrana plasmática de la célula vegetal. La interfase apoplástica situada entre la membrana plasmática fúngica y la membrana periarbuscular vegetal se denomina "espacio periarbuscular" (PAS). Dada la capacidad de ambas membranas de sintetizar componentes de la pared celular, el espacio periarbuscular contiene componentes de la pared celular de origen tanto fúngico como vegetal. Figura tomada de Parniske (2008).

4. Reorganización celular y del citoesqueleto vegetal

Para el establecimiento de la simbiosis MA es esencial que las células vegetales de la raíz, tanto epidérmicas como del córtex, sufran una profunda reorganización a fin de permitir la penetración intracelular de las hifas fúngicas. Algunas de las alteraciones morfológicas y fisiológicas que sufren las células colonizadas son la invaginación de la membrana plasmática, la fragmentación de la vacuola central, el movimiento del núcleo y otros orgánulos hacia el centro de la célula, la formación de *novo* de la llamada membrana periarbuscular y la localización de las respectivas

proteínas transmembrana específicas, así como la deposición de moléculas y proteínas específicas de la pared celular que forman parte de la interfase simbiótica (Reinhardt 2007).

En todas estas drásticas reorganizaciones celulares se cree que juega un papel esencial el citosqueleto, concretamente el formado por los microtúbulos (MTs), ya que se ha observado que dichos MTs sufren enormes cambios que acompañan el proceso de establecimiento de la simbiosis MA. Por ejemplo, desde el primer contacto de la hifa fúngica con la superficie de la raíz, la célula epidérmica contactada restructura la disposición de sus MTs corticales (aquellos situados en la periferia de la célula), los cuales cambian de una organización transversal a una orientación aleatoria (Genre et al. 2005).

De forma similar, en ausencia de hongo MA, las células corticales del parénquima muestran una disposición helicoidal oblicua de los MTs corticales, además de algunos haces de MTs envolviendo el núcleo, el cual se encuentra desplazado hacia la periferia probablemente debido a la presencia de una gran vacuola central. En cambio, cuando la raíz es colonizada, aquellas células que se convierten en hospedadoras de arbúsculos modifican profundamente la organización de sus MTs, los cuales pasan de su anterior orientación helicoidal a una disposición completamente aleatoria. Además, se ha visto que estos cambios no sólo se producen en las células con arbúsculos sino también al menos en las dos filas longitudinales de células adyacentes (Blancaflor et al. 2001). Sin embargo, parece ser que estos MTs corticales no se mantienen hasta el final de la vida del arbúsculo, sino que, por el contrario, van fragmentándose en los arbúsculos maduros hasta acabar desapareciendo y, en su lugar, aparecen otros MTs con una organización completamente nueva que consiste en MTs que discurren a lo largo de las hifas arbusculares, envolviendo todo el arbúsculo y enlazando unas hifas con otras o con el núcleo (Genre and Bonfante 1997; Genre and Bonfante 1998; Blancaflor et al. 2001). Finalmente, cuando el arbúsculo empieza la etapa de senescencia, se vuelven a formar nuevos MTs corticales que aumentan progresivamente en longitud (Blancaflor et al. 2001). En la Figura 7, se pretenden resumir estos cambios que sufre el citoesqueleto MT en las células invadidas por arbúsculos en las distintas etapas.

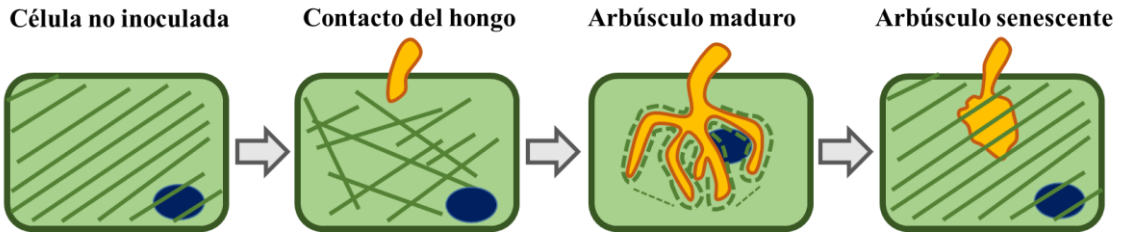

Figura 7. Distribución de los microtúbulos corticales en las células del córtex de la raíz en las distintas etapas de la micorrización. Basado en los resultados de Blancaflor et al., (2001).

Por otra parte, en las células vegetales, la envoltura nuclear actúa como centro organizador de microtúbulos (MTOC), controlando el ensamblaje y la organización de los microtúbulos. El MTOC normalmente se encuentra rodeando el núcleo, sin embargo, se ha visto que en las células colonizadas por el hongo MA, el MTOC (visualizado a través del marcaje de la γ-tubulin) pasa a una disposición difusa entorno a las ramificaciones finas del arbúsculo (Genre and Bonfante 1999).

Además, cabe mencionar que en las células colonizadas por hongos MA, parece producirse un incremento de la síntesis de tubulina. Por ejemplo, la expresión del gen de maíz *Tubα3*, codificante para una tubulina, únicamente se induce en células hospedadoras de arbúsculos (Bonfante et al. 1996). Adicionalmente, mediante marcaje con fluorescencia, se ha observado que en las células micorrizadas se incrementa la cantidad de α -tubulina correspondiente a los MTs (Genre and Bonfante 1997), así como la γ –tubulina correpondiente al MTOC (Genre and Bonfante 1999).

Aunque está menos estudiado, los filamentos de actina también sufren cambios durante la micorrización y, al igual que los MTs, se disponen envolviendo los arbúsculos maduros (Genre and Bonfante 1998; Genre et al. 2005). Al contrario de lo que ocurre en las células animales, el principal papel que está descrito para el citosqueleto de actina en las células vegetales es su implicación en el tráfico de membranas (Wang and Hussey 2015), por lo que podría tener un papel importante en la formación de la membrana periarbuscular.

Si bien no se conocen con exactitud las señales que desencadenan los cambios en el citosqueleto vegetal durante la micorrización, se cree que se trata de una combinación de estímulos químicos y mecánicos, dada la alta similitud que se ha encontrado entre la respuesta a microorganismos invasores (tanto patogénicos

como simbióticos), y la respuesta a estímulos mecánicos artificiales como el contacto con una microaguja. Tal y como se muestra en la Figura 8, en todos los casos se observa que bajo el sitio de contacto se agregan los filamentos de actina a modo de haces, se forma una zona libre de microtúbulos y se acumulan componentes endomembranales provenientes del retículo endoplasmático o de orgánulos como los peroxisomas (Jayaraman et al. 2014; Hardham et al. 2008).

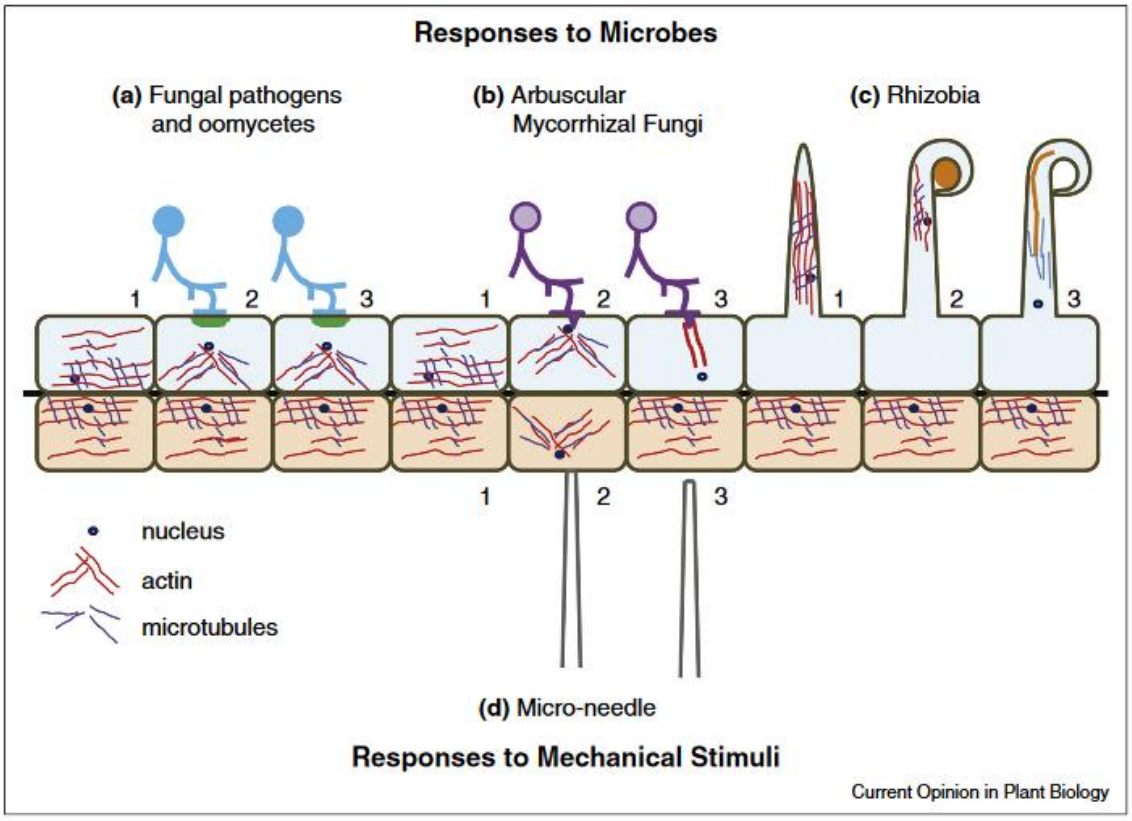

Figura 8. Comparación de los cambios en células vegetales durante la interacción con microorganismos y ante la aplicación de estímulos físicos. Imagen tomada de Jayaraman et al. (2014). Se compara la respuesta de la célula vegetal a hongos patogénicos (a), hongos MA (b), *Rhizobium* (c), o estímulos físicos (d). Para los cuatro tipos de estímulos, se ilustran las alteraciones que sufren el núcleo (punto), los filamentos de actina (en rojo) y los microtúbulos (en azul) de la célula vegetal antes de la interacción (1), durante la interacción (2) y tras la interacción (3). En todos los casos el núcleo, los filamentos de actina y los microtúbulos migran al punto de contacto, sin embargo, existen ciertas diferencias. En el caso de los hongos patógenos, en el punto de contacto se forma una estructura de resistencia denominada papila (en verde) (a2). En los hongos MA y *Rhizobium*, el movimiento de núcleo guía la formación del aparato de pre-penetración (b3) o de la hebra de infección (c3), respectivamente, mediante la fusión de membranas, formando un conducto para la infección. En los estímulos físicos, los cambios revierten una vez cesa la presión ejercida (d3).

5. Beneficios obtenidos por ambos simbiontes en la asociación MA

El hongo MA es un simbionte obligado y, como tal, no puede completar su ciclo si no es en simbiosis con las raíces de las plantas, a través de las cuales obtiene el carbono que le es esencial para su crecimiento. Sin embargo, las ventajas que obtiene la planta de esta interacción también son de gran relevancia. De hecho, se especula que los hongos MA ayudaron y fueron determinantes en la aparición de las primeras plantas terrestres, ayudando a la adquisición de nutrientes por parte de la planta en el nuevo y adverso ambiente terrestre (Pirozynski and Malloch 1975). Además, hasta día de hoy, la simbiosis MA se ha conservado en el mundo vegetal, pudiendo encontrar en cada uno de los principales biomas aproximadamente 200000 especies vegetales que presentan este tipo de simbiosis (Davison et al. 2015; Heijden et al. 2015), por lo que los hongos MA deben ser considerados como componentes integrales del ciclo de vida de la planta de gran importancia en los ecosistemas terrestres. La aportación de nutrientes a la planta aún sigue siendo considerada como la principal ventaja de las micorrizas arbusculares, sobre todo de fósforo y, en menor medida, nitrógeno y otros minerales necesarios para la nutrición de la planta. Esto es posible gracias a que las hifas fúngicas son hasta 100 veces más largas que los pelos radiculares, de modo que el hongo aumenta enormemente la superficie de absorción de la raíz, y, en segundo lugar, a que el hongo MA es capaz de movilizar nutrientes que están en el suelo pero cuya disponibilidad es muy limitada. El fósforo es el macronutriente más importante después del nitrógeno, y sin embargo constituye un elemento con una movilidad muy escasa en el suelo, lo cual lo convierte en el macronutriente más limitante de los cultivos agrícolas (Mohammadi et al. 2011; Balemi and Negisho 2012). En la agricultura convencional, esta problemática se suele abordar mediante el aporte de fertilizantes químicos a las tierras de cultivo, pero esto conlleva grandes inconvenientes medioambientales derivados del movimiento de P a superficie y a aguas subterráneas (Grant et al. 2005). En este aspecto, los hongos MA suponen una interesante alternativa a la hora de incrementar la biodisponibilidad y aprovechamiento del P endógeno de los suelos de forma sostenible, y de así mejorar el estatus nutricional de los cultivos (Aggarwal et al. 2011).

Aunque la adquisición de nutrientes es considerada la aportación más relevante de los hongos MA a las plantas, existe una lista muy larga de otros beneficios que

proporcionan los hongos MA, y seguramente muchos de ellos aún se desconocen. A continuación se pretenden resumir los más importantes:

Resistencia frente a estreses abióticos: las micorrizas arbusculares son capaces de aumentar la resistencia de las plantas frente a otras situaciones diferentes de estrés abiótico además de la deficiencia de nutrientes (Latef et al. 2016), incluyendo la salinidad (Aroca et al. 2013), bajas temperaturas (Chen et al. 2013), altas temperaturas (Gavito et al. 2005), el estrés hídrico (Zhu et al. 2012; Ruiz-Lozano et al. 2016) y la toxicidad por metales pesados (Schutzendubel and Polle 2002; Upadhyaya et al. 2010).

Resistencia frente a estreses bióticos: la simbiosis MA reduce de forma relevante el estrés biótico de la planta ocasionado por patógenos e insectos, y es capaz de reducir o incluso impedir la infección por patógenos (Cordier et al. 1998; St Arnaud and Elsen 2005). Se cree que esto se consigue a través una combinación de diferentes mecanismos:

- La competencia directa por la disponibilidad de factores de crecimiento como el carbono y el nitrógeno, así como la competencia por el mismo nicho ecológico o por determinados sitios específicos de infección podrían reducir la invasión por patógenos (Filion et al. 2003) ya que ,presumiblemente, los recursos explotados por hogos MA y los organismos patógenos en la raíz son los mismos.
- Los cambios inducidos por el hongo MA en la arquitectura del sistema radicular, en la morfología y en los exudados radiculares, también podrían alterar la dinámica de infección por el patógeno o afectar a la comunidad microbiana de la micorrizosfera, favoreciendo componentes de la microbiota que sean capaces de antagonizar a los patógenos radiculares. De hecho, se ha observado que los cambios en los exudados radiculares pueden afectar directamente a los microorganimos patógenos y a los nematodos (Vos et al. 2012).
- La capacidad de los hongos MA de reprogramar la expresión génica en la planta (Campos-Soriano et al. 2012), afectando al metabolismo primario y secundario de la planta y, por lo tanto a sus defensas.

- La capacidad de los hongos MA de preacondicionar a la planta para una activación eficiente de las defensas vegetales a la hora de un ataque por patógenos, un fenómeno conocido como "priming" (Pozo and Azcón-Aguilar 2007). Por este mecanismo de priming o preacondicionamiento se crea en la planta un estado de "alerta" en el cual las respuestas defensivas no están inducidas, pero sí que están preparadas para activarse mucho más rápidamente y/o más potentemente ante los ataques por patógenos o insectos, tanto a nivel de la raíz (Benhamou et al. 1994; Pozo et al. 1999; Yao et al. 2003; Jaiti et al. 2007; Hao et al. 2012), como a nivel sistémico (Pozo et al. 2008; Jung et al. 2012; Pozo et al. 2010). De ahí, la gran importancia ecológica de los hongos MA y su gran potencial como agentes bioprotectores.

Mejora de la estructura del suelo: Los hongos MA pueden contribuir a mejorar la estructura del suelo favoreciendo la estabilidad de los agregados del suelo, tanto directamente por el efecto físico que ejerce la red de micelio que se forma entorno a las partículas del suelo, como indirectamente por la exudación a través de la hifas de una glicoproteína con hierro tipo glomalina, que actúa a modo de pegamento biológico, ayudando a ligar las partículas finas de suelo formando agregados de distintos tamaños (Gonzalez-Chavez et al. 2004; Rillig 2004; Rillig and Mummey 2006). Así, un suelo bien agregado es resistente al viento, la erosión del agua, y tiene una mejor aireación y tasas de infiltración de agua favorables para el crecimiento de la planta y de los microorganismos (Bronick and Lal 2005; Wu et al. 2008; Miller and Jastrow 2000).

Impacto sobre la diversidad, estructura y estabilidad de la comunidad vegetal: Los hongos MA parece que afectan a numerosos aspectos de los ecosistemas. Los estudios llevados a cabo sugieren que los hongos MA permiten ampliar el nicho de las plantas (Klironomos et al. 2000), tienen una influencia sobre la diversidad vegetal (Van der Heijden et al. 1998) y sobre la resistencia y resiliencia de las comunidades (Vogelsang et al. 2006; Helgason et al. 2007), modifican las interacciones de competencia entre las plantas (Fitter 1977; Wagg et al. 2011), y muchas plantas son incluso incapaces de coexistir con otras plantas si no están presentes los hongos MA (Van Der Heijden et al. 2008). También algunas

investigaciones muestran que la introducción de hongos MA en nuevos hábitats propicia la capacidad invasora de las plantas (Nuñez et al. 2009; Dickie et al. 2010) y que, por otra parte, las plantas invasoras pueden actuar eliminando las redes micorrícicas (Stinson et al. 2006; Vogelsang and Bever 2009), modificando consecuentemente la estructura de la comunidad vegetal y perjudicando el establecimiento de las plántulas correspondientes a plantas micorrícicas. Tras revisar numerosos estudios, Liu et al. (2015) llegaron a la conclusión de que la magnitud en que la simbiosis MA afecta a la capacidad competitiva de las plantas difiere notablemente entre los diferentes grupos funcionales de plantas. Debido a todos estos aspectos en los que los hongos MA impactan en los ecosistemas, la estructura de la comunidad vegetal sufre alteraciones dependiendo de la presencia (Grime et al. 1987; Hartnett and Wilson 1999; O'Connor et al. 2002) y/o composición de comunidades micorrícicas (Van der Heijden et al. 1998; Vogelsang et al. 2006).). Además, los hongos MA parecen afectar a la estabilidad de la comunidad vegetal (Yang et al. 2014), a través de la influencia que ejercen sobre las especies vegetales y haciendo que la productividad se mantenga más constante a lo largo del tiempo .

Como entre todos los beneficios que los hongos MA proporcionan a las plantas, el más estudiado es el aporte de nutrientes, a continuación se dedica un apartado específico para describir los mecanismos moleculares que subyacen al intercambio de nutrientes entre ambos simbiontes en ambas direcciones.

El intercambio de nutrientes en la simbiosis MA

La funcionalidad de la simbiosis MA radica en el correcto intercambio de nutrientes entre la planta y el hongo, de forma que ambos organismos se beneficien de la interacción. Para ello, es imprescindible que por ambas partes se regule el transporte de nutrientes en las dos direcciones.

El fósforo, en forma de fosfato inorgánico (Pi), es el principal nutriente mineral aportado por el hongo MA a la planta. Las hifas extraradicales del hongo MA adquieren el Pi del suelo, sintetizan polifostato a partir de él, y lo transfieren a lo largo de las hifas hasta los arbúsculos, donde es catabolizado de nuevo a Pi,

exportado al espacio apoplástico periarbuscular (Tani et al. 2009; Ezawa et al. 2002; Hijikata et al. 2010), e importado por la célula vegetal a través de transportadores de fosfato específicos de la membrana periarbuscular tales como MtPT4 y OsPT11, caracterizados por Javot et al. (2007a) y Yang et al. (2012).

El hongo MA es un simbionte obligado, y la planta constituye su única fuente de carbono. Se estima que entre el 4% y el 20% del carbono fijado en la fotosíntesis es destinado al mantenimiento del hongo MA (Bago et al. 2000; Douds et al. 2000; Graham 2000). Tradicionalmente se pensaba que este aporte de carbono se producía fundamentalmente en forma de azúcares (Shachar-Hill et al. 1995; Helber et al. 2011), sin embargo, numerosos estudios más recientes avalan que gran parte, posiblemente la mayor parte, del carbono se aporta en forma de ácidos grasos y que, de hecho, los hongos MA son auxótrofos de ácidos grasos (Wewer et al. 2014; Jiang et al. 2017).

A pesar de que actualmente ha quedado desplazada a un segundo plano por los ácidos grasos, la transferencia de carbono en forma de sacarosa de la planta al hongo ha sido estudiada en bastante profundidad durante muchos años. Durante mucho tiempo se pensó que el carbono aportado al hongo MA era en forma de azúcares (hexosas) (Shachar-Hill et al. 1995; Helber et al. 2011). Todo empezó con la observación de que almacenamiento de almidón desaparecía en las células infectadas, de modo que se empezó a investigar sobre la posibilidad de que la movilización de almidón pudiese ser relevante en el aporte de azúcares al hongo MA (Kinden and Brown 1975; Smith and Gianinazzi-Pearson 1988), y esto se vio apoyado por diferentes estudios de trazabilidad con ^{14}C marcado radiactivamente (Lewis and Harley 1965; SMITH et al. 1969; Ho and Trappe 1973; Solaiman and Saito 1997).

La sacarosa, producida durante la fotosíntesis en los tejidos verdes, es transportada a través del floema hasta la raíz (Giaquinta 1983), donde es escindida en glucosa y fructosa para su uso en la producción de energía. La micorrización de la raíz supone la presencia de un consumidor extra de sacarosa para la planta colonizada, de modo que la fuerza sumidero de las raíces se incrementa (Bago et al. 2000; Graham 2000; Douds et al. 2000) y se induce la expresión de varios genes que codifican para transportadores de sacarosa (SUTs) en las hojas y en las raíces colonizadas (Boldt et al. 2011; Doidy et al. 2012). Para la exportación de la sacarosa del floema a las

células con arbúsculos es necesaria una regulación muy fina de los transportadores de sacarosa, y ésta ha de degradarse en la célula vegetal hospedadora mediante invertasas, ya que los hongos MA no tienen la capacidad de consumir ni de cortar la sacarosa (Giaquinta 1983; Schubert et al. 2004). De hecho, en las plantas micorrizadas se induce la expresión de invertasas y sacarosa sintasas vegetales (Salzer and Hager 1991; Schaarschmidt et al. 2006), y de hecho, la represión de la invertasa apoplástica produce una reducción en los niveles de micorrización (Schaarschmidt et al. 2007). Los genes correspondientes a transportadores de sacarosa (SUTs) y de monosacáridos (MSTs) se inducen mucho en el floema de las raíces micorrizadas, con una inducción aún más acentuada de algunos de estos genes en las células colonizadas por arbúsculos (Gaude et al. 2012). Además, muy recientemente se ha identificado en patata otra familia de transportadores, los SWEETS; concretamente se trata de exportadores de sacarosa y monosacáridos que también podrían ser elementos clave en la descarga de sacarosa del floema en las raíces y en la regulación del azúcar exportado hacia la interfase simbiótica durante la micorrización, ya que los genes que codifican para los transportadores SWEETs presentan una expresión diferencial en las plantas inoculadas respecto a las no inoculadas (Manck-Götzenberger and Requena 2016). Finalmente, también cabe mencionar algunos transportadores fúngicos como GpMST1 con capacidad de importar glucosa proveniente de la planta hospedadora (Schüßler et al. 2006), y *RiMST2*, que se expresa tanto en las hifas intraradicales como en los arbúsculos, y cuyo silenciamiento da lugar a una reducción en la colonización micorrícica y a la aparición de arbúsculos truncados (Helber et al. 2011). Por último, en las esporas se ha observado que se inducen dos genes, *RiMST5* y *RiMST6*, ambos codificantes para cotransportadores de H^+ posiblemente implicados en la adquisición de glucosa para la germinación (Lahmidi et al. 2016).

Estos resultados sugieren que todos estos transportadores puede que estén implicados en la descarga de sacarosa del floema hacia las células con arbúsculos y en la recuperación de azúcares de vuelta a la planta durante la simbiosis MA.

Sin embargo, el planteamiento de los carbohidratos como la única fuente de carbono suministrada por la planta se veía envuelto en una serie de contradicciones difíciles de explicar por aquel momento. Por ejemplo, los defectos en el metabolismo del almidón no afectaban significativamente al desarrollo micorrício (Gutjahr et al.

2009; Gutjahr et al. 2011), los mutantes en proteínas exportadoras de azúcar tampoco veían afectada su colonización micorrícica (Gabriel-Neumann et al. 2011), y el micelio extraradical no parecía tener capacidad de tomar azúcares (Pfeffer et al. 1999). A esto se une el hecho de que la principal forma de almacenamiento de carbono del hongo encontrada en sus compartimentos de reserva (esporas y vesículas) son los lípidos, mientras que sólo se encuentran cantidades ínfimas de glucosa polimerizada en forma de glucógeno (Beilby and Kidby 1980; Beilby 1983; Jabaji-Hare 1988; Bécard et al. 1991). De este modo, si la totalidad del carbono se transfiere al hongo en forma de azúcares, una gran parte de los azúcares tomados de la planta debería ser convertida a ácidos grasos, que en el momento de su utilización como fuente de energía deberían ser convertidos de nuevo a azúcares. Sin embargo, este modelo es completamente subóptimo desde un punto de vista energético ya que en estas transformaciones la eficiencia de conversión del carbono puede alcanzar tan solo el 50% como máximo, respecto al uso directo de los azúcares tomados de la planta (Bago et al. 2003).

Todas estas incongruencias se sumaron a la observación de que *R. irregularis* carecía de los genes que codifican para el complejo FAS, conservado en los eucariotas y esencial para la síntesis de ácidos grasos de novo (Wewer et al. 2014). Este primer indicio desencadenó que las investigaciones profundizaran en la posibilidad de que los ácidos grasos también pudiesen constituir un aporte de carbono relevante para el hongo, y que la planta fuera la fuente de esos ácidos grasos. Así se sucedieron numerosos estudios con mutantes para una serie de genes vegetales inducibles por micorrización y relacionados con el metabolismo lipídico (*DIS*, *FAT*, *RAM2* y *STR*), en los que el desarrollo del arbúsculo se veía perjudicado, los niveles de lípidos en el hongo estaban reducidos y la simbiosis no se mantenía (Keymer et al. 2017; Zhang et al. 2010; Gobbato et al. 2012; Wang et al. 2012; Bravo et al. 2016; Bravo et al. 2017; Luginbuehl et al. 2017). El análisis conjunto de los resultados derivados de estos estudios permitieron perfilar el modelo actual (MacLean et al. 2017): en los plástidos de la célula vegetal colonizada se inicia el incremento de la biosíntesis de ácidos grasos C16:00 gracias a DIS, una keto-acil ACP sintasa (Groth et al. 2013; Keymer et al. 2017), y FatM, una acil ACP-tioesterasa (Bravo et al. 2017). Los ácidos grasos C16:00 son exportados hasta el retículo endoplásmático, donde a través de la enzima RAM2, una glicerol-3-fosfato acil transferasa, son convertidos a β-

monoacilglicerol (16:0 β-MAG) (Gobbato et al. 2012), una forma típica de lípidos para exportación fuera de la célula. Finalmente, los 16:0 β-MAG son exportados al apoplasto periarbuscular mediante STR/STR2, unos transportadores ABC localizados en la membrana periabuscular (Bravo et al. 2017; Jiang et al. 2017), pasando a estar disponibles para el hongo. En la Figura 9 se esquematizan los principales procesos de intercambio nutricional conocidos por el momento que ocurren en los arbúsculos.

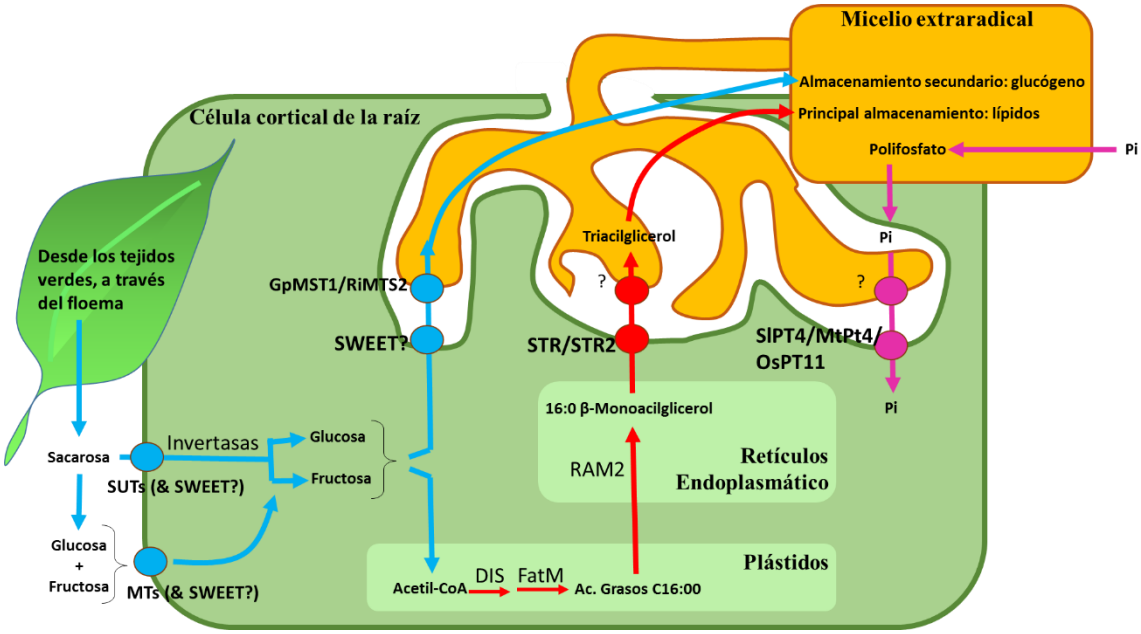

Figura 9. Intercambio de nutrientes entre el hongo MA y la planta hospedadora. Representación esquemática de los transportadores y otras proteínas descritas en la literatura implicadas en el intercambio de carbohidratos, ácidos grasos, y fosfato entre la planta y el hongo MA.

6. Regulación del proceso simbiótico

Aunque en la regulación del desarrollo de la micorriza arbuscular todos los procesos se solapan y entrecruzan dando lugar a un resultado final, conceptualmente se podría hacer una separación temporal de acontecimientos en función de los elementos reguladores. En primer lugar, los factores ambientales actúan a modo de reguladores determinantes sobre la respuesta de la planta y sobre su predisposición a establecer asociaciones simbióticas. Entre ellos, el factor ambiental cuyo efecto sobre la micorrización ha sido más estudiado es la disponibilidad de nutrientes y el estado nutricional de la planta, y por ello haremos más hincapié en este aspecto. En segundo lugar, la combinación de los diversos factores ambientales es percibida por

la planta y se traduce en una compleja amalgama de señales cuyo patrón es exclusivo y específico para cada situación ambiental concreta de las miles que pueden darse. Entre estas señales cabe destacar aquellas de naturaleza hormonal y las especies reactivas de oxígeno, las cuales serán descritas en mayor profundidad a continuación. En tercer y último lugar, la señalización culmina con la activación/represión de la expresión de los genes específicos correspondientes. Esto es conocido como regulación transcripcional, está dirigida por los factores de transcripción, y es determinante a la hora de poner en marcha toda la maquinaria proteica y enzimática requerida para el establecimiento de la simbiosis MA.

6.1. Regulación ambiental. La regulación nutricional.

Los factores ambientales son los reguladores iniciales de la simbiosis MA, y son innumerables los factores, tanto bióticos como abióticos, que afectan a la simbiosis MA (Hoeksema et al. 2010). Entre los múltiples factores que afectan a la interacción cabe destacar el genotipo de los simbiontes y su contexto biótico, el estadío de las sucesión ecológica en que se encuentran, la intensidad de luz , la disponibilidad de nutrientes y el estado nutricional de la planta (Hoeksema et al. 2010). A continuación se enumeran los más importantes:

Factores bióticos.

En el correcto establecimiento de la simbiosis MA intervienen diversos factores relacionados con la interacción entre los simbiontes y con otros organismos presentes en el medio, así como factores genéticos y anatómicos característicos de ambos simbiontes.

- **La planta hospedadora**: la eficiencia de colonización de los hongos MA puede ser bastante más eficaz en unas especies que en otras (Lambert et al. 1980), e incluso puede variar entre cultivares de la misma especie (Hall 1978). Se ha propuesto que aquellas especies o cultivares más susceptibles a la colonización son aquellas con menor capacidad de absorción de fosfato (Menge et al. 1978), además de influir otros parámetros fisiológicos y morfológicos como la anatomía de las raíces vegetales o la presencia o no de pelos radiculares (Baylis 1975; Janos 1975).

- **Interacciones con otros microorganismos**: Los hongos MA son capaces de establecer interacciones sinérgicas con otros microorganismos del suelo que promueven la colonización de la planta por el hongo MA así como el crecimiento de la planta (de Oliveira and Garbaye 1989). Estos "microorganismos auxiliares de la micorrización" pueden ser bacterias fijadoras de nitrógeno libre (Fitter and Garbaye 1994; Amora-Lazcano et al. 1998), rhizobacterias promotoras del crecimiento vegetal (Meyer and Linderman 1986), bacterias solubilizadoras de fosfato (Toro et al. 1998), actinomicetos-*Frankia* fijadores de nitrógeno (Rose and Youngberg 1981) e incluso hongos saprofíticos como los del género *Trichoderma* (Calvet et al. 1993). Aunque en menos ocasiones, también cabe mencionar que existen evidencias de microorganismos capaces de interactuar negativamente con los hongos MA, alimentándose de sus hifas o esporas, o inhibiendo la germinación de sus esporas por fungistasis (Tommerup 1985).

Factores abióticos.

Los factores climáticos y físico-químicos del suelo en el que crece la planta hospedadora determinan fuertemente el desarrollo y establecimiento de la simbiosis micorriza arbuscular.

- **Luz:** el hongo MA depende del suministro de productos fotosintéticos provenientes de la planta, cuya biosíntesis depende directamente de la disponibilidad de luz. En este sentido, Furlan and Fortin (1977) demostraron que la luz estimula el desarrollo micorrícico, mientras que la falta de luz reduce la colonización y la producción de esporas. Existen trabajos recientes que muestran una relación entre el ratio de luz roja/ roja lejana con el nivel de micorrización y atribuyen este efecto regulatorio de la micorrización a través del efecto de la intensidad lumínica sobre la vía del jasmonato y las estrigolactonas (Nagata et al. 2015),
- **Temperatura**: la temperatura del suelo es capaz de influir en la germinación de las esporas, la penetración de las hifas fúngicas en las raíces y en la extensión del hongo en el interior de las mismas. Sin embargo, el rango óptimo de temperatura es variable, y se ha visto que depende de la especie

fúngica en cuestión (Schenck et al. 1975) y de la textura del suelo (Bowen 1980).

- **pH del suelo**: el pH del suelo afecta a la geminación y desarrollo de las esporas fúngicas de los hogos MA (Daniels and Trappe 1980; Angle and Heckman 1986). Aunque el pH óptimo para la micorrización depende mucho del tipo de planta y de suelo, así como de las formas de fósforo presentes y de la especie de hongos MA implicada; parece que los niveles máximos de colonización micorrícica se obtienen en pHs neutros o ligeramente alcalinos (Postma et al. 2007; Hayman and Mosse 1971; Piotrowski et al. 2008; Zangaro et al. 2012), mientras que pHs inferiores a 5 provocan un decremento de la micorrización (Clark 1997; Coughlan et al. 2000).
- **Estrés hídrico**: el aumento de la salinidad o la sequía en el suelo reduce la capacidad de formación de propágulos y la colonización MA. Sin embargo, son muchos los estudios que indican que el uso eficiente de los hongos MA mejoran el crecimiento de las plantas en una amplia variedad de condiciones de estrés salino (Ruiz-Lozano et al. 1996; Singh et al. 1997; Azcón-Aguilar and Barea 1997; Al-Karaki et al. 2001).
- **Disponibilidad de nutrientes**: De todos los factores ambientales que afectan a la micorrización, éste es el más estudiado. La disponibilidad de nutrientes, además de ser regulada por la simbiosis MA, tiene también la capacidad de regular la propia simbiosis. En el apartado siguiente se hará una descripción de cómo los nutrientes actúan en sí mismos como señales de regulación de la simbiosis.

Nutrientes como elementos reguladores de la simbiosis MA

La mayor parte de las condiciones medioambientales tienen un impacto sobre la interacción entre los organismos simbiontes. Nosotros nos focalizaremos en los nutrientes como factor ambiental regulador de la simbiosis MA, ya que se trata del factor más estudiado.

El intercambio bidireccional de nutrientes durante la simbiosis MA se cree que sigue el "modelo de libre mercado" propuesto por Kiers et al. (2011), aunque dicho modelo debería ser reestructurado teniendo en cuenta los nuevos descubrimientos concernientes a que los ácidos grasos podrían ser la principal forma de transferencia

de carbono de las plantas hospedadoras al hongo MA (MacLean et al. 2017), y no los azúcares como hasta entonces se había pensado. Este modelo se basa en que el intercambio de nutrientes es regulado por ambos simbiontes, siguiendo un mecanismo de estimulación mutua entre la planta hospedadora y el hongo MA colonizante. Por una parte la planta hospedadora es capaz de discernir entre el hongo MA del cual puede obtener más beneficio y obsequiarle con más aporte de carbohidratos; mientras que por parte del hongo, también incrementa la transferencia de minerales a aquellas raíces que le donan más carbohidratos, y en cambio los retiene en sus hifas si la planta no le aporta cantidades suficientes (Hammer et al. 2011). Mediante este mecanismo la planta se protege contra "hongos timadores" (Fitter 2006) y, al mismo tiempo, el hongo MA sólo da su recompensa (Pi) a las plantas que le benefician. Así mismo, en el control del intercambio C-N durante la simbiosis MA muy probablemente se dé un mecanismo de recompensa mutua parecido al que ocurre para el intercambio C-P. De este modo, el incremento en la disponibilidad de carbono desde las plantas al hongo MA induce la toma y transporte del N por parte del hongo (Fellbaum et al. 2012).

Está claro que el Pi y el N presente en la planta y en el entorno, así como el Pi transferido del hongo a la planta, son factores que regulan la simbiosis MA. Aunque no se conocen en profundidad los mecanismos específicos subyacentes que permiten detectar el nivel de nutrientes y regular el intercambio bidireccional (Koide and Schreiner 1992; Breuillin et al. 2010; Hammer et al. 2011; Kiers et al. 2011; Kretzschmar et al. 2012; Yoneyama et al. 2012; Kobae et al. 2016), cada vez existe más información al respecto. Por ejemplo, algunos estudios sugieren que el fosfato además de jugar un papel nutricional para la planta, también tiene un papel esencial como regulador del mantenimiento de la simbiosis MA, y que la adquisición de Pi vía hongo está relacionada con la esperanza de vida y/o la expansión del arbúsculo. De hecho, mutantes de pérdida de función de *MtPT4* y *OsPT11* dan lugar a una degeneración prematura o fallos en el desarrollo de los arbúsculos, y a una pérdida de la simbiosis (Javot et al. 2007a; Yang et al. 2012). Hasta la fecha se han identificado algunos componentes clave que median la expresión diferencial de genes en función de los niveles de Pi disponible (Wu et al. 2013). El factor de trascripción MYB parece ser el regulador principal de la respuesta (Rubio et al. 2001; Zhou et al. 2008). En condiciones limitantes de Pi, MYB se une a los elementos

cis reguladores P1BS de promotores tales como los transportadores de Pi asociados a micorrización (Chen et al. 2011), activando la llamada "expresión génica inducible por hambre de Pi" (Rubio et al. 2001). Sin embargo, en condiciones de altos niveles de Pi, parece que las proteínas SPX1 y SPX2 podrían tener un sensor de dicha concentración de Pi y, posiblemente a través de la unión de inositol polifosfato (Wild et al. 2016), se une a MYB, impidiendo que MYB interaccione con los elementos P1BS y, de este modo, deteniendo la respuesta génica asociada a condiciones de hambre de Pi (Wang et al. 2014b; Puga et al. 2014). En la traducción de estas señales nutricionales muy probablemente jueguen un papel importante las fitohormonas. De hecho, la deficiencia de P hace que se incremente la biosíntesis de estrigolactonas y que las citoquininas sean movilizadas del tallo a la raíz, favoreciendo así la simbiosis MA (Cosme and Wurst 2013; Fusconi 2013); mientras que, por el contrario, altas concentraciones de P dan lugar a un desarrollo muy deficiente de los arbúsculos, y esto probablemente esté asociado con la desestabilización de DELLA (Floss et al. 2013). Cabe mencionar que la homeostasis celular de Pi posiblemente se mantenga gracias a un ciclo de retroalimentación negativa entre MYB y las proteínas SPX, ya que se ha observado que los genes que codifican para SPX1 y SPX2 también son inducidos por MYB en condiciones de bajo Pi (Wang et al. 2014b). Ante altos niveles de Pi, parece que además del mecanismo descrito mediado por la inhibición de MYB a través de SPX1 y SPX2, también se da una represión específica de genes dirigida hacia una reducción del flujo de Pi del hongo a la planta, así como de mecanismos para controlar el desarrollo fúngico. Por ejemplo, por condiciones de elevado Pi:

- Se reprime la expresión de genes que codifican para enzimas de la ruta de biosíntesis de carotenoides y SLs, lo cual podría acarrear la reducción den la síntesis de SLs y la consecuente inhibición de la germinación de esporas fúngicas (Balzergue et al. 2013).
- Se reprime la expresión de genes que codifican para transportadores de fosfato específicos de arbúsculos (Balzergue et al. 2013), consecuentemente reduciendo la colonización micorríciCa (Breuillin et al. 2010).
- Se reprimen STR y STR2, que median el flujo de lípidos a los hongos MA (Wang et al. 2017)

- Se afecta negativamente la señalización presimbiótica, ya que en dichas condiciones se observa una cierta inhibición en el número de picos de calcio y de las células sujetas a los mismos (Russo et al. 2013), aunque en otros estudios no se observa tal inhibición (Balzergue et al. 2013).

En definitiva, el transporte simbiótico de Pi es esencial para el mantenimiento de la simbiosis. Junto a esto, se ha visto que la colonización micorrícica, aparte de verse perjudicada por abundancia de Pi, también es favorecida, aunque en menor medida, por deficiencia de N (Nouri et al. 2014); y que el aumento de la concentración de N conlleva una disminución de la micorrización (Blanke et al. 2005). De hecho, la degeneración prematura de los arbúsuculos observada en plantas mutadas para los genes codificantes de transportadores de Pi específicos de micorrización (Javot et al. 2007a; Yang et al. 2012), se ve prevenida en condiciones de bajo N en el medio (Maldonado-Mendoza and Harrison 2017).

Sin embargo, otros nutrientes minerales esenciales como el hierro, el potasio y el calcio no parecen afectar a la formación de la micorriza (Nouri et al. 2014).

El nivel de azúcares disponible para el hongo MA también parece constituir un factor determinante para el desarrollo del mismo. Los resultados apuntan a que existe un umbral por debajo del cual el crecimiento del hongo se ve afectado; sin embargo, por encima de dicho umbral, el aumento de azúcares disponibles no supone un incremento en la colonización micorrícica (Schaarschmidt et al. 2007). Algunos estudios parecen indicar que este hecho podría deberse a que la planta hospedadora es capaz de regular los niveles de colonización modulando el flujo de azúcar hacia el hongo, por ejemplo mediante el transportador periarbuscular de sacarosa SlSUT2, que regula negativamente los niveles de micorrización, muy probablemente a través de su participación en la recuperación de parte de la sacarosa liberada a la matriz periarbuscular hacia el apoplasto vegetal, reduciendo así la disponibilidad de sacarosa para el hongo MA, y evitando que el desarrollo fúngico pueda llegar a ser perjudicial para la planta (Bitterlich et al. 2014b).

Por otra parte, los azúcares, junto con las hormonas, también están implicados en integrar los eventos moleculares locales y las respuestas sistémicas, para así ajustar los procesos de crecimiento y de defensa (Ruan 2014). Así, los azúcares también podrían desempeñar una función de este tipo durante la simbiosis MA.

Además, se ha planteado la posibilidad de que la inducción en la expresión de invertasas de la pared celular, así como transportadores SUTs y SWEETs, y la consecuente modificación de las relaciones fuente-sumidero bajo condiciones de micorrización, podría actuar como señal para la activación y regulación de mecanismos de defensa durante la simbiosis (Doidy et al. 2012), de forma análoga a como ocurre en repuesta a patógenos vegetales (Herbers et al. 1996; Lemonnier et al. 2014; Roitsch et al. 2003; Yamada et al. 2016).

El nivel de nutrientes también parece tener cierto efecto regulador sobre el simbionte fúngico. Tal es el caso de RiMST2. *RiMST2* se induce principalmente en las hifas intraradicales y los arbúculos y codifica para un transportador de azúcares bastante promiscuo pero con cierta preferencia por las moléculas de xilosa. Curiosamente, ante la adición de xilosa al medio, en el micelio extraradical se induce la expresión de *RiMST2*, lo cual hace pensar que es precisamente la presencia de xilosa en las raíces micorrícicas lo que activa la expresión de *RiMST2* en el micelio intraradical (Helber et al. 2011).

El desafío actual es comprender cómo las plantas integran las señales medioambientales y del desarrollo, y cómo generan respuestas que afectan a la simbiosis MA. La incesante mejora en las herramientas biotecnológicas muy probablemente permita dibujar en el futuro una red detallada de las interconexiones presentes entre las rutas implicadas en el intercambio de nutrientes durante la simbiosis MA, y que este conocimiento resultante pueda ser aplicable a estrategias de mejora vegetal focalizadas en promover la adquisición y utilización de nutrientes a través de la micorrización.

6.2. Regulación hormonal (y otras moléculas señal)

Las fitohormonas son pequeñas moléculas que actúan a concentraciones bajas como reguladores versátiles de casi cualquier proceso de desarrollo y defensa en las plantas. En función de los estímulos ambientales percibidos, las fitohormonas se acumulan y distribuyen en los distintos tejidos diferencialmente, interaccionan entre sí de forma sinérgica o antagonista, y son percibidas por sus receptores. Junto a los sistemas redox, este diálogo hormonal y las cascadas de señalización derivadas, permiten traducir las señales ambientales en cambios fenotípicos y en una

respuesta sistémica de la planta en términos de crecimiento y de mecanismos de defensa, de una forma completamente eficiente y coordinada (Sparks et al. 2013).
La homeostasis hormonal regula, y es regulada por, la simbiosis MA. Los cambios en los perfiles hormonales ante cambios ambientales se traducen en cambios en el proceso o eficiencia de la colonización. A su vez, la simbiosis MA puede aumentar la resistencia de la planta a condiciones de estrés alterando la homeostasis hormonal, aunque el papel preciso de las fitohormonas y los mecanismos exactos por los cuales regula la micorrización se desconocen.

La simbiosis MA regula el balance hormonal

La simbiosis MA altera la homeostasis hormonal en el hospedador y mejora así la respuesta y tolerancia a estreses ambientales (Fernández et al. 2014; Selosse et al. 2014). La mayoría de los estudios referentes a la regulación de las fitohormonas están basados en la aplicación de estímulos independientes. Sin embargo, las plantas están expuestas a múltiples señales y factores de estrés, y han de priorizar las respuestas para alcanzar la máxima eficiencia en la gestión de los recursos. Por ello, las últimas investigaciones están focalizándose en dilucidar las múltiples conexiones moleculares que median el diálogo hormonal para la integración de señales, y en cómo su regulación espaciotemporal permite afinar la respuesta. Gracias a todos estos estudios estamos tan solo empezando a comprender una pequeña parte de la total complejidad en la regulación de las fitohormonas.
El establecimiento y funcionalidad de la simbiosis MA dependen mucho de las condiciones del medio y están finamente reguladas gracias a la participación de casi todas las fitohormonas identificadas hasta día de hoy. Sin embargo, aún no se conoce en detalle cómo actúan para integrar las señales medioambientales y regular la simbiosis MA de acuerdo con dichas señales:

- Las citoquininas, auxinas y estrigolactonas actúan de forma conjunta provocando modificaciones en la arquitectura de la raíz (Fusconi 2013)
- El ABA cambia las propiedades hidráulicas de la raíz, incrementando la toma de agua ante condiciones desfavorables (Ruiz-Lozano et al. 2012). Ante estrés osmótico se incrementa el contenido de ABA en las plantas micorrizadas, posiblemente generando inmunidad en la planta frente al estrés (Aroca et al. 2013)

- Los jasmonatos participan en la inducción de la inmunidad vegetal frente a patógenos y herbívoros en las plantas micorrizadas (Jung et al. 2012), así como en todas aquellas plantas conectadas por redes comunes de micelio micorrícico (Song et al. 2014) .

Es decir, en conjunto la señalización hormonal desencadenada en las plantas en condiciones de micorrización está dirigida a la mejora de la salud vegetal, incluyendo una mejor nutrición y una mayor defensa ante factores que generan estrés.

Fitohormonas como elementos reguladores de la simbiosis MA

Las fitohormonas son reguladores centrales del desarrollo y del estrés vegetal, y orquestan las respuestas a las condiciones fluctuantes del ambiente. Así mismo, existen evidencias claras de que las fitohormonas juegan un papel clave para la regulación del establecimiento y funcionamiento de la simbiosis MA, probablemente a través de la integración de las señales ambientales y del desarrollo de la planta mediante los llamados centros moleculares ("molecular hubs") de la señalización hormonal (Foo et al. 2013; Gutjahr 2014). La mayoría de pruebas resultan del análisis de plantas con alteraciones en la biosíntesis de hormonas o en la señalización hormonal.

Hasta el momento se han identificado fitohormonas que participan tanto en la señalización presimbiótica, como en etapas más tardías para la regulación de las adaptaciones morfológicas de la raíz para el alojamiento del hongo, el control de la propagación de la colonización o la regulación de la funcionalidad de la simbiosis.

Estrigolactonas

Antes del contacto físico entre el hongo MA y la raíz vegetal, se requiere de la comunicación molecular entre ambos simbiontes. Los elementos básicos de la comunicación son las estrigolactonas (SLs) por parte de la planta y los factores Myc por parte del hongo. Las estrigolactonas son grupo de fitohormonas derivadas de carotenoides que regulan muchos otros aspectos del desarrollo vegetal (Akiyama et al. 2005b; Gomez-Roldan et al. 2008; Lopez-Obando et al. 2015). Las SLs son secretadas a la rizosfera en respuesta a condiciones deficientes de Pi (Kretzschmar et al. 2012; Yoneyama et al. 2007), y sirven cómo señal de la presencia de un hospedador receptivo a ser colonizado por hongos MA. De este modo, la detección

de las SLs por el hongo MA, hace que se induzca la germinación de las esporas fúngicas, así como que se active el metabolismo oxidativo del hongo para generar energía que es destinada a estimular su propio crecimiento y ramificación, incrementando la probabilidad de contacto físico con la raíz hospedadora y preparándolo para establecer la simbiosis (Akiyama and Hayashi 2006; Besserer et al. 2006; Besserer et al. 2008; Waters et al. 2017). De hecho, la colonización micorrícia se reduce bastante en los mutantes para la biosíntesis o exportación de SLs (Gomez-Roldan et al. 2008; Koltai et al. 2010; Kretzschmar et al. 2012; Yoshida et al. 2012; Gutjahr et al. 2012). Además, las SLs inducen la secreción de señales difusibles por parte del hongo, tales como oligómeros de quitina de cadena corta (COs) (Genre et al. 2013), que activan el CSSP para la colonización inicial de las células epidérmicas de la raíz (MacLean et al. 2017; Gutjahr 2014; Waters et al. 2017; Akiyama et al. 2005b; Oldroyd 2013). Además, se ha visto que la concentración y las características estructurales de las SLs secretadas por la planta son importantes para el desarrollo fúngico (Ruyter-Spira et al. 2013). Sin embargo, la biosíntesis de estrigolactonas se ve reducida cuando el hongo MA está bien establecido en la raíz, probablemente debido a que una vez la planta alcanza un mejor estado nutricional se dan mecanismos de autoregulación para evitar la sobrecolonización (López-Ráez et al. 2015).

Giberelinas

Se cree que le complejo giberelina-DELLA juega un papel esencial en el control de la simbiosis de acuerdo al estado fisiológico de la planta ante unas condiciones medioambientales particulares. Las giberelinas biológicamente activas tienen un efecto inhibidor sobre el desarrollo del arbúsculo, mientras que los represores DELLA son esenciales para la formación del mismo. Esto se debe a que los factores de transcripción DELLA son reguladores centrales de la señalización mediada por giberelinas, y un nodo común para otras hormonas como las auxinas, el etileno, el ácido abcísico y los brasinosteroides, lo cual permite a las plantas integrar la señalización nutricional y las señales del desarrollo para regular de forma correcta la simbiosis MA (Floss et al. 2013; Foo et al. 2013; Yu et al. 2014; Jin et al. 2016; Gutjahr 2014).

Brasinosteroides

Se cree que los brasinosteroides tienen una función señalizadora durante la simbiosis MA. De hecho la mutación de *MSBP* (Membrane Steroid-Binding Protein) en *M. truncatula* y de *DIMINUTO* en arroz, dan lugar a una reducción en la colonización micorrícica (Bitterlich et al. 2014a; Kuhn et al. 2010) .

Otra prueba que respalda la participación de los brasinosteroides durante la simbiosis MA es que componentes de la biosíntesis y señalización de brasinosteroides, concretamente BAK1-like receptor kinase, MSBP (a **m**embrane **s**teroid-**b**inding **p**rotein) y DIMINUTO (the BR biosynthetic sterol reductase), interaccionan físicamente con SUT2, un transportador que regula negativamente el desarrollo del hongo posiblemente retirando, o señalizando la retirada, de azúcares disponibles de la interfase simbiótica (Bitterlich et al. 2014b).

Otras hormonas

- El ácido salicílico, el etileno y las citoquininas tienen un efecto negativo sobre la penetración y colonización de la raíz por parte del hongo MA (Foo et al. 2013).
- El ABA y las auxinas regulan positivamente el desarrollo del arbúsculo y su funcionalidad (Martín-Rodríguez et al. 2011; Etemadi et al. 2014).
- En cuanto al ácido jasmónico, se han observado tanto efectos positivos como negativos sobre la micorrización (Wasternack and Hause 2013). En tomate se ha visto que la resistencia a enfermedades está asociada con el "priming" o preacondicionamiento inducido por los hongos MA, que activa respuestas sistémicas mediadas por ácido jasmónico (Song et al. 2015). Por otra parte, se ha visto que el pre-acondicionamiento de las respuestas inmunodefensivas dependiente de jasmonatos afecta además a otras plantas conectadas a través de redes de micelio micorrícico (Song et al. 2014).

Diálogo hormonal

Como en otros procesos vegetales, el impacto de las hormonas sobre las micorrizas depende del diálogo hormonal:

- Las interacciones fundamentalmente antagonistas ABA-etileno y ABA-giberelinas, regulan el desarrollo de la micorrización y la formación de los

arbúsculos, respectivamente (Martín-Rodríguez et al. 2011; Gutjahr 2014; Martin-Rodriguez et al. 2016)

- Componentes de la señalización por azúcares también interaccionan con los jasmonatos y los brasinosteroides para regular finamente las micorrizas (Bitterlich et al. 2014b).

Señales vegetales no hormonales reguladoras de la simbiosis MA

Además de las señales hormonales, también hay indicios de otras moléculas señal importantes durante la micorrización. Por ejemplo, en la comunicación presimbiótica, aparte de las estrigolactonas hay otros compuestos señal que podrían tener un papel esencial para la preparación del hongo y la planta, antes de que ocurra el contacto físico. Entre estos compuestos cabe destacar un compuesto hipotéticamente transportado por el exportador NOPE1 vegetal (Nadal et al. 2017) y un hipotético ligando del receptor D14L también vegetal (Gutjahr et al. 2015).

En concreto, los resultados indican la existencia de una molécula (posiblemente un derivado de la N-acetlyglucosamina) que es exportada a través de los transportadores NOPE1 (NO PERCEPTION1) de la planta y que actúa como señal esencial para que el hongo se prepare para la simbiosis; de hecho los mutantes *nope1* apenas muestran interacción con el hongo MA y sus exudados son incapaces de inducir respuestas transcripcionales en el hongo MA (Nadal et al. 2017).

Por otra parte, se cree que en la señalización presimbiótica hay otra molécula importante, aún tampoco identificada, que al unirse y ser reconocida por el receptor D14L (DWARF 14 LIKE) desencadena la respuesta transcripcional requerida para la simbiosis. Esta hipótesis se basa en los estudios de (Gutjahr et al. 2015), que identificaron al receptor D14L como una proteína esencial para la simbiosis MA en arroz y para la adecuada respuesta transcripcional asociada. El posible ligando de D14L y su mecanismo de acción durante la micorrización no están descritos. Sin embargo, sí que existe información respecto su homólogo KAI2 (KARRIKIN INSENSITIVE2) en *Arabidopsis*. KAI2 está identificado como el receptor específico de karrikinas, moléculas de tipo butenolide relacionadas con las SLs y que se generan en la quema de tejidos vegetales en los incendios. KAI2 activa MAX2, una proteína F-box que participa en la degradación, y posiblemente reciclaje, de

proteínas (Nelson et al. 2011; Waters et al. 2012). De este modo, ante un incendio, las karrikinas liberadas son detectadas por las semillas en latencia de determinadas especies, promoviendo su germinación y aportándoles capacidad competitiva tras el incendio (Flematti et al. 2015). Sin embargo, la gran conservación de KAI2 en el reino vegetal desde las plantas evolutivamente más antiguas hasta aquellas no asociadas con hábitats propensos a incendios (Waters et al. 2015; Waters et al. 2014; Conn and Nelson 2016), junto con el hecho del que el mutante *d3* de arroz (homólogo a MAX2) también es incapaz de micorrizarse (Yoshida et al. 2012), sugiere que la ruta de señalización mediada por D14L además de tener un papel posiblemente secundario en la estimulación de la germinación tras los incendios, también es necesaria para el establecimiento de la simbiosis MA. Aunque se desconoce el ligando de D14L responsable de esta señalización, ha de tener una estructura similar a las estrigolactonas o las karrikinas, y podría tener un origen o bien fúngico y ser un componente de los extractos de esporas, o bien vegetal, constituyendo un ligando endógeno de la planta, posiblemente de naturaleza hormonal, aún no identificado pero al que se le ha asignado el nombre de KL (KAI2 ligand). En cualquiera de los dos casos, se especula que la unión del ligando a D14L permite una adecuada respuesta transcripcional de la planta vía activación de MAX2/D3 y que esta señalización mediada por D14L está implicada en la simbiosis MA desde los primeros momentos de la evolución (Gutjahr et al. 2015).

Otras moléculas candidatas a constituir moléculas señalizadoras son la micorradicina y los derivados de la ciclohexanona, las cuales son apocarotenoides C13 y C14, respectivamente, que se acumulan específicamente en las raíces micorrizadas (Klingner et al. 1995; Maier et al. 1995), pero cuya función aún se desconoce. Los derivados de la ciclohexanona contienen la estructura del anillo α-ionona, por lo que también aparecen en la literatura como "derivados de los α-ionoles". Una de estos derivados de α-ionoles, la 7,8-dihydro-3-oxo-α-ionona, fue inicialmente identificada en hojas de *Podocarpus blumei*, de ahí su nombre blumenol C (Galbraith and Horn 1972), y algunos de sus derivados glicosidados, "derivados del blumenol C", son los que se han identificado en las raíces de muchas plantas colonizadas por hongos MA, y se ha visto que se empiezan a acumular al inicio de la

formación del arbúsculo y se van incrementando en cantidad durante la colonización (Strack and Fester 2006; Maier et al. 1995).

Tanto la micorradicina como los derivados de los α-ionoles son metabolitos secundarios generados en los plástidios como consecuencia de las modificaciones del metabolismo plastídico en las células invadidas por arbúsculos, y producidos por la rotura oxidativa de carotenoides precursores. Estos apocarotenoides se depositan en el citosol y la vacuola de la célula vegetal como gotas amarillas hidrófobas (Strack and Fester 2006). Los estudios de Floss et al. (2008) sugieren que la ruta del metileritriol fosfato (MEP), proveedora de las unidades C5 requeridas para la biosíntesis de todos los isoprenoides, es necesaria para la producción de los dos apocarotenoides (micorradicina y derivados de la ciclohexanona) inducidos por micorrización. Además, estos autores observaron que las deficiencias en la ruta MEP dan lugar a un aumento en el número de arbúsculos en degeneración y senescentes. Este hecho, junto con la cierta capacidad antifúngica que presentan los derivados de ciclohexanonas correspondientes (Park et al. 2004), *dio lugar a* que Walter et al. (2015) propusieran un modelo en el cual los apocarotenoides C13/C14 en la simbiois MA cumplen una función similar a la fitoalexinas, acelerando la degradación y la eliminación total de los arbúsculos en los que la transferencia de minerales del hongo a la planta no funciona adecuadamente. Por otra parte, López-Ráez et al. (2015) sugieren que la micorradicina podría ser relevante en las etapas más tardías de la micorrización, en concreto para el mantenimiento de los arbúsculos (López-Ráez et al. 2015). Sin embargo, Kobae et al. (2018) puntualizan que no se debe descartar que tengan un posible papel en las etapas tempranas, ya que la colonización micorrícica ocurre a través de la formación sucesiva de unidades de infección (Kobae et al. 2016; Sanders and Sheikh 1983); y, por lo tanto, un retraso imperceptible en la penetración de las células epidérmicas puede que esté dando lugar a la reducción del nivel de colonización a etapas tardías de la micorrización.

Como se muestra en la Figura 10, en la ruta de biosíntesis de apocarotenoides, D17/CC7 cataliza los precursores carotenoides C40 para proveer precursores C27 tanto para D10/CCD8 en la biosíntesis de estrigolactonas, como para CCD1 en la síntesis de apocarotenoides C13/C14 inducidos en micorrización (Walter et al. 2015; Maier et al. 1995; Klingner et al. 1995). *CCD1* se induce claramente en las células que contienen arbúsculos en las etapas tardías de la micorrización (Lopez

Raez et al., 2001), pero su mutación no parece afectar al desarrollo de la micorrización (Floss et al., 2008). Por otra parte, *D17* parece tener un papel bastante más importante que *D10* en el desarrollo de la colonización intraradical (Kobae et al. 2018).

En definitiva, aún queda mucho trabajo para clarificar la relación funcional entre CCD7, CCD8 y CCD1, así como para elucidar el papel que desempeñan la micorradicina y de los derivados de ciclohexanonas durante la micorrización. Sin embargo, en cualquier caso parece que está claro que muy probablemente la activación del metabolismo plastídico de los carotenoides que se da durante la micorrización no sólo sería relevante en la simbiosis debido a su rol en la biosíntesis de giberelinas, ácido abscísico y SLs (Fester 2008; Takeda et al. 2015; Walter et al. 2015), sino que adicionalmente cabría destacar el papel de los plástidos en la biosíntesis de los apocarotenoides C13/C14 para la regulación de la micorrización.

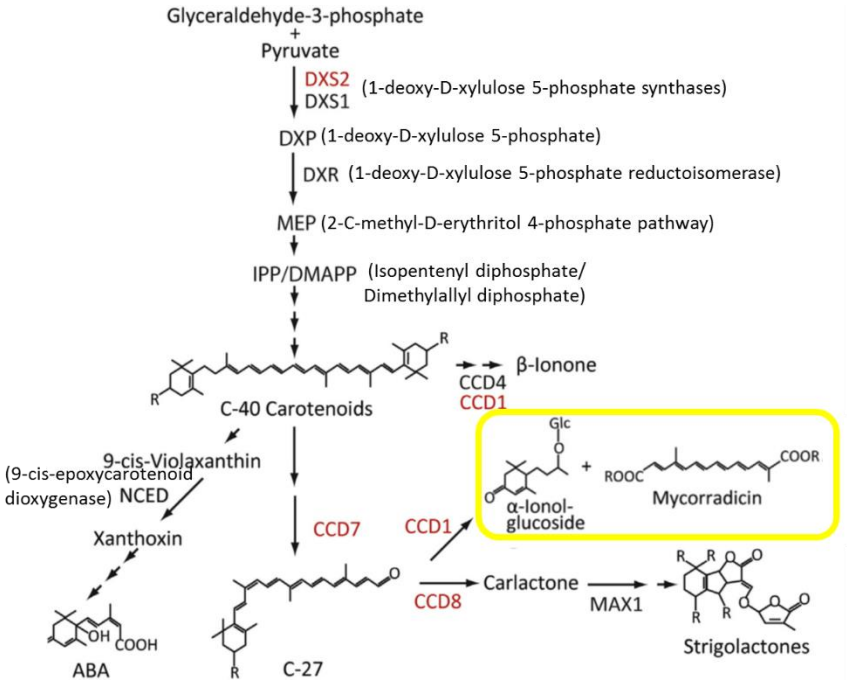

Figure 10. Síntesis de apocarotenoides en las plantas. Los apocarotenoides se forman por la rotura de los carotenoides C40, a través de la ruta independiente del mevalonato o ruta del metileritriol fosfato (MEP), mediante la acción de dioxigenasas tipo CCDs (Carotenoid Cleavage Dioxygenases). Los mutantes importantes para las interacciones planta-microorganismos están señalados en rojo. Figura modificada de Siebers et al. (2016).

Señales fúngicas reguladoras de la simbiosis MA: LCO/COs y efectores

Hoy por hoy, debido a las limitaciones metodológicas que impiden llevar a cabo aproximaciones genéticas en los hongos MA, es dificilísimo atribuir de forma inequívoca la capacidad señalizadora a una determinada molécula fúngica. Sin embargo, por el momento se han conseguido identificar dos compuestos que actúan como señales fúngicas de la señalización presimbiótica, ambos derivados de la quitina del hongo y con capacidad de disparar los picos de Ca^{++} en el núcleo de la célula hospedadora y, consecuentemente, el CSSP. Estas dos moléculas señal son los Myc-LCOs y los Myc-COs, en su conjunto conocidos como factores Myc (Gutjahr and Parniske 2013; Rich et al. 2014).

Por una parte, los Myc-LCOs son lipoquitooligosacáridos, en forma sulfatada o no sulfatada, que se encuentran en los exudados de las esporas de los hongos MA y que actúan como señales en la comunicación presimbiótica. Fueron descubiertos por Amor et al. (2003) debido a su similitud estructural con los factores Nod implicados en la señalización de la nodulación. Al igual que los factores Nod de la simbiosis *Rhizobium*-leguminosa, los Myc-LCOs desencadenan los picos de Ca^{++} nucleares (Sun et al. 2015) y son capaces de estimular el crecimiento de raíces laterales en *M. truncatula* (Maillet et al. 2011).

Prácticamente en paralelo, se vio que unos compuestos muy parecidos a los Myc-LCOs, pero constituidos por oligosacáridos de quitina de cadena más corta, también eran señales importantes durante la etapa presimbiótica, pero con una maquinaria de percepción y una actividad biológica claramente distinta. Estos compuestos son conocidos como Myc-COs, incluyen tanto tetra- como penta- quitooligosacaridos (CO4 y CO5) y, según las observaciones de Genre et al. (2013) se incrementan cuando el análogo de estrigolactonas GR24 está presente durante la germinación de las espora fúngica, y son capaces de activar el CSSP de las células hospedadoras a concentraciones submicromolares. Al contrario que los Myc-LCOs, los Myc-COs no son capaces de estimular el crecimiento de raíces laterales (Sun et al. 2015; Oláh et al. 2005).

La percepción de los Myc-LCOs/COs se da a través de unas proteínas quinasa, los LysM RLKs (Lysin-Motif Receptor-Like Kinases). Cabe destacar OsCERK1, esencial para la micorrización del arroz, así como sus homólogos en leguminosas, LjNFR1 y MtLYK3, con un papel relevante tanto en la micorrización como en la nodulación

(Zhang et al. 2015a; Amor et al. 2003), aunque no imprescindibles, posiblemente debido a que la familia de las LysM RLKs es enorme en las leguminosas y quizás haya redundancia funcional. Además, estos receptores podrían tener un papel adicional en las respuestas inmunitarias en respuesta a moléculas de quitina de microorganismos patógenos, tal y como se ha observado en el caso de CERK1 (Miyata et al. 2014), lo que sugiere la presencia de mecanismos moleculares que permiten la alternancia entre respuestas defensivas o simbióticas dependiendo de los microbios que interactúan con la planta.

La señalización por factores Myc a través de los receptores LysM RLKs y su papel relevante en desencadenar los picos de Ca^{++} y el CSSP durante la micorrización está respaldada por numerosos estudios. Por ejemplo, la mutación en los genes LjNFR1 y MtLYK3 requeridos en la percepción de factores Nod, resultan en una reducción de la colonización micorrícica (Zhang et al. 2015a), el silenciamiento del homólogo en *Parasponia andersonii*, *PaNFP*, da lugar a defectos en la formación de arbúsculos (Den Camp et al. 2011), y ante el silenciamiento por VIGS tanto del gen *PaNFP* de *Parasponia* o del homólogo de tomate *SlLYK10*, se produce un bloqueo de la entrada del hongo MA en la raíz (Buendia et al. 2016).

Así mismo, mutantes silenciados o knockout para *OsCERK1* no responden a exudados de esporas fúngicas germinadas ni a la adición de CO_4 purificado (Carotenuto et al. 2017), y tienen un defecto claro en la penetración fúngica de la epidermis radicular (Miyata et al. 2014; Zhang et al. 2015a), lo cual hace pensar que los Myc-COs de los exudados fúngicos son señales importantes durante la comunicación hongo-hospedador. En el caso de los mutantes *mtnfp*, no se nodulan (Amor et al. 2003) y, a pesar de que se micorrizan de forma aparentemente normal (Maillet et al. 2011; Zhang et al. 2015a) y los picos de Ca++ se generan de forma normal en respuesta a Myc-COs (Genre et al. 2013), la señalización nuclear por picos de Ca^{++} sí que ve impedida en el caso de que se apliquen Myc-LCOs en dichos mutantes *mtnfp* (Sun et al. 2015). Es más, hay estudios que demuestran que la expresión génica en respuesta a los Myc-LCOs depende enormemente de NFP (Camps et al. 2015; Czaja et al. 2012).

Junto con los LCOs/COs, cada vez está más claro que los hongos MA también emplean pequeñas moléculas de secreción para comunicarse con la planta

hospedadora, y que actúan como "efectores" modulando la respuesta inmune para permitir la micorrización, de modo análogo a los efectores típicos implicados en desencadenar la respuesta inmune tras la detección de los PAMPs (Patrones Moleculares Asociados a Patógenos), permitiendo la infección de la planta por parte del patógeno (kamoun et al., 2017).

De este modo, los hongos que establecen asociaciones simbióticas con las plantas, al igual que en las interacciones de tipo patogénico, han tenido que desarrollar estrategias evolutivas para una comunicación efectiva que permita:

- Manipular o "piratear" las defensas vegetales
- Redireccionar el desarrollo de la raíz en vistas a adecuar el futuro nicho ecológico del hongo

Para ambos propósitos, durante las primeras etapas de la infección es de especial importancia que haya una comunicación molecular efectiva entre ambos organismos. En esta comunicación participan proteínas o metabolitos secretados por el hongo que reciben el nombre de "efectores" [ver rev. (Kobae et al. 2018)].

Por el momento, sólo se han identificado efectores que actúan sobre la señalización hormonal. SP7 (Secreted Protein7) es secretado por el hongo *R. irregularis* e interacciona con el ERP (Factor de Respuesta a Etileno), inhibiendo la señalización por etileno (Kloppholz et al. 2011). Otro efector identificado es SIS1, el cual es inducible por SLs y es necesario para la correcta formación de los arbúsuclos (Tsuzuki et al. 2016). En cuanto a la alteración de la ruta del jasmonato, se desconoce si existe un efector liberado por los hongos MA. Sin embargo, sí que se ha visto que el hongo ectomicorrícico *Laccaria bicolor* secreta el efector MiSSP7, estabilizando JAZ, un represor de la señalización por jasmonatos (Plett et al. 2014). Se predice que existe una lista mucho más grande de efectores fúngicos, de modo que diferentes efectores podrían estar actuando sobre distintos procesos de señalización del hospedador y sobre diferentes etapas de la micorrización.

Aunque las proteínas efectoras descubiertas por el momento son muy pocas, se cree que existen muchas más. De hecho, en la secuencia genómica de *R. irregularis* DAOM197198 se predice que existen varios cientos de genes codificantes para proteínas de secreción, muchas de las cuales podrían actuar como efectores (Tisserant et al. 2013; Lin et al. 2014; Toro and Brachmann 2016) y, algunos de estos genes precisamente son inducibles por el análogo de estrigolactonas GR24 (Tsuzuki

et al. 2016). Las predicciones de los secretomas de otras especies de hongos MA como *Rhizophagus clarus* (Toro and Brachmann 2016)*, Gigaspora mar- garita* and *Gigaspora rosea* (Tang et al., 2016; Kamel et al., 2017b), sugieren que un subset de efectores putativos está conservado, mientras que hay otros efectores específicos de cada especie (Kamel et al. 2017a; Kamel et al. 2017b), o incluso específicos de los diferentes aislados dentro de la misma especie (Chen et al. 2018). Además, recientemente Zeng et al. (2018) identificaron en el genoma de *R. irregularis* los genes candidatos a codificar efectores, y llegaron a la conclusión de que hay distintos sets que se expresan diferencialmente en el micelio extrarradical, en las hifas intraradicales y en los arbúsculos y, aunque la mayoría de estos genes parecen expresarse al mismo nivel en distintas especies hospedadoras, también parece que hay determinados sets de efectores dependientes del hospedador.

6.3. Regulación transcripcional

La señalización a través del CSSP desencadena la reprogramación de la célula a todos los niveles, y las raíces colonizadas sufren numerosos cambios transcripcionales, tal y como muestran los estudios llevados a cabo en especies tales como *Medicago truncatula* (Liu et al. 2007; Gomez et al. 2009), *Lotus japonicus* (Guether et al. 2009; Handa et al. 2015), arroz (Güimil et al. 2005), patata (Gallou et al. 2012) y, en nuestra planta modelo, el tomate (Dermatsev et al. 2010; García Garrido et al. 2010; López-Ráez et al. 2010; Fiorilli et al. 2009; Ruzicka et al. 2012). Estos análisis muestran que durante la simbiosis MA se ha de dar una tremenda regulación a nivel transcripcional y, de hecho, muchos de los genes cuya expresión se ve inducida durante la micorrización codifican para factores de transcripción, con especial importancia de los factores tipo GRAS, específicos de plantas. De acuerdo con esto, se ha visto que numerosos miembros de la familia de factores de transcripción tipo GRAS están implicados en la regulación de cada una de las etapas de la simbiosis MA, desde el inicio de la colonización hasta la senescencia de los arbúsculos (Xue et al. 2015; Park et al. 2015; Heck et al. 2016; Floss et al. 2017; Pimprikar and Gutjahr 2018), del mismo modo que son relevantes en la nodulación (Udvardi and Scheible 2005). A continuación se detallan los principales mecanismos de regulación por factores de transcripción identificados por el momento en cada una de las etapas del desarrollo micorrícico.

Etapas iniciales: CYCLOPs

La percepción y transmisión de una serie de señales simbióticas externas, entre ellas los Myc-LCOs, culmina con la generación de picos de Ca^{++} en el núcleo de la célula vegetal a colonizar, los cuales constituyen la señal clave desencadenante de la respuesta transcripcional simbiótica. Justo a este nivel, CCaMK/DMI3, una quinasa dependiente de Ca^{++} y calmodulina, es la encargada principal de interpretar estos pulsos de Ca^{++} (Miller et al., 2013) y, en respuesta, fosforilar y activar CYCLOPS/IPD3 (Yano et al. 2008; Singh et al. 2014), un factor de transcripción primario y central de la respuesta transcripcional simbiótica. Como resultado, CYCLOPS/IPD3 se une directamente al promotor de *RAM1*, y muy probablemente a los promotores de otros genes inducibles por micorrización (Favre et al. 2014).

Ramificación del arbúsculo: RAM1

La ramificación del arbúsculo está regulada por una serie de factores de transcripción tipo GRAS, entre los cuales RAM1 es el mejor caracterizado (Gobbato et al. 2012; Park et al. 2015; Rich et al. 2015; Xue et al. 2015; Pimprikar et al. 2016; Luginbuehl et al. 2017). RAM1 se expresa muy fuertemente y de forma específica en las zonas de la raíz colonizadas por hongos MA (Gobbato et al. 2012; Gobbato et al. 2013; Park et al. 2015; Rich et al. 2015; Xue et al. 2015; Pimprikar et al. 2016). En las raíces mutantes *ram1* sólo se observan arbúsculos truncados o con ramificaciones muy primarias (Park et al. 2015; Rich et al. 2015; Xue et al. 2015; Pimprikar et al. 2016), y los análisis transcriptómicos de dichas raíces sugieren que RAM1 es un regulador transcripcional temprano requerido para la transición entre las ramificaciones arbusculares de primer orden y las más finas (Park et al. 2015; Rich et al. 2015; Xue et al. 2015; Pimprikar et al. 2016; Luginbuehl et al. 2017), y más concretamente podría tener un papel importante en la formación de la membrana periarbuscular y en el intercambio de nutrientes entre los simbiontes. De hecho, los mutantes *ram1* son defectuosos en la activación de la expresión de genes inducibles por micorrización presuntamente implicados en la formación de la membrana periarbuscular (*VAPYRIN* y *Exo70I*) (Feddermann et al. 2010; Pumplin et al. 2010; Zhang et al. 2015b), en el transporte de minerales del hongo a la raíz a nivel del arbúsculo (*PT4* y *AMT2.2*), y en la biosíntesis de ácidos grasos (*KASIII*, *DIS*, *FatM* and

RAM2) (Park et al. 2015; Pimprikar et al. 2016; Jiang et al. 2017; Keymer et al. 2017; Luginbuehl et al. 2017; Rich et al. 2017), que además de ser requeridos para la formación de la membrana arbuscular, actualmente también son considerados como la fuente de transferencia de carbono más importante para nutrir al hongo. Sin embargo, hay que mencionar que, al contrario de lo que ocurre en *Medicago* y *Petunia* (Park et al. 2015; Rich et al. 2015), en los mutantes *ram1* de *Lotus japonicus* no se ha observado una expresión defectuosa para genes tales como *RAM2*, *STR* y *PT4*, lo cual sugiere una posible redundancia funcional a nivel de *RAM1* en *Lotus* (Pimprikar et al. 2016).

Adicionalmente, los experimentos llevados a cabo con plantas sobreexpresadas para *RAM1* confirman que la activación de la expresión de muchos de estos genes relacionados con la funcionalidad del arbúsculo y la formación de la membrana periarbuscular es dependiente de *RAM1* pero independiente del hongo MA, (Park et al. 2015; Pimprikar et al. 2016; Luginbuehl et al. 2017), y revelan que entre los genes directamente activados por RAM1 también hay una serie de genes codificantes para factores de transcripción (Rich et al. 2017; Luginbuehl et al. 2017). Por ejemplo, cabe destacar tres genes que codifican para TFs con el dominio ERF/AP2, cuyos homólogos en *Arabidopsis* regulan la glicólisis y la biosíntesis de ácidos grasos (Luginbuehl et al. 2017; To et al. 2012), y que podrían tener un papel similar en plantas micorrícicas; de hecho, su silenciamiento da un fenotipo muy parecido a los mutantes *ram1*, incluyendo la no inducción de genes específicos para la biosíntesis de lípidos en los arbúsculos (Luginbuehl et al. 2017; Bravo et al. 2017; Jiang et al. 2017; Keymer et al. 2017; Devers et al. 2013).

Expansión de las células corticales de la raíz: MIG

MIG1 (MYCORRHIZA INDUCED GRAS 1) es otro factor de transcripción GRAS que se induce durante la micorrización, específicamente en células con arbúsculos (Heck et al. 2016). Los resultados de Heck et al. (2016) apuntan a que MIG recluta a DELLA para regular la expansión radial de las células que contienen arbúsculos, y no la formación de la membrana periarbuscular. Concretamente Heck et al. (2016) muestran que MIG es capaz de interaccionar con DELLA, que el silenciamiento simultáneo de los tres *MIGs* da lugar a arbúsculos deformados y más pequeños, que la sobreexpresión de DELLA restaura el desarrollo de los arbúsculos en dichas

plantas, que la sobreexpresión de *MIG* no desencadena la inducción de genes para la regulación del intercambio de nutrientes como *RAM1*, *RAD1*, *Exo70I* (Park et al. 2015; Zhang et al. 2015b; Floss et al. 2016), y que tanto la sobreexpression de *DELLA* como de *MIG* dan lugar a un aumento del diámetro del córtex, tanto por un mayor tamaño de las células como por un mayor número de capas celulares. Sin embargo, por ahora se desconoce el papel del tamaño celular en la ramificación del hongo.

Degeneración del arbúsculo: MYB1

Los arbúsculos están en continuo reciclaje y su vida es relativamente corta, aunque varía entre unos arbúsculos y otros y entre especies (Brown and King 1982; Alexander et al. 1989; Kobae and Hata 2010). Por ejemplo, en arroz se ha visto que el arbúsculo maduro tiene una vida de tan solo 2-3 días y que colapsa en unas pocas horas, ya que la visualización del marcador PT11-GFP desaparece rápidamente (Kobae and Hata 2010). La degeneración del arbúsculo comienza con el colapso de las ramificaciones más finas seguido de las senescencia gradual del arbúsculo completo (Kobae and Fujiwara 2014; Kobae et al. 2014). Aunque se desconoce el sentido biológico, se cree que este rápido reciclaje de arbúsculos podría servirle a la planta para eliminar rápidamente aquellos arbúsculos que no le proporcionan nutrientes y así evitar mecanismos de "engaño" o abuso por parte del hongo (Javot et al. 2007a; Gutjahr and Parniske 2017). De hecho, en plantas mutantes para transportadores arbusculares de fosfato *mtpt4* y *ospt11*, en las cuales se ve perjudicado el aporte de nutrientes del hongo a la planta, se acelera la degeneración de los arbúsculos y la inducción asociada de genes codificantes de hidrolasas (proteasas, lipasas, quitinasas) y de proteínas relacionadas con la maduración (Floss et al. 2017). Por ahora no se conoce como está conectada la percepción del Pi a la regulación transcripcional, pero esto ha de estar controlado temporalmente para activar rápidamente la degeneración de los arbúsculos cuando hayan terminado su función proveedora de nutrientes a la planta. A este respecto, se ha identificado al factor de transcripción MYB1 como elemento regulador clave de la inducción transcripcional de muchos de los genes asociados a la degeneración del arbúsculo. *MYB1* se induce durante la micorrización y acelera la degeneración del arbúsculo cuando la liberación de Pi a nivel del arbúsculo es nula (Floss et al. 2017). Mientras

que la esperanza de vida de los arbúsculos se acorta en los mutantes *mtpt4*, en los doble mutantes *pt4 myb1* se recupera el fenotipo normal. Sin embargo, en los mutantes *myb1* no se incrementa la esperanza de vida del arbúsculo en presencia de PT4, lo cual sugiere que existe redundancia funcional a nivel de MYB1 (Floss et al. 2017).

Se ha de hacer notar que en *Lotus* no se ha visto una implicación clara del homólogo de *MYB1*, *MAMI*, posiblemente porque la sobreexpresión con p35S no es muy efectiva en esta especie (Maekawa et al. 2008), o por la presencia de una segunda copia de *MYB1* en *Lotus*, que aún no se ha estudiado (Floss et al. 2017) y que quizás tenga un papel más relevante durante la micorrización.

Colonización a nivel cuantitativo: OsAM18, NSP1, NSP2, LOM1, NFYAs

En el control de la colonización a un nivel cuantitativo, se han identificado cuatro factores de transcripción tipo GRAS implicados. Estos son OsAM18 (Fiorilli et al., 2015), NSP1 y NSP2 (Shtark et al. 2016) y LOM1 (Couzigou et al. 2017). NSP1, al igual que RAM1 (Hohnjec et al. 2015), es activado por MYC-LCOs y es esencial para la inducción de un gran número de genes (Delaux et al. 2013; Camps et al. 2015; Hohnjec et al. 2015), entre los que cabe destacar genes para la biosíntesis de SL, que podrían contribuir al incremento en la longitud de raíz micorrizada dependiente de NSP1. De hecho, la inducción de genes implicados en la ruta de biosíntesis de SLs, así como la producción de SLs, se ven afectadas tanto en mutantes *nsp1* como *nsp2* (Liu et al. 2011; Takeda et al. 2013). Estos resultados sugieren que NSP1 y RAM1 podrían cooperar en la regulación de las respuestas transcripcionales a las Myc-LCOs. Por otro lado, NSP2 es regulado negativamente a nivel post-transcripcional por un microRNA llamado miR171h, posiblemente determinando en qué partes de la raíz y ante qué condiciones nutricionales se ha de inhibir la expansión de la colonización MA. Precisamente la expresión de miR171h es especialmente elevada en la zona de elongación de la raíz (Lauressergues et al. 2012) y ante condiciones de alto Pi y bajo N (Hofferek et al. 2014), pudiendo mediar en la inhibición de la micorrización en ambos casos. Otros miembros de la familia miR171 son conocidos por tener como diana los genes LOM (**LO**ST **M**ERISTEMS), también codificantes de factores de transcripción GRAS que regulan positivamente la colonización micorrícica a nivel cuantitativo (Couzigou et al. 2017). En concreto, hay seis

miembros miR127 (a, b, c, d, e y f) capaces de interactuar con el transcrito *LOM1*. Mientras que en *Arabidopsis* todos ellos se unen al transcrito de *LOM1* induciendo su degradación, en las especies vegetales micorrizables uno de los seis miR127, concretamente miR127b, tiene un cambio conservado que impide que dicho miR127b actúe cortando el RNA de *LOM1*, lo cual sugiere que podría tratarse un mecanismo específico de la simbiosis MA para proteger al tránscrito *LOM1* del resto de los miembros miR127, para así evitar la degradación de *LOM1* y permitir la acción promotora de LOM1 sobre los niveles de colonización (Couzigou et al. 2017). Además, en las plantas hay mecanismos de regulación sistémicos para el control de la colonización. Este fenómeno es el llamado "autorregulación de la micorrización", e incluye la participación de un receptor kinasa tipo CLAVATA denominado NARK (**N**ODULATION **A**UTOREGULATION **R**ECEPTOR **K**INASE) (Meixner et al. 2005; Schaarschmidt et al. 2013), que parece reprimir la expresión de genes que codifican para factores de transcripción de la familia NFYA, reguladores positivos de la colonización micorrícica a nivel cuantitativo (Schaarschmidt et al. 2013), presumiblemente mediante su interacción con factores de transcripción GRAS.

El papel múltiple de DELLA

DELLA constituye un gen simbiótico común a la micorrizacion y a la nodulación, aparte de tener múltiples roles en el desarrollo vegetal y en la adaptación medioambiental (Fonouni-Farde et al. 2016; Davière and Achard 2013, 2016). La importancia de DELLA radica en que este factor de transcripción, o más concretamente el módulo DELLA/GAs, es un regulador central en la señalización mediada por giberelinas (GAs), unas hormonas que promueven numerosas procesos del desarrollo y del crecimiento en las plantas en respuesta a las condiciones ambientales (Harberd et al. 1998; Achard et al. 2006; Achard et al. 2007; Achard et al. 2008; Jiang et al. 2007). Así, las proteínas DELLA actúan reprimiendo la respuesta a GAs y, en cambio, una alta concentración de GAs provoca la degradación de DELLA, ya que las GAs son percibidas por GID1, un receptor de la familia de las alfa/beta hidrolasas, activándose la interacción de GID1 con DELLA, así como la degradación de DELLA vía el proteosoma 26S (Willige et al. 2007; McGinnis et al. 2003; Gomi et al. 2004; Griffiths et al. 2006). En cuanto a la simbiosis

MA, parece que DELLA actúa al inicio de la colonización micorrícica, así como en las etapas tempranas de la formación del arbúsculo y de su generación.

En las etapas tempranas de la simbiosis micorrícica, DELLA tiene un papel fundamental en el desarrollo de la micorrización, mientras que las GAs tienen un efecto inhibidor. En concreto se ha visto que *DELLA1* y *DELLA2* de *M. truncatula* son imprescindibles en el establecimiento de ambos tipos de simbiosis (Floss et al. 2013; Jin et al. 2016; Fonouni-Farde et al. 2016) y que además, el tratamiento con GAs así como la mutación de DELLA dan lugar a la inhibición de la formación de la micorriza (El Ghachtouli et al. 1996; Floss et al. 2013; Foo et al. 2013; Yoshida et al. 2014; Takeda et al. 2015). Asimismo, la eliminación de los dominios de DELLA responsables de su unión a GID1 da lugar a la insensibilidad a tratamiento por GAs (Willige et al. 2007) y a que se anule el efecto inhibidor de las GAS sobre la micorrización (Floss et al. 2013; Takeda et al. 2015).

El papel esencial de DELLA en la micorrización radica en su participación en la activación de genes inducibles por micorrización. El mecanismo más conocido por el que DELLA induce la expresión de genes simbióticos es a través de su interacción con el factor de transcripción CYCLOPS, promoviendo la capacidad de CYCLOPS de transactivar el promotor de *RAM1* y posiblemente de otros genes (Takeda et al. 2015; Pimprikar et al. 2016; Park et al. 2015; Floss et al. 2016; Feng et al. 2008). Así, el complejo CYCLOPS-DELLA seguramente constituye un integrador importante de la señalización simbiótica con la señalización por GAs, para conseguir un ajuste adecuado entre la formación de la micorriza arbuscular y el estado fisiológico de la planta según las condiciones ambientales. Por otra parte, los resultados de Floss et al. (2013) y Pimprikar et al. (2016) sugieren que, en ausencia de CYCLOPS, DELLA es capaz de interaccionar con otra proteína de unión a ADN alternativa, y de desencadenar la respuesta transcripcional asociada a micorrización de forma independiente a la señalización vía CCaMK y CYCLOPS. Se cree que un posible candidato podría ser algún factor de transcripción de la familia IDD (INDETERMINATE DOMAIN) (Yoshida et al. 2014; Fukazawa et al. 2014; Fukazawa et al. 2017). De hecho, numerosos factores de transcripción de este tipo se ven inducidos por micorrización (Gutjahr et al. 2015; Rich et al. 2015; Takeda et al. 2015; Luginbuehl et al. 2017) y, curiosamente se ha visto que otros factores de transcripción tipo GRAS (SHR y SCR) regulan la expresión génica a través de su

unión a determinados factores de transcripción de tipo IDD que son los que sí establecen una interacción directa con el ADN (Hirano et al. 2017). Por ello, en el desarrollo micorrícico, quizás DELLA también actúe como un cofactor transcripcional y la activación transcripcional de DELLA independiente de CYCLOPS pueda estar mediada por una proteína IDD. A pesar del papel esencial de DELLA al inicio de la micorrización, cabe mencionar que aparentemente DELLA no está implicada en la formación del aparato de prepenetración (Ivanov and Harrison 2014), posiblemente debido a que quizás dicho proceso no esté regulado transcripcionalmente y, por lo tanto, no dependa del complejo CCaMK-CYCLOPS-DELLA. De hecho se ha visto que la formación del PPA es independiente de CCaMK (Genre et al. 2009).

Aparte de la acción de DELLA en la activación de genes simbióticos para el inicio de la colonización MA, los resultados apuntan a un papel adicional de DELLA en el desarrollo del arbúsculo, que además es a tres niveles, tanto en la expansión de las células hospedadoras de arbúsculos, como en el inicio de la formación del arbúsculo y en su degeneración. En concreto, como ya hemos visto, posiblemente a través de la interacción DELLA-MIG1, se aumenta el tamaño de las células del córtex, lo cual parece ser importante para que el arbúsculo se desarrolle de forma correcta en el futuro (Heck et al. 2016). Además, DELLA1 y DELLA2 son muy importantes en el inicio de la formación de los arbúsculos en *M. truncatula*, así como en la degeneración del arbúsculo, ya que es capaz de interaccionar con el factor de transcripción MYB1, el cual regula el colapso de los arbúsculos. Por el contrario, DELLA no parece participar en la ramificación del arbúsculo ni en la formación de hifas intrarradicales (Floss et al. 2013; Floss et al. 2017). Para explicar este comportamiento de DELLA, Pimprikar and Gutjahr (2018) han propuesto un modelo en el cual las GAs juegan un papel dual, siendo los niveles de GAs bajos al inicio y al final de la vida del arbúsculo para promover la formación o degradación del mismo, respectivamente; e incrementándose los niveles de GAs en células con arbúsculos maduros (posiblemente en respuesta al mayor Pi en circulación; (Jiang et al. 2017) para permitir su mantenimiento. Además esta hipótesis justificaría la curiosa activación de promotores de genes implicados tanto en la biosíntesis como el la degradación de GAs en las células con arbúsculos (Takeda et al. 2015).

Complejos de factores de transcripción

Los factores de transcripción GRAS tienen tendencia a formar complejos (Hirano et al., 2017). Aunque se desconoce el significado biológico de todas estas interacciones, se especula que los distintos complejos de factores de transcripción podrían regular distintos grupos de genes dependo del contexto. El caso de DELLA es el más conocido, ya que se ha observado que, aparte de interaccionar con el receptor de GAs GID1, también es capaz de interactuar con diversos factores de transcripción tales como CYCLOPS (Pimprikar et al. 2016), DIP1 (Yu et al. 2014), MYB1 (Floss et al. 2017) y MIG1 (Heck et al. 2016). A continuación destacamos las posibles interacciones de RAM1 y MYB1 con otros factores de transcripción, y que podrían ser relevantes en la regulación de la simbiosis MA.

En el caso de RAM1, que como hemos visto es esencial para la activación de genes implicados en la formación de las ramificaciones finas del arbúsculo, se ha observado que es capaz de interaccionar con DIP1 y RAD1, ambos factores de transcripción tipo GRAS. DIP1 (DELLA INTERACTING PROTEIN) interacciona además, como su nombre indica, con DELLA (Yu et al. 2014). Sin embargo, parece que RAM1 no necesita interaccionar con DELLA para inducir el programa transcripcional para el desarrollo del arbúsculo, y que RAM1 actúa aguas abajo de DELLA (Pimprikar et al. 2016). Por otra parte, RAD1 es el homólogo más cercano a RAM1, y ambos factores de transcripción son capaces de interaccionar (Park et al. 2015; Xue et al. 2015). Además, los mutantes para los genes que codifican ambos TFs tienen un fenotipo similar en *L. japonicus*, con arbúsculos truncados (Xue et al. 2015), aunque no en *Medicago* (Park et al. 2015), lo que sugiere que la importancia relativa de RAM1 y RAD1 varía entre estas dos leguminosas.

Por otra parte, el factor de transcripción MYB1 es capaz de interaccionar con NSP1 y con DELLA (Floss et al., 2017), por lo que dichas interacciones podrían mediar en el papel de MYB1 en la degeneración del arbúsculo. Sin embargo, se desconoce si MYB1, NSP1 y DELLA interaccionan formando un mismo complejo, o si se forman dos complejos distintos por separado (MYB1-NSP1 y MYB1-DELLA), cada uno de ellos encargado de regular un grupo diferente de genes.

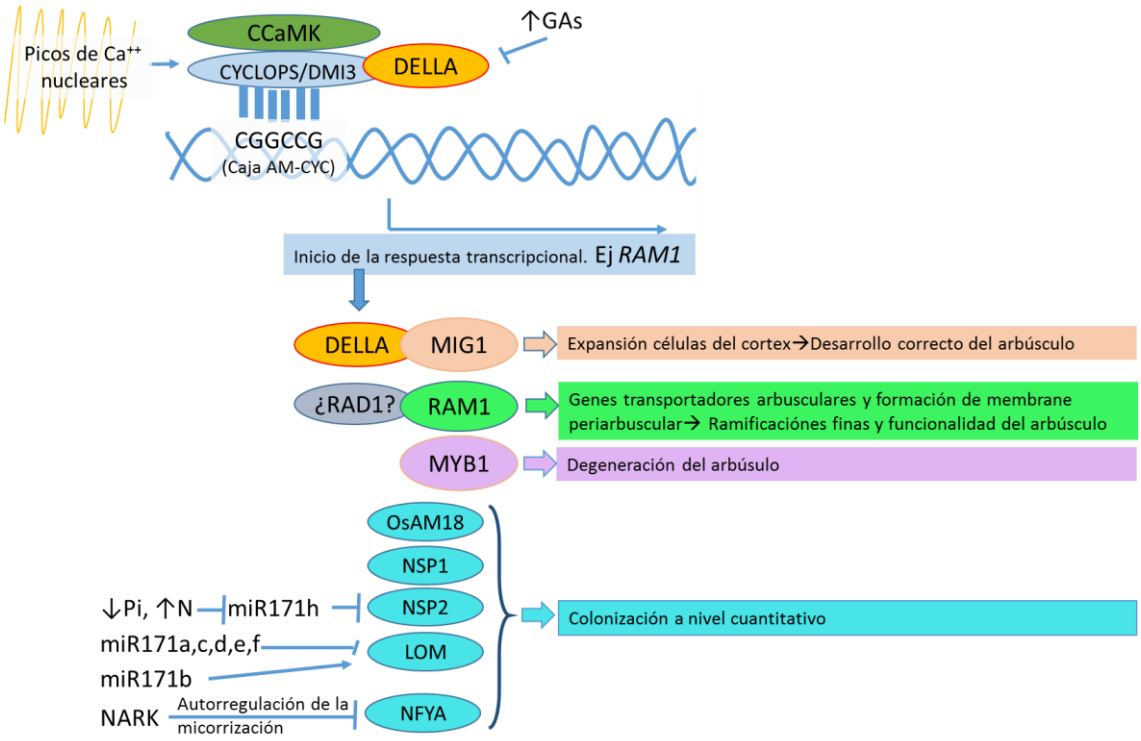

Figura 11. Representación esquemática de los factores de transcripción implicados en la regulación de la simbiosis MA. En la última parte de la ruta común de señalización simbiótica (CSSP) se generan picos de calcio en el núcleo que hacen que CCaMK fosforile y active el factor de transcripción CYCLOPS y, tras la unión de DELLA, CYCLOPS se une a la caja AM-CYC perteneciente a promotores de genes inducibles por micorrización, tales como RAM1, que desencadenan las respuestas simbióticas. En dicha respuestas son muchos los factores de transcripción y las interacciones entre ellos que están implicados para cada una de las etapas de la simbiosis MA. Además, existen mecanismos que regulan finamente la acción de estos factores de transcripción durante la micorrización.

Objectives /Objetivos

OBJETIVES

Arbuscular Mycorrhizal (MA) fungi constitute a natural resource useful as an alternative to the chemical fertilizers which have a high environmental impact. AM fungi establish symbiosis interactions with the roots of most land plants, improving plant nutrition and plant defense against biotic and abiotic stresses. In order to improve the efficiency of AM functionality, it is essential to understand the fundamental processes and to identify the key components involved in the regulation of AM development.

At this respect, it is necessary to better understand the processes involved in the regulation of AM formation, with a special interest in the formation and functioning of the arbuscules, the symbiotic structures for nutrient exchange. In this manner, it is very valuable the knowledge concerning the mechanisms involved in the regulation of the arbuscular cycle, including regulator genes, plant hormones (mainly ABA and giberellins), DELLA and other GRAS transcription factors, and apocarotenoid compounds.

In the lab team where the Doctoral Thesis has been performed, the research is focused in the study of the molecular processes taking place during AM symbiosis in tomato. In addition to its importance as a crop, this plant species is a biological model for plant physiology and genetic studies, and a very suitable plant for mycorrhizal studies because, among other reasons, in contrast to legume plants tomato is unable to nodulate, and then the signaling processes of AM symbiosis do not overlap with those concerning the root-nodule symbiosis.

In our laboratory, a comparative transcriptomic study was performed, comparing non inoculated and inoculated plants with the AM fungus *Rhizophagus irregularis*, together with tomato mutants with an impaired arbuscule formation (the ABA-deficient mutant *sitiens*) (García Garrido et al. 2010). As a result of this microarray analysis, several highly AM-induced genes whose induction upon mycorrhization

was damaged in the *sitiens* mutants were identify as candidate genes to encode proteins with a relevant role during the symbiotic process, and more specifically, in arbuscule formation. From this list, we decided to select two genes and, as a **general objective** for the present thesis, we proposed the **functional analysis of these two tomato genes induced during mycorrhization, *tsb* and *SlDLK2***. The *tsb* gene was chosen because of its possible involvement in the cytoskeleton rearrangements occurring in the root cells upon AM colonization; while the *SlDLK2* gene, which encodes for an α,β-hydrolase protein, was selected because of its possible role a hormonal receptor involved in signaling during mycorrhization.

The *tsb* gene encodes for a putative MAP (Microtubule Associated Protein) that belongs to a family of MAPs unique from Solanaceae plants. Some of the members of this MAP family have been previously described as pollen specific and with a function in cytoskeleton rearrangements and the formation of the pollen tube (Zhao et al. 2006; Huang et al. 2007; Liu et al. 2013). Although there is not information about the possible involvement of this group of MAPs during mycorrhization, it is well known that the cytoskeleton or root cells is strongly altered upon AM colonization. The study of microtubule associated proteins (MAPs) and actin filament binding proteins (ABPs) is probably the best approach to elucidate the cause-effect relation between cytoskeleton rearrangements occurring in the colonized cells and the development and functioning of mycorrhizas, as previously suggested by Timonen and Peterson (2002). For this reason, we decided to focus on the functional study of *tsb* during AM symbiosis.

The second gene selected for its functional analysis was a gene that encodes for a protein belonging to the α.β-hydrolase family, particularly to the DLK2 group. For this reason, it was named as *SlDLK2*. The α.β-hydrolase (ABH) superfamily is constituted by a group of proteins widely distributed across all kingdoms of life, and shows a high functional variety. In some plants, some of these proteins possess a catalytic activity associated to their action as receptors, mainly of plant hormones, such as giberellins, strigolactones and karrikins (Mindrebo et al., 2016). Curiously, the DLK2 protein group is phylogenetically very close to the strigolactone receptors (D14) and the karrikin receptors (KAI2). Strigolactones are plant hormones exudated by the roots and important for presymbiotic signaling during

mycorrhization. In addition, a recent discovery showed that the karrikin receptor KAI2 is essential for the AM symbiosis (Gutjahr et al. 2015). However, DLK2 α.β-hydrolases are shortly characterized, and no relation has yet been found between DLK2 and the mycorrhization process. As the α.β-hydrolases closely related to DLK2 are essential receptors during mycorrhization (KAI2) or are able to perceive signals important for the mycorrhization (SLs), we thought that SlDLK2 might also be a receptor protein with a relevant role in signaling during the AM symbiosis.

Based on all the above, and considering as a priority to have a methodology suitable to evaluate in a quickly and efficient manner gene functionality during mycorrhization, the following **specific objectives** were proposed for the presented thesis work:

1.- Setting up a procedure that allow us to evaluate the functionality of plant genes during the mycorrhization of tomato plants in a quickly and efficient way.

2.- Analysis of the expression pattern and cell localization of *tsb* gene expression.

3.- Functional analysis of *tsb* gene during AM development. Study of the possible role of TSB in the rearrangements of microtubules in root cells.

4.-Analysis of the expression pattern and cell localization of *SlDLK2* gene expression.

5.-Functional analysis of the *SlDLK2* gene during AM colonization. Elucidate the possible action of SlDLK2 as a hormonal receptor

6.-Elucidate the possible role of SlDLK2 in mycorrhizal signaling through the analysis of transcriptional alterations (and metabolic associated pathways) underlying to SlDLK2 silencing in mycorrhizal roots.

OBJETIVOS

Los hongos formadores de Micorriza Arbuscular (MA) son un recurso natural, cuyo aprovechamiento y gestión permitiría reducir en gran medida el uso de fertilizantes químicos y el impacto medioambiental de los mismos. Dichos hongos forman simbiosis con las raíces de la mayoría de las plantas terrestres, mejorando su nutrición e incrementando su capacidad de defensa frente a estreses tanto bióticos como abióticos. El conocimiento de los procesos fundamentales que regulan el desarrollo de la simbiosis MA, así como la identificación del papel de elementos reguladores específicos implicados en su funcionalidad, nos permitirá desarrollar en un futuro procedimientos para mejorar la eficiencia de la misma.

En este sentido, es muy necesario que se lleven a cabo estudios encaminados al conocimiento de los procesos implicados en la regulación de la formación de la asociación MA, concretamente en un paso esencial como es la formación y función del arbúsculo, la estructura simbiótica de intercambio de nutrientes. El conocimiento de los mecanismos por los que genes reguladores, hormonas vegetales, esencialmente ABA y Giberelinas (GAs), proteínas DELLA, TFs GRAS, y compuestos apocarotenoides participan en la regulación del ciclo arbuscular será valioso para desarrollar procedimientos de mejora a fin de lograr una simbiosis MA más eficaz.

Parte de la investigación que realiza el grupo de trabajo que acoge esta Tesis doctoral está focalizada en desgranar los procesos moleculares que ocurren en la simbiosis MA en la planta de tomate. Dicha especie vegetal, además de ser un cultivo de interés agrícola, es un modelo biológico para estudios de fisiología y genética vegetal, y es una planta muy adecuada para el estudio de la micorrización, entre otras razones porque a diferencia de las leguminosas, no es capaz de nodularse y, por lo tanto, se evita la interferencia en la señalización con el proceso de nodulación, lo que resulta útil según el tipo de estudios que llevemos a cabo.

En el seno de dicho grupo de investigación se realizó un estudio trasncriptómico comparativo de plantas de tomate inoculadas y no inoculadas con el hongo formador

de MA *Rhizophagus irregularis*, así como en mutantes de tomate *sitiens* defectuosos en la formación de arbúsculos como consecuencia de su déficit en ABA (García Garrido et al. 2010). Como fruto de dicho microarray, se pudieron identificar una serie de genes altamente inducidos en micorrización, pero en los que dicha inducción se veía gravemente afectada en los mutantes *sitiens* y, por lo tanto, eran candidatos a codificar proteínas con un papel relevante en el proceso simbiótico, preferentemente en la fase de formación de arbúsculos. De esta lista de genes se decidieron seleccionar dos de ellos, y como **objetivo general** de la presente tesis se planteó el **análisis funcional de estos dos genes de tomate inducidos por micorrización, *tsb* y *SlDLK2*.** Concretamente, el *tsb* se eligió por ser posiblemente importante para la reorganización del citosqueleto de las células de la raíz durante la micorrización, y el segundo de ellos, codificante para una proteína de la familia α/β-hidrolasa, aquí denominada SlDLK2, por ser un posible receptor hormonal relevante en la señalización durante la micorrización.

El gen *tsb* codifica para una putativa MAP (Proteína Asociada a Microtúbulos), perteneciente a una familia de MAPs exclusiva de Solanáceas, dentro de la cual algunos miembros han sido anteriormente descritos como específicos del polen y con una función en la restructuración del citosqueleto y en la formación del tubo polínico (Zhao et al. 2006; Huang et al. 2007; Liu et al. 2013). Aunque por el momento no existe ninguna información referente al posible papel de este grupo de MAPs durante la micorrización, sí que se sabe que el citosqueleto de las células vegetales de la raíz sufre grandes cambios en el proceso de la colonización MA. El estudio de proteínas de unión a microtúbulos (MAPs) y filamentos de actinas (ABPs) problablemente sea la mejor aproximación a la hora de elucidar las relaciones causa-efecto entre las reorganizaciones del citosqueleto que sufren las células colonizadas y el desarrollo y función de las micorrizas, tal y como ya apuntó con anterioridad Timonen and Peterson (2002), por lo que decidimos focalizarnos en realizar un estudio funcional de *tsb* durante la simbiosis MA.

Por otra parte, el otro gen seleccionado para su análisis funcional, tal y como ya se ha mencionado, fue un gen que codifica para una proteína perteneciente a la familia α,β-hidrolasa, concretamente al grupo DLK2, de ahí que haya sido nombrada aquí como SlDLK2. La superfamilia α.β-hidrolasa (ABH) la constituye un grupo de

proteínas ampliamente distribuidas entre los seres vivos y con una gran variedad funcional. En plantas, algunas de estas proteínas poseen actividad catalítica asociada a su acción como receptores, sobre todo de hormonas vegetales y ligandos en la señalización por giberelinas, estrigolactonas y karrikinas (Mindrebo et al., 2016). Curiosamente, el grupo de proteínas DLK2 está muy cercano filogenéticamente a los receptores de estrigolactonas (receptores D14) y de karrikinas (receptores KAI2). Las estrigolactonas son unas hormonas vegetales exudadas por las raíces de las plantas e importantes en la señalización presimbiótica durante la micorrización. Por otra parte, recientemente se ha descubierto que el receptor de karrikinas KAI2 parece ser esencial para la micorrización (Gutjahr et al. 2015). Sin embargo, las □□□-hidrolasas de tipo DLK2 están poco caracterizadas, y no existe en la literatura ninguna mención sobre su ligando específico ni sobre su posible relación con la micorrización. Debido a que las α.β--hidrolasas muy cercanas a SlDLK2 son receptores importantes durante la micorrización (KAI2) o perciben señales importantes para la micorrización (SLs), nos planteamos la posibilidad de que SlDLK2 pudiese ser también una proteína receptora con un papel relevante en la señalización durante el proceso de la simbiosis MA.

En base a todo lo anterior y considerando también prioritario disponer de una metodología apropiada para evaluar de manera rápida y eficaz la funcionalidad de estos genes durante la micorrización, se ha propuesto los siguientes **objetivos específicos** para el trabajo de tesis presentado:

1.- Puesta a punto de un procedimiento que permita evaluar la funcionalidad de genes vegetales durante la micorrización en plantas de tomate de una manera rápida y eficaz.

2.- Análisis del patrón de expresión y de la localización celular de la expresión del gen *tsb.*

3.- Análisis funcional del gen *tsb* durante el desarrollo de la colonización micorrícica. Estudio del posible papel de TSB en la restructuración del citoesqueleto de microtúbulos en las células del raíz.

4.- Análisis del patrón de expresión y de la localización celular de la expresión del gen *SLDLK2*.

5.- Análisis funcional del gen *SLDLK2* durante el desarrollo de la colonización micorrícica. Elucidar la posible acción de SlDLK2 como receptor hormonal.

6.- Elucidar el posible papel de SlDLK2 en la señalización micorrícica mediante el análisis de las alteraciones transcripcionales (y rutas metabólicas asociadas) que subyacen al silenciamiento de *SlDLK2* en raíces micorrizadas.

General Material & Methods

1. Biological material and growth conditions

1.1. Fungal material and production

Rhizophagus irregularis (Ri; formerly known as *Glomus intraradices*) DAOM 197198 was used for most of the experiments. As an obligate symbiont, it was cultivated in a monoxenic culture together with actively growing Ri T-DNA carrot (*Daucus carota* L.) hairy roots clone DC2, previously transformed from *Agrobacterium rhizogenes*

Table 1. Minimal (M) medium and Modified White´s (MW) medium, Bécard and Fortin (1988):

	M medium		MW medium	
	mg l^{-1}	µM	mg l^{-1}	µM
Macroelements				
$MgSO_4 \cdot 7H_2O$	731	2965.75	731	2965.75
KNO_3	80	791.21	80	791.21
KCl	65	871.78	65	871.78
KH_2PO_4	4.8	35.27	-	-
Na_2SO_4	-	-	199	1401.01
$NaH_2PO_4 \cdot H_2O$	-	-	19	158.34
$Ca(NO_3)_2 \cdot 4H_2O$	288	1219.56	288	1219.56
EDTA-NaFe	8	21.79	8	21.79
KI	0.75	4.51	0.75	4.51
Microelements				
$MnCl_2 \cdot 4H_2O$	6	30.31	6	30.31
$ZnSO_4 \cdot 7H_2O$	2.65	9.21	2.65	9.21
H_3BO_3	1.50	24.26	1.50	24.26
$CuSO_4 \cdot 5H_2O$	0.13	0.52	0.13	0.52
$Na_2MoO_4 \cdot 2H_2O$	0.0024	0.0099	0.0024	0.0099
Organic constituents				
Glycine	3	39.96	3	39.96
Thiamine hydrochloride	0.1	0.2965	0.1	0.2965
Pyridoxine hydrochloride	0.1	0.4863	0.1	0.4863
Nicotinic acid	0.5	4.0614	0.5	4.0614
Myo-inositol	50	277.51	50	277.51
Sucrose	10000	29214.13	30000	87642.4189

The pH of the media was adjusted to 5.5. The medium was solidified with 0.4% gellan gum (Gel Gro: ICN Biochemical, Aurora, OH, USA). Sterilization was done at 120ºC for 15 min.

strain A4. The dual culture was stablished according to Chabot et al. (1992) in petri dishes (150 mm) on Minimal (M) medium previously described by Bécard and Fortin (1988) but solidified with 0.4% (w\v) gellan gum (Gel Gro: ICN Biochemical, Aurora, OH, USA). The fungal material used as inouculum was a mixture of M medium, spores, hyphae and root fragments. As a negative control for non-inoculated treatments, we also grew axenic cultures of only uninfected carrot hairy roots in Modified White´s (MW) medium, also described by the same authors. Composition of MM and MW media is detailed in Table 1.

1.2. Surface sterilization and germination of seeds

For our experiments *Solanum lycopersicum* cv Moneymaker (accession LA2706, Tomato Genetics Resource Center, TGRC, University of California, USA) was used. Seeds of *S. lycopersicum* L. were surface sterilized with a 5 min soaking using 2.35% w/v sodium hypochloride (50% v/v commercial bleach) and then washed with sterile distilled water.

In order to improve the vigor of the seeds in terms of percentage, speed and uniformity in germination, seeds were allowed to 1 day imbibition with distilled water in the dark at room temperature with slight shaking.

Seeds were then placed and incubated in sterile and sealed Petri dishes with wet filter paper at the dark and at 25-28ºC during 4 days. After this period, germinated seeds were ready to use for both in vitro and growth chamber plant assays.

1.3. Plant growth conditions

Both, 1 week old *S. lycopersicum* seedlings grown in vermiculite, and hairy root tomato plant seedlings obtained in vitro, were grown in an autoclave-sterilized (20 min at 120ºC) mixture of expanded clay, washed vermiculite and coconut fiber (2:2:1, by volume). The components of the substrate were chosen as more suitable for proper plant growth, better mycorrhizal colonization and easier reproducibility of the experiments compared to other tested substrates as soil and sand. The substrate mixture used provided high water holding capacity, aeration and available organic matter. In addition expanded clay (Lecaton, 3-8 mm particle size; Leca-

Deutschland, Halstenbek, Germany) is recommended as a carrier for spores and mycelia of arbuscular mycorrhizal fungi (Baltruschat 1987).

Plant growth and treatments took place in a growth chamber (day: night cycle, 16h, 24ºC: 8h, 20ºC; relative humidity 50%) %) with an average photosynthetic photon flux density of 350 µmol m^{-2} s^{-1}.

Inoculation with *Glomus irregulare* (DAOM 197198) was carried out in 500-ml pots. Each seedling was grown in a separate pot and was inoculated with a piece of monoxenic culture in Gel-Gro medium containing 50 spores of *R. irregularis* and infected carrot roots (see *Fungus material and Production*). In the non-inoculated treatment the plants were inoculated with a piece of Gel-Gro medium containing only uninfected carrot roots.

As hairy root tomato plants suffered strongly their transfer from in vitro to pot culture, plastic glasses or humidity domes were set on top of these plants and they were sprayed with water every two days to keep moisture and prevent wilting during the first weeks.

One week after planting and weekly thereafter, the pots were given 20 ml of a modified Long Ashton nutrient solution containing 25% of the standard phosphorus (P) concentration (Hewitt 1966) (Table 2), as low-phosphate conditions have been shown to stimulate hyphal branching, consequently improving the colonization rate by the AM fungi (Nagahashi and Douds 2000; Akiyama et al. 2005a). In the case of non-mycorrhizal plants, a complete Long Ashton solution was used in the same manner. Plants were harvested at different times after inoculation, and the root system was washed and rinsed several times with tap water.

In the case of the hairy root tomato plants, screening and removal of DsRed-negative (non-transformed roots) was done by observation under a fluorescent stereomicroscope Leica M165F, keeping the root system submerged in water during the procedure.

The root system was weighed and used for the different measurements according to the nature of the experiments. In each experiment, at least five independent plants were analyzed per treatment.

Table 2. Modified Long Ashton nutrient solution, Hewitt (1966)

	mg l^{-1}	Complete µM
Macroelements		
KNO_3	303	2990.03
$Ca(NO_3)_2$	1416	8629.52
$MgSO_4 \cdot 7H_2O$	368	1493.68
$Na_2HPO_4 \cdot 2H_2O$*	231*	1298.04*
EDTA-Fe(II)	25	72.24
Microelements		
$MnSO_4 \cdot 4H2O$	2.20	9.86
H_3BO_3	1.86	30.08
$CuSO_4 \cdot 5H_2O$	0.24	0.96
$ZnSO_4 \cdot 2H_2O$	0.29	1.47
$Na_2MoO_4 \cdot 2H_2O$	0.03	0.12

The pH of the media was adjusted to 7 with NaOH. *For watering of mycorrhizal plants, the amount of Na_2HPO_4 of the nutrient solution was reduced to ¼ (final concentration 324 µM) in order to prevent mycorrhizal inhibition due to an excess of P.

1.4. AM inoculation and plant growth

Germinated seeds were placed on vermiculite for hypocotyl elongation for 1 week. Each seedling was transferred to a 500-ml pot containing an autoclave-sterilized (20 min at 120ºC) mixture of expanded clay, washed vermiculite and coconut fiber (2:2:1, by volume). In the AM inoculated (I) treatments, the plants were inoculated with a piece of monoxenic culture in Gel-Gro medium produced according to Chabot et al. (1992), containing 50 spores of *R. irregularis* (DAOM 197198) and infected carrot roots. For the non-inoculated (NI) treatment a piece of Gel-Gro medium containing only uninfected carrot roots was used. Plant growth took place in a growth chamber (day: night cycle, 16h, 24ºC: 8h, 20ºC; relative humidity 50%).

One week after planting and weekly thereafter, the pots were given 20 ml of a modified Long Ashton nutrient solution containing 25% of the standard phosphorus (P) concentration to prevent mycorrhizal inhibition as a result of excess of phosphorous. In the case of non-mycorrhizal plants, a complete Long Ashton solution was used in the same manner. Plants were harvested at different times after inoculation. The root system was washed and rinsed several times with tap water, weighed and used for the different measurements according to the nature of the experiments. In each experiment, at least five independent plants were analyzed per treatment.

2. Staining of the AM fungus

AM fungus was stained using two different procedures depending of the purpose. The trypan blue staining was used for an overview of the mycorrhizal colonization phenotype and for the estimation of AM colonization and mycorrhizal parameters; while the WGA fluorescent staining was used for a detailed imaging of arbuscule morphology by confocal microscopy.

2.1. The trypan blue staining for estimation of AM colonization

The non-vital trypan blue histochemical staining was used to determine total colonization and it was performed following the method described by Phillips and Hayman (1970) with some modifications. Root segments were cleared with 10% KOH for 10 min in a boiling water bath. This remove the cell root cytoplasm and most of the nuclei, and the roots become very clear with the vascular cylinder distinctly visible. The roots were then rinsed several times with tap water and acidified by an incubation with 0.1N HCl for 3 min. Excess of HCl was removed and roots were stained by simmering for 10-15 min with 0.05% trypan blue in lactic acid. Excess stain was removed by replacing the staining solution with clear lactic acid.

Mycorrhiza development was evaluated in terms of percentage of mycorrhizal root length, by the gridline intersect method described by Giovannetti and Mosse (1980). This method is used to estimate both the proportion of infected roots and their total infected and uninfected root length.

The counting of the infected and uninfected root is summarized in Figure 1. The root sample was spread out evenly in a grid-lined Petri dish and observed under a stereomicroscope. Vertical and horizontal gridlines were scanned and the presence or absence of infection was recorded at each point where the roots intersected a line. At least 100 root-gridline intersects were recorded.

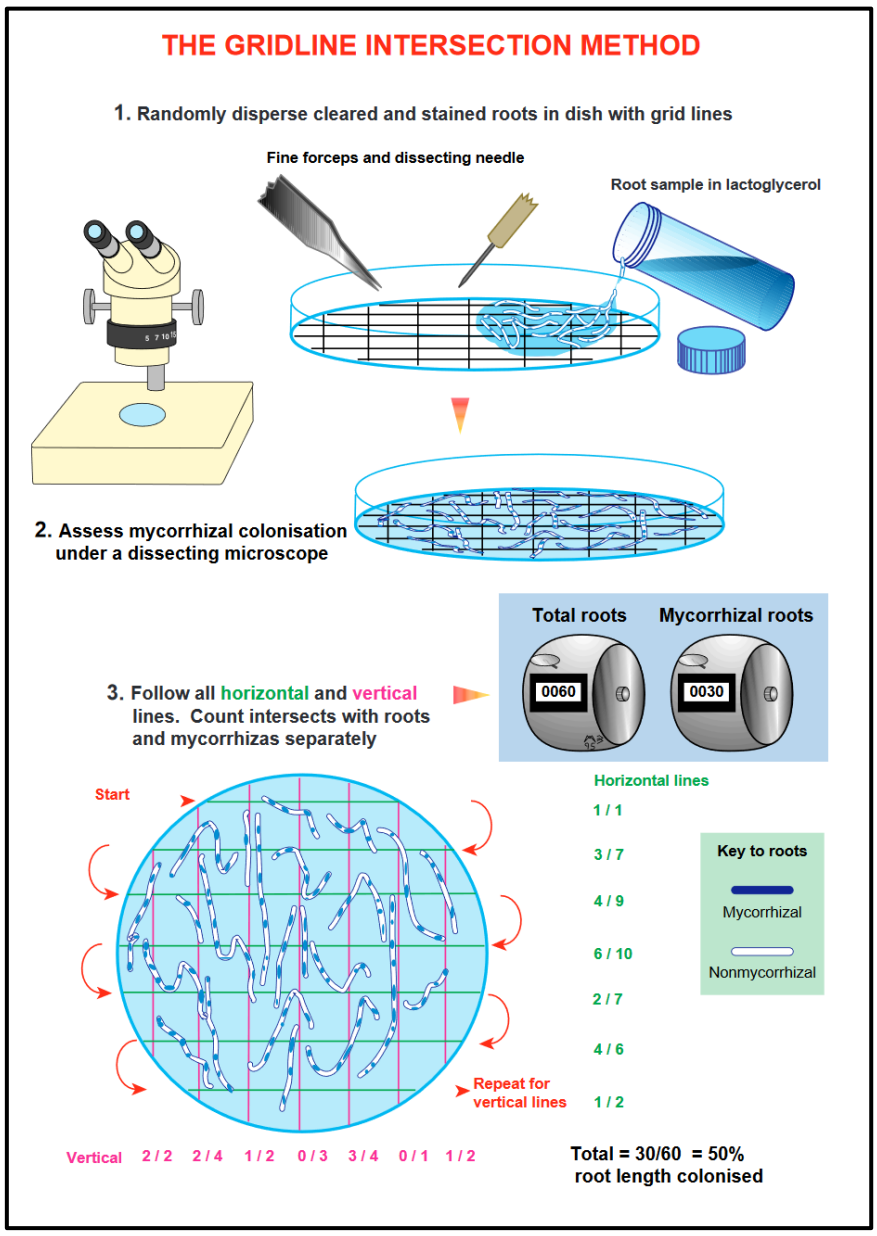

Figure 1. The gridline intersection method of Giovannetti and Mosse (1980) illustrated by Brundrett et al. (1996).

In some plant assays, stained roots were observed with a light microscope, and the intensity of root cortex colonization by AM fungus was determined according to the procedure of Trouvelot (1986) and quantified using MYCOCALC software (http://www.dijon.inra.fr/mychintec/Mycocalc-prg/download.html). Three microscope slides were analyzed per biological replicate, and each slide contained thirty 1-cm root pieces. The root fragments were rated according to the range of classes indicated in Figure 2, and these rate values were used to calculate the mycorrhization parameters through the following formulas:

- **Frecuency of mycorrhiza in the root system**
  (Frequency of colonization, "F%"):
  F%= (Number of mycorrhized fragments/Number of total fragments)*100

- **Intensity of the mycorrhizal colonization in the entire root system**
  (Relative mycorrhizal root length, relative mycorrhizal intensity, "M%"):
  M%=$(95*n_5 + 70*n_4 + 30*n_3 + 5*n_2 + n_1)$/(number of total fragments)
  where n_5 = number of fragments rated 5 according to mycorrhizal colonization; n_4 = number of fragments rated 4 etc.

- **Intensity of the mycorrhizal colonization in the root fragments**
  (Absolute mycorrhizal root lengh, absolute mycorrhizal intensity, "m%"):
  m% = M%*(number of total fragments)/(number of mycorrhized fragments)

- **Arbuscule abundance in mycorrhizal parts of root fragments**
  (Absolute arbuscule richness, "a%"):
  a% = (100*mA3+50*mA2+10*mA1)/100
  where mA3, mA2, mA1 are the % of m, rated A3, A2, A1, respectively, with
  mA3=(($95*n_5A3 + 70*n_4A3 + 30*n_3A3 + 5*n_2A3 + n_1A3$)/nb myco)*100/m and the same for A2 and A1.
  Where e. g. n_5A3= number of fragments rated 5 according to mycorrhizal colonization and rated 3 depending on the arbuscule abundance

- **Arbuscule abundance in the entire root system**
  (Relative arbuscule richness, "A%"):
  A% = a*M/100)

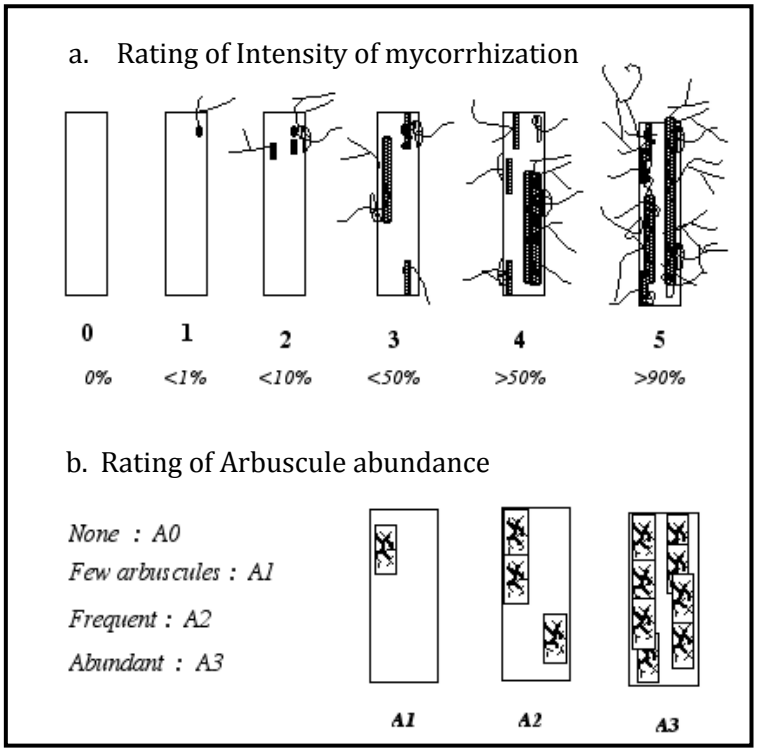

Figure 2. Scoring scale to evaluate the level of mycorrhizal colonization (a) and the arbuscule abundance (b) in roots fragments. Figure from Trouvelot et al. (1986).

2.2. WGA-fluorescent staining for arbuscule morphology analysis

Inoculated roots were subjected to staining of the AM fungal structures with Wheat Germ Agglutinin (WGA)-Alexa Fluor 488, a lectin that has a strong affinity for oligomers and polymers of N-acetylglucosamine residues, especially chitin (Peters and Latka 1986) on the hyphal cell wall, allowing the imaging of arbuscules. AM inoculated root fragments were previously cut with a sharp blade in 1-cm segments and embedded in hot (~60ºC) liquid 4% agarose in PBS 1X. When the agarose was solidified, the blocks were resized and glued on a vibratome plate with a thin film of cyanoacrylate (Super Glue). 60µm longitudinal and 120 µm transverse sections were cut on a vibratome (Leica VT1200S). Sections were retrieved with the wide end of a Pasteur pipette and carefully washed with PBS 1X. Sections were inspected under a stereomicroscope (Zeiss Stemi 2000-C) and selected cuttings were vacuum-infiltrated with 10µg ml^{-1} WGA-Alexa Fluor 488 conjugate (Molecular Probes, Eugene, Oreg., USA) in PBS 1X for 60 min in the dark. Sections were incubated overnight at 4ºC in the same fluorescence staining solution. Cuttings were washed

with PBS 1X, selected under an epifluorescence stereomicroscope (Leica M165FC), mounted on glass slides with a drop of glycerol and cover slipped. Bright-field and fluorescence optical images of GUS-activity localization and AM fungal structures were performed with an epifluorescence stereomicroscope (Leica M165FC) and inverted transmission microscope (Leica DMI600B). Z-stack images were acquired with a laser scanning confocal fluorescence microscope (C-1, Nikon).

3. Expression Analysis of *tsb* and *SlDLK2* genes in tomato organs

Tomato *tsb* and *SlDLK2* gene expressions were analyzed by qPCR in various organs of *S. lycopersicum* cv Moneymaker plants. Tomato plants of 100 days old were used to analyze *tsb* and *SlDLK2* expression in roots, leaves, young flower buds, mature flower buds, open flowers, green fruits and young stems. 125 days old plants were used to measure *tsb* and *SlDLK2* gene expression in developing fruits turning red, mature fruits in red and seeds.

4. RNA extractions and gene expression quantification

For the qPCR experiments, representative root samples from each root system were collected, immediately frozen in liquid nitrogen, and stored at -80ºC until RNA extraction. Total RNA was isolated from about 0.2 g samples using the RNeasy Plant Mini Kit (Qiagen, Hilden, Germany) following the manufacturer´s instructions, and treated with RNase-Free DNase. 1µg of DNAse-treated RNA was reverse-transcribed into cDNA using the iScriptTM cDNA synthesis kit (Bio-Rad, Hercules, CA, USA) following the supplier´s protocol. For the qPCR, it was prepared a 20 µL PCR reaction containing 1 µL of diluted cDNA (1:10), 10 µL 2x SYBR Green Supermix (Bio-Rad, Hercules, CA, USA) and 200 nM of each primer using a 96-well plate. The PCR program consisted of a 3 min incubation at 95ºC, followed by 35 cycles of 30 s at 95ºC, 30 s at 58-63ºC, and 30 s at 72ºC. The specificity of the PCR amplification procedure was checked using a melting curve after the final PCR cycle (70 steps of 30 s, from 60 to 95ºC, at a heating rate of 0.5ºC). Experiments were carried out on three biological replicates, and the threshold cycle (Ct) was determined in triplicate. The relative transcription levels were calculated by using the $2^{-\Delta\Delta Ct}$ method (Livak

and Schmittgen, 2001). The Ct values of all genes were normalized to the Ct value of the *LeEF-1α* housekeeping gene.

The qPCR data for each gene were shown as relative expression with respect to the control treatment ("reference treatment") to which it was assigned an expression value of 1. The reference treatment generally corresponded to the non-AM inoculated treatment. All genes whose transcript abundance was measured by qPCR and the corresponding primers used are listed in Table 3.

Table 3. Primers used in this study for quantitative reverse transcription polymerase chain reaction (qPCR) experiments

Target gene [GenBank/RefSeq /SolDB accession number]	Primer name	Primer sequence (5´→3´)	Reference
Rhizoglomus irregulare			
GinGS [DQ063587]	qGinGS-F qGinGS-R	(5´-CCTCAAGGTCCCTATTATTGTTCTG-3´) (5´-ACGATAATGAGCTTCCACAACGT-3´)	Govindarajulu et al. (2005)
GinEF [DQ282611]	qGinEF-F qGinEF-R	(5´-GCTATTTTGATCATTGCCGCC-3´) (5´-TCATTAAAACGTTCTTCCGACC-3´)	Benabdellah et al. (2009)
GinAMT1 [AJ880327]	qGinAMT1-F qGinGS-R	(5´-TGTGTCAGCATTGTCTTCAGT-3´) (5´-GGCAAGTGCGGGTGTAATAG-3´)	López-Pedrosa et al. (2006)
GinAMT2 [FM993985]	qGinEF-F qGinEF-R	(5´-AGTGCCAATGCCGCTAACATA -3´) (5´-TGATGTACCTCCAACAATTCCA -3´)	Pérez-Tienda et al. (2011)
Solanum lycopersicum			
LeEF-1α [NM_001247106]	qLeEF1α-F qLeEF1α-R	(5´-GGTGGCGAGCATGATTTTGA-3´) (5´-CGAGCCAACCATGGAAAACAA-3´)	García Garrido et al. (2010)
ccd7 [Solyc01g090660]	qccd7-F qccd7-R	(5´-AGCCAAGAATTCGAGATCCC-3´) (5´-GGAGAAAGCCCACATACTGC-3´)	(López-Ráez et al. 2010)
MAX1 [Solyc08g062950]	qMAX1-F qMAX1-R	(5´- CGCCCTTAGTTGCCAGAGAA -3´) (5´- GCCAACCAAACCCATGTTCC -3´)	Guillotin et al. (2017)
SlDLK2 [AW622368]	qα,βHydro-F qα,βHydro-R	(5´-GGGAGTTGAAATTGCATTACCT-3´) (5´-TAGTGAAATGGGCACCACAA-3´)	García Garrido et al. (2010)
SlPT4 [Solyc06g051850.1]	qSlPT4-F qSlPT4-R	(5´-GAAGGGGAGCCATTTAATGTGG-3´) (5´-ATCGCGGCTTGTTTAGCATTTCC- 3´)	Balestrini et al. (2007)
SlRAM1 [Solyc02g094340.1]	qGRAS27-F qGRAS27-R	(5´- CTCAGAATGTCAGAGGAAGAT- 3´) (5´- CCAGCAGCAGTATCAGAA-3´)	This work
SlEXO84 [Solyc09g072720.2]	qEXO84-F qEXO84-R	(5´- CGGCTAAGATCTCAATTCTG-3´) (5´- ATAAGAGTGTCATCAGCATG-3´)	This work
SlAMT2.2 [Solyc08g067080.1]	qAMT2-F qAMT2-R	(5´- CTCAGAATGTCAGAGGAAGAT- 3´) (5´- CCAGCAGCAGTATCAGAA-3´)	This work
SlSTR [Solyc01g097430.3]	qSTR-F qSTR-R	(5´- TAGTCCCAAGTTACATCAC-3´) (5´- ACCATCTCCAAACCAAAG-3´)	This work
SlD27 [Solyc09g065750]	qD27-F qD27-R	(5´-TTGGCTAGTTGGACCTTGTG -3´) (5´- CAAAGTTTGGCACCATATTCA-3´)	Torres-Vera et al. (2016)
SlCYP707A3-like [Solyc04g071150]	qCYP707A3-like-F qCYP707A3-like-R	(5´- GGAATCAACTTAGCCAAACTGG - 3´) (5´- GATACTTGTTCTTCAGCATCCTAA -3´)	Fiorilli et al. (2009) This work
SlGA3ox1 [Solyc06g066820]	qSlGA3ox1-F qSlGA3ox1-R	(5´-TCACTGTCCCTCCAATACCC -3´) (5´-ATCGTGTTCGGTTTACGACC -3´)	García Garrido et al. (2010)
SlGAST1 [Solyc02g089350]	qSlGAST1-F qSlGAST1-R	(5´- CAACAACAGAGAAATAACCAAC -3´) (5´- TTATACGATGTCTTTGAACACC -3´)	Serrani et al. (2007)
SlNCED1 [Solyc07g056570]	qNCED1-F qNCED1-R	(5´- AGGCAACAGTGAAACTTCCATCAAG - 3´) (5´-TCCATTAAAGAGGATATTACCGGGGAC -3´)	Ji et al. (2014)

SlCCaMK [Solyc01g096820]	qCCaMK-F qCCaMK-R	(5´- GAAGAGGTGTTAAGAGCAATG -3´) (5´- CTCATATCAACCGTTCCATC -3´)	This work
SlCyclops [Solyc08g075760]	qCyclops-F qCyclops-R	(5´- CAAGGGACATATCAGGAC - 3´) (5´- AGGGAGCCATAATACTTTC -3´)	This work
SlSYMRK [Solyc02g091590]	qSYMRK-F qSYMRK-R	(5´- AGCAGCAGGATTCATATTAG -3´) (5´- GCAGACCACAGAGATAAC -3´)	This work
SlVapyrin [Solyc10g081500]	qVapyrin-F qVapyrin-R	(5´- GAGAGTCTTTAATTGTTGAGC -3´) (5´- TTAGCACCATTGAGTAAGAG -3´)	This work
SlRAM2 [Solyc02g087500]	qRAM2-F qRAM2-R	(5´- CATGAATCCTAGCCCATC - 3´) (5´- GCACTCATACGATAATGTTG -3´)	This work
SlD14 [XP_004238093] [Solyc04g077860]	qSlD14-F qSlD14-R	(5´-GACATTTGCCACATCTTAGC-3´) (5´-TTTTGGTTTGGTTGACGC-3´)	Torres-Vera et al. (2016)
"SlKAI2cA" [XP_004233449] [Solyc02g064770]	qABHF1105-F qABHF1105-R	(5´-TTGCCTCATGTGTCTGTCCC -3´) (5´-GAGCTGCGGAAGATGTCCTT-3´)	This work
"SlKAI2cB" [XP_004231894] [Solyc02g092770]	qKAI2cB-F qKAI2cB-R	(5´- TCTAGTTGAGGATTATAAGGTT -3´) (5´- TCACATCATAGGCGTATC -3´)	This work
"SlKAI2iA" [Solyc02g064760]	qKAI2iA-F qKAI2iA-R	(5´- GATTTTGAACGATATGCCTATG -3´) (5´- AGGACGAAATATAGAAGCAA -3´)	This work
"SlKAI2iB" [XP_004233607] [Solyc02g092760]	qABHF1106-F qABHF1106-F	(5´-CGGTGGGAGGTGACATGAAT-3´) (5´-CAGGGGTTGTTGTTTCATTCTTCG-3´)	This work

5. Plasmid Construction and hairy root transformation

For *tsb* and *SlDLK2* genes, the full-length cDNA gene sequence and a RNAi fragment were amplified from *S. lycopersicum* cDNA of roots infected by the AM fungus *R. irregularis*. The respective putative promoters (an approximately 1500-pb fragment immediately upstream of the start codon) were amplified from genomic DNA of *S. lycopersicum* cv Craigella. Amplifications were carried out by PCR using the iProof High Fidelity DNA-polymerase (BioRad) and specific primers (Table 4). PCR fragments were introduced in pENTR/D-TOPO (Invitrogen) vector and sequenced. pENTR/D-TOPO containing the corresponding genes, RNAi fragments and promoters, were subsequently recombined into pUBIcGFP-DR (Kryvoruchko et al. 2016), pK7GWIWG2_II-RedRoot (http://gateway.psb.ugent.be) and pBGWFS7:: pAtUbq10::DsRed (modified from Karimi et al. 2002) vectors, respectively, using the GATEWAY technology (Invitrogen).

Table 4. Primers used in this study for PCR amplifications and plasmid constructions

Target sequence	Primer name	Primer sequence (5´→3´)
SlDLK2 **OE**	Hydro-caccATG Hydro _stop-R	(5´-CACCATGGTGATATTGGATTTATT-3´) (5´-CTAAGAAGTTAAGATTCTATGAATTAC-3´)
SlDLK2 **RNAi**	Hydro -caccATG iHydro -R	(5´-CACCATGGTGATATTGGATTTATT-3´) (5´-CATCAGCAAAAGGCTCATAGG-3´)
SlDLK2 **promoter**	promHydro -F promHydro -R	(5´-CACCATATTGTGGATTAGGCCTG-3´) (5´-CTACTTATGCTATTCTAACTATACT-3´)
tsb **OE**	TSB-caccATG TSBstop-R	(5´-CACCATGGGTTGTGGGGAATC-3´) (5´-CTAATCTGTTTTTGAATCTGTTGT TGC-3´)
tsb **RNAi**	TSB-caccATG qTSB-R	(5´-CACCATGGGTTGTGGGGAATC-3´) (5´-ACAGAAACAGGGGTTGTTGC-3´)
tsb **promoter**	promTSB-F promTSB-R	(5´-CACCCAAGTAGTCGACACCCATTAATG-3´) (5´-ATATCTAGAAAATAAACAGGGGAAAGGG-3´)
PT4 **promoter**	promPT4 -F promPT4 -R	(5´-CACCAATCGCGACTTCATTGA-3´) (5´-CAATTGCTCTAAATTGCTCAATTTAC-3´)

For hairy root transformation, *Agrobacterium rhizogenes* MSU440 cultures harboring the corresponding overexpression, RNAi, and promoter-GUS constructs, were used to transform *S. lycopersicum* cv Moneymaker plantlets according to a protocol developed and published as part as this thesis (Ho-Plágaro et al. 2018) (see Chapter 1). Composite plants were transferred to pots and followed the same plant growth conditions as explained before. Screening and selection of DsRed (transformed) roots was done by observation under a fluorescent stereomicroscope Leica M165F.

6. Gene expression localization

In order to localize the expression of the studied genes, *tsb* and *SlDLK2,* transgenic roots carrying the corresponding promoter-GUS fusions were used, based on a technique originally developed by (Jefferson 1989).The method is based on the activity of the GUS enzyme (β-glucuronidase), which is encoded by the *Escherichia coli gusA* (*uid A*) gene firstly isolated by (Jefferson et al. 1986). Using GUS to report the activity of promoters and genes is advantageous because GUS assays are straightforward and, with few exceptions, plants lack GUS activity.

Endogenous β-glucuronidase activity is absent from most higher plants, allowing the detection of low levels of GUS activity in transformed tissues.

There are different possible glucuronides that can be used as substrates for the β-glucuronidase, depending on the type of detection needed (histochemical, spectrophotometrical, fluorimetrical). We used the most common of them, the chromogenic substrate X-Gluc (5-bromo-4-chloro-3-indoyl-D-glucuronic acid). The GUS enzyme cleaves X-Gluc to produce colorless glucuronic acid and an intense blue precipitate (as shown in Figure 3).

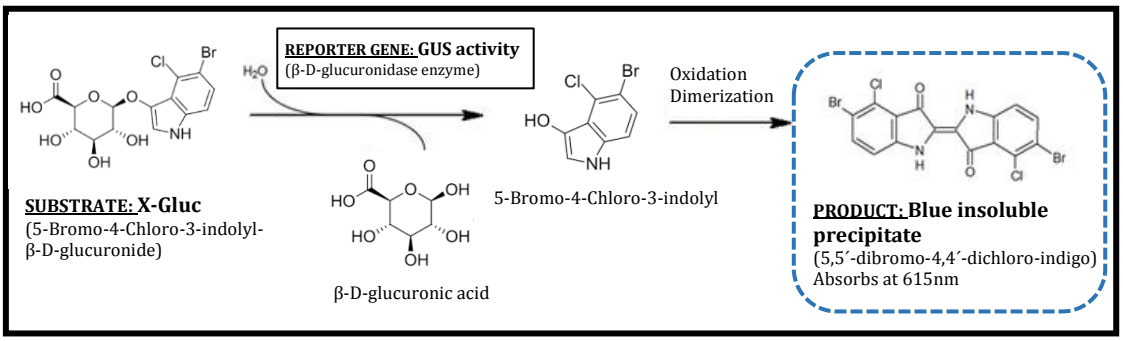

Figure 3. Indigogenic reaction scheme occurring during GUS staining. X-Gluc (5-bromo-4-chloro-3-indolyl-β-D-glucuronide) is hydrolyzed and cleaved by GUS (β-glucuronidase) to produce glucuronic acid and an unstable, soluble, colorless primary product (5-bromo-4-chloro-3-indolyl). The 5-bromo-4-chloro-3-indolyl undergoes an oxidative dimerization to produce the insoluble blue precipitate 5,5´-dibromo-4,4´-dichloro-indigo, which immediately precipitates upon formation, allowing precise cellular localization of enzymatic activity.

Transgenic roots carrying the promoter-GUS fusions were vacuum-infiltrated with a GUS staining solution composed of 0.05 M sodium phosphate buffer, 1mM potassium ferrocyanide, 1 mM potassium ferricyanide, 0.05% Triton X-100, 10.6 mM EDTA-Na and 5µg/mL X-gluc cyclohexylammonium salt (previously dissolved in N, N-dimethylformamide) for 30 minutes to improve the penetration of the substrate. Then, the tissues were incubated in the dark at 37ºC from 1 hour to overnight or until the staining was satisfactory in the same staining solution. Afterwards, the roots were rinsed with H_2O, mounted on glass slides and cover slipped with glycerol. For co-staining of the AM fungus, AM inoculated roots were submitted to WGA staining following the procedure explained in section 2.2.

7. Statistical analysis

Gaussian distribution was assumed. When two means were compared, the data was analysed using a two tailed Student´s *t*-test. For comparisons among all means, a one-way or two-way ANOVA was performed followed by the LSD multiple comparison test. The Graphpad Prim version 6.01 (Graphpad Software, San Diego, California, USA) was used to determine statistical significance. Differences at $P<0.05$ were considered significant. Data represent the mean ± SE.

Chapter 1. An improved method for *Agrobacterium rhizogenes*-mediated transformation of tomato suitable for the study of arbuscular mycorrhizal symbiosis

Published in 2018 in *Plant methods*, *14*(1), 34. https://doi.org/10.1186/s13007-018-0304-9

Tania Ho-Plágaro[1], Raúl Huertas[2], María I. Tamayo-Navarrete[1], Juan A. Ocampo[1], José M. García-Garrido[1]*.

1Department of Soil Microbiology and Symbiotic Systems, Estación Experimental del Zaidín (EEZ), CSIC, Calle Profesor Albareda nº1, 18008 Granada, Spain. 2Noble Research Institute LLC, 2510 Sam Noble Parkway, Ardmore, OK 73401, USA.

Abstract

Background: *Solanum lycopersicum*, an economically important crop grown worldwide, has been used as a model for the study of arbuscular mycorrhizal (AM) symbiosis in non-legume plants for several years and several cDNA array hybridization studies have revealed specific transcriptomic profiles of mycorrhizal tomato roots. However, a method to easily screen candidate genes which could play an important role during tomato mycorrhization is required.

Results: We have developed an optimized procedure for composite tomato plant obtaining achieved through *Agrobacterium rhizogenes*-mediated transformation. This protocol involves the unusual *in vitro* culture of composite plants between two filter papers placed on the culture media. In addition, we show that *DsRed* is an appropriate molecular marker for the precise selection of cotransformed tomato hairy roots*. S. lycopersicum* composite plant hairy roots appear to be colonized by the AM fungus *Rhizophagus irregularis* in a manner similar to that of normal roots, and a modified construct useful for localizing the expression of promoters putatively associated with mycorrhization was developed and tested.

Conclusions: In this study, we present an easy, fast and low-cost procedure to study AM symbiosis in tomato roots.

Background

The *Solanum lycopersicum* (tomato) is an economically important crop grown worldwide. Tomato production accounts for 16% of global vegetable production and constitutes the largest vegetable category. The total tomato crop is forecast to reach 38.6 million tons in 2017 and is expected to continue growing (https://www.wptc.to/).

Tomato crops are susceptible to many insects, bacteria and nematodes which cause significant reductions in fruit yields under current production practices (Engindeniz 2006). Rhizosphere symbiotic microorganisms are increasingly proposed as a possible alternative to overcoming these problems (Haldar and Sengupta 2016), with particular emphasis on arbuscular mycorrhizal (AM) fungi which form mutualistic symbiotic association with most higher plants. Although tomato growth is not very responsive to AM fungi (Smith et al. 2009), mycorrhization significantly reduces tomato infection and disease severity caused by several root pathogens (Akköprü and Demir 2005; Berta et al. 2005; Cordier et al. 1996; Diedhiou et al. 2003) and is regarded as a potential beneficial crop management tool to reduce pathogen populations in the soil which positively impacts crop health, quality and production (Copetta et al. 2011).

In addition to its cultivation and economic importance worldwide, *S. lycopersicum* has become a convenient model for research into plant genetics and physiology due to several features such as its relatively compact genome (950 Mb), the availability of a marker-saturated genetic linkage map and the annotated genome sequence (http://solgenomics.net), rich germplasm collections (Tomato Genetics Resource Center, http://tgrc.ucdavis.edu) and highly efficient transformation protocols (Pino et al. 2010).

Several microarray analyses (López-Ráez et al. 2010; García Garrido et al. 2010; Fiorilli et al. 2009) have produced specific transcriptomic profiles of mycorrhizal tomato roots. However, the development of a procedure to easily screen candidate genes performing important functions during mycorrhization is required.

Agrobacterium rhizogenes-mediated transformation offers a fast and reliable alternative to stable transformation when research is focused on root biology. Unlike *A. tumefaciens*, *A. rhizogenes* contains root locus (*rol*) genes, which, on induction, trigger the development of adventitious, genetically transformed so-called hairy roots due to the conspicuous abundance of their root hairs, a term first used in the literature by Stewart et al. (Stewart et al. 1900).

Using *A. rhizogenes*-mediated transformation, healthy composite plants consisting of untransformed shoots with transgenic hairy roots can be generated. Protocols for obtaining composite plants have been proposed in order to easily pinpoint genes resistant to root pathogens in coffee (Alpizar et al. 2006), peanuts (Geng et al. 2012), soybean (Kereszt et al. 2007; Kuma et al. 2015; Li et al. 2010), potato (Horn et al. 2014), and even tree species such as avocado (Prabhu et al. 2017) and *Prunus* (Bosselut et al. 2011). These techniques have also been developed to assess genes predicted to function in the plant parasitism of neighboring roots (Tomilov et al. 2007) and to study root symbiotic interactions including AM and *Rhizobium* symbiosis in legume species such as soybean (Kereszt et al. 2007), pea (Clemow et al. 2011) and *Medicago truncatula* (Floss et al. 2013; Chabaud et al. 2006; Boisson-Dernier et al. 2001).

Although some molecular studies have been carried out using *in vitro* tomato hairy root cultures, e.g. for the study of *Fusarium* tolerance (Bettini et al. 2016) or of changes in cell wall ligno-suberization associated with salt stress (Talano et al. 2006), no reports exist regarding the use of this system to study AM symbiosis in tomato and, to our knowledge, no specific protocol currently exists for obtaining composite tomato plants *in vitro*. Only one paper have previously reported the obtaining of composite tomato plants (Collier et al. 2005), however the protocol was not specific for tomato and the authors did not used *in vitro* conditions.

The aim of this work was to show the difficulties found for *in vitro* composite tomato plant obtaining and we set up a method to overcome these problems. The major challenges we encountered were the excessive handling required and the consequent high level of contamination-related loss. The main factor which hampered composite tomato plant obtaining was the specific growth of tomato

hairy roots which penetrate deeply into the culture media. In order to assist in tracking the success of the transformation procedure and to distinguish between non-cotransformed and transgene-containing roots, we used DsRed as a visual marker protein that delivers red fluorescence, and we tested that it can be successfully used as a marker to undoubtedly identify and select tomato cotransformed hairy roots from the beginning of the *in vitro* culture until the harvesting time. In this paper, we present a strategy for fast and efficient production of *S. lycopersicum* composite plants using *A. rhizogenes* MSU440, in which the transgenic roots of the composite plants showed the expression of the red fluorescence protein marker (DsRed). We demonstrated that these plants are efficiently mycorrhized by *Rhizophagus irregularis* and also showed the utility of this method for localizing the expression of AM-induced promoters. The procedure developed would now favor undertaking further research into the molecular mechanisms involved in AM symbiosis in tomato.

Methods

Binary vectors and *A. rhizogenes* strain

We selected three different binary vectors to facilitate transgenic overexpression, RNAi silencing and localization of promoter-GUS expression. The three vectors, all of which contained the *DsRed* marker gene for identification and selection of cotransformed hairy roots, used GATEWAY technology (Invitrogen) for transgene and promoter cloning. The following vectors were selected: pUBIcGFP-DR (Kryvoruchko et al. 2016) for overexpression, pK7GWIWG2_II-RedRoot (http://gateway.psb.ugent.be) for RNAi silencing and pBGWFS7::pAtUbq10::DsRed for promoter-GUS expression analysis. The latter vector was obtained by cloning the pAtUbq10::DsRed fragment in the pBGWFS7 vector (Karimi et al. 2002) using the In-Fusion HD Cloning Kit (Takara). In order to check the proper functioning of this plasmid, the arbuscular-induced phosphate transporter 4 promoter (p*SlPT4*) was subcloned. The empty binary vectors pUBIcGFP-DR, pK7GWIWG2_II-RedRoot and pBGWFS7::pAtUbq10::DsRed, as well as the construct pBGWFS7::

pAtUbq10::DsRed::p*SlPT4* were introduced into *A. rhizogenes* MSU440 by electroporation, and transformants were selected by resistance to streptomycin and spectinomycin.

Generation of composite *S. lycopersicum* plants

Figures 1 and 2 highlight the important steps of the procedure which most easily achieved the highest transformation efficiencies. *A. rhizogenes* MSU440 cultures harboring the corresponding overexpression, RNAi and promoter-GUS constructs were used to transform *S. lycopersicum* plantlets according to a technique adapted from a previously described protocol (Boisson-Dernier et al. 2001). *S. lycopersicum* cv Moneymaker plant seeds were surface sterilized by soaking for 5 min using 2.35% w/v sodium hypochloride (50% v/v commercial bleach) and then washed three times with sterile distilled water. In order to improve the germination percentage, speed and uniformity, seeds were subjected to 1-day imbibition in distilled water in the dark at RT with slight shaking. Seeds were then placed and incubated in sterile and sealed Petri dishes with wet filter paper in the dark at 25-28ºC for 4 days. After this period, germinated seeds were placed on filter paper on 0.5x MS agar medium (0.8% agar) plates which included vitamins to allow for favorable conditions at seedling emergence and during the first days following infection. The germinated seeds were left to emerge in a growth chamber for 4 days at 24ºC, with a 16h light/8h dark photoperiod and ~115 µmol m^{-2} s^{-1} of light intensity. To generate hairy roots (genetically transformed), the radicle and the bottom part of the hypocotyl from these 4-day-old seedlings were removed, while maintaining the 1-cm apical portion of the hypocotyl. A sterile syringe tip coated with transgenic *A. rhizogenes* was used to puncture the stem of the cutting 3-4 times. Alternatively, diagonally cut radicles were coated with *A. rhizogenes*. These wounded seedlings were kept on the same 0.5x MS agar plates, and their hypocotyls were covered with a humid filter paper strip to maintain moisture. The seedlings were left to root in a growth chamber under the same conditions as before.

Roots grown during the first week (adventitious laterals, non-transformed roots) were removed, and plantlets were transferred to 0.5x MS agar medium (0.8% agar) plates without vitamins in order to boost new root development. During the

following 3-4 weeks, screening and removal of DsRed-negative roots (non-transformed) were carried out weekly by observation under a fluorescent Leica M165F stereomicroscope. Plantlets with at least one cotransformed hairy root were transferred to 0.5x MS agar medium (0.8% agar) with vitamins. Finally, seedlings with selected DsRed-positive roots (hairy roots) were transplanted to pots and allowed to grow in a growth chamber.

Additional methods used in this chapter but previously described in the *General Materials and Methods* section:

- **Plant growth and AM inoculation**
- **AM fungal staining**
- **Histochemical localization of GUS activity and the AM fungus**
- **RNA extractions and gene expression quantification**

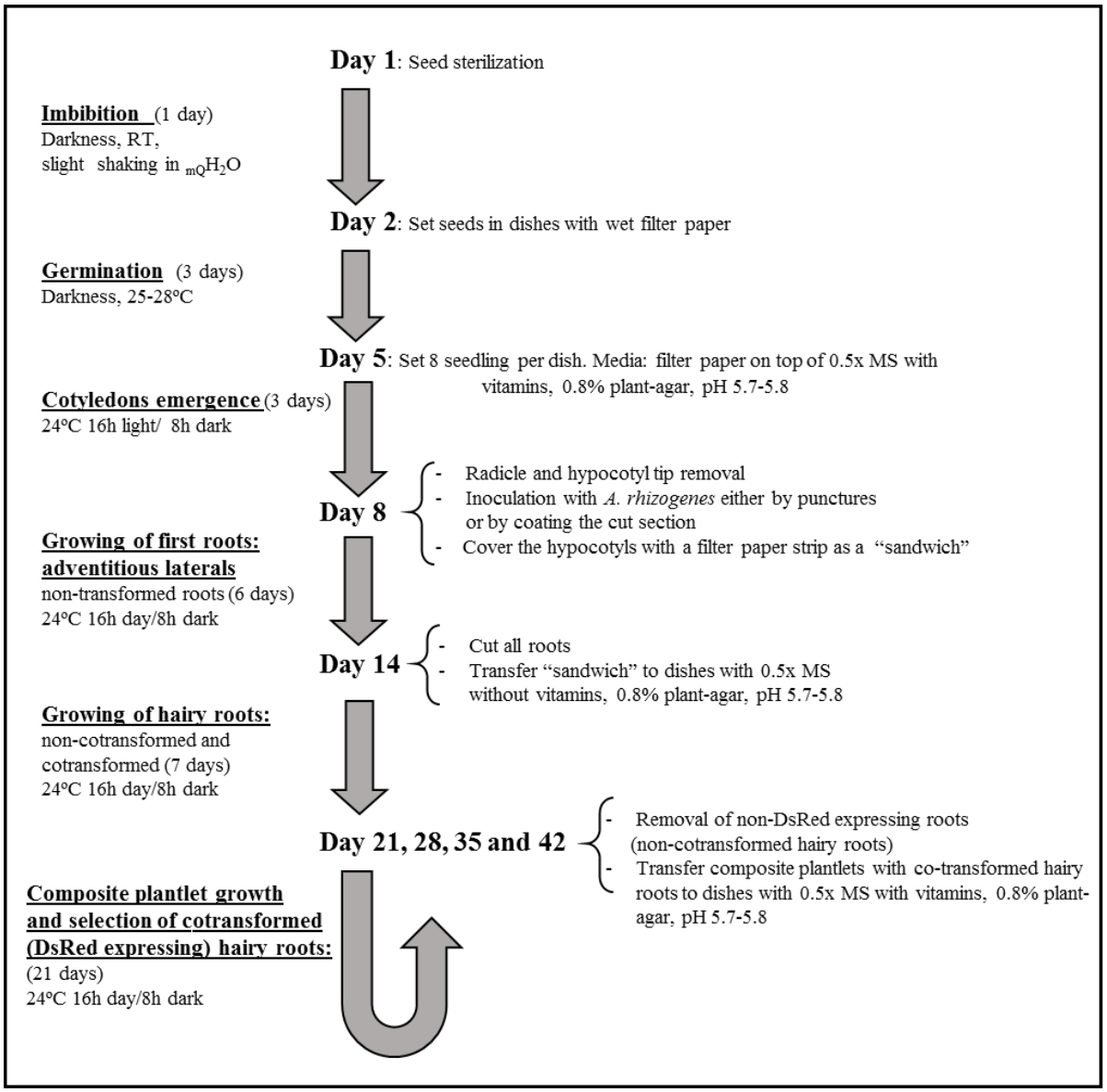

Figure 1. Schematic representation of the time-line required for the generation of composite tomato plants, with an emphasis on the parameters which must be optimized

Figure 2. Important steps for tomato composite plant production. Seed germination (A) and germinated seeds placed in petri dishes with MS media (B). *A. rhizogenes* bacterial culture and syringe used to inoculate tomato hypocotyls by punctures (C). Setting of the filter paper strip (D) and easy transfer of the plants to new/fresh media using the "sandwich" method (E). Resulting vigorous composite tomato plantlets (F) and derived composite plants growing in pots (G).

Results

A. rhizogenes-mediated tomato transformation

Most of the *in vitro* procedures used for generating composite plants involve placing the *A. rhizogenes* inoculated sectioned seedlings on slanted agar (Boisson-Dernier et al. 2001). We found that *S. lycopersicum* roots, in contrast to *M. trucatula* roots, deeply penetrated the agar media; it was extremely difficult to remove untransformed adventitious laterals and non-cotransformed hairy roots and to detach the derived composite plantlets from the media without breaking the roots. To cope with this problem, we placed a filter paper on the plate media as previously recommended by certain researchers (Limpens et al. 2004; Tomilov et al. 2007). After using this method, drying and detrimental effects on shoot growth were observed, and only 26 ± 8 % of the composite seedlings could be transferred to pots, many of which subsequently died after transfer to pots. Using this method, we obtained a final survival rate of only 9 ± 1 %. We tested a modified method involving the placement of an additional filter paper strip on the hypocotyls in sandwich mode during the whole *in vitro* culture process as illustrated in Figure 3. Using this protocol, transformation efficiency was maintained, while seedling drying was totally prevented, and a significant improvement in composite seedling fitness was observed. With this modification, it was possible to transfer and successfully grow 93 ± 2 % of the initial transformed seedlings in pots (Fig. 4A).

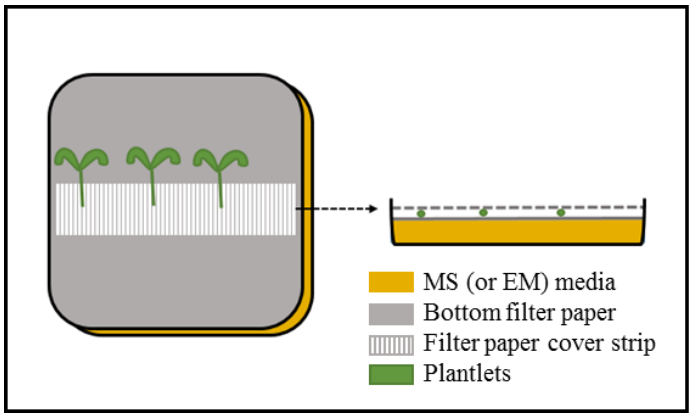

Figure 3. Illustration of the "sandwich" method for *in vitro* culture of tomato composite plants. Hypocotyl location in between of two filter papers was the best choice found for easy handling and to produce vigorous composite plants.

A. rhizogenes inoculation method

The most common inoculation procedure used for generating composite plants involves stab inoculation (Quandt et al. 1993). However, many authors have found that growth is significantly improved when *A. rhizogenes* is inoculated directly on freshly sectioned seedling radicles or hypocotyls in some species (Boisson-Dernier et al. 2001; Tomilov et al. 2007; Martirani et al. 1999). In order to determine the most appropriate method for tomato transformation, *S. lycopersicum* plants were inoculated with *A. rhizogenes* either by puncturing the seedlings with a glass needle containing bacteria or by coating the fresh diagonally-cut ends of hypocotyls into bacterial cultures. During the first week following inoculation, a small number of non-transformed adventitious laterals appeared just above the hypocotyl section regardless of the *A. rhizogenes* inoculation method used, which is a normal response of tomato seedlings to removal of the root apical meristem. Two weeks after inoculation, puncture inoculation resulted in approximately 50 % of the plantlets developing cotransformed hairy roots, while only 25 % of the coated-inoculated seedlings had regenerated cotransformed hairy roots by that time. However, four weeks after *A. rhizogenes* inoculation and consecutive weekly removal of non-cotransformed hairy roots (non-DsRed expressing roots), at least 90 % of plantlets had developed cotransformed hairy roots in both punctured and coated-inoculated seedlings. Although transgenic root growth was boosted by the puncture method, both methods were found to be effective for obtaining composite plants, with the final test showing similar success (Fig. 4B). These results are different to those obtained with *M. truncatula* (Boisson-Dernier et al. 2001) and *Triphysaria versicolor* (Tomilov et al. 2007), where transformation efficiency increased by dipping the freshly sectioned hypocothyls into *Agrobacterium* cultures. We therefore conclude that the effectiveness of the type of wound for *A. rhizogenes* infection is species-dependent.

Elimination of *A. rhizogenes* is not required

Most protocols proposed for obtaining composite plants include the use of antibiotics, such as timentin, cefotaxime or augmentin depending on the *A. rhizogenes* strain used, in order to inhibit *A. rhizogenes* growth on the media of the *in vitro* composite plant culture (Boisson-Dernier et al. 2001; Tomilov et al. 2007). We noticed that, in the absence of cefotaxime, *A. rhizogenes* did not spread out in the *in vitro* culture used in this study, in which the filter paper is placed on the MS media and sucrose is lacking, and the percentage of composite plants obtained is not significantly affected (Fig. 4C).

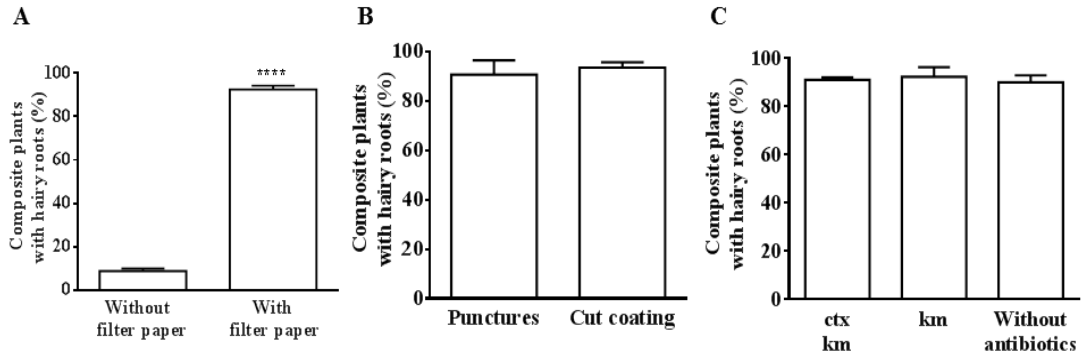

Figure 4. **Efficiency of different methods for tomato composite plant production.** The percentage of 30 day-old vigorous composite plants grown in pots with respect to the initially *A. rhizogenes* inoculated seedlings is shown. The effectiveness of a filter paper strip covering the wounded *A. rhizogenes* inoculated hypocotyls in sandwich mode was proved (A), and we compare two *A. rhizogenes* inoculation methods: by punctures or by coating the bottom part of the hypocotyl with the bacterial culture (B). The requirement of cefotaxime (500 μg ml^{-1}) and kanamycin (100 μg ml^{-1}) antibiotics was tested (C). When not specified, standard conditions were used, which include the sandwich mode, *A. rhizogenes* inoculation by punctures and the use of antibiotics. Data corresponds to at least three independent experiments starting from 100 germinated seeds. *A. rhizogenes* carried the empty vectors pK7GWIWG2_II-RedRoot (A,B,C), pUBIcGFP-DR (A,B) or pBGWFS7::pAtUbq10::DsRed (A,B). Values correspond to mean ± SE. Significant differences (Student´s t test) between treatments are indicated with asterisks (****P<0.0001).

Molecular markers: Selection for cotransformed hairy roots by DsRed

In general, *A. rhizogenes* transformation protocols involve cotransformation, with both the Ri T-DNA and T-DNA of a binary vector containing the transgene of interest together with molecular markers to allow selection of cotransformed hairy roots. We decided to use the *DsRed* gene driven by the *A. thaliana* ubiquitin promoter (p*AtUbq10*) as a molecular marker to select cotransformed hairy roots and to facilitate quantification of transformation efficiency. The excitation wavelength for DsRed range from 554 to 563 nm and the emission wavelength range from 582 to 592 nm. We demonstrated that inspection and selection through visual observation of DsRed expression under a green fluorescence stereomicroscope fully ensure selection of cotransformed hairy roots. Red auto-fluorescence of tomato roots did not cause problems for interpreting the fluorescence, even in young composite plantlets (Fig. 5A,B), as auto-fluorescence was very weak compared to the fluorescence signal from DsRed. The unmistaken appearance of *DsRed* overexpressing roots compared to DsRed negative roots in adult plants was also observed (Fig. 5C,D). If a fluorescent stereomicroscope is unavailable, root exposure to a green LED bulb (492 – 577 nm wavelength) and visualization through a red-orange photography filter (~585nm) which blocks UV, blue, yellow and green light but passes longer wavelengths, can also be used (Fig. 5E).

Antibiotic counterselection is often used to increase the percentage of hairy roots cotransformed with the binary vector T-DNA and to inhibit growth of non-transformed adventitious laterals and non-cotransfromed hairy roots. After testing a range of kanamycin (Km) concentrations for the growth of hairy roots cotransformed with the plasmid pK7GWIWG2_II-RedRoot, we found that 100 μg ml^{-1} Km was insufficient to totally inhibit non-transformed hairy root initiation and, over this level of concentration, Km began to negatively affect the shoot growth of composite plants. It was not possible to set an optimal

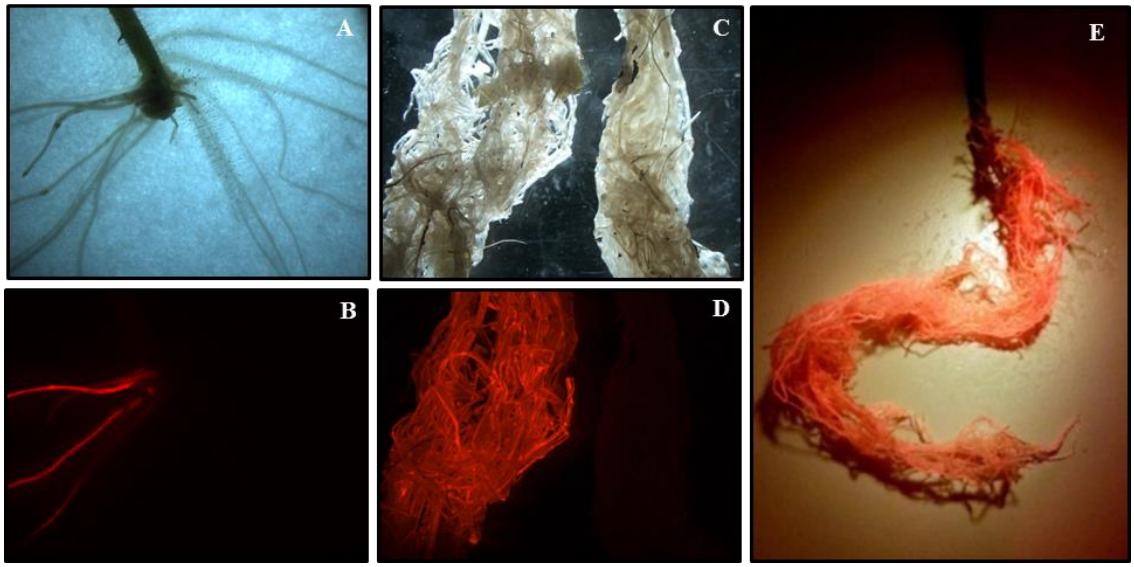

Figure 5. Screening of cotransformed hairy roots expressing the DsRed marker gene in composite tomato plants. Roots of *in vitro* composite plantlet (A,B) and composite plants harvested after 45 days growing in a pot (C,D,E) were visualized with a stereomicroscope under bright light (A,C) and under green fluorescence (B,D) for selection of cotransformed hairy roots. Composite plant exposed to a green fluorescent lamp and visualized through a red-orange photography filter (E). Similar results were obtained independently of the binary vector tested: pUBIcGFP-DR, pK7GWIWG2_II-RedRoot or pBGWFS7::pAtUbq10::DsRed.

concentration for complete inhibition of non-transformed root development without interfering with shoot growth. In order to determine whether additional antibiotic selection is appropriate in order to enhance cotransformed hairy root growth, experimental trials were carried out both with and without kanamycin (100 µg ml^{-1}). The number of plantlets, which developed uncotransformed hairy roots, increased by 30% in the absence of Km as compared to those in the presence of Km (100 µg ml^{-1}) two weeks after infection. However, once they had developed more than two cotransformed hairy roots, regardless of the presence or absence of the antibiotic, after removal of non-cotransformed hairy roots, the composite seedlings rarely developed new untransformed hairy roots and achieved similar final success rates (Fig. 4C). These results show that, although antibiotic selection slightly boosts the growth of cotransformed hairy roots initially, the presence of the antibiotic does not totally eliminate untransformed root development and does not implies a superior efficiency of the method. We show that *S. lycopersicum* transformed roots with pK7GWIWG2_II-RedRoot, pUBIcGFP-DR and the new plasmid

pBGWFS7,0::pUbq::DsRed developed in this study are highly suitable for tomato hairy roots obtaining and selection without requiring selective co-transformation antibiotics.

Transfer of composite tomato plantlets to pots

One of the critical steps of the procedure involves the transfer of composite plantlets from *in vitro* conditions to pots. In this step, most of the plantlets were not sufficiently strong to acclimate to the new *ex vitro* conditions and died after a few days. We performed a trial for pre-acclimatization and growth of composite plants before transferring to pots, in which the aerial part was exposed to *ex vitro* conditions, while keeping the root system *in vitro* as explained as follows. A hole was melted in the side and the lid of the Petri dish containing the 0.5x MS medium (0.8% agar) using a hot metal rod. The obtained 4 week old composite tomato plantlets were transferred (one plantlet in each Petri plate), with the roots placed on the surface of the medium and the shoot extending beyond the hole. The gap around shoot emerging from the hole of the Petri dish was sealed with silicone grease. Petri dishes were placed vertically in a growth chamber. In this way, larger and stronger composite plants pre-acclimated to *ex vitro* conditions were obtained. However, this procedure was discarded because it greatly increased contamination of the media. Alternatively, composite plantlets were directly transferred from *in vitro* conditions to pots, and immediately covered with translucent plastic or fitted with a humidity chamber to maintain humidity for the first three weeks, which resulted in survival rates of virtually 100% for the plantlets transferred.

Symbiotic phenotype and molecular characterization of AM composite plants

AM development in *S. lycopersicum* cotransformed hairy roots was studied. Composite plantlets cotransformed with the pK7GWIWG2_II-RedRoot vector were transferred to pots and inoculated with the AM fungus *R. irregularis*. Composite plants were starved of exogenous phosphate to promote mycorrhization. Trypan blue staining revealed that tomato roots began to be colonized by *R. irregularis* fifteen days after AM inoculation, that mature arbuscules were present in some areas of the root at 30 dpi and that hairy roots reached roughly 35%

mycorrhization at 45 dpi. We did not find any abnormalities in the mycorrhizal phenotype. Apparently, the same mycorrhizal rates (Fig. 6A) and arbuscular morphology were observed in cotransformed hairy roots (Fig. B,C) with respect to non-cotransformed hairy roots and adventitious laterals (Fig. 6D,E). In order to confirm the correct functionality of mycorrhization by *R. irregularis* in composite tomato plants, mycorrhizal activity was checked at the molecular level. The *S. lycopersicum SlPT4* marker gene previously described as associated with the mycorrhization process (Gomez et al. 2009; Balestrini et al. 2007) was selected. A similar induction of *SlPT4* was found in both types of AM-inoculated roots (non-cotransformed and cotransformed) with respect to the uninoculated roots, indicating normal mycorrhiza-associated activity in the cotransformed hairy roots (Fig. 6F). These results suggest that transgenic hairy roots can be used to study AM symbiosis.

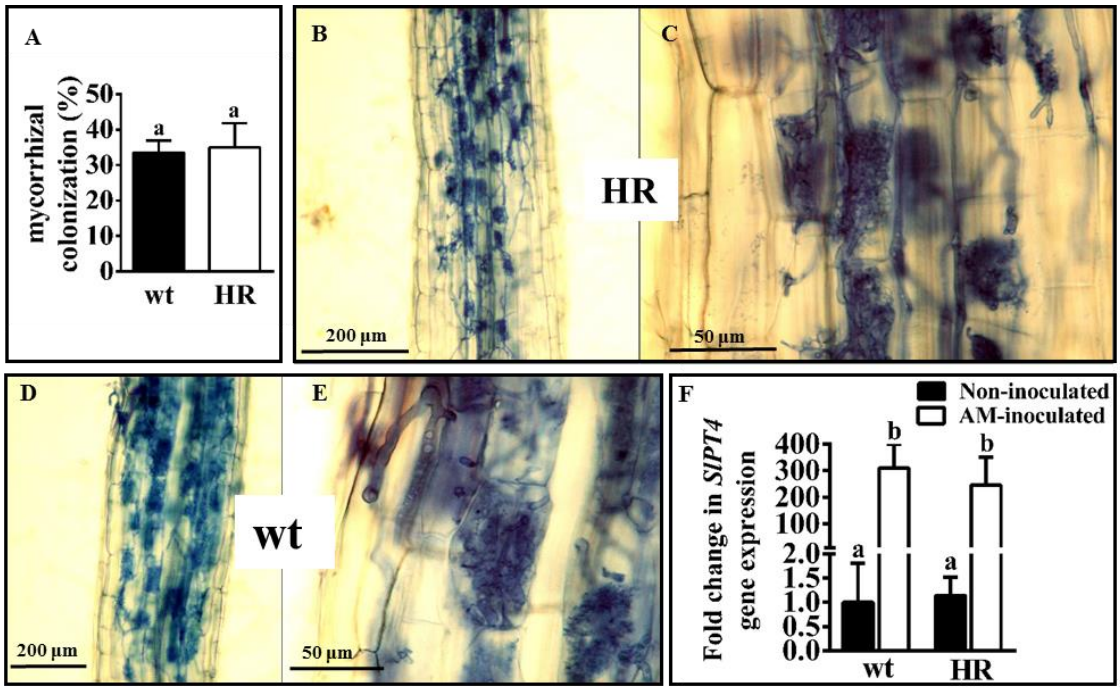

Figure 6. Phenotype and molecular characterization of tomato AM-composite plant roots. Percentage of total root length colonized in wt (adventitious laterals and non-cotranformed hairy roots) and HR (cotransformed hairy roots) from composite plants 45 days after inoculation with *R. irregularis* (A). Trypan blue staining showing AM fungal colonization and arbuscule morphology in HR (B,C) and wt roots (D,E). Expression of the AM associated gene *SlPT4* in the corresponding roots with respect to the non-inoculated roots (F). Values correspond to mean ± SE. Bars with a same letter are not significantly different (P>0.05) according to LSD multiple comparison test.

Promoter-GUS analysis of AM-composite tomato plants

The pBGWFS7,0 plasmid (Karimi et al. 2002) used to localize promoter expression was modified in this study to include *DsRed* marker gene overexpression. In order to test the usefulness of the resulting vector (pBGWFS7,0::pUbq::DsRed) for promoter expression studies of AM fungal colonized tomato hairy roots, we chose the phosphate transporter 4 promoter (p*SlPT4*), which is demonstrated to have an induced expression associated with AM arbuscules (Nagy et al. 2005). We obtained *in vitro* composite tomato plantlets with hairy roots cotransformed with the pBGWFS7,0::pAtUbq::DsRed::p*SlPT4* plasmid, which were subsequently AM-inoculated with *R. irregularis* and transferred to pots. 50-dpi cotransformed hairy roots were identified by DsRed fluorescence and collected. As expected, GUS staining was absent in the non-inoculated plants (Fig. 7A) and apparently limited to arbuscule containing cells (Fig. 7B,C), which are located in the root cortex as observed in the cross-sections (Fig. 7D). Counterstaining with WGA-alexa 488 to visualize fungal structures corroborated that p*SlPT4* induction is clearly associated with arbuscules, as shown in Figure 7E. The results confirm that the pBGWFS7,0::pUbq::DsRed plasmid can be used for *A. rhizogenes*-mediated transformation, DsRed detection of cotransformed hairy roots and promoter-GUS expression analysis of AM roots.

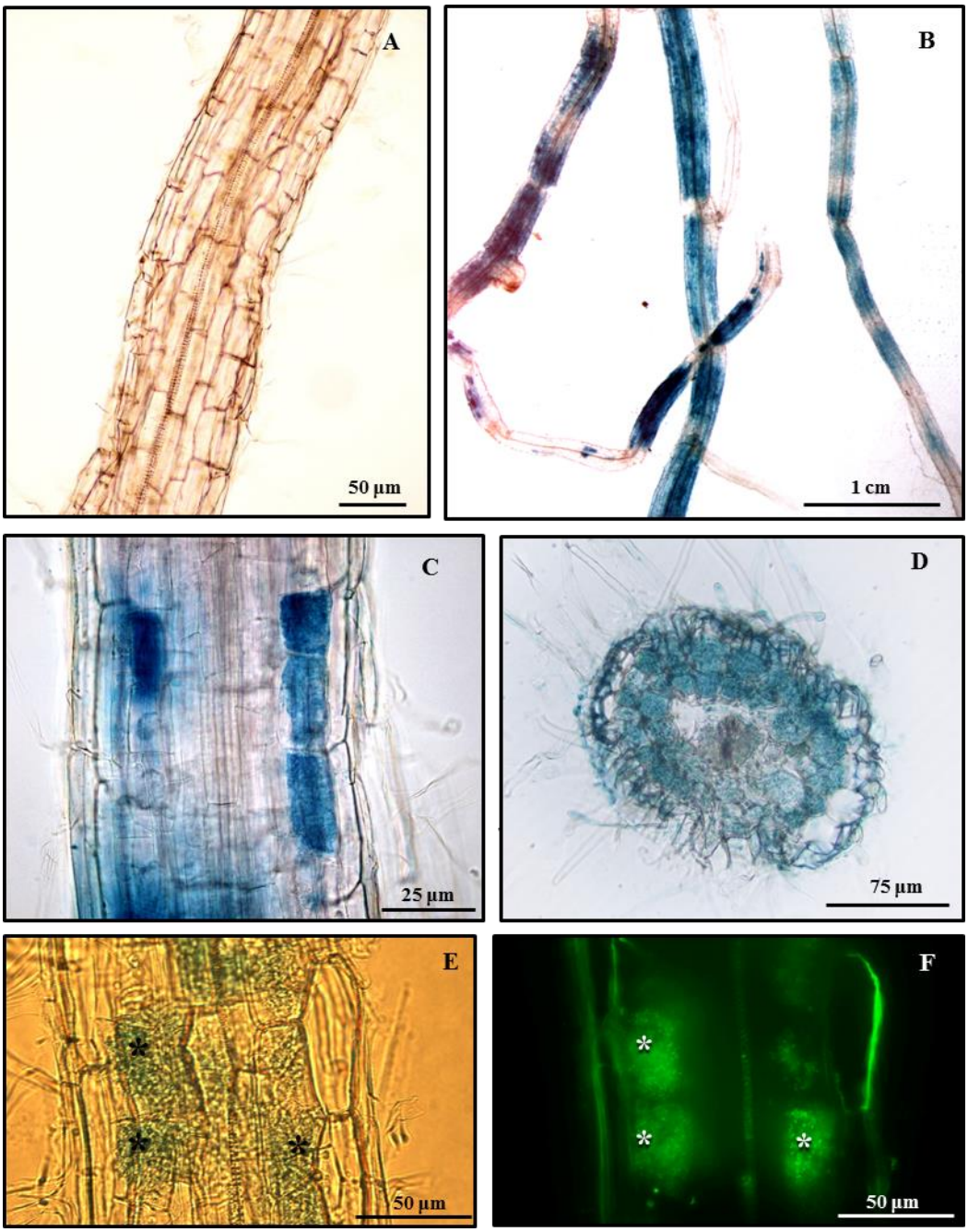

Figure 7. Expression analysis of *SlPT4* promoter activity in cotransformed mycorrhized tomato hairy roots after GUS staining. GUS activity in *A. rhizogenes*-transformed roots expressing the *SlPT4* promoter β-glucuronidase fusion was assessed 45 days after inoculation with *R. irregularis* (B-D), and without *R. irregularis* (A). GUS stained roots were vibratome sectioned (D,E,F) and the AM fungus was counterstained with WGA-Alexa Fluor488 to visualize fungal structures (E,F). Root cells with GUS activity (*SlPT4* promoter expression marker) observed under bright-field (E) are coincident to cells containing arbuscules, which deliver green fluorescence due to AM hyphae staining with WGA-Alexa Fluor488 (F). Asterisks indicate arbuscules in the host cortical cells. All images were taken with an inverted fluorescent microscope, except in B, which was taken with a stereomicroscope.

Discussion

In the protocol developed in this work, we firstly provide experimental evidence that slanted culture of seedlings is not required. Alternatively, the placing of seedlings between two filter papers in sandwich mode is also successful and useful for the composite seedling culture of species such as tomato, whose roots tend to penetrate the culture media. In addition, the tedious task of detaching the agar from roots when transferring plantlets to pots is avoided by using this method.

The other major challenge we overcame in the *in vitro* culture of composite plants was the frequent contamination of the culture media. Weekly transfer of the plantlets to maintain fresh media and antibiotic activity, as well as taking out the aerial part of the plant greatly increased contamination of the culture media. Procedure modifications introduced, driven to reduce changes in the culture media and to minimize composite plant handling, virtually reduced *in vitro* culture contamination to zero and simplified the method considerably.

In view of our results, we conclude that large amounts of composite tomato plants can be obtained by using this low-cost and user-friendly handling method, which avoids the use of antibiotics and the tedious task of detaching agar from the roots, and also minimizes the transfer of plantlets to different media and plant manipulation, thus reducing contamination to virtually zero and achieving success rates of 90% and almost 100% at times. In addition, selection of cotransformed tomato hairy roots is completely ensured through the use of the fluorescent molecular marker DsRed. This method provides an improved tool to rapidly assess gene functions in tomato roots without the need for stable transformation plant production. In particular, we showed that the proposed technique is extremely useful for mycorrhizal studies and screening of candidate genes for involvement in AM symbiosis. However, it is important to note that this method might also be suitable for molecular studies of root pathogen interactions affecting tomato, which is an extremely important agricultural species.

References

Akiyama K, Matsuzaki K, Hayashi H (2005) Plant sesquiterpenes induce hyphal branching in arbuscular mycorrhizal fungi. Nature 435 (7043):824-827. doi:10.1038/nature03608

Akköprü A, Demir S (2005) Biological control of Fusarium wilt in tomato caused by *Fusarium oxysporum* f. sp. lycopersici by AMF *Glomus intraradices* and some rhizobacteria. J Phytopathol 153 (9):544-550

Alpizar E, Dechamp E, Espeout S, Royer M, Lecouls A-C, Nicole M, Bertrand B, Lashermes P, Etienne H (2006) Efficient production of *Agrobacterium rhizogenes*-transformed roots and composite plants for studying gene expression in coffee roots. Plant Cell Rep 25 (9):959-967

Balestrini R, Gómez-Ariza J, Lanfranco L, Bonfante P (2007) Laser microdissection reveals that transcripts for five plant and one fungal phosphate transporter genes are contemporaneously present in arbusculated cells. Mol Plant-Microbe Interact 20 (9):1055-1062

Berta G, Sampo S, Gamalero E, Massa N, Lemanceau P (2005) Suppression of *Rhizoctonia* root-rot of tomato by *Glomus mossae* BEG12 and *Pseudomonas fluorescens* A6RI is associated with their effect on the pathogen growth and on the root morphogenesis. Eur J Plant Pathol 111 (3):279-288

Bettini PP, Santangelo E, Baraldi R, Rapparini F, Mosconi P, Crinò P, Mauro ML (2016) *Agrobacterium rhizogenes rolA* gene promotes tolerance to *Fusarium oxysporum*. J Plant Biochem Biotechnol 25 (3):225-233

Boisson-Dernier A, Chabaud M, Garcia F, Bécard G, Rosenberg C, Barker DG (2001) *Agrobacterium rhizogenes*-transformed roots of *Medicago truncatula* for the study of nitrogen-fixing and endomycorrhizal symbiotic associations. Mol Plant-Microbe Interact 14 (6):695-700

Bosselut N, Van Ghelder C, Claverie M, Voisin R, Onesto J-P, Rosso M-N, Esmenjaud D (2011) *Agrobacterium rhizogenes*-mediated transformation of *Prunus* as an alternative for gene functional analysis in hairy-roots and composite plants. Plant Cell Rep 30 (7):1313

Clemow SR, Clairmont L, Madsen LH, Guinel FC (2011) Reproducible hairy root transformation and spot-inoculation methods to study root symbioses of pea. Plant Methods 7 (1):46

Collier R, Fuchs B, Walter N, Kevin Lutke W, Taylor CG (2005) Ex vitro composite plants: an inexpensive, rapid method for root biology. Plant J 43 (3):449-457

Copetta A, Bardi L, Bertolone E, Berta G (2011) Fruit production and quality of tomato plants (*Solanum lycopersicum* L.) are affected by green compost and arbuscular mycorrhizal fungi. Plant Biosyst 145 (1):106-115. doi:10.1080/11263504.2010.539781

Cordier C, Gianinazzi S, Gianinazzi-Pearson V (1996) Colonisation patterns of root tissues by *Phytophthora nicotianae* var. parasitica related to reduced disease in mycorrhizal tomato. Plant Soil 185 (2):223-232

Chabaud M, Boisson-Dernier A, Zhang J, Taylor CG, Yu O, Barker DG (2006) *Agrobacterium rhizogenes*-mediated root transformation. The *Medicago truncatula* handbook, version November

Diedhiou P, Hallmann J, Oerke E-C, Dehne H-W (2003) Effects of arbuscular mycorrhizal fungi and a non-pathogenic *Fusarium oxysporum* on *Meloidogyne incognita* infestation of tomato. Mycorrhiza 13 (4):199-204

Engindeniz S (2006) Economic analysis of pesticide use on processing tomato growing: a case study for Turkey. Crop Protect 25 (6):534-541

Fiorilli V, Catoni M, Miozzi L, Novero M, Accotto GP, Lanfranco L (2009) Global and cell-type gene expression profiles in tomato plants colonized by an arbuscular mycorrhizal fungus. New Phytol 184 (4):975-987

Floss DS, Schmitz AM, Starker CG, Gantt JS, Harrison MJ (2013) Gene silencing in *Medicago truncatula* roots using RNAi. Legume genomics: methods and protocols:163-177

García Garrido JM, León Morcillo RJ, Martín Rodríguez JA, Ocampo Bote JA (2010) Variations in the mycorrhization characteristics in roots of wild-type and ABA-deficient tomato are accompanied by specific transcriptomic alterations. Mol Plant-Microbe Interact 23 (5):651-664. doi:10.1094/MPMI-23-5-0651

Geng L, Niu L, Gresshoff PM, Shu C, Song F, Huang D, Zhang J (2012) Efficient production of *Agrobacterium rhizogenes*-transformed roots and composite plants in peanut (*Arachis hypogaea* L.). Plant Cell Tiss Org Cult 109 (3):491-500

Gomez SK, Javot H, Deewatthanawong P, Torres-Jerez I, Tang Y, Blancaflor EB, Udvardi MK, Harrison MJ (2009) *Medicago truncatula* and *Glomus intraradices* gene expression in cortical cells harboring arbuscules in the arbuscular mycorrhizal symbiosis. BMC Plant Biol 9:10. doi:10.1186/1471-2229-9-10

Haldar S, Sengupta S (2016) Microbial Ecology at Rhizosphere: Bioengineering and Future Prospective. In: Choudhary DK, Varma A, Tuteja N (eds) Plant-Microbe Interaction: An Approach to Sustainable Agriculture. Springer Singapore, Singapore, pp 63-96. doi:10.1007/978-981-10-2854-0_4

Hewitt EJ (1966) Sand and water culture methods used in the study of plant nutrition. Commenwealth Agricultural Bureaux,

Horn P, Santala J, Nielsen SL, Hühns M, Broer I, Valkonen JP (2014) Composite potato plants with transgenic roots on non-transgenic shoots: a model system for studying gene silencing in roots. Plant Cell Rep 33 (12):1977-1992

Jefferson R (1989) The GUS reporter gene system. Nature 342 (6251):837

Karimi M, Inze D, Depicker A (2002) GATEWAY vectors for *Agrobacterium*-mediated plant transformation. Trends Plant Sci 7 (5):193-195

Kereszt A, Li D, Indrasumunar A, Nguyen CD, Nontachaiyapoom S, Kinkema M, Gresshoff PM (2007) *Agrobacterium rhizogenes*-mediated transformation of soybean to study root biology. Nat Protoc 2 (4):948-952

Kryvoruchko IS, Sinharoy S, Torres-Jerez I, Sosso D, Pislariu CI, Guan D, Murray J, Benedito VA, Frommer WB, Udvardi MK (2016) *MtSWEET11*, a Nodule-Specific Sucrose Transporter of *Medicago truncatula*. Plant Physiol 171 (1):554-565. doi:10.1104/pp.15.01910

Kuma K, Lopes-Caitar V, Romero C, Silva S, Kuwahara M, Carvalho M, Abdelnoor R, Dias W, Marcelino-Guimarães F (2015) A high efficient protocol for soybean root transformation by *Agrobacterium rhizogenes* and most stable reference genes for RT-qPCR analysis. Plant Cell Rep 34 (11):1987-2000

Li J, Todd TC, Trick HN (2010) Rapid in planta evaluation of root expressed transgenes in chimeric soybean plants. Plant Cell Rep 29 (2):113-123

Limpens E, Ramos J, Franken C, Raz V, Compaan B, Franssen H, Bisseling T, Geurts R (2004) RNA interference in *Agrobacterium rhizogenes*-transformed roots of *Arabidopsis* and *Medicago truncatula*. J Exp Bot 55 (399):983-992

Livak KJ, Schmittgen TD (2001) Analysis of relative gene expression data using real-time quantitative PCR and the 2− ΔΔCT method. methods 25 (4):402-408

López-Ráez JA, Verhage A, Fernandez I, Garcia JM, Azcón-Aguilar C, Flors V, Pozo MJ (2010) Hormonal and transcriptional profiles highlight common and differential host responses to arbuscular mycorrhizal fungi and the regulation of the oxylipin pathway. J Exp Bot 61 (10):2589-2601. doi:10.1093/jxb/erq089

Martin-Rodriguez JA, Huertas R, Ho-Plagaro T, Ocampo JA, Tureckova V, Tarkowska D, Ludwig-Muller J, Garcia-Garrido JM (2016) Gibberellin-Abscisic Acid Balances during Arbuscular Mycorrhiza Formation in Tomato. Frontiers in plant science 7:1273. doi:10.3389/fpls.2016.01273

Martirani L, Stiller J, Mirabella R, Alfano F, Lamberti A, Radutoiu SE, Iaccarino M, Gresshoff PM, Chiurazzi M (1999) T-DNA tagging of nodulation-and root-related genes in *Lotus japonicus*: expression patterns and potential for promoter trapping and insertional mutagenesis. Mol Plant-Microbe Interact 12 (4):275-284

Nagahashi G, Douds DD (2000) Partial separation of root exudate components and their effects upon the growth of germinated spores of AM fungi. Mycol Res 104 (12):1453-1464

Nagy R, Karandashov V, Chague V, Kalinkevich K, Tamasloukht MB, Xu G, Jakobsen I, Levy AA, Amrhein N, Bucher M (2005) The characterization of novel mycorrhiza-specific phosphate transporters from *Lycopersicon esculentum* and *Solanum tuberosum* uncovers functional redundancy in symbiotic phosphate transport in solanaceous species. Plant J 42 (2):236-250

Phillips JM, Hayman D (1970) Improved procedures for clearing roots and staining parasitic and vesicular-arbuscular mycorrhizal fungi for rapid assessment of infection. Trans Br Mycol Soc 55 (1):158IN116-161IN118

Pino LE, Lombardi-Crestana S, Azevedo MS, Scotton DC, Borgo L, Quecini V, Figueira A, Peres LE (2010) The *Rg1* allele as a valuable tool for genetic transformation of the tomato'Micro-Tom'model system. Plant methods 6 (1):23

Prabhu SA, Ndlovu B, Engelbrecht J, Van den Berg N (2017) Generation of composite *Persea americana* (Mill.)(avocado) plants: A proof-of-concept-study. PloS one 12 (10):e0185896

Quandt HJ, Pühler A, Broer I (1993) Transgenic root nodules of *Vicia hirsuta*: a fast and efficient system for the study of gene expression in indeterminate-type nodules. Mol Plant Microbe Interact 6 (6):699-706

Smith FA, Grace EJ, Smith SE (2009) More than a carbon economy: nutrient trade and ecological sustainability in facultative arbuscular mycorrhizal symbioses. New Phytol 182 (2):347-358

Stewart FC, Rolfs FM, Hall FH (1900) A fruit-disease survey of western New York in 1900. vol 191. New York Agricultural Experiment Station,

Talano MA, Agostini E, Medina MI, Reinoso H, del Carmen Tordable M, Tigier HA, de Forchetti SM (2006) Changes in ligno-suberization of cell walls of tomato hairy roots produced by salt treatment: the relationship with the release of a basic peroxidase. J Plant Physiol 163 (7):740-749

Tomilov A, Tomilova N, Yoder JI (2007) *Agrobacterium tumefaciens* and *Agrobacterium rhizogenes* transformed roots of the parasitic plant *Triphysaria versicolor* retain parasitic competence. Planta 225 (5):1059-1071. doi:10.1007/s00425-006-0415-9

Trouvelot A (1986) Mesure du taux de mycorhization VA d'un systeme radiculaire. Recherche de methodes d'estimation ayant une significantion fonctionnelle. Mycorrhizae: physiology and genetics:217-221

Chapter 2. *Tsb*, a novel upregulated gene in tomato roots colonized by AM fungi encoding a Microtubule Associated Protein: Cloning, Expression, and Characterization

Part of this Chapter has has been submitted for publication in the *Physiologia plantarum* scientific journal and is under review

Abstract

Arbuscular mycorrhizal (AM) symbiosis formation requires plant root host cells to undergo major structural and functional modifications in order to house a new highly branched fungal structure for the reciprocal exchange of nutrients called arbuscule. These morphological and physiological modifications are associated with changes in the cytoskeleton, and microtubule (MT) and actin filament remodelling has been observed in host cells colonized by AM fungi. The identification and functional analysis of microtubule and actin filament dynamics during AM symbiosis may help to elucidate the role of cytoskeleton during mycorrhization. In this sense, microtubule-associated proteins (MAPs) play a crucial role in the regulation of microtubule dynamics. In the present study, we found out that the tomato *tsb* gene, belonging to a *Solanaceae* group of genes encoding MAPs for pollen development, is also highly expressed in tomato roots colonized by AM fungi, particularly in cells containing AM arbuscules. In order to analyse the function of *tsb* in the mycorrhization process, hairy root tomato plants harbouring overexpression and RNAi constructs were generated. Overexpression of *tsb* gene enhanced expression of genes encoding for specialized transporter proteins located at the periarbuscular membrane and proteins involved in exocytosis that have been reported to provide a specific exocytotic capacity necessary for membrane proliferation. In addition *tsb* overexpression triggered changes in microtubule arrangements in cortical root cells. These results strongly suggest that *tsb* encodes a MAP that induces modifications in the microtubule cortical arrays of arbuscule-containing cells, and has an essential role in AM functionality. The relation between *tsb*, the cytoskeleton and the formation of the specialized periarbuscular membrane and the symbiotic interface is discussed.

Introduction

During the establishment of the arbuscular mycorrhizal (AM) symbiosis, plant cells undergo morphological and functional changes, suggesting that there is a high degree of interaction between both partners at the cellular, molecular and genetic levels. AM development, including penetration and growth of the AM fungi in roots, activate symbiotic programs for functional mycorrhization in both symbionts, resulting in a complex sequence of events, and triggering substantial morphological, physiological and functional changes in both partners (Gutjahr and Parniske 2013; Parniske 2008).

Morphological and physiological changes occurring include invagination of the plasma membrane, fragmentation of the central vacuole, movement of the nucleus and other organelles towards the center of the cell, de novo formation of the so-called periarbuscular membrane, location of new transmembrane proteins in this membrane and deposition of specific cell wall molecules and proteins at the interface compartment between the two partners. In this regard, we need to highlight the key role that must be played by cytoskeleton in order to accomplish all these modifications in the host cell during mycorrhization, as previously suggested by Timonen and Peterson (2002). In fact, microtubule (MT) and actin filament rearrangements have been observed in host cells colonized by AM fungus, both developing a basketlike structure around the arbuscule. First insights were obtained in tobacco cortex cells infected with the AM fungus *Gigaspora margarita* (Genre and Bonfante 1998; Genre and Bonfante 1997). Later, Blancaflor et al. (2001) reported a similar pattern of the MT cytoskeleton in *Medicago* root cells occupied by arbuscules of the mycorrhizal fungus *Glomus versiforme*, reporting an extensive remodeling of the MT cytoskeleton from the early stages of arbuscule development until arbuscule collapse and senescence, and, in addition, they showed that non-colonized cortical cells adjacent to arbuscule-containing cells also suffer a rearrangement of their MTs from an oblique to a random array, indicating that the cortical cells initiate the modification of their cytoskeleton prior to the entry of the fungus, and suggesting that some kind of signaling between the AM fungus and plant cortical cells occurs before penetration.

Further investigation carried out by Genre et al. (2005) with *Medicago* plants and the AM fungus *Gigaspora margarita*, revealed that MT organization not only changes in the cortex cells, but also in epidermal cells, even before penetration of the fungal hyphae. Upon contact of the hyphae with the epidermal root cell, the cell nucleus of the epidermal cell moves to the appressorium contact site and, around it, it is assembled a transient intracellular donut-shaped structure named the prepenetration apparatus (PPA), which comprises a novel cytoskeletal organization of microtubules and microfilaments, as well as the accumulation of endoplasmic reticulum. Afterwards, the nucleus moves to the cortical side of the cell, leaving a tunnel of PPA material behind it, whose attributed function is to synthetize an apoplastic compartment, and a membrane invagination to guide and allow the growth and penetration of the hyphae.

In plant cells, the role of the Microtubule Organizing Center (MTOC) is accomplished by the nuclear envelope, which acts controlling the MT assembly and organization. Curiously, Genre and Bonfante (1999) showed that, when the tobacco cell is colonized by the AM fungus *G. margarita*, the MTOC (visualized by γ-tubulin labelling) also changes its distribution from a perinuclear location to a diffuse occupation at the perifungal membrane surrounding exclusively the thin branches.

An overall increase of the tubulin synthesis also seems to occur in the AM colonized cells. The maize tubulin gene *Tubα3* is exclusively activated in the arbuscule-containing cells (Bonfante et al. 1996), and an increase in the fluorescent signals labelling the α -tubulin of the MTs (Genre and Bonfante 1997), and the γ -tubulin of the MTOC (Genre and Bonfante 1999) was also observed in AM infected tobacco cells, suggesting that new MTOCs and MTs are synthesized during AM colonization.

MTs and microfilaments are well-known for its role in determining the structure of the cell and organelles but, additionally, they are known to be involved in transport mechanisms, acting as “tracks” for intracellular traffic of clathrin coating vesicles (CCVs), the major transport means in the cell, and then determining the exocytosis and endocytosis pathways. In this manner, the cytoskeleton is responsible for subsequent establishment of cell polarity, plasma membrane expansion, membrane differentiation, secretion, cell wall formation and membrane recycling, all of them processes that are reported to take place in the host cells invaded by AM arbuscules

and to be required for a functional symbiosis. In this regard, several modifications in the secretion pathway have been observed (Harrison and Ivanov 2017) during the formation of the arbuscule, and the plasma membrane of the host cell harbouring the arbuscule undergoes around a 10-fold expansion (Alexander et al. 1989) in order to form the periarbuscular membrane, which surrounds the arbuscule. In addition, the periarbuscular membrane shows an asymmetric distribution of transport proteins with respect to the peripheral plasma membrane (Harrison et al. 2002; Harrison et al. 2010), as well as the cell-wall of the symbiotic interphase has a specific composition (Balestrini and Bonfante 2014), indicating an specific exocytosis towards the periarbuscular membrane.

However, so far, it is not clear if the strong cytoskeletal modifications observed in cells of mycorrhizal roots are related to the high intracellular trafficking,and to the membrane and cell wall polarization in these AM colonized roots. And it is also unknown if these cytoskeletal rearrangements are involved in AM development, facilitating the penetration of the hyphae and supporting the completely new cell structure required in the arbuscule-containing cells or, in the other hand, if the cytoskeletal changes are mainly involved in the establishment of a functional symbiotic interphase between both partners.

For a better understanding of the cause and effect relationship between cytoskeleton rearrangements undergoing in the AM colonized roots and the mycorrhizal development and/or function, the study of microtubule-associated proteins (MAPs) and actin-binding proteins (ABPs), is probably the best approach, as previously proposed by Timonen and Peterson (2002). Identification and functional analysis of these instrumental elements for microtubule and actin filament dynamics during AM symbiosis,may help to elucidate the role of cytoskeleton during mycorrhization.

Interestingly, two microarray hybridizations comparing arbuscular mycorrhizal tomato roots and non-mycorrhizal roots (García Garrido et al. 2010; López-Ráez et al. 2010) revealed that a tomato gene called *tsb* (GenBank AF515615, SGN-U565479, Tomato Affymetrix ID Les.3682.1.S1_at), encoding a lysine-rich protein, was up-regulated in roots colonized by the AM fungus *Rhizopahgus irregularis*. The study of García Garrido et al. (2010) revealed that it was the third gene whose expression

was induced the most (41-fold) in wild type tomato roots (cv. Rheinlands Ruhm) inoculated by *R. irregularis* after 50 days (52% mycorrhization approximately) with respect to non-inoculated roots. In addition, García Garrido et al. (2010) also observed that this induction of *tsb* gene expression was reduced by more than 89% in inoculated roots of tomato mutants with an impairment in arbuscule formation (*sitiens*, an ABA-deficient mutant) with respect to inoculated wild type roots, which suggest that *tsb* gene could play an essential role in the arbuscular mycorrhiza formation or functioning. Similar results were obtained in the microarray hybridization performed by López-Ráez et al. (2010), that also showed that *tsb* gene expression was up-regulated 3.67-fold in tomato roots inoculated with *R. irregularis* after 63 days (41% mycorrhization) with respect to un-inoculated roots. They also perform the same experiment with another species of AM fungi, *G. mosseae*, obtaining that *tsb* gene expression was also increased (3.18-fold induction) in the inoculated roots 63 days after inoculation (23% mycorrhization) comparing to non-mycorrhized roots.

Surprisingly, *tsb* has been previously described as a gene expressed exclusively in pollen (Zhao et al. 2003) and *tsb* gene encodes a protein which is homolog to several pollen-specific proteins from the *Solanaceae* family that have been characterized to function as MAPs involved in the cytoskeleton rearrangement during pollen development: SBgLR and ST901 from *Solanum tuberosum*, and SB401 from *Solanum berthaultii*. The imperfect repetitive motif V-V-E-K-K-N/E-E is conserved across all these *Solanaceae* MAPs. This domain resembles the repetitive K-K-E-E and K-K-E-I/V motifs, demonstrated to be responsible for the *in vivo* interaction between the mouse neural protein MAP1B and the microtubules (Noble et al. 1989). Actually, it has been demonstrated that SBgLR from potato and SB401 from wild potato are able to bind and bundle microtubules (Huang et al. 2007; Liu et al. 2013, respectively). All these MAPs are specifically expressed in pollen and are suggested to play a crucial role related to late-pollen development through its role organizing the cytoskeleton. Suppression of *st901* gene in potato resulted in aberrant pollen at maturation and a high reduction of pollen viability (Zhao et al. 2006). In the same manner, pollen abortion occurred when the potato gene *SBgLR* was constitutively expressed in transgenic tobacco (Liu et al. 2013) . SB401 also may have an important

role in organizing the cytoskeleton in pollen tubes, as it co-localized with cortical microtubules of the pollen tube in the wild potato *S. berthaultii* (Huang et al. 2007).

In summary, all these genes homologous to *tsb* (*st901*, *SBgLR* and *sb401*) are described as essential pollen specific genes involved in cytoskeleton rearrangements during pollen tube development, and it is unknown whether they are also specifically expressed in AM roots, as *tsb*. In a similar manner as it must occur during the mycorrhization process, the cytoskeleton plays a crucial role in pollen tube development, through controlling the intracellular traffic of organelles and vesicles, in order to build the dynamic cell wall required to get a highly adapted specialized shape and allow the apex-constrained growth of the pollen tube (Cai et al. 2017).

In this work we try to clarify the possible role of the microtubule cytoskeleton rearrangements during arbuscular mycorrhization through the functional analysis of *tsb,* a *S. lycopersicum* gene encoding a novel mycorrhizal-specific putative MAP. The effect of *tsb* on microtubule rearrangements as well as its role on mycorrhizal development and functional symbiosis will be assessed.

Methods

Bioinformatic Analysis

TSB amino acid sequence was subjected to a homology search against the *Viridiplantae* database (taxid:33090) using the on-line BLASTP server at NCBI (www.ncbi.nlm.nih.gov) with all default settings. From the resulting blastp output, putative homologs for TSB were subjected to phylogenetic analysis. Phylogenetic relationships were determined using Geneious software to create a neighbor-joining tree using the Jukes-Cantor model. Those possible homologs that had been previously characterized in the literature, were selected for further alignment using Clustal Omega (Sievers et al. 2011). The imperfect repetitive V-V-E-K-K-N/E-E motifs were identified. Putative N-linked glycosylation sites were predicted using the NetNGlyc 1.0 program (http://www.cbs.dtu.dk/services/NetNGlyc/). Potential casein kinase II phosphorylation sites were detected using the KinasePhos 2.0

(Wong et al. 2007) and NetPhos 3.1 (Blom et al. 2004) servers, and the plant-specific phosphorylated site predictors PlantPhos (Lee et al. 2011) and PhosPhAt 4.0 (Durek et al. 2010). Prediction of TSB subcellular localization was performed by TargetP 1.1 Server (Emanuelsson et al. 2000). Hydrophobicity of TSB protein was estimated with Protscale server of ExPASy (http://web.expasy.org/protscale/) using the Kyte–Doolittle algorithm (Kyte and Doolittle 1982) and default parameters.
Putative functional promoter elements were identified by the PlantCARE (Plant Cis-Acting Regulatory Element) database (Lescot et al. 2002).

Identification of the potato *tsb* ortholog in AM roots

S. tubersosum ssp. Andigena plants was grown and inoculated with the AM fungus *R. irregularis* in the same manner as explained before for the tomato plants. Plants were harvested at 36 and 56 dpi, mycorrhizal colonization was measured by tripan blue staining and expression of the potato *tsb* homologs *st901*, *SBgLR* and *STtLR* was analyzed at 36 and 56 dpi in inoculated and non-inoculated plants by qPCR, to check if any of them was mycorrhizal-induced as the *tsb* gene.

Microtubule inmunofluorescence staining and WGA co-staining

A combined staining of the microtubule cytoskeleton and the AM fungus of colonized and non-colonized tomato hairy roots overexpressing and downregulating *tsb* gene was carried out based on the protocol carried out by Blancaflor et al. (2001) and detailed described in Dyachok et al. (2009).
Hairy roots were selected under a stereomicroscope and fixated for 2h with PME buffer (50mM piperazine-di-ethanesulfonic acid, 2mM MgCl2 and 10mM EGTA, pH7) containing 3.7% formaldehyde and 5% dimethyl sulfoxide (v/v). Roots were washed with PME buffer, attached to an aluminium block using cyanocrylate and cut longitudinally with a vibratome (Vibratome 1000 Plus, Vibratome Company, St. Louis, Mo., U.S.A.). 60µm sections were transferred onto glass cover slips and secured with a thin film of agar as described by Brown and Lemmon (1995). Root sections were digested for 10 min with 1% cellulose Y-C (Karlan Research Products, Santa Rosa, CA, USA) in PME buffer, washed, incubated for 20 min in 1% Triton X-100 also in PME buffer and washed again. Sections were subjected to a 2 hours incubation with monoclonal rat anti-yeast alpha tubulin (clone YOL1/34; 1:50

dilution, Accurate Chemicals, Westbury, NY, USA), washed, and followed by a 2 hours incubation with goat anti-rat IgG (H+L) conjugated with Alexa Fluor 488 (1:100 dilution, Molecular Probes, Life Technologies, Eugene, Oregon, USA) and washed again. Root sections corresponding to mycorrhized roots were incubated for 15 min in 0.1mg/mL of wheat germ agglutinin (WGA)-Texas Red-x (Molecular Probes, Life Technologies, USA) and washed. All sections were mounted in 20% Mowiol 4-88 (Calbiochem, La Jolla, Calif., U.S.A.) and observed under a Perkin Elmer Ultraview ERS spinning disk confocal microscope (Norwalk, CT).

Additional methods used in this chapter but previously described in the *General Materials and Methods* section:

- **Plant growth and AM inoculation**
- **Expression Analysis of *tsb* gene in tomato organs**
- **Plasmid Construction and Hairy root transformation**
- **Gene expression localization**
- **Estimation of root colonization by AM fungus**
- **RNA extractions and gene expression quantification**

Results and Discussion

Expression Analysis of *tsb* gene expression in mycorrhizal roots

In order to corroborate that *tsb* shows an expression pattern associated with AM symbiosis, as previously characterized in the microarray hybridizations of García Garrido et al. (2010) and López-Ráez et al. (2010), the expression of *tsb* gene in mycorrhizal and non-mycorrhizal tomato roots was quantified at 32, 42, 52 and 62 dpi (days post-inoculation) using qPCR. For each sample, we calculated the fold change for *tsb* gene expression with respect to non-mycorrhizal plant roots at 32 dpi. As expected, the expression of *tsb* gene was higher in mycorrhizal than in non-mycorrhizal plant roots at all times evaluated, and the gene was significantly up-regulated as root length colonization by *R. irregularis* increased through time (Fig. 1A,B), reaching its maximum expression (18.6-fold) at the last time analyzed (62 dpi). A similar experiment was repeated for a second time (Fig. 2) and, again, we

observed that increases in *tsb* gene expression were parallel to increases of mycorrhization level. Data from both experiments were analyzed together comparing the two variables (percentage of mycorrhizal colonization and *tsb* gene expression) for each biological replicate, and a highly significant positive correlation (r=0.759, P<0.0001) was found between mycorrhizal colonization and *tsb* gene expression (Fig. 1C), suggesting that this gene is tightly regulated during arbuscular mycorrhizal development and thus could play an important role in the colonization process.

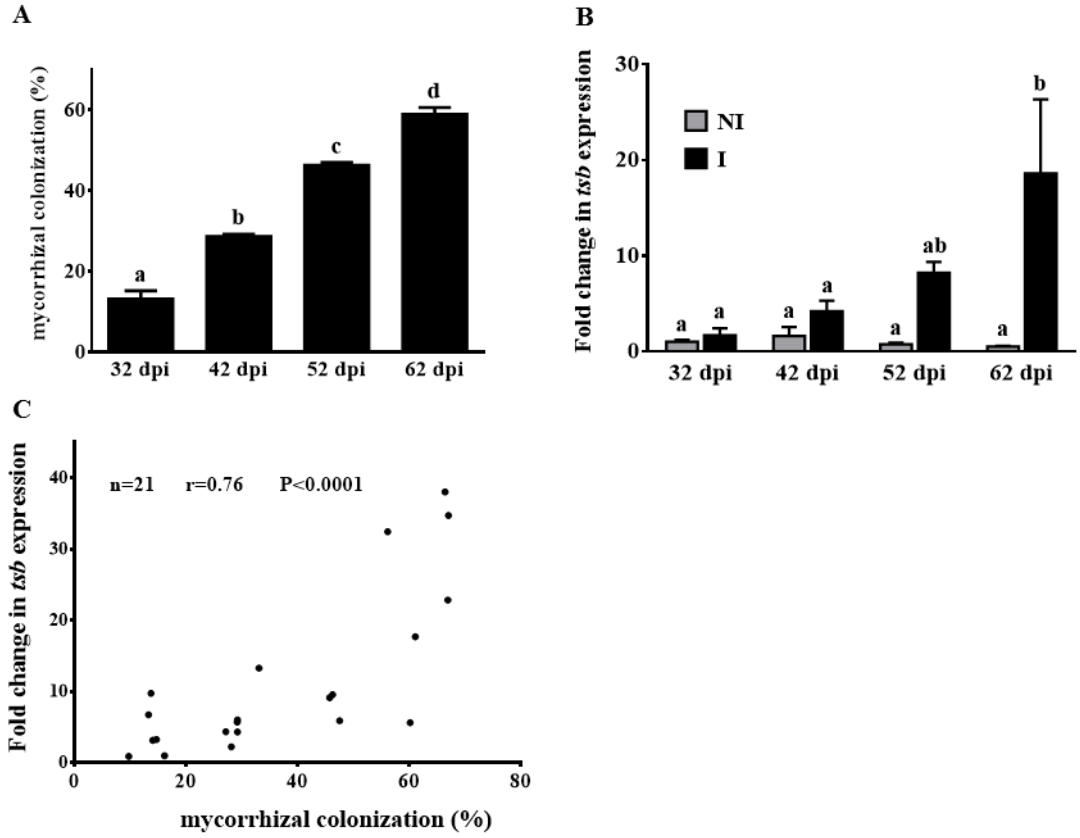

Figure 1. Mycorrhizal colonization and expression analysis of *tsb* gene in Money Maker tomato plants non-inoculated (NI) and inoculated (I) with the AM fungi *R. irregularis.* After 32, 42, 52 and 62 dpi (days post-inoculation), the percentage of total root length colonized by *R. irregularis* was measured (A) and *tsb* gene expression was analyzed by qPCR (B). qPCR data represents the relative expression of the *tsb* gene in plants with respect to expression in non-colonized plants at 32 dpi , in which expression was designated as 1. Values correspond to mean±SE (n=3). Bars with a same letter are not significantly different (*P*=0.05) according to LSD multiple comparison test. (C) is the scatter plot depicting the relationship between *tsb* expression level and mycorrhizal colonization. The Pearson correlation coefficient (*r*) determining the relationship between two variables is indicated.

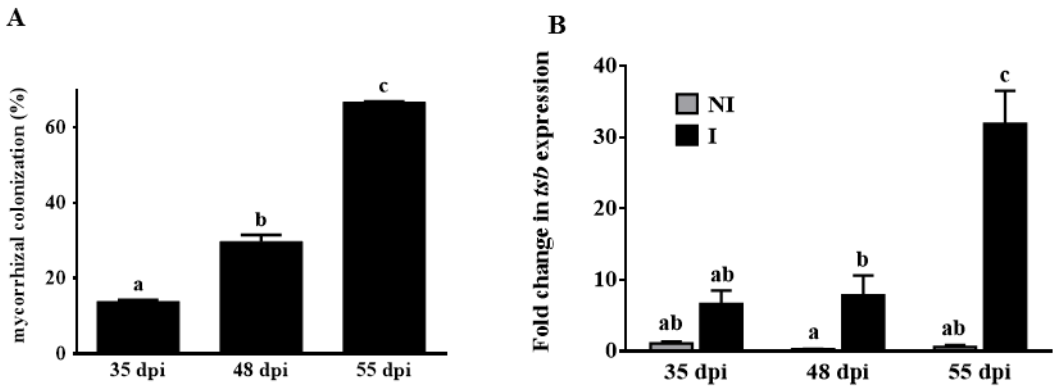

Figure 2. Mycorrhizal colonization and expression analysis of *tsb* gene in Money Maker tomato plants non-inoculated (NI) and inoculated (I) with the AM fungus *R. irregularis*. Data used for Fig. 1C. An experiment similar to that one showed in Figure 1 was performed for a second time and the percentage of total root length colonized by *R. irregularis* (A) and *tsb* gene expression analyzed by qPCR (B) were measured at 35, 48 and 55 dpi. qPCR data represents the fold change *tsb* gene expression with respect to non-colonized plants at 35 dpi, in which expression was designated as 1. Values are the mean±SE of three biological replications. Bars with a same letter are not significantly different (P=0.05) according to LSD multiple comparison test.

Promoter reporter activity of *tsb* in tomato roots

To analyse *tsb* promoter activity, tomato composite plants were generated. The 1.5 kp upstream region of *tsb* (p*tsb*) was fused to a GUS reporter construct. We observed the blue dye (that corresponds to GUS activity) in mycorrhizal transgenic hairy roots carrying the p*tsb*-GUS eight weeks after inoculation, and it was apparently detectable in the cortex zones affected by AM fungal root colonization (Fig. 3C-F). However, the non-mycorrhizal roots showed a promoter activity only restricted to the central cylinder and pericycle (Fig. 3A, B). The promoter of the tomato phosphate transporter 4 (*SlPT4*), previously described to be specifically expressed in arbuscule-containing cells (Nagy et al. 2005), was used as a positive control for the GUS staining (Fig. 4).

Longitudinal roots sections were stained for GUS activity and counterstained with WGA-alexa488 to visualize fungal structures (Figure 5). Colonization by *R. irregularis* redirected *tsb* expression to arbusculated cells, whereas non-colonized neighboring cells were not stained. Thus, the expression of *tsb* is AM-dependent and is associated with cortex cells colonized by AM fungal arbuscules.

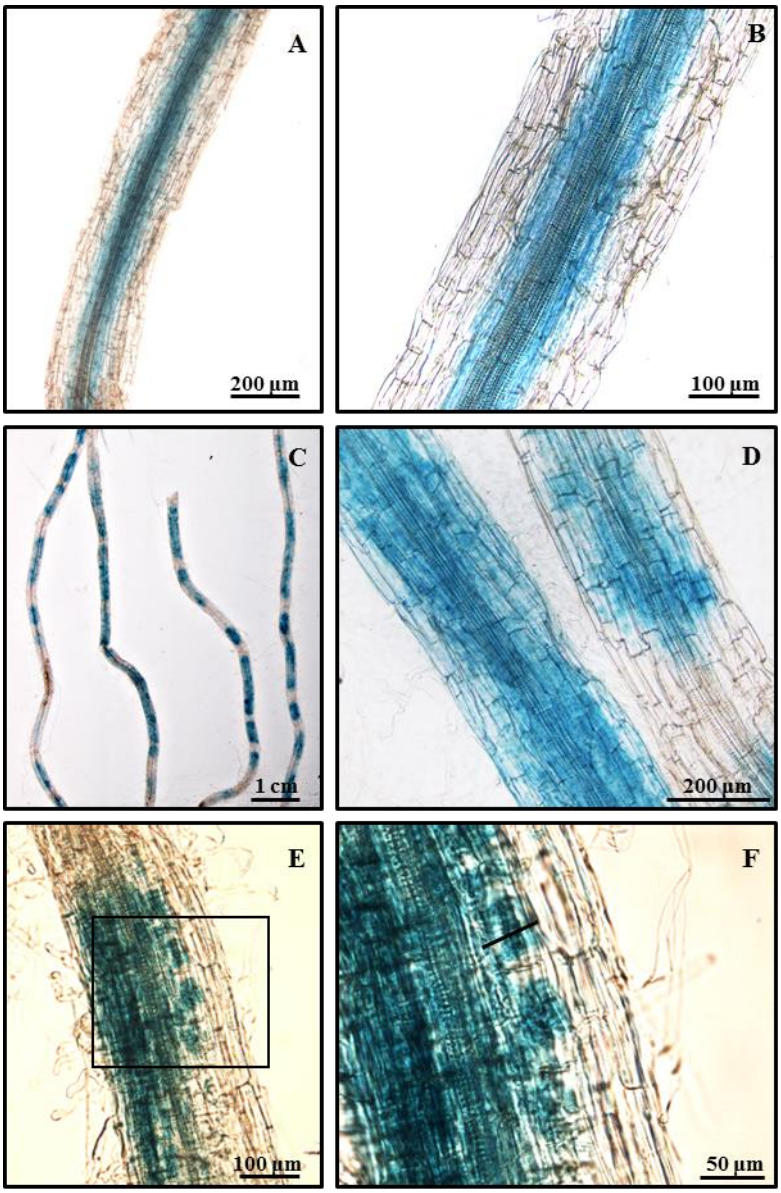

Figure 3. Expression analysis of the *tsb* promoter in transgenic *Solanum lycopersicum* whole (not sectioned) roots after GUS staining. GUS activity in *A. rhizogenes*-transformed roots expressing the *tsb* promoter *β-glucuronidase* fusion was assesed 8 weeks after inoculation with *R. irregularis* (C-F), and without *R. irregularis* (A and B). (F) is the higher magnification image of the squared area in image (E). All images were taken with an inverted microscope, except (C), which was taken with a stereomicroscope.

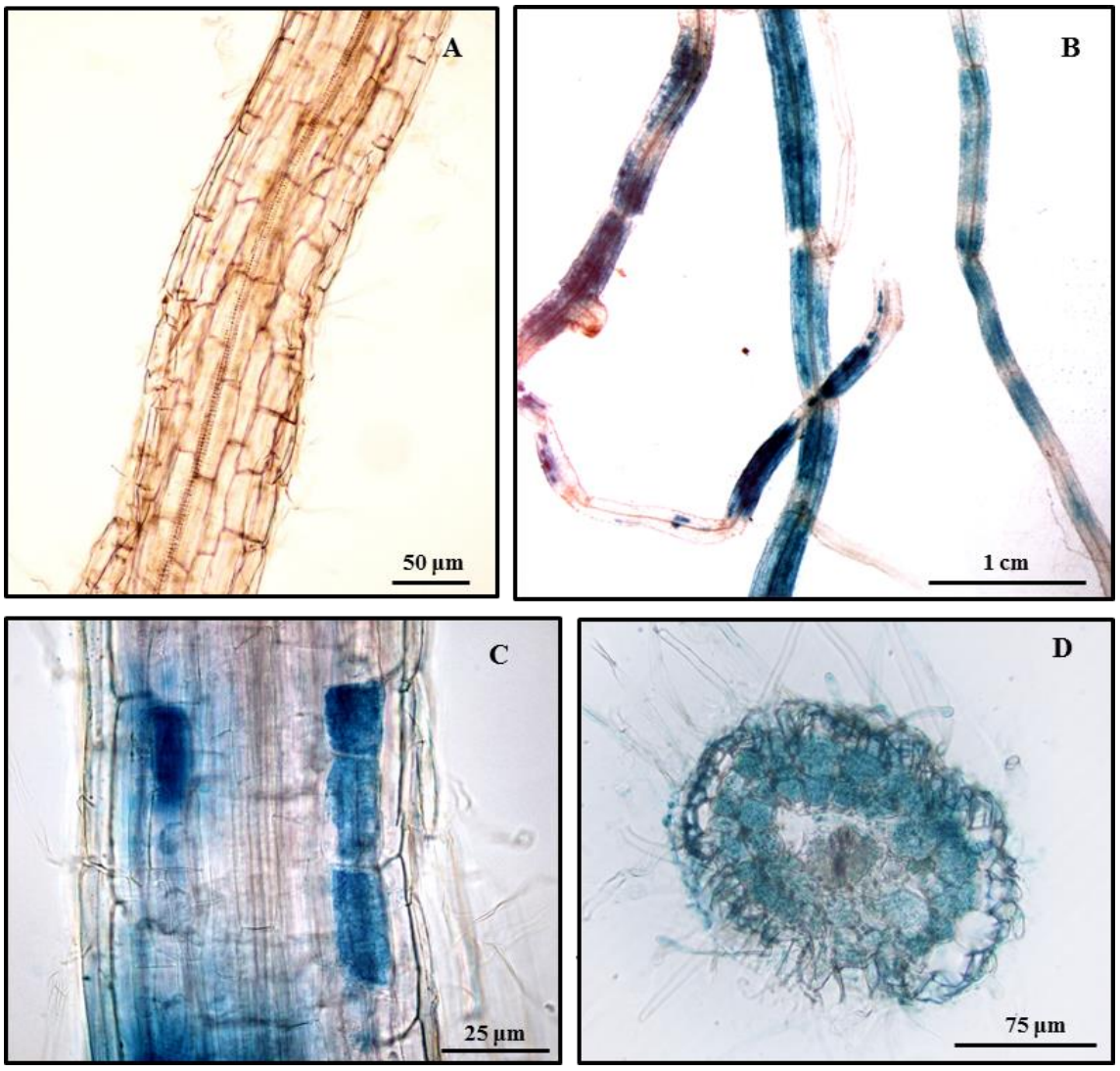

Figure 4. Expression analysis of the positive control *SlPT4* promoter in transgenic *Solanum lycopersicum* roots after GUS staining. GUS activity in *A. rhizogenes*-transformed roots expressing the *SlPT4* promoter *β-glucuronidase* fusion was assesed 8 weeks after inoculation with *R. irregularis* (B-D), and without *R. irregularis* (A). All images were taken with an inverted microscope, except (B), which was taken with a stereomicroscope.

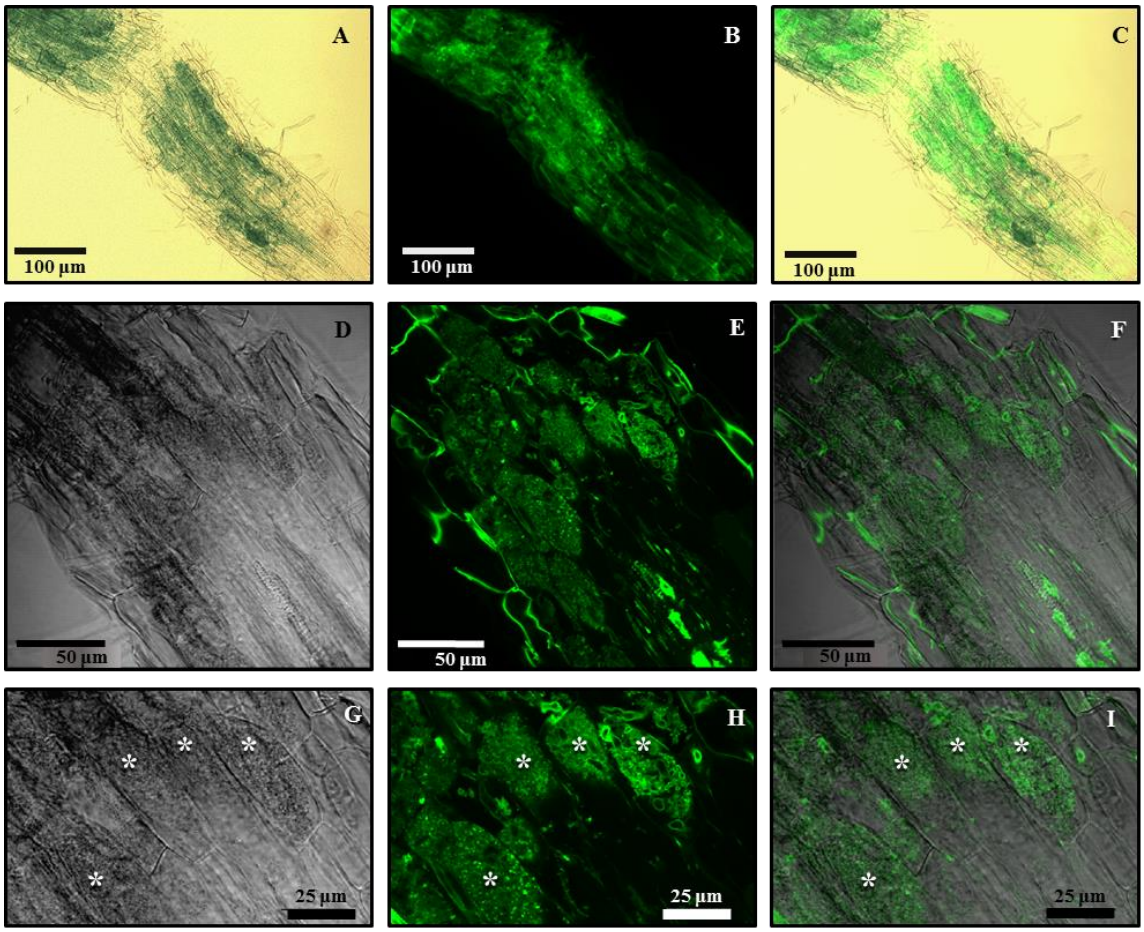

Figure 5. Histochemical analysis of *tsb* promoter expression in AM colonized transformed roots 8 weeks after inoculation with *R. irregularis*. GUS stained roots were vibratome sectioned and the AM fungus was labeled with WGA. B, E and H show *R. irregularis* hyphae stained with WGA-Alexa Fluor 488, which fluoresces green, and A, D and G are the corresponding bright-field images, which show exclusively GUS activity. C, F and I are the merged images of GUS staining and WGA-Alexa 488 images. White asterisks indicate arbuscules in the host cortical cells. Images were acquired by CLSM.

Expression Analysis of *tsb* gene in tomato organs

The expression pattern of *tsb* gene was analyzed by qPCR in different organs of tomato, showing that *tsb* gene is strongly upregulated in flowers, particularly after anthesis, reaching 112±49-fold induction in open flowers with respect to roots, as illustrated in Fig. 6. Actually, *tsb* has been previously described as a gene only expressed in pollen (Zhao et al. 2003). This result is also in agreement with the RNA-Seq data of tomato organs downloaded through the tomato eFP browser at bar.utoronto.ca (Fig. 7), where fully opened flower exhibited a RPKM fold change of ⩾120. It is also worth mentioning that after open flowers, the next organ showing

the highest *tsb* expression level are the roots (non-mycorrhized) according to both the qPCR carried out and the downloaded RNA-Seq data.

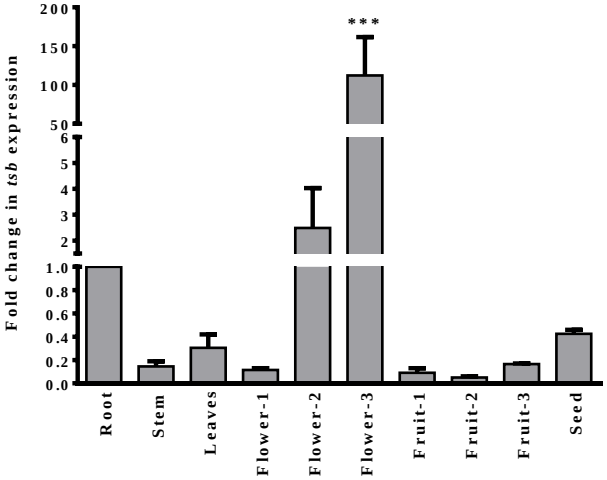

Figure 6. Data of *tsb* gene expression pattern in different organs of *Solanum lycopersicum* cv Moneymaker. *tsb* gene expression was measured by qPCR in roots, young stems, leaves, young flower buds ("Flower-1"), mature flower buds ("Flower-2"), open flowers ("Flower-3"), green fruits ("Fruit-1"), developing fruits turning red ("Fruit-2") , mature red fruits ("Fruit-3") and seeds. qPCR data represents the fold change of *tsb* gene expression in plant organs with respect to roots, in which expression was designated as 1. Values are the mean ± SE of two biological replications. Significant differences (LSD multiple comparison test) between *tsb* gene expression in different plant organs are indicated with asterisks (*$P < 0.05$).

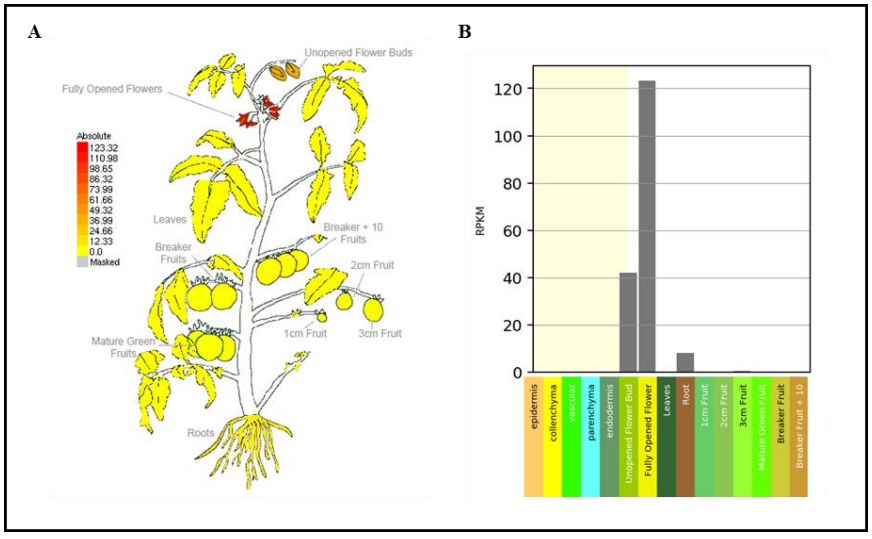

Figure 7. Data of *tsb* gene expression pattern in various organs/tissues of *Solanum lycopersicum* cv Heinz 1706 according to RNA-Seq analysis previously performed by Matas et al. (2011). Electronic fluorescent pictographic representation of absolute *tsb* gene expression pattern (A) and the corresponding chart (B). These electronic expression data were downloaded from the Tomato eFP Browser (at http://bar.utoronto.ca). Shown data is Illumina-derived and RPKM-normalized. The expression levels are presented using absolute fold-change values.

The *tsb* homologs *st901* and *SBgLR* from potato, and *sb401* from wild potato, are also reported to have a similar expression pattern, being specifically expressed in pollen. In addition, we observed that all of these homologs are expressed as well at late stages of pollen development. During male gametophyte development, gene expression have been proposed to be tightly regulated by two consecutive major gene expression programs (Twell et al. 2006) that require two gene sets: the "early" genes, which are expressed in the microspore and are downregulated before pollen maturation; and the "late" genes, that are expressed after pollen mitosis and are accumulated until maturity in mature pollen or pollen tubes (Mascarenhas 1990). In *S. tuberosum*, *st901* is described to be specifically expressed in mature pollen grains (Zhao et al. 2006); and *SBgLR* is also exclusively expressed in anthers at late developmental stages, as well as GFP expression driven by the *SBgLR* promoter in transgenic tobacco indicated that it is specifically expressed in the pollen tube (Lang et al. 2008). In the same manner, *sb401* from *S. berthaultii* is specifically expressed in mature and germinating pollen (Liu et al. 1997). In conclusion, all *tsb* homologs studied so far are found to be "late" pollen-specific genes. This fact, together with the data obtained in our qPCR in different organs of tomato (Fig. 6) and the RNA-Seq data downloaded through the tomato eFP browser (Fig. 7), suggest that the *tsb* gene also belong to this class of "late" pollen-specific genes.

Sequence and structure analysis of TSB protein

To find potential homologs in plants for the TSB protein we used BLASTP. Ten homolog proteins were obtained for TSB, with an E-value below 10^{-12}, and all of them belonged to species from the *Solanaceae* family. No homolog proteins were found outside the *Solanaceae* family, as the other matching proteins from the BLASTP query had an E-value higher than 0.03. Thus, it seems that TSB-like proteins constitute a *Solanaceae* family-specific group of proteins. The phylogenetic analysis is showed in Fig. 8.

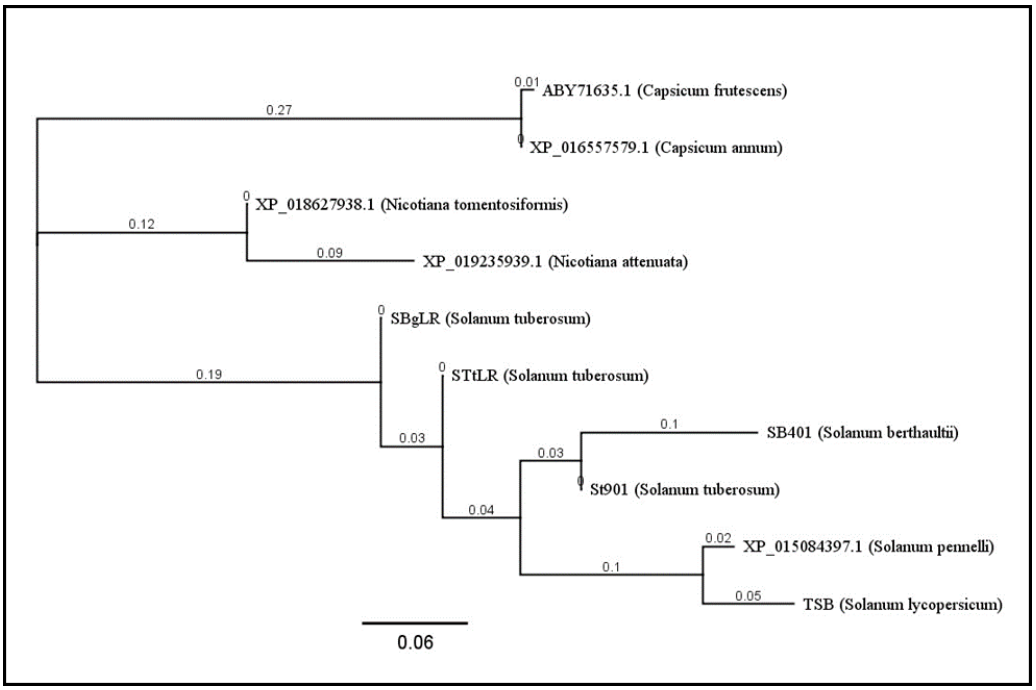

Figure 8. Phylogenetic analysis of putative TSB homolog proteins: the "TSB-like" *Solanaceae*-specific protein group. Phylogenetic relationships among amino acid sequences with high similarity to TSB from various plants previously identified by BLASTP: XP_015084397.1 from *Solanum pennelli*; ST401 from *Solanum berthaultii*; ST901, SBgLR and STtLR from *Solanum tuberosum*; XP_018627938.1 from *Nicotiana tomentosiformis*; XP_019235939.1 from *Nicotiana attenuate*; XP_016557579.1 from *Capsicum annum*; and ABY71635.1 from *Capsicum frutescens*. The common protein name or the GenBank/RefSeq accession numbers are indicated, followed by the species name between brackets. The scale bar represents the number of substitutions per site.

Based on our qPCR data from different organs of tomato and the bibliography regarding the TSB-homologs, we can speculate that TSB has biological function in pollen, binding microtubules, and probably also actin, triggering cytoskeleton rearrangements and having a role in pollen development or pollen tube formation (Huang et al. 2007; Zhao et al. 2006; Liu et al. 2013). However, a detailed bioinformatic analysis of TSB amino acid sequence was performed.

The *tsb* gene contains two exons and three introns (Fig. 9A), like its close potato homologs *st901* (Zhao et al. 2006) and *SBgLR* (Liu et al. 2013). The two proteins encoded by these genes from *S. tuberosum* (ST901 and SBgLR) and a protein from the wild potato *S.berthaultii* (ST401) were selected for further alignment and amino acid sequence analysis (Fig. 9C), as previous studies have been conducted to characterize these proteins (Huang et al. 2007; Zhao et al. 2006; Liu et al. 2013; Liu

et al. 2009) . The corresponding phylogenetic analysis is shown in Fig. 9B. The alignment reveals several common features between TSB and its putative homologs. TSB, ST901, SBgLR and SB401 proteins contain several imperfect repeated motifs of the sequence V-V-K-K-N/E-E. Additionally, many potential casein kinase II phosphorylation sites and all putative glycosylation sites are conserved.

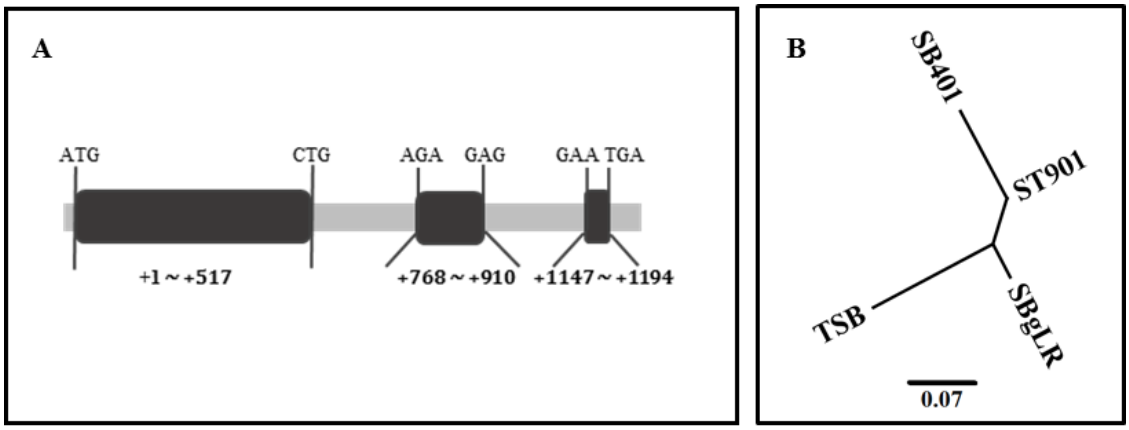

C

```
TSB       MGCGESKHAVATANATIPKNKRSLSSKSESRKGENIVKTENG--------EKMEEEKELI 52
ST901     MGCGESKHAVATENATIPKNKRSLSSKSESTKGENVVKTENGVAEIGSHDEKVEEEKELI 60
SBgLR     MGCGESKHAVATENATIPKNKRSLSSKSESTKGE------NGVAEIVSRDEKVEEEKELI 54
SB401     MGCGESKHAVATENATIPKNKRSLSSKSESTKGENVVKTENGV---GS-DEKVEEEKELI 56
          *********** ***************** ***      **        **:*******

TSB       APKMVAVEKEKEE---------------------EVVEPKNETIPVAVVETKKNENDEAT 91
ST901     APKVVAVEKEKSEKKEMVELEKAKEDEV--------IETKNETIHVAVVE-KKNENDETT 111
SBgLR     APKVVAVEKEKSEKKEMVELEKAKEDEVVEKKEEKVVETKNET---------------T 98
SB401     APKVVAVEKEKSEKKEMVELEKAKEDEVVEKKEEKVVETKNETIHVAVVE-KKNENDETT 115
          ***:*******.*                        :* ****              *

TSB       TPVSVVEKENTTPVAVVEKKNENEEMAPVSVVEKKNAIDETIPVPAVEKKNENEETASPV 151
ST901     APVSVVENDETTPVAVVEKKNENEETV-----------------------------PV 140
SBgLR     TPVSVVENDETTPVAVVEKKNENEETS-----------------------------PV 127
SB401     TPVSVIENDETTPVAVVEKKNENEETV-----------------------------PV 144
          :****:*:::***************                                 **

TSB       SVVAVVEKKESVEEIKAEEKT-EIIKPIEEVKEKAEEKEEVIAVSEATDAAKPETVKDDD 210
ST901     SV---VEKKESVEEIKVEEKTEETIKPIEEVKEK--EKEEVIAVSEATDAAKPETVKDDD 195
SBgLR     SVVAVVEKK-------AEEKTEETIKPIEEVKEK--EKEEVIAVSEATNAAKPETVKDDD 178
SB401     SVVAVVEKKESVEEIKVEEKTEETIKPIEEVKDK--EKEEVIAISEATDATKPETVKDDD 202
          **   ****       .**** * ********:*  *******:****:*:*********

TSB       KPET---------EEKPKEENATETSATTDSKTD-------------     235
ST901     KPET---------EEKPKEENATETS---DSKTD-------------     217
SBgLR     KPETAKDADKPETEEKPKEENATETSAT-DSKTD-------------     211
SB401     KPET---------EEKPKEEEQLKQQQRQTQKQIKVQAWEYGRKSVY    240
          ****         *******:  : .    .
```

Figure 9. Gene structure of *tsb*, and phylogenetic analysis and amino acid comparison of TSB and its homologs. (A) Gene structure of TSB. Three exons were illustrated in black. (B) Phylogenetic analysis of the TSB amino acid sequences with its homologs from various plants: ST901 and SBgLR (*Solanum tuberosum*), and SB401 (*Solanum berthaultii*). The scale

bar represents the number of substitutions per site. (C) Amino acid comparison between TSB and its related proteins. The imperfect repeated motifs V-V-E-K-K-N/E-E responsible for microtubule binding are shadowed in gray. Bold underlined sequences correspond to putative glycosylation sites. Bold, not underlined residues indicate predicted casein kinase II phosphorylation sites. The consensus symbols of the Clustal Omega aligment are used: the identical residues are indicated with "*", residues of strongly similar properties are labelled with ":", and residues of weakly similar properties are indicated with ".".

In particular, TSB contains seven imperfect repeated V-V-K-K-N/E-E motifs. This domain resembles the repetitive K-K-E-E and K-K-E-I/V motifs, demonstrated to be responsible for the *in vivo* interaction between the mouse neural protein MAP1B and the microtubules (Noble et al. 1989). Actually, it has been demonstrated that SBgLR from potato and SB401 from wild potato are able to bind and bundle microtubules (Liu et al. 2013; Huang et al. 2007, respectively), although experimental evidence is required to prove that the V-V-E-K-K-N/E-E motif is responsible for that function.

Many plant MAPs bind both microtubules and actin filaments. Such is the case of MAP18 (Zhu et al. 2013; Wang et al. 2007), AtFH4 (Deeks et al. 2010), MDP25 (Li et al. 2011; Qin et al. 2014) and the TSB homolog SB401 (Huang et al. 2007), the two last ones having a role regulating the organization and dynamics of actin filaments during pollen tube growth (Petrasek and Schwarzerova 2009). The actin-binding ability of MAP18 from *Arabidopsis thaliana* have been attributed to the richness of proline (P), glutamate (E), valine (V) and lysine (K) residues throughout its amino acid sequence (Kato et al. 2010), as it reminds to the PEVK domain of the giant intrasarcomeric protein titin in humans, which is responsible for the interaction with actin filaments in the muscles (Linke et al. 2002; Nagy et al. 2004). However, again, it is not proved if the PEVK-rich domain of MAP18 from *Arabidopsis* is the source of its actin-binding ability. Then, although TSB protein is also rich in these four amino acids (56% of the residues) as seen in Fig. 10, we should carefully consider it as an indicator of a possible interaction of TSB with actin filaments.

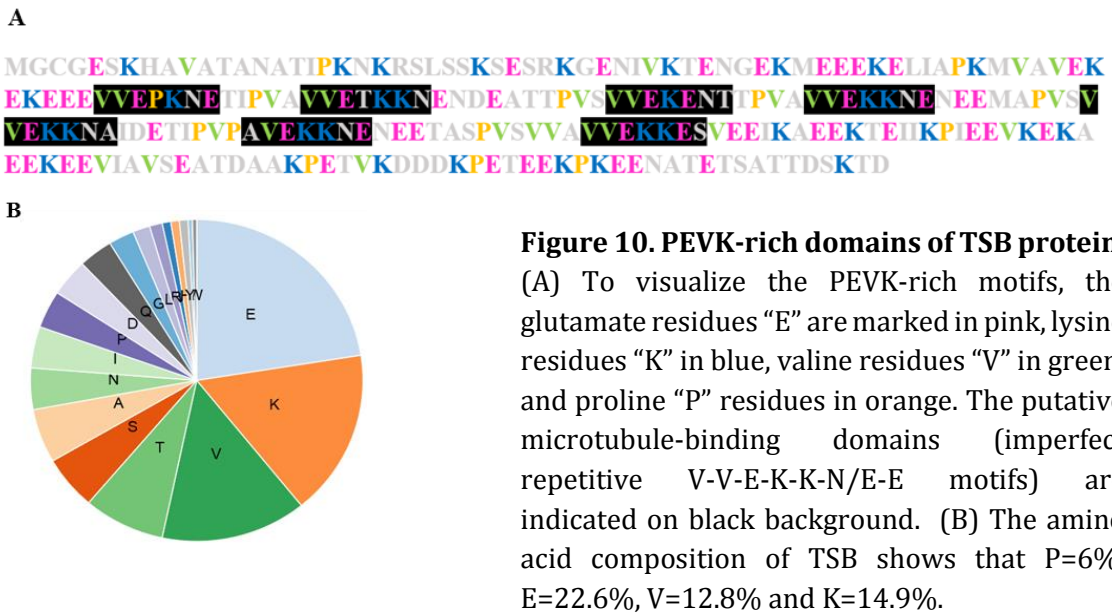

Figure 10. PEVK-rich domains of TSB protein. (A) To visualize the PEVK-rich motifs, the glutamate residues "E" are marked in pink, lysine residues "K" in blue, valine residues "V" in green, and proline "P" residues in orange. The putative microtubule-binding domains (imperfect repetitive V-V-E-K-K-N/E-E motifs) are indicated on black background. (B) The amino acid composition of TSB shows that P=6%, E=22.6%, V=12.8% and K=14.9%.

Prediction of casein kinase II phosphorylation sites revealed eleven potential residues in the TSB protein. Three of them are located within the V-V-K-K-N/E-E repeats. It has been shown that the activity of many animal MAP s on the control of microtubule dynamics if often regulated by phosphorylation, as occurs in MAP1B (reviewed in: Gordon-Weeks 2004), MAP2 (Sánchez et al. 2000), MAP6 (Baratier et al. 2006) and MAP9 (Venoux et al. 2008). Some plant MT-associated proteins (MAPs) are also known to change their MT binding properties by phosphorylation, as is the case of MAP65 family proteins (Komis et al. 2011). Similar results have been observed for the putative TSB homolog SB401 in *S.berthaultii*. Liu et al. (2009) demonstrated that phosphorylation of SB401 by casein kinase II (CKII) markedly reduced its ability to bundle microtubules and to polymerize tubulin. However, they did not observed any effect on its bundling of F-actin, thus, they proposed that phosphorylation by CKII may regulate the effects of SB401 on microtubules and the actin cytoskeleton. A similar regulation by phosphorylation may occur for TSB protein. In fact, the alignment shows that most of the predicted CKII phosphorylation sites are conserved (Fig. 9C). Although considerable variability was found in the predictions of the various servers used (Fig. 11), we must highlight that the only consensus prediction was for the residue S-162, which actually is situated within the V-V-K-K-N/E-E repeats and it was conserved in ST901 and SB401, being also the only consensus phosphorylation site predicted for those proteins. Together

with S-162, another residue that could play an important role in the regulation of TSB by phosphorylation is the amino acid S-95, which is conserved across all the TSB homologs (Fig 9C, Fig. 11).

TSB

Position	KinasePhos	NetPhos	PlantPhos	PhosPhAt
95	-	+	+	-
102	+	-	+	-
162	+	+	+	+
195	+	+	-	-
198	+	-	+	+
205	+	-	+	+
214	-	+	+	+
227	+	-	-	-
229	+	-	-	+
230	+	+	-	-
234	-	+	-	-

ST901

Position	KinasePhos	NetPhos	PlantPhos	PhosPhAt
30	+	-	+	-
31	+	-	+	-
48	-	+	+	+
91	-	+	+	-
115	+	+	+	-
141	-	+	+	-
148	+	+	+	+
180	+	+	-	-
183	+	-	+	+
190	+	-	+	+
199	-	+	+	+
211	-	+	-	+
212	-	+	-	-
216	-	+	-	-

SBgLR

Position	KinasePhos	NetPhos	PlantPhos	PhosPhAt
30	+	-	+	+
31	+	-	+	+
42	-	+	+	+
93	-	+	+	+
102	-	+	+	-
163	-	+	+	-
166	+	-	+	+
173	+	-	+	+
182	+	+	+	+
191	-	+	+	+
203	-	+	-	+
204	+	-	-	-
210	-	+	-	-

SB401

Position	KinasePhos	NetPhos	PlantPhos	PhosPhAt
30	+	-	+	-
31	+	-	+	-
45	-	+	+	+
95	-	+	+	-
119	-	+	+	-
155	+	+	+	+
187	+	+	-	+
190	+	-	+	+
197	+	-	+	+
206	-	+	+	+

Figure 11. Prediction of potential casein kinase II phosphorylated sites for TSB protein and its homologs. Aminoacid position of the casein kinase II phosphorylated sites predicted by KinasePhos and/or NetPhos are shown for TSB protein and its homologs ST901, SBgLR and SB401. It is also indicated if those sites were also predicted as putative phosphorylation sites by plant-specific phosphorylation site predictors (PlantPhos and PhoPhAt). Predicted sites by each program are marked with "+", while not predicted sites are marked with "-". Predicted phosphorylated sites located in the repeated microtubule binding domains that are conserved residues among protein homologs are indicated with the same color.

Prediction with NetNGlyc 1.0 server revealed three potential N-glycosylation sites for TSB, which were well conserved across its homologs (Fig. 9C). N-glycosylation targeting only occurs on proteins that are going to be secreted or membrane bounded, then we wondered if TSB follows the secretory pathway. However,

subcellular localization predicted by TargetP 1.1 indicated that TSB protein apparently lacks a signal peptide to drive it into the endoplasmic reticulum, and the hydrophilicity plot for TSB (Fig. 12) shows that TSB protein is hydrophilic throughout. Thus, TSB is likely to be localized in the cytoplasm, and then N-glycosylation of TSB may not occur, despite having three potential N-glycosylation sites apparently conserved. This is supported by the observations of Liu et al. (1997) with respect to SB401 from *S. berthaultii* in pollen. They obtained a similar mobility on SDS-polyacrylamide gel for *E.coli*-expressed protein and the endogenous pollen SB401 protein, indicating that N-linked glycosylation of SB401 may not occur *in vivo* in pollen.

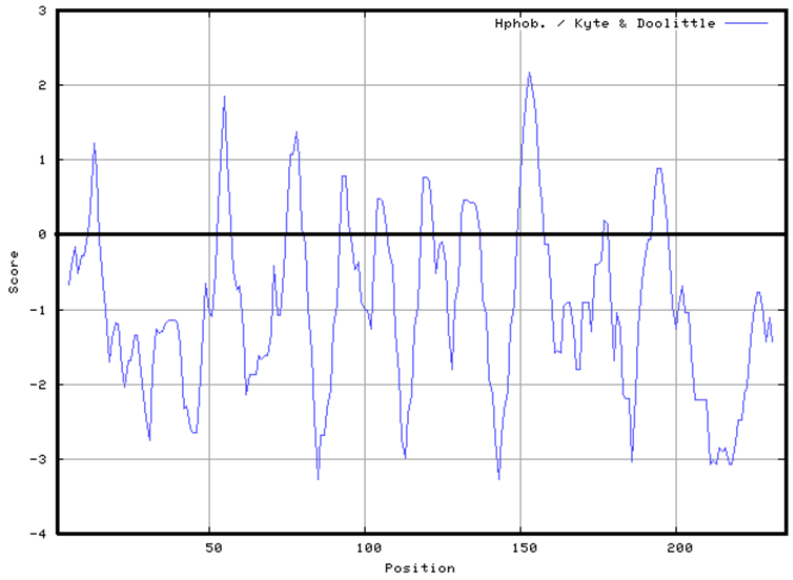

Figure 12. Hydropathy plot of the TSB protein. TSB amino acid sequence exhibits a generally hydrophilic profile according to Kyte and Doolite (1982) prediction.

In silico analysis of the *tsb* promoter

Lack of information about the *tsb* promoter encouraged us to look for putative motifs responsible of its upregulation in pollen and AM-colonized root cells. As the promoter regions of the potato *tsb* homologs *SBgLR* and *st901* are available at the potato genome database (solanaceae.plantbiology.msu.edu/pgsc_download.shtml), and the *SBgLR* promoter has been deeply studied (Lang et al. 2008; Zhou et al. 2010; Chang et al. 2017), we decided to predict the putative regulatory cis-elements in the

tsb promoter based on homology with the *SBgLR* and *st901* promoter regions, together with the information provided by the PlantCARE database (Lescot et al. 2002). The corresponding alignment and the putative cis-regulatory elements identified in our study are presented in Fig. 13.

We examined the -1493 to -1 region of the *tsb* gene. Many putative cis-element motifs related to pollen-specific activity have been characterized in different plant species. Particularly, we identified nine AGAAA elements, six TTTCT, four GTGA and one AAATGA in the *tsb* promoter. Eight of these elements are localized in the 200 nt upstream of the *tsb* start codon. All these motifs have been reported to act as cis-regulatory elements specific to late pollen expressed genes. The AGAAA element has been described as responsible for the pollen-specificity of the tomato *lat52* promoter (Eyal et al. 1995; Bate and Twell 1998) and its reverse complementary sequence TTTCT also directs the pollen-specific expression of the maize *ZM13* promoter (Hamilton et al. 1998) and the potato *SBgLR* promoter (Chang et al. 2017). The putative late pollen-specific motif GTGA has been identified in the tobacco *g10* gene (Rogers et al. 2001) and in the tomato *lat56* (Twell et al. 1991). Also, the AAATGA motif was described as a pollen-specific cis-regulatory element in the promoter of *NTP303* from tobacco, within which TGA is the functional core (Weterings et al. 1995). Curiously, in the -207 to -190 region of the *tsb* promoter, two of these pollen-specific motifs, TTTCT and AGAAA, surround a unique putative TATA box, giving place to the quasi-palindromic sequence TTTCTATTATATTAGAA. This sequence is nearly identical to the palindromic repressor found in the -227 to -209 promoter region of the *SBgLR* potato late-pollen specific gene (Zhou et al. 2010); and the authors of the finding suggested that this palindromic repressor could be involved in inhibiting *SBgLR* gene expression in other tissues different from pollen and/or during early stages of pollen development. Other similarities were found between the *tsb* promoter and the deeply studied *SBgLR* promoter. The 24 pb sequence upstream of the *SBgLR* palindromic repressor was shown to play a role inhibiting the palindrome (Zhou et al. 2010) and it is highly conserved in the *tsb* promoter. The -156 to -127 region of the *SBgLR* promoter, which belongs to the 5´UTR of the transcript, is reported as a crucial region for pollen-specific gene expression and it is also very well conserved in the *tsb* promoter. This region

includes two conserved motifs; the TTTCT motif at -149 position, demonstrated to be crucial for pollen-specific *SBgLR* expression, and the ARR TF binding site AATC at -139 position, which was probed to partially affect *SBgLR* expression in pollen (Chang et al. 2017). In summary, many putative pollen-specific elements where found in the *tsb* promoter and, for several of them, their possible regulatory role played during pollen development is supported by their homology with the well-studied *SBgLR* promoter.

By contrast, we found much less information regarding the localization of mycorrhizal-related cis-regulators in the *tsb* promoter. Only a few motifs have been reported as mycorrhizal-associated cis-elements so far. These are the CTTC element (Karandashov et al. 2004), the CTTC-like motif named MYCS (Chen et al. 2011) and the P1BS element (Rubio et al. 2001). We identified a putative P1BS site (GAATATAC at -266 position) and a probable MYCS site (TTTCTTCTTAT at -27 position) in the *tsb* promoter. In the *tsb* promoter sequence alignment with the *st901* and *SBgLR* promoters, it is remarkable that the *tsb* promoter possess two unique sequences that are not present in the other promoters (-1132 to -996 and -163 to -417 upstream of the starting codon) and, attending to the microarray carried out by Gallou et al. (2012), none of the three *tsb* ortholog genes (*STtLR*, *SBgLR* and *st901*) appear to be induced by mycorrhization in potato roots. Then, key regulatory elements responsible for the *tsb* expression during mycorrhization could be placed in these regions. To confirm that the potato *tsb*-homologs are not upregulated under AM fungal infection, we decided to analyse the expression of these three genes in mycorrhizal potato roots, with respect to non-mycorrhizal roots. Again, we did not detect an induction of *STtLR*, *SBgLR* nor *st901* genes in the mycorrhizal potato roots (Fig. 14). Gene expression in I vs NI roots was not significantly different, with P values of $P>0.6$, except for *SBgLR* at 56 dpi ($P=0.1$). Then, we suggest that indeed some additional motifs must be exclusively present in the promoter region of the *tsb* to allow its specific induction in colonized cells, and they may be located at the candidate regions -1132 to -996 and -163 to -417 upstream of the *tsb* starting codon. However, further analysis is required to confirm this observation.

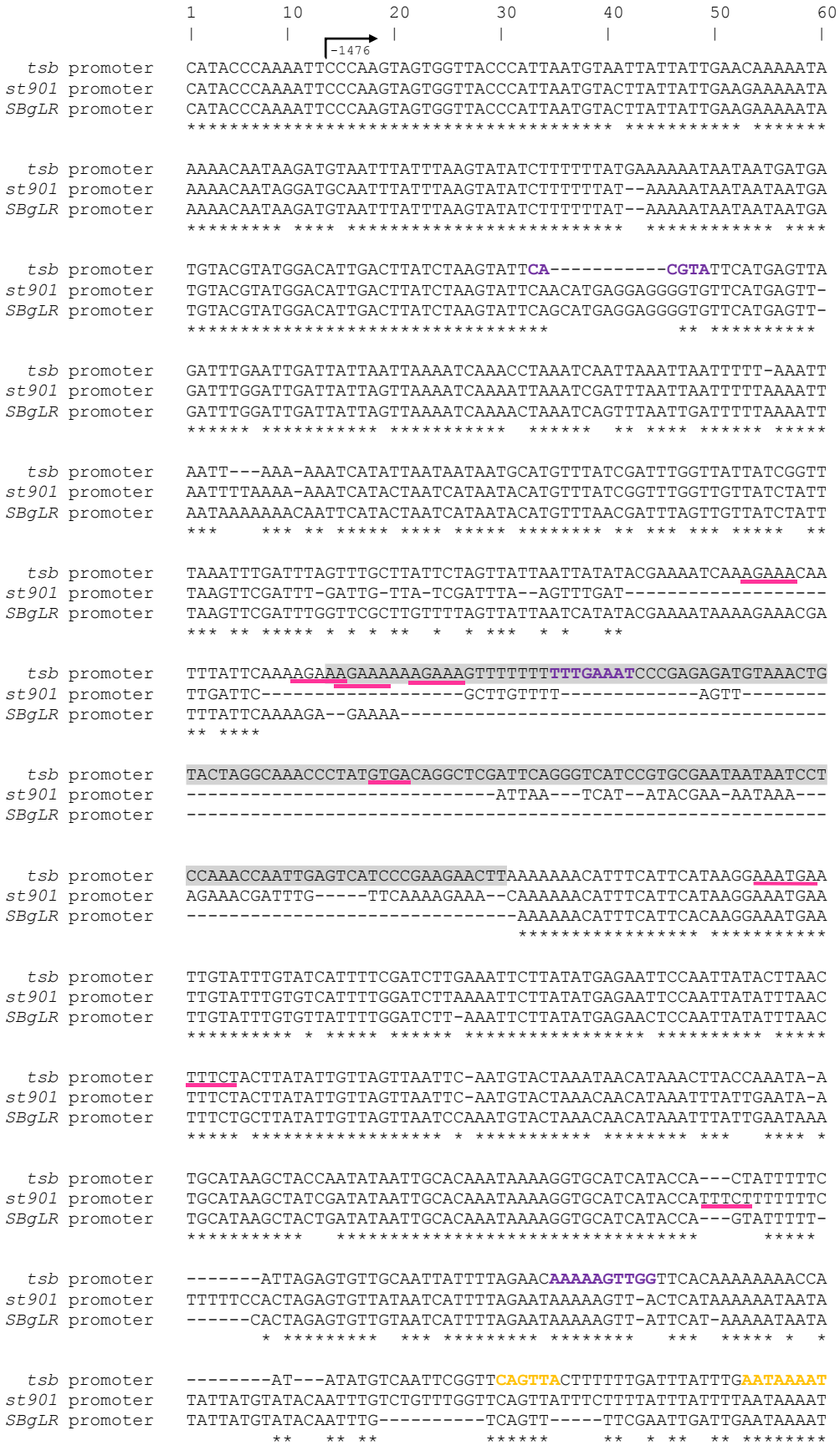
1 10 20 30 40 50 60
-1476
tsb promoter CATACCCAAAATTCCCAAGTAGTGGTTACCCATTAATGTAATTATTATTGAACAAAAATA
st901 promoter CATACCCAAAATTCCCAAGTAGTGGTTACCCATTAATGTACTTATTATTGAAGAAAAATA
SBgLR promoter CATACCCAAAATTCCCAAGTAGTGGTTACCCATTAATGTACTTATTATTGAAGAAAAATA
tsb promoter AAAACAATAAGATGTAATTTATTTAAGTATATCTTTTTTATGAAAAAATAATAATGATGA
st901 promoter AAAACAATAGGATGCAATTTATTTAAGTATATCTTTTTTAT--AAAAATAATAATAATGA
SBgLR promoter AAAACAATAAGATGTAATTTATTTAAGTATATCTTTTTTAT--AAAAATAATAATAATGA
tsb promoter TGTACGTATGGACATTGACTTATCTAAGTATTCA----------CGTATTCATGAGTTA
st901 promoter TGTACGTATGGACATTGACTTATCTAAGTATTCAACATGAGGAGGGGTGTTCATGAGTT-
SBgLR promoter TGTACGTATGGACATTGACTTATCTAAGTATTCAGCATGAGGAGGGGTGTTCATGAGTT-
tsb promoter GATTTGAATTGATTATTAATTAAAATCAAACCTAAATCAATTAAATTAATTTTT-AAATT
st901 promoter GATTTGGATTGATTATTAGTTAAAATCAAAATTAAATCGATTTAATTAATTTTTAAAATT
SBgLR promoter GATTTGGATTGATTATTAGTTAAAATCAAAACTAAATCAGTTTAATTGATTTTTAAAATT
tsb promoter AATT---AAA-AAATCATATTAATAATAATGCATGTTTATCGATTTGGTTATTATCGGTT
st901 promoter AATTTTAAAA-AAATCATACTAATCATAATACATGTTTATCGGTTTGGTTGTTATCTATT
SBgLR promoter AATAAAAAAACAATTCATACTAATCATAATACATGTTTAACGATTTAGTTGTTATCTATT
tsb promoter TAAATTTGATTTAGTTTGCTTATTCTAGTTATTAATTATATACGAAAATCAAAGAAACAA
st901 promoter TAAGTTCGATTT-GATTG-TTA-TCGATTTA--AGTTTGAT----------
SBgLR promoter TAAGTTCGATTTGGTTCGCTTGTTTTAGTTATTAATCATATACGAAAATAAAAGAAACGA
tsb promoter TTTATTCAAAAGAAAGAAAAAAGAAAGTTTTTTTTTTGAAATCCCGAGAGATGTAAACTG
st901 promoter TTGATTC----------GCTTGTTTT----------AGTT--------
SBgLR promoter TTTATTCAAAAGA--GAAAA----------
tsb promoter TACTAGGCAAACCCTATGTGACAGGCTCGATTCAGGGTCATCCGTGCGAATAATAATCCT
st901 promoter ----------ATTAA---TCAT--ATACGAA-AATAAA---
SBgLR promoter ----------
tsb promoter CCAAACCAATTGAGTCATCCCGAAGAACTTAAAAAAACATTTCATTCATAAGGAAATGAA
st901 promoter AGAAACGATTTG-----TTCAAAAGAAA--CAAAAAACATTTCATTCATAAGGAAATGAA
SBgLR promoter ----------AAAAAACATTTCATTCACAAGGAAATGAA
tsb promoter TTGTATTTGTATCATTTTCGATCTTGAAATTCTTATATGAGAATTCCAATTATACTTAAC
st901 promoter TTGTATTTGTGTCATTTTGGATCTTAAAATTCTTATATGAGAATTCCAATTATATTTAAC
SBgLR promoter TTGTATTTGTGTTATTTTGGATCTT-AAATTCTTATATGAGAACTCCAATTATATTTAAC
tsb promoter TTTCTACTTATATTGTTAGTTAATTC-AATGTACTAAATAACATAAACTTACCAAATA-A
st901 promoter TTTCTACTTATATTGTTAGTTAATTC-AATGTACTAAACAACATAAATTTATTGAATA-A
SBgLR promoter TTTCTGCTTATATTGTTAGTTAATCCAAATGTACTAAACAACATAAATTTATTGAATAAA
tsb promoter TGCATAAGCTACCAATATAATTGCACAAATAAAAGGTGCATCATACCA---CTATTTTTC
st901 promoter TGCATAAGCTATCGATATAATTGCACAAATAAAAGGTGCATCATACCATTTCTTTTTTTC
SBgLR promoter TGCATAAGCTACTGATATAATTGCACAAATAAAAGGTGCATCATACCA---GTATTTTT-
tsb promoter -------ATTAGAGTGTTGCAATTATTTTAGAACAAAAAGTTGGTTCACAAAAAAAACCA
st901 promoter TTTTTCCACTAGAGTGTTATAATCATTTTAGAATAAAAAGTT-ACTCATAAAAAATAATA
SBgLR promoter ------CACTAGAGTGTTGTAATCATTTTAGAATAAAAAGTT-ATTCAT-AAAAATAATA
tsb promoter --------AT---ATATGTCAATTCGGTTCAGTTACTTTTTTGATTTATTTGAATAAAAT
st901 promoter TATTATGTATACAATTTGTCTGTTTGGTTCAGTTATTTCTTTTATTTATTTTAATAAAAT
SBgLR promoter TATTATGTATACAATTTG----------TCAGTT-----TTCGAATTGATTGAATAAAAT

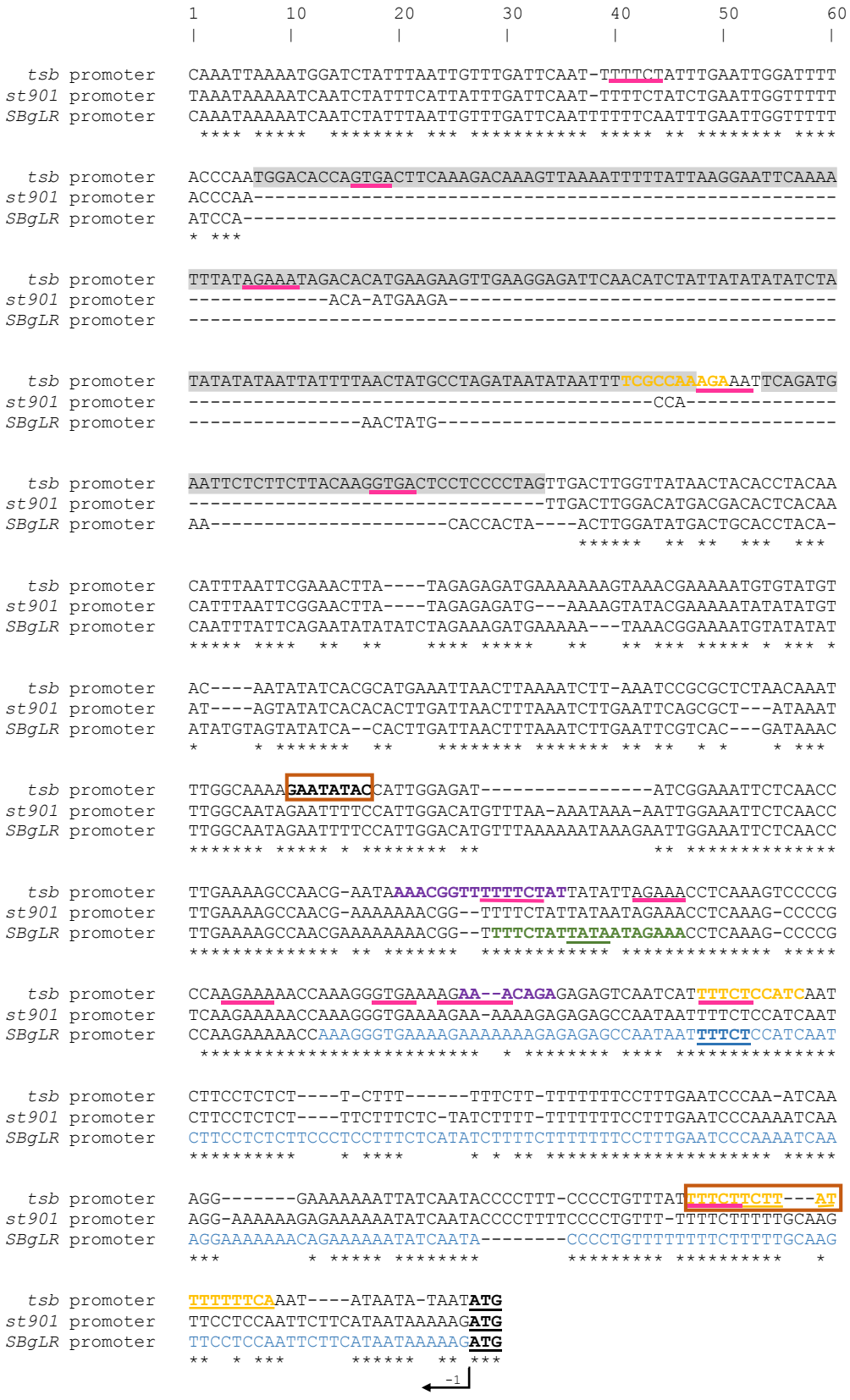
1 10 20 30 40 50 60
tsb promoter CAAATTAAAATGGATCTATTTAATTGTTTGATTCAAT-TTTTCTATTTGAATTGGATTTT
st901 promoter TAAATAAAAATCAATCTATTTCATTATTTGATTCAAT-TTTTCTATCTGAATTGGTTTTT
SBgLR promoter CAAATAAAAATCAATCTATTTAATTGTTTGATTCAATTTTTTCAATTTGAATTGGTTTTT
tsb promoter ACCCAATGGACACCAGTGACTTCAAAGACAAAGTTAAAATTTTTATTAAGGAATTCAAAA
st901 promoter ACCCAA----------
SBgLR promoter ATCCA----------
tsb promoter TTTATAGAAATAGACACATGAAGAAGTTGAAGGAGATTCAACATCTATTATATATATCTA
st901 promoter ----------ACA-ATGAAGA----------
SBgLR promoter ----------
tsb promoter TATATATAATTATTTTAACTATGCCTAGATAATATAATTTTCGCCAAAGAAATTCAGATG
st901 promoter ----------CCA----------
SBgLR promoter ----------AACTATG----------
tsb promoter AATTCTCTTCTTACAAGGTGACTCCTCCCCTAGTTGACTTGGTTATAACTACACCTACAA
st901 promoter ----------TTGACTTGGACATGACGACACTCACAA
SBgLR promoter AA----------CACCACTA----ACTTGGATATGACTGCACCTACA-
tsb promoter CATTTAATTCGAAACTTA----TAGAGAGATGAAAAAAAGTAAACGAAAAATGTGTATGT
st901 promoter CATTTAATTCGGAACTTA----TAGAGAGATG---AAAAGTATACGAAAAATATATATGT
SBgLR promoter CAATTTATTCAGAATATATATCTAGAAAGATGAAAAA---TAAACGGAAAATGTATATAT
tsb promoter AC----AATATATCACGCATGAAATTAACTTAAAATCTT-AAATCCGCGCTCTAACAAAT
st901 promoter AT----AGTATATCACACACTTGATTAACTTTAAATCTTGAATTCAGCGCT---ATAAAT
SBgLR promoter ATATGTAGTATATCA--CACTTGATTAACTTTAAATCTTGAATTCGTCAC---GATAAAC
tsb promoter TTGGCAAAAGAATATACCATTGGAGAT----------ATCGGAAATTCTCAACC
st901 promoter TTGGCAATAGAATTTTCCATTGGACATGTTTAA-AAATAAA-AATTGGAAATTCTCAACC
SBgLR promoter TTGGCAATAGAATTTTCCATTGGACATGTTTAAAAAATAAAGAATTGGAAATTCTCAACC
tsb promoter TTGAAAAGCCAACG-AATAAAACGGTTTTTTCTATTATATTAGAAACCTCAAAGTCCCCG
st901 promoter TTGAAAAGCCAACG-AAAAAAACGG--TTTTCTATTATAATAGAAACCTCAAAG-CCCCG
SBgLR promoter TTGAAAAGCCAACGAAAAAAAACGG--TTTTCTATTATAATAGAAACCTCAAAG-CCCCG
tsb promoter CCAAGAAAAACCAAAGGGTGAAAAGAA--ACAGAGAGAGTCAATCATTTTCTCCATCAAT
st901 promoter TCAAGAAAAACCAAAGGGTGAAAAGAA-AAAAGAGAGAGCCAATAATTTTCTCCATCAAT
SBgLR promoter CCAAGAAAAACCAAAGGGTGAAAAGAAAAAAAGAGAGAGCCAATAATTTTCTCCATCAAT
tsb promoter CTTCCTCTCT----T-CTTT------TTTCTT-TTTTTTTCCTTTGAATCCCAA-ATCAA
st901 promoter CTTCCTCTCT----TTCTTTCTC-TATCTTTT-TTTTTTTCCTTTGAATCCCAAAATCAA
SBgLR promoter CTTCCTCTCTTCCCTCCTTTCTCATATCTTTTCTTTTTTTCCTTTGAATCCCAAAATCAA
tsb promoter AGG-------GAAAAAAATTATCAATACCCCTTT-CCCCTGTTTATTTTCTTCTT---AT
st901 promoter AGG-AAAAAAGAGAAAAAATATCAATACCCCTTTTCCCCTGTTT-TTTTCTTTTTGCAAG
SBgLR promoter AGGAAAAAAACAGAAAAAATATCAATA--------CCCCTGTTTTTTTTCTTTTTGCAAG
tsb promoter TTTTTTCAAAT----ATAATA-TAATATG
st901 promoter TTCCTCCAATTCTTCATAATAAAAAGATG
SBgLR promoter TTCCTCCAATTCTTCATAATAAAAAGATG
-1

Format code	Motif (consensus sequence is indicated when different to the found one)	Sequence (5´→3´)	Prediction/ Demonstrated	Source
–●–	Late pollen-specific cis-regulatory elements.	AGAAA (x9)	Predicted	Eyal et al., 1995; Bate and Twell, 1998
		TTTCT (x6)	Predicted	Hamilton et al., 1998; Chang et al., 2017
		GTGA (x4)	Predicted	Rogers et al., 2001; Twell et al., 1991
		AAATGA (x1)	Predicted	Weterings et al., 1995
–●–	Palindromic repressor	TTTCTATTATAATAGAAA	Demonstrated	Chang et al., 2017
–●–	Defense and stress responsiveness motifs (TC-rich repeats). Consensus ATTTTCTTCA	AATAAAAT (reversed) TCGCCAAAGA TTTCTCCATC TTTCTTCTT ATTTTTTTCA	Predicted	PlantCARE database
	MYB binding site involved in drought-inducibility	TAACTG (reversed)	Predicted	PlantCARE database
–●–	ABA responsive element (ABRE)	TACGTG (reversed)	Predicted	PlantCARE database
	Ethylene responsive element (ERE)	ATTTCAAA (reversed)	Predicted	PlantCARE database
	Salicylic Acid responsive element (TCA element). Consensus CCATCTTTTT	CCAACTTTTT (reversed)	Predicted	PlantCARE database
	MYB binding site for flavonoid synthesis. Consensus aaaAaaC(G7C)GTTA	ATAGAAAAAACCGTTT (reversed)	Predicted	PlantCARE database
	GA responsive element (GARE)	AACAGA	Predicted	PlantCARE database
–●–	Mycorrhizal responsive element MYCS. Consensus TTTCTTGTTCT	TTTCTTCTTAT	Predicted	Chen et al., 2011
	Phosphate starvation response-associated Binding site (PHR1 binding site, P1BS). Consensus GnATATnC	GAATATAC	Predicted	Rubio et al., 2001

Figure 13. Cis-regulatory elements predicted in the *tsb* promoter and alignment with the promoter of its potato homologs *st901* and *SBgLR*. Alignment of the *tsb* promoter with the promoter region of its potato homologs *st901* and *SBgLR*, both non-mycorrhizal induced genes. Putative cis-regulatory elements are marked, including those involved in pollen-specific expression or mycorrhizal-associated expression, as well as those predicted to respond to defense, stress, drought or hormones. Prediction is supported on the PlantCARE database, as well as on sequence homology with the well-studied *SBgLR* promoter, and the identification of some putative motifs of interest previously described in the literature. Cloned region of the *tsb* promoter from -1494 to -1, numbered from the starting translation site (+1) is indicated with arrows. 5´UTR of *SBgLR* gene (Chang et al., 2017) is indicated in blue. The two grey dashed regions indicate zones with lack of homology with the other *tsb*-like promoters and are suggested to contain mycorrhizal-specific cis-elements. The identical residues are indicated with "*".

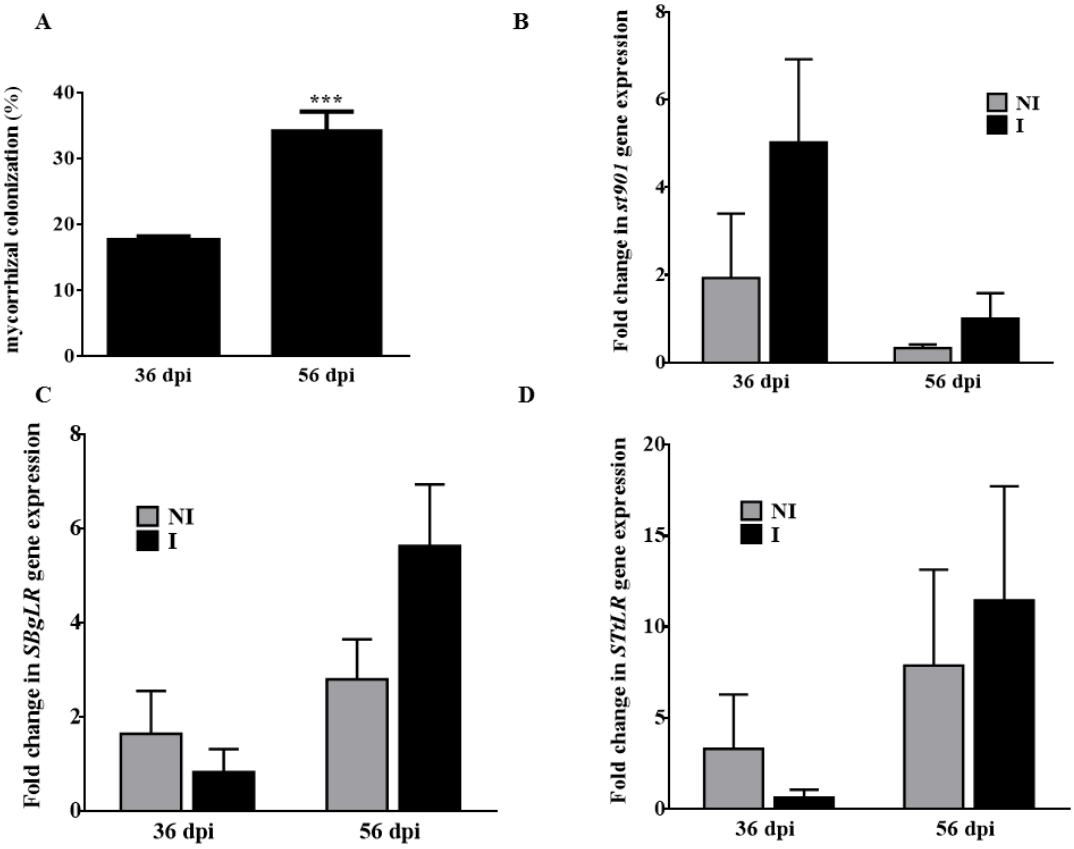

Figure 14. Mycorrhizal colonization and expression analysis of the potato *tsb* homolog genes *st901*, *SBgLR* and *STtLR* in *Solanum tuberosum* ssp. Andigena plants non-inoculated (NI) and inoculated (I) with the AM fungi *R. irregularis*. After 36 and 56 dpi (days post-inoculation), the percentage of total root length colonized by *R. irregularis* was measured (A) and *st901* (B), *SBgLR* (C) and *STtLR* (D) gene expression was analyzed by qPCR. qPCR data represents the relative gene expression in plants with respect to expression in non-colonized plants at 32 dpi , in which expression was designated as 1. Values correspond to mean±SE (n=3). Significant differences (Student´s *t*-test) between the mutant and the control are indicated with asterisks (*$P < 0.05$).

Functional analysis of *tsb* gene in tomato RNAi and overexpression composite plants

Tomato RNAi and overexpressing plants for the *tsb* gene were obtained in order to perform a functional analysis of this gene. The RNAi experiment was carried out using composite plants with hairy roots transformed with the control empty vector (pK7GWIWG2_II-RedRoot) and the *tsb* RNAi construct (pK7GWIWG2_II-RedRoot::i*tsb*). We tested the expression level of the *tsb* gene in the roots of these

RNAi plants after 45 dpi and we obtained a successful repression of the *tsb* gene by 77.66%±4.70, as shown in Fig. 15.

For the overexpression (OE) experiment the control empty vector (pUBIcGFP-DR) and the *tsb* OE vector (pUBIcGFP-DR) were used for the transient transformation, and 45 days after inoculation with the AM fungus *R. irregularis* a significant upregulation of *tsb* by 619%±1.77 was obtained in the OE hairy roots (Fig. 15B).

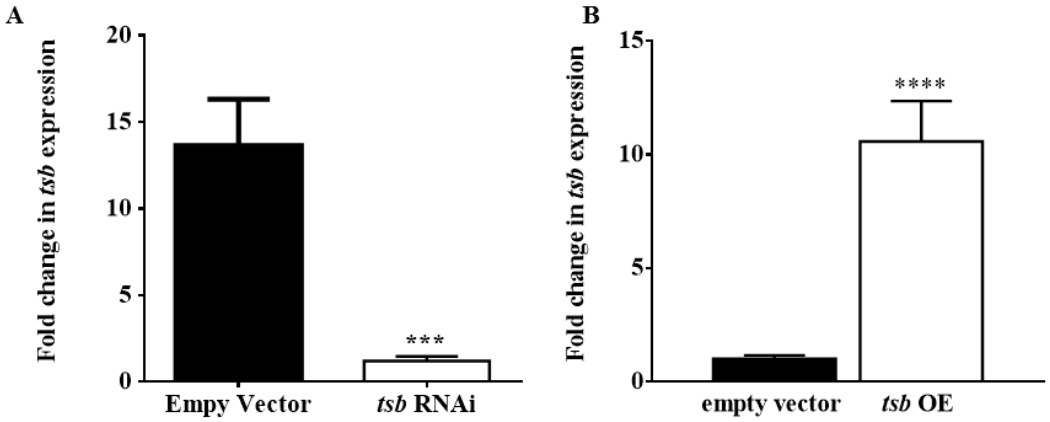

Figure 15. *tsb* gene expression in hairy roots of *tsb* RNAi and *tsb* overexpressing AM colonized composite plants. The transcript abundance of the *tsb* gene was quantified by qPCR of hairy roots from *tsb* RNAi (A) and *tsb* overexpressing (B) composite plants 45 days after infection with *R. irregularis*. The *tsb* gene expression data was represented with respect to *tsb* RNAi roots in (A), and to the control plants containing the empty vector pUBIcGFP-DR in (B), in which the expression level was designated as 1 (n≥6). Values correspond to mean ± SE. Significant differences (Student´s t test) between the mutant and the control are indicated with asterisks (***$P < 0.001$; ****$P < 0.0001$).

In the *tsb* RNAi and *tsb* OE hairy roots we observed alterations in hairy root development, modifications in the mycorrhization pattern, as well as changes in the cortical microtubule array of root cells. Particular changes are detailed below.

tsb has a role in root development

We observed that growth of new hairy roots was much more difficult in the *tsb* RNAi composite plants than in the control plants. In fact, 48% (39 out of 80) of composite control seedlings resulted to develop positively transformed roots with the empty vector two weeks after inoculation with *A. rhizogenes*, while, in contrast, only 22% of seedlings (18 plants with hairy roots/80 total plants) had developed transformed *tsb* RNAi roots by the same time. Older composite plants also kept this pattern. 45 days after transferring the plants to pots, growth of transformed *tsb* RNAi roots was impaired (not significant, P=0.138) (Fig. 16A), while it was observed a significant induced growth of hairy roots in the *tsb* overexpressing composite plants both in the non-inoculated and in the *R. irregularis*-inoculated plants (Fig. 16B). Although the main role of *tsb* may be related to pollen development and AM root colonization, this gene might also have some function in root development, probably mainly in the first stages. This possible role is in agreement with our results regarding some expression of the *tsb* gene in non-mycorrhizal roots, as seen in the *tsb* organ analysis (Fig. 6), the RNAseq data from the eFP tomato brower (Fig. 7), and the *tsb* promoter activity observed in the central cylinder and pericycle of non-inoculated roots (Fig. 3A, B).

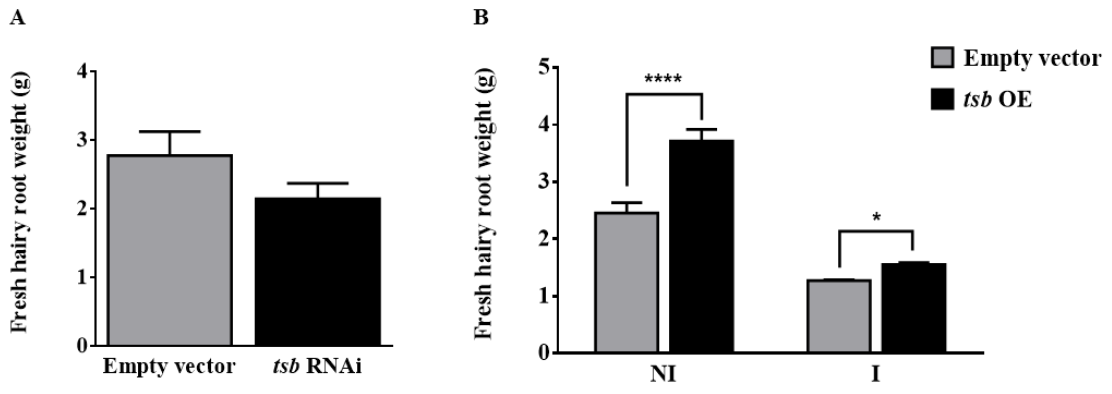

Figure 16. Fresh weight of hairy root system in *tsb* RNAi and *tsb* OE composite plants. Amount of developed hairy roots was measured in terms of fresh weight in *tsb* RNAi (A) and *tsb* OE (B) composite non-inoculated (NI) and inoculated (I) plants by *R. irregularis* after 45 dpi. Values are the mean ± SE (n>7). Significant differences (LSD multiple comparison test) between *tsb* gene expression in different plant organs are indicated with asterisks (*P < 0.05; ****P < 0.0001).

tsb plays a role during AM mycorrhization

Analysis of the percentage of mycorrhization in the *tsb* RNAi and *tsb* overexpressing roots revealed important changes. *tsb* RNAi roots, compared to the control roots presented a significant increase (144.6%±10.81, $P<0.05$) in the percentage of root length colonized by the AM fungus (Fig. 17A), as well as a significant increase in arbuscule abundance in colonized roots, as shown in Fig 17B.

In view of these results, we wondered if the contrary response occurred in the *tsb* overexpressing inoculated composite plants harvested after 43 and 65 days post-inoculation (dpi) with the AM fungus *R. irregularis*. Although not significant, overexpression of *tsb* tends to have the opposite effect in root length colonization with respect to *tsb* RNAi at two harvest times. Attending to the average values, it was observed a 21% and a 6.52% decrease in *tsb* expression in the mycorrhized root length of *tsb* OE roots at 43 and 65 dpi, respectively (Fig. 18A). Similarly, measurements of mycorrhization parameters did not reveal significant changes between control and *tsb* OE plants (Fig. 18B).

In order to check if the mycorrhization response in the *tsb* OE roots was specific of the AM fungus species, a similar assay was performed with another AM fungus, named *Funneliformis mosseae* (Schüßler and Walker 2010), formerly known as *Glomus mosseae*. Composite tomato plants overexpressing the *tsb* gene and inoculated with the AM fungus *F. mosseae* were collected at 66 dpi and the percentage of root colonized was analyzed. In this case a significant increase (28.64%, $P<0.05$) in the percentage of colonized root was observed in the *tsb* OE hairy roots (Fig. 18A).

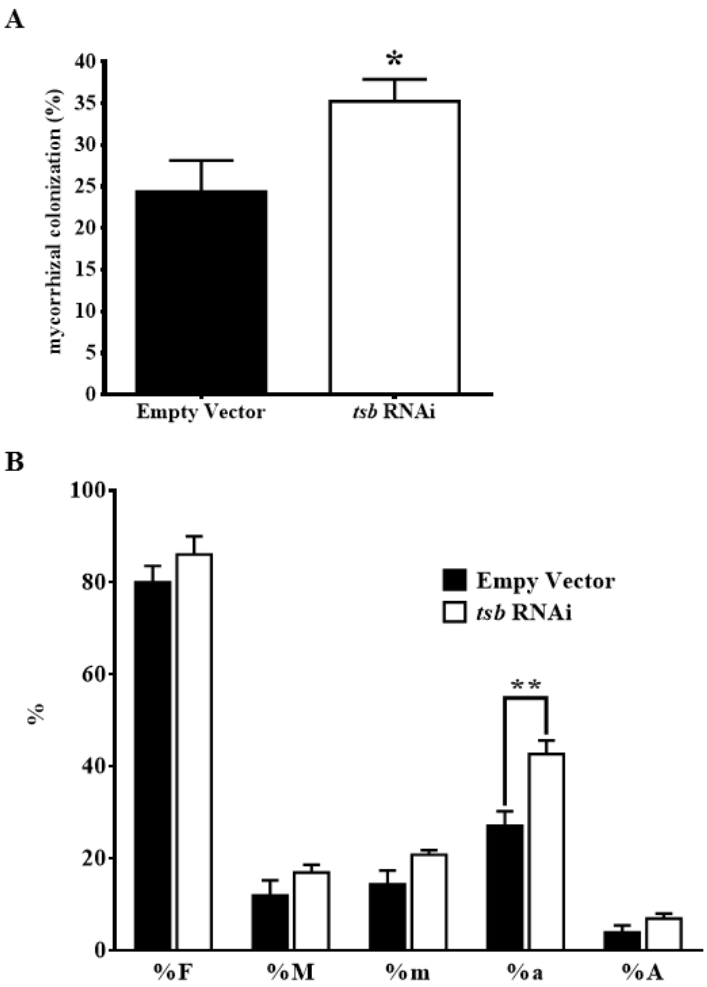

Figure 17. Mycorrhizal colonization at the histological level in *tsb* RNAi composite tomato plants 45 days after inoculation with AM fungus *R. irregularis.* After 45 dpi (days post-inoculation) the percentage of total root length colonized by *R. irregularis* was measured (A) and the mycorrhization parameters were analyzed (B) by visualization of tripan blue stained hairy roots transformed with the empty vector or the *tsb* RNAi vector (n=8). Values correspond to mean ± SE. Significant differences (Student´s *t*-test) between the mutant and the control are indicated with asterisks (*$P < 0.05$; **$P < 0.01$).

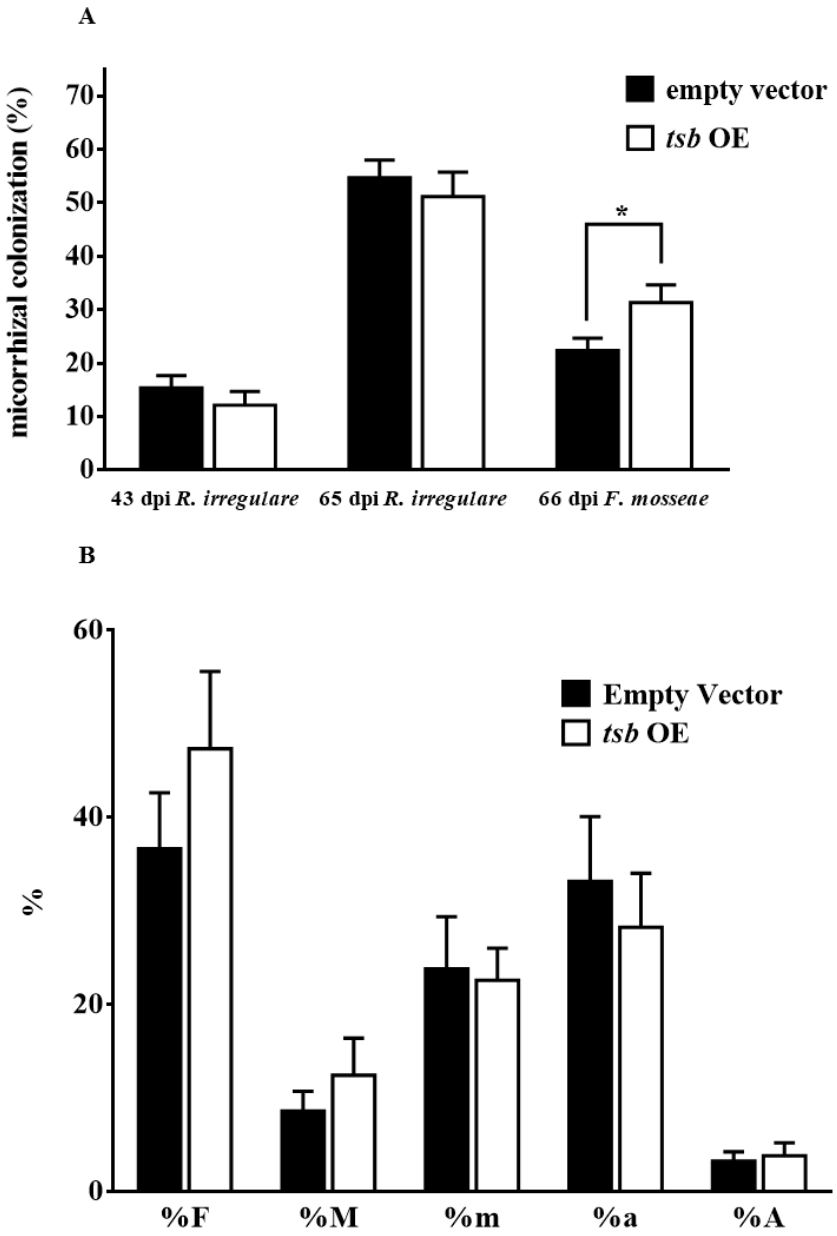

Figure 18. Mycorrhizal colonization in *tsb* overexpressing roots of composite tomato plants after inoculation with the AM fungi *R. irregularis* and *F. mosseae.* (A) is the percentage of total root length colonized by *R. irregularis* measured at 43 and 65 dpi (n=11) of control and *tsb* OE hairy roots. The corresponding data for an independent experiment with *Funneliformis mossae* infected roots at 66 dpi is shown in the same graph. (B) are the mycorrhizal parameters in the 43 dpi - *R. irregularis* inoculated roots. Values correspond to mean ± SE. Significant differences (Student´s t test) between the mutant and the control are indicated with asterisks (*$P < 0.05$).

In order to corroborate these results at a molecular level, we decided to test if the overall increase in the mycorrhization of the *tsb* RNAi hairy roots was accompanied by an increase in the *R. irregularis* (*GinEF*) and the *S. lycopersicum* (*SlPT4*) marker genes associated to the mycorrhization process. Surprisingly, we obtained the

opposite result to the expected one. *GinEF* and *SlPT4* were somewhat downregulated in the *tsb* RNAi roots (Fig. 19), indicating a decrease in both the AM fungal and the mycorrhizal root-associated activity. In view to the unexpected results concerning a decrease trend of AM functional activity in *tsb* RNAi roots, despite an observable increase in the colonized root length and the arbuscule abundance, we decided to analyse the expression of other tomato marker genes that are also upregulated during the mycorrhization process. The expression of those genes which were putative orthologues to previously described gene markers for arbuscule functionality was unaffected or somewhat diminished in *tsb* RNAi mycorrhizal roots (Fig. 19). These genes included the mycorrhiza-induced *RAM1* (Gobbato et al. 2012), the *EXO84*, a gene coding for a protein which ,together with *EXO70i*, is implicated in the exocytosis program associated with arbuscule development (Zhang et al. 2015b; Genre et al. 2011), and an ammonium transporter gene from the *AMT2-2* family also involved in arbuscule development and life span (Breuillin-Sessoms et al. 2015). The results suggest that the arbuscule functionality were moderately repressed in the *tsb* RNAi hairy roots, despite the observable increase in AM colonization and arbuscule abundance.

As done for the *tsb* RNAi hairy roots, the expression of a sub-set of genes required for arbuscule functionality (*SlPT4, RAM1, EXO84,* and *AMT2-2*) was quantified in the *tsb* OE hairy roots, this time including also a *STR* gene coding for an ABC transporter essential for arbuscule development (Zhang et al. 2010). Due to the different colonization dynamics of both fungi used, plants inoculated with *F. mosseae* collected at 65 dpi had a similar colonization level to those inoculated with *R. irregularis* at 43dpi. For this reason, we decided to analyze gene expression in parallel for these two sets of plants. Transcripts accumulation was detected only in mycorrhizal plant roots and a similar expression pattern was noted for all genes examined, independently of the fungal inoculum. In most cases the expression of marker genes in *tsb* OE mycorrhizal hairy roots at least doubled the expression achieved in control mycorrhizal hairy roots (Fig. 20). This result indicated that *tsb* is clearly involved in arbuscule activity and *tsb* OE facilitate the functionality of arbuscules.

These results confirm that the AM symbiotic responses in the host plant were repressed in the *tsb* RNAi and induced in *tsb* OE hairy roots, despite the observable opposite effect on AM colonization and arbuscule abundance.

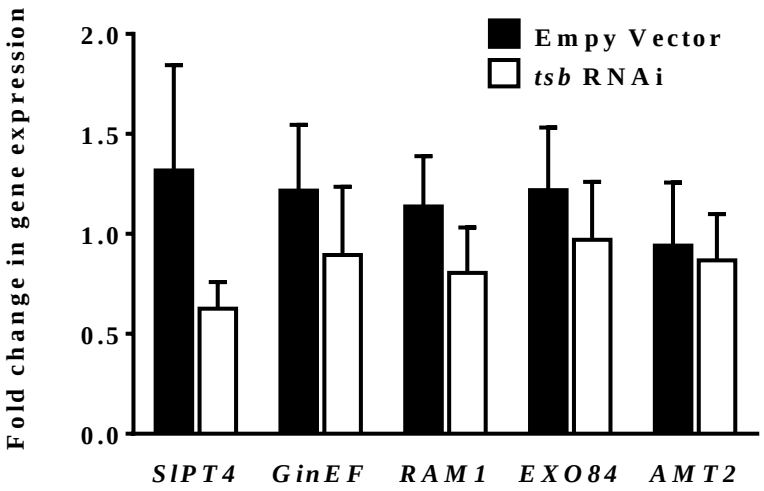

Figure 19. Expression of AM-related genes in *tsb* RNAi hairy roots of composite tomato plants inoculated with the AM fungus *R. irregularis.* After 45 dpi, expression of *GinEF* fungal activity-marker gene and *SlPT4* tomato arbuscule activity marker, were measured by qPCR in *tsb* RNAi hairy roots (A) . The expression of several other AM-upregulated tomato genes was also analyzed in the same *tsb* RNAi hairy root samples (B). qPCR data represents the relative transcript abundance for each gene measured in hairy root systems of *tsb* RNAi composite plants with respect to the expression in the control plants transformed with the empty vector, in which expression was designated as 1 (n>5). The common GenBank/RefSeq accession number for each gene is indicated between brackets. Values correspond to mean ± SE. A gene repression trend in *tsb* RNAi hairy roots is observed for all marker genes analyzed. However, significant differences (Student´s t test) between the mutant and the control were not found.

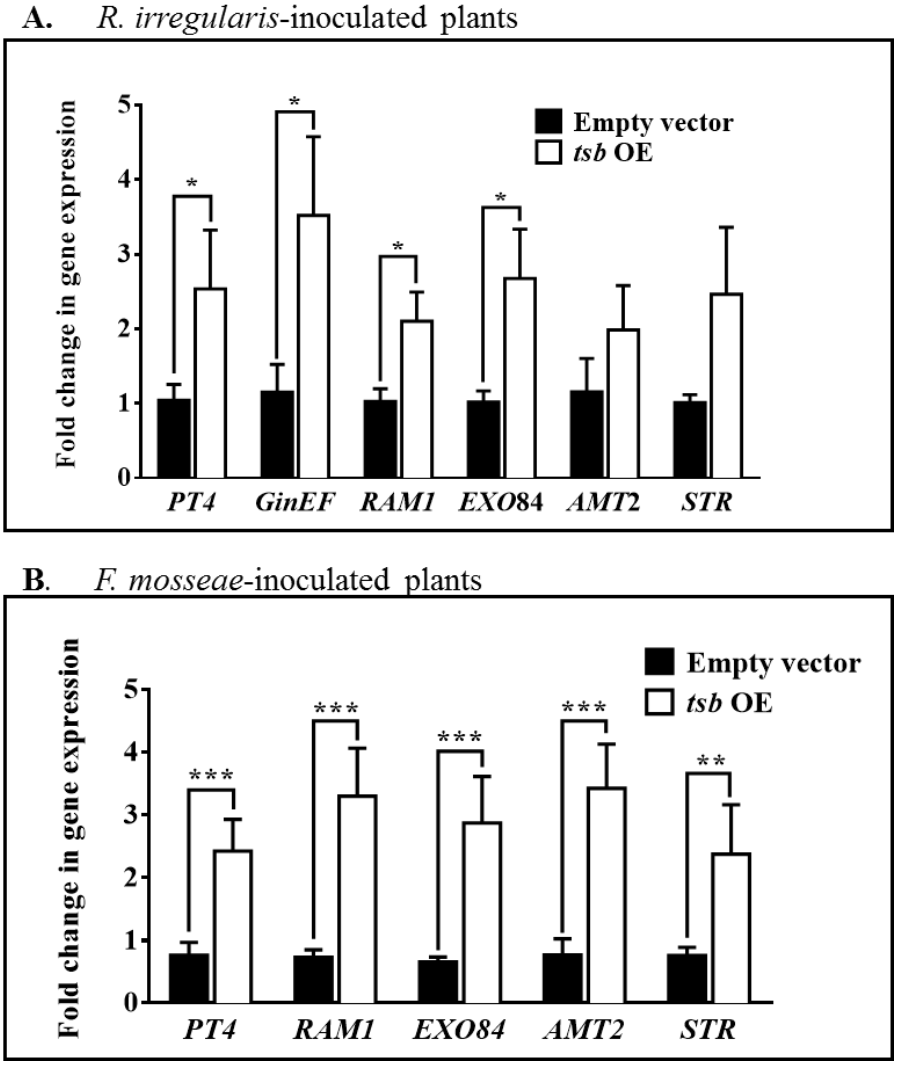

Figure 20. Expression of AM-related genes in *tsb* OE hairy roots of composite tomato plants inoculated with the AM fungus *R. irregularis* or *F. mosseae.* Expression of *GinEF* fungal activity-marker gene, the *SlPT4* tomato arbuscule activity marker, and several other AM-upregulated tomato genes were measured by qPCR in *tsb* overexpressing hairy roots inoculated with the AM fungus *R. irregularis* (A) and *F. mosseae* (B) at 43 and 66 dpi, respectively. qPCR data represents the relative transcript abundance for each gene measured in hairy root systems of mutated composite plants with respect to the expression in the control plants transformed with the empty vector, in which expression was designated as 1 (n>5). Values correspond to mean ± SE. Significant differences (Student´s t test) between the mutant and the control are indicated with asterisks (*$P < 0.05$; **$P < 0.01$; ***$P < 0.001$).

tsb is involved in MT cytoskeleton rearrangements in root cortex cells

Microtubule staining was carried out in order to check if TSB, as a putative MAP (Microtubule Associated Protein) induced during mycorrhization, has a role in microtubule rearrangements The control hairy roots containing the empty vector showed the typical helicoidal arrangement of MTs in the mature cortex cells already described for tomato roots (Genre and Bonfante 1997; Genre and Bonfante 1998). In contrast, non-inoculated roots overexpressing the *tsb* gene showed a differential array of MTs, consisting in more spaced MTs following a random organization(Fig. 21). A similar MT pattern modification was observed by Blancaflor et al. (2001) in *M. truncatula* roots when colonized by the AM fungus *G.versiforme*. They notified that the neighboring cortex cells to those infected by arbuscules or bordered by intercellular hyphae reorganized their cortical MTs from an helical orientation to a random orientation, suggesting that some kind of signaling between the fungus and the plant cortical cells must occur prior to penetration of the fungus, probably in order to make the non-colonized cells more susceptible to fungal penetration attempts. Blancaflor et al. (2001) also observed that this random array of cortical MTs is maintained during the initial stage of arbuscule development, but it tends to disappear as soon as the arbuscule develops and, in turn, it is formed a continuous coat of microtubules closely outlining the perifungal membrane and linking the arbuscule branches to each other, as also observed in tobacco root cells colonized by the AM fungus *G. margarita* (Genre and Bonfante 1997; Genre and Bonfante 1998). In view of these results, we may hypothesize that the specific induction of *tsb* in arbusculated cells of mycorrhizal roots, as revealed by our GUS *tsb* promoter reporter assay, might be important in cell wall loosening and facilitate the colonization by the AM fungus.

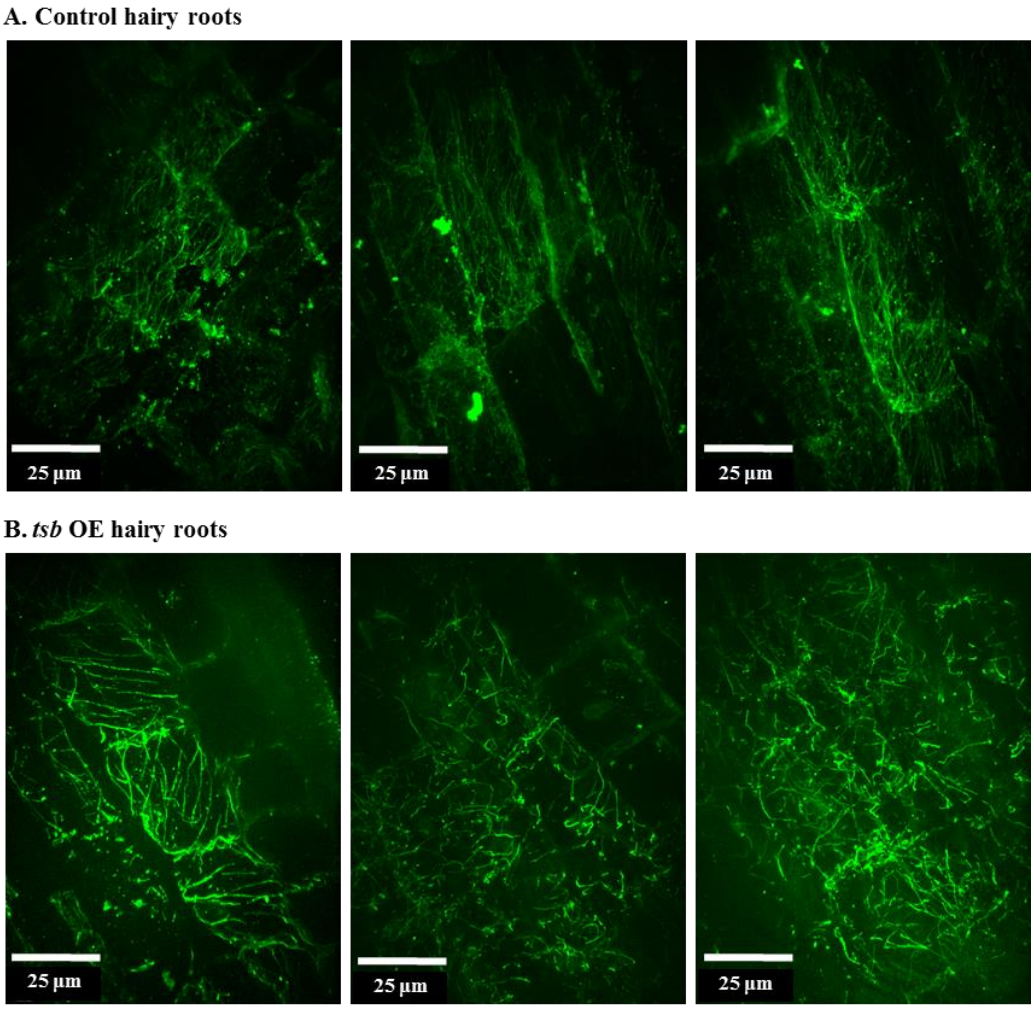

Figure 21. Microtubule immunostaining in mature cortical root cells of control and *tsb* overespressing hairy roots. Images correspond to the cortex zone of hairy roots of 40 days old-composite tomato plants subjected to vibratome sectioning and microtubule immunostaining. Control roots transformed with the empty vector pUBIcGFP-DR exhibited a tipical helicoidal MT array (A), while *tsb* overexpressing roots showed less MTs displaying a more disorganized arrangement (B). Images taken at the Perkin Elmer Ultraview ERS spinning disk confocal microscope.

Microtubule staining of *tsb* RNAi hairy roots from non-inoculated plants was also performed, but it did not revealed any noticeable difference with respect to the control plants containing the empty vector pK7GWIWG2II-RedRoot (data not shown). This could be due to the fact that *tsb* in roots is mainly a mycorrhizal induced gene, and then both the *tsb* RNAi and the control roots under non-inoculation conditions presented similar low levels of *tsb*, unable to provoke an observable structural change on the cortical microtubule array.

As the *tsb* is induced in roots during the mycorrhization process, we proceeded to test if the silencing of *tsb* affects the MT array in *R. irregularis* colonized roots by a co-localization fluorescent staining of the MTs and the AM fungus of arbusculated cortex cells. The same experiment was performed with *tsb* OE AM colonized roots. We did not find any difference in either the *tsb* RNAi and *tsb* OE arbuscule containing cells with respect to the control ones (Fig. 22). The MT pattern observed is similar in the three cases, consisting in a net of MTs enveloping the arbuscule branches and the trunk, as previously described by other authors (Genre and Bonfante 1998; Blancaflor et al. 2001). This result suggest that once the fungal hyphae penetrates the cortex root cells, the MT cytoskeleton tend to surround the arbuscule, making it difficult to observe the possible differences in the MT organization and/or the amount of MTs in the mutant hairy roots.

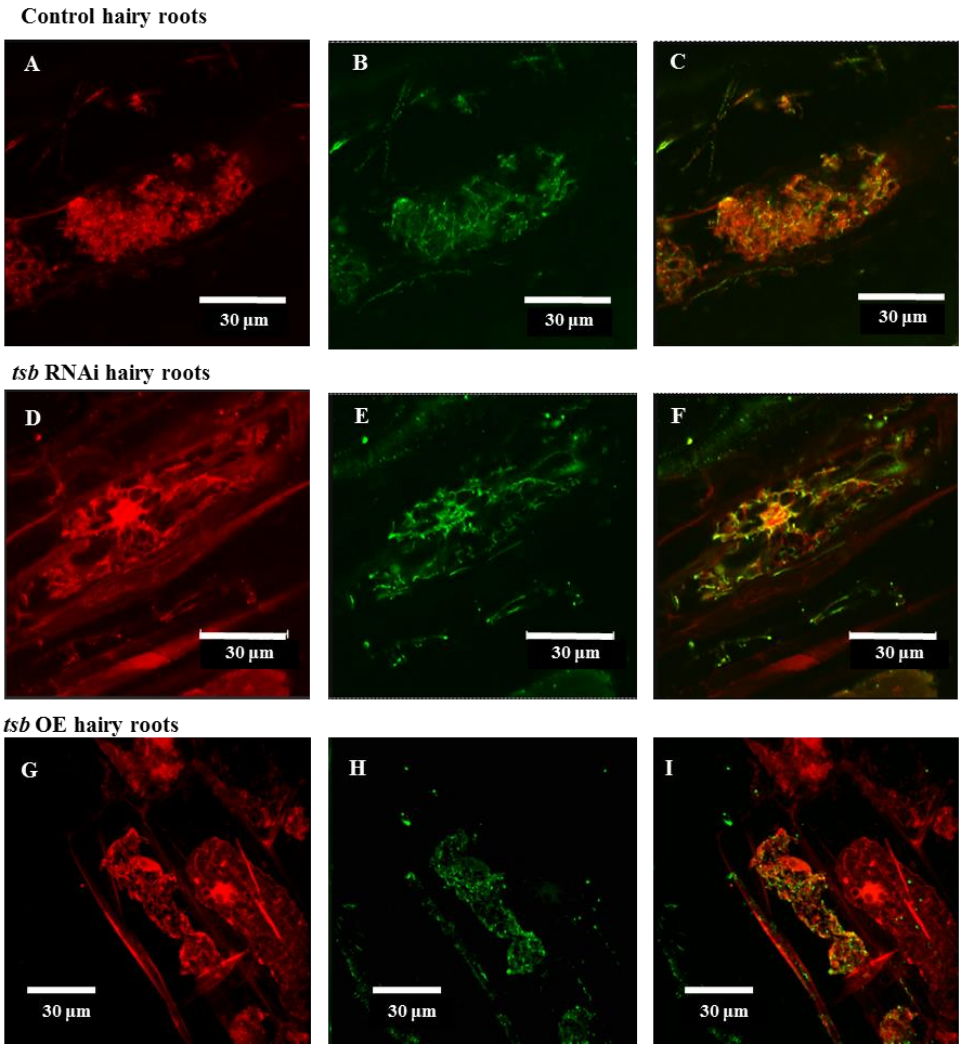

Figure 22. Microtubule and AM fungus co-localization staining in arbuscule-containing cortical root cells of control, *tsb* RNAi and *tsb* OE hairy roots. Images

correspond to vibratome sections of arbuscule-containing cells 40 days after inoculation with *R. irregularis*. Sections were subjected to microtubule green inmunostaining (B, E, H) and AM fungal fluorescent WGA-Texas red stanining (A, D, G). The merge images (C, F, I) are shown. Images were taken at the Perkin Elmer Ultraview ERS spinning disk confocal microscope.

Discussion

tsb gene is highly induced during mycorrhization (García Garrido et al. 2010; López-Ráez et al. 2010) and encodes a putative MAP, as predicted here by homology search and amino acid motif analysis. Orthologs of the encoded protein TSB are only found in species from the *Solanaceae* family, indicating that this gene belongs to a family-specific group of proteins, here named as TSB-like proteins (Fig. 8).

In view of all the results regarding the functional analyses performed here, we propose a model for the role of *tsb* during mycorrhization, which is summarized in Fig. 23.

During mycorrhization the *tsb* gene expression is induced (Fig. 1). This *tsb* upregulation is specific of the arbuscule-containing cells, as shown by the *tsb* promoter-GUS transformed roots obtained in this work (Fig. 3 and 4). The encoded protein, TSB, is a putative MAP, and then it may function binding the microtubules of these arbuscule-infected cells and changing its conformation (Struk and Dhonukshe 2014), probably to a more random array, as we probed using *tsb* OE composite plants and MT immunostaining (Fig. 19). This switch from an helicoidal cortical MT arrangement to a random one has also been previously observed in root cortex cells at the initial steps of arbuscule development and in the adjacent cells to the infected ones (Blancaflor et al. 2001).

It is well-documented that MTs play a crucial role in the transport of vesicles and organelles through the animal cells (Phaire-Washington et al. 1980; Allen et al. 1985). In plants, the major role ascribed to cortical MTs in interphase cells is to embed the cellulose synthase complexes in the plasma membrane (Crowell et al. 2009; Gutierrez et al. 2009) and guide their movement along the membrane

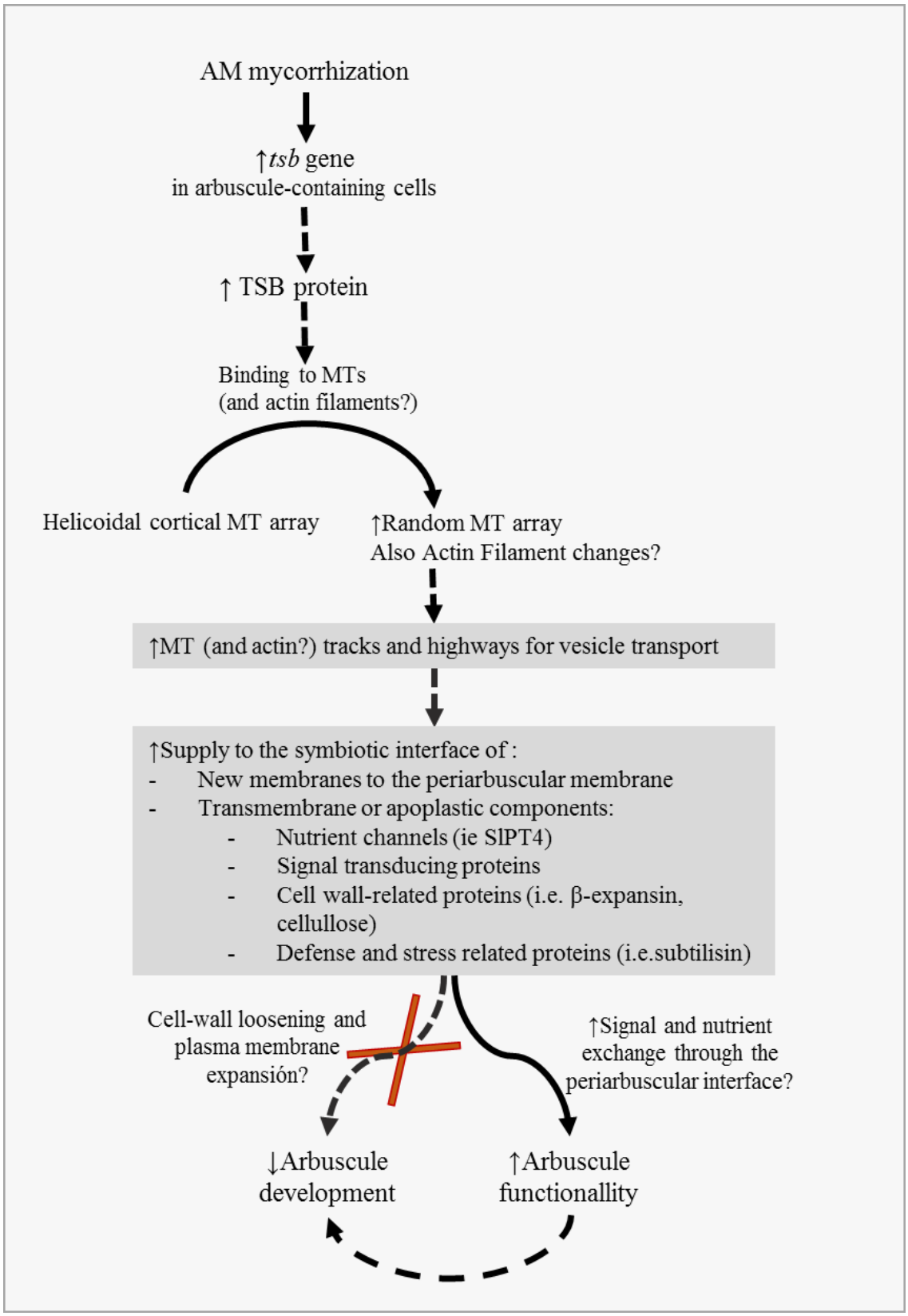

Figure 23. Hypothetical model of action of *tsb* gene during the AM symbiosis. *tsb* induction occurs in cells colonized by arbuscules. The putative MAP encoded by *tsb* might be involved in the MT (and probably also actin) cytoskeleton rearrangements occuring in the arbuscule-containing cells. Very likely, *tsb* mediated-cytoskeleton modifications might be headed for establisment of a new net of MT (and maybe also actin) that allow the proper

transport (or embedding) via vesicles of membranes, as well as transmembrane and apoplastic proteins or compounds, to the symbiotic interfase comparment required for arbuscule functionallity. Solid arrows indicate proved effects of *tsb*-induction during mycorrhization, while dashed arrows indicate expected effects of *tsb* induction (also accompained with a question mark "?") or causal associations previously reported. The strikethrough arrow indicate not observed effects.

(Paredez et al. 2006; Bringmann et al. 2012; Li et al. 2012), and it has been proposed that MTs determine the orientation of cellulose microfibrils (Baskin 2001; Lloyd 2011). Moreover, some evidences also exist about the involvement of cortical MTs in non-cellulosic polysaccharide release or assembling during cell wall biogenesis (Swamy et al. 2015; McFarlane et al. 2008), and their participation in vesicle trafficking in plant cells of cell wall material (Zhu et al. 2015; Oda et al. 2014; Kong et al. 2015) and membranous cargoes (Yamada et al. 2017).

A particular array of microtubules is found in cells subjected to a strong polarization, such as root hairs, pollen tubes and cells undergoing cytokinesis, and -/with the required directional growth, the expansion of plasma membrane, and/or the specific deposition of cell wall and membrane components at the growing tip and at the cell plate (Muller and Jurgens 2016; Sieberer et al. 2005; Cai et al. 2017). In fact, *tsb* gene is pollen-specific expressed as previously described by Zhao et al. (2003) and corroborated by our data (Fig. 6), and it is expected to encode a MAP involved in microtubule rearrangements during pollen development. However, our finding related to its additional mycorrhizal-specific expression raise the idea of *tsb* as a player in MT reorganization also in AM infected cells.

In cells containing AM arbuscules is also crucial the establishment of a specialized cell wall and membrane surrounding the arbuscule for mycorrhizal development and functioning (Balestrini and Bonfante 2014). Thus, it is required a polarized and asymmetric delivery of cell wall components (Balestrini et al. 2005; Takeda et al. 2009) and intrinsic membrane proteins (Pumplin et al. 2012; Kobae and Hata 2010). In fact, it is reported that arbuscule development is accompanied by a specific vesicle trafficking (Harrison and Ivanov 2017; Gavrin et al. 2016; Huisman et al. 2016; Zhang et al. 2015b). Strong cytoskeletal rearrangements are also reported in arbuscule-containing cells, and its relation with the modification of the

periarbuscular membrane and the apoplastic compartment has been previously suggested (Blancaflor et al. 2001; Genre and Bonfante 1999). Nevertheless, so far, lack of evidence supports this hypothesis and, in addition, Timonen et al. (2006) reported that disruption of microtubules with oryzalin in tomato AM infected roots did not have a clear effect on AM colonization or hyphal growth. In this regard, the identification of the tomato mycorrhizal-responsive MAP, *tsb*, possessing a MT rearrangement ability (Fig. 21) and the study of its functional role on mycorrhization could help us to decipher the role of MT alterations during mycorrhization.

The observed switch in *tsb* OE root cortex cells from a helicoidal cortical MT arrangement to a random one was not apparently related to cell wall loosening or to facilite the arbuscule development in the infected cells. Moreover, arbuscule abundance and mycorrhizal intensities were found to be even higher in the *tsb* RNAi than in the control plants (Fig. 17). Then, we discard the role of *tsb* as an essential gene for cell wall loosening or to allow arbuscule development.

By contrast, the examination of expression levels of arbuscule functionality marker genes (Fig. 19 and 20), indicated that *tsb* is clearly involved in arbuscule activity. The *tsb* OE mycorrhizal roots showed an overall upregulation in the expression level of several tomato genes associated to the functionality of arbuscules, such as genes coding for the mycorrhizal phosphate transporter SlPT4, the transcription factor RAM1, the ammonium transporter AMT2-2, the exocytosis-related protein EXO84, and the ABC transporter STR (Fig.20).

Then, putting together our results and previous evidences regarding the role of the MT cytoskeleton modifying the cell wall in plant cells, and the cytoskeleton rearrangements in arbuscule containing cells, we suggest that *tsb* could be a MAP responsible of developing and/or keeping a suitable MT arrangement in the arbuscule-containing cells for the required transport of vesicles or for the proper delivering, embedding or positioning of specific compounds in the periarbuscular membrane and the interface compartment.

According to the raised hypothesis it was expected that the AM fungus, as an obligate symbiont, would suffered from nutrient deficiencies under the impossibility to establish fully functional arbuscules in the *tsb* RNAi roots. At this respect, it was observed a clear decrease in the activity of the AM fungus colonizing *tsb* RNAi roots (*GinEF*) (Fig. 19A). Given the carbohydrate starvation in the AM fungus under these conditions, together with a probable impairment of plant defense responses in the disable arbuscule, it is not surprising that the AM fungus tends to colonized new root cortex cells, trying to stablish a functional symbiotic interface between the two partners in order to fulfil its nutritional requirements. These reasons could explain the higher root colonization rates that we observed in the mutated roots (Fig. 17).

In addition, it is worth mentioning that TSB amino acid sequence also contains the putative motives described for actin filament binding (Fig. 10). Several MAPs in plants have also been reported as actin binding proteins (ABPs) (Li et al. 2010; Petrasek and Schwarzerova 2009; Tsvetkov et al. 2007), including the TSB homolog SB401 (Huang et al. 2007), and interactions between actin filaments and microtubules are common in plants (Takeuchi et al. 2017). Actin filaments are also known to act as tracks or highways during for the transportation of vesicles in plant cells; moreover, the actin cytoskeleton is postulated as the major cytoskeletal component involved in membrane trafficking, in contrast to animal cells (Wang and Hussey 2015). Actin cytoskeleton rearrangements has also been previously observed in AM colonized cells (Genre and Bonfante 1998; Genre et al. 2005), then the proposed model for the action of the TSB protein on mycorrhization could be played through the organization of both the MTs and the actin filaments in order to establish the required net of transportation “tracks” towards the symbiotic interface and allow the activity and functioning of the arbuscule.

Conclusion

Among a *Solanaceae*-specific group of pollen-specific genes encoding MAPs with an essential function in pollen development, we identified the mycorrhizal-responsive *tsb* gene. This gene is specifically expressed in the arbuscule containing cells and has the ability to rearrange the MT cytoskeleton, although we do not discard an additional role on the actin cytoskeleton.

Functional analysis indicated that *tsb* has an essential role in AM functionality. Then, this work provides the first hint of the role of the microtubule cytoskeleton rearrangements during mycorrhization. At the same time, it is relevant the fact that this paper provides insights pointing to the existence of a specific biological machinery commonly shared between two types of cells undergoing a strong membrane polarization, the arbuscule-containing cells and the pollen tube, as previously suggested by other authors (Nguema-Ona et al. 2012; Nouri and Reinhardt 2015).

Future perspectives

Further research is needed to effectively confirm that TSB protein is a MT or Actin Binding protein (ABP). Although *in vitro* assays of binding and bundling of tubulin and actin to and by TSB-homologs have been performed (Huang et al. 2007; Liu et al. 2013), no data exists regarding to TSB. Furthermore, the *in vivo* localization of the TSB protein is still unknown, and future research about hairy root transformation of the TSB-tagged protein to test putative microtubular location in combination with appropriate cellular markers, would be useful.

If it is the case that TSB is also an ABP, it would be interesting to test if TSB acts as a connector between both cytoskeletal components (MTs and actin filaments), as occurs with its close homolog SB401 from *Solanum berthaultii* (Huang et al. 2007), and it would be worth to check if actin cytoskeleton arrays are perturbed in *tsb* mutated roots.

In our study we report a*tsb* role for arbuscule functionality. We hypothesize that it is caused through the *tsb* cytoskeleton modifying action, that allow proper transport of vesicles for membrane expansion, cell wall material deposition and location of new transmembrane proteins in the symbiotic interface. However, it would be necessary to elucidate the specific changes in cytoskeleton remodeling during mycorrhization in disturbed *tsb* RNA interference or overexpressing hairy roots. These changes should also be correlated with specific alterations in the periarbuscular membrane.

Tsb signals regulation pathway during mycorrhization remains unknown, and the specific common induction of the *tsb* gene in both arbuscule-containing cells and the pollen tube opens the question whether some common regulatory mechanisms regulate both processes, and whether *tsb* is differently regulated in mycorrhized roots and pollen tubes. Analysis of the *tsb* promoter and the promoter of its close homologs, all of them pollen-specific genes, reveal high degree of similarity , but some extra domains are present in the *tsb* promoter, pointing out to the possibility that these additional domains were evolutionary inserted in order to allow *tsb*-response to mycorrhization. Current research is being performed in this direction, and a series of *tsb* promoter-GUS deletion constructs would give some light on the regulation mechanisms of this gene expression during mycorrhization and the putative identification of new AM-responsive cis-elements.

Bibliography

Alexander T, Toth R, Meier R, Weber HC (1989) Dynamics of arbuscule development and degeneration in onion, bean, and tomato with reference to vesicular–arbuscular mycorrhizae in grasses. Can J Bot 67 (8):2505-2513

Allen RD, Weiss DG, Hayden JH, Brown DT, Fujiwake H, Simpson M (1985) Gliding movement of and bidirectional transport along single native microtubules from squid axoplasm: evidence for an active role of microtubules in cytoplasmic transport. J Cell Biol 100 (5):1736-1752

Balestrini R, Bonfante P (2014) Cell wall remodeling in mycorrhizal symbiosis: a way towards biotrophism. Front Plant Sci 5:237. doi:10.3389/fpls.2014.00237

Balestrini R, Cosgrove DJ, Bonfante P (2005) Differential location of alpha-expansin proteins during the accommodation of root cells to an arbuscular mycorrhizal fungus. Planta 220 (6):889-899. doi:10.1007/s00425-004-1431-2

Baratier J, Peris L, Brocard J, Gory-Faure S, Dufour F, Bosc C, Fourest-Lieuvin A, Blanchoin L, Salin P, Job D, Andrieux A (2006) Phosphorylation of microtubule-associated protein STOP by calmodulin kinase II. J Biol Chem 281 (28):19561-19569. doi:10.1074/jbc.M509602200

Baskin TI (2001) On the alignment of cellulose microfibrils by cortical microtubules: a review and a model. Protoplasma 215 (1-4):150-171

Bate N, Twell D (1998) Functional architecture of a late pollen promoter: pollen-specific transcription is developmentally regulated by multiple stage-specific and co-dependent activator elements. Plant Mol Biol 37 (5):859-869

Blancaflor EB, Zhao L, Harrison MJ (2001) Microtubule organization in root cells of *Medicago truncatula* during development of an arbuscular mycorrhizal symbiosis with *Glomus versiforme*. Protoplasma 217 (4):154-165

Blom N, Sicheritz-Ponten T, Gupta R, Gammeltoft S, Brunak S (2004) Prediction of post-translational glycosylation and phosphorylation of proteins from the amino acid sequence. Proteomics 4 (6):1633-1649. doi:10.1002/pmic.200300771

Bonfante P, Bergero R, Uribe X, Romera C, Rigau J, Puigdomenech P (1996) Transcriptional activation of a maize α-tubulin gene in mycorrhizal maize and transgenic tobacco plants. Plant J 9 (5):737-743

Breuillin-Sessoms F, Floss DS, Gomez SK, Pumplin N, Ding Y, Levesque-Tremblay V, Noar RD, Daniels DA, Bravo A, Eaglesham JB (2015) Suppression of arbuscule degeneration in *Medicago truncatula* phosphate transporter4 mutants is dependent on the ammonium transporter 2 family protein *AMT2;3*. Plant Cell 27 (4):1352-1366

Bringmann M, Li E, Sampathkumar A, Kocabek T, Hauser MT, Persson S (2012) POM-POM2/cellulose synthase interacting1 is essential for the functional association of cellulose synthase and microtubules in *Arabidopsis*. Plant Cell 24 (1):163-177. doi:10.1105/tpc.111.093575

Cai G, Parrotta L, Cresti M (2017) The Cytoskeleton of Pollen Tubes and How It Determines the Physico-mechanical Properties of Cell Wall. In: Pollen Tip Growth. Springer, pp 35-62

Crowell EF, Bischoff V, Desprez T, Rolland A, Stierhof Y-D, Schumacher K, Gonneau M, Höfte H, Vernhettes S (2009) Pausing of Golgi bodies on microtubules regulates secretion of cellulose synthase complexes in *Arabidopsis*. Plant Cell 21 (4):1141-1154

Chang Y, Yan M, Yu J, Zhu D, Zhao Q (2017) The 5' untranslated region of potato *SBgLR* gene contributes to pollen-specific expression. Planta. doi:10.1007/s00425-017-2695-7

Chen A, Gu M, Sun S, Zhu L, Hong S, Xu G (2011) Identification of two conserved cis-acting elements, MYCS and P1BS, involved in the regulation of mycorrhiza-activated phosphate transporters in eudicot species. New Phytol 189 (4):1157-1169

Deeks MJ, Fendrych M, Smertenko A, Bell KS, Oparka K, Cvrckova F, Zarsky V, Hussey PJ (2010) The plant formin AtFH4 interacts with both actin and microtubules, and contains a newly identified microtubule-binding domain. J Cell Sci 123 (Pt 8):1209-1215. doi:10.1242/jcs.065557

Durek P, Schmidt R, Heazlewood JL, Jones A, MacLean D, Nagel A, Kersten B, Schulze WX (2010) PhosPhAt: the *Arabidopsis thaliana* phosphorylation site database. An update. Nucleic Acids Res 38 (Database issue):D828-834. doi:10.1093/nar/gkp810

Emanuelsson O, Nielsen H, Brunak S, von Heijne G (2000) Predicting subcellular localization of proteins based on their N-terminal amino acid sequence. J Mol Biol 300 (4):1005-1016. doi:10.1006/jmbi.2000.3903

Eyal Y, Curie C, McCormick S (1995) Pollen specificity elements reside in 30 bp of the proximal promoters of two pollen-expressed genes. Plant Cell 7 (3):373-384

Gallou A, Declerck S, Cranenbrouck S (2012) Transcriptional regulation of defence genes and involvement of the WRKY transcription factor in arbuscular mycorrhizal potato root colonization. Funct Integr Genomics 12 (1):183-198. doi:10.1007/s10142-011-0241-4

García Garrido JM, León Morcillo RJ, Martín Rodríguez JA, Ocampo Bote JA (2010) Variations in the mycorrhization characteristics in roots of wild-type and ABA-deficient tomato are accompanied by specific transcriptomic alterations. Mol Plant-Microbe Interact 23 (5):651-664. doi:10.1094/MPMI-23-5-0651

Gavrin A, Chiasson D, Ovchinnikova E, Kaiser BN, Bisseling T, Fedorova EE (2016) VAMP721a and VAMP721d are important for pectin dynamics and release of bacteria in soybean nodules. New Phytol 210 (3):1011-1021. doi:10.1111/nph.13837

Genre A, Bonfante P (1997) A mycorrhizal fungus changes microtubule orientation in tobacco root cells. Protoplasma 199 (1):30-38

Genre A, Bonfante P (1998) Actin versus tubulin configuration in arbuscule-containing cells from mycorrhizal tobacco roots. New Phytol 140 (4):745-752

Genre A, Bonfante P (1999) Cytoskeleton-related proteins in tobacco mycorrhizal cells: gamma-tubulin and clathrin localisation. Eur J Histochem 43:105-111

Genre A, Chabaud M, Timmers T, Bonfante P, Barker DG (2005) Arbuscular mycorrhizal fungi elicit a novel intracellular apparatus in *Medicago truncatula* root epidermal cells before infection. Plant Cell 17 (12):3489-3499. doi:10.1105/tpc.105.035410

Genre A, Ivanov S, Fendrych M, Faccio A, Žárský V, Bisseling T, Bonfante P (2011) Multiple exocytotic markers accumulate at the sites of perifungal membrane biogenesis in arbuscular mycorrhizas. Plant Cell Physiol 53 (1):244-255

Gobbato E, Marsh JF, Vernié T, Wang E, Maillet F, Kim J, Miller JB, Sun J, Bano SA, Ratet P (2012) A GRAS-type transcription factor with a specific function in mycorrhizal signaling. Curr Biol 22 (23):2236-2241

Gordon-Weeks PR (2004) Microtubules and growth cone function. J Neurobiol 58 (1):70-83. doi:10.1002/neu.10266

Gutierrez R, Lindeboom JJ, Paredez AR, Emons AMC, Ehrhardt DW (2009) *Arabidopsis* cortical microtubules position cellulose synthase delivery to the plasma membrane and interact with cellulose synthase trafficking compartments. Nat Cell Biol 11 (7):797-806

Gutjahr C, Parniske M (2013) Cell and developmental biology of arbuscular mycorrhiza symbiosis. Annu Rev Cell Dev Biol 29

Hamilton DA, Schwarz YH, Mascarenhas JP (1998) A monocot pollen-specific promoter contains separable pollen-specific and quantitative elements. Plant Mol Biol 38 (4):663-669

Harrison MJ, Dewbre GR, Liu J (2002) A phosphate transporter from *Medicago truncatula* involved in the acquisition of phosphate released by arbuscular mycorrhizal fungi. Plant Cell 14 (10):2413-2429

Harrison MJ, Ivanov S (2017) Exocytosis for endosymbiosis: membrane trafficking pathways for development of symbiotic membrane compartments. Curr Opin Plant Biol 38:101-108

Harrison MJ, Pumplin N, Breuillin FJ, Noar RD, Park H-J (2010) Phosphate transporters in arbuscular mycorrhizal symbiosis. In: Arbuscular mycorrhizas: physiology and function. Springer, pp 117-135

Huang S, Jin L, Du J, Li H, Zhao Q, Ou G, Ao G, Yuan M (2007) SB401, a pollen-specific protein from *Solanum berthaultii*, binds to and bundles microtubules and F-actin. Plant J 51 (3):406-418. doi:10.1111/j.1365-313X.2007.03153.x

Huisman R, Hontelez J, Mysore KS, Wen J, Bisseling T, Limpens E (2016) A symbiosis-dedicated SYNTAXIN OF PLANTS 13II isoform controls the formation of a stable host-microbe interface in symbiosis. New Phytol 211 (4):1338-1351. doi:10.1111/nph.13973

Karandashov V, Nagy R, Wegmüller S, Amrhein N, Bucher M (2004) Evolutionary conservation of a phosphate transporter in the arbuscular mycorrhizal symbiosis. Proc Natl Acad Sci USA 101 (16):6285-6290

Kato M, Nagasaki-Takeuchi N, Ide Y, Maeshima M (2010) An *Arabidopsis* Hydrophilic Ca2+-Binding Protein with a PEVK-Rich Domain, PCaP2, is Associated with the Plasma Membrane and Interacts with Calmodulin and Phosphatidylinositol Phosphates. Plant Cell Physiol 51 (3):366-379. doi:10.1093/pcp/pcq003

Kobae Y, Hata S (2010) Dynamics of periarbuscular membranes visualized with a fluorescent phosphate transporter in arbuscular mycorrhizal roots of rice. Plant Cell Physiol 51 (3):341-353. doi:10.1093/pcp/pcq013

Komis G, Illes P, Beck M, Samaj J (2011) Microtubules and mitogen-activated protein kinase signalling. Curr Opin Plant Biol 14 (6):650-657. doi:10.1016/j.pbi.2011.07.008

Kong Z, Ioki M, Braybrook S, Li S, Ye Z-H, Lee Y-RJ, Hotta T, Chang A, Tian J, Wang G (2015) Kinesin-4 functions in vesicular transport on cortical microtubules and regulates cell wall mechanics during cell elongation in plants. Mol plant 8 (7):1011-1023

Kyte J, Doolittle RF (1982) A simple method for displaying the hydropathic character of a protein. J Mol Biol 157 (1):105-132

Lang Z, Zhou P, Yu J, Ao G, Zhao Q (2008) Functional characterization of the pollen-specific *SBgLR* promoter from potato (*Solanum tuberosum* L.). Planta 227 (2):387-396. doi:10.1007/s00425-007-0625-9

Lee TY, Bretana NA, Lu CT (2011) PlantPhos: using maximal dependence decomposition to identify plant phosphorylation sites with substrate site specificity. BMC Bioinformatics 12:261. doi:10.1186/1471-2105-12-261

Lescot M, Dehais P, Thijs G, Marchal K, Moreau Y, Van de Peer Y, Rouze P, Rombauts S (2002) PlantCARE, a database of plant cis-acting regulatory elements and a portal to tools for in silico analysis of promoter sequences. Nucleic Acids Res 30 (1):325-327

Li J, Wang X, Qin T, Zhang Y, Liu X, Sun J, Zhou Y, Zhu L, Zhang Z, Yuan M, Mao T (2011) MDP25, a novel calcium regulatory protein, mediates hypocotyl cell elongation by destabilizing cortical microtubules in *Arabidopsis*. Plant Cell 23 (12):4411-4427. doi:10.1105/tpc.111.092684

Li S, Lei L, Somerville CR, Gu Y (2012) Cellulose synthase interactive protein 1 (CSI1) links microtubules and cellulose synthase complexes. Proceedings of the National Academy of Sciences of the United States of America 109 (1):185-190. doi:10.1073/pnas.1118560109

Li Y, Shen Y, Cai C, Zhong C, Zhu L, Yuan M, Ren H (2010) The type II *Arabidopsis* formin14 interacts with microtubules and microfilaments to regulate cell division. Plant Cell 22 (8):2710-2726

Linke WA, Kulke M, Li H, Fujita-Becker S, Neagoe C, Manstein DJ, Gautel M, Fernandez JM (2002) PEVK domain of titin: an entropic spring with actin-binding properties. Journal of structural biology 137 (1-2):194-205. doi:10.1006/jsbi.2002.4468

Liu BQ, Jin L, Zhu L, Li J, Huang S, Yuan M (2009) Phosphorylation of microtubule-associated protein SB401 from *Solanum berthaultii* regulates its effect on microtubules. J Integr Plant Biol 51 (3):235-242. doi:10.1111/j.1744-7909.2008.00797.x

Liu C, Qi X, Zhao Q, Yu J (2013) Characterization and functional analysis of the potato pollen-specific microtubule-associated protein SBgLR in tobacco. PloS one 8 (3):e60543. doi:10.1371/journal.pone.0060543

Liu J, Seul U, Thompson R (1997) Cloning and characterization of a pollen-specific cDNA encoding a glutamic-acid-rich protein (GARP) from potato *Solanum berthaultii*. Plant Mol Biol 33 (2):291-300

López-Ráez JA, Verhage A, Fernandez I, Garcia JM, Azcón-Aguilar C, Flors V, Pozo MJ (2010) Hormonal and transcriptional profiles highlight common and differential host responses to arbuscular mycorrhizal fungi and the regulation of the oxylipin pathway. J Exp Bot 61 (10):2589-2601. doi:10.1093/jxb/erq089

Lloyd C (2011) Dynamic microtubules and the texture of plant cell walls. Int Rev Cell Mol Biol 287 (287):287-329

Mascarenhas JP (1990) Gene activity during pollen development. Annu Rev Plant Biol 41 (1):317-338

McFarlane HE, Young RE, Wasteneys GO, Samuels AL (2008) Cortical microtubules mark the mucilage secretion domain of the plasma membrane in *Arabidopsis* seed coat cells. Planta 227 (6):1363-1375

Muller S, Jurgens G (2016) Plant cytokinesis-No ring, no constriction but centrifugal construction of the partitioning membrane. Semin Cell Dev Biol 53:10-18. doi:10.1016/j.semcdb.2015.10.037

Nagy A, Cacciafesta P, Grama L, Kengyel A, Malnasi-Csizmadia A, Kellermayer MS (2004) Differential actin binding along the PEVK domain of skeletal muscle titin. J Cell Sci 117 (Pt 24):5781-5789. doi:10.1242/jcs.01501

Nagy R, Karandashov V, Chague V, Kalinkevich K, Tamasloukht MB, Xu G, Jakobsen I, Levy AA, Amrhein N, Bucher M (2005) The characterization of novel mycorrhiza-specific phosphate transporters from *Lycopersicon esculentum* and *Solanum tuberosum* uncovers functional redundancy in symbiotic phosphate transport in solanaceous species. Plant J 42 (2):236-250

Nguema-Ona E, Coimbra S, Vicré-Gibouin M, Mollet J-C, Driouich A (2012) Arabinogalactan proteins in root and pollen-tube cells: distribution and functional aspects. Ann Bot 110 (2):383-404

Noble M, Lewis SA, Cowan NJ (1989) The microtubule binding domain of microtubule-associated protein MAP1B contains a repeated sequence motif unrelated to that of MAP2 and tau. J Cell Biol 109 (6 Pt 2):3367-3376

Nouri E, Reinhardt D (2015) Flowers and mycorrhizal roots–closer than we think? Trends Plant Sci 20 (6):344-350

Oda Y, Iida Y, Nagashima Y, Sugiyama Y, Fukuda H (2014) Novel coiled-coil proteins regulate exocyst association with cortical microtubules in xylem cells via the conserved oligomeric golgi-complex 2 protein. Plant Cell Physiol 56 (2):277-286

Paredez AR, Somerville CR, Ehrhardt DW (2006) Visualization of cellulose synthase demonstrates functional association with microtubules. Science 312 (5779):1491-1495. doi:10.1126/science.1126551

Parniske M (2008) Arbuscular mycorrhiza: the mother of plant root endosymbioses. Nat Rev Microbiol 6 (10):763-775

Petrasek J, Schwarzerova K (2009) Actin and microtubule cytoskeleton interactions. Curr Opin Plant Biol 12 (6):728-734. doi:10.1016/j.pbi.2009.09.010

Phaire-Washington L, Wang E, Silverstein SC (1980) Phorbol myristate acetate stimulates pinocytosis and membrane spreading in mouse peritoneal macrophages. J Cell Biol 86 (2):634-640

Pumplin N, Zhang X, Noar RD, Harrison MJ (2012) Polar localization of a symbiosis-specific phosphate transporter is mediated by a transient reorientation of secretion. Proc Natl Acad Sci USA 109 (11):E665-672. doi:10.1073/pnas.1110215109

Qin T, Liu X, Li J, Sun J, Song L, Mao T (2014) *Arabidopsis* microtubule-destabilizing protein 25 functions in pollen tube growth by severing actin filaments. Plant Cell 26 (1):325-339. doi:10.1105/tpc.113.119768

Rogers H, Bate N, Combe J, Sullivan J, Sweetman J, Swan C, Lonsdale D, Twell D (2001) Functional analysis of cis-regulatory elements within the promoter of the tobacco late pollen gene g10. Plant Mol Biol 45 (5):577-585

Rubio V, Linhares F, Solano R, Martín AC, Iglesias J, Leyva A, Paz-Ares J (2001) A conserved MYB transcription factor involved in phosphate starvation signaling both in vascular plants and in unicellular algae. Genes Dev 15 (16):2122-2133

Sánchez C, Díaz-Nido J, Ávila J (2000) Phosphorylation of microtubule-associated protein 2 (MAP2) and its relevance for the regulation of the neuronal cytoskeleton function. Prog Neurobiol 61 (2):133-168

Schüßler A, Walker C (2010) The Glomeromycota: a species list with new families and new genera. The Royal Botanic Garden Kew, Botanische Staatssammlung Munich, and Oregon State University

Sieberer BJ, Ketelaar T, Esseling JJ, Emons AM (2005) Microtubules guide root hair tip growth. New Phytol 167 (3):711-719. doi:10.1111/j.1469-8137.2005.01506.x

Sievers F, Wilm A, Dineen D, Gibson TJ, Karplus K, Li W, Lopez R, McWilliam H, Remmert M, Soding J, Thompson JD, Higgins DG (2011) Fast, scalable generation of high-quality protein multiple sequence alignments using Clustal Omega. Mol Syst Biol 7:539. doi:10.1038/msb.2011.75

Struk S, Dhonukshe P (2014) MAPs: cellular navigators for microtubule array orientations in *Arabidopsis*. Plant Cell Rep 33 (1):1-21

Swamy PS, Hu H, Pattathil S, Maloney VJ, Xiao H, Xue LJ, Chung JD, Johnson VE, Zhu Y, Peter GF, Hahn MG, Mansfield SD, Harding SA, Tsai CJ (2015) Tubulin perturbation leads to unexpected cell wall modifications and affects stomatal behaviour in Populus. J Exp Bot 66 (20):6507-6518. doi:10.1093/jxb/erv383

Takeda N, Sato S, Asamizu E, Tabata S, Parniske M (2009) Apoplastic plant subtilases support arbuscular mycorrhiza development in *Lotus japonicus*. Plant J 58 (5):766-777. doi:10.1111/j.1365-313X.2009.03824.x

Takeuchi M, Staehelin LA, Mineyuki Y (2017) Actin-Microtubule Interaction in Plants. In: Cytoskeleton-Structure, Dynamics, Function and Disease. InTech,

Timonen S, Drew E, Smith S (2006) Effect of cytoskeletal inhibitors on mycorrhizal colonisation of tomato roots. Symbiosis (Rehovot) 41 (2):81-86

Timonen S, Peterson RL (2002) Cytoskeleton in mycorrhizal symbiosis. Plant Soil 244 (1):199-210

Tsvetkov AS, Samsonov A, Akhmanova A, Galjart N, Popov SV (2007) Microtubule-binding proteins CLASP1 and CLASP2 interact with actin filaments. Cell Motil Cytoskeleton 64 (7):519-530. doi:10.1002/cm.20201

Twell D, Oh S-A, Honys D (2006) Pollen development, a genetic and transcriptomic view. The pollen tube:15-45

Twell D, Yamaguchi J, Wing RA, Ushiba J, McCormick S (1991) Promoter analysis of genes that are coordinately expressed during pollen development reveals pollen-specific enhancer sequences and shared regulatory elements. Genes Dev 5 (3):496-507

Venoux M, Basbous J, Berthenet C, Prigent C, Fernandez A, Lamb NJ, Rouquier S (2008) ASAP is a novel substrate of the oncogenic mitotic kinase Aurora-A: phosphorylation on Ser625 is essential to spindle formation and mitosis. Hum Mol Genet 17 (2):215-224. doi:10.1093/hmg/ddm298

Wang P, Hussey PJ (2015) Interactions between plant endomembrane systems and the actin cytoskeleton. Front Plant Sci 6

Wang X, Zhu L, Liu B, Wang C, Jin L, Zhao Q, Yuan M (2007) *Arabidopsis* MICROTUBULE-ASSOCIATED PROTEIN18 functions in directional cell growth by destabilizing cortical microtubules. Plant Cell 19 (3):877-889. doi:10.1105/tpc.106.048579

Weterings K, Schrauwen J, Wullems G, Twell D (1995) Functional dissection of the promoter of the pollen-specific gene NTP303 reveals a novel pollen-specific, and conserved cis-regulatory element. Plant J 8 (1):55-63

Wong YH, Lee TY, Liang HK, Huang CM, Wang TY, Yang YH, Chu CH, Huang HD, Ko MT, Hwang JK (2007) KinasePhos 2.0: a web server for identifying protein kinase-specific phosphorylation sites based on sequences and coupling patterns. Nucleic Acids Res 35 (Web Server issue):W588-594. doi:10.1093/nar/gkm322

Yamada M, Tanaka-Takiguchi Y, Hayashi M, Nishina M, Goshima G (2017) Multiple kinesin-14 family members drive microtubule minus end–directed transport in plant cells. J Cell Biol 216 (6):1705-1714

Zhang Q, Blaylock LA, Harrison MJ (2010) Two *Medicago truncatula* half-ABC transporters are essential for arbuscule development in arbuscular mycorrhizal symbiosis. Plant Cell 22 (5):1483-1497

Zhang X, Pumplin N, Ivanov S, Harrison MJ (2015) EXO70I Is Required for Development of a Sub-domain of the Periarbuscular Membrane during Arbuscular Mycorrhizal Symbiosis. Curr Biol 25 (16):2189-2195. doi:10.1016/j.cub.2015.06.075

Zhao Q, Yu J, Zhu D, Ao G (2003) Cloning and characterization of a pollen-specific lysine-rich protein cDNA (*tsb*) from tomato. Chin J Biochem Mol Biol 20 (2):275-279

Zhao Y, Zhao Q, Ao G, Yu J (2006) Characterization and functional analysis of a pollen-specific gene st901 in *Solanum tuberosum*. Planta 224 (2):405-412. doi:10.1007/s00425-006-0226-z

Zhou P, Yang F, Yu J, Ao G, Zhao Q (2010) Several cis-elements including a palindrome involved in pollen-specific activity of *SBgLR* promoter. Plant Cell Rep 29 (5):503-511. doi:10.1007/s00299-010-0839-3

Zhu C, Ganguly A, Baskin TI, McClosky DD, Anderson CT, Foster C, Meunier KA, Okamoto R, Berg H, Dixit R (2015) The fragile Fiber1 kinesin contributes to cortical microtubule-mediated trafficking of cell wall components. Plant Physiol 167 (3):780-792

Zhu L, Zhang Y, Kang E, Xu Q, Wang M, Rui Y, Liu B, Yuan M, Fu Y (2013) MAP18 regulates the direction of pollen tube growth in *Arabidopsis* by modulating F-actin organization. Plant Cell 25 (3):851-867. doi:10.1105/tpc.113.110528

Chapter 3. *SlDLK2*, a Novel Upregulated gene in Tomato Roots Colonized by AM fungi, encoding an α, β-hydrolase that acts as a negative regulator of arbuscule branching

Part of this Chapter is in preparation for publishing.

Abstract

The establishment of an arbuscular mycorrhizal (AM) symbiotic interaction is a successful strategy for the promotion of substantial plant growth, development, and fitness. Numerous studies have supported the hypothesis that plant hormones play an important role in the establishment of functional AM symbiosis. Strigolactones (SLs) are plant hormones lately identified and known to be relevant in the AM hyphal branching. Also, the receptor of a similar signal molecule, karrikin, has been recently shown to be essential for mycorrhizal colonization. Here, we perform a functional analysis of *SlDLK2*, a tomato gene highly upregulated in tomato roots colonized by AM fungi, which encodes an α, β-hydrolase gene closely related to SLs and karrikin receptors, indicating that SlDLK2 could be a receptor playing a signalling role during the mycorrhization process. The examination of a promoter-reporter construct in tomato hairy roots revealed that *SlDLK2* is specifically expressed in cells containing arbuscules. In order to analyze the function of *SlDLK2* during mycorrhization, hairy root tomato plants harboring overexpression and RNAi constructs were generated. Interference of *SlDLK2* gene expression resulted in a significant increased AM development and functionality (at a transcriptomic level), while the *SlDLK2* overexpressing AM roots presented a significant decrease in both AM development and AM functionality, associated with an anomalous arbuscule development, with lack of branching, elucidating a clear negative role played by SlDLK2 on arbuscule development. SlDLK2 shows a conservation of the hydrolytic triad described for the SL and karrikin receptor proteins, and SlDLK2 keeps some activity to interact and hydrolyze SL-analog molecules. Although the specific ligand remains unknown, C13 α-ionol derivative molecules are proposed here as potential candidates for further research.

Introduction

The Arbuscular mycorrhizal (AM) symbiosis is the most prevalent (Smith and Read 2008) and widespread symbioses in the plant kingdom. This microbe-plant mutualistic association is established between the endosymbiotic AM fungi, soil microscopic fungi of the phylum Glomeromycota (Smith and Read 2008), and higher plants, including most of crop species. In the cortical cells of the roots, the AM fungi develops specialized intraradical, highly branched structures, called arbuscules, where bidirectional exchange of nutrients between plant and fungi partners occurs (Bonfante and Requena 2011; Gutjahr and Parniske 2013). The AM fungus increases the plant's exploratory capacity through an extensive external hyphal network in the rhizosphere, which is able to efficiently uptake water and nutrients, mainly Pi (inorganic phosphate), from soil areas inaccessible to the roots (Smith and Read 2008). Then, these nutrients and water are transported to the arbuscules to be provided to the plant. In return, the fungus obtains the required carbon from the host plant in the form of plant photosynthetic products (Javot et al. 2007; Harrison 1999; Govindarajulu et al. 2005; Smith and Read 2008).

During establishment of the AM symbiosis plant cells undergo morphological and functional changes which could be related with the known fine hormone regulation that occurs in these cells (Foo et al. 2014; Pozo et al. 2015). Strigolactones (SLs) are important plant signals for AM symbiosis. Although the SL receptor in AM fungi is not yet known, SL-signalling in AM fungi triggers an induction of mitochondrial activity and density (energy production), associated to an increase in hyphal branching, consequently facilitating the mycorrhization process (Besserer et al. 2008; Besserer et al. 2006b; Akiyama et al. 2005a). In addition, the perception of SLs by germinated spores of *R. irregularis* promotes the production of short-chain chito-oligosaccharides (COs; CO4– CO5) (Genre et al. 2013), in turn activating the symbiotic signalling pathway in the root epidermis (Genre et al. 2013; Sun et al. 2015).

The expression of SL biosynthesis genes is partly up-regulated in AM colonized roots (Kobae et al. 2018). Several studies have shown that mutants or antisense lines impaired in SL biosynthesis or transport exhibit reduced mycorrhization, although morphology of intercellular hyphae and arbuscules was not affected (Kretzschmar et al. 2012; Koltai et al. 2010; Vogel et al. 2010; Yoshida et al. 2012; Gomez-Roldan et al. 2008). Moreover, recent observations from Kobae et al. (2018) established that SL biosynthethic genes are also required for efficient hypopodium formation, suggesting a role of SLs in both the pre-symbiotic chemical dialog and the subsequent hyphal entry into the roots.

D14 protein is the only plant SL receptor known to date, but D14 involvement during mycorrhization has not yet been established. Studies of Nakamura et al. (2013) suggest a possible role of D14 on mycorrhization through alteration of the gibberellin (GA) signalling, as they observed that, in a SL-dependent manner, D14 of rice is able to interact with the DELLA protein SLR, a GRAS transcription factor that inhibits GA signalling and positively regulates mycorrhization and nodulation (Yu et al. 2014; Jin et al. 2016; Floss et al. 2013).

In the other hand, the D14-related protein KAI2, a component of an intracellular receptor complex involved in the detection of the smoke compound karrikin, have been recently found to be essential for initiating the AM symbiosis in rice roots by the AM fungi *R. irregularis* and *Gigaspora rosea* (Gutjahr et al. 2015). Actually, the authors of the finding suggest that this new role could be the main role for the conserved KAI2 protein group, as AM symbiosis is also highly conserved in the plant kingdom, involving more than 80% of all plant species, as opposed to 1200 smoke-responsive plant species (Chiwocha et al. 2009). Nevertheless, the endogenous ligand of the KAI2 receptor is still unknown.

Then, it is clear that the SL and karrikin receptors, D14 and KAI2, respectively, are someway related to the regulation of AM symbiosis. These two proteins belong to the α,β-hydrolase fold superfamily, particularly to the RsbQ-like family. This family is divided in three protein clades (Delaux et al. 2012; Hamiaux et al. 2012; Waters et al. 2012):

- D14/DAD2 (Dwarf14/Decreased in Apical Dominance2) clade, which is composed by α, β-hydrolase proteins that bind to strigolactones.
- KAI2/HTL (Karrikin-Insensitive 2/Hyposensitive To Light) clade, comprising karrikin binding α, β-hydrolases. In the literature, this clade is often designated as "D14-like".
- DLK2 (Dwarf14-Like2) clade, with unknown strigolactone or karrikin binding ability. This group was named DAD2-like by Hamiaux et al. (2012), who identified it as a divergent clade from the D14/KAI2 groups. However later studies of Delaux et al. (2012), Waters et al. (2012), and Bythell-Douglas et al. (2017) established this group as a sister clade of the core D14, and designated it as DLK2 clade.

Surprisingly, a tomato gene belonging to this last group, here named *SlDLK2* (*Solanum lycopersicum DLK2*), was found to be highly upregulated by arbuscular mycorrhizal fungi in the microarray hybridizations and data analysis carried out by García Garrido et al. (2010) and López-Ráez et al. (2010). The study of García Garrido et al. (2010) revealed that this gene (GenBank AW622368, SGN-U583796, Tomato Affymetrix ID LesAffx.28554.1.S1_at) was the most induced in wild type tomato roots inoculated by *R. irregularis* with respect to un-inoculated roots. Particularly, the tomato α,β-hydrolase *SlDLK2* increased its gene expression by 128-fold in roots inoculated with *R. irregularis* after 50 days (52% mycorrhization approximately) with respect to non-inoculated roots. They confirmed this result by qPCR, which showed an expression of 724-fold induction in mycorrhized roots. In addition, García Garrido et al. (2010) also observed that the *SlDLK2* induction was reduced by 88% (array analysis) or 94% (qPCR) in inoculated roots of *sitiens*, an ABA-deficient tomato mutant with an impaired AM formation with respect to inoculated wild type roots, which suggest that α,β-hydrolase gene could play an essential role in the arbuscular mycorrhiza symbiosis formation. Similar results were obtained in the microarray hybridization performed by López-Ráez et al. (2010), that also showed that the most induced gene in tomato roots inoculated with *R. irregularis* after 63 days (41% mycorrhization) was an α, β-hydrolase corresponding to *SlDLK2*, which was up-regulated 42.64-fold with respect to un-inoculated roots. They also perform the same experiment with another species of

AM fungi, *G. mosseae*, obtaining that *SlDLK2* gene expression was also increased (>17-fold induction), becoming the fourth most induced gene in *G. mosseae* inoculated roots (63 days after inoculation, 23% mycorrhization) comparing to non-mycorrhized roots.

Some reports exists recognizing *DLK2* gene expression as an excellent marker for SL or KAR action (Waters et al. 2012; Sun et al. 2016), maybe because its transcription is mostly accomplished through MAX2-mediated signalling (Végh et al. 2017). However, very little is known about the DLK2 group physiological function. Recent reports show that DLK2 from *Arabidopsis thaliana* does not affect SL responses, can regulate seedling photomorphogenesis and might function in light signalling pathways (Végh et al. 2017).

In this work we analyse the role of *SlDLK2*, a tomato gene highly induced during mycorrhization encoding an α, β-hydrolase protein closely related to the D14 and KAI2 receptors. Functional analyses using the AM fungus *R. irregularis* and tomato composite plants overexpressing and silenced for the *SlDLK2* gene were performed, and efforts to envisage the possible ligand of SlDLK2 were made.

Methods

Promoter sequence identification

SlDLK2 promoter was obtained using the Universal Genome Walker 2.0 Kit (Clontech), following the manufacturer instructions. Genomic DNA from *S. lycopersicum* cv Craigella GCR26 was extracted using the DNAeasy Plant Mini Kit (Qiagen), digested with four restriction enzymes (DraI, EcoRV, PvuII and StuI), purified, and ligated to the Genome Walker adapters provided with the Universal Genome Walker kit. A primary PCR with GSP1 and Ap1 primers, and a secondary (or "nested") PCR with GSP2 and Ap2 primers, were performed. Primers used were two designed reverse Gene Specific Primers (GSP1 5´CATCAGCAAAAGGCTCATA GGAGGAGTA3´ and GSP2 5´CCCAAACTGATTGATCTCCTCCATATCC3´), and two

Adaptator Specific Primers (Ap1 and Ap2) provided in the kit. PCR products were purified and sequenced, and the fragment corresponding to the *SlDLK2* promoter was selected for cloning.

Expression Analysis of *SlDLK2* gene in hormone treated roots

20-day old plants grown in 25 mL-Falcon tubes with vermiculite, and watered twice a week with Long Ashton nutrient solution, were treated with an exogenous hormone application at the following concentrations: 0.5 mM salicylic acid (SA), 50 µM methyl jasmonate (MeJA), 10 µM GA_3, 75 µM abscisic acid (ABA), 0.1 mM indol acetic (IAA) or 70 µM ethephon (Et) for the different treatments. Plant root systems were harvested at 12, 24 and 48 hours after hormone treatments and *SlDLK2* gene expression was analyzed by qPCR.

***Agrobacterium*-mediated transient expression for SlDLK2 protein localization**

Agrobacterium-mediated transient expression in *Nicotiana benthamiana* was performed as previously described by Li (2011). The bacterial suspension was adjusted to a final OD_{600} of 0.5 and *N. benthamiana* leaves were infiltrated with *A. tumefaciens GV3101* carrying plasmids to induce the expression of SlDLK2-GFP ($pGWB_5$). Samples were taken at 40 h post-infiltration for analysis. Confocal laser scanning microscopy was performed employing the abaxial side of *Agrobacterium*-infiltrated *N. benthamiana* leaves, and the green channel was recorded, signal saturation was avoided and several fields of view were inspected to obtain a global overview of the putative localization of SlDLK2-GFP.

Protein expression and purification

SlDLK2 protein was purified as previously done for AtD14L (Kagiyama et al. 2013). *SlDLK2* cDNA sequence was cloned into pET49b(+) (Novagen), and the protein was expressed in *E. coli* BL21 Star (DE3) (Invitrogen) as a fusion protein with an N-terminal glutathione S-transferase (GST) tag. Cells were grown at 37ºC in Luria-Bertani (LB) medium containing 30 µg/mL kanamycin. When the OD_{600} of the cell culture reached 0.8, isopropyl-β-thiogalactopyranoside (IPTG) was added to 100 µM concentration and grown at 16ºC for 20h to induce *GST-SlDLK2* gene fusion

expression. Cells were collected by centrifugation at 3993 xg for 15 min at 4ºC, suspended in 20 mM HEPES, 150 mM NaCl (pH 7.5) (Buffer A) and disrupted by sonication a 4ºC. The soluble portion of the cell extract was loaded onto a GST-affinity column comprising Glutathione Sepharose 4B resin (GSH resin) (GE Healthcare) and then washed with Buffer A. Bound GST-fusion protein was eluted with Buffer A containing 20 mM glutathione and then cleaved by overnight treatment with HRV3C protease (Novagen) at 4 °C. The cleaved protein sample was purified by ion exchange chromatography using HiTrap Q HP, GST-affinity chromatography to remove the cleaved GST and gel filtration using Hi Load 26/60 Superdex 75 prep grade. The ion exchange and gel filtration chromatographies were performed on an AKTA prime system. Purified protein was concentrated using an Amicon 10K filter unit (Merck Millipore) up to 4 mg/mL with Buffer A. The protein sample was divided into 50-µL aliquots in 0.5-mL tubes (Eppendorf) and immediately frozen in liquid nitrogen. Frozen samples were stored at -80 °C until use. The identity of the purified protein was verified using matrix-assisted laser desorption/ionization time-of-flight mass spectroscopy (MALDI–TOF MS; Bruker Daltonics).

Site Directed Mutagenesis

Codons codifying for putative residues belonging to the catalytic triad of SlDLK2 were mutated to alanine using the QuickChange Site-Directed Mutagenesis kit (Agilent Technologies). Sequence of mutagenic primers used were 5´GTTGGTCATGCTATGTCTGGCATCATTGGTTGCATTGC 3´ and 5´GCAATGCAACCAA TGATGCCAGACATAGCATGACCAAC 3´ for Ser98Ala mutation, 5´ CAAACCAAG GTTGCTTTTGCTGTTCCAAACTCGGTTCCC 3´and 5´GGGAACCGAGTTTGGAACAGCA AAAGCAACCTTGGTTTG 3´ for the Asp219Ala mutation, and 5´ CAACACTCA TGGCGCTTTTCCGCAGCTCACTGC3´ and 5´ GCAGTGAGCTGCGGAAAAGCGCCATGA GTGTTG 3´ for the His248Ala mutation. Mutant strand synthesis was performed with the *PfuUltra* polymerase, and then methylated and hemimethylated parental DNA strand were digested with DpnI. *E. coli* competent cells were transformed with the mutated DNA for nick repair. Protein expression and purification were performed in the same manner as for wildtype SlDLK2.

Isothermal Titration Calorimetry (ITC)

Binding studies using Isothermal Titration Calorimetry (ITC) were carried out using a calorimeter (MicroCal iTC200, GE Healthcare). Based on Kagiyama et al. (2013) experiments conducted with *Arabidopsis* and rice SlDLK2 related proteins, ITC was performed at 20 °C. SlDLK2 purified protein was dialyzed overnight in a 20 mM Na-HEPES (pH 7.5) and 300 mM NaCl buffer. Given the poor solubility of GR24 and GR5, reverse titration was used whereby concentrated protein solution (450-650 μM) was injected (2 μL each, 5-min pause) into the ligand aqueous solution (45-65 μM), reaching a final molar concentration of 2:1 (protein:ligand). Although KAR1 solubility is described to be sufficient for calorimetry assays (Kagiyama et al. 2013), SlDLK2 was found to became aggregated at concentrations >700μM, then reverse titration was also used for binding assays with KAR1 in the same manner as for GR24 and GR5. Some trials with other molar ratios, alternative incubation buffers and forward titration were performed. Details of each titration are given in Fig. 28 and Fig. 29.

Thin Layer Chromatography

Thin Layer Chromatography (TLC) was performed in a similar way as Hamiaux et al. (2012) in order to analyze the time course GR24 and GR5 hydrolysis and cleavage by SlDLK2 purified protein, as well as by the corresponding catalytic site mutant proteins.

125 μL reactions of 20 mM HEPES 300mM NaCl buffer containing 5% DMSO, 50 μM SlDLK2 (or mutant proteins) and 1 mM GR24 (or GR5) in PBS buffer were incubated at 22 °C. At different incubation time points (3h, 8h, 20h, 30h, 48h), reaction mixtures were transferred to glass vials and extracted by 1 min vortexing with 1 mL ethyl acetate, 5 min centrifugation at 3500 xg, and collection of the organic phase in a new glass vial. This organic phase was evaporated under nitrogen, resuspended into 20 μL acetone containing 5/1000 acetic acid and analyzed by TLC on a pre-coated silica gen 60 F254 plate (Merck) using chloroform/acetone (4:1, v/v, containing 5/1000 acetic acid) as developing solvent. Spots were visualized under

UV light (254 nm). Fresh GR24 and GR5 in acetone were used as a reference. AtD14 protein was used as a positive control of GR24 and GR5 cleavage.

Thermal Shift Assay (TSA)

Reaction mixtures for the Themal Shift Assays (TSAs) were prepared in a 96-well plate, and each reaction was carried out in 25- µL scale in 20 mM TRIS, 150 mM NaCl, pH 8 buffer containing 20 µM protein, 0 to 2 mM ligand, 5% (v/v) acetone, and 5x reporter dye Sypro Orange (Ex/Em: 490/610 nm). In the control reaction, acetone was added instead of chemical solution. Plates were set in an iQ5 real-time PCR detection system. After incubation at 23 °C for 5 min in darkness, samples were heated from 23 °C to 85 °C, with a rate of temperature increase of ~0.5°C every 11 seconds, with the corresponding fluorescence data acquisition. The curve data for each sample was imported into Microsoft Excel, where averages of the technical replicates were calculated and the graphs generated. Each protein-ligand combination was replicated three times on the same plate, and each experiment was performed at least twice.

Bioinformatic Analysis

The protein encoded by *SlDLK2* was blasted against the ESTHER server at http://bioweb.ensam.inra.fr/ESTHER/ general?what=index (Hotelier et al., 2004), an α,β-hydrolase protein specific database, to identify the group of α,β-hydrolases to which it belonged.

Amino acid sequence was also subjected to a homology search against the *Viridiplantae* database (taxid:33090) using the on-line BLASTP server at NCBI (www.ncbi.nlm.nih.gov) with all default settings. Another BLASTP search was performed against a series of selected dicot (*S. lycopersicum*, *Solanum tuberosum*, *Arabidopsis thaliana*, *Coffea canephora, Sesamum indicum, Daucus carota, Lactuca sativa, Beta vulgaris, Brassica rapa*, *Glycine max*, *Medicago truncatula*, *Nicotiana benthamiana*, *Vitis vinifera*, *Petunia hybrida*, *Ricinus communis*, *Prunus persica and Asparagus officinalis*) and monocot (*Oriza sativa* and *Zea mays*) species in order to obtain a wide view of the putative homologs in angiosperms plants. Blast output sequences with an alignment score ≥ 200 were considered as putative homologs and

were subjected to phylogenetic analysis. Phylogenetic relationships were determined with Geneious software to create a neighbor-joining tree using the Jukes-Cantor model. Those possible homologs that had been previously characterized in the literature were selected for further alignment using Clustal Omega (Sievers et al. 2011). Three-dimensional (3D) structure protein prediction was generated using the I-TASSER server (http://zhanglab.ccmb.med.umich.edu/I-TASSER/) (Yang et al. 2015), and superimpositions with the crystallized structures of AtD14 and AtKAI2 were performed with Chimera software (Pettersen et al. 2004). Putative functional promoter elements were identified by the PlantCARE (Plant Cis-Acting Regulatory Element) database (Lescot et al. 2002). In silico expression of *SlDLK2* and its tomato homologous genes were downloaded from the tomato eFP browser at bar.utoronto.ca. Genome, gene and protein sequences from tomato lacking at the NCBI database, were downloaded from the Sol Genomics Network database (http://solgenomics.net, version 3.2 updated in June 2017), and the respective annotations from the international Tomato Annotation Group (iTAG 3.2) were used.

Additional methods used in this chapter but previously described in the *General Materials and Methods* section:

- **Plant growth and AM inoculation**
- **Expression Analysis of *SlDLK2* gene in tomato organs**
- **Estimation of root colonization by AM fungus**
- **Plasmid Construction and Hairy root transformation (Chapter 2)**
- **Gene expression localization**
- **RNA extractions and gene expression quantification**
- **Statistical analysis**

Results

Sequence identification of the SlDLK2 tomato AM-induced *α,β-hydrolase* gene and its promoter

The putative cDNA sequence of the tomato *α,β-hydrolase* induced during mycorrhization (Tomato Affymetrix ID probe LesAffx.28554.1.S1_at) (García Garrido et al. 2010) corresponded with the 384 bp-putative gene Solyc00g170200.1 of the Tomato Genome Sequence ITAG3.0 (https://solgenomics.net). The fact that this 384 bp-sequence is mapped to "chromosome 00", a place holder for tomato sequences that could not be mapped to any of the 12 tomato chromosomes, together with a blastn homology search which revealed that all putative paralog genes in the plant kingdom had a longer length (data not shown), suggested that Solyc00g170200.1 might not correspond to the complete tomato *α,β-hydrolase* sequence. A BLASTN against the putative 384 bp-cDNA sequence was performed against the *S. lycopersicum* database (taxid:4081) using the online server at NCBI (www.ncbi.nlm.nih.gov), and a 1092 bp sequence with 100% identity was output (GenBank ID AK319425.1). This sequence was previously obtained in the RNA-seq performed by Aoki et al. (2010) in *S. lycopersicum* cv MicroTom leaves. In order to confirm that this 1092 bp sequence corresponded with the full-length cDNA sequence of the tomato *α, β-hydrolase* induced by mycorrhization, 5´and 3´primers were design and amplification by PCR was performed using a cDNA sample from a tomato AM-colonized root. The amplicon was sequenced, and it was effectively confirmed that the *α, β-hydrolase* studied, here named SlDLK2, corresponded to the AK319425.1, with a CDs of 807 bp length instead of 384 bp (Fig. 1).

The promoter sequence could not be found 5´upstream of the *α,β-hydrolase* at the Tomato Genome Sequence 3.0 database. Using the Universal Genome Walking 2.0 kit, a 1600 bp amplified product, coming from the tomato genomic DNA digested with PvuII, was purified and sequenced, and it was successfully checked its correspondence to the *α,β-hydrolase* promoter sequence. A blastn against the Tomato Genome Sequence 3.0 revealed that most of the promoter sequence was located, again, in the place holder "chromosome 00" (SL3.0ch00: 15883672 -

15882392), as shown in Fig. 1. A 1509 bp fragment just upstream of the *SlDLK2* gene was selected for subsequent cloning and promoter expression analysis.

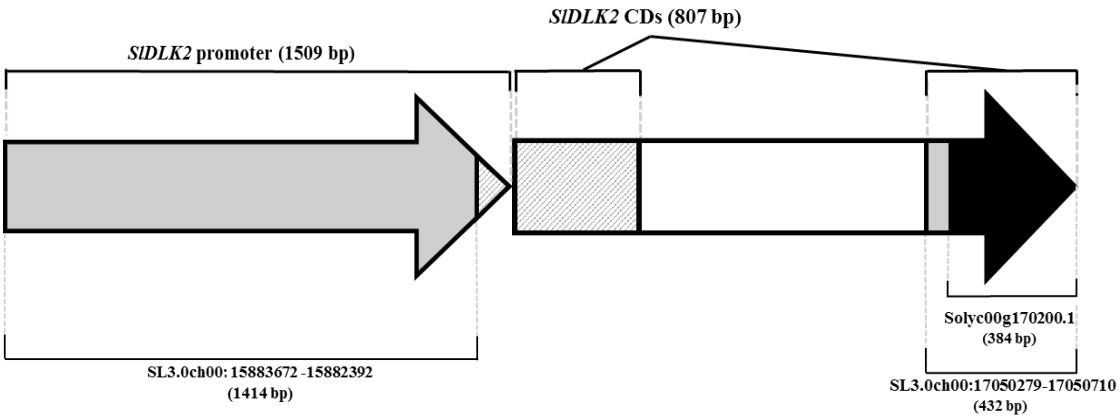

Figure 1. Scheme of sequence identification of full-length CDs and the corresponding promoter of the tomato AM-induced α, β-hydrolase *SlDLK2.* Sequence initially identified in the Tomato Genome Sequence 2.40 as the tomato α,β-hydrolase gene responsive to mycorrhization *SlDLK2* is shown in black (Solyc00g170200.1). Additional sequences present (grey) or lacking (dashed grey) at the Tomato Genome Sequence 2.40 and found out here to belong to the *SlDLK2* CDs and its promoter are shown. The *SlDLK2* ORF contains an intron (white). The corresponding base pair-lengths are indicated between brackets.

Phylogenetic analysis and sequence alignment

The protein encoded by the tomato *α,β-hydrolase* gene responsive to mycorrhization belongs to the alpha/beta hydrolase superfamily, which includes all proteins containing the α, β-fold, extensively widespread across all three domains of life. In plants, the α, β-hydrolase superfamily is sparsely characterized, but it is remarkable the characterization of the α, β-fold as the core structure for phytohormone and ligand receptors in the gibberellin, strigolactone and karrikin signaling pathways.

A BLASTP using the ESTHER sever (ESTerases and alpha/beta-Hydrolase Enzymes and Relatives, http://bioweb.ensam.inra.fr/ESTHER/general?what=index) revealed that our protein belongs to the RsbQ-like family of α,β-hydrolase folds, known to include the karrikin and strigolactone receptors, KAI2/HTL2 and DAD2/D14, respectively.

Putative protein homologs belonging to *S. lycopersicum* and eighteen more different plant species were identified using BLASTP at NCBI. Subsequent phylogenetic analysis (Fig. 2) showed that the tomato α,β-hydrolase protein studied here belongs to a third clade of RsbQ-like α,β-hydrolases previously named as "D14-like2 group" (DLK2) (Waters et al. 2012), of very little known function. Thus, we decided to name the corresponding tomato *α,β-hydrolase* gene induced during AM symbiosis as *SlDLK2* (*Solanum lycopersicum* D14-like2). The only member of this group that has been studied so far is DLK2 from *Arabidopsis thaliana* (ID) (Végh et al. 2017).

Then, the *SlDLK2* analyzed here encodes a protein belonging to the α,β-hydrolase superfamily, particularly to the RsbQ-like family and the low characterized D14-like2 group.

Three proteins from the DAD2/D14 clade (the *Oriza sativa* OsD14, *Arabidopsis thaliana* AtD14 and *Petunia hybrida* PhDAD2), as well as one protein from the KAI2/HTL2 group (*AtKAI2*) were selected for further alignment and amino acid sequence analysis (Fig. 3), as previous information is available referred to their protein structure, essential residues and catalytic ability (Hamiaux et al. 2012; Kagiyama et al. 2013; Zhao et al. 2015; Yao et al. 2016b).

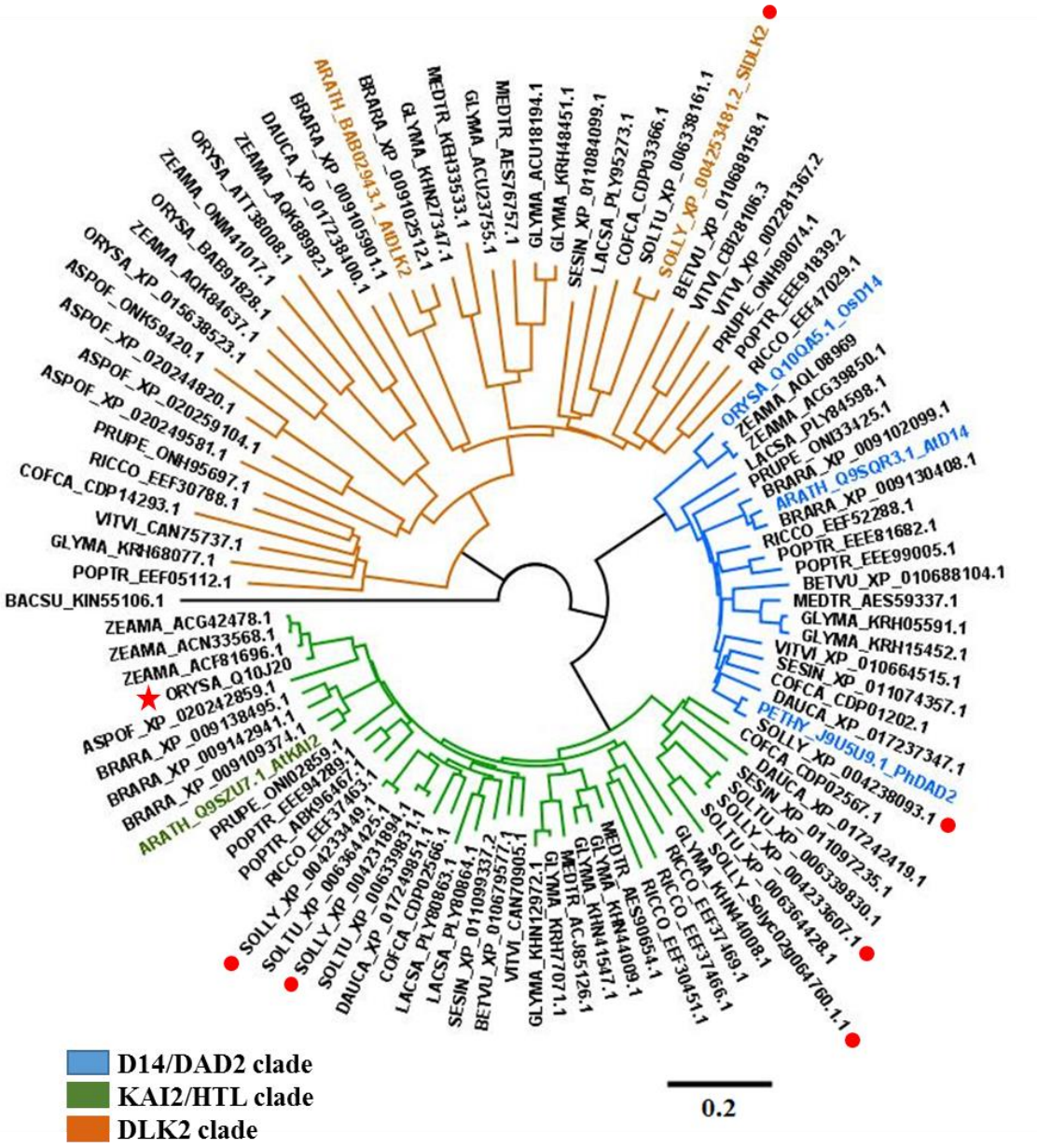

Figure 2. Phylogenetic analysis of putative homolog proteins for *the Solanum lycopersicum* AM-induced α,β-hydrolase SlDLK2: the RsbQ-like family of α,β-hydrolase folds. Phylogenetic relationships among amino acid sequences with high similarity to the tomato SlDLK2 from various plants: *Solanum lycopersicum* (labelled with a red spot), *Solanum tuberosum*, *Arabidopsis thaliana*, *Coffea canephora*, *Sesamum indicum*, *Daucus carota*, *Lactuca sativa*, *Beta vulgaris*, *Brassica rapa*, *Glycine max*, *Medicago truncatula*, *Nicotiana benthamiana*, *Vitis vinifera*, *Petunia hybrida*, *Ricinus communis*, *Prunus persica*, *Oryza sativa*, *Zea mays* and *Asparagus officinalis*. Proteins are named with the first three letters of the genus name, the first two letters of the species name and the GenBank/RefSeq accession number, except for one *S. lycopersicum* protein , which uses the SolDB accession (http://solgenomics.net/). Common protein names are also indicated for proteins previously characterized. A protein with known function in mycorrhization is labelled with a red star. Three clades were identified in the RsbQ-like family of α,β-hydrolases. Colour branches correspond to each clade as indicated in the legend. The scale bar represents the number of substitutions per site. The tree is rooted on the RsbQ from *Bacillus subtilis*.

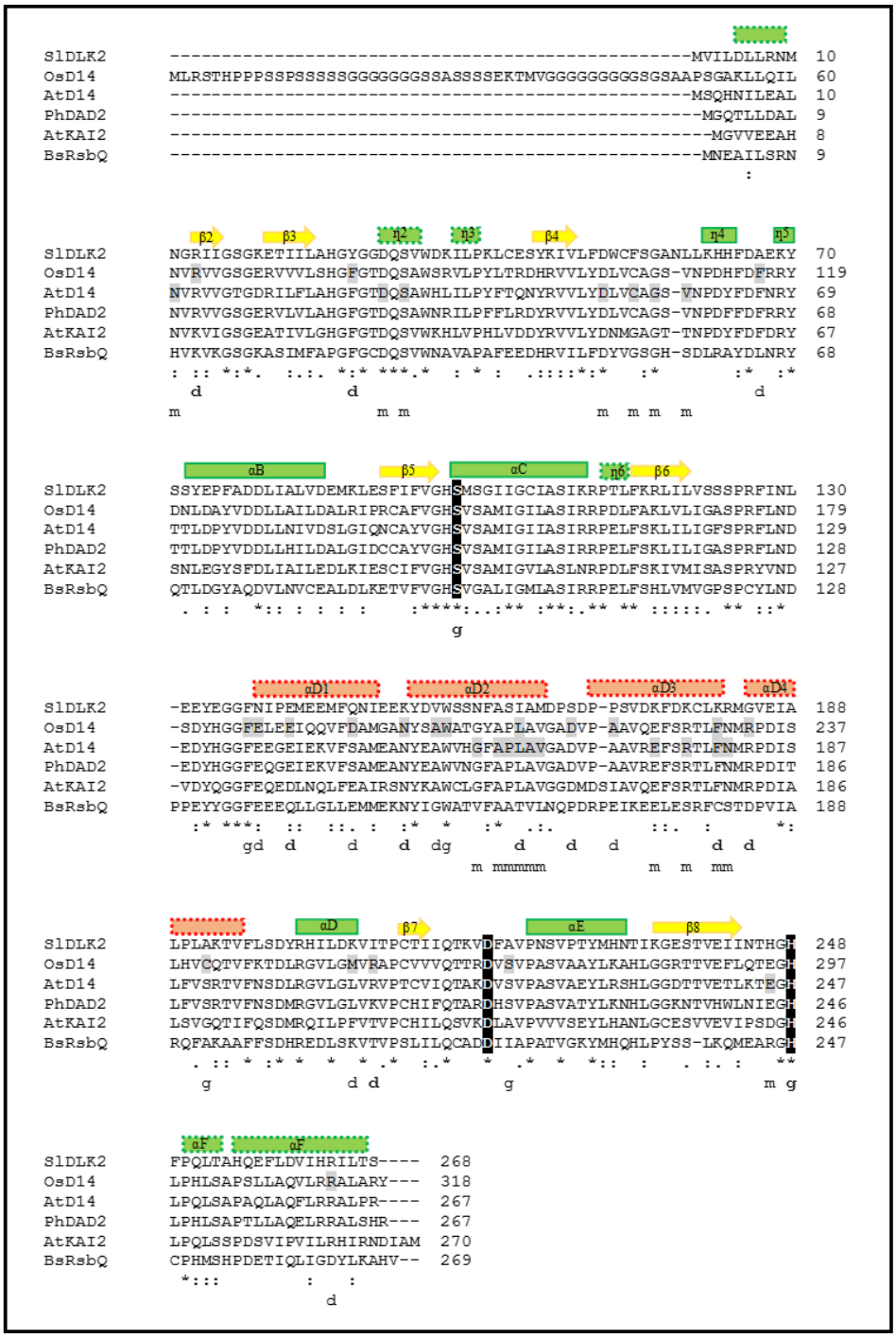

Figure 3. Amino acid comparison of SlDLK2 and its homologs. Amino acid comparison between SlDLK2 and its related proteins. The residues from the catalytic triad are shadowed in black. Important (or essential if bold labels) residues for MAX2/D3 and GR24 binding are shadowed in grey and labelled below by *m*/*d* and *g*, respectively, based on Zhao et al. (2015) and Yao et al. (2016) results. Predicted alpha helices from the core domain (green bars) and lid domain (red bars), as well as beta strands (yellow bars with an arrow) are indicated, based on crystal structure of OsD14 and AtKAI2 (Kagiyama et al., 2013). Additional or modified domains form the canonical α,β-hydrolase are indicated with dashed outline bars. The consensus symbols of the Clustal Omega alignment are used: the identical residues are indicated with "*", residues of strongly similar properties are labelled with ":", and residues of weakly similar properties are indicated with ".".

SlDLK2 amino acid sequence only shares a 37.45%, 40.07%, 40.23% and 39.62% identity with OsD14, AtD14, PhDAD2 and AtKAI2 proteins, respectively. Members of the α,β-hydrolase superfamily show an extremely low sequence identity. Nevertheless, they keep a highly conserved three dimensional structure. The "core domain" of the canonical α,β-hydrolase is composed by a 8-stranded central beta-sheet surrounded by six alpha helices, being the most conserved feature the loops containing the catalytic triad residues Ser-His-Asp/Asn (Heikinheimo et al. 1999; Nardini and Dijkstra 1999). Structural and functional variation is typically dependent on additional structural elements named "lid domains". Previous crystallization and functional analyses of three α,β-hydrolases belonging to the RsbQ-like group (i.e. OsD14 from *Oryza sativa*, PhDAD2 from *Petunia hybrida* and AtD14 and AtKAI2 from *Arabidopsis thaliana*) revealed that the lid domain in the three proteins is constituted by a four-helical V shaped domain important for binding and ligand recognition, and the core domain lacks a beta strand and has an extra alpha helix (Hamiaux et al. 2012; Kagiyama et al. 2013; Guo et al. 2013; Zhao et al. 2015; Zhao et al. 2013), as shown in Fig. 4A. The predicted structure for SlDLK2 was obtained with the I-TASSER server and revealed that SlDLK2 contains a predicted ligand-binding pocket with the catalytic residues facing inward (Fig. 4B), as typically found in the D14-family proteins. The generated 3D model of SlDLK2 (Fig. 4C) was superimposed to the crystal structures AtD14 and AtKAI2 (Fig. 4D,E, respectively), showing high structural similarity among paralogs.

Amino acid sequence alignment showed that SlDLK2 lid domain is similar in length (80 bp approximately), but shows low identity (33.8%, 40.3% and 35.4%) with respect to its homolog proteins OsD14, PhDAD2 and AtKAI2, respectively. Crystallization and structural studies should be performed to confirm the conservation of the topology described for D14 and KAI2 receptors in SlDLK2 (Hamiaux et al. 2012), and to obtain a more detailed structure.

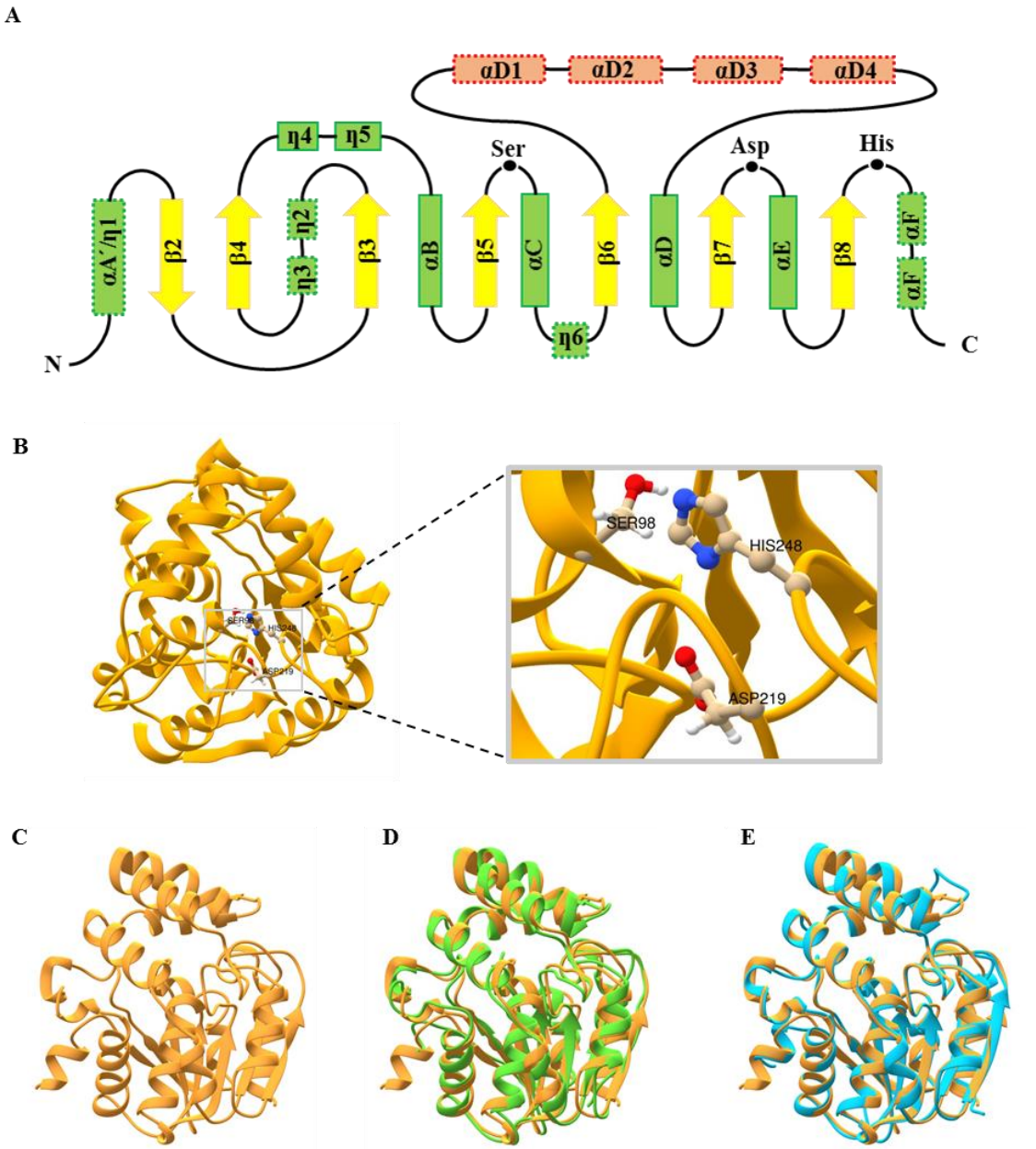

Figure 4. SlDLK2 shares high structural similarity with AtD14 and AtKAI2. Topology diagram of the SlDLK2 homologs D14 and KAI2 (A), showing alpha helices from core domain (green bars) and lid domain (red bars), as well as beta strands (yellow bars with an arrow), based on crystal structure of OsD14 and AtKAI2 (Kagiyama et al., 2013). The active site residues Ser, Asp and His are labelled. Domains modified from the canonical α,β-hydrolase are indicated with dashed outline. The predicted structure of SlDLK2 by the I-TASSER server (Yang et al. 2015) is shown in (B-C), including an expanded view of the catalytic triad residues of SlDLK2 (Ser98-Asp219-His248) in (B). The predicted structure of SlDLK2 (orange) was superimposed with the crystallized structures of AtD14 (D, green; PDB code 4IH4) or of AtKAI2 (C, blue; PDB code 4IH1) using the Chimera software (Pettersen et al. 2004)

The catalytic triad residues are conserved in SlDLK2 (Ser98-Asp219-His248). It is established that these residues not only provide hydrolase activity to proteins belonging to the α,β-hydrolase superfamily (Long and Cravatt 2011), but it has also been reported that the putative catalytic triad in RsbQ-like α,β-hydrolases is required for ligand binding, protein destabilization and subsequent interaction with other proteins. For example the putative catalytic residue Ser147 of OsD14 has an essential role on GR24 binding (Zhao et al. 2015), and the catalytic triad of PhDAD2 participates in protein destabilization and GR24-dependent interaction with PhMAX2A in vitro (Hamiaux et al. 2012).

Zhao et al. (2015) performed a series of independent mutations for the pocket residues of OsD14 expected to interact with GR24 by bioinformatics modelling. From the six residues that negatively affected GR24 binding by more than 50%, four of them are conserved in SlDLK2, while the other two are substituted by smaller size residues (Table 3). However, amino acid size comparison of residues belonging to the catalytic pocket based on OsD14 crystal structure (Zhao et al. 2015; Kagiyama et al. 2013) are generally of bigger size in SlDLK2 (Table 3), expectedly making the pocket smaller, as reported to occur in AtKAI2 and suggested to be the reason for AtKAI2 impossibility to bind GR24 (Kagiyama et al. 2013).

Putative pocket residues are mostly conserved among the plant-DLK2 proteins, with the exception of F127, M145, F220 and A221, that seem to be specific from the Solanaceae family (Fig. 5). From these four pocket residues, F127 and A221 might determine the binding of the Solanaceae-DLK2 members to an specific ligand different from the ligand bound by the other DLK2 plant proteins, as the aligned residues for F127 and A221 in OsD14 have been demonstrated to affect its binding ability to GR24 (Zhao et al. 2015).

OsD14	AtKAI2	SlDLK2
F78	F26	Y28 (↑)
S147	S95	S98
V148	V96	M99 (↑)
F176	Y124 (↑)	F127
F186	F134	F137
V194	L142 (↑)	M145 (↑↑)
W205	W153	W156
Y209	F157 (↑)	F160 (↑)
C241	G190 (↓)	A192 (↓)
V244	I193 (↑)	V195
F245	F196	F196
D268	D217	D219
V269	L218 (↑)	F220 (↑↑)
S270	A221 (↓)	A221 (↓)
H297	H246	H248

Table 3. Catalytic pocket residues size analysis. Residues reported to face the catalytic pocket of OsD14 are shown (Zhao et al., 2015; Kagiyama et al., 2012), indicating in bold letters those demonstrated to affect binding ability to GR24 (Zhao et al., 2015). Residues belonging to the putative catalytic triad are underlined. Aligned residues in AtKAI2 and SlDLK2 show that the catalytic pocket is expected to be smaller than in OsD14. Residues exhibiting a higher size are orange shadowed, while those with a smaller size are blue shadowed. Small size differences are indicated with one are arrow (↑ or ↓), while bigger differences in size are labelled with double arrow (↑↑ or ↓↓).

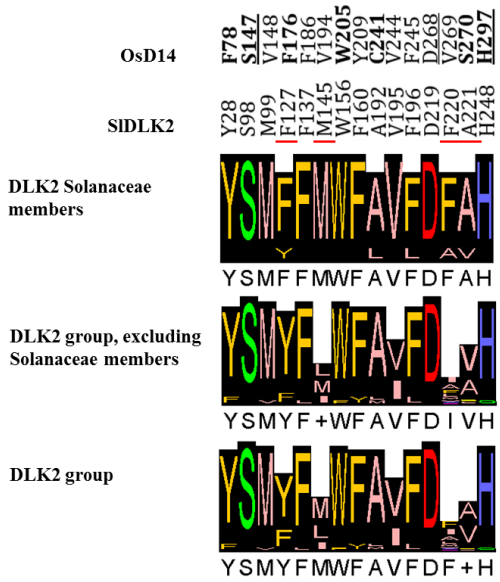

Figure 5. Conservation of putative pocket residues in DLK2 proteins from the plant kingdom and Solanaceae family. Residues reported to face the catalytic pocket of OsD14 are shown (Zhao et al., 2015; Kagiyama et al., 2012), indicating those demonstrated to affect the binding ability to GR24 (Zhao et al., 2015) in bold letters, and those belonging to the putative catalytic triad underlined. Below, aligned residues in SlDLK2 are shown, together with the conservation histogram and the consensus residues corresponding to the alignment of DLK2 proteins from representative plant species: *Solanum lycopersicum*, *Solanum tuberosum*, *Solanum pennelli*, *Nicotiana tabacum*, *Nicotiana benthamiana*, *Arabidopsis thaliana*, *Coffea canephora*, *Sesamum indicum*, *Daucus carota*, *Lactuca sativa*, *Beta vulgaris*, *Brassica rapa*, *Glycine max*, *Medicago truncatula*, *Vitis vinifera*, *Petunia hybrida*, *Ricinus communis*, *Prunus persica*, *Oryza sativa*, *Zea mays* and *Asparagus officinalis*. Pocket residues from SlDLK2 which are apparently specific from the Solanaceae-DLK2 proteins are red underlined.

In summary, it is expected that the conserved triad Ser98-Asp219-His248 in SlDLK2 has a hydrolase activity and we suggest that SlDLK2 has a smaller size catalytic pocket able to bind SL-like or KAR-like ligands smaller than GR24, despite conservation of some residues involved in GR24 binding (Zhao et al. 2015).

Similarly to other hormonal signaling mechanisms, SL and karrikin signal transduction are proposed to be based upon hormone-activated proteolysis. In each of these mechanisms, an F-box protein component of a Skp1–Cullin–F-box (SCF) E3 ubiquitin ligase complex targets specific protein substrates for polyubiquitination and degradation by the 26S proteasome. What distinguishes each signaling mechanism are the targets of the F-box protein and how SCF-mediated polyubiquitination is activated by the hormone. Particularly, OsD14 is reported to undergo conformational changes during SL binding or hydrolysis that enable SL signal transduction through binding the F-box protein OsD3 in a SL-dependent manner (Hamiaux et al. 2012; Zhao et al. 2015), and the subsequent ubiquitination and degradation of targeted proteins, such as the repressors Os53 and AtSMXL6/7/8 (Jiang et al. 2013; Zhou et al. 2013; Wang et al. 2015). A similar mechanism has been suggested for the karrikin receptor AtKAI2 in *Arabidopsis*, through the interaction with the F-box homolog AtMAX2 and the resulting degradation of SMAX1, as AtMAX2 has been identified as essential for the karrikin response (Nelson et al. 2011), *max2* mutants exhibit phenotypes common to *kai2* (Waters et al. 2012), and *smax1* mutants resembled wild-type seedlings treated with karrikins (Stanga et al. 2013). However, identified residues for D3/MAX2 binding (Zhao et al. 2015; Yao et al. 2016b) are mostly not conserved in SlDLK2 (Fig. 3, Table 4), suggesting that SlDLK2 is unable to bind D2/MAX2. It is probable that SlDLK2 binds other types of F-box proteins or maybe it is not involved in protein degradation.

AtD14	OsD14	AtKAI2	SlDLK2
N11	N61	N9	N11
R13	**R63**	K11	R13
F28	**F78**	F26	Y28
D32	D81	D29	D31
S33	S83	S31	S33
D52	D102	D50	D52
C55	C105	G53	F55
G57	G107	G55	G57
V59	V109	T57	L60
F66	**F116**	F64	A67
D131	**D181**	D129	E132
E137	**E187**	E135	N138
E140	**E190**	D138	E141
N151	**N201**	N149	K152
A154	**A204**	A152	V155
G158	G208	G156	N159
A160	A210	A158	A161
P161	P211	P159	S162
L162	**L212**	L160	I163
A163	A213	A161	A164
V164	V214	V162	M165
D167	**D217**	D165	S168
A170	**A220**	I169	P171
E174	E224	E173	K175
R177	R227	R176	K178
F180	**F230**	F179	K181
N181	N231	N180	R182
R183	**R233**	R182	G184
L205	**M255**	F204	K206
R207	**R257**	T206	I208
E245	E295	D244	H246
R263	**R313**	R262	R264

Table 4. Residues involved in MAX2/D3 binding. Residues of AtD14 that based on crystal structure are facing towards the interface mediating AtD14-MAX2 interaction, are shown (Yao et al., 2016). It is also included G158 of AtD14, reported to be involved in construction of a π-turn structure that contributes to stabilizing the proper conformation of the AtD14 lid, that is essential for binding of MAX2 (Yao et al., 2016). Those residues of AtD14 or OsD14 whose substitution has been reported to compromise MAX2/D3 binding based on Yao et al. (2016) and Zhao et al. (2015) studies are indicated in bold letters. All residues are surface residues with the exception of F78 of OsD14, which is a pocket residue. The aligned residues for AtKAI2 and SlDLK2 proteins are shown. Residues shadowed in dark blue, light blue or white are identical, similar or different, respectively, to the aligned one of AtD14, showing bigger differences in SlDLK2 residues.

SlDLK2-GFP localizes in the nucleus and cytoplasm in *N. benthamiana* cells

To determine the subcellular localization of SlDLK2 in plant cells, we carried out an *Agrobacterium*-mediated transient expression of SlDLK2 fused to a green fluorescent protein (GFP) tag in epidermal cells of *N. benthamiana*. Visualization of the samples through confocal microscopy indicated a cytoplasmic and nuclear localization of SlDLK2-GFP (Fig. 6). In a parallel experiment we transiently expressed free GFP, and observed that free GFP also displayed a cytoplasmic and nuclear location (Fig. 7A). A western blot analyses of SlDLK2-GFP overexpressing leaves together with the control tissues expressing free GFP, allowed us to confirm that most of the green fluorescent signal observed in the SlDLK2-GFP transformed tissues was associated with the full-length SlDLK2-GFP fusion protein, and not to presence of free GFP (Fig. 7B).

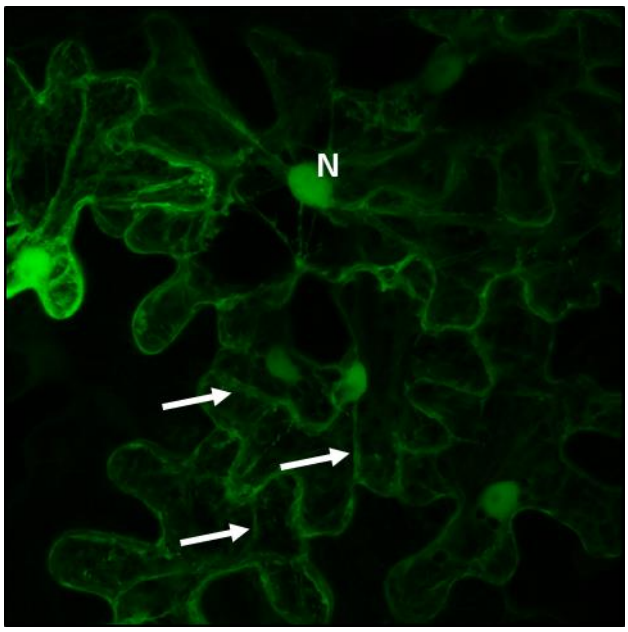

Figure 6. SlDLK2-GFP localizes to cytoplasmic and nuclear plant cell compartments. A representative confocal microscopy image of *Nicotiana benthamiana* epidermal cells expressing SlDLK2-GFP. N, nucleus; arrows, cytoplasmic strands.

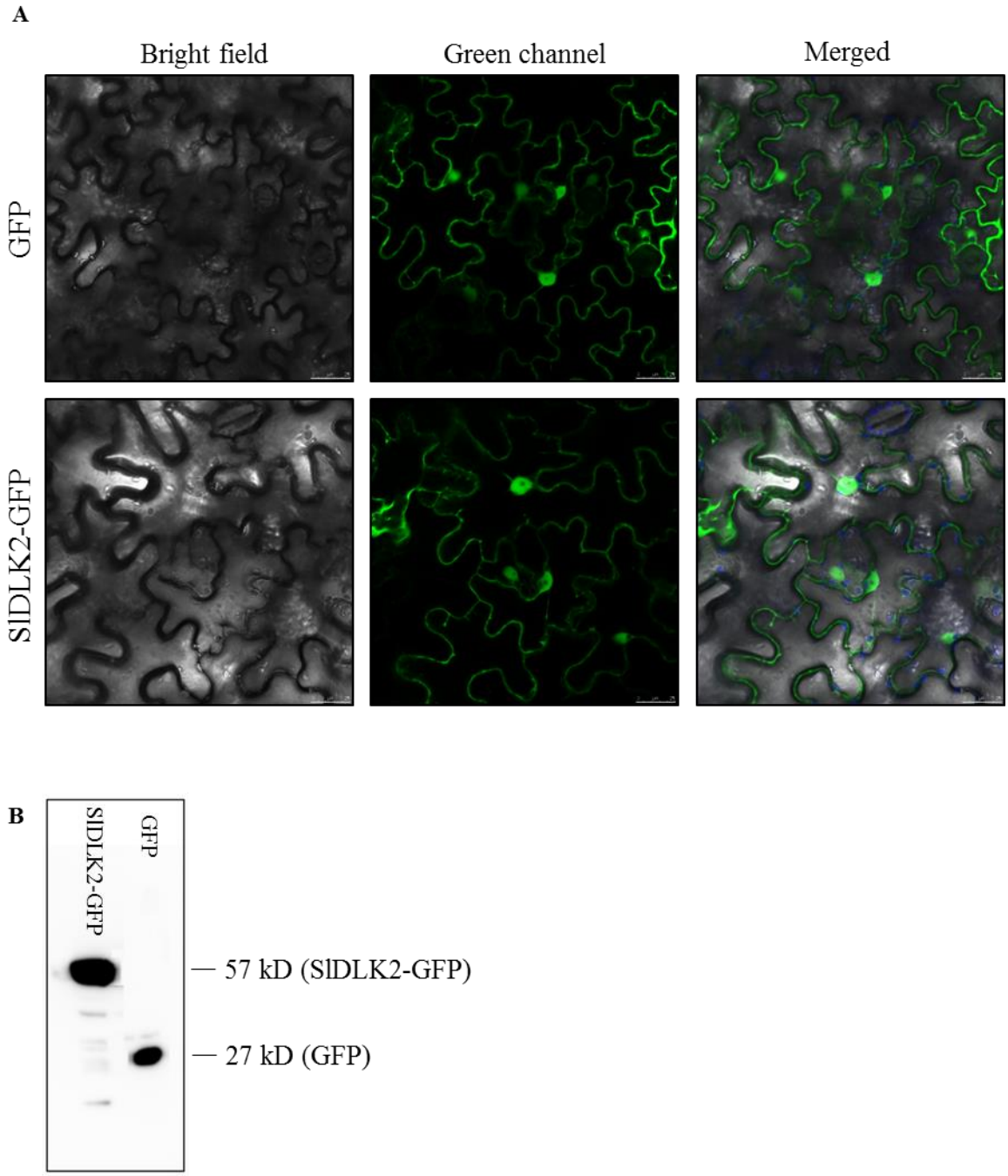

Figure 7. Subcellular localization and western blot analysis of SlDLK2. Images from the observation of SlDLK2-GFP and GFP transformed *Nicotiana benthamiana* leaf cells (A). Images taken in the green channel show the localization of both, SlDLK2-GFP and the control GFP, with a cytoplasmic and nuclear localization. Each square has a real-life size of 164 µm. Western blot analysis of the *N. benthamiana* transformed tissues used in the experiment (B). The expected sizes of the SlDLK2-GFP fusion protein and free GFP are indicated for reference. This representative experiment indicates that most of the signal observed under the confocal microscope in the SlDLK2-GFP transient expressing tissues is associated with the full-length SlDLK2-GFP.

Analysis of *SlDLK2* gene expression in mycorrhizal roots

In order to corroborate that *SlDLK2* expression is associated with AM symbiosis, as previously characterized in the microarray hybridizations of García Garrido et al. (2010) and López-Ráez et al. (2010), the expression pattern of *SlDLK2* gene in mycorrhizal and non-mycorrhizal tomato roots was quantified at 32, 42, 52 and 62 dpi (days post-inoculation) using qPCR. For each sample, we calculated the fold change for *SlDLK2* gene expression with respect to non-mycorrhizal plant roots at 32 dpi. As expected, the expression of *SlDLK2* gene was higher in mycorrhizal than in non-mycorrhizal plant roots at all times evaluated, and the gene was significantly up-regulated as root length colonization by *R. irregularis* increased through time (Fig. 8A,B), reaching its maximum expression (8.92-fold) at the last time analyzed (62 dpi). A similar experiment was repeated for a second time (Fig. 9) and, again, we observed that increases in *SlDLK2* gene expression were parallel to increases in the mycorrhization level. Data from both experiments were analyzed together comparing the two variables (percentage of mycorrhizal colonization and *SlDLK2* gene expression) for each biological replicate, and a highly significant positive correlation ($r=0.70$, $P<0.001$) was found between mycorrhizal colonization and *SlDLK2* gene expression (Fig. 8C), what suggest that this gene is tightly regulated during arbuscular mycorrhizal development and thus could play an important role in the AM symbiosis.

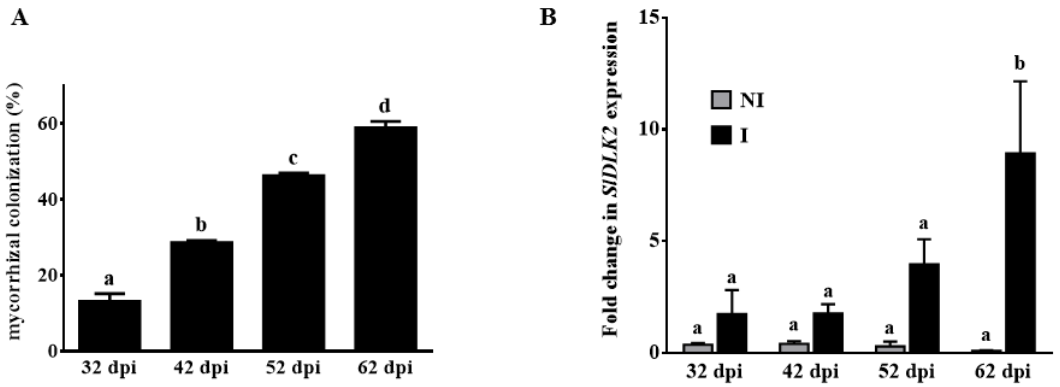

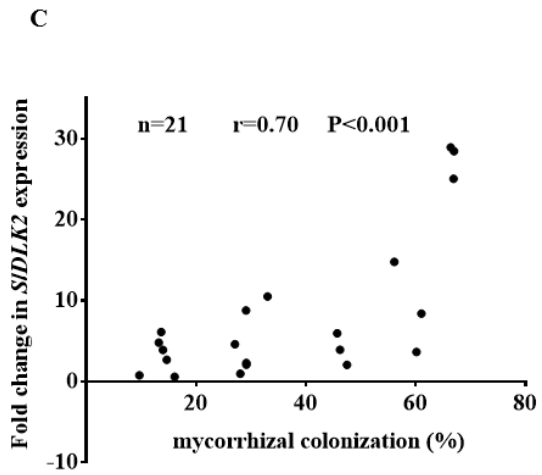

Figure 8. Mycorrhizal colonization and expression analysis of *SlDLK2* gene in Money Maker tomato plants non-inoculated (NI) and inoculated (I) with the AM fungi *R. irregularis.* After 32, 42, 52 and 62 dpi (days post-inoculation), the percentage of total root length colonized by *R. irregularis* was measured (A) and *SlDLK2* gene expression was analyzed by qPCR (B). qPCR data represents the relative expression of the *SlDLK2* gene in plants with respect to expression in non-colonized plants at 32 dpi , in which expression was designated as 1. Values correspond to mean ± SE (n=3). Bars with a same letter are not significantly different (P>0.05) according to LSD multiple comparison test. The scatter plot depicting the relationship between *SlDLK2* expression level and mycorrhizal colonization is shown (C). The Pearson correlation coefficient (r) determining the relationship between two variables is indicated.

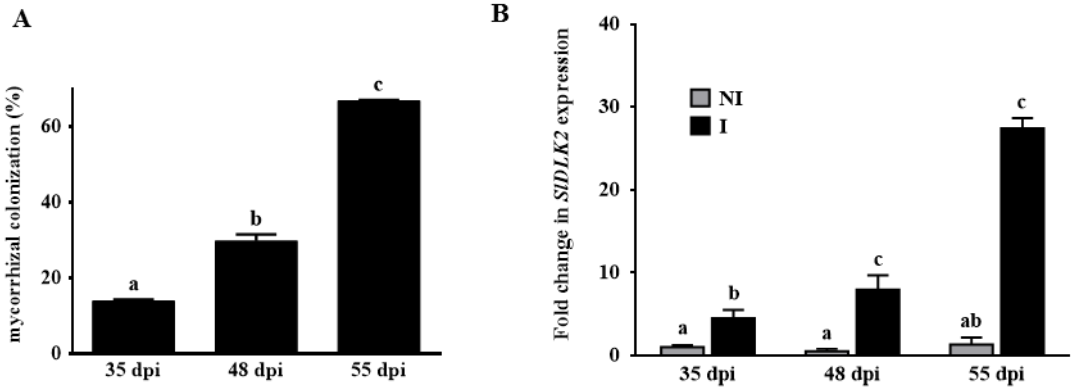

Figure 9. Mycorrhizal colonization and expression analysis of *SlDLK2* gene in Money Maker tomato plants non-inoculated (NI) and inoculated (I) with the AM fungus *R. irregularis* (Repeated experiment). An experiment similar to that showed in Fig. 8 was performed for a second time and the percentage of total root length colonized by *R. irregularis* (A) and *SlDLK2* gene expression analyzed by qPCR (B) were measured at 35, 48 and 55 dpi. qPCR data represents the fold change *SlDLK2* gene expression in plants with respect to non-colonized plants at 35 dpi, in which expression was designated as 1. Values are the mean±SE of three biological replications. Bars with similar letters are not significantly different (P>0.05) according to LSD multiple comparison test.

Expression Analysis of *SlDLK2* gene in tomato organs

The expression pattern of *SlDLK2* gene was analyzed by qPCR in different organs of tomato, showing that *SlDLK2* is upregulated in leaves, with a 5.75 ± 0.20-fold induction with respect to non-mycorrhizal roots, followed by gene induction in flowers at all stages (with 2.5 to 4 fold change values), as illustrated in Fig. 10. By contrast, fruits exhibited the highest repression of *SlDLK2*. This result is in agreement with the RNA-Seq data of tomato organs downloaded through the tomato eFP browser at bar.utoronto.ca (Fig. 11), where *SlDLK2* exhibited a RPKM fold change of ≥200 in leaves, followed by both unopened and opened flowers (about 50 RPKM), while no expression is shown in fruits. It is also worth mentioning that the third organ showing the highest *SlDLK2* expression level are the roots (non-mycorrhized) according to both the qPCR carried out and the downloaded RNA-Seq data.

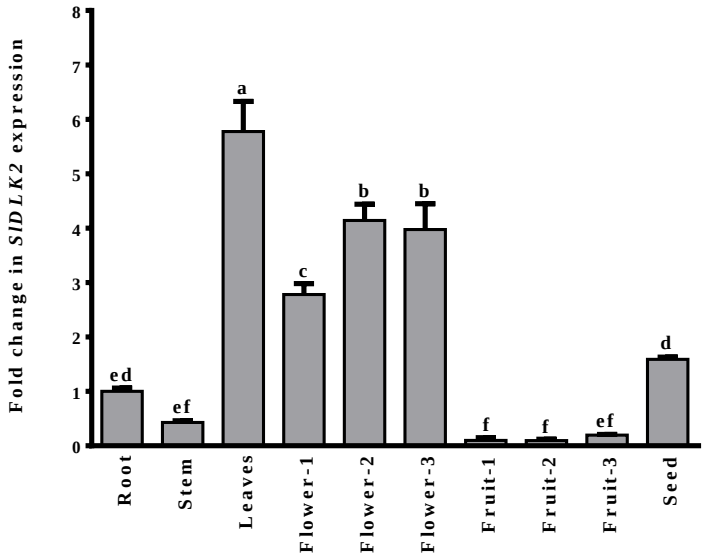

Figure 10. Data of *SlDLK2* gene expression pattern in different organs of *S. lycopersicum* cv Moneymaker. *SlDLK2* gene expression was measured by qPCR in roots, young stems, leaves, young flower buds ("Flower-1"), mature flower buds ("Flower-2"), open flowers ("Flower-3"), green fruits ("Fruit-1"), developing fruits turning red ("Fruit-2"), mature fruits in red ("Fruit-3") and seeds. qPCR data represents the fold change of *SlDLK2* gene expression in plant organs with respect to roots, in which expression was designated as 1. Values are the mean ± SE of two biological replications. Bars with a same letter are not significantly different (P>0.05) according to LSD multiple comparison test.

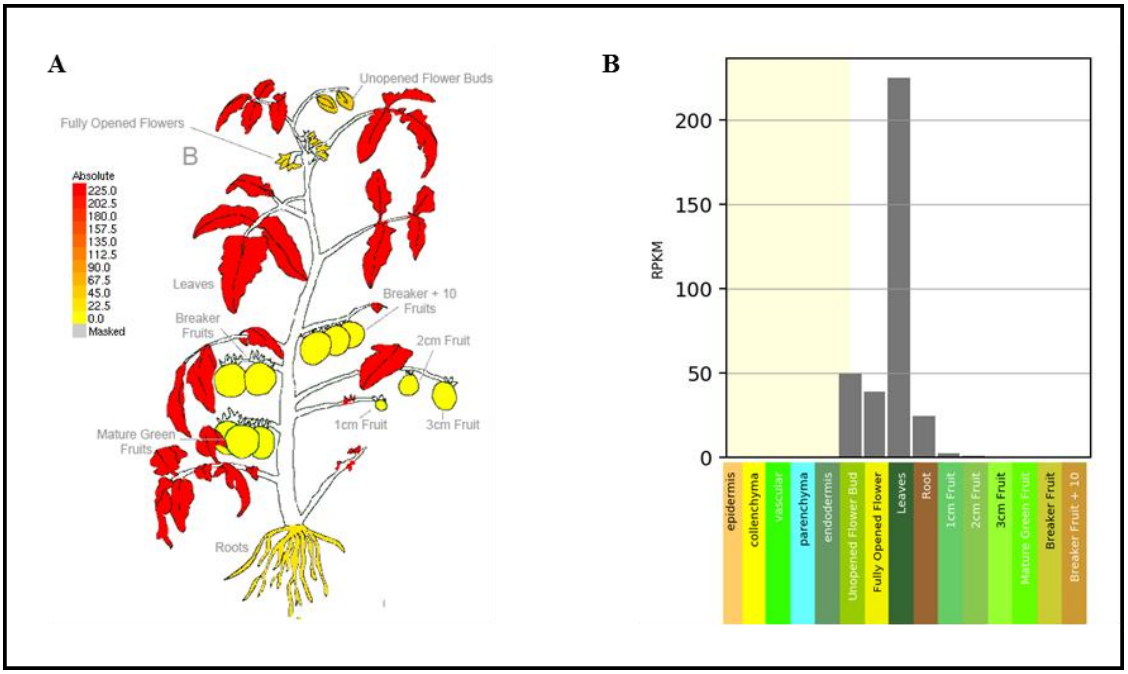

Figure 11. Data of *SlDLK2* gene expression pattern in various organs/tissues of *S. lycopersicum* cv Heinz 1706 according to RNA-Seq analysis previously performed by Matas et al. (2011). Electronic fluorescent pictographic representation of absolute *SlDLK2* gene expression pattern (A) and the corresponding chart (B). These electronic expression data were downloaded from the Tomato eFP Browser (at http://bar.utoronto.ca). Shown data is Illumina-derived and RPKM -normalized. The expression levels are presented using absolute fold-change values.

Expression of other *RsbQ-like α,β-hydrolase* genes in tomato organs and AM roots

The BLASTP homology search at NCBI and Solgenomics revealed the presence of five other tomato α,β-hydrolases belonging to the RsbQ-like group, in addition to SlDLK2 (Fig. 3). Only one tomato α,β-hydrolase (XP_004238093.1, here named "SlD14") takes part from the D14/DAD2 clade, while four α,β-hydrolases belonged to the KAI2/HTL clade. Particularly two pairs were found in the KAI2/HTL clade. One pair is phylogenetically closer to the previously characterized KAR1 receptor AtD14L (Kagiyama et al. 2013), and it is constituted by the XP_004233449.1 and the XP_004231894.1 proteins (here named "SlKAI2c", KAI2 conserved, pair). The other

pair is composed by the XP_004233607.1 and the Solyc02g064760 ("SlKAI2i" KAI2 intermediate pair). Gene localization in the Tomato Genome Sequence 3.0 and the proposed names used in this paper are shown in Fig. 12. In silico expression of the corresponding cDNAs was downloaded from the Tomato eFP Browser (at http://bar.utoronto.ca), showing a completely different expression pattern among the different α,β-hydrolases (Fig 13). This result is in agreement with lack of similarity found among putative promoter sequences of all six RsbQ-like α,β-hydrolases, downloaded from the Tomato Genome Sequence 3.0 (https://solgenomics.net) (data not shown), suggesting a completely different gene regulation. qPCR analyses were performed in *R. irregularis* colonized roots compared to non-inoculated roots, and revealed that apart from *SlDLK2*, another tomato RsbQ-like α,β-hydrolase, corresponding to the putative tomato receptor of canonical SLs, *SlD14*, might also be someway responsive to mycorrhization, and it actually seems to be induced at the first stages of the mycorrhization. Interestingly, apart from the particularly important role of SL signaling for pre-symbiotic fungal growth and hyphal branching (Mori et al. 2016; Akiyama et al. 2005b; Besserer et al. 2006b), the activation of SL biosynthetic genes is reported to be required for efficient hyphopodium formation (Kobae et al. 2018). Then, the observed up-regulation of *SlD14* might take part in this process for the punctual entry of AM fungi into the roots.

We observed *SlKAI2cB*, the closest tomato homolog to the rice karrikin receptor *OsD14L* reported by Gutjahr et al. (2015) to be essential for mycorrhization in rice, is not induced by AM fungal colonization in tomato at 35 and 48 dpi, supporting the lack of alteration of *OsD14L* transcript expression during AM colonization previously observed by Gutjahr et al. (2015). However, *SlKAI2cB* is curiously repressed in old roots under mycorrhizal conditions, what could be related to a negative regulatory mechanism of mycorrhization at later stages.

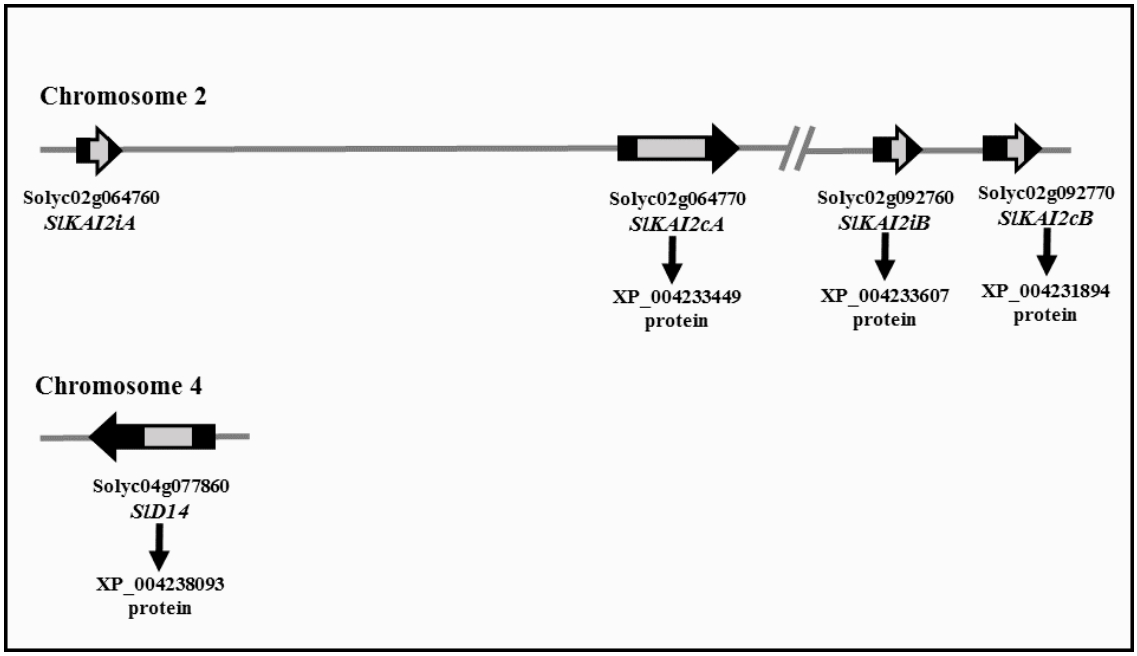

Figure 12. Localiza-tion diagram of tomato RsbQ-like α,β-hydrolase genes in the Tomato Genome Sequence 3.0. The four tomato α,β-hydrolases belonging to the KAI2 group are located in chromosome 2, while the putative *SlD14* is located in chromosome 4. Arrows represent tomato RsbQ-like α,β-hydrolases, with intron sequences shadowed in grey. SolDB accessions and common gene name used in this work are indicated, together with the RefSeq accession number of the encoded protein.

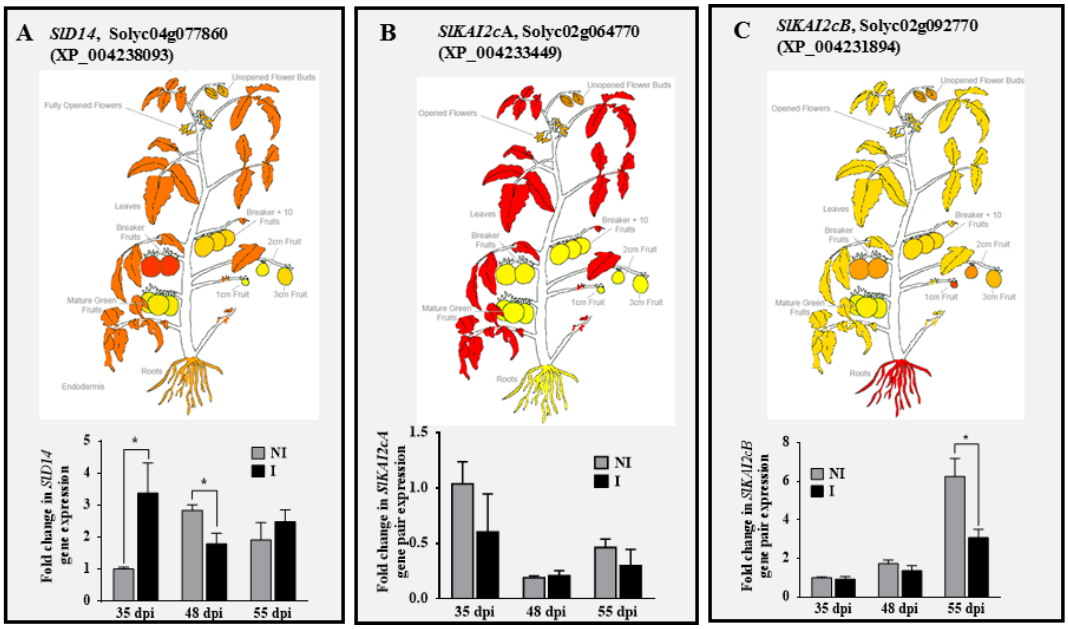

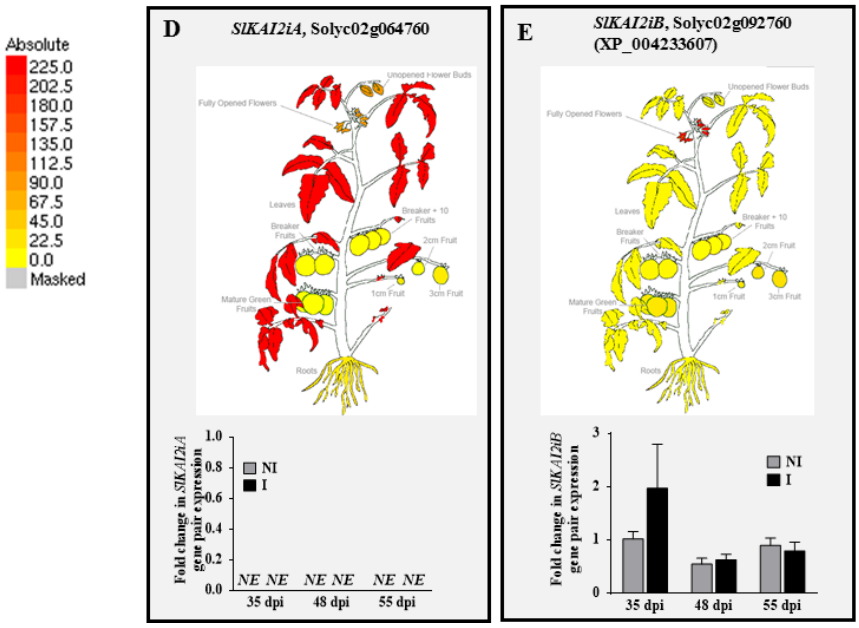

Figure 13. Data of tomato *RsbQ-like α,β-hydrolases* gene expression pattern in various organs/tissues and in mycorrhizal roots. In silico differential organ gene expression and qPCR-analyzed time course gene expression in AM inoculated roots are shown for the *SlDLK2* closely related tomato genes coding for the putative SlD14 (A), SlKAI2cA(B), SlKAI2cB (C), SlKAI2iA (D) and SlKAI2iB (E) proteins. Electronic fluorescent pictographic representation of absolute fold change gene expression values, corresponding to the RNA-Seq analysis previously performed by Matas et al. (2011) in *S. lycopersicum* cv Heinz 1706, was downloaded from the Tomato eFP Browser (at http://bar.utoronto.ca). Graphs represent gene expression analyzed by qPCR at 35, 48 and 55 dpi in plants inoculated with *G. irregularis* (I). qPCR data represents the fold change gene expression in plants with respect to non-colonized (NI) plants at 35 dpi, in which expression was designated as 1. Values correspond to mean ± SE. *NE*; no expression detected. Significant differences (Student´s t test) between the mutant and the control are indicated with asterisks (*$P \leq 0.1$, **$P \leq 0.05$, ***$P \leq 0.01$).

Expression analysis of *SlDLK2* gene in non-mycorrhizal roots subjected to hormone treatment

Exogenous hormone application was performed and its effect on *SlDLK2* gene expression was analysed at 12, 24 and 48h after treatment. The results are illustrated in Fig. 14, where fold change gene expression is expressed as log2 (M-value) in order to equally visualize gene induction and repression, with respect to the control treated with water. Three different gene expression patterns were observed. Methyl jasmonate and GA_3 significantly reduced *SlDLK2* gene expression. Salycilic acid, the ethylene-releasing compound ethephon (2-chloroethyl phosphonic acid) and abscisic acid initially (12h after treatment) induced and later

(24 and 48h) repressed *SlDLK2* gene expression, suggesting a slower negative regulation. The only hormone exhibiting a clear inducing role on *SlDLK2* gene expression was the IAA, which provoked a >7 fold change induction at 48h after treatment with respect to the control at the same time.

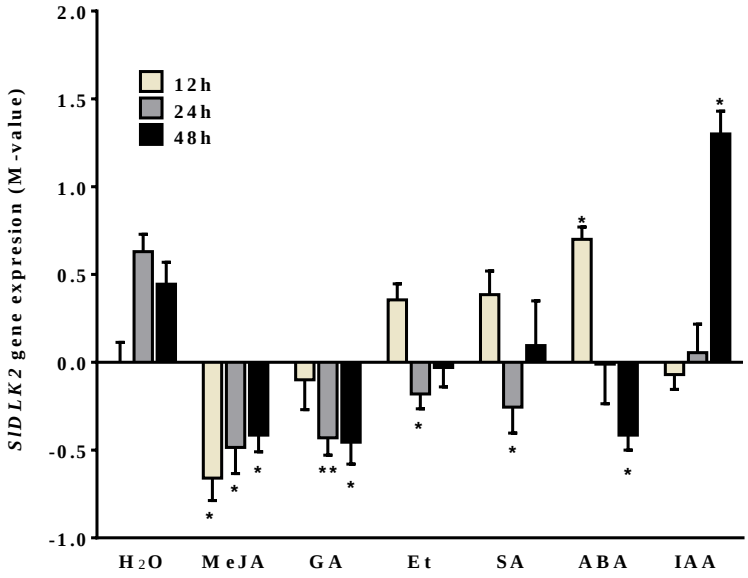

Figure 14. Hormone treatment effect on *SlDLK2* gene expression in tomato non-inoculated roots. *SlDLK2* gene expression analyzed by qPCR in roots treated with water (H_2O), methyl jasmonate (MeJA), gibberellin (GA_3), ethephon (Et), salicylic acid (SA), abscisic acid (ABA) and indol acetic acid (IAA). Gene expression was analyzed at 12, 24 and 48 hours after hormone treatment. qPCR data represents the M value (log2 fold change) of *SlDLK2* gene expression in roots with respect to H_2O treated plants at the first time analyzed (12h), in which expression was designated as 1. Values correspond to mean ± SE. Significant differences (Student´s t test) between the treated root and the control root at the same time analyzed are indicated with asterisks (*P < 0.05, **<0.01).

Gene expression and AM fungus localization

To analyze the *SlDLK2* promoter activity, the 1560 bp region upstream of *SlDLK2* (p*SlDLK2*) was fused to a GUS reporter construct and tomato composite plants were generated. Transgenic roots were checked for the presence of the blue dye that corresponds to GUS activity. In non-mycorrhizal hairy roots of eight week old plants carrying the p*SlDLK2*-GUS, lack of staining was found, with the exception of some roots showing a promoter activity restricted to the central cylinder and pericycle (Fig. 15 A-C). However, under mycorrhizal conditions, the promoter activity was

also detectable in the cortex zones affected by AM fungal root colonization (Fig. 15 D-H). The promoter of the tomato phosphate transporter 4 (*PT4*), previously described to be specifically expressed in arbuscule-containing cells (Nagy et al. 2005), was used as a positive control for the GUS staining (Chapter 1, Fig. 4).

Longitudinal roots sections were stained for GUS activity and counterstained with WGA-alexa488 to visualize fungal structures (Fig. 16). Colonization by *R. irregularis* redirected *SlDLK2* expression to arbusculated cells, whereas non-colonized neighboring cells were not stained. Thus, the expression of *SlDLK2* is AM-dependent and is associated with cortex cells colonized by AM fungal arbuscules.

It is worth mentioning that the induced expression pattern of *SlDLK2* in the vascular cylinder of the control roots (Fig. 15A-C) is different to that one shown by its homolog gene *DLK2* in *Arabidopsis*, characterized by a strong activity associated to root hairs and the cortex (Végh et al. 2017). Then, *SlDLK2* in the vascular tissues of tomato roots might be involved in transport rather than in the speculated role for *Arabidopsis DLK2* in nutrient uptake and edaphic stress responses (Végh et al. 2017). However, we must not discard such a role for *SlDLK2* because, in the particular case of mycorrhizal roots, *SlDLK2* expression is highly induced in arbusculated cells (Fig. 15D-F), where a high nutrient uptake is known to be required.

Curiously, the expression pattern of *SlDLK2* in the un-inoculated tomato roots is very similar to that one found for the gene *SMXL4*. SMXL4 protein is reported to be involved in phloem formation and transport as well as in carbohydrate accumulation (Wallner et al. 2017; Wu et al. 2017), and it is speculated to be negatively regulated upon interaction with DLK2 in *Arabidopsis* (Végh et al. 2017). Following this hypothesis, *SMXL4* might have a role in carbohydrate transfer to the AM fungus in arbucule-containing cells, and *SlDLK2* induction in arbuscule-containing cells might be required to inactivate SMXL4 proteins in order to restrict AM fungal development. In this manner, *SlDLK2* silencing might trigger an inefficient inactivation of SMXL4, favoring carbohydrate transport to the AM fungus and, consequently, favoring carbohydrate availability and development of the AM fungus, which is in agreement with the higher mycorrhizal colonization in the *SlDLK2* RNAi composite plants (see later).

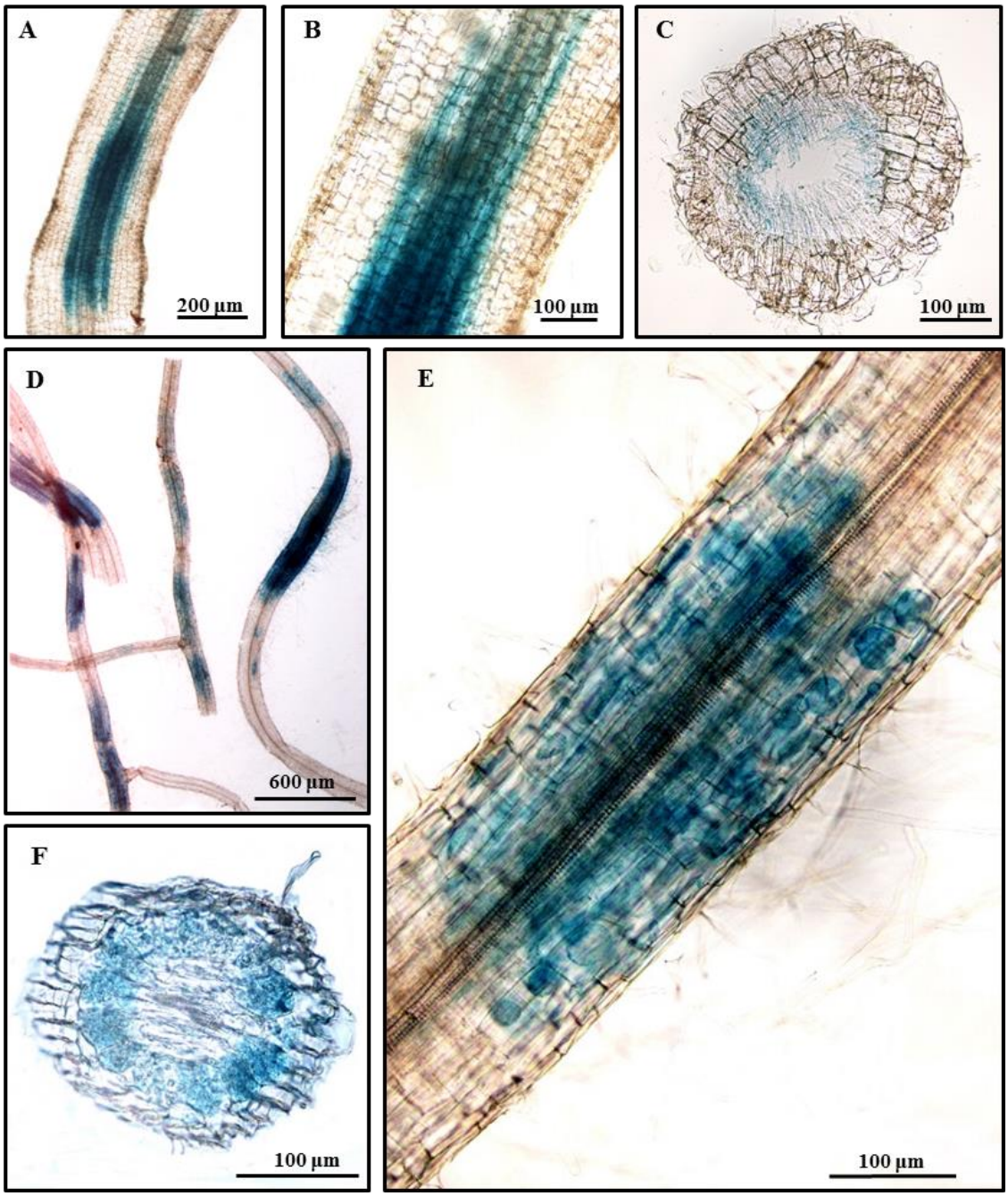

Figure 15. Expression analysis of the *SlDLK2* promoter in transgenic *S. lycopersicum* roots after GUS staining. GUS activity in *A. rhizogenes*-transformed roots expressing the *SlDLK2* promoter *β-glucuronidase* fusion was assessed 8 weeks after inoculation with *R. irregularis* (whole root in D, E; cross-section in F), and without *R. irregularis* (whole root in A and B, cross-section in C). All images were taken with an inverted microscope, except D, which was taken with a stereomicroscope.

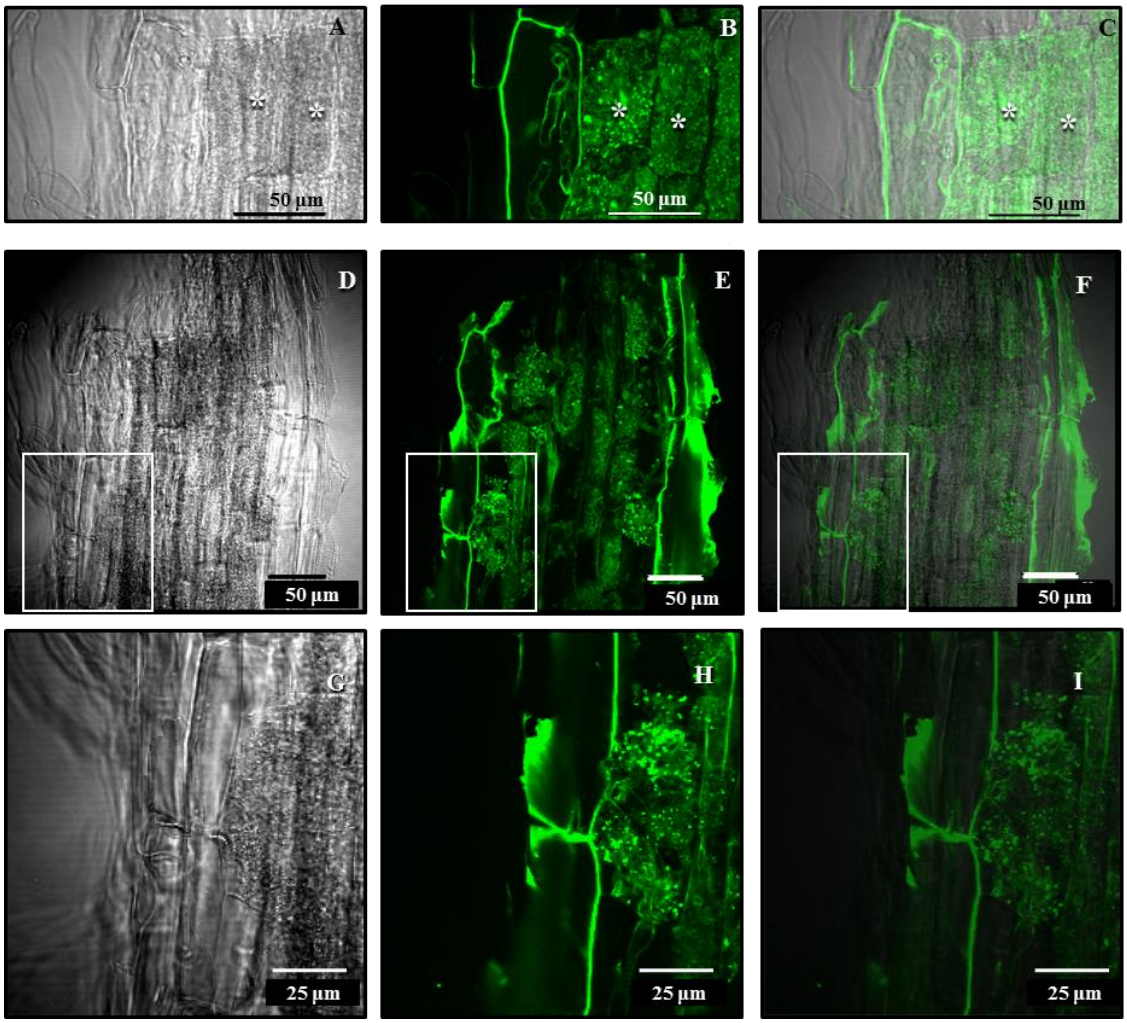

Figure 16. Histochemical analysis of *SlDLK2* promoter expression in AM colonized transformed roots 8 weeks after inoculation with *R. irregularis*. GUS stained roots were vibratome sectioned and the AM fungus was labelled with WGA. (B), (E) and (H) show *R. irregularis* hyphae stained with WGA-Alexa Fluor 488, which fluoresces green; and (A), (D) and (G) are the corresponding bright-field images, which show exclusively GUS activity. (C), (F) and (I) are the merged images of GUS staining and WGA-Alexa 488 images. (G), (H) and (I) are the higher magnification images of the squared area in images (D), (E) and (F). White asterisks indicate arbuscules in the host cortical cells. Images were acquired by CLSM.

Theoretical and bioinformatics analysis of the *SlDLK2* promoter

We examined the -1560 to -1 region upstream of the *SlDLK2* coding region in order to look for mycorrhizal-induced elements (Fig. 17). Only a few motifs have been reported as mycorrhizal-associated cis-elements so far. Among these are the CTTC element (Karandashov et al. 2004), the CTTC-like motif named MYCS (Chen et al. 2011) and the P1BS element (Rubio et al. 2001). We identified a putative P1BS site (GGATAATC at -104 position) and a probable MYCS site (TCTCTTTTTCT at -159 position) in the *SlDLK2* promoter. We also found a putative AT-rich motif at -459 position, an element demonstrated to be essential for the high-level expression of *MtENOD11* during mycorrhization and nodulation in *Medicago truncatula* (Boisson-Dernier et al. 2005). It is also remarkable the identification of a putative auxin responsive element (AuxRE, TGTCAC) at -618 position, which could be responsible of the *SlDLK2* induction observed 48 hours after exogenous auxin application (Fig. 14). In fact, the AuxRE element is located in a similar position in the *SlGH3.4* promoter (-654), and it was recently shown to contribute to induce *SlGH3.4* gene expression in the AM-colonized cells through its response to auxin (Chen et al. 2017), which suggest that the AuxRE element might have an analogous role in regulating *SlDLK2* expression. Finally, at (Boisson-Dernier et al. 2005)-73 position we identified the GCCGGC palindrome, which was predicted as a possible cis-regulatory element associated to mycorrhization by Favre et al. (2014).

The promoter sequence was also subjected to the PlantCARE database (Lescot et al. 2002) for prediction of other cis-regulatory elements (Fig. 17). Two putative methyl jasmonate responsive elements (CGTCA) were found at -987 and -484 positions, which probably act as repressor binding sites in response to methyl jasmonate. Other stress-responsive cis-acting elements were predicted, including the MBS element for drought stress, the HSE element involved in heat stress and the TC-rich repeats for defense and stress responsiveness.

Some cis-elements related to leaf development and differentiation were also predicted by the PlantCARE database, what is in agreement with the upregulation of the *SlDLK2* gene observed in leaves in our qPCR analysis (Fig. 10) and in the RNA-Seq data downloaded through the tomato eFP browser (Fig. 11).

-1476

-1560 CCATATTGTGGATTAGGCCTGTAAACTTTACTTTTATTTACTAACTTATA
-1510 AAACTTAAACAAGAATAAACAATATATTGATTTTGATTATCAATGAATGT
-1460 TATTGAAGTCCGAAATGCTAAAGCATAAACGATTAGTCCATATTTAAGGA
-1410 GTTTGAGGCTAGGTTATAATTACCCCATTTTAGTTATCTATTTTAAAACC
-1360 ACTTTGTGGTTACGGGTTTTGGAGTAAATTTTATTCTATTATGATTTTTT
-1310 TAAAGAAGATTGTAAAAGTGTTTATTTGAACCCCTTTTACATGAATTGAT
-1260 GATCCTTCATTAGTATAAGTCGAATCATTATGATGGATTACAATTGTAAA
-1210 GTATATAGTAACATATGAGTTATGCTCCTTGACAAATACAAGTCAATTGA
-1160 ATGCGATTATATATGCATGATCAAGCTATAATTGGGTAATACAATTAGCT
-1110 ACGGTATATGTCACCCTTACATCTATTAACTTCACATTTTAGGATTGATA
-1060 AGACCATATTTATTGAAATTTCATAGTGATTTTCATCAAACAACTGATAT
-1010 GAAATAGCAAAAAAATTTCTTCGTCAATATGAACGAATGTTATTGCAGAG
-960 TGAATGGCTTAGGTTAATCGATTAGTCTATAGGTTACAAGTTTGAATCTA
-910 GGATAGACCACAATTTTAAGTAATTTTTTTAAAAATAAACTATTTGAATG
-860 TTTTAGGATTTAAATAATTTTTAATTTCATATTTTTTTTCTTAAATAAGA
-810 TTGTAAAAGTATATATTTGATCAACTTCAAAATAATTGAAGATTTTTAAG
-760 TCGAATCATTATGGTGAAAATAAACCTAAAGTGTATAGTAAAATATAAGT
-710 TACGCTCCCTCACAAATACAAGTTAATTGAATGTGATTATATATACATGA
-660 TCAAGTTTATAATGGGGTAATAACAATTAGTTACGTATATGTCACTCTTA
-610 CATCTATTAACTTCACATTTTAGGATTGATTAGACCATATTGATTGATAA
-560 TGTCTCATTTTTATAAAATTTCATAGTGATTTTCATTAAAAAACTAATATG
-510 AAGTAGACTAAATAAATTTTCCTTCGTCAATATAAACCAATGTTATTGCA
-460 GCGCGAATAATTTAGTGTCAATCGATTAGTCTATAAGTCACGAGTTTTAA
-410 TCTAGGATAGGCCACAATTTAAAGTATTTTTTTTCAAAAATAGACTATGT
-360 GAATATTTTAGTATTTAAGTAATTTATGATTTCATATATTTTTTCCTTAA
-310 ATAAGATTGTAAAAGTGTATATTTGATCAACTTCACAATAATTGAAGATT
-260 TTCACTATTTTAAGTCGAATCATTATAATGAATCCATAACAAAATTGACA
-210 GACCCTAAAAATGCCTTTCACGCTAGAATTGTAGCTCTGAACTCACTCTC
-160 TTTTTCTTAAAAGAAAATTTAGAATTAACTTTTAATCTTTGATCCGCCTC
-110 TAGGATAATCAATACGTTGCATTATATAGTGTTGGCCGGCCAATAAACCT
-60 CTTCCCTTTGCTATATATATAAATATATAGTAAGTATAGTTAGAATAGCA
-10 TAAGTAGAAAATGGTGATATTGGATTTATTAAGAAATATGAATGGAAGAA

Format code	Motif (consensus sequence is indicated when different to the found one)	Sequence (5´→3´) (Position)	Source
-●-	HD-Zip 1 element involved in differentiation of the palisade mesophyll cells.Consensus CAAT (T/A) ATTG.	CAATAATTG (-271)	PlantCARE database
	HD-Zip 2 element involved in the control of leaf morphology development.Consensus CAAT (G/C) ATTG.		
-●-	Defense and stress responsiveness motifs (TC-rich repeats). Consensus ATTTTCTTCA	AATTTACTCCA (reversed) (-1336) ATTTTCACCA (reversed) (-744)	PlantCARE database
	MYB binding site involved in drought-inducibility (MBS)	CAACTG (-1017)	PlantCARE database
	Heat stress responsiveness motif (HSE)	AAAAAATTTC (-997) AAAAAATTAC (reversed) (-886) GAAATTTTAT (reversed) (-545)	PlantCARE database
-●-	Methyl jasmonate responsive element (CGTCA)	CGTCA (-987) CGTCA (-484)	PlantCARE database
	Auxin responsive element (AuxRE)	TGTCAC (-1099) TGTCAC (-618)	Chen et al. (2017)
-●-	Mycorrhizal responsive element MYCS. Consensus TTTCTTGTTCT	TCTCTTTTTCT (-159)	Chen et al. (2011)
	Phosphate starvation response-associated Binding site (PHR1 binding site, P1BS). Consensus GnATATnC	GGATAATC (-104)	Rubio et al. (2001)
	AT-rich motif. Consensus TTATT(N)7-12AATAA	TTATTGCAGCGCGAATAA (-459)	Boisson-Dernier et al. (2005)
	GCC-box	GCCGGC (-73)	Favre et al. (2014)

Figure 17. Cis-regulatory elements predicted in the *SlDLK2* promoter. Nucleotide sequence of the *SlDLK2* promoter cloned region, from position -1560 to -1, numbered from the starting translation site (+1). Putative cis-regulatory elements are marked, including those likely involved in mycorrhizal-associated expression and those predicted to respond to defense, stress, drought, heat or hormones. Prediction is supported on the PlantCARE database, as well as on the identification of some putative motifs of interest previously described in the literature. The translation start codon is underlined.

Functional analysis of *SlDLK2* gene in tomato RNAi and overexpressing composite plants

Tomato RNAi and overexpressing (OE) hairy roots for the *SlDLK2* gene were obtained in order to perform a functional analysis of this gene. The RNAi experiment was carried out using composite plants with hairy roots transformed with the control empty vector (pK7GWIWG2_II-RedRoot) and the *SlDLK2* RNAi construct (pK7GWIWG2_II-RedRoot::¡*SlDLK2*). We tested the expression level of the *SlDLK2* gene in the roots of these RNAi plants after 45 dpi and we obtained a successful repression of the *SlDLK2* gene by 90.66%, as shown in Fig. 18A.

For the OE experiment, the control empty vector (pUBIcGFP-DR) and the *SlDLK2* OE vector (pUBIcGFP-DR) were used for the transient transformation, and 62 days after inoculation with the AM fungus *R. irregularis* a significant upregulation of *SlDLK2* by 487.33% was obtained in the OE mycorrhizal hairy roots (Fig. 18B). We must highlight that the OE produced in AM-roots was significantly much higher in AM roots than in uninoculated roots. We speculate that *SlDLK2* gene expression might be auto-regulated by a positive feedback mechanism that only occurs under mycorrhizal conditions, then overexpression would trigger an increased activation of the endogenous *SlDLK2* promoter in AM roots.

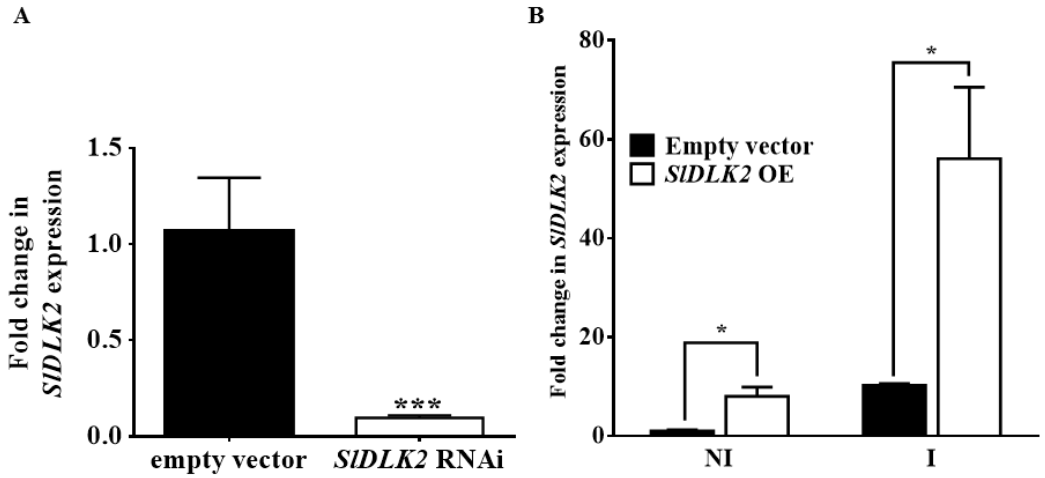

Figure 18. *SlDLK2* gene expression in hairy roots of *SlDLK2* RNAi and OE AM colonized composite plants. The transcript abundance of the *SlDLK2* gene was quantified by qPCR in hairy roots from *SlDLK2* RNAi (A) and *SlDLK2* overexpressing (B) composite plants 45 and 62 days after infection with *R. irregularis*, respectively. The *SlDLK2* gene expression data in RNAi and OE roots is represented with respect to its expression in the control plants containing the corresponding empty vector (pK7GWIWG2_II-RedRoot and pUBIcGFP-DR, respectively), in which the expression level was designated as 1 (n=3). Values correspond to mean ± SE. Significant differences (Student´s t test) between the mutant and the control are indicated with asterisks (*$P < 0.05$; ****P<0.0001).

In the *SlDLK2* RNAi and *SlDLK2* OE hairy roots we observed alterations in the mycorrhization pattern and arbuscule morphology, as well as changes in AM-associated and hormone metabolism-related gene expression. Particular changes are detailed below.

SlDLK2 plays a negative role during AM mycorrhization

Analysis of the percentage of mycorrhization in the *SlDLK2* RNAi and overexpressing (OE) roots revealed important changes. *SlDLK2* RNAi roots, compared to the control roots presented a significant increase (58.23%, $P \leq 0.001$) in the percentage of root length colonized by the AM fungus (Fig. 19A), as well as a significant increase for all the mycorrhizal parameters, indicating that *SlDLK2* gene silencing positively affects the relative and absolute mycorrhizal intensities (M% and m%) and arbuscule abundances (A% and a%, respectively), as shown in Fig. 19B.

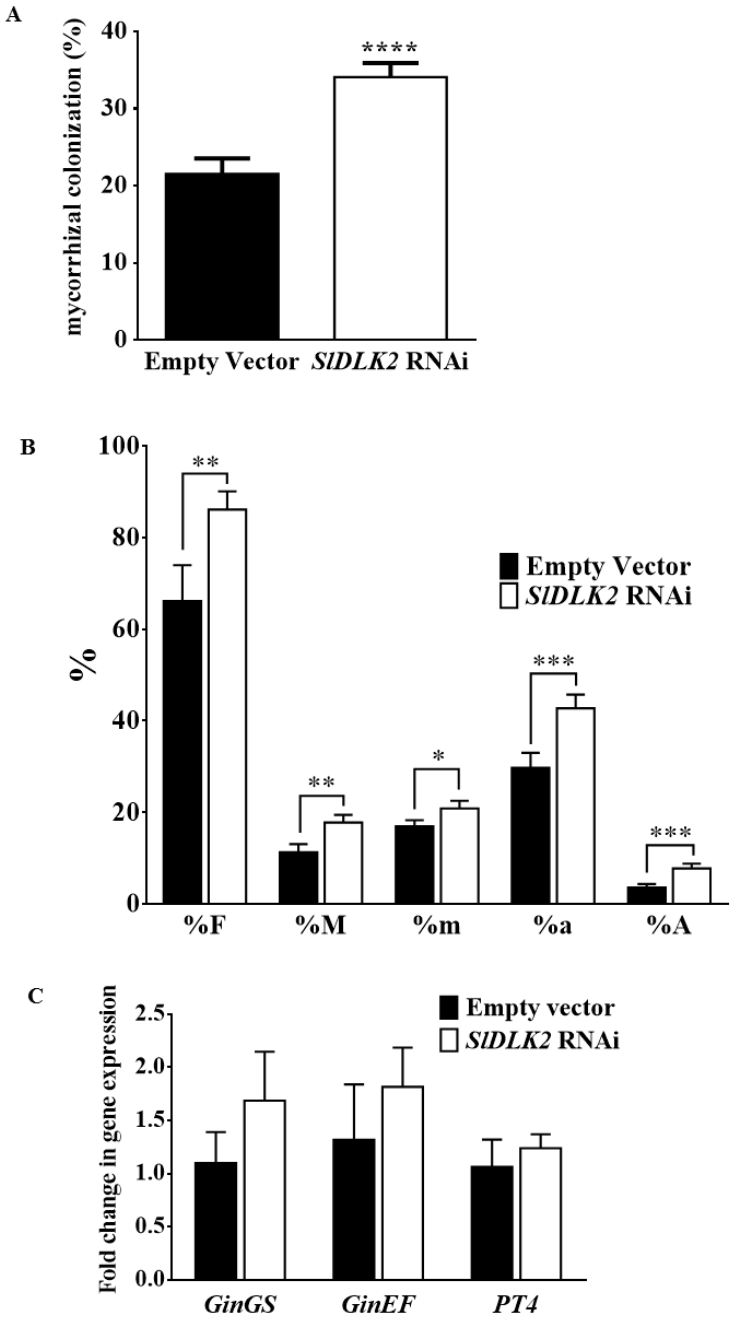

Figure 19. Mycorrhizal colonization at the histological and molecular levels in *SlDLK2* RNAi composite tomato plants 45 days after inoculation with AM fungus *R. irregularis*. After 45 dpi (days post-inoculation) the percentage of total root length colonized by *R. irregularis* was measured (A) and the mycorrhizal parameters were analyzed (B) by visualization of trypan blue stained hairy roots transformed with the empty vector or the *SlDLK2* RNAi vector (n=8). Expression of arbuscule activity-marker genes belonging to the AM fungus (*GinGS* and *GinEF*) and to the tomato plants (*PT4*) was measured by qPCR (C). qPCR data represents the relative expression of genes in hairy root systems of *SlDLK2* RNAi composite plants with respect to expression in the control plants, in which expression was designated as 1 (n=3). Values correspond to mean ± SE. Significant differences (Student´s *t*-test) between the mutant and the control are indicated with asterisks (ns $P>0.1$, *$P \leq 0.1$, **$P \leq 0.05$, ***$P \leq 0.01$, ****$P \leq 0.001$).

In view of these results, we wondered if the contrary response occurred in the *SlDLK2* OE composite plants. We did not observe any significant difference on root length colonized in the OE roots with respect to the control roots at 50 dpi after inoculation with *R. irregularis*. However, at 62 dpi, the mycorrhizal colonization of the root significantly decreased by a 21.22% in the *SlDLK2* OE roots with respect to the control roots (Fig. 20A). In addition, a significant decrease for all the mycorrhizal parameters except m% was observed at that time, indicating that *SlDLK2* gene OE negatively affects the relative mycorrhizal intensity (M%), and relative and absolute arbuscule abundances (A% and a%, respectively), as presented in Fig 20B.

In order to corroborate these results at a molecular level, we decided to test if the overall increase in the mycorrhization of the *SlDLK2* RNAi hairy roots was accompanied by an increase in the *R. irregularis* (*GinGS* and *GinEF*) and the *S. lycopersicum* (*PT4*) marker genes associated to the mycorrhization process. As expected, *GinGS*, *GinEF* and *PT4* were tentatively upregulated in the *SlDLK2* RNAi roots (Fig. 19C), suggesting an increase in both the AM fungal and the mycorrhizal root-associated activity. Consistent with this result, we observed the opposite effect in AM *SlDLK2* OE mycorrhizal hairy roots for the *PT4* gene (Fig. 20C). However, controversial results were obtained with respect the AM fungal genes analyzed. Although *GinGS* was not differentially expressed, *GinEF* was curiously significantly (P<0.1) upregulated in AM *SlDLK2* OE roots (Fig. 20D), suggesting that AM fungal activity might be someway induced despite its impaired development in *SlDLK2* OE roots.

These results confirm that the AM colonization, the arbuscule abundance and the AM symbiotic functional responses in the host plant were induced in the *SlDLK2* RNAi hairy roots and repressed by *SlDLK2* overexpression, suggesting a negative role of *SlDLK2* during AM symbiosis.

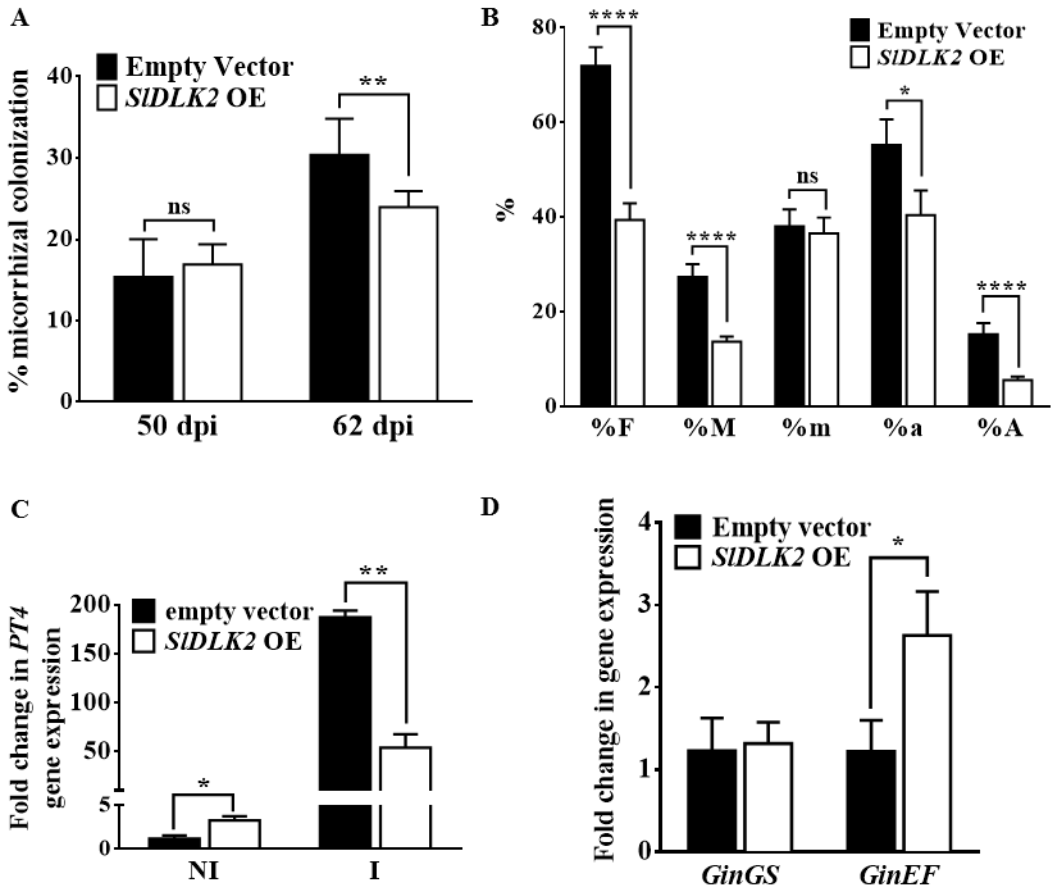

Figure 20. Mycorrhizal colonization in *SlDLK2* overexpressing roots of composite tomato plants after inoculation with the AM fungi *R. irregularis.* Percentage of total root length colonized by *R. irregularis* was measured at 50 and 62 dpi in control (n=11) and *SlDLK2* OE (n=15) hairy roots stained with trypan blue (A). The mycorrhization parameters were also measured at the last time i.e. 62 dpi (B). Expression of the *PT4* arbuscule activity-marker gene belonging to the tomato plant (C) and the *GinGS* and *GinEF* from the AM fungus (D) were measured by qPCR. qPCR data represents the relative expression of genes in hairy root systems of *SlDLK2* OE composite plants with respect to the control non-inoculated (C) and inoculated (D) roots containing the empty vector, in which expression was designated as 1 (n=3). Values correspond to mean ± SE. Significant differences (Student´s t test) between the mutant and the control are indicated with asterisks (ns P>0.1, *P ≤0.1, **P ≤ 0.05, ****P ≤ 0.001).

Is *SlDLK2* involved in SL, ABA and GA hormone regulation?

We screened a few genes related to hormone regulation and response and some interesting preliminary results were obtained (Fig. 21). The SL biosynthetic gene D27 was highly induced in *SlDLK2* RNAi mycorrhizal roots. The ABA biosynthetic

gene, *NCED1*, encoding a 9-cis-epoxy-carotenoid dioxygenase involved in ABA biosynthesis is repressed in the *SlDLK2* RNAi mycorrhizal roots; while *CYP707A3-like* (SGN-U223227) encoding a putative cytochrome P450 involved in ABA catabolism is highly induced. Finally, as for gibberellins (GAs), although not significant differences were observed with respect to the GA biosynthetic gene *GAox1* and the Gibberellic Acid- Stimulated Transcript 1 *GAST1*, a repression trend was observed.

Then, our results suggest that *SlDLK2* impairment during mycorrhization triggers several changes at a hormonal level, including the induction of SL biosynthesis, the signaling for reduction of ABA contents and, probably, a repression of GA signaling. This issue will be analyzed in more detailed in the next chapter.

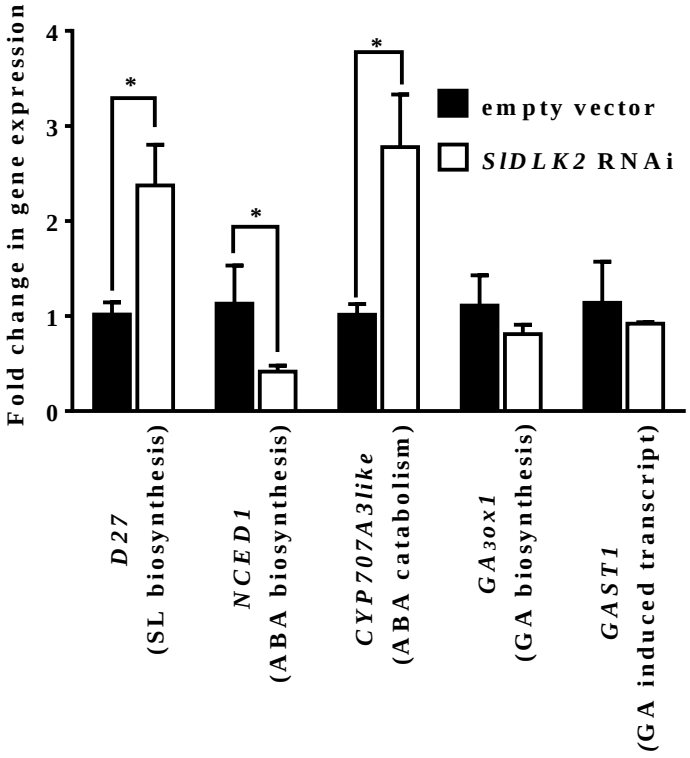

Figure 21. Expression of hormone-related genes in *SlDLK2* RNAi composite tomato plants 45 days after inoculation with AM fungus *R. irregularis.* After 45 dpi (days post-inoculation) the expression of hormone metabolism or response genes was measured by qPCR. qPCR data represents the relative gene expression in hairy root systems of *SlDLK2* RNAi composite plants with respect to expression in the control plants, in which expression was designated as 1 (n=3). Values correspond to mean ± SE. Significant differences (Student´s *t*-test) between the mutant and the control are indicated with asterisks (*P ≤ 0.05).

Is the mycorrhizal phenotype of *SlDLK2* RNAi hairy roots affected by the use of a constitutive promoter for silencing?

Experiments performed with non-inoculated and inoculated roots carrying the *SlDLK2* promoter GUS construct (Fig. 15) suggested that *SlDLK2* might have an additional role in the central cylinder. Consequently, *SlDLK2* RNAi under the constitutive 35S promoter might trigger dysfunctionalities associated to the role of *SlDLK2* in the vascular cylinder and not to mycorrhization. For this reason, in order to restrict and strengthen silencing to the arbuscule-containing cells, we decided to carry out an alternative approximation by interfering the *SlDLK2* gene under the control of the arbuscule-specific *PT4* promoter. As in the previous experiment, mycorrhizal colonization was significantly increased in the p*PT4-SlDLK2* RNAi roots with respect to the control mycorrhizal roots (Fig. 22A). Again, arbuscule morphology apparently showed no abnormalities and the marker gene of arbuscular activity *PT4* was not significantly altered (Fig. 22B). However, this time *GinEF* expression was significantly increased, together with other AM associated genes analysed including *RAM1* and *D27* (Fig. 22B), what suggest that induction of some AM related genes could be accompanying the increased mycorrhizal colonization in the *SlDLK2* silenced roots.

In view of our results, we might say that, in general, mycorrhizal-related transcriptomic alterations turned to be significant by using a p*PT4*-directed silencing. Then, we propose that RNA interference under the control of the *PT4* promoter might be more suitable for functional studies concerning arbuscule-associated genes (e. g. *SlDLK2*) than using a constitutive promoter. For this reason, we decided to subsequently select and submit these p*PT4-SlDLK2* RNAi roots for a transcriptomic RNA-seq analyses, which is shown and deeply dissected in a separate chapter (Chapter 4)

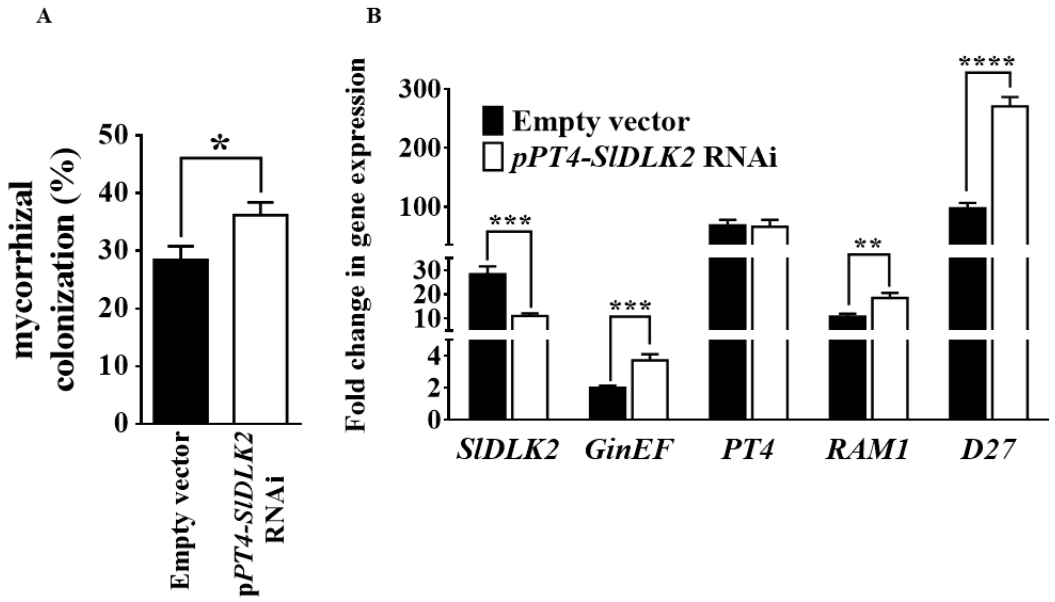

Figure 22. Mycorrhizal colonization and expression of AM related genes in p*PT4-SlDLK2* RNAi composite tomato plants 50 days after inoculation with the AM fungus *R. irregularis*. After 50 dpi (days post-inoculation) mycorrhizal development was measured (A) and the expression of hormone metabolism or hormone response genes was measured by qPCR (B). qPCR data represents the relative gene expression in hairy root systems with respect to the non-inoculated composite plants transformed with the empty vector, in which expression was designated as 1 (not shown) (n=3). Values correspond to mean ± SE. Significant differences (Student´s *t*-test) between the mutant and the control are indicated with asterisks (**P ≤ 0.01; ***P ≤ 0.001; ****P ≤ 0.0001).

SlDLK2 involvement in supressing arbuscule hyphal branching

While lack of abnormalities were found in arbuscules of *SlDLK2* RNAi roots, observation of trypan blue stained hairy roots overexpressing *SlDLK2* (Fig. 23) and control roots (data not shown), revealed that *SlDLK2* OE apparently showed some alterations in arbuscule morphology, and the presence of arbuscules containing thick body-shape structures was often found in these roots. To confirm this impression, the AM fungus of *SlDLK2* OE hairy roots was stained with WGA and visualized by confocal microscopy. A clear perturbation on the arbuscule development was observed. In most cases, the arbuscules in *SlDLK2* OE roots were composed of a long arbuscule trunk growing inside the host cortex cell with lack of bifurcation into fine branches, suggesting that *SlDLK2* overexpression leads to the impossibility of arbuscules to branch, as clearly illustrated in Fig. 24.

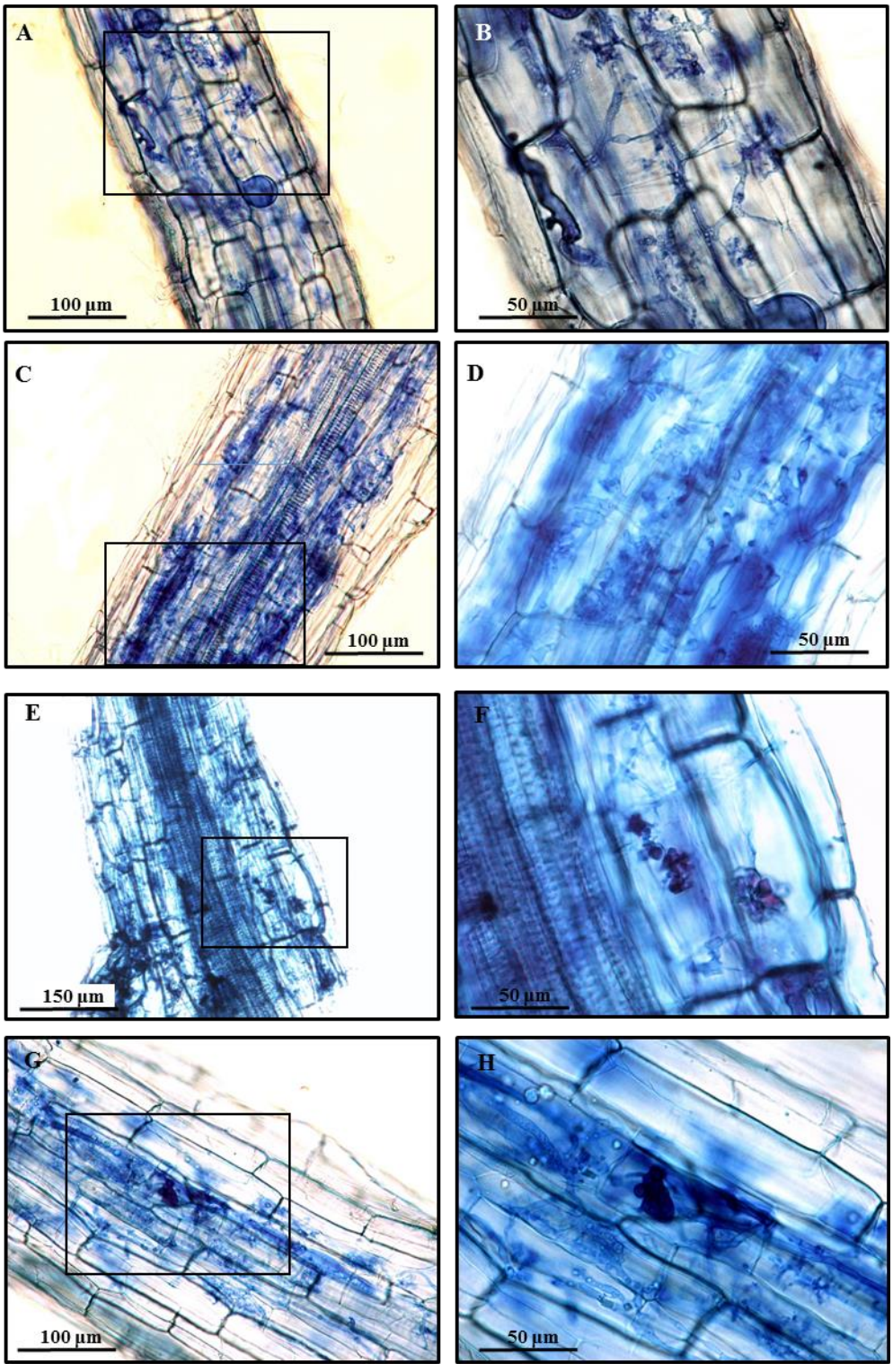

Figure 23. AM fungal trypan blue staining of control and *SlDLK2* OE mycorrhizal hairy roots. Images correspond to tomato hairy roots 62 days after inoculation with *R. irregularis,* subjected to trypan blue staining. Highly mycorrhized root fragments (A and C) with not fully developed arbuscules (B and D). Anomalous arbuscules with body-shaped structures (F and H). B, D, F and H images are the higher magnification of the squared area in A, C, E, G images. All images were taken with an optical microscope. The corresponding control images are shown in Fig 4 (Chapter 2).

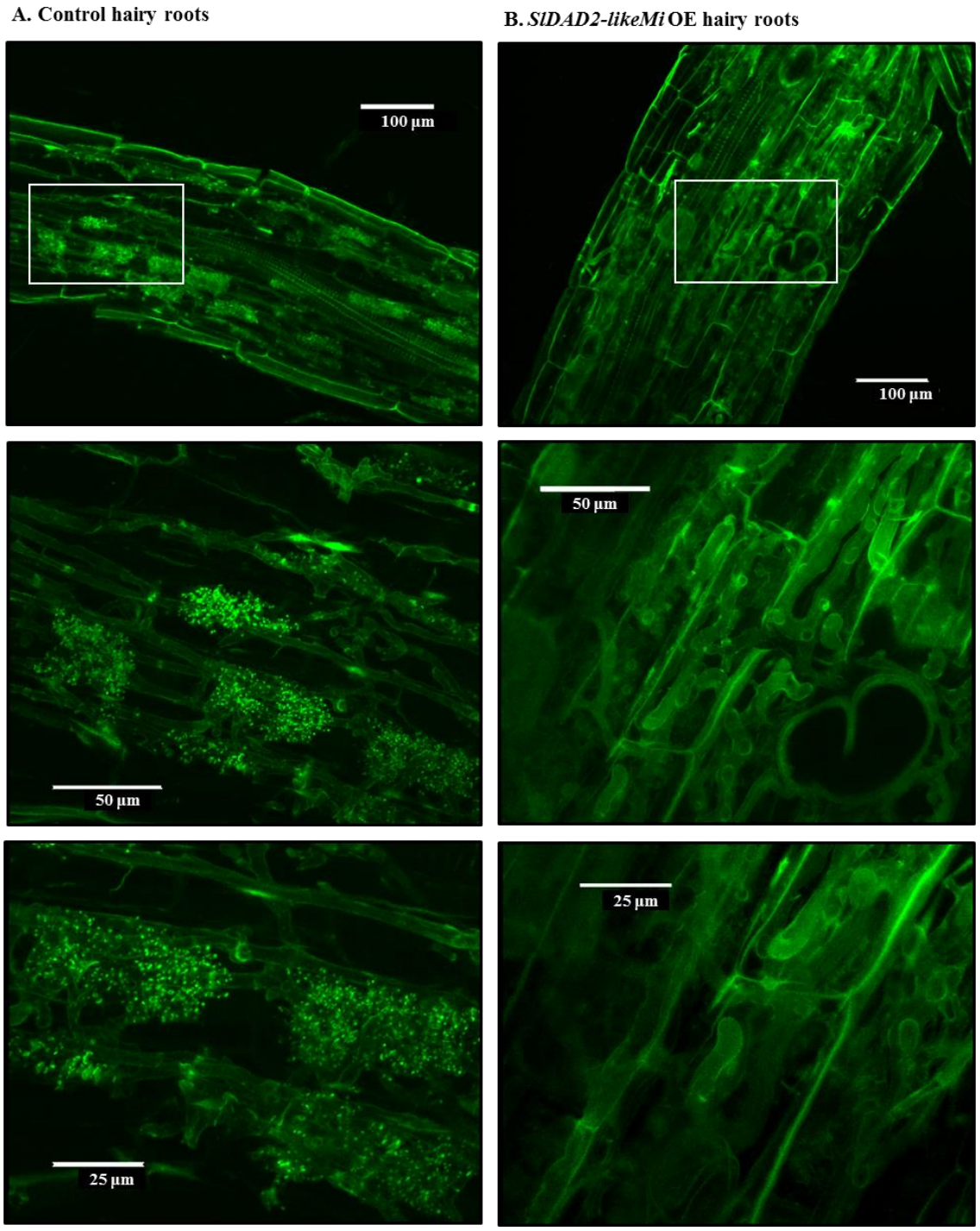

Figure 24. AM fungal fluorescent staining of control and *SlDLK2* overexpressing mycorrhizal hairy roots. Images correspond to the cortex zone of tomato hairy roots 62 days after inoculation with *R. irregularis,* and subjected to hyphal staining with WGA-Alexa Fluor 488, which fluoresces green. Control roots transformed with the empty vector pUBIcGFP-DR exhibited formation of mature highly branched arbuscules (A, left), while *SlDLK2* overexpressing roots showed lack of branching for most of the arbuscules (B, right). Each image is the higher magnification from its above image. Images were acquired by CLSM.

How *SlDLK2* overexpresssion affects the expression pattern of AM related genes?

In view that *SlDLK2* overexpression negatively affects mycorrhizal intensity and arbuscule abundances, together with the fact that a clear perturbation on arbuscule development was observed in *SlDLK2* OE hairy roots, we decided to study the expression pattern of AM-responsive genes in order to correlate morphological disorders with putative alterations in the expression patterns. Several putative orthologues of genes described to be involved in different stages of the mycorrhization process were analyzed. Early genes required at the beginning of AM colonization were selected, including the strigolactone biosynthetic genes *D27*, *ccd7* and *MAX1* (Fig. 25), as well as the common symbiosis signaling pathway genes *CCaMK*, *CYCLOPS* and *SYMRK* (Demchenko et al. 2004; Lévy et al. 2004; Yano et al. 2008) (Fig. 26). It was also analyzed the expression of *RAM1* (Gobbato et al. 2012)(Fig. 27A), a regulator of arbuscule branching that modulates arbuscule-related gene expression (Pimprikar et al. 2016). Other arbuscule-related genes were selected for qPCR determination, including *Vapyrin* and *EXO84,* involved in cellular rearrangements and membrane trafficking (Pumplin et al. 2010; Zhang et al. 2015; Genre et al. 2011); *RAM2*, encoding an AM-inducible glycerol-3 phosphate-O-acyltransferase (GPAT) that is required to support a full arbuscule development (Wang et al. 2012; Gobbato et al. 2012); and *AMT2.2* (ammonium transporter) and *STR* (ABC transporter) genes, encoding periarbuscular membrane transporters for arbuscule functionality (Breuillin-Sessoms et al. 2015; Zhang et al. 2010; Wang et al. 2012) (Fig. 27).

Under mycorrhizal conditions, two well-defined patterns of gene expression could be established. The first one is characterized by the unregulation or small affectation in the expression between control and *SlDLK2* OE hairy roots. This kind included all genes related to early stages (Fig. 26), as well as *RAM1*, *RAM2*, *Vapyrin* (Fig. 27A) and SL biosynthesis-related genes (Fig. 25). Only *ccd7* showed a slight but significant reduction in transcript abundance among all genes analyzed involved in early stages of AM development (Fig. 25). The second well-defined pattern is characterized by a marked reduction in the levels of expression in mycorrhizal *SlDLK2* OE hairy roots. This category includes all the genes encoding for periarbuscular membrane

transporters or membrane trafficking components (*AMT2.2*, *STR*, and *EXO84*) (Fig. 27A,B) whose expression pattern is similar to that one shown by *PT4* (Fig. 20). This result apparently indicated that *SlDLK2* is involved in arbuscule functionality rather than in signaling mycorrhizal colonization or arbuscule development and suggest an impairment or shortage in the periarbuscular membrane that is in agreement with the results obtained on the morphology of the arbuscules in *SlDLK2* OE roots, lacking bifurcation into fine branches.

At the same time, we studied the expression levels of genes encoding fungal transporters in control and *SlDLK2* OE mycorrhizal hairy roots (Fig. 27C). The results obtained clearly show that overexpression of *SlDLK2* gene did not significantly affect the transcription of the *GinAMT1* and *GinAMT2* fungal genes that encode for symbiotic membrane ammonium transporters (López-Pedrosa et al. 2006; Pérez-Tienda et al. 2011). As arbuscule branching greatly diminished in *SlDLK2* OE mycorrhizal roots, our results suggest that the expression of the fungal genes *GinAMT* and *GinAMT2* is not restricted to the fine arbuscular branches, which is in agreement with the study of Pérez-Tienda et al. (2011).

However, contrary results were curiously found with respect to non-inoculated plants. Overexpression of *SlDLK2* in un-inoculated roots tend to increase AM-associated gene expression. Particularly, expression of *MAX1*, *CYCLOPS*, *SYMRK*, *RAM1*, *AMT2.2* and *STR* was significantly induced in OE *SlDLK2* hairy roots.

The opposite result in un-inoculated and AM colonized plants suggest a different behavior of the SlDLK2 protein and/or the expression of AM-analyzed genes under both conditions. We speculate that AM-associated gene expression in mycorrhizal plants overexpressing *SlDLK2* might be a result of an indirect effect of lack of functional branched arbuscules in *SlDLK2* OE roots (Fig. 24), rather than a direct effect of an induced signaling through *SlDLK2*. Differential expression of some AM-associated genes observed in un-inoculated plants could suggest that SlDLK2 might be able to signal for gene regulation during mycorrhization without requirement of additional mycorrhizal signals. An RNA-seq analysis of *SlDLK2* OE in non-inoculated roots could shed light on potential direct targets of *SlDLK2* signaling.

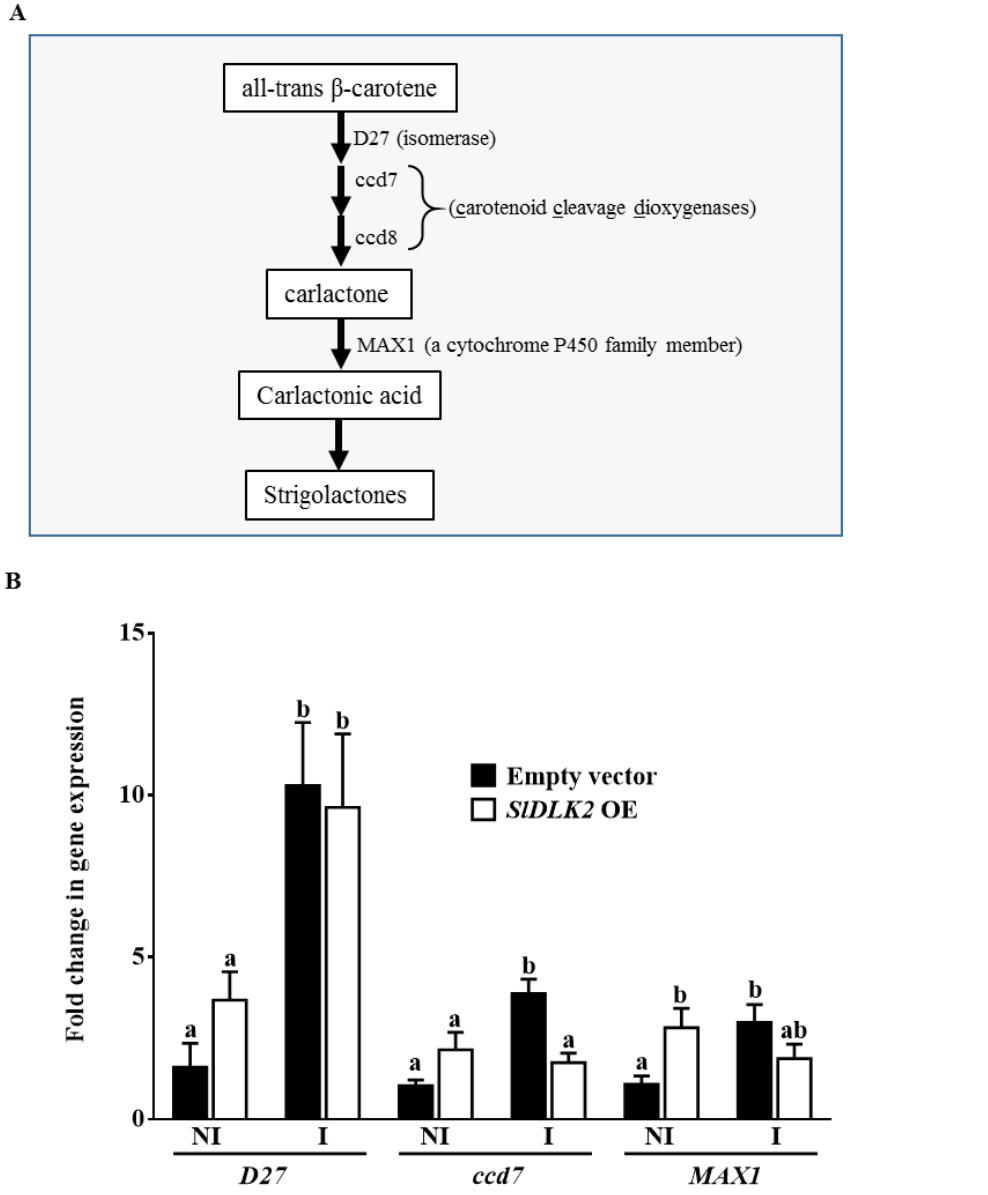

Figure 25. Gene expression of SL biosynthesis-related genes in *SlDLK2* OE roots. A simple depiction of the SL synthesis pathway (A). The transcript abundance of the *D27*, *ccd7* and *MAX1***,** involved in SL biosynthesis, was quantified by qPCR in control and *SlDLK2* OE hairy roots, non-inoculated (NI) and inoculated (I) with *R. irregularis*, 62 days after infection. The gene expression data is represented with respect to its expression in the control non-inoculated roots containing the empty vector (pUBIcGFP-DR), in which the expression level was designated as 1. Values are the mean ± SE of three biological replications. For each gene analyzed, bars with similar letters are not significantly different (*P*=0.05) according to LSD multiple comparison test.

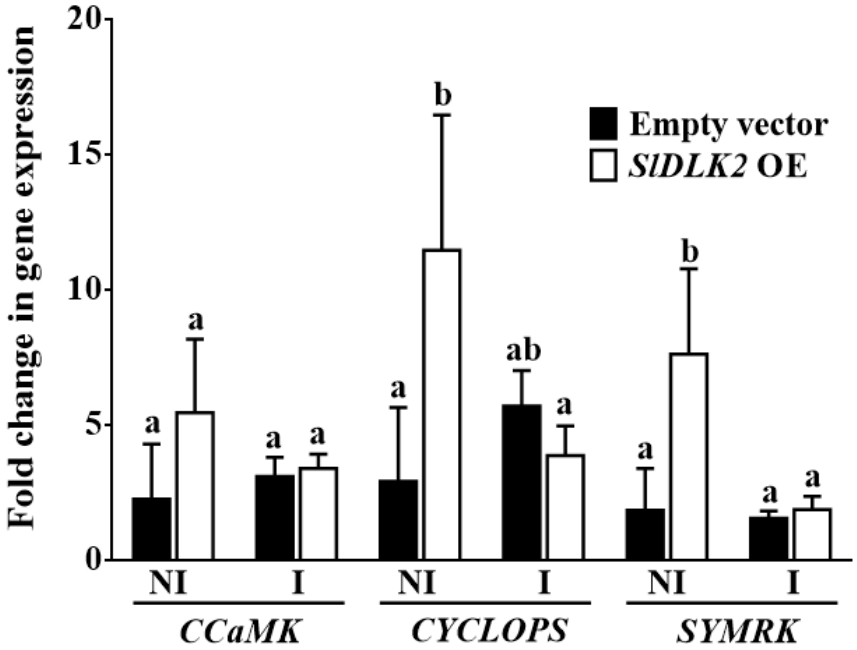

Figure 26. Gene expression of tomato genes for AM - signaling in *SlDLK2* OE roots. Transcript abundances of the putative *CCaMK, SYMRK and CYCLOPS* genes involved in the common symbiosis signaling pathway (CSSP) were quantified by qPCR in control and *SlDLK2* OE hairy roots, non-inoculated (NI) and inoculated (I) with *R. irregularis*, 62 days after fungal infection. The gene expression data is represented with respect to its expression in the control NI roots containing the empty vector (pUBIcGFP-DR), in which the expression level was designated as 1. Values are the mean ± SE of five biological replications. For each gene analyzed, bars with similar letters are not significantly different (P>0.05) according to LSD multiple comparison test.

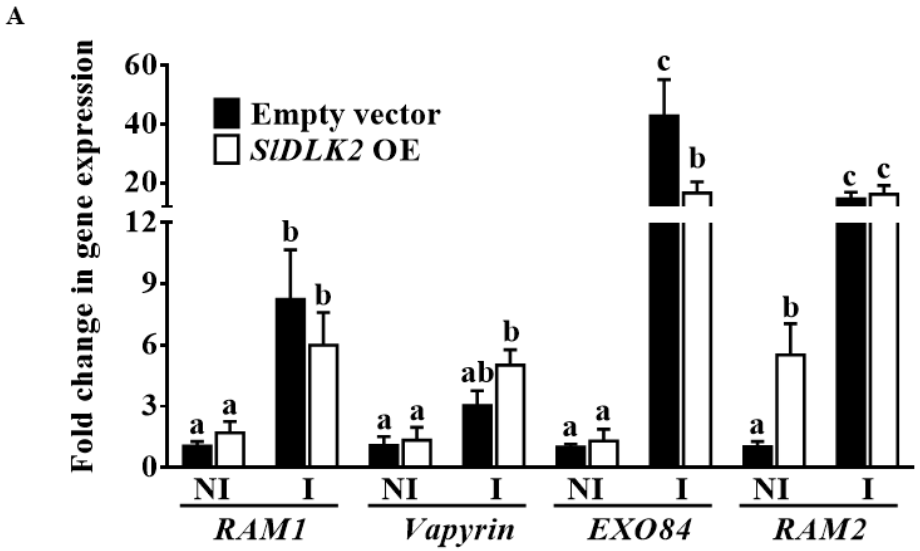

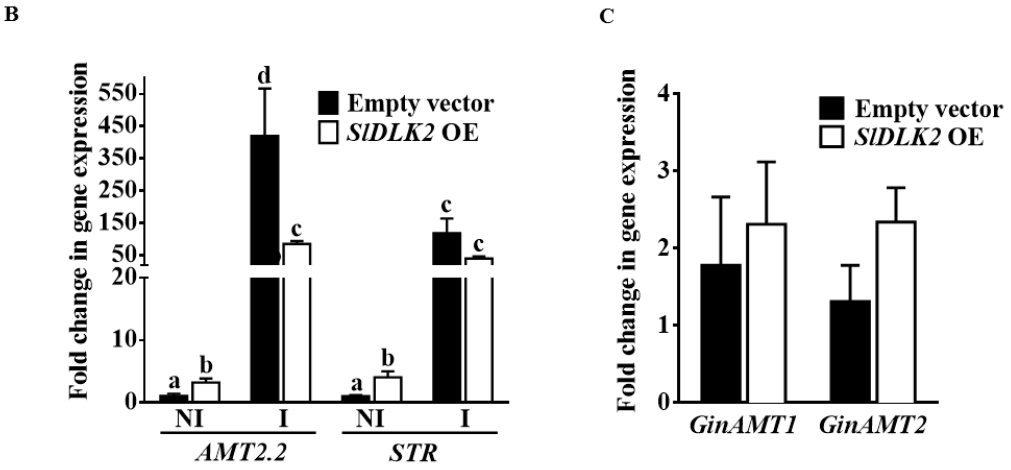

Figure 27. Gene expression of tomato arbuscule-related genes. Transcript abundance of putative *RAM1*, *Vapyrin*, *EXO84* and *RAM2* arbuscule-associated genes (A), as well as of genes encoding plant (B) and fungal (C) transporters for arbuscule functionality. Gene expression was analyzed by qPCR in control and *SlDLK2* OE hairy roots, non-inoculated (NI) and inoculated (I) with *R. irregularis*, 62 days after fungal infection. The *SlDLK2* gene expression data is represented with respect to its expression in the NI (A, B) or I (C) roots containing the empty vector, in which the expression level was designated as 1. Values are the mean ± SE of five biological replications. For each gene analyzed, bars with similar letters are not significantly different (P>0.05) according to LSD multiple comparison test.

SlDLK2 has a weak affinity towards SL analogs

Binding studies of the purified SlDLK2 protein to the SL analogs GR24 and GR5, and the bioactive karrikin KAR1, were conducted by isothermal titration calorimetry (ITC), revealing that SlDLK2 exhibits a weak heat curve when interacting with GR24 and GR5, but not with KAR1 (Fig. 28). The data was analyzed with Origin 7.0 software. Nevertheless, the dissociation constant (K_D) could not be determined, as long as the heat curve generated did not fit a sigmoidal curve. Additional calorimetry assays were performed for GR24 and GR5, modifying the ITC conditions (Fig. 29). Again, a weak heat curve was generated, being impossible to measure the K_D. This result suggest that SlDLK2 possess a slight ability to interact with the SL-analogs GR24 and GR5, but in a very weak way, indicating that they are not the specific ligands of SlDLK2 protein, although the biological ligand might be similar to these kind of molecules. As for KAR1, although a completely lack of binding was found in our experiment, we must not discard some SlDLK2 protein ability to interact with KAR1 in other experimental conditions, as residues aligning with those reported to

face the catalytic pocket in OsD14 suggest that the putative ligand of SlDLK2 should be more similar to KAR1 than to SL (see Table 3).

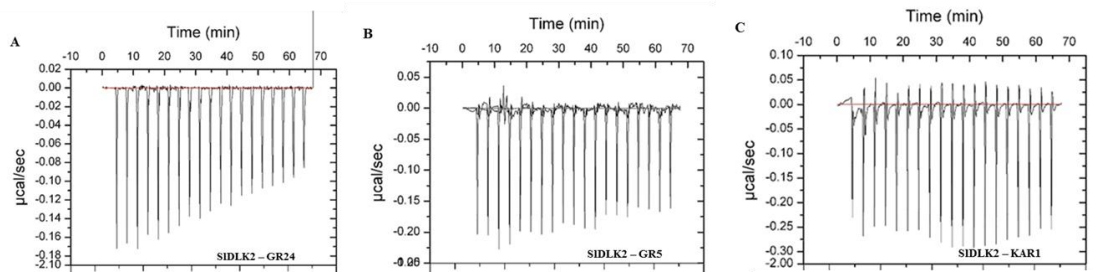

Figure 28. Analysis of GR24, GR5 and KAR1 binding to SlDLK2. Binding assay of GR24, GR5 and KAR1 to SlDLK2 purified protein was performed with 20 injections of 2 µL of SlDLK2 into 200 µL of GR24, GR5 or KAR1 (A, B and C, respectively). The injections were performed over a period of 6 s with a 300-s interval between injections, and the final molar ratio reached was 2 : 1 (protein: ligand). Original protein and ligand solutions were 466 µM protein and 46 µM GR24 (A), 640 µM protein and 64 µM GR5 or KAR1 (B, C). The final protein: ligand molar concentration reached was 78 µM : 38.3 µM (A) , 106 µM : 53µM (B, C). K_D value could not be measured for any binding assay.

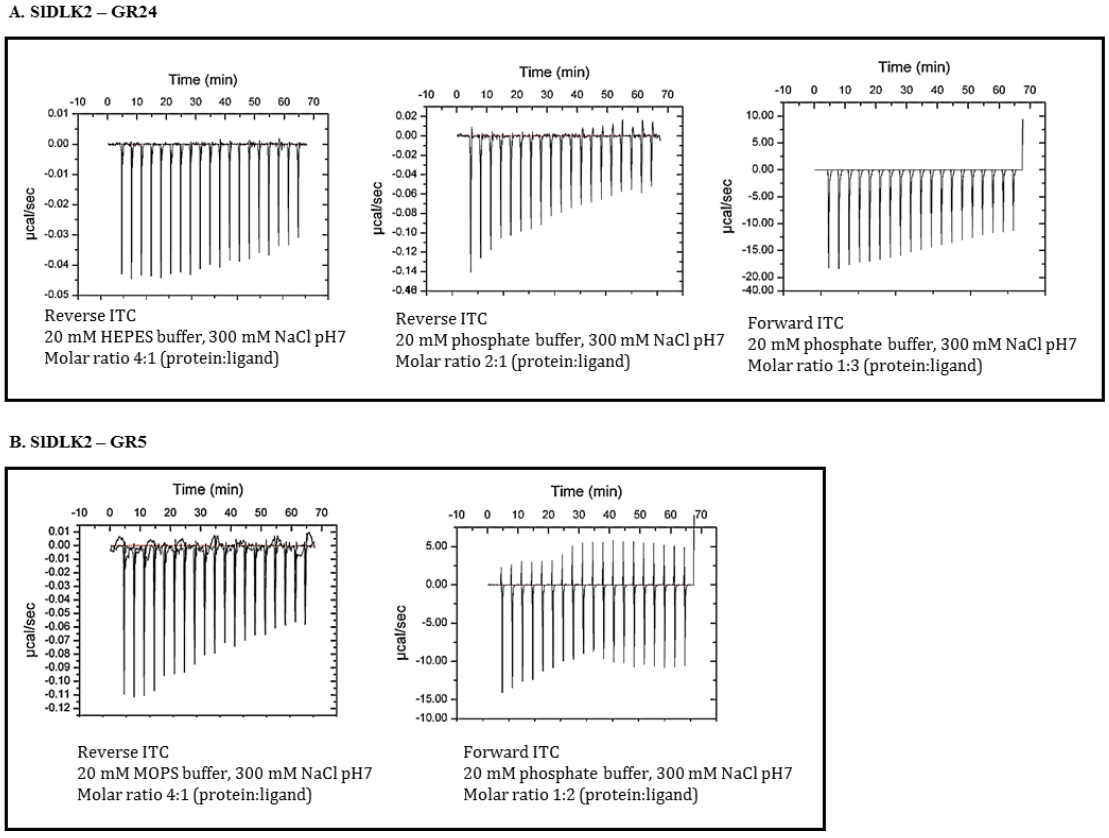

Figure 29. Additional assays for GR24 and GR5 binding to SlDLK2. Binding assay of GR24 and GR5 to SlDLK2 using alternative buffer solutions and molar ratios. Forward and reverse titrations were tried. ITC was performed with 20 injections of 2 µL into 200 µL. The

injections were performed over a period of 6 s with a 300-s interval between injections. Buffer solution, final molar ratio and the use of forward/reverse titration are indicated in each ITC diagram. K_D value could not be measured for any binding assays.

SlDLK2 has a weak hydrolytic activity towards SL analogs

Hydrolytic activity of SlDLK2 protein towards the SL analogs GR24 and GR5 was analyzed by a time course TLC experiment. We observed that SlDLK2 possesses some hydrolyzing activity towards GR24 and GR5, but the catalytic activity was much slower than that one for the control AtD14 (Fig. 30B), a reported SL-binding α,β-hydrolase (Kagiyama et al. 2013). While the spots corresponding to the two resulting molecules from GR24 cleavage were clearly detected 8, 20, 30 and 48 h after incubation with AtD14, only weak spots were detected at the same time points when incubating GR24 with SlDLK2 (Fig. 30B). In a similar manner, GR5 was completely hydrolyzed by AtD14 after 20 h, while SlDLK2 was not able to fulfill GR5 hydrolysis after 38 hours (Fig. 31B.). To confirm if the SlDLK2 hydrolytic activity resides in the catalytic triad residues, the same experiment was repeated with three different SlDLK2 mutant proteins, independently mutated in the Ser98, Asp219 and His248 putative catalytic residues. Effectively, a decreased in the hydrolytic activity was observed in the three SlDLK2 mutants, towards both the GR5 and GR24 molecules (Fig 30C and 31C, respectively). Ser98 and His248 were apparently more important than Asp219 for GR24 hydrolytic activity (Fig 30C). Then, our results confirm the presence of the catalytic triad Ser98-Asp219-His248 in the α,β-hydrolase SlDLK2, responsible for the slight hydrolytic activity observed towards SL compounds. However, deeper studies are needed to find the specific substrate that SlDLK2 binds *in planta*.

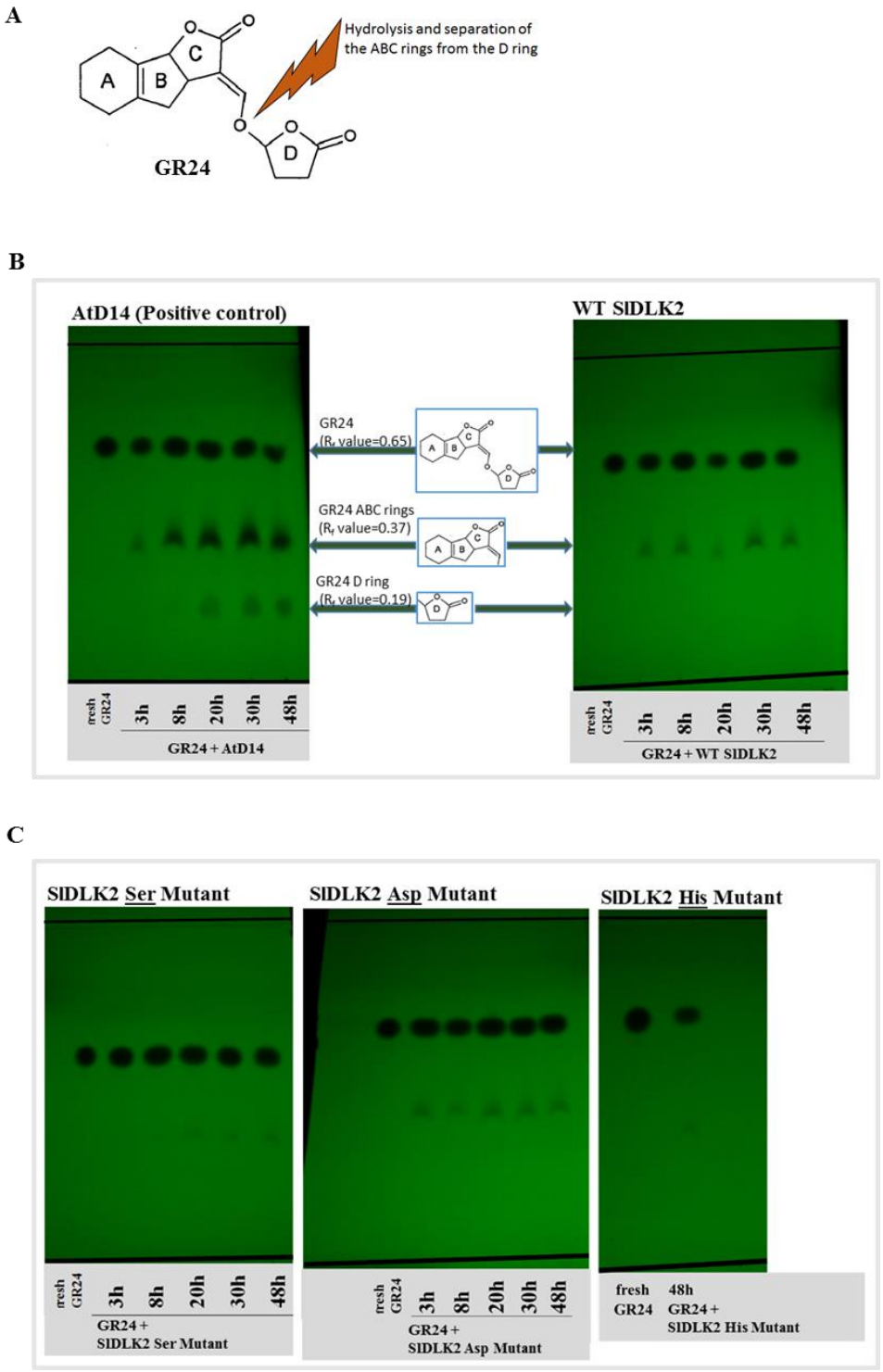

Figure 30. Cleavage of GR24 by SlDLK2 and involvement of the catalytic triad. (A) Hydrolysis cleavage site of GR24 molecule is indicated. (B) TLC analysis of GR24 time course hydrolysis by SlDLK2 (right plate) and by the corresponding positive control AtD14 (left plate). Rf values of the spots are indicated between brackets. GR24 and GR24-derivative cleavage rings expected to correspond to each spot are also showed. (C) TLC analyses of GR24 time course hydrolysis by SlDLK2 mutant proteins for the catalytic triad residues Ser98, Asp219 and His248. Times points (3, 8, 20, 30 and 48 h) are indicated. Fresh GR24 was used as a reference (first lane) in each TLC plate.

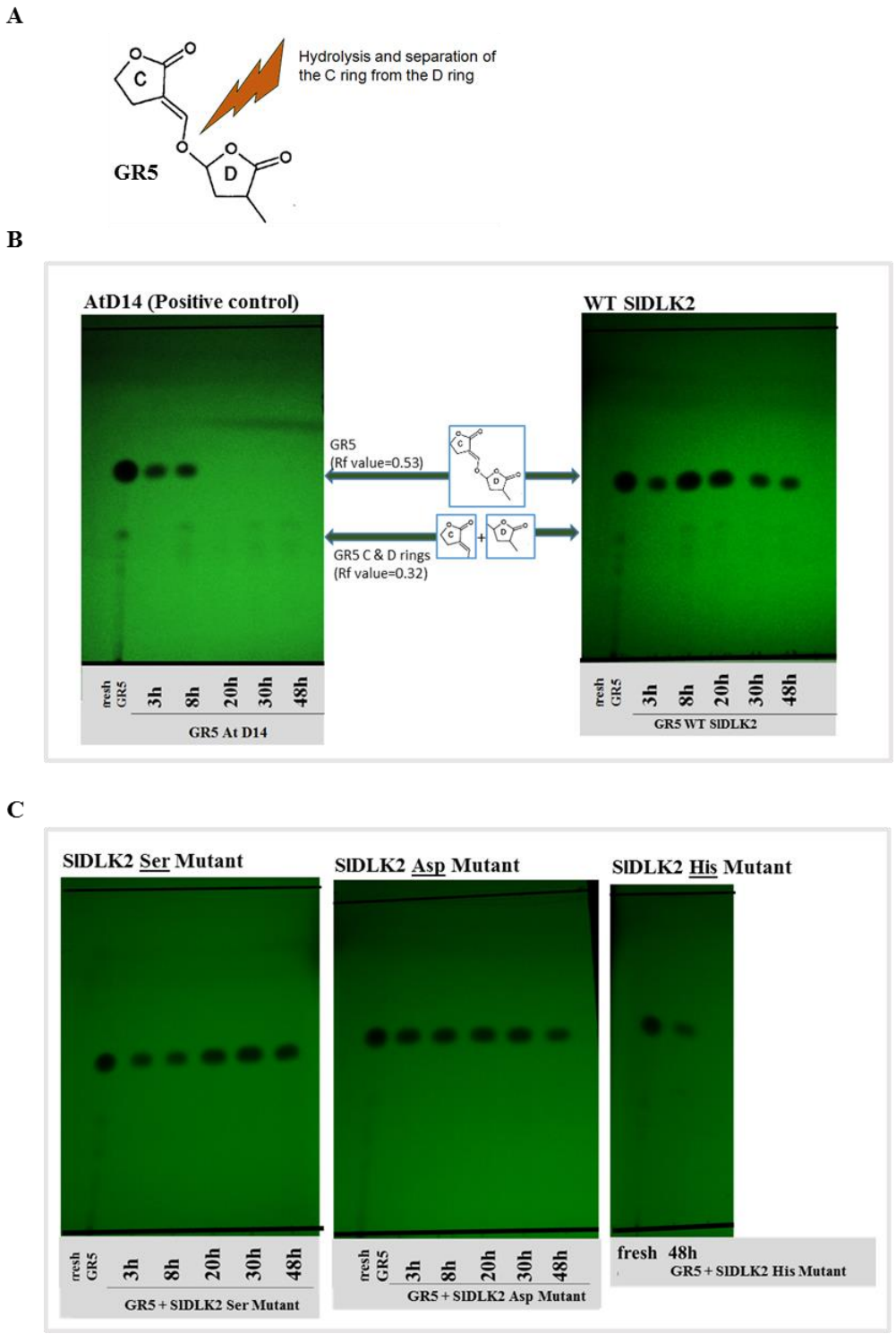

Figure 31. Cleavage of GR5 by SlDLK2 and involvement of the catalytic triad. (A) Hydrolysis cleavage site of GR5 molecule is indicated. (B) TLC analysis of GR5 time course hydrolysis by SlDLK2 (right plate), accompanied by the corresponding positive control AtD14 (left plate). Rf values of the spots are indicated between brackets. GR5 and GR5-derivative cleavage rings expected to correspond to each spot are also showed. (C) TLC analyses of GR5 time course hydrolysis by SlDLK2 mutated proteins for the catalytic triad residues Ser98, Asp219 and His248 . Time points (3, 8, 20, 30 and 48 h) are indicated. Fresh GR5 was used as a reference (first lane) in each TLC plate.

Does SlDLK2 signaling occur through protein destabilization upon ligand binding?

Thermal Shift Assay (TSA) has been established as a reliable method to infer alterations of protein thermal stability in the presence of small-molecule interaction partners (Niesen et al. 2007). Protein binding normally induces thermal stability of the protein. However, studies performed with the α,β-hydrolase SLs receptor proteins DAD2, AtD14 and OsD14 in the presence of SLs (Waters et al. 2015; Zhao et al. 2015; Hamiaux et al. 2012) have revealed a distinct hormone signaling mechanism, where the systematic destabilization of both the hormone and the receptor occurs upon interaction. Although our ITC assays show that neither GR24 nor KAR1 are specific ligands for SlDLK2, ITC revealed that GR24 is able to slightly interact with SlDLK2 (Fig. 28A). In order to elucidate if that interaction also triggers the destabilization of SlDLK2, as occurs with D14, we performed TSA experiments.

With increasing amounts of the GR24 racemic mixture (*rac*-GR24), the melting temperature for SlDLK2 decreased up to 2ºC and, curiously, the highest concentrations of rac-GR24 triggered high fluorescence signals from the beginning of the experiment, indicative of lack of binding and an unfolded state of the protein (Fig. 32A). Performing TSAs with the different GR24 enantiomers separately (Fig. 32B), we observed that the thermal transition in *rac*-GR24 might be caused by the enantiomer $GR24^{5DS}$, which showed a weak thermal transition of 2ºC, while enantiomers $GR24^{ent\text{-}5DS}$, $GR24^{4DO}$, and $GR24^{ent\text{-}4DO}$ might cause the protein unfolding at high concentrations or *rac*-GR24. We measured the pH of the TSA reaction mixture with the corresponding enantiomer or *rac*-GR24 concentrations and we did not observed a perturbation of the pH due to ligand concentration, what allowed us to discard a protein unfolding as an effect of pH modification. It is described in the literature that SL signaling occurs through destabilization of the D14 receptor (Hamiaux et al. 2012), in the same manner, our observations indicate that a SlDLK2 –mediated signaling could also occur through its own destabilization upon ligand binding.

As for KAR1, TSA did not reveal any thermal shift (Fig. 32C), which confirm the ITC results concerning lack of interaction between SlDLK2 and KAR1 (Fig. 28C).

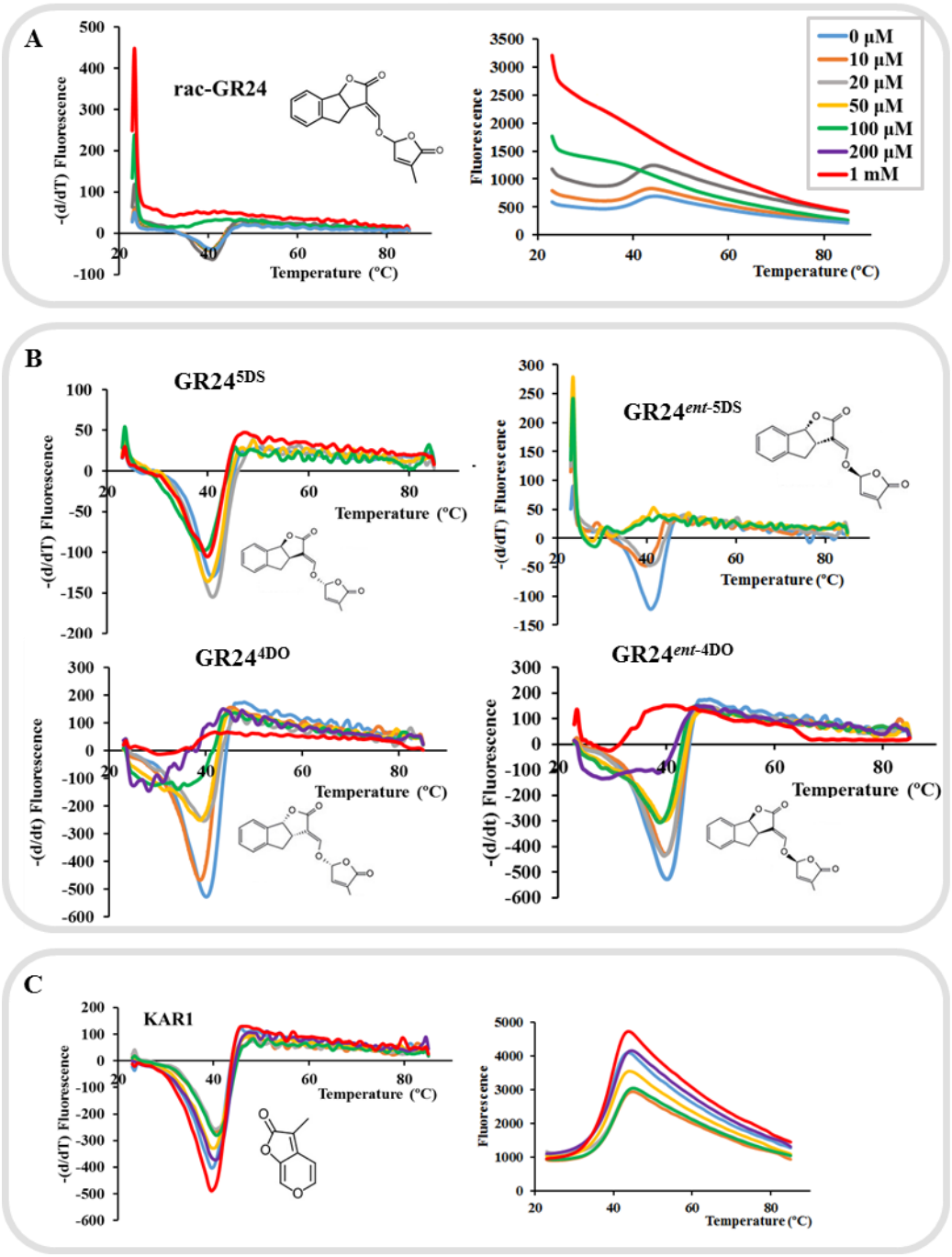

Figure 32. Analysis of KAR1 and GR24binding to SlDLK2 by Thermal Shift Assay (TSA). Melting temperature curves of SlDLK2 at varying concentrations of GR24 racemic mixture (A), GR24 enantiomers (B) and KAR1 (C) were assessed by TSA. Protein unfolding was monitored by detecting changes in Sypro Orange fluorescence on a Bio-Rad iQ5 real-time PCR detection system. The inflection point of the fluorescence versus temperature curves was determined and the minima referred to as the melting temperature (Tm). For KAR1 and rac-GR24, changes in fluorescence with temperature are shown (right), together with the respective derivatives (left).

SlDLK2 candidate ligand screening

We also used the TSA methodology as a tool which allows us to evaluate the interaction between SlDLK2 protein and several candidate ligand compounds. SlDLK2 exhibited thermal stability in the presence of natural SLs compounds such as orobanchol, solanacol, (+)-strigone, (-)-*ent*-strigone and (+/-)-5-deoxystrigol, with melting temperatures decreasing less than 1ºC at increasing concentrations of compounds. For (-)-*ent*-strigone and (+/-)-5-deoxystrigol we observed that they triggered protein unfolding at 200 µM, as occurred for *rac*-GR24 and, again, this result was not an effect of a perturbation of the pH in the reaction mixture (Fig. 33).

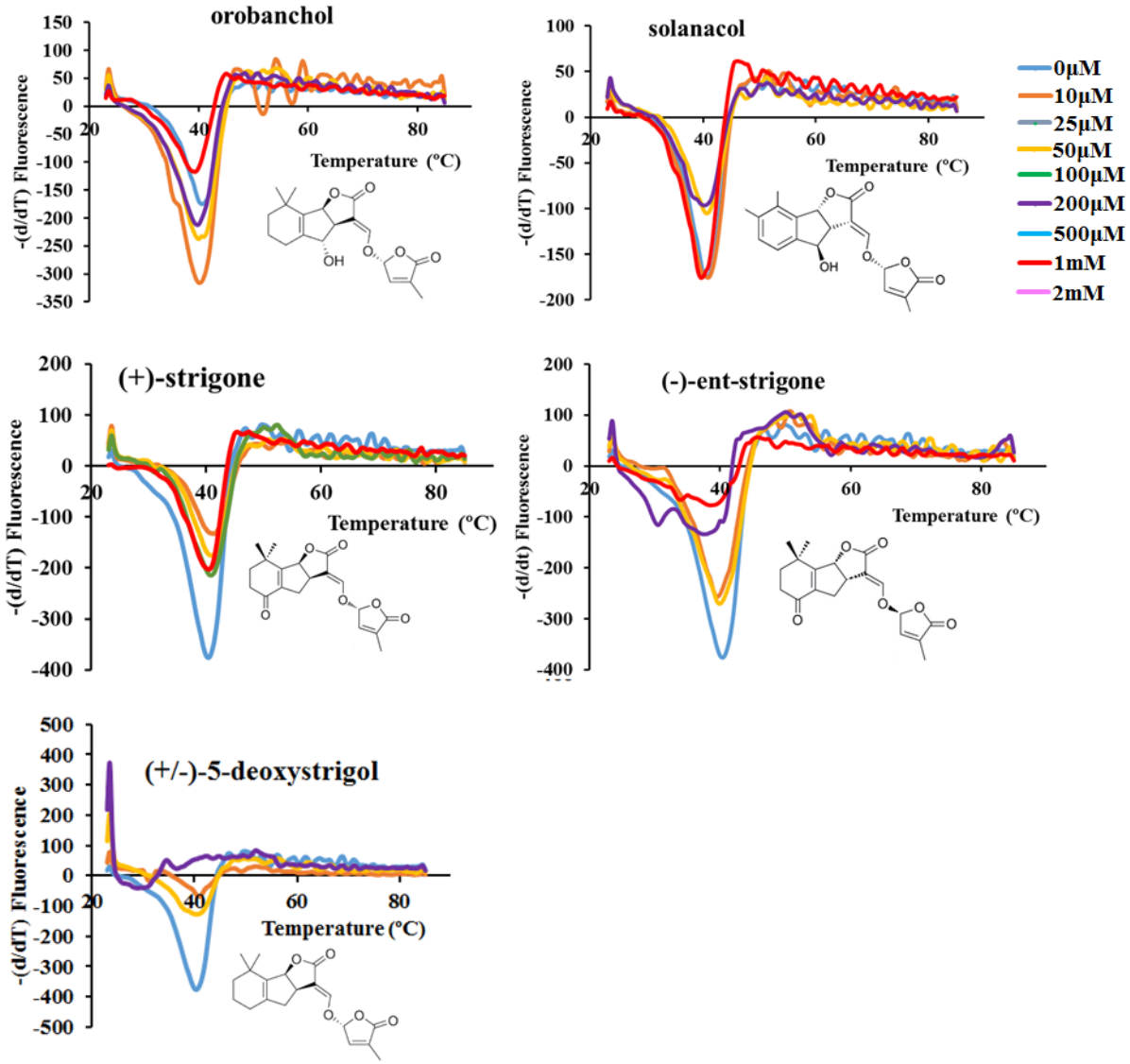

Figure 33. Binding analysis of candidate natural SL compounds to SlDLK2 by Thermal Shift Assay (TSA). Melting temperature curves of SlDLK2 at varying concentrations of different natural SLs were assessed by TSA. Protein unfolding was monitored by detecting

changes in Sypro Orange fluorescence on a Bio-Rad iQ5 real-time PCR detection system. The inflection point of the fluorescence versus temperature curves was determined and the minima referred to as the melting temperature (Tm).

The results obtained using natural SLs, as well as those previously obtained using the GR24 synthetic SL, suggest that the possible ligand of SlDLK2 protein is not a canonical SL. Therefore, we decided to carry out experiments using two kinds of ligand molecules which represent core structures in apocarotenoids. The first one was the 3-methyl-2(5*H*)-furanone, that is the common structural unit in natural and several synthetic strigolactones, and the second ones were α- and β-ionone, two apocarotenoids derived from α-and β-carotene, respectively, and whose structure resembles C13-apocarotenids which accumulate in mycorrhizal roots (Maier et al. 1995; Strack and Fester 2006; Walter et al. 2007).

As for GR24 and natural SLs, the TSA experiment using 3-methyl furanone is indicative of lack of binding (Fig. 34). Interestingly, the TSA experiments using α-ionone and β-ionone were found to induce a marked decrease (4.5ºC) on SlDLK2 melting temperature. Particularly, increasing amounts of α- or β-ionone varying up to 2 mM, caused a decrease on melting temperature of SlDLK2 from 40ºC to 35.5ºC. This result prompt us to consider that SlDLK2 could be the specific receptor of some of the C13-apocarotenoid blumenin-related compounds that have been described to accumulate during mycorrhization but with still unknown function (Strack and Fester 2006). However, we could not confirm this hypothesis, in spite of our TSA trials carried out with trans-3-oxo-α-ionol, which is the core structure shared among all blumenin-related AM-associated compounds, and with the blumenol-C-glucoside, a glycosylated form of blumenin found in several mycorrhizal species (Strack and Fester 2006)(data not shown). In this manner, further research is required in order to check if SlDLK2 is or is not a receptor of AM-specific C13-apocarotenoids.

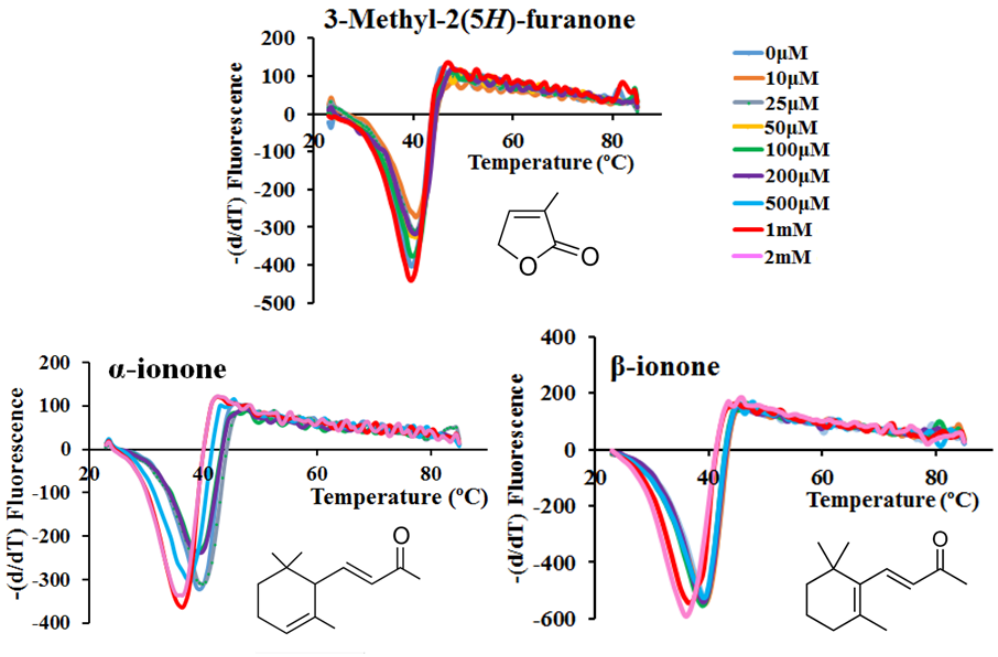

Figure 34. Binding analysis of alternative apocarotenoid core structures to SlDLK2 by Thermal Shift Assay (TSA). Melting temperature curves of SlDLK2 at varying concentrations of 3-methyl-2(*5H*)-furanone, α-ionone and β-ionone were assessed by TSA. Protein unfolding was monitored by detecting changes in Sypro Orange fluorescence on a Bio-Rad iQ5 real-time PCR detection system. The inflection point of the fluorescence versus temperature curves was determined and the minima referred to as the melting temperature (Tm).

Discussion

We identified here a tomato α,β-hydrolase gene induced during mycorrhization (*SlDKL2*) as a plant component associated with cortex cells developing fungal arbuscules and involved in supressing/regulating arbuscule hyphal branching during the establishment of AM symbiosis.

The α, β-hydrolase superfamily (ABH) is a widespread and functionally malleable protein superfamily recognized for its diverse biochemical activities. In plants, ABH enzymes possess an α, β-fold that serves as the core structure for phytohormone and ligand reception in the gibberellin, strigolactone and karrikin signaling pathways (GID1, DAD2/D14 and KAI2/HTL2 receptors, respectively) (Mindrebo et al. 2016). Particularly, *SlDLK2* is closely related to the SL and karrikin receptors.

It is demonstrated that D14 and KAI2 α,β-hydrolases from *Arabidopsis* are able to bind SLs and KAR1, in the sub-micromolar and micromolar range, respectively (Kagiyama et al. 2013), and that GR24 is also hydrolysed by the D14 protein PhDAD2 after binding (Hamiaux et al. 2012). However, so far it has not been reported any information about the probable ligand of the third un-studied group of RsbQ α,β-hydrolases, i.e. DLK2 group. Here, our ITC and TLC results suggest that SlDLK2 and probably, by extension, all the α,β-hydrolases belonging to the DLK2 group, are able to bind and hydrolyse a similar, but different compound to strigolactones and karrikins. The residues putatively belonging to the pocket binding site are more similar to those described for the karrikin binding protein AtKAI2 (Table 3), however we did not observe any binding of KAR1 to SlDLK2. Nevertheless, some kind of un-specific interaction was detected between SlDLK2 and the SL-analogues GR24 and GR5 (Fig. 28). What it is clear is that SlDLK2 has the typical catalytic hydrolysing activity residing in the catalytic triad Ser-Asp-His, main functional feature of the α,β-hydrolase superfamily (Fig. 4B, 30).

OsD14 and AtKAI2 receptor hydrolases are reported to act together with F-box protein OsD3/AtMAX2, which takes part of an SCF (SKP1-CULLIN-F-BOX) E3 ubiquitin ligase, in the perception of strigolactones and karrikins, respectively (Hamiaux et al. 2012; Zhao et al. 2015), and some residues have been identified for D3/MAX2 binding (Zhao et al. 2015; Yao et al. 2016a). These residues are mostly not conserved in SlDKL2 suggesting that it is unable to bind D2/MAX2. It is probable that SlDKL2 binds other types of F-box proteins or maybe it is not involved in protein degradation.

Some efforts have been carried out in this work in order to elucidate the nature of the specific ligand of SlDLK2. Although we initially speculated that the specific biological ligand of SlDLK2 might be a molecule with a butenolide ring, such as SLs or karrikins, our results raised the idea of C13 α-ionol derivatives (formerly called C13 cyclohexanone derivatives) as potential candidates to bind SlDLK2 (Fig. 34). Curiously, these apocarotenoids, containing the α-ionone ring structure, start to accumulate after beginning of arbuscule formation, and progressively increase during colonization (Maier et al. 1995; Strack and Fester 2006; Walter et al. 2007), as occurs with *SlDLK2* gene expression. Although their role during mycorrhization

has not been elucidated, it has been demonstrated that mycorrhization stimulates the 2-C-methyl-D-erythritol-4-phosphate (MEP) pathway and the metabolism of apocarotenoids in the root, and that at least a group of them, derived from cyclohexanones (CH) are specific from mycorrhizal roots and they can have a regulatory role in the life cycle of arbuscules. Thus, it has been proposed that these compounds accelerate the senescence of mature arbuscules and make possible the replacement of old arbuscules by young and functional ones, maintaining a high population of active arbuscules (Walter 2013). Nothing is known about the molecular signalling responsible for the metabolic activation of CH production, neither if it is induced by some signal generated in mature arbuscules or whether it is nonspecific and inherent in the development of the arbuscule. If it is true, however, that phosphorus deficiency stimulates the expression of apocarotenoid metabolism genes, including strigolactones (SLs), which code for carotenoid cleavage enzymes (carotenoid cleavage dioxygenases-CCDs) responsible for generation of apocarotenoids compounds.

In both plants and animals, apocarotenoids are responsible for the regulation of gene expression (Moise et al. 2005). Apocarotenoids also play a key role in allelopathic interactions and plant defence mechanism (Bouvier et al. 2005). In this sense, the α-ionone isomer, β-ionone, has been reported as a feeding deterrent for the crucifer flea beetle in *Arabidopsis* (Wei et al. 2011), and as a sporulation inhibitor of the pathogenic fungus *Peronospora tabacina* in tobacco (Salt et al. 1986). Then, in the same manner, ionone-related compounds may be likely important for a negative signaling of the mycorrhization process and it is tenting to speculate that this signaling might be accomplished through binding to the SlDLK2 receptor, as supported by our thermal shift assays with the SlDLK2 protein and the α- and β-ionone compounds. In addition, *SlDLK2* gene is constitutively expressed in leaves and flowers of tomato plants, suggesting the existence of a specific ligand generated in the plant.

qPCR analyses were performed in *R. irregularis* colonized roots compared to non-inoculated roots, revealing that, apart from *SlDLK2* , another two tomato RsbQ-like α,β-hydrolases might be someway responsive to mycorrhization. One of them is the canonical SL receptor SlD14, which is significantly upregulated at early stages of

mycorrhization, suggesting that it might have a role in SL signaling for the pre-symbiotic fungal growth and hyphal branching (Mori et al. 2016; Akiyama et al. 2005b; Besserer et al. 2006b) and/or might facilitate hyphopodium formation (Kobae et al. 2018). In addition, the gene encoding for SlKAI2cB, putative homolog of the OsD14L receptor reported to be essential for mycorrhization in rice (Gutjahr et al. 2015), was significantly repressed at late stages, what might account for a negative regulation of mycorrhizal development.

In order to get insights into the functional characterization of *SlDLK2* we performed experiments of mycorrhization with overexpressed (OE) and downregulated (RNAi) composite plants. In both, *SlDLK2* RNAi and *SlDKL2* OE hairy roots we observed alterations in the mycorrhization pattern and arbuscule morphology, as well as changes in AM-associated gene expression. *SlDLK2* RNAi hairy roots, compared to the control roots presented a significant increase in the percentage of root length colonized by the AM fungus, as well as a significant increase for all the mycorrhizal parameters, indicating that *SlDKL2* gene silencing positively affects mycorrhizal intensities and arbuscule abundance. An opposite trend was observed for *SlDKL2* OE composite plants where AM colonization of the root significantly decreased with respect to the control roots indicating that *SlDKL2* overexpression negatively affects the relative mycorrhizal intensity and arbuscule abundance.

Observation of stained hairy roots overexpressing *SlDKL2* and control roots revealed important alterations in arbuscule morphology, and it was often found the presence of mycorrhizal roots with no branched arbuscules or little-branched distorted arbuscules in *SlDKL2* OE mycorrhizal roots. In most cases, the arbuscules in *SlDKL2* OE roots were composed of a long arbuscule trunk growing inside the host cortex cell with lack of bifurcation into fine branches, suggesting that *SlDKL2* overexpression leads to the impossibility of arbuscules to branch. In agreement, comparative qPCR analysis reveals that this specific gene overexpression led to a down regulation in the expression of arbuscule-related genes encoding for periarbuscular membrane transporters or proteins involved in membrane trafficking, what might be related to the loss of periarbuscular membrane. Our results apparently indicated that *SlDLK2* is involved in arbuscule functionality

rather than in initial signaling events for mycorrhizal colonization or arbuscule development.

It is known that a fine hormone regulation occurs during AM symbiosis (Foo et al. 2014; Pozo et al. 2015), and here we show that the AM induced *SlDLK2* gene responds to exogenous hormone application and is also probably involved in regulation of hormone metabolism during mycorrhization. *SlDLK2* gene expression is repressed by MeJA and GA treatment. Ethylene, salicylic acid and ABA initially (12h) induce and later (48h) repress *SlDLK2* expression; while, auxin treatment activate *SlDLK2* gene expression (Fig. 14). In fact, two putative cis regulatory elements for MeJA and two auxin responsive elements were identified in the *SlDLK2* promoter sequence (Fig. 17), suggesting that *SlDLK2* might be directly repressed by MeJA and activated by auxins. In addition, *SlDLK2* is likely involved in regulating hormone balance during mycorrhization, as an alteration in gene expression associated to hormone metabolic pathways and SL-biosynthetic genes is observed *SlDLK2* RNAi AM roots and SlDLK2 OE roots, respectively (Fig. 21, 25). However these results must be taken carefully as a contrary regulation is observed in inoculated and non-inoculated roots upon *SlDLK2* overexpression (Fig. 25).

In this sense, it is also worth noting that differential gene expression observed in non-inoculated roots upon *SlDLK2* overexpression suggests that SlDLK2 is able to trigger transcriptomic changes without the requirement of an AM-derived molecule. Then, we speculate that at least some amount of the SlDLK2 ligand must be constitutively present in the non-inoculated roots. As mentioned above, the expression of *SlDLK2* in leaves and flowers suggests a role of SlDLK2 in these organs mediated by the interaction with the endogenous ligand. Maybe, the induction of AM-associated genes by *SlDLK2* overexpression in un-inoculated roots could be unspecific and mediated by the induction in *SlDLK2* OE roots of signaling molecules and/or transcription factors that overlap with the mycorrhization signaling.

Based on the critical discussion of our results and the evaluation of the previous contributions, we propose different hypothesis trying to explain this negative

impact on AM-formation through SlDLK2 (Fig. 35). The first possibility to consider is a competitive model in which the ligand bound by SlDLK2 is a plant molecule that signals for arbuscule hyphal branching, probably through a receptor of fungal nature. As mycorrhizal colonization goes on, the plant synthesizes SlDLK2, a competitive inhibitor (not a signalling receptor) able to bind and retain the same ligand, reducing the free availability and the inductor action on hyphal branching of this compound, and consequently the branching effect disappear. This model is quite similar to what has been described at pre-symbiotic stages, where the exudation of SLs by the root induces hyphae branching (Akiyama et al. 2005b).

The second possibility contemplates the option in which the ligand is a repressor of arbuscule branching that signals through its binding to the specific plant receptor SlDLK2. In this case, there is not a direct effect on fungal hyphae, but rather the effect is mediated via *planta* and could require other molecular actors and a more complex signalling pathway that includes other regulators of the arbuscular cycle.

Obviously, a combination of the two models in which the ligand has a dual role, due to the presence of two different receptors, one in the fungus and the other one in the plant cannot be discarded. In this sense, this combined model of action is the one that resembles the most to the strigolactone signalling, a plant hormone that is produced under nutrient starvation, specially phosphate deprivation conditions (Decker et al. 2017; Yoneyama et al. 2012), and suggested to have two receptors, D14 in the plant, that signals for shoot and root architecture (Jiang et al. 2015; Kapulnik et al. 2011; Rasmussen et al. 2012), and a putative receptor in the fungus, that signals for induction of hyphal branching and mitochondrial density (Akiyama et al. 2005a; Besserer et al. 2006a). Surely the future discovery of the natural ligand of SlDLK2 could give us key information to clarify and decipher the veracity of the proposed models.

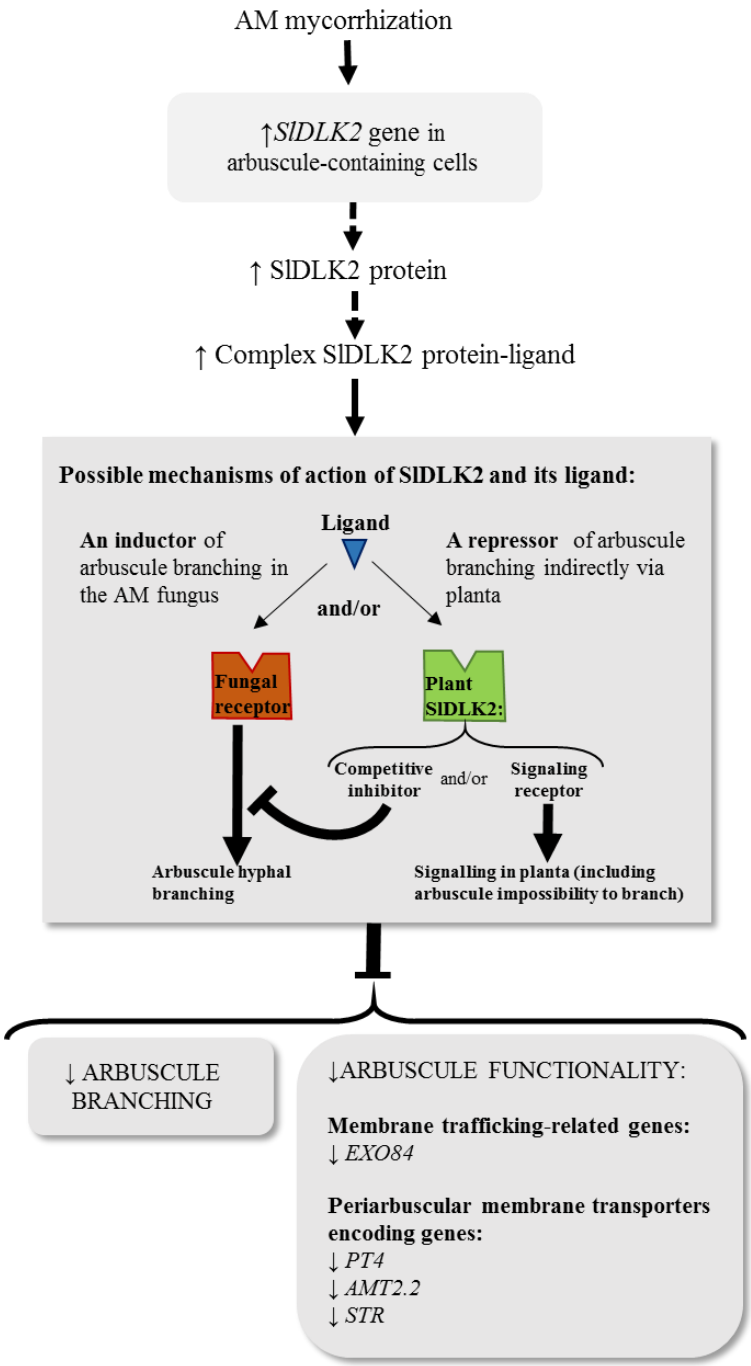

Figure 35. Hypothetical models of action of *SlDLK2* gene during the AM symbiosis. *SlDLK2* gene induction occurs in cells colonized by arbuscules. SlDLK2 protein might act as a signalling receptor that binds an hormonal compound and/or as a competitive inhibitor of a fungal receptor which specifically binds a branching inductor molecule. In any case, SlDLK2 is apparently involved in negatively regulate AM development (and probably AM functioning) upon ligand binding, as a repression of arbuscule branching and an impaired expression of tomato genes associated to transport and membrane trafficking in the periarbuscular membrane are observed in SlDLK2 OE mycorrhizal roots. Solid arrows indicate proved effects of *SlDLK2*-induction during mycorrhization, while dashed arrows indicate expected or proposed effects of *SlDLK2* induction.

Conclusion

SlDLK2, a tomato gene highly induced during mycorrhization encoding an α, β-hydrolase protein closely related to the D14 and KAI2 receptors belongs to a third clade of RsbQ-like α,β-hydrolases previously named as "D14-like2 group" (DLK2). Functional analysis and molecular studies of RNAi and OE hairy roots, point out to a negative role of the AM inducible gene *SlDLK2* during mycorrhization, likely focused on inhibiting arbuscule hyphal branching, and then controlling mycorrhizal colonization at late stages of the symbiosis. Although it cannot be ruled that the specific biological ligand of SlDLK2 might be a molecule with a butenolide ring, such as SLs or karrikins, our results raised the idea of C13 α-ionol (β-ionone) derivatives as potential candidates to bind SlDLK2

Future perspectives

We speculate that an increased accumulation of the putative ligand at free stage should be present in *SlDLK2* RNAi roots. Then, the comparison of differential metabolomic profiles between control and *SlDLK2* RNAi mycorrhizal roots might help us to elucidate the chemical structure of the biological ligand of the SlDLK2 receptor. In order to get closer to the specific ligand of the SlDLK2 receptor, a deeper screening of potential candidates by TSA, focusing on C13 α-ionol derivatives-related molecules, and confirmation of the interaction by isothermal titration calorimetry and nuclear magnetic resonance are being performed.

An RNA-seq analysis in non-inoculated and inoculated roots could shed light on potential direct targets of *SlDLK2* signaling. We have already perform an RNA-seq analysis in order to elucidate transcriptomic alterations due to RNA silencing in tomato roots during mycorrhization (next chapter). This study will be completed with an RNA-seq analyses in *SlDLK2* overexpressed plants, in which a transcriptomic study of the alterations in the expression of fungal genes will be also included. This experiment will allow us to elucidate transcriptomics changes in both symbionts and to clarify in a direct way the possible alterations in the expression of fungal genes caused by the limitation in the formation of arbuscules in OE plants.

Additionally, given the binding capacity of D14 receptors to interact with regulatory proteins such as DELLA or F-box proteins, it would be interesting to investigate putative SlDKL2 protein interactors using co-IP, BiFC or yeast-two hybrid techniques.

Bibliography

Akiyama K, Matsuzaki K-i, Hayashi H (2005a) Plant sesquiterpenes induce hyphal branching in arbuscular mycorrhizal fungi. Nature 435 (7043):824-827

Akiyama K, Matsuzaki K, Hayashi H (2005b) Plant sesquiterpenes induce hyphal branching in arbuscular mycorrhizal fungi. Nature 435 (7043):824-827. doi:10.1038/nature03608

Aoki K, Yano K, Suzuki A, Kawamura S, Sakurai N, Suda K, Kurabayashi A, Suzuki T, Tsugane T, Watanabe M, Ooga K, Torii M, Narita T, Shin IT, Kohara Y, Yamamoto N, Takahashi H, Watanabe Y, Egusa M, Kodama M, Ichinose Y, Kikuchi M, Fukushima S, Okabe A, Arie T, Sato Y, Yazawa K, Satoh S, Omura T, Ezura H, Shibata D (2010) Large-scale analysis of full-length cDNAs from the tomato (*Solanum lycopersicum*) cultivar Micro-Tom, a reference system for the Solanaceae genomics. BMC Genomics 11:210. doi:10.1186/1471-2164-11-210

Balestrini R, Gómez-Ariza J, Lanfranco L, Bonfante P (2007) Laser microdissection reveals that transcripts for five plant and one fungal phosphate transporter genes are contemporaneously present in arbusculated cells. Mol Plant-Microbe Interact 20 (9):1055-1062

Benabdellah K, Merlos MA, Azcon-Aguilar C, Ferrol N (2009) GintGRX1, the first characterized glomeromycotan glutaredoxin, is a multifunctional enzyme that responds to oxidative stress. Fungal Genet Biol 46 (1):94-103. doi:10.1016/j.fgb.2008.09.013

Besserer A, Bécard G, Jauneau A, Roux C, Séjalon-Delmas N (2008) GR24, a synthetic analog of strigolactones, stimulates the mitosis and growth of the arbuscular mycorrhizal fungus Gigaspora rosea by boosting its energy metabolism. Plant Physiol 148 (1):402-413

Besserer A, Puech-Pagès V, Kiefer P, Gomez-Roldan V, Jauneau A, Roy S, Portais J-C, Roux C, Bécard G, Séjalon-Delmas N (2006a) Strigolactones stimulate arbuscular mycorrhizal fungi by activating mitochondria. PLoS Biol 4 (7):e226

Besserer A, Puech-Pages V, Kiefer P, Gomez-Roldan V, Jauneau A, Roy S, Portais JC, Roux C, Becard G, Sejalon-Delmas N (2006b) Strigolactones stimulate arbuscular mycorrhizal fungi by activating mitochondria. PLoS Biol 4 (7):e226. doi:10.1371/journal.pbio.0040226

Boisson-Dernier A, Andriankaja A, Chabaud M, Niebel A, Journet E-P, Barker DG, de Carvalho-Niebel F (2005) MtENOD11 gene activation during rhizobial infection and mycorrhizal arbuscule development requires a common AT-rich-containing regulatory sequence. Mol Plant-Microbe Interact 18 (12):1269-1276

Bonfante P, Requena N (2011) Dating in the dark: how roots respond to fungal signals to establish arbuscular mycorrhizal symbiosis. Curr Opin Plant Biol 14 (4):451-457

Bouvier F, Isner J-C, Dogbo O, Camara B (2005) Oxidative tailoring of carotenoids: a prospect towards novel functions in plants. Trends Plant Sci 10 (4):187-194

Breuillin-Sessoms F, Floss DS, Gomez SK, Pumplin N, Ding Y, Levesque-Tremblay V, Noar RD, Daniels DA, Bravo A, Eaglesham JB (2015) Suppression of arbuscule degeneration in *Medicago truncatula* phosphate transporter4 mutants is dependent on the ammonium transporter 2 family protein *AMT2;3*. Plant Cell 27 (4):1352-1366

Bythell-Douglas R, Rothfels CJ, Stevenson DWD, Graham SW, Wong GK, Nelson DC, Bennett T (2017) Evolution of strigolactone receptors by gradual neo-functionalization of KAI2 paralogues. BMC Biol 15 (1):52. doi:10.1186/s12915-017-0397-z

Chabaud M, Boisson-Dernier A, Zhang J, Taylor CG, Yu O, Barker DG (2006) *Agrobacterium rhizogenes*-mediated root transformation. The *Medicago truncatula* handbook, version November

Chabot S, Bécard G, Piché Y (1992) Life cycle of *Glomus intraradix* in root organ culture. Mycologia:315-321

Chen A, Gu M, Sun S, Zhu L, Hong S, Xu G (2011) Identification of two conserved cis-acting elements, MYCS and P1BS, involved in the regulation of mycorrhiza-activated phosphate transporters in eudicot species. New Phytol 189 (4):1157-1169

Chen X, Liao D, Yang X, Ji M, Wang S, Gu M, Chen A, Xu G (2017) Three cis-Regulatory Motifs, AuxRE, MYCRS1 and MYCRS2, are Required for Modulating the Auxin- and Mycorrhiza-Responsive Expression of a Tomato GH3 Gene. Plant Cell Physiol 58 (4):770-778. doi:10.1093/pcp/pcx013

Chiwocha SD, Dixon KW, Flematti GR, Ghisalberti EL, Merritt DJ, Nelson DC, Riseborough J-AM, Smith SM, Stevens JC (2009) Karrikins: a new family of plant growth regulators in smoke. Plant Sci 177 (4):252-256

Decker EL, Alder A, Hunn S, Ferguson J, Lehtonen MT, Scheler B, Kerres KL, Wiedemann G, Safavi-Rizi V, Nordzieke S (2017) Strigolactone biosynthesis is evolutionarily conserved, regulated by phosphate starvation and contributes to resistance against phytopathogenic fungi in a moss, Physcomitrella patens. New Phytol 216 (2):455-468

Delaux PM, Xie X, Timme RE, Puech-Pages V, Dunand C, Lecompte E, Delwiche CF, Yoneyama K, Becard G, Sejalon-Delmas N (2012) Origin of strigolactones in the green lineage. New Phytol 195 (4):857-871. doi:10.1111/j.1469-8137.2012.04209.x

Demchenko K, Winzer T, Stougaard J, Parniske M, Pawlowski K (2004) Distinct roles of Lotus japonicus SYMRK and SYM15 in root colonization and arbuscule formation. New Phytol 163 (2):381-392

Favre P, Bapaume L, Bossolini E, Delorenzi M, Falquet L, Reinhardt D (2014) A novel bioinformatics pipeline to discover genes related to arbuscular mycorrhizal symbiosis based on their evolutionary conservation pattern among higher plants. BMC Plant Biol 14 (1):333

Fiorilli V, Catoni M, Miozzi L, Novero M, Accotto GP, Lanfranco L (2009) Global and cell-type gene expression profiles in tomato plants colonized by an arbuscular mycorrhizal fungus. New Phytol 184 (4):975-987

Floss DS, Levy JG, Lévesque-Tremblay V, Pumplin N, Harrison MJ (2013) DELLA proteins regulate arbuscule formation in arbuscular mycorrhizal symbiosis. Proc Natl Acad Sci 110 (51):E5025-E5034

Foo E, Ferguson BJ, Reid JB (2014) Common and divergent roles of plant hormones in nodulation and arbuscular mycorrhizal symbioses. Plant Signal Behav 9 (9):1037-1045

García Garrido JM, León Morcillo RJ, Martín Rodríguez JA, Ocampo Bote JA (2010) Variations in the mycorrhization characteristics in roots of wild-type and ABA-deficient tomato are accompanied by specific transcriptomic alterations. Mol Plant-Microbe Interact 23 (5):651-664. doi:10.1094/MPMI-23-5-0651

Genre A, Chabaud M, Balzergue C, Puech-Pagès V, Novero M, Rey T, Fournier J, Rochange S, Bécard G, Bonfante P (2013) Short-chain chitin oligomers from arbuscular mycorrhizal fungi trigger nuclear Ca2+ spiking in *Medicago truncatula* roots and their production is enhanced by strigolactone. New Phytol 198 (1):190-202

Genre A, Ivanov S, Fendrych M, Faccio A, Žárský V, Bisseling T, Bonfante P (2011) Multiple exocytotic markers accumulate at the sites of perifungal membrane biogenesis in arbuscular mycorrhizas. Plant Cell Physiol 53 (1):244-255

Gobbato E, Marsh JF, Vernié T, Wang E, Maillet F, Kim J, Miller JB, Sun J, Bano SA, Ratet P (2012) A GRAS-type transcription factor with a specific function in mycorrhizal signaling. Curr Biol 22 (23):2236-2241

Gomez-Roldan V, Fermas S, Brewer PB, Puech-Pagès V, Dun EA, Pillot J-P, Letisse F, Matusova R, Danoun S, Portais J-C (2008) Strigolactone inhibition of shoot branching. Nature 455 (7210):189

Govindarajulu M, Pfeffer PE, Jin H, Abubaker J, Douds DD, Allen JW, Bücking H, Lammers PJ, Shachar-Hill Y (2005) Nitrogen transfer in the arbuscular mycorrhizal symbiosis. Nature 435 (7043):819-823

Guillotin B, Etemadi M, Audran C, Bouzayen M, Bécard G, Combier JP (2017) Sl-IAA27 regulates strigolactone biosynthesis and mycorrhization in tomato (var. MicroTom). New Phytol 213 (3):1124-1132

Guo Y, Zheng Z, La Clair JJ, Chory J, Noel JP (2013) Smoke-derived karrikin perception by the alpha/beta-hydrolase KAI2 from Arabidopsis. Proceedings of the National Academy of Sciences of the United States of America 110 (20):8284-8289. doi:10.1073/pnas.1306265110

Gutjahr C, Gobbato E, Choi J, Riemann M, Johnston MG, Summers W, Carbonnel S, Mansfield C, Yang SY, Nadal M, Acosta I, Takano M, Jiao WB, Schneeberger K, Kelly KA, Paszkowski U (2015) Rice perception of symbiotic arbuscular mycorrhizal fungi requires the karrikin receptor complex. Science 350 (6267):1521-1524. doi:10.1126/science.aac9715

Gutjahr C, Parniske M (2013) Cell and developmental biology of arbuscular mycorrhiza symbiosis. Annu Rev Cell Dev Biol 29

Hamiaux C, Drummond RS, Janssen BJ, Ledger SE, Cooney JM, Newcomb RD, Snowden KC (2012) DAD2 is an alpha/beta hydrolase likely to be involved in the perception of the plant branching hormone, strigolactone. Curr Biol 22 (21):2032-2036. doi:10.1016/j.cub.2012.08.007

Harrison MJ (1999) Molecular and cellular aspects of the arbuscular mycorrhizal symbiosis. Annu Rev Plant Biol 50 (1):361-389

Heikinheimo P, Goldman A, Jeffries C, Ollis DL (1999) Of barn owls and bankers: a lush variety of α/β hydrolases. Structure 7 (6):R141-R146

Javot H, Pumplin N, Harrison MJ (2007) Phosphate in the arbuscular mycorrhizal symbiosis: transport properties and regulatory roles. Plant, Cell Environ 30 (3):310-322

Jefferson R (1989) The GUS reporter gene system. Nature 342 (6251):837

Ji K, Kai W, Zhao B, Sun Y, Yuan B, Dai S, Li Q, Chen P, Wang Y, Pei Y (2014) SlNCED1 and SlCYP707A2: key genes involved in ABA metabolism during tomato fruit ripening. J Exp Bot 65 (18):5243-5255

Jiang L, Liu X, Xiong G, Liu H, Chen F, Wang L, Meng X, Liu G, Yu H, Yuan Y, Yi W, Zhao L, Ma H, He Y, Wu Z, Melcher K, Qian Q, Xu HE, Wang Y, Li J (2013) DWARF 53 acts as a repressor of strigolactone signalling in rice. Nature 504 (7480):401-405. doi:10.1038/nature12870

Jiang L, Matthys C, Marquez-Garcia B, De Cuyper C, Smet L, De Keyser A, Boyer F-D, Beeckman T, Depuydt S, Goormachtig S (2015) Strigolactones spatially influence lateral root development through the cytokinin signaling network. J Exp Bot 67 (1):379-389

Jin Y, Liu H, Luo D, Yu N, Dong W, Wang C, Zhang X, Dai H, Yang J, Wang E (2016) DELLA proteins are common components of symbiotic rhizobial and mycorrhizal signalling pathways. Nat Commun 7

Kagiyama M, Hirano Y, Mori T, Kim SY, Kyozuka J, Seto Y, Yamaguchi S, Hakoshima T (2013) Structures of D14 and D14L in the strigolactone and karrikin signaling pathways. Genes Cells 18 (2):147-160. doi:10.1111/gtc.12025

Kapulnik Y, Delaux P-M, Resnick N, Mayzlish-Gati E, Wininger S, Bhattacharya C, Séjalon-Delmas N, Combier J-P, Bécard G, Belausov E (2011) Strigolactones affect lateral root formation and root-hair elongation in Arabidopsis. Planta 233 (1):209-216

Karandashov V, Nagy R, Wegmüller S, Amrhein N, Bucher M (2004) Evolutionary conservation of a phosphate transporter in the arbuscular mycorrhizal symbiosis. Proc Natl Acad Sci USA 101 (16):6285-6290

Karimi M, Inze D, Depicker A (2002) GATEWAY vectors for *Agrobacterium*-mediated plant transformation. Trends Plant Sci 7 (5):193-195

Kobae Y, Kameoka H, Sugimura Y, Saito K, Ohtomo R, Fujiwara T, Kyozuka J (2018) Strigolactone biosynthesis genes of rice is required for the punctual entry of arbuscular mycorrhizal fungi into the roots. Plant Cell Physiol

Koltai H, LekKala SP, Bhattacharya C, Mayzlish-Gati E, Resnick N, Wininger S, Dor E, Yoneyama K, Yoneyama K, Hershenhorn J (2010) A tomato strigolactone-impaired mutant displays aberrant shoot morphology and plant interactions. J Exp Bot 61 (6):1739-1749

Kretzschmar T, Kohlen W, Sasse J, Borghi L, Schlegel M, Bachelier JB, Reinhardt D, Bours R, Bouwmeester HJ, Martinoia E (2012) A petunia ABC protein controls strigolactone-dependent symbiotic signalling and branching. Nature 483 (7389):341

Kryvoruchko IS, Sinharoy S, Torres-Jerez I, Sosso D, Pislariu CI, Guan D, Murray J, Benedito VA, Frommer WB, Udvardi MK (2016) *MtSWEET11*, a Nodule-Specific Sucrose Transporter of *Medicago truncatula*. Plant Physiol 171 (1):554-565. doi:10.1104/pp.15.01910

Lescot M, Dehais P, Thijs G, Marchal K, Moreau Y, Van de Peer Y, Rouze P, Rombauts S (2002) PlantCARE, a database of plant cis-acting regulatory elements and a portal to tools for in silico analysis of promoter sequences. Nucleic Acids Res 30 (1):325-327

Lévy J, Bres C, Geurts R, Chalhoub B, Kulikova O, Duc G, Journet E-P, Ané J-M, Lauber E, Bisseling T (2004) A putative Ca2+ and calmodulin-dependent protein kinase required for bacterial and fungal symbioses. Science 303 (5662):1361-1364

Li X (2011) Infiltration of Nicotiana benthamiana protocol for transient expression via Agrobacterium. Bio Protoc 1:e95

Long JZ, Cravatt BF (2011) The metabolic serine hydrolases and their functions in mammalian physiology and disease. Chem Rev 111 (10):6022-6063

López-Pedrosa A, González-Guerrero M, Valderas A, Azcón-Aguilar C, Ferrol N (2006) *GintAMT1* encodes a functional high-affinity ammonium transporter that is expressed in the extraradical mycelium of *Glomus intraradices*. Fungal Genet Biol 43 (2):102-110

López-Ráez JA, Verhage A, Fernandez I, Garcia JM, Azcón-Aguilar C, Flors V, Pozo MJ (2010) Hormonal and transcriptional profiles highlight common and differential host responses to arbuscular mycorrhizal fungi and the regulation of the oxylipin pathway. J Exp Bot 61 (10):2589-2601. doi:10.1093/jxb/erq089

López-Ráez JA, Kohlen W, Charnikhova T, Mulder P, Undas AK, Sergeant MJ, Verstappen F, Bugg TD, Thompson AJ, Ruyter-Spira C (2010) Does abscisic acid affect strigolactone biosynthesis? New Phytol 187 (2):343-354

Maier W, Peipp H, Schmidt J, Wray V, Strack D (1995) Levels of a terpenoid glycoside (blumenin) and cell wall-bound phenolics in some cereal mycorrhizas. Plant Physiol 109 (2):465-470

Mindrebo JT, Nartey CM, Seto Y, Burkart MD, Noel JP (2016) Unveiling the functional diversity of the alpha/beta hydrolase superfamily in the plant kingdom. Curr Opin Struct Biol 41:233-246. doi:10.1016/j.sbi.2016.08.005

Moise AR, Von Lintig J, Palczewski K (2005) Related enzymes solve evolutionarily recurrent problems in the metabolism of carotenoids. Trends Plant Sci 10 (4):178-186

Mori N, Nishiuma K, Sugiyama T, Hayashi H, Akiyama K (2016) Carlactone-type strigolactones and their synthetic analogues as inducers of hyphal branching in arbuscular mycorrhizal fungi. Phytochemistry 130:90-98. doi:10.1016/j.phytochem.2016.05.012

Nagy R, Karandashov V, Chague V, Kalinkevich K, Tamasloukht MB, Xu G, Jakobsen I, Levy AA, Amrhein N, Bucher M (2005) The characterization of novel mycorrhiza-specific phosphate transporters from *Lycopersicon esculentum* and *Solanum tuberosum* uncovers functional redundancy in symbiotic phosphate transport in solanaceous species. Plant J 42 (2):236-250

Nakamura H, Xue Y-L, Miyakawa T, Hou F, Qin H-M, Fukui K, Shi X, Ito E, Ito S, Park S-H (2013) Molecular mechanism of strigolactone perception by DWARF14. Nat Commun 4:2613

Nardini M, Dijkstra BW (1999) α/β Hydrolase fold enzymes: the family keeps growing. Curr Opin Struct Biol 9 (6):732-737

Nelson DC, Scaffidi A, Dun EA, Waters MT, Flematti GR, Dixon KW, Beveridge CA, Ghisalberti EL, Smith SM (2011) F-box protein MAX2 has dual roles in karrikin and strigolactone signaling in Arabidopsis thaliana. Proc Natl Acad Sci 108 (21):8897-8902

Niesen FH, Berglund H, Vedadi M (2007) The use of differential scanning fluorimetry to detect ligand interactions that promote protein stability. Nat Protoc 2 (9):2212-2221

Pérez-Tienda J, Testillano PS, Balestrini R, Fiorilli V, Azcón-Aguilar C, Ferrol N (2011) *GintAMT2*, a new member of the ammonium transporter family in the arbuscular mycorrhizal fungus *Glomus intraradices*. Fungal Genet Biol 48 (11):1044-1055

Pettersen EF, Goddard TD, Huang CC, Couch GS, Greenblatt DM, Meng EC, Ferrin TE (2004) UCSF Chimera—a visualization system for exploratory research and analysis. Journal of computational chemistry 25 (13):1605-1612

Phillips JM, Hayman D (1970) Improved procedures for clearing roots and staining parasitic and vesicular-arbuscular mycorrhizal fungi for rapid assessment of infection. Trans Br Mycol Soc 55 (1):158IN116-161IN118

Pimprikar P, Carbonnel S, Paries M, Katzer K, Klingl V, Bohmer MJ, Karl L, Floss DS, Harrison MJ, Parniske M (2016) A CCaMK-CYCLOPS-DELLA complex activates transcription of *RAM1* to regulate arbuscule branching. Curr Biol 26 (8):987-998

Pozo MJ, López-Ráez JA, Azcón-Aguilar C, García-Garrido JM (2015) Phytohormones as integrators of environmental signals in the regulation of mycorrhizal symbioses. New Phytol 205 (4):1431-1436

Pumplin N, Mondo SJ, Topp S, Starker CG, Gantt JS, Harrison MJ (2010) Medicago truncatula Vapyrin is a novel protein required for arbuscular mycorrhizal symbiosis. Plant J 61 (3):482-494. doi:10.1111/j.1365-313X.2009.04072.x

Rasmussen A, Mason MG, De Cuyper C, Brewer PB, Herold S, Agusti J, Geelen D, Greb T, Goormachtig S, Beeckman T (2012) Strigolactones suppress adventitious rooting in Arabidopsis and pea. Plant Physiol 158 (4):1976-1987

Rubio V, Linhares F, Solano R, Martín AC, Iglesias J, Leyva A, Paz-Ares J (2001) A conserved MYB transcription factor involved in phosphate starvation signaling both in vascular plants and in unicellular algae. Genes Dev 15 (16):2122-2133

Salt S, Tuzun S, Kuć J (1986) Effects of β-ionone and abscisic acid on the growth of tobacco and resistance to blue mold. Mimicry of effects of stem infection by Peronospora tabacina Adam. Physiol Mol Plant Pathol 28 (2):287-297

Serrani JC, Sanjuán R, Ruiz-Rivero O, Fos M, García-Martínez JL (2007) Gibberellin regulation of fruit set and growth in tomato. Plant Physiol 145 (1):246-257

Sievers F, Wilm A, Dineen D, Gibson TJ, Karplus K, Li W, Lopez R, McWilliam H, Remmert M, Soding J, Thompson JD, Higgins DG (2011) Fast, scalable generation of high-quality protein multiple sequence alignments using Clustal Omega. Mol Syst Biol 7:539. doi:10.1038/msb.2011.75

Smith S, Read D (2008) Mycorrhizal Symbiosis. 3 th. Academic Press. London.,

Stanga JP, Smith SM, Briggs WR, Nelson DC (2013) SUPPRESSOR OF MORE AXILLARY GROWTH2 1 controls seed germination and seedling development in Arabidopsis. Plant Physiol 163 (1):318-330

Strack D, Fester T (2006) Isoprenoid metabolism and plastid reorganization in arbuscular mycorrhizal roots. New Phytol 172 (1):22-34

Sun J, Miller JB, Granqvist E, Wiley-Kalil A, Gobbato E, Maillet F, Cottaz S, Samain E, Venkateshwaran M, Fort S (2015) Activation of symbiosis signaling by arbuscular mycorrhizal fungi in legumes and rice. Plant Cell 27 (3):823-838

Sun YK, Flematti GR, Smith SM, Waters MT (2016) Reporter gene-facilitated detection of compounds in Arabidopsis leaf extracts that activate the Karrikin signaling pathway. Front Plant Sci 7

Torres-Vera R, García JM, Pozo MJ, López-Ráez JA (2016) Expression of molecular markers associated to defense signaling pathways and strigolactone biosynthesis during the early interaction tomato-Phelipanche ramosa. Physiol Mol Plant Pathol 94:100-107

Trouvelot A (1986) Mesure du taux de mycorhization VA d'un systeme radiculaire. Recherche de methodes d'estimation ayant une significantion fonctionnelle. Mycorrhizae: physiology and genetics:217-221

Végh A, Incze N, Fábián A, Huo H, Bradford KJ, Balázs E, Soós V (2017) Comprehensive Analysis of DWARF14-LIKE2 (DLK2) Reveals Its Functional Divergence from Strigolactone-Related Paralogs. Front Plant Sci 8:1641

Vogel JT, Walter MH, Giavalisco P, Lytovchenko A, Kohlen W, Charnikhova T, Simkin AJ, Goulet C, Strack D, Bouwmeester HJ (2010) SlCCD7 controls strigolactone biosynthesis, shoot branching and mycorrhiza-induced apocarotenoid formation in tomato. Plant J 61 (2):300-311

Walter MH (2013) Role of carotenoid metabolism in the arbuscular mycorrhizal symbiosis. Molecular Microbial Ecology of the Rhizosphere: Volume 1 & 2:513-524

Walter MH, Floß DS, Hans J, Fester T, Strack D (2007) Apocarotenoid biosynthesis in arbuscular mycorrhizal roots: contributions from methylerythritol phosphate pathway isogenes and tools for its manipulation. Phytochemistry 68 (1):130-138

Wallner E-S, López-Salmerón V, Belevich I, Poschet G, Jung I, Grünwald K, Sevilem I, Jokitalo E, Hell R, Helariutta Y (2017) Strigolactone-and Karrikin-Independent SMXL Proteins Are Central Regulators of Phloem Formation. Curr Biol 27 (8):1241-1247

Wang E, Schornack S, Marsh JF, Gobbato E, Schwessinger B, Eastmond P, Schultze M, Kamoun S, Oldroyd GE (2012) A common signaling process that promotes mycorrhizal and oomycete colonization of plants. Curr Biol 22 (23):2242-2246

Wang L, Wang B, Jiang L, Liu X, Li X, Lu Z, Meng X, Wang Y, Smith SM, Li J (2015) Strigolactone Signaling in Arabidopsis Regulates Shoot Development by Targeting D53-Like SMXL Repressor Proteins for Ubiquitination and Degradation. Plant Cell 27 (11):3128-3142. doi:10.1105/tpc.15.00605

Waters MT, Nelson DC, Scaffidi A, Flematti GR, Sun YK, Dixon KW, Smith SM (2012) Specialisation within the DWARF14 protein family confers distinct responses to karrikins and strigolactones in Arabidopsis. Development 139 (7):1285-1295. doi:10.1242/dev.074567

Waters MT, Scaffidi A, Moulin SL, Sun YK, Flematti GR, Smith SM (2015) A Selaginella moellendorffii ortholog of KARRIKIN INSENSITIVE2 functions in Arabidopsis development but cannot mediate responses to karrikins or strigolactones. Plant Cell 27 (7):1925-1944

Wei S, Hannoufa A, Soroka J, Xu N, Li X, Zebarjadi A, Gruber M (2011) Enhanced β-ionone emission in Arabidopsis over-expressing AtCCD1 reduces feeding damage in vivo by the crucifer flea beetle. Environ Entomol 40 (6):1622-1630

Wu YY, Hou BH, Lee WC, Lu SH, Yang CJ, Vaucheret H, Chen HM (2017) DCL2-and RDR6-dependent transitive silencing of SMXL4 and SMXL5 in Arabidopsis dcl4 mutants causes defective phloem transport and carbohydrate over-accumulation. Plant J

Yang J, Yan R, Roy A, Xu D, Poisson J, Zhang Y (2015) The I-TASSER Suite: protein structure and function prediction. Nat Methods 12 (1):7

Yano K, Yoshida S, Müller J, Singh S, Banba M, Vickers K, Markmann K, White C, Schuller B, Sato S (2008) CYCLOPS, a mediator of symbiotic intracellular accommodation. Proc Natl Acad Sci 105 (51):20540-20545

Yao R, Ming Z, Yan L, Li S, Wang F, Ma S, Yu C, Yang M, Chen L, Chen L (2016a) DWARF14 is a non-canonical hormone receptor for strigolactone. Nature 536 (7617):469-473

Yao R, Ming Z, Yan L, Li S, Wang F, Ma S, Yu C, Yang M, Chen L, Chen L, Li Y, Yan C, Miao D, Sun Z, Yan J, Sun Y, Wang L, Chu J, Fan S, He W, Deng H, Nan F, Li J, Rao Z, Lou Z, Xie D (2016b) DWARF14 is a non-canonical hormone receptor for strigolactone. Nature 536 (7617):469-473. doi:10.1038/nature19073

Yoneyama K, Xie X, Kim HI, Kisugi T, Nomura T, Sekimoto H, Yokota T, Yoneyama K (2012) How do nitrogen and phosphorus deficiencies affect strigolactone production and exudation? Planta 235 (6):1197-1207

Yoshida S, Kameoka H, Tempo M, Akiyama K, Umehara M, Yamaguchi S, Hayashi H, Kyozuka J, Shirasu K (2012) The D3 F-box protein is a key component in host strigolactone responses essential for arbuscular mycorrhizal symbiosis. New Phytol 196 (4):1208-1216

Yu N, Luo D, Zhang X, Liu J, Wang W, Jin Y, Dong W, Liu J, Liu H, Yang W (2014) A DELLA protein complex controls the arbuscular mycorrhizal symbiosis in plants. Cell Res 24 (1):130

Zhang Q, Blaylock LA, Harrison MJ (2010) Two *Medicago truncatula* half-ABC transporters are essential for arbuscule development in arbuscular mycorrhizal symbiosis. Plant Cell 22 (5):1483-1497

Zhang X, Pumplin N, Ivanov S, Harrison MJ (2015) EXO70I Is Required for Development of a Sub-domain of the Periarbuscular Membrane during Arbuscular Mycorrhizal Symbiosis. Curr Biol 25 (16):2189-2195. doi:10.1016/j.cub.2015.06.075

Zhao L-H, Zhou XE, Wu Z-S, Yi W, Xu Y, Li S, Xu T-H, Liu Y, Chen R-Z, Kovach A (2013) Crystal structures of two phytohormone signal-transducing α/β hydrolases: karrikin-signaling KAI2 and strigolactone-signaling DWARF14. Cell Res 23 (3):436

Zhao LH, Zhou XE, Yi W, Wu Z, Liu Y, Kang Y, Hou L, de Waal PW, Li S, Jiang Y, Scaffidi A, Flematti GR, Smith SM, Lam VQ, Griffin PR, Wang Y, Li J, Melcher K, Xu HE (2015) Destabilization of strigolactone receptor DWARF14 by binding of ligand and E3-ligase signaling effector DWARF3. Cell Res 25 (11):1219-1236. doi:10.1038/cr.2015.122

Zhou F, Lin Q, Zhu L, Ren Y, Zhou K, Shabek N, Wu F, Mao H, Dong W, Gan L, Ma W, Gao H, Chen J, Yang C, Wang D, Tan J, Zhang X, Guo X, Wang J, Jiang L, Liu X, Chen W, Chu J, Yan C, Ueno K, Ito S, Asami T, Cheng Z, Wang J, Lei C, Zhai H, Wu C, Wang H, Zheng N, Wan J (2013) D14-SCF(D3)-dependent degradation of D53 regulates strigolactone signalling. Nature 504 (7480):406-410. doi:10.1038/nature12878

Chapter 4. Transcriptomic changes undergoing *SlDLK2* silencing during arbuscular mycorrhizal symbiosis in tomato

Part of this paper is in preparation for publishing

Abstract

SlDLK2, a tomato gene encoding an α, β-hydrolase protein closely related to the SLs and karrikin receptors, is highly upregulated in tomato roots colonized by arbuscular mycorrhizal (AM) fungi. Previous studies suggest that the SlDLK2 protein is involved in signaling inhibition of arbuscule branching in tomato (chapter 2), and then might function as a negative regulator of the mycorrhization process. A transcript profiling experiment by RNA-seq, performed with *SlDLK2* RNAi directed by the arbuscule-specific promoter p*PT4*, revealed important changes in the metabolic pathways. Biggest changes observed were associated to a nutrient starvation and induced defense signature in the *SlDLK2* RNAi mycorrhizal roots, probably as a consequence of the higher AM development in these plants. However, examination of many other differentially expressed genes supports the idea of SlDLK2 as a negative regulator of mycorrhization. In view of our results, we propose that SlDLK2 might be important to activate GA signaling, restrict hexose production and supply to the AM fungus, and induce a number of resistance mechanisms, in order to control AM fungal development.

Introduction

The arbuscular mycorrhizal (AM) symbiosis is a widespread association between terrestrial plants and fungi of the phylum Glomeromycota. AM endosymbiosis infection and establishment involves the intracellular accommodation of the AM fungus in the root cells. In this process the host cells need to be fundamentally reprogrammed for the new symbiosis-related functions, such as suppression of defense, intracellular accommodation of the microbe, and nutrient exchange. A high degree of conservation is observed at the cellular (Genre and Bonfante 1998; Bonfante-Fasolo 1984; Genre et al. 2005; Pumplin and Harrison 2009) and

transcriptomic (Breuillin et al. 2010; Guether et al. 2009; Güimil et al. 2005; Hohnjec et al. 2005; Liu et al. 2003; Manthey et al. 2004; Siciliano et al. 2007; Rich et al. 2017) levels in different AM host species, and between the mycorrhizal and the rhizobium-nodule symbiosis, with remarkable conservation of the common symbiotic signaling pathway (CSSP) (Gutjahr and Parniske 2013; Oldroyd 2013). Several microarrays have been performed to study transcriptome alterations of tomato roots stablishing AM symbiosis (López-Ráez et al. 2010; García Garrido et al. 2010; Fiorilli et al. 2009; Ruzicka et al. 2012). However, transcriptome data from microarray analyses is restricted to a limited number of target genes.

In this chapter we describe the transcriptomic analysis of *S. lycopersicum* AM inoculated roots by RNA-seq, what expands the transcriptome information previously provided by the microarrays performed so far. In parallel to this study, we analyzed the transcriptome of *SlDLK2 RNAi* mycorrhizal tomato roots. *SlDLK2* (*Solanum lycopersicum D14-LIKE2*) is a tomato gene found to be highly induced during mycorrhization that encodes an α, β-hydrolase highly related to the D14 and KAI2 receptors of the strigolactone and karrikin compounds, respectively. The possible ligand and the signaling mechanism of SlDlK2 is still unknown, but a previous functional study suggests a role of *SlDLK2* in inhibiting arbuscule branching, and to negatively regulate AM development and functionality (chapter 2). *SlDKL2* gene silencing positively affects mycorrhizal intensities and arbuscule abundance. Nevertheless, *SlDKL2* overexpression leads to important alterations in arbuscule morphology what makes it very interesting the study of transcriptome alterations associated with this altered AM-phenotype. In this work, we present the results of the transcriptomic analysis comparing control and *SlDLK2* RNAi mycorrhizal composite plants, in order to analyze possible mechanisms impaired by *SlDLK2* silencing, as well as to envisage specific pathways probably regulated through *SlDlK2*-mediated signaling during mycorrhization. We are currently conducting a second round of experiments that will address the study of transcriptomic alterations in *SlDKL2* overexpressing plants. The critical analysis of the results as a whole will allow us to define with high degree of confidence those alterations in gene expression linked to the function of the SlDLK2 protein.

Methods

RNA preparation and Illumina sequencing

Nine different root pools were collected for the RNA-seq analysis: three pools containing a mixture of *SlDLK2* RNAi and control roots from non-inoculated plants (NI); three pools of roots from AM-inoculated control plants (wt-I); and three pools of roots from AM-inoculated *SlDLK2* silenced plants (*iDLK2*-I). Total RNA was extracted using the Rneasy Plant Mini Kit (Qiagen, Hilden, Germany). The quality and quantity of total RNA samples were assessed using a NanoDrop 1000 spectrophotometer (Thermo Scientific) and samples were normalized at the same concentration (6 µg, 300 ng/µL). Later, samples were sent to Sistemas Genómicos S.L. (Paterna, Valencia, Spain) for cDNA library preparation and sequencing using an Illumina HiSeq1000 machine.

RNA-seq sequence processing

The TopHat v2.1.0 algorithm (Trapnell et al. 2009) was used to align reads from the RNA-Seq experiment to the Tomato Genome Reference Sequence SL3.0 provided by the Sol Genomics consortium at (https://solgenomics.net/organism/Solanum lycopersicum/genome), using the last ITAG 3.10 annotation. Then, low quality reads were removed from the map through Picard Tools (http://picard.sourceforge.net), and high quality reads were selected for assembly and identification through Bayesian inference using the Cufflinks v2.2.1 algorithm proposed by Trapnell et al. (2010).

Gene quantification process was performed by the htseq-count 0.6.1p1 tool (Anders et al. 2015). Isoform quantification and differential expression was carried out through the DESeq2 method (Anders and Huber 2010).

To elucidate the biological processes and significantly altered pathways that were involved in the response to AM inoculation on tomato roots, overrepresentation analyses on the differentially expressed genes (DEGs) were performed using MetGenMap (Joung et al. 2009).

GAs quantification

Samples were analyzed for GA content according to Urbanová et al. (2013) with some modifications. A representative portion of each tomato whole root system (10 mg lyophilized dry weight) was homogenized in 2-ml Eppendorf tubes with 1ml 80% acetonitrile containing 5% formic acid and 19 internal GA standards ([$^2H_2$]GA_1 , [^{2} H_2]GA_3, [$^2H_2$]GA_4, [$^2H_2$]GA_5, [$^2H_2$]GA_6, [$^2H_2$]GA_7, [$^2H_2$]GA_8, [$^2H_2$]GA_9, [$^2H_2$]GA_{15}, [$^2H_2$]GA_{19}, [$^2H_2$]GA_{20}, [$^2H_2$]GA_{24}, [$^2H_2$]GA_{29}, [$^2H_2$]GA_{34}, [$^2H_2$]GA_{44}, [$^2H_2$]GA_{51} and [$^2H_2$]GA_{53}) (OlChemIm, Olomouc, Czech Republic) using an MM 301 vibration mill (www.retsch.de) set at 27 Hz for 3 min, adding 2-mm zirconium oxide beads to each tube to increase the extraction efficiency. The tubes were then placed in a fridge (4ºC) and extracted overnight with stirring using a bench top laboratory rotator Stuart SB 3 at 15 r.p.m. (www.bibby-scientific.com). The homogenates were centrifuged at 33095 g for 10 min at 4 ºC using Beckman Avanti™ 30 centrifuge (Beckman Coulter Inc., Brea, CA). Supernatants were further purified using mixed mode anion exchange cartridges (www.waters.com) and analyzed by ultra-high performance chromatography (Acquity UPLC™ System; Waters MS Technologies, Manchester, UK) coupled to triple-stage quadrupole mass spectrometer (Xevo® TQ MS, Waters MS Technologies) equipped with electrospray interface (ESI). GAs were detected using multiple-reaction monitoring mode (MRM) based on transition of the precursor ion $[M–H]^-$ to the appropriate product ion. Data were acquired and processed by MASSLYNX 4.1 software (Waters MS Technologies) and GA levels were calculated using standard isotope-dilution method (Rittenberg and Foster 1940).

Additional methods used in this chapter but previously described in the *General Materials and Methods* section:

- **Plasmid Construction and Hairy root transformation**
- **Plant growth and AM inoculation**

Results and Discussion

Experimental design

Here, we selected *SlDLK2* hairpin interference samples directed by the arbuscular specific *SlPT4* promoter (whose expression pattern is coincident to the *SlDLK2* promoter) because in the previous chapter we observed that silencing of *SlDLK2* directed by the *SlPT4* promoter apparently enhanced changes at a transcriptional level with respect to the use of *SlDlK2* RNAi controlled by the constitutive *35S* promoter. Particularly, control plants transformed with the empty vector (wt-I) exhibited a 28.44 ± 2.39 % (n=12) mycorrhizal colonization, while *SlDLK2* RNAi inoculated composite plants (i*DLK2*-I) showed a 36.21 ± 2.22% mycorrhization (n=12). From these plants, *SlDLK2* gene expression was measured to select wt-I root pools with a representative *SlDLK2* induction upon mycorrhization, and i*DLK2*-I root pools with an effective *SlDLK2* silencing (Fig. 1A). In addition, although the average mycorrhizal development was higher in the i*DLK2*-I roots, we selected wt-I and i*DLK2*-I samples with similar mycorrhizal colonization levels (Fig. 1B) and similar mycorrhizal functionality (Fig. 1C) for the RNA-seq in order to limit transcriptome changes to *SlDLK2* silencing, and reduce changes due to the higher mycorrhization of i*DLK2*-I plants.

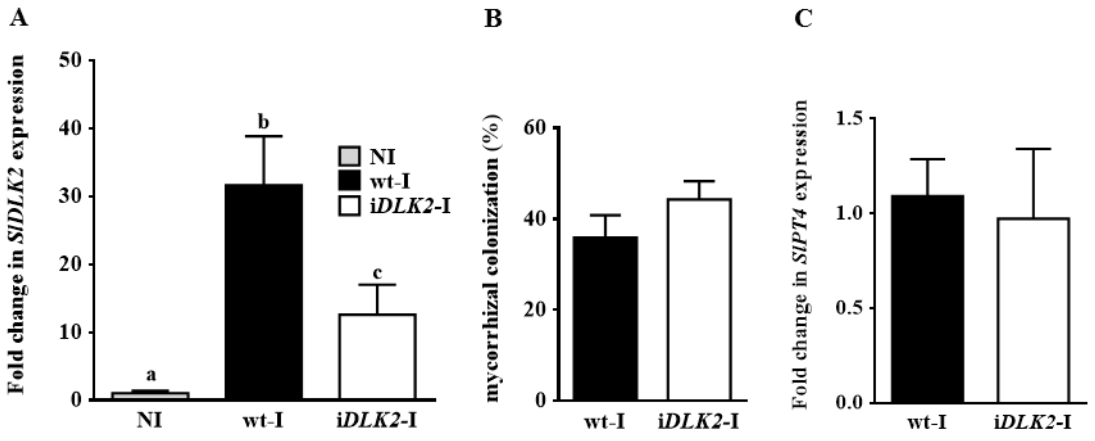

Figure 1. *SlDLK2* gene expression, mycorrhizal development and arbuscule activity in root samples selected for the RNA-seq analysis. *SlDLK2* gene expression (A), mycorrhizal colonization (B) and the expression of the arbuscular tomato marker *SlPT4* (phosphate-transporter 4) (C), are shown for samples used in the RNA-seq analysis. NI, non-inoculated; wt-I, control inoculated plants transformed with the empty vector; i*DLK2*-I, *SlDLK2* RNAi

inoculated plants. Values are the mean ± SE of three biological replications. Bars with similar letters are not significantly different (P>0.05) according to LSD multiple comparison test.

Raw sequencing data and mapping of RNA-seq reads to *S. lycopersicum* genome

To reveal the AM symbiosis-associated transcriptional responses in tomato, as well as the involvement of the AM-induced gene *SlDLK2* during mycorrhization, AM-inoculated control composite plants transformed with the empty vector pK7GWIWG2_II-RedRoot ("I"), as well as AM- *SlDLK2* silenced plants carrying the vector pK7GWIWG2_II-RedRoot::i*SlDLK2* ("i*DLK2*-I"), and a mix of these two groups of plants under non-inoculated conditions ("NI") were subjected to total RNA extraction and RNA-seq analysis. We used a single treatment of non-inoculated plants, composed of a mixture of control and *iSlDKL2* transformants, because in both types the RNA interference is not effective in the absence of mycorrhization, due to the AM-associated expression of *SlDLK2*.

Three sample replicates per treatment were used. The single lane of Illumina HiSeq2000 high-throughput sequencing generated about 74.21 million total reads for each sample, being mapped a number of 68.97 million reads (92.95 %), with 51.77 million (69.81 %) of high quality properly paired reads and 15.60 millions (20.99 %) of spliced reads (Table 1).

Table 1. Number of mapped reads, high quality reads and splices reads for each sample.

		Mapped reads		HQ reads		Splice reads	
Sample name	**Total reads**	**Number**	**%**	**Number**	**%**	**Number**	**%**
NI (1)	66527294	62760196	94.34	49085600	73.78	15215113	22.87
NI (2)	73665122	69071215	93.76	53872098	73.13	16092139	21.84
NI (3)	72685452	67501805	92.87	52016044	71.56	16316428	22.45
wt-I (1)	79125452	74786703	94.52	52926152	66.89	16096014	20.34
wt-I (2)	100333076	91843848	91.54	68676632	68.45	21296683	21.23
wt-I (3)	58014180	53700605	92.56	39662344	68.37	11585053	19.97
i*DLK2*-I (1)	71221312	66155665	92.89	50265956	70.58	15183303	21.32
i*DLK2*-I (2)	62717190	56965880	90.83	41821406	66.68	11833885	18.87
i*DLK2*-I (3)	83626738	77957049	93.22	57609988	68.89	16770618	20.05
Average ± SE	74.21 million ± 4.18	68.97 million ± 3.84	92.95 % ± 0.40	51.77 million ± 2.84	69.81 % ± 0.86	15.60 million ± 0.95	20.99 % ± 0.43

The obtained reads were mapped to the Tomato Genome Reference Sequence SL3.0 using TopHat, and the generated output was processed by Cufflinks toolkits for transcript assembly and differential gene expression analysis. In general, a total of 35905 expressed genes were detected from the tomato root samples. These 35905 discovered gene transcripts included 34761 well-known protein coding genes in tomato, as well as 1144 non-coding RNA genes, such as miRNA genes, siRNA genes and long non-coding RNA genes.

A look at the whole root transcriptome and DEGs

Using the DESeq2 algorithm, normalized read counts were obtained for each sample and the fold change induction or repression was calculated for each gene in the following treatment comparisons: "wt-I vs NI", "i*DLK2*-I vs NI" and "i*DLK2*-I vs wt-I". Detailed results are shown in Supplementary Tables 1, 2 and 3, respectively. Using a cuttof value of fold change >2 or <-2 to declare a gene as expressed, 7664 genes were differentially regulated in at least one of the comparisons, from a total of 35905 detected gene transcripts in the RNA-seq analysis. A Venn diagram is shown if Figure 2, indicating the number of differentially expressed genes (DEGs) between treatments.

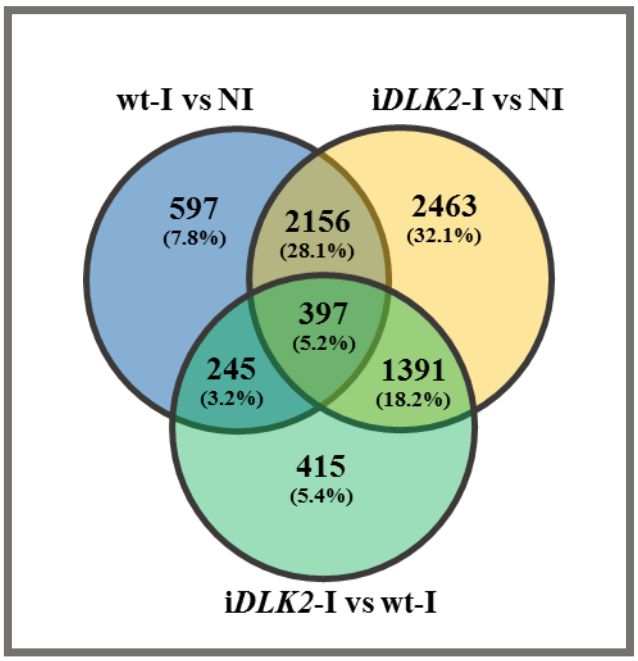

Figure 2. Venn diagram of DEGs. The Venn diagram shows the number of tomato genes detected in the RNA-seq to be differentially and significantly expressed (fold change ≤-2 or ≥2, and $P<0.05$) for the corresponding comparisons between the three treatments: non-inoculated roots (NI), control inoculated roots (wt-I) and *SlDLK2* silenced inoculated roots (DLK2-I).

Validation of the RNA-seq data analysis

Fourteen putative homolog genes to AM-induced genes previously described in the literature were selected, and all of them were found to be upregulated in wt-I roots with respect to NI roots in the RNA-seq (Table 2). Gene induction of five of these genes was successfully confirmed by qPCR (Fig. 3). Additionally, most of the genes reported to be highly AM-induced in previous microarray analyses of García Garrido et al. (2010) and López-Ráez et al. (2010), were also upregulated in the RNA-seq (Tables 3 and 4, respectively), what validates the data from the RNA-seq analysis.

Table 2. Gene expression data in the RNA-seq in mycorrhizal roots with respect to un-inoculated roots of putative AM-induced genes described in the literature.

Gene ID (SolDB)	Fold change	p-value	Description	Common name	Reference
Solyc08g067080.2.1	49.92	3.52E-25	Ammonium transporter	AMT2-2	Breuillin-Sessoms et al. (2015)
Solyc04g077760.1.1	27.50	9.76E-21	Exocyst complex component 7	EXO70i	Zhang et al. (2015b)
Solyc09g072720.2.1	27.18	6.85E-18	Exocyst complex component 8	Exo84	Genre et al. (2011)
Solyc02g087500.2.1	20.07	ns	Glycerol-3-phosphate acyltransferase	RAM2	Wang et al. (2012)
Solyc10g081500.1.1	13.67	7.98E-22	Ankyrin repeat-containing protein	Vapyrin (PAM1)	Pumplin et al. (2010)
Solyc02g094340.1.1	12.52	6.97E-20	GRAS family transcription factor	RAM1	Gobbato et al. (2012)
Solyc01g097430.3.1	11.18	3.94E-08	ABC transporter	STR	Zhang et al. (2010)
Solyc02g091590.3.1	4.74	2.64E-20	symbiosis receptor-like kinase (SYMRK)	SYMRK	Demchenko et al. (2004)
Solyc09g098410.2.1	4.52	6.36E-04	ABC transporte	STR-2	Zhang et al. (2010)
Solyc08g075760.3.1	4.49	9.00E-15	CYCLOPS/IPD3-like protein	CYCLOPS (IPD3)	Yano et al. (2008)
Solyc04g071150.3.1	4.35	8.11E-08	Cytochrome P450 family protein	CYP707A3-like	Martin-Rodriguez et al. (2016)
Solyc06g051860.2.1	4.25	2.91E-04	mycorrhiza-inducible inorganic phosphate transporter 5	PT5	Balestrini et al. (2007) and Chen et al. (2011)
Solyc01g096820.3.1	3.41	1.18E-09	Calcium/calmodulin dependent protein kinase	CCaMK (DMI3)	Lévy et al. (2004)
Solyc08g080010.2.1	2.69	2.37E-03	Subtilisin-like protease	Subtilase	Takeda et al. (2009)

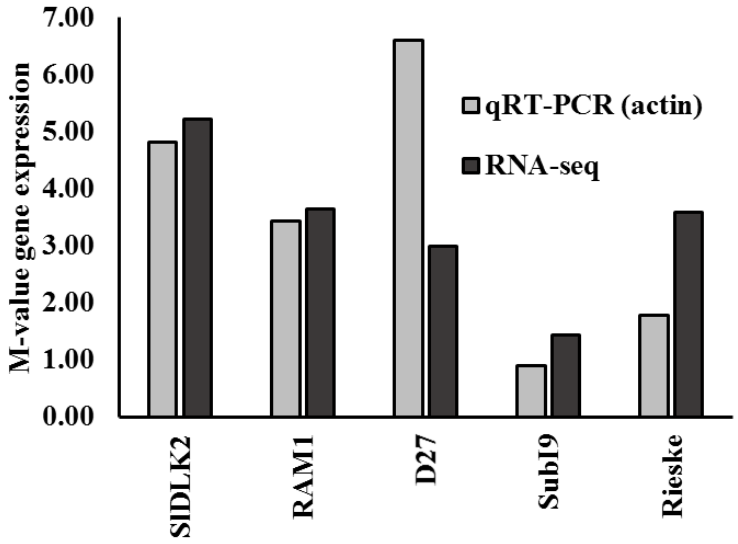

Figure 3. Gene expression of AM-induced genes: comparison between RNA-seq and qPCR data. mRNA levels of marker AM-induced genes was quantified by qPCR and compared with our RNA-Seq data set. Expression values are presented as M-value (log_2FoldChange) in wt-I vs NI root samples. In the qPCR data the mRNA expression values were normalized to the expression of housekeeping actin gene.

Table 3. Comparison between the mRNA expression of AM-induced genes found in the microarray data of García Garrido et al. (2010), and our RNA-seq data set. Both are experiments performed in mycorrhizal tomato roots colonized with *R. irregularis,* with respect to un-inoculated roots.

Gene (SolDB ID)	Gene (GenBank ID)	Fold change in microarray (García-Garrido et al., 2010)	Fold change in RNA-seq (This work)	Description
Solyc00g170200	AW622368	133.00	37,003	alpha,beta-hydrolase
Solyc10g085280	X72729	106.5	2,30	(ERT 1b) ripening-related mRNA. UDP glucosyl transferase
Solyc01g067370	AF515615	41.35	23,85	LOC54371. TSB protein
Solyc09g072700	AW928514	24.38	107,50	putative peroxidase III
Solyc03g098720	BG631366	24.14	Does not appear	putative miraculin protease
Solyc05g007950	X79337	24.08	2,21	rnale | ribonuclease
Solyc04g078730	BT014524	20.77	1,05	subtilase (protease)
Solyc03g098710	AI897365	17.57	24,05	putative Kunitz-type protease inhibitor
Solyc04g040160	BG626023	16.55	12,01	Rieske [2Fe-2S] region, oxidoreductase activity
Solyc01g104950	AB041811	14.88	2,48	hydrolase activity, hydrolyzing O-glycosyl compounds. LEXYL1 | LEXYL1 protein
Solyc01g097950	BT014016	14.62	Dos not appear	putative cysteine synthase (cs1 gene)

Solyc10g078740	BG625959	11.72	2,15	putative enoyl-acyl-carrier-protein reductase
Solyc04g011910	AW626187	11.53	2,20	unknown
Solyc03g098720	BI931127	10.84	4,29	putative miraculin protease
Solyc02g078950	BG630947	10.43	3,91	putative beta-galactosidase
Solyc02g078570	BT014379	9.51	13,05	hdc | Histidine decarboxylase
Solyc11g010850	BI933750	9.18	20,86	putative 1-deoxy-D-xylulose 5-phosphate synthase 2
Solyc06g084240	AB015675	9.05	12,65	CPS | copalyl diphosphate synthase

Table 4. Comparison between the mRNA expression of AM-induced genes found in the microarray data of López-Ráez et al. (2010), and our RNA-seq data set. Both are experiments performed in mycorrhizal tomato roots colonized with *R. irregularis*, with respect to un-inoculated roots.

Gene (SolDB ID)	Gene (GenBank ID)	Fold change in microarray (Lopéz-Ráez et al., 2010)	Fold change in RNA-seq (This work)	Description
Solyc08g014000	U09026	2,78	66,70	Lipoxygenase A (LoxA)
Solyc10g007960	AF454634	3,42	35,50	Allene oxide synthase (AOS3)
Solyc03g044200	AI771939	5,04	1,96	Class III alcohol dehydrogenase 5
Solyc05g025780	AF243040	4,85	4,85	Receptor-like protein kinase (PRK3)
Solyc03g044200	BI922195	3,85	19,62	Class III alcohol dehydrogenase 5
Solyc01g008620	M80604	3,31	10,98	Beta-1,3-glucanase
Solyc04g078660	BM409727	3,26	37,44	N-hydroxycinnamoyl/ benzoytransferase

Identification of the most differentially expressed genes (DEGs) and related metabolic pathways associated to AM symbiosis formation in tomato.

Complete information regarding the differential gene expression in AM-roots with respect to un-inoculated roots, is given in Supplementary Table S1. As the DEG list in this "wt-I" *vs* "NI" comparison was too large using a cuttof value of fold change >2 or <-2 and $P<0.05$ (3395), we decided to narrow it down by selecting the genes with at least 10-fold change (FC) increase/decrease for further investigation. There were 297 DEGs in total, from which only 16 genes were down-regulated, compared to 281 up-regulated genes (Fig. 4). In addition, the down-regulation was also much weaker than the upregulation in wt-I *vs* NI roots, i.e. the maximum repression observed was by 29.81 fold change, while the most upregulated gene reached up to a 273.80 fold change induction. This is in agreement with previous studies pointing that gene repression is not relevant in AM-related gene expression reprogramming (Rich et al. 2017; Breuillin et al. 2010).

A

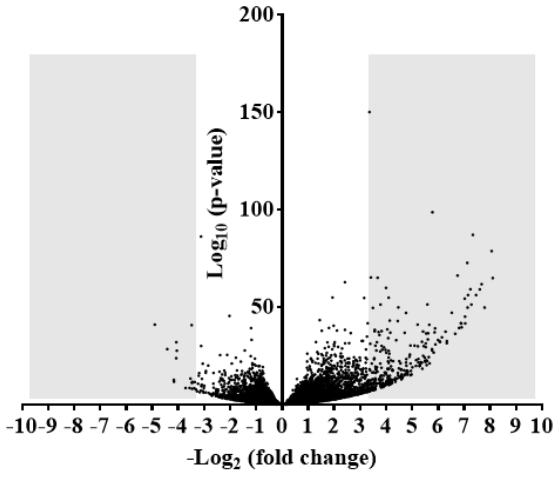

B

Classification	Number
All detected genes	35905
Up-regulated genes (Fold change >10)	281
Down-regulated genes (Fold change <10)	16

Figure 4. Transcriptome analysis of RNA-seq data of AM-inoculated *vs* un-inoculated tomato roots. (A) Volcano plot to inspect DEGs under different condition between wt-I and NI roots. Genes located in the grey shaded area represent the differentially expressed genes (DEGs) under conditions of fold change >10 or <-10, and $P<0.05$, selected for further analyses. (B) Number of all the detected genes and DEGs for the selected conditions.

For Gene Ontology (GO) analyses, the 297 DEGs were submitted to the Panther database. As shown in Figure 5 (upper pie charts), most of the genes were associated

to a catalytic function, to develop metabolic or cellular biological process, and to be components of the cell or organelles. GO enrichment analysis was additionally performed for the 297 DEGs list using MetGenMap. 14582 GO terms were assigned by MetGenMap, and the fraction percentages for biological processes (12727), cellular component (1038) and molecular function (817) were 87.28%, 7.12% and 5.60%, respectively. The nine GO terms more represented for these three fractions revealed similar results to those of PhanterDB, however a more relevant representation of membrane components was shown this time (Fig. 5, bottom graphs).

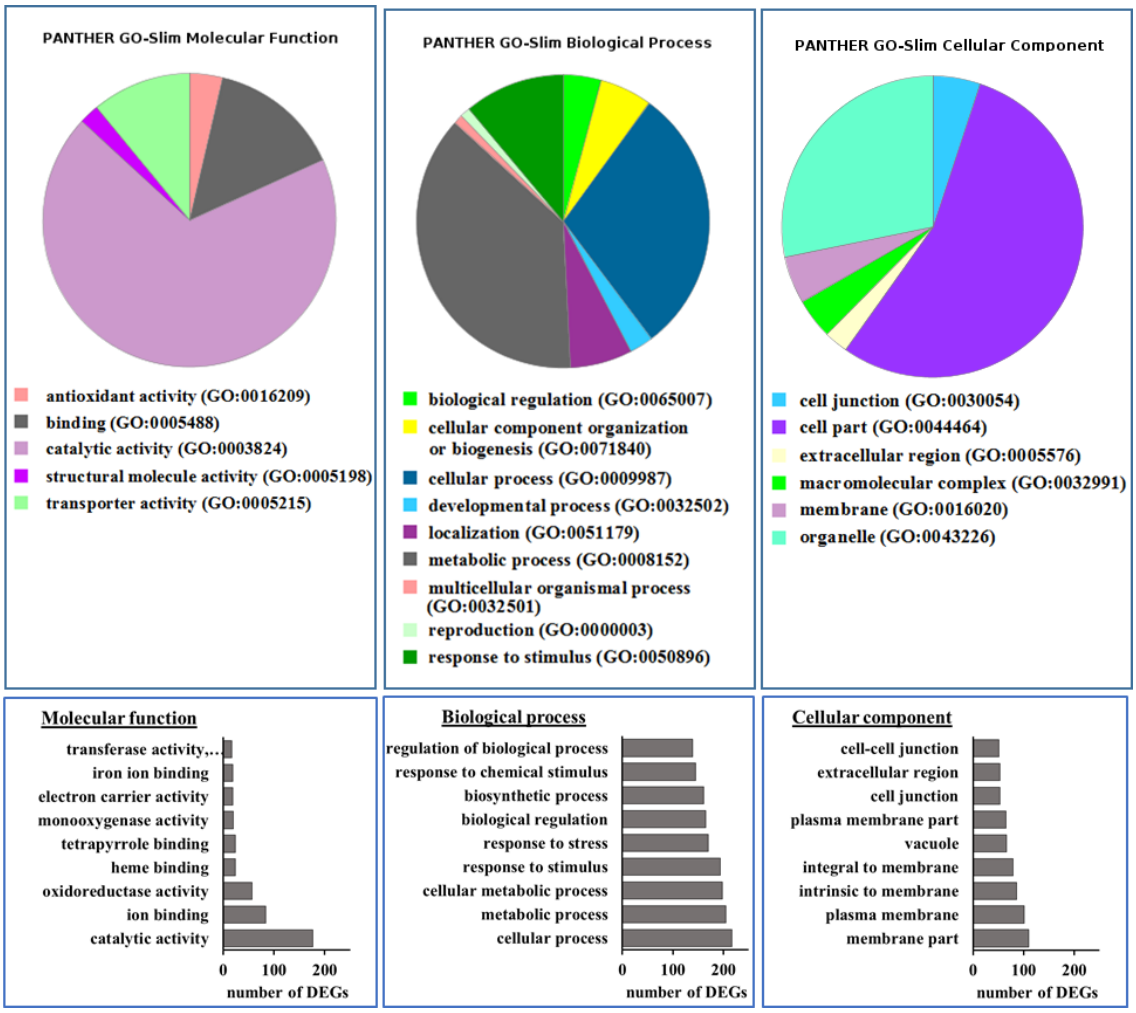

Figure 5. Gene ontology of DEGs in AM-inoculated vs un-inoculated tomato roots. Gene Ontology (GO) categories of DEGs (fold change >10 or <-10, $P<0.05$) in "wt-I" *vs* "NI" conditions, regarding the molecular function, the biological process and the cellular component, are summarized. Analysis was performed using PhanterDb (upper pie charts),

as well as MetGenMap (bottom bar graphs). For the MetGenMap analysis, the 9 most represented GOs for each category are shown.

Pathways associated to highly up-/down- regulated genes upon mycorrhization (wt-I *vs* NI comparison, fold change >10 or <-10, and $P< 0.05$) were analyzed by MetGenMap. Pathways predicted to be differentially regulated in AM plants with $P < 0.1$ are shown in Table 5. A clear upregulation of genes associated to gibberellin, abcisic acid and cytokinin biosynthesis pathways was observed in mycorrhizal plants. In addition, there was a remarkable induction of genes related to biosynthesis of many secondary metabolites including alkaloids (hyosciamine, scopolamine), poliamides, carotenoids (trans-lycopene), glycosides (trans-cinnamoyl-beta-D-glucoside, saponin) and phenolics such as hydroxycinammic acid derivatives (sinapaldehyde, ferulate, sinapate), flavonols (syringetin, quercetin, myricetin), dihydroflavonols (dihydroquerectin, dihydromyriciten), flavones (luteolin) and anthocyanins.

Table 5. MetGeneMap analysis of wt-I *vs* NI tomato plants. Pathways most significantly changed ($P<0.1$) between wt-I and NI treatments, using as input data all DEGs from the RNA-seq with a fold change cutoff value of 10 and $P< 0.05$.

Number	Pathway name	p-value
1	superpathway of GA_{12} biosynthesis	0.001
2	abscisic acid biosynthesis	0.001
3	GA_{12} biosynthesis	0.003
4	coenzyme A biosynthesis	0.015
5	pantothenate and coenzyme A biosynthesis III	0.018
6	syringetin biosynthesis	0.021
7	ferulate and sinapate biosynthesis	0.024
8	hyoscyamine and scopolamine biosynthesis	0.024
9	free phenylpropanoid acid biosynthesis	0.027
10	cinnamate esters biosynthesis	0.036
11	simple coumarins biosynthesis	0.040
12	superpathway of anthocyanin biosynthesis (from delphinidin 3-O-glucoside)	0.047
13	gentiodelphin biosynthesis	0.047
14	betanidin degradation	0.047
15	luteolin biosynthesis	0.051
16	saponin biosynthesis II	0.051
17	flavonol biosynthesis	0.061
18	cytokinins-O-glucoside biosynthesis	0.064
19	acyl-ACP thioesterase pathway	0.068
20	sanguinarine and macarpine biosynthesis	0.068
21	palmitoleate biosynthesis	0.068
22	phenylpropanoid biosynthesis	0.078
23	saponin biosynthesis I	0.085
24	gibberellin biosynthesis III (early C-13 hydroxylation)	0.085
25	superpathway of gibberellin biosynthesis	0.085
26	trans-lycopene biosynthesis	0.100

Network of GRAS Transcription Factors in the AM symbiosis

Transcriptional mechanisms underlying the cellular reprogramming occurring in root cells for the establishment of the AM symbiosis is poorly understood. However, it has been reported that many members of the GRAS transcription factor family, which have an important role in regulation in plants, are involved in the regulation of the AM symbiosis and nodulation, and it has been suggested that a formation of multicomponent GRAS transcription factor complexes are essential for elicitation of nodulation or mycorrhization (Oldroyd 2013).

The GRAS gene family has been previously identified and characterized in tomato (Huang et al. 2015; Niu et al. 2017). In Figure 6 we show a phylogenetic tree comprising the GRAS protein family in tomato, together with the GRAS proteins from *Arabidopsis* (Tian et al. 2004), and members from other species whose involvement during the mycorrhization process have been reported, including DELLAs (Floss et al. 2013; Foo et al. 2013; Yu et al. 2014; Takeda et al. 2015), RAM1 (Gobbato et al. 2012; Rich et al. 2015; Xue et al. 2015), RAD1 (Xue et al. 2015) and MIG1 (Heck et al. 2016).

In the RNA-seq analysis performed here, we found a number of these genes to be significantly induced upon AM inoculation in tomato. From the 53 GRAS tomato genes previously identified by Huang et al. (2015), 18 GRAS genes were found to be significantly induced (fold change >2) in the AM-inoculated roots in the RNA-seq data (Table 6; red star labels from Fig. 6).

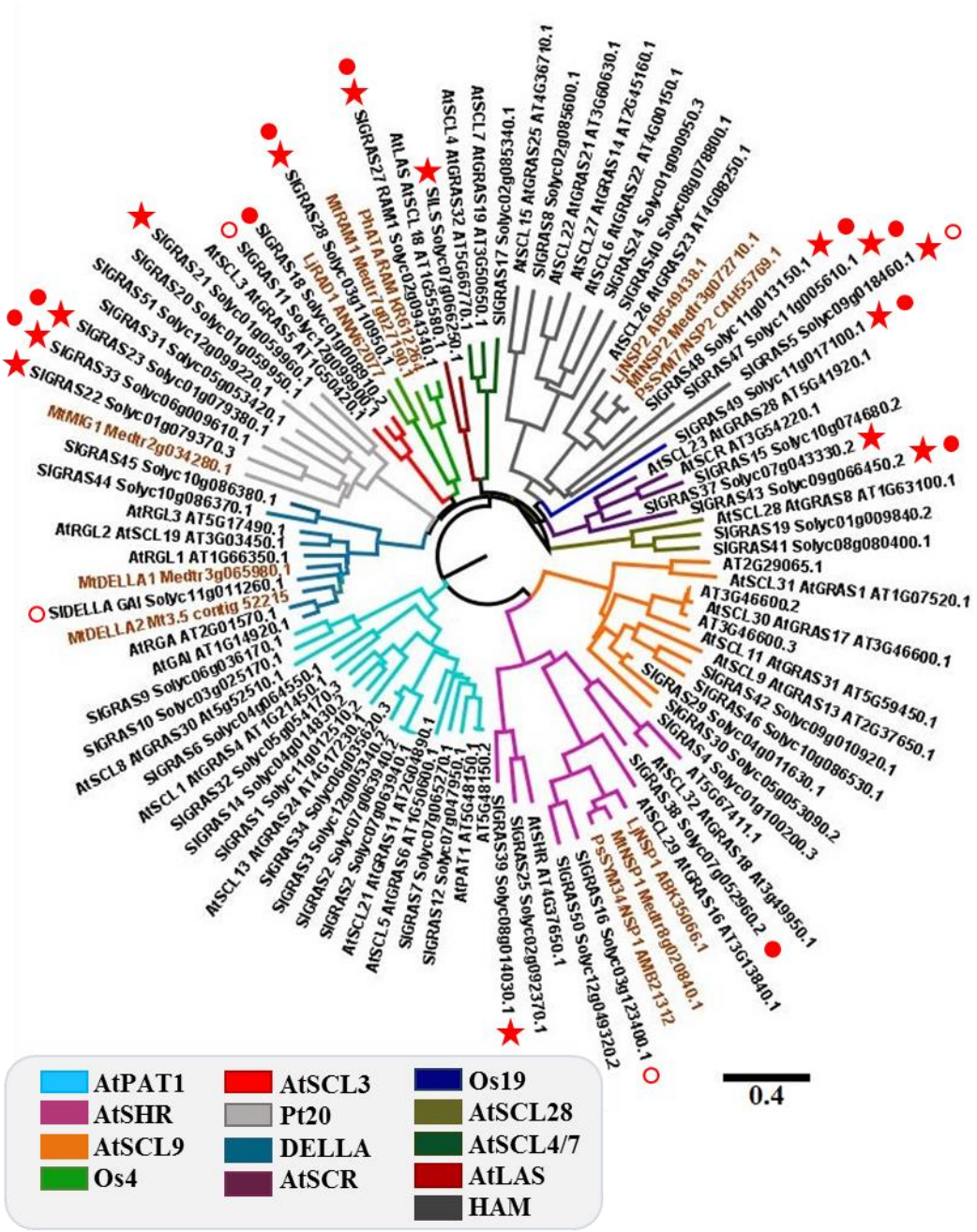

Figure 6. Phylogenetic analysis of the GRAS protein family in *Solanum lycopersicum*. An unrooted phylogenetic tree was generated based on amino acid alignment of GRAS proteins from tomato and *Arabidopsis*, together with proteins previously reported to be involved in the AM symbiosis (brown typed) from *Lotus japonicus* (LjRAD1, LjNSP1 and LjNSP2), *Petunia hybrida* (PhATA/RAM), *Medicago truncatula* (MtDELLA1, MtDELLA2, MtMIG1, MtRAM1, MtNSP1 and MtNSP2) and pea (PsSYM7, PsSYM34). Induced expression upon mycorrhization of the corresponding tomato GRAS protein-coding genes are labeled with a red star (RNA-seq data) or a red spot (qPCR data). Not-AM induced genes based on qPCR results are labeled with a white spot. Common protein names assigned by Tian et al. (2004) and Huang et al. (2015) are indicated. The SolDB accessions (http://solgenomics.net/) for tomato proteins, and the PlantGDB IDs (http://www.plantgdb.org) for *Arabidopsis* and *Medicago* proteins are also shown. GenBank/RefSeq accession number are used for proteins from other species. Colour

branches correspond to each clade from the GRAS family as indicated in the legend. The scale bar represents the number of substitutions per site.

Table 6. Effect of mycorrhization on expression of GRAS gene family. RNA-seq fold change and p-values of GRAS genes upregulated (fold change >2) in the control mycorrhizal plants (wt-I) with respect to the non-inoculated plantas (NI)

GRAS gene		wt-I *vs* NI	
Huang et al., 2015 nomenclature	SolycDB ID	Fold change	p value
SlGRAS36	Solyc06g082530	2.023	1.51E-06
SlGRAS46	Solyc10g086530	2.079	2.38E-04
SlGRAS26	Solyc02g092570	4.905	6.22E-10
SlGRAS38	Solyc07g052960	24.058	1.28E-15
SlGRAS39	Solyc08g014030	2.215	6.55E-03
SlGRAS5	Solyc09g018460	2.039	1.03E-02
SlGRAS47	Solyc11g005610	11.123	1.59E-09
SlGRAS48	Solyc11g013150	2.111	1.99E-04
SlLS	Solyc07g066250	4.383	3.54E-04
SlGRAS37	Solyc07g043330	2.002	2.20E-03
SlGRAS43	Solyc09g066450	49.088	2.15E-37
SlGRAS21	Solyc01g059960	4.006	1.40E-03
SlGRAS22	Solyc01g079370	3.233	2.80E-04
SlGRAS23	Solyc01g079380	2.117	4.54E-02
SlGRAS33	Solyc06g009610	14.588	8.72E-14
SlGRAS27	Solyc02g094340	12.524	6.97E-20
SlGRAS28	Solyc03g110950	35.716	-
SlGRAS49	Solyc11g017100	8.205	-

Based on these results, we decided to screen a set of GRAS genes, focusing in those putative orthologs of GRAS genes known to be involved in mycorrhization. Particularly, the expression of fourteen tomato GRAS genes was assessed through qPCR in a time-course experiment with *S. lycopersicum* plants 32, 42, 52 and 62 days after inoculation with the AM fungus *Rhizophagus irregularis* (Fig. 7). qPCR data confirmed the upregulation of *SlGRAS23*, *SlGRAS27*, *SlGRAS28*, *SlGRAS33*, *SlGRAS43*, *SlGRAS47*, *SlGRAS48* and *SlGRAS49* genes under mycorrhizal conditions; and two other GRAS that were not found to be activated in the RNA-seq, i.e. SlGRAS18 and

SlGRAS38, turned to be induced by the AM fungus inoculation in the time-course experiment (red spot labels from Fig. 6).

The AM-induced genes *SlGRAS21*, *SlGRAS22*, *SlGRAS23* and *SlGRAS33* are putative homologs to *MtMIG1*, a gene actually reported to be induced in arbuscule-containing cells and that encodes for a transcription factor suggested to have a role in cell remodeling during AM fungal accommodation (Heck et al. 2016). *SlGRAS27* is also induced upon mycorrhization, and is the putative homolog of *MtRAM1* and *PhATA/RAM* from *Medicago* and *Petunia*, respectively. *PhATA/RAM* is required for the morphogenesis of arbuscules (Rich et al. 2015), and *MtRAM1* was reported as needed either for hyphopodia formation (Gobbato et al. 2012) or to support arbuscule branching (Park et al. 2015). *SlGRAS28* was observed also to increase its gene expression under mycorrhizal conditions, and is the homolog gene to *LjRAD1* from *Lotus japonicus,* whose mutation trigger an accelerated degeneration and a strongly reduced number of arbuscules (Xue et al. 2015). In the HAM subfamily, we found that *SlGRAS47*, *SlGRAS48* (and *SlGRAS5* in the RNA-seq) are AM-activated genes. *MtNSP2* and the pea gene *PsSYM7* also belong to this clade, and their mutation caused a decrease in AM fungal colonization (Maillet et al. 2011; Shtark et al. 2016). Finally, *SlGRAS38* and *SlGRAS39* transcripts were also increased upon mycorrhization as occurs with other members from the AtSHR subfamily from other species, such as *MtNSP1, OsNSP1, LjNSP and PsSYM34/NSP1.* The mutation or silencing of *NSP1* gives place to an impaired response to Myc-LCOs at the pre-symbiotic stage and a reduced frequency of mycorrhizal colonization in *Medicago* (Delaux et al. 2013; Hohnjec et al. 2015), a delay in AM development in pea (Shtark et al. 2016), and a decreased frequency of *Lotus japonicus* plants colonized by AM fungi (Takeda et al. 2013). In summary, our data suggest that a network of GRAS transcription factors could have a relevant role in mediating the transcriptional program underlying the tomato response to AM colonization in tomato.

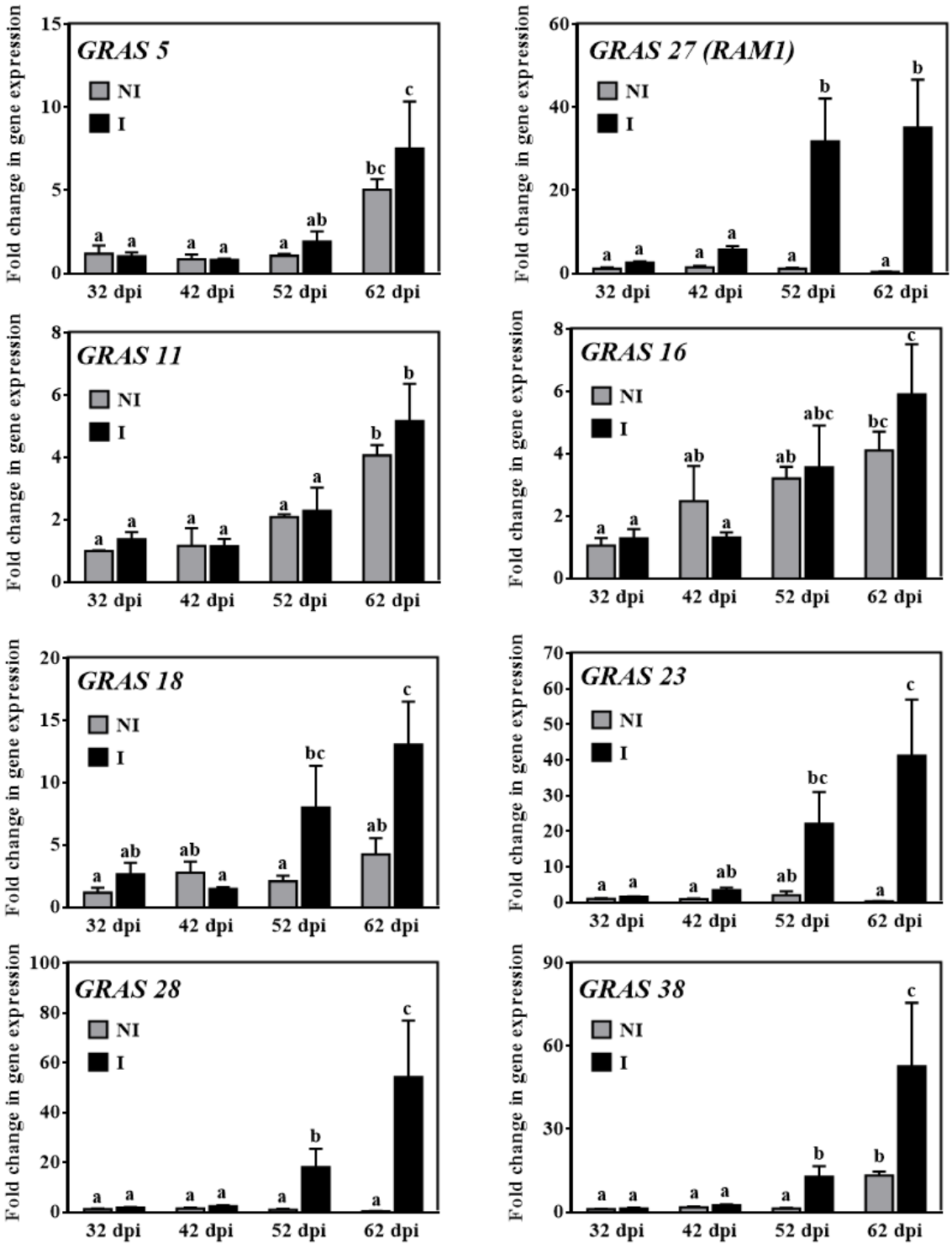
GRAS 5
GRAS 27 (RAM1)
GRAS 11
GRAS 16
GRAS 18
GRAS 23
GRAS 28
GRAS 38
NI
I
Fold change in gene expression
32 dpi
42 dpi
52 dpi
62 dpi

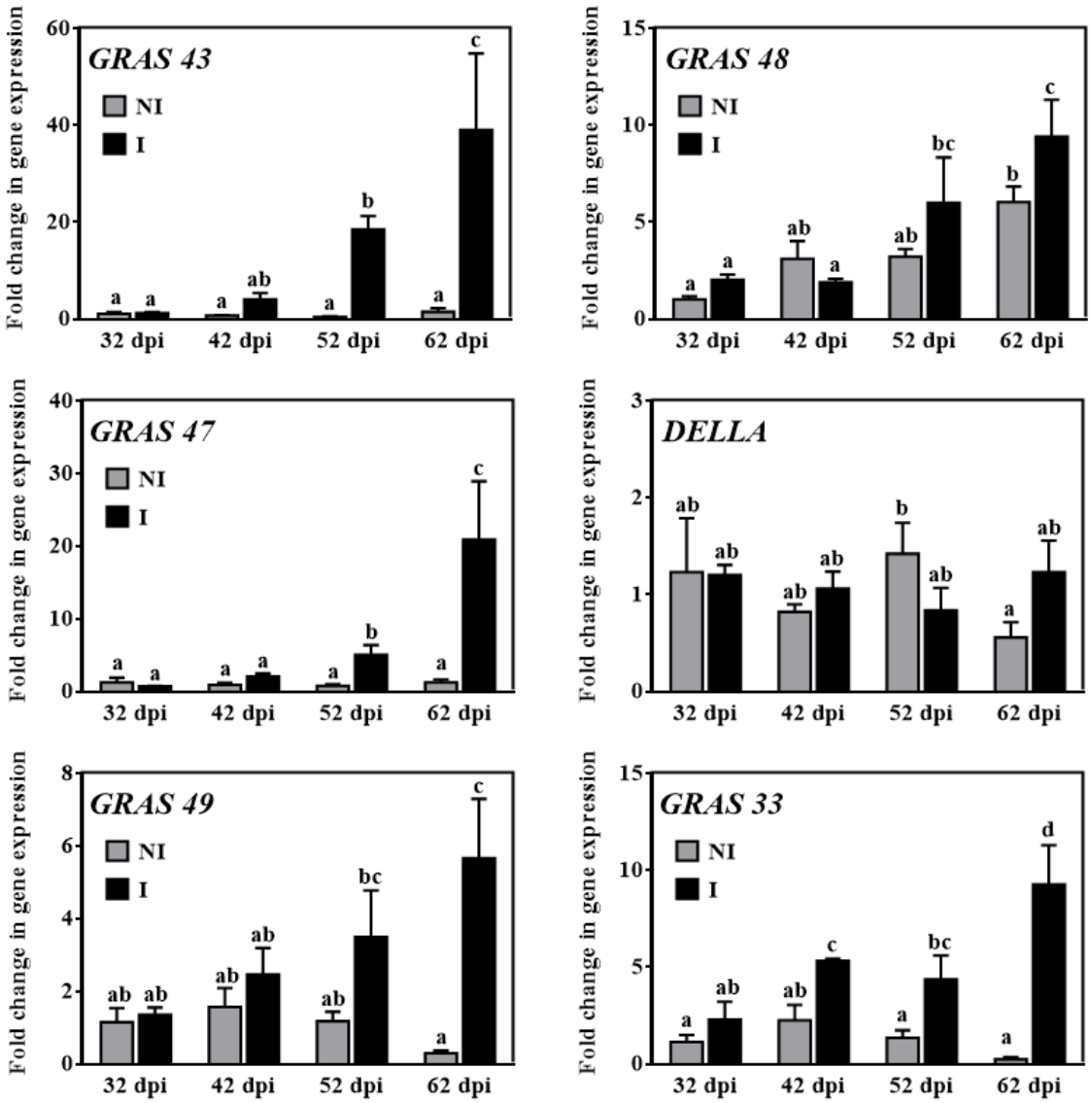

Figure 7. Characterization of expression of GRAS genes during mycorrhization in tomato roots. After 32, 42, 52 and 62 dpi (days post-inoculation) with the AM fungus *R. irregularis*, the expression of several putative *GRAS* genes was analyzed by qPCR. qPCR data represents the relative gene expression in roots of AM inoculated plants (I) with respect to its expression in non-colonized (NI) plants at 32 dpi , in which its expression was designated as 1. Values correspond to mean ± SE (n=3). Bars with a same letter are not significantly different (P>0.05) according to the LSD multiple comparison test.

General transcriptomic changes and associated pathways in AM roots throughout *SlDLK2* silencing

Using MetGenMap software, transcriptome of AM-inoculated control roots (wt-I) was compared to *SlDLK2* RNAi AM roots (i*DLK2*-I), in order to detect alteration of

pathways caused by *SlDLK2* interference during mycorrhization. The complete list of 35905 genes detected, with the corresponding fold change and p-values, was used as input data (Supplementary Table 3). Up-regulation and down-regulation cutoffs were set at 5 and -5, and the p-value cutoff at 0.05. Significantly regulated pathways are shown in Table 7. Silencing of *SlDLK2* in mycorrhizal tomato roots triggered the activation of genes associated to degradation of amino acids and chlorophyll, as well as the pyruvate fermentation to ethanol, all of them processes directed to the production of alternative respiratory substrates to cope energy crisis conditions (Mithran et al. 2014; Araújo et al. 2011), probably due to the glucose starvation condition induced by a higher mycorrhization in the *SlDLK2* RNAi plants. However, the activation of other pathways such as the dopamine degradation and the thiosulfate disproportionation could be involved in the cause, and not the effect, of the higher mycorrhization in *SlDLK2* silenced plants, because dopamine is an alkaloid with strong antioxidant properties and with the ability to alleviate nutrient deficiency (Liang et al. 2017), and thiosulfate shows some toxicity that might affect the fungus (Cipollone et al. 2007). Then, the degradation of antioxidant and/or antifungal metabolites in *SlDLK2* RNAi plants might contribute to facilitate their mycorrhization.

Table 7. MetGeneMap analysis of i*DLK2*-I *vs* wt-I tomato plants (Cutoff value 5). Pathways significantly ($P < 0.1$) changed between i*DLK2*-I *vs* wt-I treatments using as input data all DEGs from the RNA-seq with a fold change cutoff value of 5 and a $P< 0.05$.

Number	Pathway name	p value
1	pyruvate fermentation to ethanol II	0.0095
2	dopamine degradation	0.0132
3	valine degradation II	0.0146
4	leucine degradation III	0.0146
5	thiosulfate disproportionation III (rhodanese)	0.0279
6	cytokinins degradation	0.0416
7	glutamate degradation II	0.0506
8	chlorophyll a degradation	0.0551
9	N-methyl-Δ1-pyrrolinium cation biosynthesis	0.0551
10	phenylethylamine degradation	0.0684
11	free phenylpropanoid acid biosynthesis	0.0684
12	arsenate detoxification II	0.0684
13	threonine degradation III (to methylglyoxal)	0.0728
14	phenylpropanoid biosynthesis, initial reactions	0.0772
15	aspartate degradation II	0.0902
16	anthocyanin biosynthesis (delphinidin 3-O-glucoside)	0.0902
17	leucopelargonidin and leucocyanidin biosynthesis	0.0914
18	leucodelphinidin biosynthesis	0.0914
19	anthocyanin biosynthesis (pelargonidin 3-O-glucoside, cyanidin 3-O-glucoside)	0.0988
20	sucrose biosynthesis	0.1031

Extending the up- and down- regulation cutoffs to 2 and -2, respectively, other modified pathways emerged (Table 8). The hydroxycinnamic acid tyramine amides and suberin pathways were induced, while the scopolamine, phosphatidylcholine, monolignol, and trehalose biosynthetic pathways were repressed. Other differentially regulated pathways were the leucoanthocyanidin, cytokinin, gibberellin and flavonol biosynthetic pathways. The repression and induction of many of these pathways could be responsible of the higher mycorrhization in the *SlDLK2* RNAi composite plants. For example, an increase production of suberin could be related to a more efficient formation of AM hypopodia (Wang et al. 2012), also probably via hydroxycinnamic acids such as feruloyltiramine, a putative component of the aromatic domain of suberin. In addition, phosphatidylcholine is the precursor of glycine betaine, reported to be involved in stress resistance (Sakamoto and Murata 2002), and it has been shown the antifungal properties of scopolamine (Abdel-Motaal et al. 2010). Then, the repression of phosphatidylcholine and scopolamine biosynthesis could produce some defects in the defense against the AM fungal infection, facilitating AM development.

Table 8. MetGeneMap analysis of i*DLK2*-I *vs* wt-I tomato plants (Cutoff value 2). Pathways significantly ($P < 0.1$) changed between i*DLK2*-I *vs* wt-I treatments using as input data all DEGs from the RNA-seq with a fold change cutoff value of 2 and a p-value of 0.05.

Number	Pathway name	p value
1	hydroxycinnamic acid tyramine amides biosynthesis	7.46 E-07
2	suberin biosynthesis	5.80 E-04
3	lysine degradation I	0.0039
4	leucodelphinidin biosynthesis	0.0059
5	leucopelargonidin and leucocyanidin biosynthesis	0.0059
6	cytokinins-O-glucoside biosynthesis	0.0110
7	glutamate degradation IV	0.0170
8	pyruvate fermentation to ethanol II	0.0183
9	ternatin C5 biosynthesis	0.0244
10	gibberellin biosynthesis III (early C-13 hydroxylation)	0.0267
11	superpathway of gibberellin biosynthesis	0.0267
12	phenylethanol biosynthesis	0.0496
13	flavonol biosynthesis	0.0503
14	hyoscyamine and scopolamine biosynthesis	0.0571
15	phosphatidylcholine biosynthesis III	0.0610
16	phosphatidylcholine biosynthesis IV	0.0610
17	valine degradation II	0.0624
18	leucine degradation III	0.0624
19	betanidin degradation	0.0650
20	monolignol glucosides biosynthesis	0.0652
21	linoleate biosynthesis II (animals)	0.0691
22	linoleate biosynthesis I (plants)	0.0691
23	saponin biosynthesis II	0.0698
24	phenylethylamine degradation	0.0714
25	cinnamate esters biosynthesis	0.0792
26	threonine degradation III (to methylglyoxal)	0.0874
27	trehalose biosynthesis V	0.0945
28	4-aminobutyrate degradation I	0.0945
29	glutamate dependent acid resistance	0.0945

In summary, we suggest that genes showing a stronger up- and down- regulation in i*DLK2*-I *vs* wt-I roots are mostly associated to pathways activated as a consequence of the slightly higher mycorrhization or the higher arbuscule abundance in the *SlDLK2* RNAi roots with respect to the control roots, rather than to a direct effect of an *SlDLK2* defective expression. However, enlarging the DEG list and including weaker differentially regulated genes by setting the cutoff gene fold change at 2 and -2, revealed several regulated pathways that could be directly perturbed by defective signaling through *SlDLK2* in the i*DLK2*-I plants. It is possible that *SlDLK2* negatively regulates the mycorrhization process by repressing the production of AM-inductors (e.g. suberin), and promoting the biosynthesis or repressing the degradation of antifungal metabolites (e.g. scopolamine and thiosulfate, respectively) and stress resistance compounds (e.g. glycine betaine and dopamine, respectively).

Specific alterations in plant root transcriptome by *SlDLK2* silencing and mycorrhization.

2790 tomato genes were found to be differentially expressed genes (DEGs) in i*DLK2*-I *vs* wt-I treatments (fold change >2 or <-2, $P<0.05$). In order to better understand the effect of *SlDLK2* silencing during mycorrhization, we classified the 2790 DEG list depending on their up- or down- regulation by *SlDLK2* silencing (i*DLK2*-I *vs* wt-I fold change), and on their corresponding AM-responsiveness (wt-I *vs* NI fold change) (see Fig. 8). 1588 genes were induced in i*DLK2* mycorrhizal roots with respect to the wildtype mycorrhizal roots (i*DLK2*-I *vs* wt-I roots), from which 344 genes were AM-induced in wildtype roots ($_i$*DLK2↑Myc*$^+$ group), 97 genes were AM-repressed in wt roots ($_i$*DLK2↑Myc*$^-$*),* and 1147 genes were not significantly altered by mycorrhization in wt roots ($_i$*DLK2↑Myc*^{ns}). In the other hand, 1202 genes resulted to be significantly repressed by *SlDLK2* silencing in mycorrhizal roots with respect to the wildtype AM roots, from with 284 genes were AM-induced ($_i$*DLK2↓Myc*$^+$), 71 genes were AM-repressed ($_i$*DLK2↓Myc*$^-$) and 847 genes did not respond to mycorrhization ($_i$*DLK2↓Myc*^{ns}). For simplicity these six groups were numbered from 1 to 6, as indicated in Fig. 8.

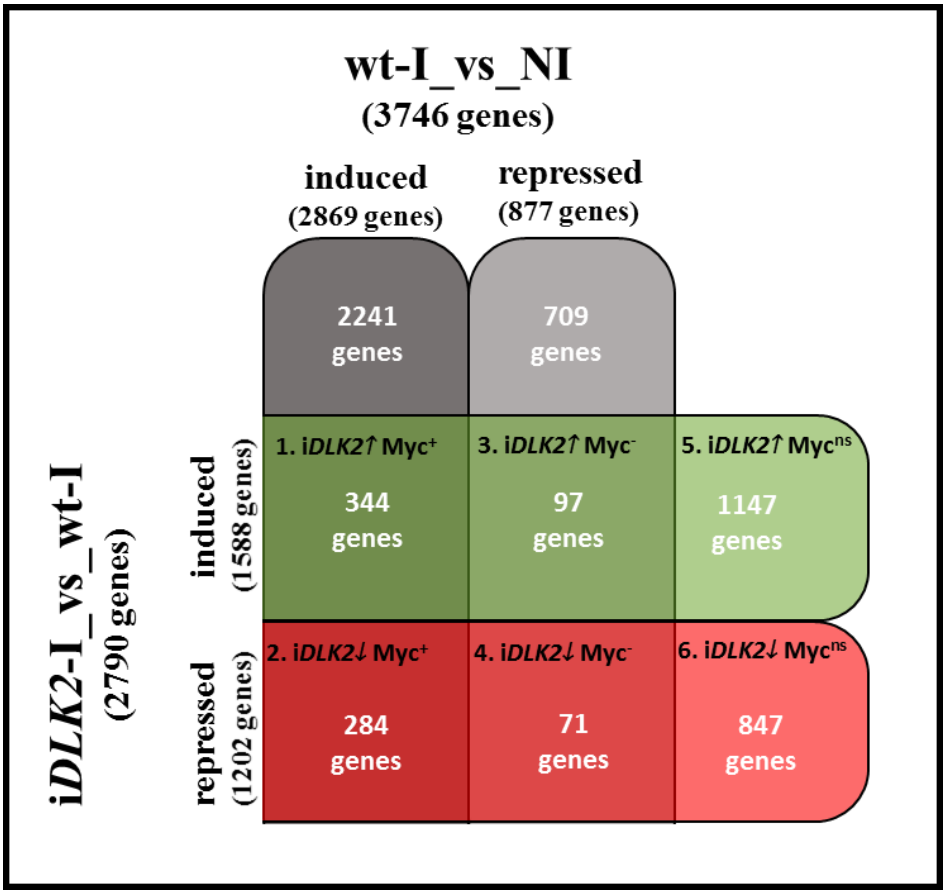

Figure 8. Classification of transcripts detected in the RNA-seq depending on their regulation by AM inoculation and by *SlDLK2* RNAi silencing. From the 35905 genes detected in the RNA-seq, a list of 6536 DEGs was selected upon their significant regulation (fold change >2 or <-2 and $P<0.05$) upon mycorrhization (based on comparison between treatments wt-I *vs* NI), and by *SlDLK2* silencing (comparison of treatments i*DLK2*-I *vs* wt-I). The 6536 DEGs list was classified depending on their up-, down- or not significant-regulation in the two comparisons: "i*DLK2*-I *vs* wt-I" and "wt-I *vs* NI". The six examined groups are numbered as follows: $_{i}DLK2{\uparrow}Myc^{+}$ (group 1), $_{i}DLK2{\downarrow}Myc^{+}$ (group 2), $_{i}DLK2{\uparrow}Myc^{-}$ (group 3), $_{i}DLK2{\downarrow}Myc^{-}$ (group 4), $_{i}DLK2{\uparrow}Myc^{ns}$ (group 5) and $_{i}DLK2{\downarrow}Myc^{ns}$ (group 6).

Using MetGenMap, associated differentially regulated pathways were calculated for Groups 1 to 6. The results are shown in Tables 9 to 14 , respectively. The six groups were examined in order to analyzed the effect of *SlDLK2* silencing. Special attention was focused in the groups where the regulatory effect of *SlDLK2* silencing on genes was opposite to the regulatory effect exerted by mycorrhization, i.e $_{i}DLK2{\downarrow}Myc^{+}$ (Group 2) and $_{i}DLK2{\uparrow}Myc^{-}$ (Group 3), as genes belonging to these groups are

expected to be differentially regulated by *SlDLK2* silencing in AM-roots in a direct way, and not as an indirect effect of the weakly high mycorrhization observed in these mutant composite plants.

GROUP1 (i*DLK2*↑Myc⁺). *SlDLK2* silencing triggers the induction of several genes induced during mycorrhization. One of these genes is Solyc09g008560 (FC 10.35), encoding a putative 2-oxoglutarate and iron dependent oxygenase that might be involved in antioxidant production, particularly in anthocyanin and leucoanthocyanidin (leucodelphinin, leucopelagornidin and leucocyanidin) biosynthesis. Also are highly induced Solyc07g062670 (FC 9.12) and Solyc10g086630 (FC 8.43), two genes described to be related to nodulation. Solyc07g062670 putatively encodes a Clavata3/ESR (CLE) peptide, reported to be induced in rhizobium colonized roots, and demonstrated to be involved in the autoregulation of nodulation, a negative feedback to regulate nodulation (Hastwell et al., 2015), while Solyc10g086630 is homologous to a described legume-specific protein. The pathways more significantly induced were the gibberellin inactivation; fatty acid β-oxidation; the biosynthesis of suberin, hydroxycinnamic acid tyramine amides (a phenylpropanoid), linoleate, sphingolipid, trans-cinnamate (intermediate of the phenylpropanoid pathway), salicylate, monoterpene and chorismate; as well as the degradation of the alkaloid betanidin and dopamine (Table 9).

Table 9. MetGeneMap analysis of Group 1. Pathways significantly (*P*>0.1) changed between i*DLK2*-I and wt-I treatments using genes from the group 1 of the RNA-seq with a fold change cutoff value of 2. Specific genes significantly regulated in each pathway are shown.

Changed pathways: *iDLK2*-I_vs_wt-I			**Changed genes in the pathway**			
Number	**Pathway name**	**p-value**	**Gene (ID SolDB)**	**Fold change (RNA-seq)**	**p-value**	**Common gene name**
1	gibberellin inactivation	0.001	Solyc02g080120	3.826	7.54E-06	Gibberellin 2-beta-dioxygenase 7
			Solyc06g082030	2.507	1.45E-05	Gibberellin 2-beta-dioxygenase 7
			Solyc07g061720	3.833	3.49E-04	Gibberellin 2-oxidase
			Solyc07g061730	2.221	2.35E-02	Gibberellin 2-oxidase
2	suberin biosynthesis	0.002	Solyc06g035960	2.289	1.92E-09	4-coumarate-CoA ligase-like protein
			Solyc00g272810	2.357	1.70E-02	Caffeoyl CoA 3-O-methyltransferase
			Solyc08g006730	3.472	6.05E-05	Caffeoyl-CoA 3-O-methyltransferase
			Solyc12g096840	3.263	4.21E-13	Caffeoyl-CoA O-methyltransferase
			Solyc05g056170	2.728	7.33E-06	Caffeoyl-CoA O-methyltransferase
			Solyc10g011920	2.497	1.89E-03	Caffeoyl-CoA O-methyltransferase
3	fatty acid β-oxidation II (core pathway)	0.003	Solyc09g061840	2.027	1.47E-06	3-ketoacyl CoA thiolase 1
			Solyc06g035960	2.289	1.92E-09	3-ketoacyl CoA thiolase 2

			Solyc04g054890	2.888	1.07E-13	4-coumarate CoA ligase-like
			Solyc03g032210	3.43	2.40E-04	4-coumarate-CoA ligase-like protein
			Solyc01g109180	2.214	1.15E-03	Acyl-CoA dehydrogenase
4	hydroxycinnamic acid tyramine amides biosynthesis	0.003	Solyc00g272810	2.357	1.70E-02	N-acetyltransferase
			Solyc08g006730	3.472	6.05E-05	N-acetyltransferase
			Solyc12g096840	3.263	4.21E-13	N-acetyltransferase
5	betanidin degradation	0.011	Solyc01g105070	2.101	2.81E-04	Peroxidase
			Solyc05g050890	2.244	2.84E-02	Peroxidase
			Solyc05g050870	2.34	1.90E-02	Peroxidase
			Solyc01g015080	2.269	9.13E-03	Peroxidase
			Solyc02g090470	2.351	1.56E-04	Peroxidase
			Solyc11g007220	2.056	2.80E-02	Peroxidase
6	1,3,5-trimethoxybenzene biosynthesis	0.017	Solyc10g008120	2.09	2.36E-04	O-methyltransferase 3
7	linoleate biosynthesis I (plants)	0.018	Solyc06g035960	2.289	1.92E-09	4-coumarate-CoA ligase-like protein
			Solyc01g109180	2.214	1.15E-03	Acyl-CoA synthetase/AMP-acid ligase II
			Solyc04g040130	2.053	4.74E-03	Acyl-CoA synthetase/AMP-acid ligase II
8	fatty acid β-oxidation I	0.019	Solyc09g061840	2.027	1.47E-06	3-ketoacyl CoA thiolase 1
			Solyc06g035960	2.289	1.92E-09	4-coumarate-CoA ligase-like protein
			Solyc03g032210	3.43	2.40E-04	Acyl-CoA synthetase/AMP-acid ligase II
			Solyc01g109180	2.214	1.15E-03	Long-chain-fatty-acid-CoA ligase
9	dopamine degradation	0.024	Solyc12g006370	2.512	6.22E-09	Amine oxidase family protein
			Solyc07g061720	3.833	3.49E-04	Gibberellin 2-oxidase
			Solyc07g061730	2.221	2.35E-02	Gibberellin 2-oxidase
10	sphingolipid biosynthesis (plants)	0.025	Solyc06g072320	2.701	5.60E-03	8-amino-7-oxononanoate synthase
			Solyc08g066020	2.023	3.05E-03	Serine C-palmitoyltransferase like protein
11 and 12	phenylpropanoid biosynthesis, initial reactions and salicylate biosynthesis	0.031	Solyc05g056170	2.728	7.33E-06	Phenylalanine ammonia-lyase
			Solyc10g011920	2.497	1.89E-03	Phenylalanine ammonia-lyase
13	monoterpene biosynthesis	0.039	Solyc01g105920	2.293	3.83E-04	(E)-beta-ocimene synthase
			Solyc01g105940	2.405	1.36E-03	Limonene synthase
14	chorismate biosynthesis	0.043	Solyc01g067750	2.935	1.55E-10	Shikimate dehydrogenase
			Solyc10g038080	2.339	2.25E-07	Shikimate dehydrogenase
15	mevalonate pathway	0.047	Solyc09g061840	2.027	1.47E-06	3-ketoacyl CoA thiolase 1
			Solyc08g007790	2.098	8.05E-05	Hydroxymethylglutaryl-CoA synthase
16	fatty acid activation	0.059	Solyc06g035960	2.289	1.92E-09	4-coumarate-CoA ligase-like protein
			Solyc01g109180	2.214	1.15E-03	Long-chain-fatty-acid-CoA ligase
17	phytate degradation	0.065	Solyc09g009610	2.319	2.59E-06	Purple acid phosphatase
18	polyhydroxybutyrate biosynthesis	0.080	Solyc10g008120	2.09	2.36E-04	O-methyltransferase 3
19	volatile cinnamoic ester biosynthesis	0.080	Solyc09g061840	2.027	1.47E-06	3-ketoacyl CoA thiolase 1
20	phenylethanol biosynthesis	0.096	Solyc12g006370	2.512	6.22E-09	Amine oxidase family protein
			Solyc08g006740	2.58	6.74E-05	Decarboxylase family protein
			Solyc08g006750	2.257	1.35E-03	Decarboxylase family protein
21	divinyl ether biosynthesis II (13-LOX), and and 13-LOX and 13-HPL pathway	0.098	Solyc08g029000	2.422	1.86E-02	Lipoxygenase
			Solyc02g087070	3.228	6.68E-04	Peroxidase family protein

GROUP 2 (ᵢ*DLK2*↓Myc⁺). Some AM-induced genes are repressed by *SlDLK2* silencing. Several of them are involved in biosynthesis pathways including the cytokinin, monolignol glucoside, coniferin, cellulose, phosphatidilcoline, coline, saponin, scopolamine, cinnamate, putrescine, nicotianamine, geraniol and geranial biosynthetic pathways, as well as the betanidin degradation and the ascorbate-gluthation pathways (Table 10).

Table 10. MetGeneMap analysis of Group 2. Pathways significantly (*P*>0.1) changed between i*DLK2*-I and wt-I treatments using genes from the group 2 of the RNA-seq with a fold change cutoff value of 2. Specific genes significantly regulated in each pathway are shown.

Changed pathways: *iDLK2*-I_vs_wt-I			**Changed genes in the pathway**			
Number	**Pathway name**	**p-value**	**Gene (ID SolDB)**	**Fold change (RNA-seq)**	**p-value**	**Common gene name**
1	cytokinins-O-glucoside biosynthesis	0.000	Solyc05g053400	-4.784	1.99E-08	Glucosyltransferase
			Solyc00g006560	-2.449	1.82E-02	Glucosyltransferase-12
			Solyc10g079320	-3.361	2.76E-07	Glucosyltransferase-5
			Solyc11g006100	-2.374	2.28E-02	UDP-glucosyltransferase
			Solyc07g043490	-4.22	6.24E-25	UDP-glucosyltransferase family 1 protein
			Solyc04g016200	-3.58	2.92E-09	UDP-glucosyltransferase HvUGT5876
			Solyc01g105350	-2.336	1.90E-02	UDP-glucuronosyltransferase
			Solyc04g074340	-2.34	6.56E-03	UDP-glucuronosyltransferase
			Solyc12g009930	-2.138	1.26E-19	UDP-glucuronosyltransferase 1-6
2	monolignol glucosides biosynthesis	0.000	Solyc05g053400	-4.784	1.99E-08	Glucosyltransferase
			Solyc05g053120	-3.349	1.20E-06	Glucosyltransferase
			Solyc07g043480	-2.892	2.59E-12	UDP-glucose glucosyltransferase
3	hyoscyamine and scopolamine biosynthesis	0.002	Solyc11g010400	-2.582	1.06E-05	1-aminocyclopropane-1-carboxylate oxidase
			Solyc02g070080	-2.606	9.67E-03	1-aminocyclopropane-1-carboxylate oxidase 1
			Solyc11g072200	-2.64	6.09E-03	1-aminocyclopropane-1-carboxylate oxidase 3
4	phosphatidylcholine biosynthesis III	0.002	Solyc12g040790	-3.665	5.18E-26	Menaquinone biosynthesis methyltransferase ubiE
			Solyc06g068950	-2.497	2.25E-10	Phosphoethanolamine N-methyltransferase
5	phosphatidylcholine biosynthesis IV	0.002	Solyc12g040790	-3.665	5.18E-26	Menaquinone biosynthesis methyltransferase ubiE
			Solyc06g068950	-2.497	2.25E-10	Phosphoethanolamine N-methyltransferase
6	coniferin metabolism	0.002	Solyc05g053400	-4.784	1.99E-08	Glucosyltransferase
			Solyc05g053120	-3.349	1.20E-06	Glucosyltransferase
			Solyc07g043480	-2.892	2.59E-12	UDP-glucose glucosyltransferase
7	choline biosynthesis I	0.005	Solyc12g040790	-3.665	5.18E-26	Menaquinone biosynthesis methyltransferase ubiE
			Solyc06g068950	-2.497	2.25E-10	Phosphoethanolamine N-methyltransferase
8	saponin biosynthesis II	0.006	Solyc10g079320	-3.361	2.76E-07	Glucosyltransferase-5
			Solyc01g105350	-2.336	1.90E-02	UDP-glucuronosyltransferase
			Solyc04g074340	-2.34	6.56E-03	UDP-glucuronosyltransferase
9	glucosinolate biosynthesis from homomethionine	0.009	Solyc11g072130	-2.406	2.15E-03	1-AMINOCYCLOPROPANE-1-CARBOXYLATE OXIDASE-like protein
			Solyc01g090610	-2.266	2.29E-02	2-oxoglutarate-dependent dioxygenase
			Solyc06g066830	-2.233	1.00E-05	2-oxoglutarate-dependent dioxygenase
			Solyc03g031940	-2.717	5.25E-04	Acyl-CoA synthetase/AMP-acid ligase II
10	phosphatidylcholine biosynthesis II	0.011	Solyc12g040790	-3.665	5.18E-26	Menaquinone biosynthesis methyltransferase ubiE
			Solyc06g068950	-2.497	2.25E-10	Phosphoethanolamine N-methyltransferase
11 and 12	leucopelargonidin and leucocyanidin biosynthesis, leucodelphinidin biosynthesis	0.014	Solyc01g108860	-2.626	9.31E-05	1-aminocyclopropane-1-carboxylate oxidase
			Solyc11g010400	-2.582	1.06E-05	1-aminocyclopropane-1-carboxylate oxidase
			Solyc02g070080	-2.606	9.67E-03	1-aminocyclopropane-1-carboxylate oxidase 1
			Solyc11g072200	-2.64	6.09E-03	1-aminocyclopropane-1-carboxylate oxidase 3
			Solyc11g072130	-2.406	2.15E-03	1-AMINOCYCLOPROPANE-1-CARBOXYLATE OXIDASE-like protein
			Solyc10g018140	-2.772	1.32E-04	Dihydroflavonol 4-reductase
13	saponin biosynthesis I	0.014	Solyc10g079320	-3.361	2.76E-07	Glucosyltransferase-5
			Solyc01g105350	-2.336	1.90E-02	UDP-glucuronosyltransferase
			Solyc04g074340	-2.34	6.56E-03	UDP-glucuronosyltransferase
14	nicotianamine biosynthesis	0.018	Solyc01g100490	-2.535	4.12E-05	Nicotianamine synthase
15	superpathway of phosphatidylcholine biosynthesis	0.023	Solyc12g040790	-3.665	5.18E-26	Menaquinone biosynthesis methyltransferase ubiE
			Solyc06g068950	-2.497	2.25E-10	Phosphoethanolamine N-methyltransferase
16	cinnamate esters biosynthesis	0.040	Solyc07g043480	-2.892	2.59E-12	UDP-glucose glucosyltransferase
			Solyc11g006100	-2.374	2.28E-02	UDP-glucosyltransferase
			Solyc07g043500	-3.547	2.45E-18	UDP-glucosyltransferase
17	cellulose biosynthesis	0.045	Solyc03g070390	-2.391	1.03E-03	Alpha-1 4-glucan-protein synthase
			Solyc02g065740	-2.006	2.07E-03	Alpha-1 4-glucan-protein synthase
			Solyc10g079860	-2.797	6.57E-07	Beta-1 3-glucanase
			Solyc09g010210	-2.299	6.11E-05	Endoglucanase 1
18	geraniol and geranial biosynthesis	0.054	Solyc11g010990	-2.333	4.39E-04	Alcohol dehydrogenase
19	putrescine biosynthesis III	0.054	Solyc03g098300	-2.828	2.02E-10	Ornithine decarboxylase

20	betanidin degradation	0.056	Solyc05g046010	-3.42	1.43E-15	Peroxidase
			Solyc01g006290	-2.107	4.78E-02	Peroxidase
			Solyc01g006300	-2.219	7.40E-03	Peroxidase
			Solyc01g108320	-2.825	4.82E-05	Peroxidase
			Solyc03g080150	-2.538	4.19E-09	Peroxidase 1
21	ascorbate glutathione cycle	0.068	Solyc09g009830	-2.065	2.27E-03	Carbonic anhydrase
			Solyc12g094470	-2.296	3.78E-03	Laccase-2
			Solyc02g080670	-2.599	6.08E-08	Laccase-22
22	superpathway of polyamine biosynthesis II	0.081	Solyc03g098300	-2.828	2.02E-10	Ornithine decarboxylase
			Solyc06g053520	-2.244	3.01E-02	Spermidine synthase
23	4-aminobutyrate degradation I	0.088	Solyc12g006470	-2.124	5.67E-07	Aminotransferase-like protein
24	menaquinone-8 biosynthesis	0.088	Solyc12g040790	-3.665	5.18E-26	Menaquinone biosynthesis methyltransferase ubiE
25 and 26	wound-induced proteolysis I and seed germination protein turnover	0.088	Solyc12g010020	-2.711	4.03E-03	Leucyl aminopeptidase
27	GA12 biosynthesis	0.088	Solyc12g006460	-2.374	4.98E-12	Cytochrome P450
28 and 29	gibberellin biosynthesis III (early C-13 hydroxylation) and superpathway of gibberellin biosynthesis	0.092	Solyc06g066830	-2.233	1.00E-05	2-oxoglutarate-dependent dioxygenase
			Solyc12g042980	-2.691	2.88E-03	2-oxoglutarate-dependent dioxygenase
30	molybdenum cofactor (sulfide) biosynthesis	0.105	Solyc08g080180	-2.86	3.87E-05	Molybdenum cofactor sulfurase

GROUP 3 (i*DLK2*↑Myc$^-$). Genes induced by *SlDLK2* silencing in mycorrhizal roots, but repressed in wt upon fungal inoculation were predicted by MetGenMap to be associated to pathways related to carbohydrate metabolism, such as the pentose phosphate pathway (6-phosphogluconolactonase Solyc05g012110), the mannitol degradation (alcohol dehydrogenase Solyc11g011340), the sucrose biosynthesis (sucrose phosphate synthase Solyc09g092130), the Calvin cycle and the glycolysis-gluconeogenesis pathway (fructose-1,6-bisphosphatase Solyc04g071340). In addition genes belonging to Group 3 showing the highest fold change expression in i*DLK2*-I *vs* wt-I encode a putative P-loop containing nucleoside triphosphate hydrolase (Solyc01g049820, FC 11.27), a putative glutamate-1-semialdehyde 2,1-aminomutase 2 (Solyc07g054810, FC 6.84), a glucan endo-1,3-beta-glucosidase 8 (Solyc01g066200, FC 6.68) and a WAT1-related protein (Solyc01g104750, FC 6.58).

Glutamate-1-semialdehyde 2,1-aminomutases are the enzymes required for rate-limiting step in the synthesis for the precursor of tetrapirroles (Tanaka and Tanaka 2007), including chlorophylls, crucial for photosynthesis. Glucan endo-1,3-beta-glucosidases are enzymes known to be involved in defense by disrupting the cell wall polysaccharides of fungal pathogens (Datta and Muthukrishnan 1999). WAT1 is a tonoplast-localized transporter that exports auxin from the vacuole to the cytoplasm required for auxin homoeostasis (Ranocha et al. 2013).

It is worth mentioning that also several genes encoding proteins related with stress defense were induced by *SlDLK2* silencing in Group 3, such as genes encoding a disease resistance protein (Solyc03g123770, FC 6.28), a BAG family molecular chaperone regulator (Solyc06g072430, FC 5.11), a SAUR-like auxin-responsive protein family (Solyc01g110847, FC 5.08), a chaperone protein DNAj (Solyc07g065970, FC 4.74), a wound-responsive family protein (Solyc07g054790, FC 4.60), a class 2 small heat shock protein Le-HSP17.6 (Solyc03g007890, 4.37), a dehydration responsive element binding protein 1 (Solyc06g050520 FC 4.29), an ethylene-responsive transcription factor (Solyc11g045690, FC 4.26) and a heat shock protein (Solyc03g082420, FC 3.63). The induction of these stress defense mechanisms typically repressed in AM roots may indicate the requirement of extra defense mechanisms to fight against the AM fungus in the *SlDLK2* RNAi plants (Table 11).

Table 11. MetGeneMap analysis of Group 3. Pathways significantly (*P*>0.1) changed between i*DLK2*-I and wt-I treatments using genes from the group 3 of the RNA-seq with a fold change cutoff value of 2. Specific genes significantly regulated in each pathway are shown.

Changed pathways: : *iDLK2*-I_vs_wt-I			**Changed genes in the pathway**			
Number	**Pathway name**	**p value**	**Gene (ID SolDB)**	**Fold change (RNA-seq)**	**p-value**	**Common gene name**
1	mannitol degradation II	0.015	Solyc11g011340	3.056	1.09E-13	Alcohol dehydrogenase
2	pentose phosphate pathway (oxidative branch)	0.030	Solyc05g012110	2.293	1.83E-07	6-phosphogluconolactonase
3	sucrose biosynthesis	0.038	Solyc09g092130	5.48	1.96E-10	Sucrose phosphate synthase
4	pentose phosphate pathway	0.050	Solyc05g012110	2.293	1.83E-07	6-phosphogluconolactonase
5	formaldehyde assimilation III (dihydroxyacetone cycle)	0.086	Solyc04g071340	4.249	7.28E-11	Fructose-1 6-bisphosphatase class 1
6	Calvin-Benson-Bassham cycle	0.090	Solyc04g071340	4.249	7.28E-11	Fructose-1 6-bisphosphatase class 1

GROUP 4 (ᵢ*DLK2*↓Myc⁻). This group includes AM-repressed genes that are even more repressed under *SlDLK2* silencing. Among the genes and associated pathways belonging to this group we found a phytoene desaturase (Solyc02g081330) involved in trans-lycopene biosynthesis, a putative nucleoredoxin (Solyc04g081900) participating in the thioredoxin pathway, the photosystem II polypeptide (Solyc12g017250) of photosynthesis light reactions, a phosphoenolpyruvate carboxylase (Solyc07g062530) involved in oxaloacetate biosynthesis (associated to the C4 photosynthetic carbon assimilation cycle, the

gluconeogenesis and the TCA cycle), a Stearoyl-CoA 9-desaturase (Solyc03g116730) for oleate biosynthesis, CER1 (Solyc03g065250) implicated in cuticular wax biosynthesis and a putative aldose 1-epimerase family protein (Solyc10g011760) which encodes the enzyme responsible of the interconversion between alpha-D-glucose-6-P and beta-D-glucose-6-P, a step important in the biosynthesis pathways of GDP-glucose, sucrose and starch biosynthesis, as well as in degradation of trehalose and starch (Table 12).

Table 12. MetGeneMap analysis of Group 4. Pathways significantly (*P*>0.1) changed between i*DLK2*-I and wt-I treatments using genes from the group 4 of the RNA-seq with a fold change cutoff value of 2. Specific genes significantly regulated in each pathway are shown.

Changed pathways: *iDLK2*-I_vs_wt-I			**Changed genes in the pathway**			
Number	**Pathway name**	**p value**	**Gene (ID SolDB)**	**Fold change (RNA-seq)**	**p-value**	**Common gene name**
1	trans-lycopene biosynthesis	0.015	Solyc02g081330	-2.481	1.25E-02	Phytoene synthase 2
2	thioredoxin pathway	0.017	Solyc04g081900	-2.067	3.86E-02	Nucleoredoxin 1
3	C4 photosynthetic carbon assimilation cycle	0.034	Solyc07g062530	-3.598	1.22E-04	Phosphoenolpyruvate carboxylase 2
4	photosynthesis light reactions	0.037	Solyc12g017250	-2.316	1.65E-02	photosystem II polypeptide
5	GDP-glucose biosynthesis	0.042	Solyc10g011760	-2.309	2.91E-03	Aldose 1-epimerase family protein
7	trehalose degradation V	0.054				
8	sucrose biosynthesis	0.056				
10	starch biosynthesis	0.095				
6	oleate biosynthesis II (animals)	0.051	Solyc03g116730	-2.026	4.00E-04	Stearoyl-CoA 9-desaturase
9	cuticular wax biosynthesis	0.061	Solyc03g065250	-2.068	1.90E-02	CER1

GROUP 5 (i*DLK2*↑Myc^{ns}). In *SlDLK2* silencing plants it is remarkable the activation of genes putatively related with amino acid degradation. Particularly, the following related genes are activated: an amine oxidase Solyc03g03188 probably involved in tryptophan and threonine degradation, and aspartate aminotransferase Solyc10g075170 associated to aspartate and glutamate degradation, and finally, seven enzymes putatively involved in leucine and valine degradation, which include three pyruvate descarboxylases (Solyc10g076510, Solyc02g077240, Solyc09g005110) and four alcohol deshydrogenases (Solyc08g005120, Solyc06g059740, Solyc04g064710, Solyc08g083280). The last seven enzymes are also candidates playing a role in the fermentation of pyruvate to ethanol.

Other genes with a high induction in Group 5 are a Chlorophyllase (Solyc09g082600, FC 16.16) putatively involved in chlrophyll *a* degradation , an expansin-like protein

(Solyc08g077330, FC 16.15), a gibberellin 2-oxidase (Solyc07g056670, FC 14.58) predicted to participate in gibberellin inactivation, a dehydration responsive element-binding factor protein (Solyc06g033850, FC 12.57), a kunitz trypsin inhibitor (Solyc06g072210, FC 12.42) involved in defense strategies (García-Olmedo et al. 1998; Ussuf et al. 2001), a 1,4-beta-D-glucanase (Solyc11g027840, FC 11.22), a putative nodulation-related protein early nodulin-93 (Solyc12g006560, FC 10.28) and a glutaredoxin (Solyc09g074600, FC 9.31), proteins that participate in ROS scavenging and key players in cellular redox homoeostasis (Rouhier et al. 2004) (Table 13).

Table 13. MetGeneMap analysis of Group 5. Pathways significantly (*P*>0.1) changed between i*DLK2*-I and wt-I treatments using genes from the group 5 of the RNA-seq with a fold change cutoff value of 5. Specific genes significantly regulated in each pathway are shown.

Changed pathways: *iDLK2*-I_vs_wt-I			**Changed genes in the pathway**			
Number	**Pathway name**	**p value**	**Gene (ID SolDB)**	**Fold change (RNA-seq)**	**p-value**	**Common gene name**
1	pyruvate fermentation to ethanol II	0.006	Solyc08g083280	2.294	2.71E-04	Alcohol dehydrogenase 2
			Solyc06g059740	3.521	2.94E-04	Alcohol dehydrogenase 2
			Solyc04g064710	2.451	1.53E-02	Alcohol dehydrogenase 2
			Solyc08g005120	4.295	7.05E-08	Cinnamoyl-CoA reductase-like protein
			Solyc10g076510	5.65	3.86E-10	Pyruvate decarboxylase
			Solyc02g077240	5.005	7.94E-08	Pyruvate decarboxylase
			Solyc09g005110	3.017	9.79E-09	Pyruvate decarboxylase 1
2	dopamine degradation	0.009	Solyc03g031880	5.57	1.17E-09	Amine oxidase family protein
			Solyc07g056670	14.586	5.98E-23	Gibberellin 2-oxidase 2
3	valine degradation II	0.010	Solyc08g083280	2.294	2.71E-04	Alcohol dehydrogenase 2
			Solyc06g059740	3.521	2.94E-04	Alcohol dehydrogenase 2
			Solyc04g064710	2.451	1.53E-02	Alcohol dehydrogenase 2
			Solyc08g005120	4.295	7.05E-08	Cinnamoyl-CoA reductase-like protein
			Solyc10g076510	5.65	3.86E-10	Pyruvate decarboxylase
			Solyc02g077240	5.005	7.94E-08	Pyruvate decarboxylase
			Solyc09g005110	3.017	9.79E-09	Pyruvate decarboxylase 1
4	leucine degradation III	0.010	Solyc08g083280	2.294	2.71E-04	Alcohol dehydrogenase 2
			Solyc06g059740	3.521	2.94E-04	Alcohol dehydrogenase 2
			Solyc04g064710	2.451	1.53E-02	Alcohol dehydrogenase 2
			Solyc08g005120	4.295	7.05E-08	Cinnamoyl-CoA reductase-like protein
			Solyc10g076510	5.65	3.86E-10	Pyruvate decarboxylase
			Solyc02g077240	5.005	7.94E-08	Pyruvate decarboxylase
			Solyc09g005110	3.017	9.79E-09	Pyruvate decarboxylase 1
5	thiosulfate disproportionation III (rhodanese)	0.023	Solyc02g083730	6.044	3.32E-30	Thiosulfate sulfurtransferase rhodanese domain protein
			Solyc02g083280	4.297	1.05E-10	Thiosulfate sulfurtransferase/rhodanese-like domain-containing protein 1
6	cytokinins degradation	0.034	Solyc04g016430	5.531	2.01E-10	Cytokinin oxidase/dehydrogenase 1
7	glutamate degradation II	0.042	Solyc10g075170	8.762	1.98E-23	Aspartate aminotransferase
8	chlorophyll a degradation	0.046	Solyc09g082600	16.156	3.78E-17	Chlorophyllase 2
9	N-methyl-Δ1-pyrrolinium cation biosynthesis	0.046	Solyc03g031880	5.57	1.17E-09	Amine oxidase family protein
10	free phenylpropanoid acid biosynthesis	0.057	Solyc00g247300	5.225	1.12E-32	Cytochrome P450
11	arsenate detoxification II	0.057	Solyc02g077580	2.099	3.79E-02	Glutaredoxin
			Solyc06g008750	5.762	3.00E-06	Glutaredoxin
12	phenylethylamine degradation	0.057	Solyc03g031880	5.57	1.17E-09	Amine oxidase family protein
13	threonine degradation III (to methylglyoxal)	0.060	Solyc03g031880	5.57	1.17E-09	Amine oxidase family protein

14	phenylpropanoid biosynthesis, initial reactions	0.064	Solyc05g047530	6.63	1.75E-07	Cytochrome P450
15	aspartate degradation II	0.075	Solyc10g075170	8.762	1.98E-23	Aspartate aminotransferase
16	anthocyanin biosynthesis (delphinidin 3-O-glucoside)	0.075	Solyc10g085190 Solyc10g076670 Solyc10g076660 Solyc10g085190 Solyc10g076670 Solyc10g076660	7.146 2.701 2.097 7.146 2.701 2.097	1.82E-10 5.53E-03 8.54E-04 1.82E-10 5.53E-03 8.54E-04	Anthocyanidin synthase Anthocyanidin synthase Anthocyanidin synthase Anthocyanidin synthase Anthocyanidin synthase Anthocyanidin synthase
17	gibberellin inactivation	0.093	Solyc07g056670	14.586	5.98E-23	Gibberellin 2-oxidase 2
18	abscisic acid biosynthesis	0.107	Solyc12g056710	6.263	6.95E-08	Xanthoxin dehydrogenase
19	tryptophan degradation VI (via tryptamine)	0.107	Solyc03g031880	5.57	1.17E-09	Amine oxidase family protein

GROUP 6 (i*DLK2*↓Myc^{ns}). Many genes that are not differentially expressed upon mycorrhization (wt-I *vs* NI), are downregulated in i*DLK2*-I *vs* wt-I. In fact, this group is the one representing the largest number of DEGs. Many of the associated changed pathways are coincident to pathways predicted in group 2, including a repression of cellulose, gibberellin and leucoanthocyanindin biosynthesis genes. In addition it is remarkable the repression of five genes related with flavonol biosynthesis (Table 14).

Table 14. MetGenMap analysis of Group 6. Pathways significantly (*P*>0.1) changed between i*DLK2*-I and wt-I treatments using genes from the group 6 of the RNA-seq with a fold change cutoff value of 2. Specific genes significantly regulated in each pathway are shown.

Changed pathways: : *iDLK2*-I_vs_wt-I			**Changed genes in the pathway**			
Number	**Pathway name**	**p value**	**Gene (ID SolDB)**	**Fold change (RNA-seq)**	**p-value**	**Common gene name**
1	trehalose biosynthesis V	0.009	Solyc09g014400 Solyc07g014590	-2.082 -2.01	3.16E-05 1.11E-05	Alpha-amylase Glycogen debranching enzyme
2	leucopelargonidin and leucocyanidin biosynthesis	0.017	Solyc01g105660	-2.357	1.68E-03	1-aminocyclopropane-1-carboxylate oxidase
3	leucodelphinidin biosynthesis	0.017	Solyc07g043420 Solyc11g013110 Solyc06g061280 Solyc03g097170 Solyc03g115220 Solyc03g122360 Solyc03g116260	-2.624 -2.105 -2.451 -3.134 -2.03 -2.185 -2.967	1.04E-18 4.43E-02 7.88E-04 4.70E-06 1.63E-05 1.33E-03 1.54E-03	2-oxoglutarate-dependent dioxygenase Anthocyanidin synthase Cinnamoyl-CoA reductase-like protein Cinnamoyl-CoA reductase-like protein Cytochrome P450 Cytochrome P450 Gibberellin 2-beta-dioxygenase 7
4	hypoglycin biosynthesis	0.017	Solyc05g051780 Solyc10g083540	-2.337 -2.301	1.33E-11 2.81E-02	Gamma-glutamyltransferase-like protein Threonine dehydratase biosynthetic
5	flavonol biosynthesis	0.020	Solyc07g043420 Solyc11g013110 Solyc03g115220 Solyc03g122360 Solyc03g116260	-2.624 -2.105 -2.03 -2.185 -2.967	1.04E-18 4.43E-02 1.63E-05 1.33E-03 1.54E-03	2-oxoglutarate-dependent dioxygenase Anthocyanidin synthase Cytochrome P450 Cytochrome P450 Gibberellin 2-beta-dioxygenase 7
6	cellulose biosynthesis	0.024	Solyc05g012070 Solyc09g075550 Solyc03g097050 Solyc12g055970 Solyc08g083210 Solyc11g040340	-2.299 -2.58 -3.629 -2.591 -2.842 -2.121	4.09E-22 1.96E-13 3.41E-11 1.19E-07 1.81E-08 1.02E-03	Alpha-1 4-glucan-protein synthase Cellulose synthase-like D6 Cellulose synthase-like protein Endoglucanase 1 Endoglucanase 1 Endoglucanase 1

7	demethylmenaquinone-8 biosynthesis	0.030	Solyc01g105460	-2.046	1.61E-04	1 4-dihydroxy-2-naphthoate octaprenyltransferase
8	UDP-D-galacturonate biosynthesis I (from UDP-D-glucuronate)	0.035	Solyc12g010540	-2.742	9.31E-06	NAD dependent epimerase/dehydratase family protein expressed
			Solyc07g006220	-2.007	1.25E-09	UDP-D-glucuronate 4-epimerase 1
9	syringetin biosynthesis	0.037	Solyc07g043420	-2.624	1.04E-18	2-oxoglutarate-dependent dioxygenase
			Solyc11g013110	-2.105	4.43E-02	Anthocyanidin synthase
			Solyc03g115220	-2.03	1.63E-05	Cytochrome P450
			Solyc03g122360	-2.185	1.33E-03	Cytochrome P450
			Solyc03g116260	-2.967	1.54E-03	Gibberellin 2-beta-dioxygenase 7
10	lysine degradation I	0.042	Solyc09g007830	-2.224	4.09E-04	Cytokinin riboside 5'-monophosphate phosphoribohydrolase LOG
			Solyc10g084150	-2.082	6.50E-04	Cytokinin riboside 5'-monophosphate phosphoribohydrolase LOG
11	gibberellin biosynthesis III (early C-13 hydroxylation)	0.052	Solyc06g066860	-2.016	4.17E-02	2-oxoglutarate-dependent dioxygenase
			Solyc03g116260	-2.967	1.54E-03	Gibberellin 2-beta-dioxygenase 7
			Solyc01g058250	-2.827	4.94E-03	Gibberellin 3-beta-hydroxylase (Fragment)
12	superpathway of gibberellin biosynthesis	0.052	Solyc06g066860	-2.016	4.17E-02	2-oxoglutarate-dependent dioxygenase
			Solyc03g116260	-2.967	1.54E-03	Gibberellin 2-beta-dioxygenase 7
			Solyc01g058250	-2.827	4.94E-03	Gibberellin 3-beta-hydroxylase (Fragment)
13	calystegine biosynthesis	0.060	Solyc04g007400	-2.074	1.92E-05	Tropinone reductase II
14	homoserine and methionine biosynthesis	0.066	Solyc06g064550	-2.633	1.56E-09	Aspartokinase-homoserine dehydrogenase
			Solyc02g067180	-2.034	2.02E-06	Cystathionine gamma synthase
15	starch degradation	0.072	Solyc09g014400	-2.082	3.16E-05	Alpha-amylase
			Solyc05g009470	-2.644	2.64E-16	Alpha-glucosidase
			Solyc07g014590	-2.01	1.11E-05	Glycogen debranching enzyme
			Solyc02g091830	-2.39	3.96E-04	Hexokinase
16	cardenolide biosynthesis	0.089	Solyc01g091670	-2.55	1.18E-04	Progesterone 5-beta-reductase
17	phospholipases	0.109	Solyc02g077160	-2.558	6.47E-05	Lipase-like protein
			Solyc03g019670	-2.506	5.77E-10	Phosphoesterase family protein
			Solyc07g014730	-2.563	9.64E-04	Phospholipase A2
			Solyc08g066800	-2.17	3.04E-02	Phospholipase D

Summary of results groups 1 to 6

A first overview of the predicted altered pathways suggest that some differentially regulated pathways such as the impaired biosynthesis of cell wall-related compounds and GAs, as well as the apparent induction in hexose production, might be a direct effect of i*DLK2* silencing and might be responsible for the increased mycorrhization of these plants. However, many other DEGs and predicted altered pathways are apparently differentially expressed as a consequence of the increased mycorrhizal colonization, rather than being the cause of the different mycorrhization pattern in i*DLK2* plants. That is the case of the activation of several genes involved in stress resistance to diseases or pathogens, and the induction of genes probably related to the production of alternative respiratory substrates to cope stress. In Figure 9, the main pathways altered in the six groups are summarized, and we indicate if they are hypothetically speculated as a cause or an effect of the decreased mycorrhizal development observed in the *SlDLK2* RNAi roots. All these genes and associated pathways were subsequently examined in detail in order to get more exact conclusions.

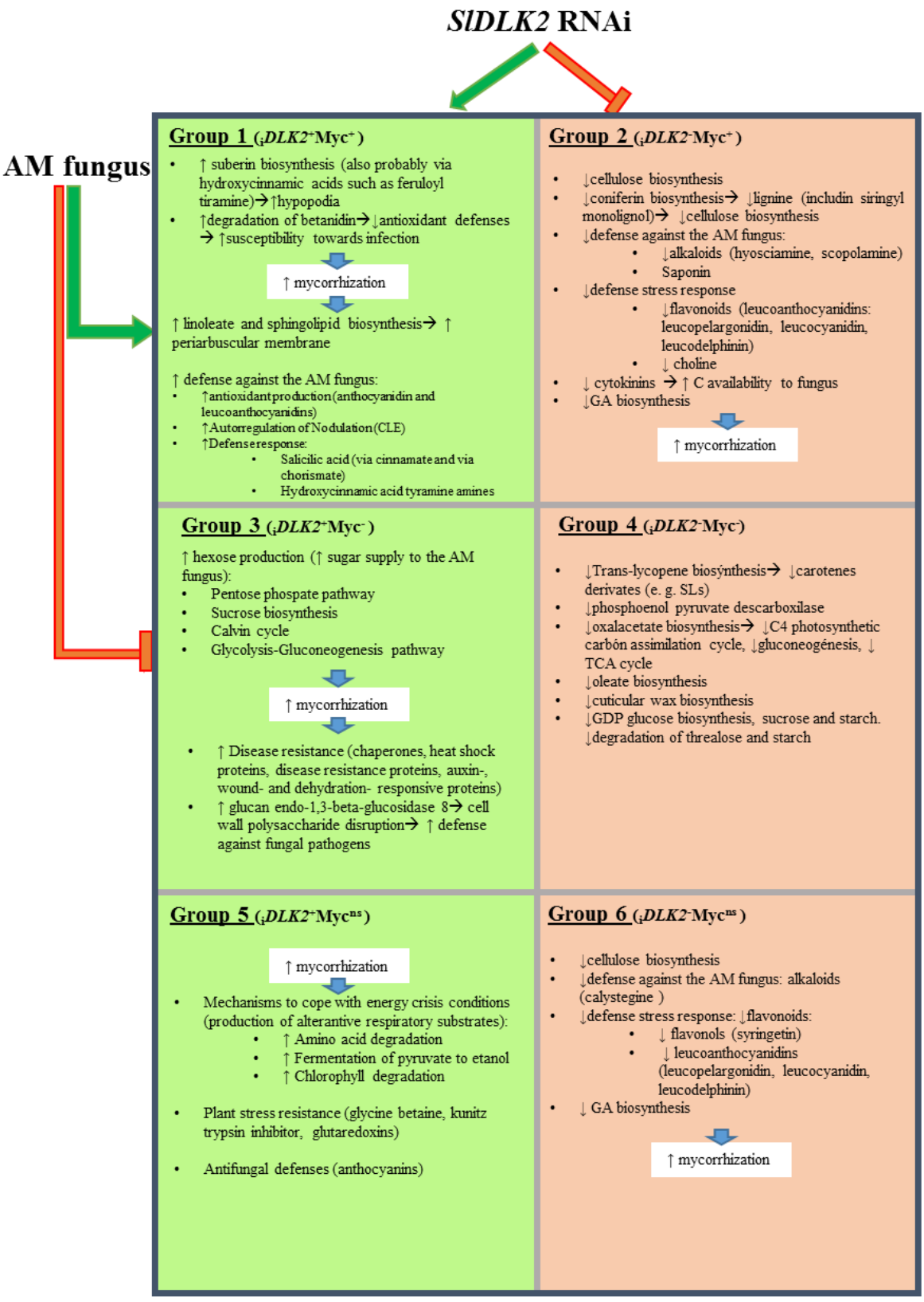

Figure 9. Classification of predicted pathways associated to transcripts detected in the RNA-seq depending on their regulation by AM inoculation and by *SlDLK2* RNAi silencing. Main pathways altered in the six groups, predicted by MetGenMap, are summarized. Red arrows/green lines represent the predicted induction/repression effect, respectively, of mycorrhization (wt-I *vs* NI data from RNA-seq) and of *SlDLK2* silencing

(i*DLK2*-I *vs* wt-I data) on changed pathways. Pathways induced or repressed in i*DLK2*-I *vs* wt-I are in green or red shadowed boxes, respectively. It is also indicated if the pathways are hypothetically considered as a cause or an effect of the decreased mycorrhizal development observed in the *SlDLK2* RNAi roots.

SlDLK2 silencing reinforces and alters the impact of mycorrhization in defense response

The RNA-seq data showed that many AM-differentially regulated genes encode for serine proteases, cysteine-rich antifungal proteins (defensins), Kunitz-type trypsin inhibitors, and subtilisin inhibitors. *SlDLK2* RNAi reinforces the up- and down-regulation of defensin genes that are AM-induced and AM-repressed, respectively (Fig. 10A). However, regarding to gene expression of putative Kunitz trypsin inhibitors, an opposite effect was observed between *SlDLK2* silencing and mycorrhization. While in *SlDLK2* RNAi AM roots the putative AM-induced Kunitz trypsin inhibitor Solyc06g072210 is AM-repressed, the AM-repressed Kunitz trypsin inhibitor Solyc04g008075 is induced (Fig. 10B). In addition, several putative genes encoding subtilisin-like proteases were differentially regulated (Fig. 10C).

The biological role of these defense genes is a paradox (García-Garrido and Ocampo 2002). However, our observations reinforces the role of these defense-related proteins as players in the developmental reprogramming of colonized cell contents or in nonspecific symptoms of a general stress response to cell colonization, rather than a role in controlling intracellular fungal development, because mycorrhization levels observed in *SlDLK2* RNAi roots were even higher despite the higher levels of many genes encoding defensins and subtilisin proteases. This is in agreement with the results of Gianinazzi-Pearson et al. (1996) and Turrini et al. (2004), who observed that overexpression of defense genes, including defensins, in plants, increases resistance to fungal pathogens but does not affect establishment of AM fungi within root tissues.

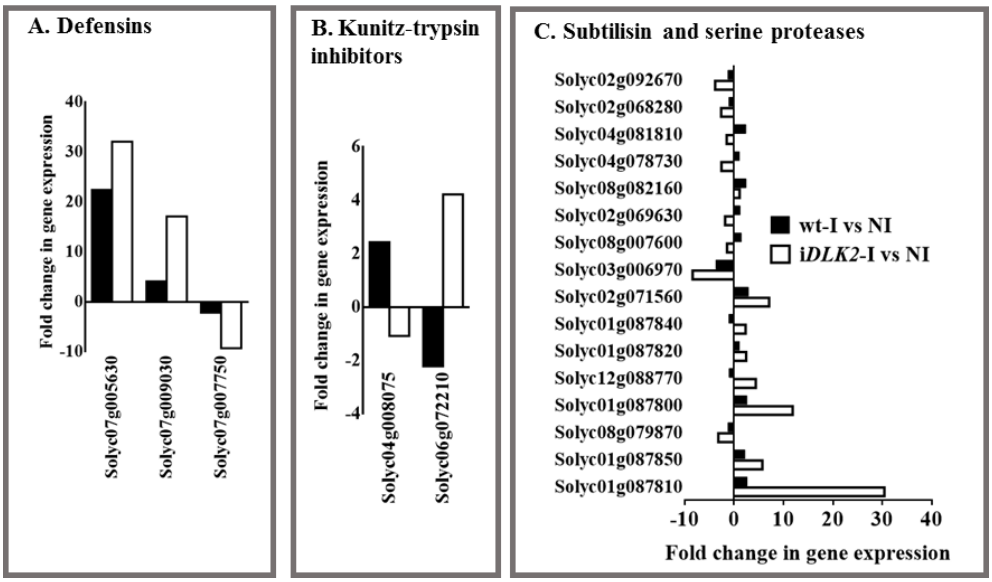

Figure 10. Effect of mycorrhization and *SlDLK2* silencing on defense-related genes. DEGs from the RNA-seq (fold change >2 or <-2 and *P*=0.05) corresponding to genes encoding defensins (A), Kunitz-trypsin inhibitors (B) and subtilisin-like or serine proteases (C), in i*DLK2*-I *vs* wt-I treatments, were selected, and their fold change gene expression in the control (wt-I) and *SlDLK2* RNAi (i*DLK2*-I) AM-plants with respect to the un-inoculated (NI) plants was graphed.

AM parasitism signature in *SlDLK2* RNAi AM roots: Nutrient starvation, induced stress, and activation of defense responses

We have chosen for the RNA-seq analysis plants with slight differences in the mycorrhization level and the expression of the typical AM marker genes was quite similar in control and i*DLK2* AM hairy roots (i*DLK2*-I *vs* wt-I, Table 15). Nevertheless, i*DLK2*-I roots are a little more colonized than wt-I roots and showed greater arbuscule abundance. Therefore, it is reasonable that we found a differential expression of other genes associated to biosynthesis of plant symbiotic structural components. For example, in i*DLK2*-I *vs* wt-I, expression changes were observed in genes putatively involved in the linoleate and sphingolipid biosynthesis pathway (Tables 8 and 9), maybe related to the requirement of new lipids for periarbuscular membrane formation. In this regard, sphingolipids compose an estimated ~40 % of the total lipids in plasma membrane of plants (Sperling et al. 2005) and the induction of genes related to linoleate and sphingolipid biosynthesis was also found in the transcriptome of mycorrhizal lichi plants (Shu et al. 2016).

Table 15. Effect of mycorrhization and *SlDLK2* silencing on AM marker genes. Fold change and p-values of several AM-associated genes for the three comparisons analyzed in the RNA-seq.

Gene common name (SolDB ID)	wt-I *vs* NI		i*DLK2*-I *vs* NI		i*DLK2*-I *vs* wt-I	
	Fold change	p value	Fold change	p value	Fold change	p value
CCaMK (Solyc01g096820)	3.41	1.17E-09	3.51	3.13E-36	-1.01	0.92
SYMRK (Solyc02g091590)	4.74	2.64E-20	3.43	2.00E-14	-1.39	0.01
Cyclops (Solyc08g075760)	4.49	9.00E-15	3.10	8.30E-10	-1.47	0.02
RAM1 (Solyc02g094340)	12.52	6.97E-20	16.95	7.91E-29	1.11	0.66
Vapyrin (Solyc10g081500)	13.66	7.97E-22	14.27	2.82E-4	-1.17	0.49
PT5 (Solyc06g051860)	4.25	2.91E-4	5.68	1.65E-4	1.02	0.94
AMT2 (Solyc08g067080)	49.92	3.51E-25	36.25	-	1.17	0.67
STR (Solyc01g097430)	11.18	3.94E-08	58.99	1.89E-17	-1.12	7.57E-01
RAM2 (Solyc02g087500)	20.07	-	37.44	3.79E-17	1.00	9.97E-01
Exo70i (Solyc04g077760)	27.50	9.76E-21	39.18	1.17E-19	-1.17	5.48E-01
Exo84 (Solyc09g072720)	27.18	6.85E-18	73.01	2.43E-21	1.33	3.42E-01

The corresponding transcriptomic profile obtained here suggests that the mycorrhizal colonization of the i*DLK2*-I roots leads to an increased nutrient starvation and stress condition, and the activation of defense mechanisms against the AM fungus. Accordingly, the AM-activated genes associated to fatty acid oxidation are more induced in *SlDLK2* RNAi roots (Table 9) and most DEGs related to amino acid and chlorophyll degradation that were not differentially expressed or downregulated in AM-roots, appeared to be upregulated in i*DLK2*-I *vs* wt-I (Table

13, Fig. 11). Degradation of amino acids, lipids and chlorophyll is thought to occur as a result of the use of these biomolecules as alternative respiratory substrates under stress conditions, when carbohydrates are scarce, i.e. darkness (Araújo et al. 2011; Hildebrandt et al. 2015). Although in our knowledge there are no reports of a carbohydrate starvation condition induced by the AM fungus in colonized plants, it is not surprising that the increased, partially uncontrolled, AM colonization in *SlDLK2* RNAi roots could lead to that situation, as glucose and fructose are the main nutrients demanded by the AM fungus (Solaiman and Saito 1997).

Pyruvate decarboxylases are considered to be rate limiting in ethanol fermentation, and their upregulation has been reported to be associated to survival to the oxidative stress conditions occurring under anoxia (Ismond et al. 2003; Mithran et al. 2014). Genes encoding for these enzymes are not differentially expressed in AM roots, however three of them are clearly induced (Solyc10g076510 FC=5.6, Solyc02g077240 FC>5, and Solyc09g005110 FC=3) in i*DLK2*-I (Table 13, Fig. 11). It is tenting to speculate that the transient ROS signaling occurring in wild type AM roots at the beginning of the colonization process (Kapoor and Singh 2017) might be extended to an increasing accumulation of ROS at later stages in *SlDLK2* RNAi roots due to a possible ineffective regulation of the AM fungus in i*DLK2* roots, where the microorganism could turn to be detected as pathogenic. In fact, three lipoxygenases are induced during mycorrhization, and one of them (Solyc08g029000) is highly more expressed in the i*DLK2*-I roots, reaching a FC value=38.5 with respect to un-inoculated roots, suggesting an induction in ROS production.

Then, we suggest that i*DLK2*-I roots showed symptoms resembling those present under energy crisis conditions due to mitochondrial disturbance under hypoxia, including an increase production of ROS and a decreased activity of the TCA cycle, as well as the subsequent activation of glycolysis, pyruvate metabolism and anaerobic respiration or fermentation in order to cope with energy crisis (Mittler et al. 2004; Ophir et al. 2009).

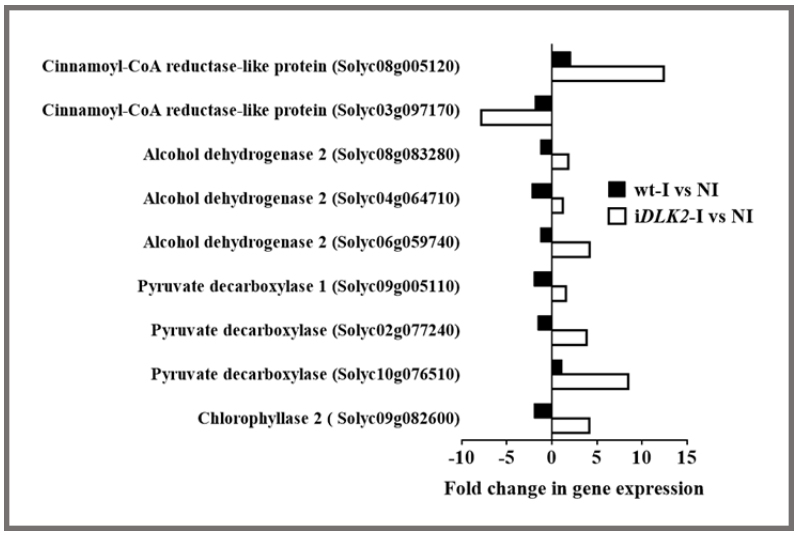

Figure 11. Effect of mycorrhization and *SlDLK2* silencing on genes related to degradation of amino acids and chlorophyll, and pyruvate fermentation to ethanol. DEGs from the RNA-seq (fold change >2 or <-2 and *P*=0.05) related to amino acid and chlorophyll degradation, as well as pyruvate fermentation to ethanol, in i*DLK2*-I *vs* wt-I treatments were selected, and their fold change gene expression in the control (wt-I) and *SlDLK2* RNAi (i*DLK2*-I) AM-plants with respect to the un-inoculated (NI) plants was graphed.

Maybe, to cope with an increased oxidative stress taking place in i*DLK2*-I plants, an induction of genes putatively related to production of metabolites with antioxidant properties could occur. For example, it is observed an increased upregulation of genes putatively involved in the leucoantocyanidins biosynthetic pathway and the activation of genes encoding glutaredoxins. In addition, in the i*DLK2*-I roots we observed an induction of several genes related to stress defense, including heat shock proteins, chaperones, wound-responsive and disease-resistance proteins, found to be AM-repressed in the wt-I roots, as well as the activation of a Kunitz trypsin inhibitor probably associated to defense strategies and the higher induction of genes for monoterpene and salicylic acid biosynthesis.

Also, six AM-induced peroxidases putatively involved in betanidin degradation are even more up-regulated under *SlDLK2* silencing conditions (Tables 9 and 10). Previous experiments showed that high amounts of a peroxidase putatively related to betanidin degradation was also found in *Monalbo* tomato roots susceptible *to Fusarium oxysporum* (Mazzeo et al. 2014). In addition, betanidin degradation is downregulated in rice resistant to the planthopper (Zhang et al. 2015a). The relation

between an increase in betanidin degradation and associated peroxidase gene expression with the increase susceptibility towards infection is in agreement with our observation in i*DLK2*-I roots. Although betanidin is reported to be an alkaloid with strong antioxidant properties probably involved in defense against oxidative stress (Taira et al. 2015), the underlying mechanisms of action in susceptibility or resistance towards pathogen or symbiont organisms are unknown.

In the *SlDLK2* RNAi tomato AM roots, it was also found the induction of other several genes associated to pathways activated during mycorrhization related to defense, including the monoterpene, salicylic acid and hydroxycinnamic acid tyramine amines biosynthesis (Table 9).

Particularly two genes related to the production of monoterpenes, encoding an (E)-beta-ocimene synthase (Solyc01g105920) and a limonene synthase (Solyc01g105940), showed an increased transcription level in *SlDLK2* RNAi AM roots. Monoterpenes are suggested to be induced in AM roots of plants at a late developmental stage (Fontana et al. 2009; Gange and West 1994; Wurst et al. 2004), and could be involved in similar roles to terpenes emitted from aerial parts (Keeling and Bohlmann 2006; Yoshitomi et al. 2016; Arimura et al. 2000; Farré-Armengol et al. 2017), acting as direct antimicrobial defenses of below- ground tissue or playing roles such as attractants or deterrents in interactions with other rhizosphere organisms, as suggested by Chen et al. (2004).

In addition, in the S*lDLK2* RNAi AM roots, it is apparently observed a higher induction of genes for salicylic acid biosynthesis with respect to the control AM roots. Salicylic acid defense responses are reported to participate in the AM symbiosis, probably mainly at early stages of AM fungal infection (Medina et al. 2003; Gutjahr and Paszkowski 2009). Plants synthesize salicylic acid through two distinct enzymatic pathways. One is from phenylalanine via cinnamate and the other is from chorismate via isochorismate. Both pathways are induced in *SlDLK2* RNAi roots (Table 9), with a specific induction of a chorismate synthase (Solyc04g049350), two shikimate dehydrogenases (Solyc01g067750 and Solyc10g038080), and two phenylalanine ammonia-lyases (Solyc10g011920 and

Solyc05g056170), indicating a possible induction of the salicylic acid biosynthesis due to their higher mycorrhization.

The hydroxycinnamic acid tyramine amide biosynthesis and the suberin biosynthesis pathways were the two most differentially regulated pathways in Sl*DLK2*-I *vs* wt-I treatments (Table 9, Fig. 12). A clear overall upregulation of genes putatively involved in suberin biosynthesis, through the hydroxicinammic acid precursor feruloyl tyramine, was observed in the i*DLK2*-I plants (Fig. 12). Another gene also reported to participate in cutin/suberin biosynthesis is *RAM2* (Wang et al. 2012; Beisson et al. 2007), also more upregulated in the *SlDLK2* RNAi mycorrhizal roots. Suberin is important for plant stress resitance against abiotic and biotic stresses (Franke and Schreiber 2007; Schreiber 2010), however, it has been reported that cutin/suberin monomers are also signaling molecules that promote AM hyphopodia formation (Wang et al. 2012). Then, the deregulated mycorrhization in i*DLK2*-I plants, could cause an activation of suberin synthesis as a defense response and, indirectly, it might be detected by the AM fungus as a signal for activating hyphopodia formation, positively feeding back mycorrhizal colonization.

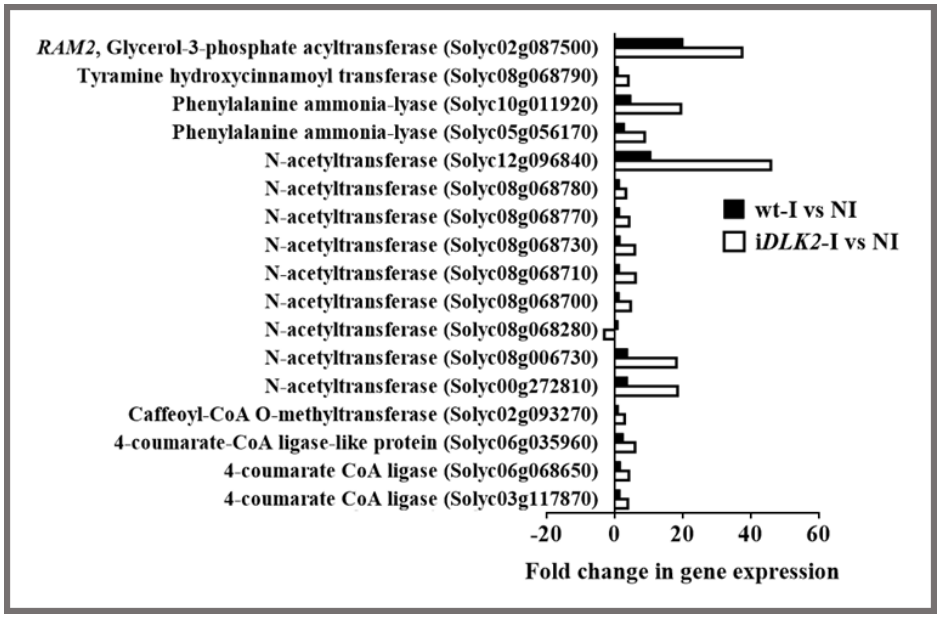

Figure 12. Effect of mycorrhization and *SlDLK2* silencing on suberin biosynthesis-related genes. *RAM2* and DEGs from the RNA-seq (fold change >2 or <-2 and *P*=0.05) related to suberin metabolism (via the hydroxicinammic acid precursor feruloyl tyramine) in i*DLK2*-I *vs* wt-I treatments were selected, and their fold change gene expression in the control (wt-I) and *SlDLK2* RNAi (i*DLK2*-I) AM-plants with respect to the uninoculated (NI) plants was graphed.

Is *SlDLK2* involved in the regulation of GA signalling?

Gibberellins (GAs) are known to accumulate in AM roots (Martin-Rodriguez et al. 2016; Martín-Rodríguez et al. 2015) and to develop a mainly negative regulatory role on arbuscule formation (Floss et al. 2013; Martin-Rodriguez et al. 2016). In particular, exogenous GA treatment inhibits AM hyphal entry into the host root and suppress arbuscule formation (Martín-Rodríguez et al. 2015; Takeda et al. 2015). Nevertheless, inhibition of GA biosynthesis or suppression of GA signaling also affects AM development in the host root and it has been shown that low GA conditions reduce hyphal branching in the host root (Takeda et al. 2015). Regarding wt inoculated plants, *SlDLK2* RNAi mycorrhizal roots showed a slight repression of several genes involved in GA biosynthesis and GA perception (Fig. 13A), as well as a clear induction of genes for GA inactivation (Fig. 13B). To confirm these results at a metabolomic level, GA content was measured (Fig. 14). Several GAs were found to be AM-induced, including GA_{53}, GA_{19}, GA_{24}, GA_{9}, GA_{29}, GA_{6} and GA_{34}, some of them already reported to be increased during mycorrhization (Martín-Rodríguez et al. 2015). As for the i*DLK2*-I roots *vs* wt-I roots, we only found an increase of GA_{29} and GA_{8}, both catabolic GA isoforms from the early-13-hydroxilation pathway, what supports the induction of GA catabolism-related genes in the i*DLK2*-I roots. In the non-inoculated plants, an unexpected increase in the bioactive GA_{3} was found in *SlDKL2* RNAi roots; however we cannot explain this result. In summary, our data suggest an overall inhibition of GA signaling in i*DLK2*-I, mainly through GA catabolism, what could consequently promote mycorrhizal development, as observed in the *SlDLK2* RNAi composite tomato plants. We propose that *SlDLK2* action could mediate the induction of GA signaling during mycorrhization, through activation of GA biosynthesis and perception, as well as by repressing GA catabolism.

GA signaling is described to proceed through GA binding to the GID1 receptor, triggering the binding and degradation of the DELLA transcription factor (Hirano et al. 2008). Interestingly, GID1 belongs to the α, β-hydrolase superfamily. The D14 α, β-hydrolase, closely related to SlDLK2, has been also reported to bind DELLA proteins upon ligand binding, and probably upon D3/MAX2 interaction, in rice

(Zhao et al. 2015; Nakamura et al. 2013). Although key residues for D3/MAX2 binding (Yao et al. 2016; Zhao et al. 2015) are not conserved in SlDLK2, we should not discard the possibility that SlDLK2 might retain some ability to bind DELLA, contributing to the negative regulation of the mycorrhization through increasing GA signaling.

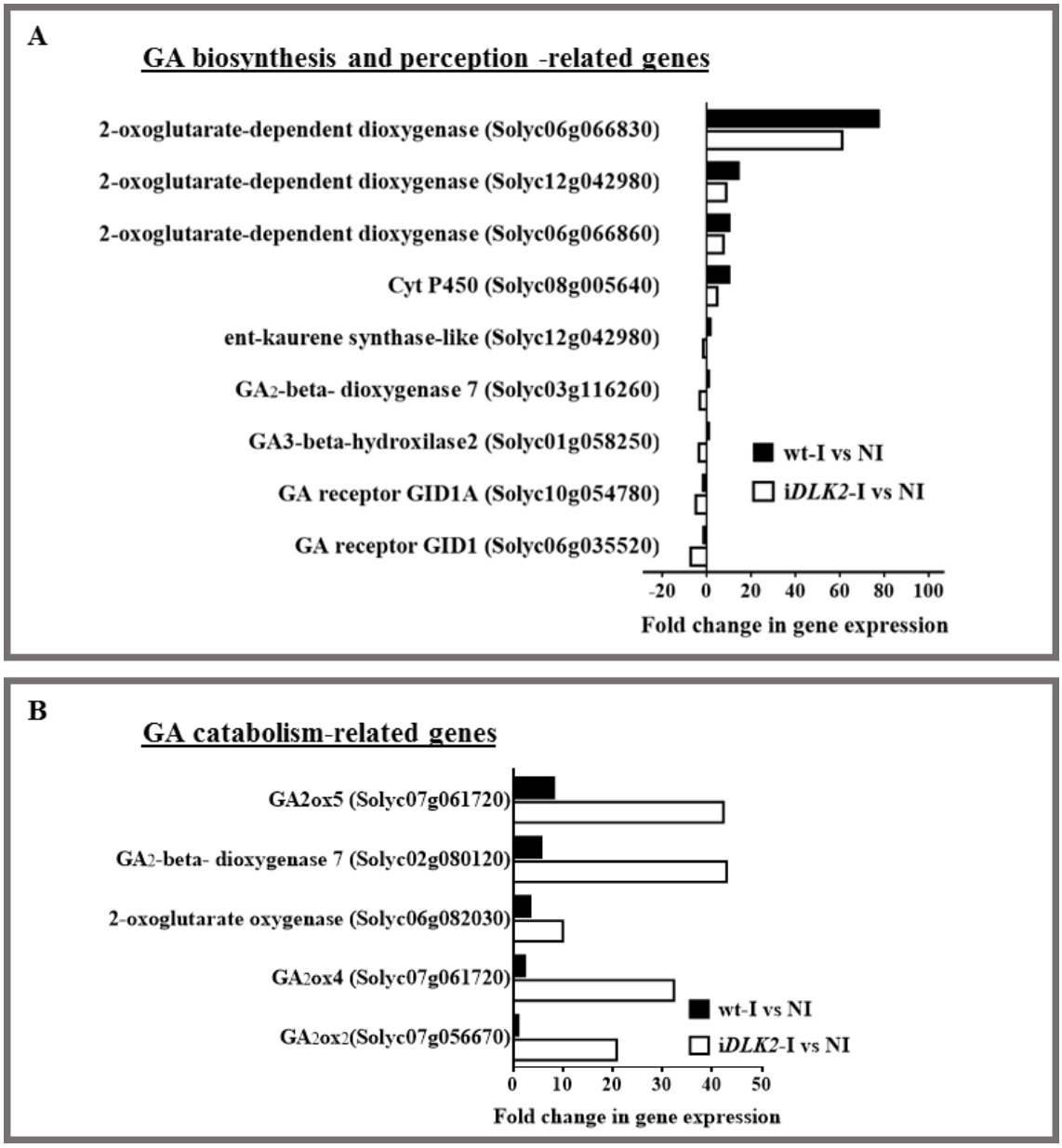

Figure 13. Effect of mycorrhization and *SlDLK2* silencing on GA metabolism-related genes. DEGs from the RNA-seq (fold change >2 or <-2, and *P*=0.05) related with GA metabolism in i*DLK2*-I *vs* wt-I treatments were selected, and their fold change gene expression in the control (wt-I) and *SlDLK2* RNAi (i*DLK2*-I) AM-plants with respect to the uninoculated (NI) plants was graphed. Genes associated to GA biosynthesis and perception are shown in (A). GA catabolism-related genes are shown in (B).

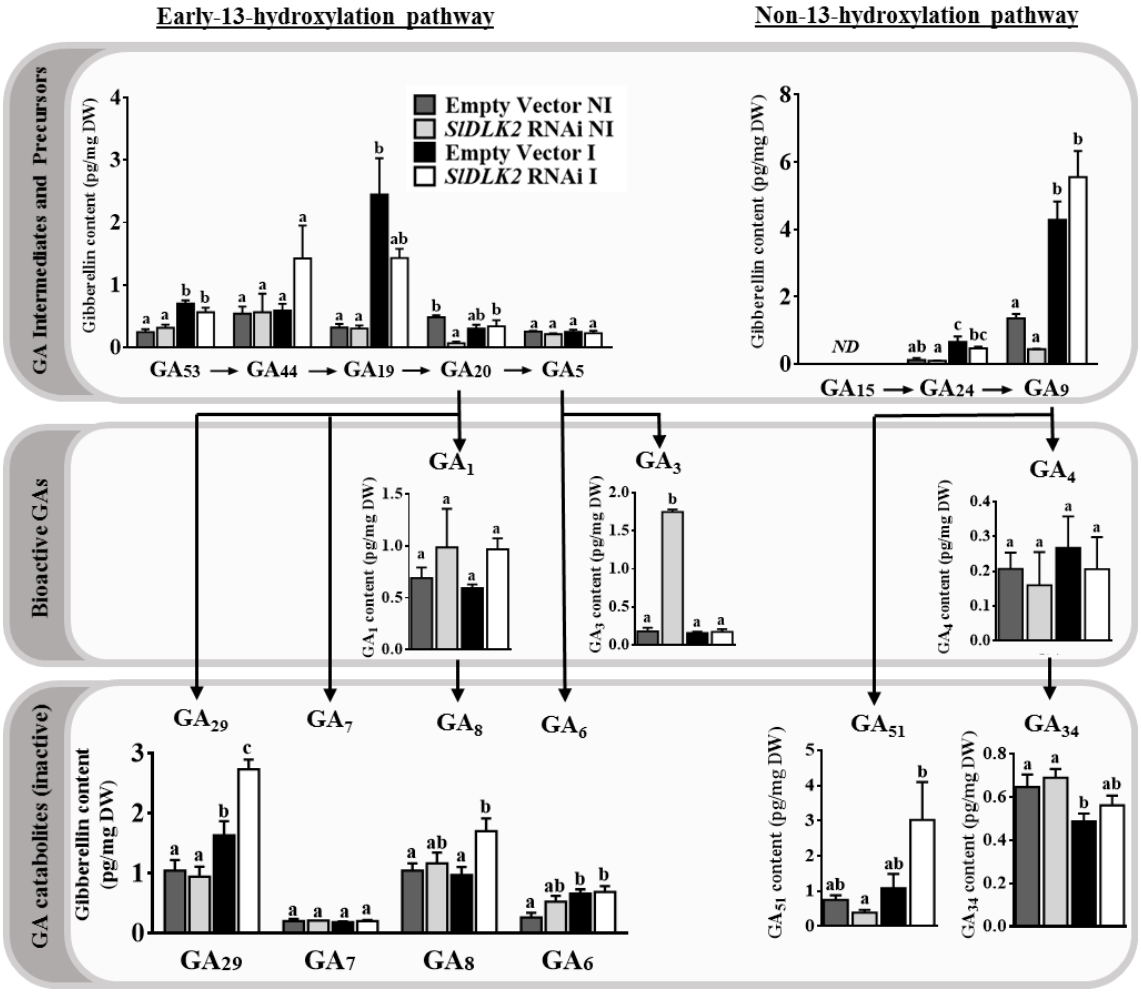

Figure 14. Effect of mycorrhization and *SlDLK2* silencing on GAs content. The GA content of precursor, bioactive and catabolite GAs from the early-13-hydrolxylation pathway (left) and the non-13-hydrolxylation pathway (right) were measured in hairy roots of both control and *SlDLK2* RNAi composite tomato plants non-colonized (NI) or colonized with *R. irregularis* (I), 50 days after infection. Values are the mean ± SE of five biological replications. For each GA analyzed, bars with similar letters are not significantly different (P=0.05) according to LSD multiple comparison test. ND, not detected.

Does *SlDLK2* restrict hexose production and supply to the AM fungus?

None of the pathways related to carbohydrate metabolism were significantly differentially regulated upon mycorrhization. However, in the i*DLK2*-I vs NI roots, the expression of many genes putatively belonging to these pathways was altered (Table 11, Fig. 15).

AM fungi are obligate biotrophic fungi, whose growth and development depend on photosynthetic products of the host plant transported from the source to the sink (Hodge et al. 2001). Sucrose, the major product of photosynthesis and the plant carbon source is used as energy carrier (Sauer 2007), but it is not absorbed directly by the AM fungus. The AM intraradical hyphae uptake carbohydrates in form of hexoses, specially glucose and, in a lower extent, fructose (Solaiman and Saito 1997). Conversion of sucrose to hexoses is required and occurs in the AM-roots through sucrose-cleaving enzymes, i.e. apoplastic invertases, as well as sucrose synthases, whose gene products have been localized in colonized cortex cells (Ravnskov et al. 2003; Schubert et al. 2004; Schaarschmidt et al. 2007; Boldt et al. 2011). Another way used by the AM fungus to obtain glucose is the oxidization of mannitol to mannose-6-P by a mannitol dehydrogenase, to produce fructose-6-P and glucose-6-P, that are used by *R. irregularis* to form trehalose, glycogen, and storage lipid (Shachar-Hill et al. 1995).

In the i*DLK2*-I roots, a sucrose-phosphate-synthase (Solyc09g092130) is repressed, and mannitol catabolism is increased through induction of mannitol dehydrogenase (Solyc11g011340), respectively. Also, the pentose phosphate pathway and the glycolysis might be activated for supply of hexoses such as fructose-6-P and β-D-glucose-6-P, respectively (Fig. 15). We may speculate that, following colonization of tomato plants with *R. irregularis*, the energy and carbon demand might be higher in *SlDLK2* RNAi roots, so sugars can be depleted and become limiting. Under these conditions, in order to produce hexose sugars for assimilation and growth, these enzymes are activated. However, an alternative explanation cannot be ruled out. AM-induced gene *SlDLK2* might have a role in repressing hexose-synthesis during mycorrhization in order to limit the sugar supply to the fungus, consequently controlling fungal development. In this context, the increased hexose production in *SlDLK2* RNAi AM roots can be a direct consequence of *SlDLK2* silencing.

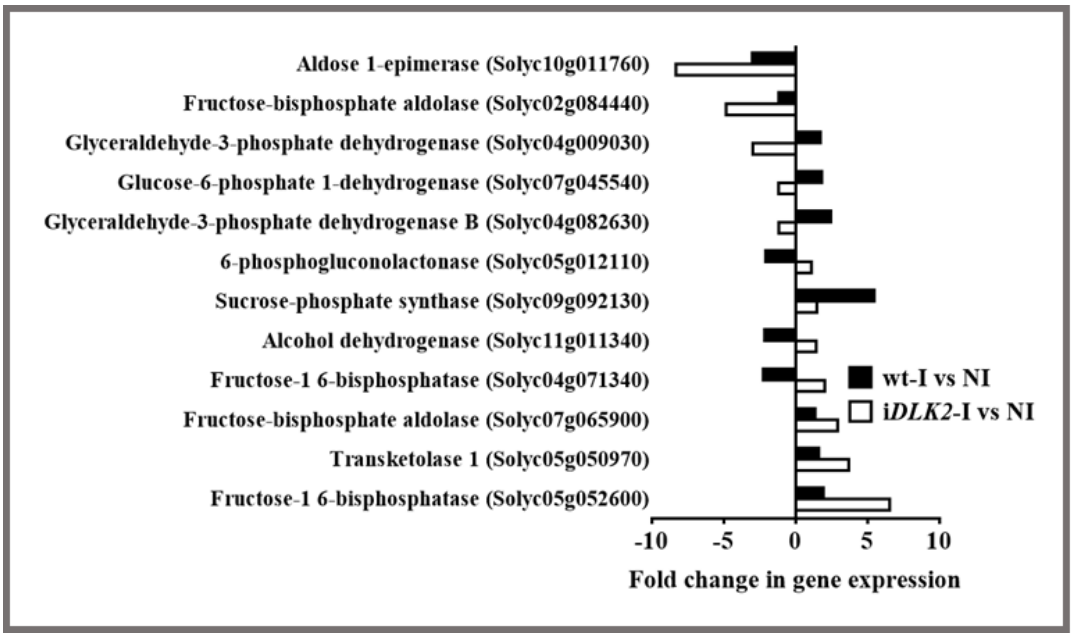

Figure 15. Effect of mycorrhization and *SlDLK2* silencing on carbohydrate metabolism-related genes. DEGs from the RNA-seq (fold change >2 or <-2 and *P*=0.05) related with carbohydrate metabolism in i*DLK2*-I *vs* wt-I treatments were selected, and their fold change gene expression in the control (wt-I) and *SlDLK2* RNAi (i*DLK2*-I) AM-plants with respect to the uninoculated (NI) plants was graphed.

In addition, our RNA-seq data showed that cytokinin (CK) biosynthesis pathway is induced during mycorrhization (Table 5), which is in agreement with the increased CK content previously reported in AM roots (Allen et al. 1980; Barker and Tagu 2000; Shaul-Keinan et al. 2002). A contradictory effect of *DLK2* RNA interference on cytokinin pathway was observed in the i*DLK2*-I roots. Although a higher activation of many of the genes involved in CK biosynthesis was observed (Fig. 16A), several other AM-induced genes putatively involved in CK biosynthesis are repressed in the i*DLK2*-I roots (Fig. 16B). Although the CK role in AM regulation is controversial (Jones et al. 2015; Laffont et al. 2015; Cosme and Wurst 2013), in our study, we can predict a defect in CK biosynthesis in the i*DLK2*-I roots which is accompanied by an increased in the AM colonization, what is in agreement with the results of the studies performed by Cosme and Wurst (2013) with CK-deficient mutant plants. Curiously, Cosme et al. (2016) suggested that root CK may restrict the C availability from the roots to the fungus thus averting parasitism by AM fungi. Following this hypothesis, in the *SlDLK2* RNAi plants, the predicted increase in hexose production, together with a defective CK biosynthesis in the roots, could increase C supply to the AM

fungus, and then promote parasitism by the fungal partner in the *SlDLK2* silencing roots.

Although a role of *SlDLK2* in the downregulation of hexose production and induction of cytokinin biosynthesis in order to restrict carbon supply to the AM fungus can be envisaged, further research is required, mainly at a metabolomic level

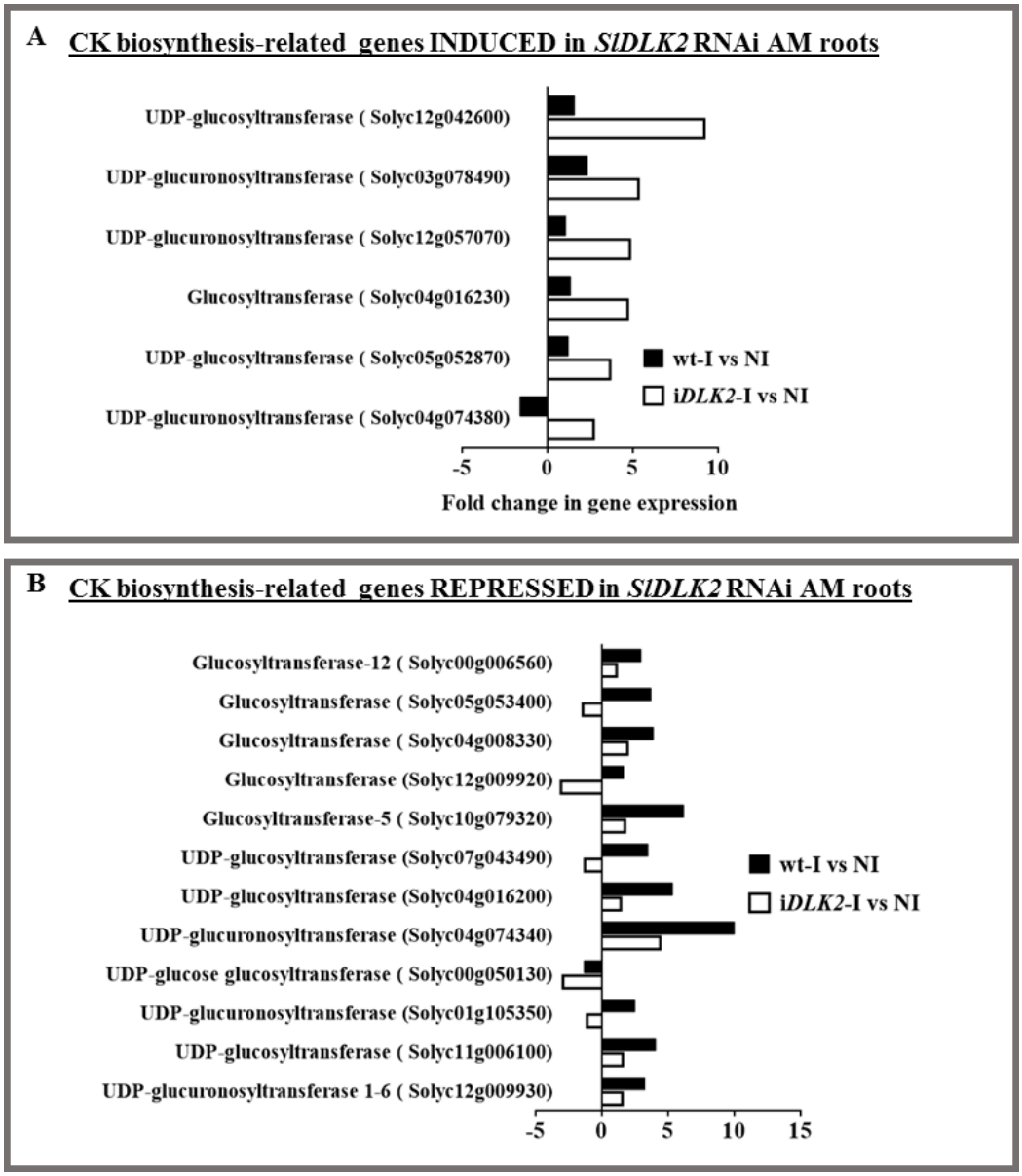

Figure 16. Effect of mycorrhization and *SlDLK2* silencing on CK metabolism-related genes. Upregulated (A) and downregulated (B) DEGs from the RNA-seq (fold change >2 or <-2 and *P*=0.05) related with CK metabolism in i*DLK2*-I *vs* wt-I treatments were selected, and their fold change gene expression in the control (wt-I) and *SlDLK2* RNAi (i*DLK2*-I) AM-plants with respect to the uninoculated (NI) plants was graphed.

Is the activation of cellulose biosynthesis mediated by *SlDlK2* during mycorrhization?

The RNA-seq data showed that cellulose biosynthesis-related genes are induced during mycorrhization, which is in agreement with previous studies reporting the induction of these genes in AM colonized cells (Siciliano et al. 2007; Guether et al. 2009; Liu et al. 2003). The role of lignin and cellulose during mycorrhization is still unknown, but it is thought that these biomolecules could have a role in strength the building up of the cell wall and make more difficult AM colonization, as susceptibility to fungal pathogens is increased upon lignin production impairment as previously shown (Wróbel-Kwiatkowska et al. 2007; Carver et al. 1994). *SlDLK2* silencing triggers a downregulation of several genes encoding enzymes involved in cellulose biosynthesis that are AM-induced in the wt-I roots (Table 14, Fig. 17). This includes most genes from the cellulose biosynthesis pathway *perse*, and three genes from the monolignol and coniferin biosynthesis pathways, including two glucosyltransferases (Solyc05g053400 and Solyc05g053120), and an UDP-glucose glucosyltransferase (Solyc07g043480) (Table 10). Coniferin alcohol, a coniferin derivative, is the precursor of lignine, and the monolignol is one of the constituents of the lignine, that actually participates in the degradation of the other lignine compounds for the cellulose production. Then, the results suggest that the overall AM-induction of cellulose biosynthesis is repressed in i*DLK2*-I roots, indicating a possible requirement of *SlDLK2* during mycorrhization for cellulose biosynthesis.

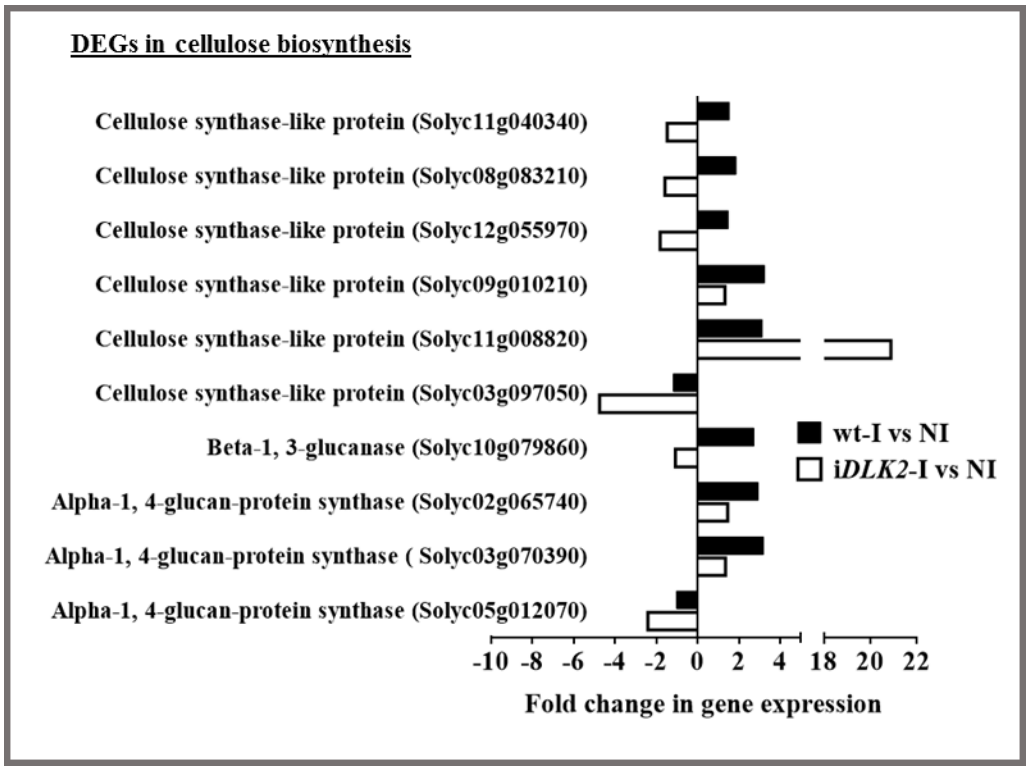

Figure 17. Effect of mycorrhization and *SlDLK2* silencing on cellulose biosynthesis-related genes. DEGs from the RNA-seq (fold change >2 or <-2 and *P*=0.05) related with cellulose biosynthesis in i*DLK2*-I *vs* wt-I treatments were selected, and their fold change gene expression in the control (wt-I) and *SlDLK2* RNAi (i*DLK2*-I) AM-plants with respect to the uninoculated (NI) plants was graphed.

Does antifungal defense and stress resistance fail in *SlDLK2* RNAi AM roots?

In view of the results obtained in the RNA-seq, roots of composite plants with *SlDLK2* silencing showed a repression of several genes involved in the synthesis of metabolites probably required to fight against the AM fungus, such as saponins (Szakiel et al. 2011; Schliemann et al. 2008).

Three AM-induced genes putatively involved in saponin biosynthesis are repressed in i*DLK2*-I silencing roots (Table 10). Saponins are part of the constitutive plant defense system but are also qualitative-changed in response to AM-fungi (Szakiel et al. 2011; Schliemann et al. 2008), so a defective production of saponins in the i*DLK2*-I roots could be involved in an inefficient defense against AM fungus, allowing the AM fungus to easily colonize the root.

Two AM-induced methyltransferases (Solyc12g040790 and Solyc06g068950) putatively involved in the biosynthesis of phosphatidylcholine and choline are repressed in the i*DLK2*-I plants (Table 10). Choline plays a critical role in plant stress resistance, mainly for enhancing glycine betaine synthesis and accumulation (Zeisel, 2006; Zhang et al., 2010), and choline biosynthesis is actually enhanced in PGPR inoculated plants (McNeil et al., 2001). Then, we suggest that *SlDLK2* silencing might be affecting choline levels, causing a defective plant stress resistance, and then a higher susceptibility of *SlDLK2* RNAi plants to AM-colonization.

Additionally, the possible deficit in certain defensive strategies against the AM fungus is accompanied by a lack in some of the mechanism of stress resistance. For example, a few genes from the i*DLK2*↓myc^{+} group (Table 10) are putatively involved in hyosciamine and scopolamine biosynthesis, as well as in biosynthesis of leucoanthocyanidins (leucopelargonidin, leucocyanidin and leucodeophinin); particularly five 1-aminocyclopropane-1-carboxyulate oxidases (Solyc01g108860, Solyc11g010400, Solyc02g070080, Solyc11g072200 and Solyc11g072130) and a dihydroflavonol-4-reductase (Solyc10g018140). Hyosciamine and scopolamine are alkaloids that might be involved in the defense against the AM fungus, as it has been previously described the antimicrobial and antifungal properties of these compounds (Abdel-Motaal et al. 2010), as well as their increased contents in AM plants (Honggang 1989) and PGPR colonized roots (Ghorbanpour et al. 2013). In the other hand, leucoanthocyanidins are flavonoid compounds and precursor metabolites of anthocyanins, which could have a role as antioxidants and stress resistance in AM-roots (Dangles et al. 2000; Chalker-Scott 1999).

Conclusions

The RNA-seq analysis presented here reveals transcriptomic alterations in tomato roots upon mycorrhization. In addition, it was performed a comparison with AM inoculated roots silenced for the *SlDLK2* gene, previously suggested to be a receptor involved in the negative regulation of mycorrhization and arbuscule branching. For the interpretation of the results it was especially difficult to distinguish between genes altered as a direct effect of the *SlDLK2* silencing, and gene changes comprising an indirect consequence of the altered mycorrhizal process in the *SlDLK2* RNAi roots. However, we made an effort to deeply study modifications in gene expression and their associated pathways in the mutant roots in order to find clues that allow us to shed light into the possible signaling role of *SlDLK2* in AM development.

In this work we firstly performed an RNA-seq to analyze transcriptomic patterns of tomato roots establishing symbiosis with AM fungi, what provides additional and more detailed information to previous microarray analysis (López-Ráez et al. 2010; García Garrido et al. 2010; Fiorilli et al. 2009; Ruzicka et al. 2012). We found a remarkable differential expression of genes related with GA, CK and ABA hormone biosynthesis, as well as secondary metabolite biosynthesis genes. The activation of GA and CK are supported by previous studies showing the activation of GA-related biosynthesis genes and the increased GA and CK content in mycorrhizal roots (Martin-Rodriguez et al. 2016; Fusconi 2013; Yurkov et al. 2017). Although controversial results have been obtained with respect to the ABA levels in AM roots (Aroca et al. 2013; Jahromi et al. 2008), our data points to an induction of the ABA biosynthetic pathway. In addition, the accumulation of several kinds of secondary metabolites is known to occur in AM roots (Rivero et al. 2015; Pedone-Bonfim et al. 2015; Zubek et al. 2015), however it is unclear if it is an effect of an improved mineral nutrition by AM symbiosis and/or a result of general plant defense reaction to fungal colonization and the accompanied oxidative stress. Finally, we also observed an overall alteration in the expression of genes encoding for GRAS transcription factors, suggesting that the GRAS network have an essential role in the transcriptional reprogramming occurring in the host cell during mycorrhization, as reported for other species (Xue et al. 2015; Gobbato et al. 2012; Rich et al. 2015).

It is important to highlight that the results obtained here must be taken carefully, as the mycorrhizal plants were watered with a Pi deficient nutrient solution in order to promote mycorrhization, keeping the uninoculated plants watered with the complete nutrient solution. This procedure is sometimes found in the experimental design of previous mycorrhizal studies (Martín-Rodríguez et al. 2015; Martin-Rodriguez et al. 2016). However, in our experience, the obtained AM plants grown under low Pi concentrations are always smaller plants and at a younger physiological stage than the uninoculated ones, watered with the complete nutrient solution. In this manner, the Pi starvation condition in AM plants with respect to the uninoculated plants could overlap and/or mask the effect of the mycorrhizal inoculation treatment. For future experiments comparing mycorrhizal and non-mycorrhizal plants we recommend to use a Pi deficient nutrient solution for both AM and non-AM plants, as done in most of the mycorrhizal studies, in order to obtain plants with a similar low Pi availability and at a similar physiological stage, and to obtain significant differences limited to the effect of the mycorrhization.

Simultaneously to the comparison between AM-inoculated (wt-I) and uninoculated (NI) plants, we included a third treatment in the RNA-seq analyses (i*DLK2*-I) in order to elucidate the role of a tomato α, β-hydrolase protein SlDLK2, suggested to function as a negative regulator that controls mycorrhizal development (unpublished). Analysis of differential expressed genes (DEGs) between mycorrhizal *SlDLK2* RNAi and control composite tomato plants (i*DLK2*-I *vs* wt-I) revealed transcriptomic changes apparently associated to two events: on the one hand the direct effect of a deficient *SlDLK2* gene expression and, on the other, the effect of the slight increased mycorrhization in *SlDLK2* RNAi plants. We tried to identify alterations associated to each one of the events and we proposed a model that is illustrated in Fig. 18.

The *SlDLK2* silencing might directly trigger an increase catabolism of gibberellins, consequently decreasing the GA signaling; a higher hexose production and supply to the AM fungus (probably with the involvement of a decreased cytokinin signaling); a decreased cellulose biosynthesis, what could facilitate the penetration of the fungus through the plant cell wall; and a possible failure of specific antifungal

defenses and stress resistance mechanisms. Altogether might contribute to a higher mycorrhizal colonization in these *SlDLK2* RNAi composite plants.

The increased mycorrhization in the *SlDLK2* RNAi roots is associated to a higher induction of typical AM-activated pathways. However, it is remarkable the upregulation of other additional pathways involved in the generation of alternative respiratory substrates and the apparent activation of extra-antioxidant responses, indicating a nutrient starvation condition and a higher oxidative stress. In this way, our data suggest that the AM fungus in the *SlDLK2* RNAi roots changes from a symbiotic to a parasitic mode. Then, the increased mycorrhization obtained through *SlDLK2* silencing might be detrimental, rather than beneficial for the plant fitness.

Although D14 and KAI2 related pathways converge upon MAX2, they diverge at the level of the SMXL family proteins, and then regulate different physiological events. KAI2 signaling occurs through its interaction with SMAX1 and SMXL2 (Stanga et al. 2016; Stanga et al. 2013), while D14 signalling is mediated by binding and degradation of SMXL 6, 7 and 8 proteins (Wang et al. 2015; Soundappan et al. 2015) or D53 in rice (Zhou et al. 2013). In the same manner, the three remaining proteins of the SMXL family, i. e. SMXL3, 4 and 5 have been suggested as candidates to be co-opted by proteins belonging to the DLK2 group (Végh et al. 2017). Little is known about the SMXL3, 4 and 5 members, but some recent studies reveal a vascular-bundle specific expression (Zhang et al. 2014) and a role in phloem formation and transport, as well as carbohydrate accumulation (Wallner et al. 2017; Wu et al. 2017). Following this hypothesis, *SlDLK2* silencing might trigger an excess of SMXL proteins at free stage, favoring phloem formation and transport and, consequently, favoring carbohydrate availability and development of the AM fungus, which is supported by the higher mycorrhizal colonization observed in the *SlDLK2* RNAi composite plants, and the predicted increased of hexose production and carbon supply to the AM fungus through induction of CK signaling. In addition, it is also worth mentioning that curiously the putative tomato *SMXL4* gene is highly repressed in the RNAi *SlDLK2* mycorrhizal roots, probably as a mechanism of negative autoregulation of SMXL4 at the transcriptional level.

Here, our RNA-seq data revealed that *SlDLK2* impairment in AM roots is accompanied by an increased GA catabolism, pointing to a possible role of *SlDLK2* in activating GA signalling during mycorrhization. Curiously, this function has also been suggested to be accomplished by the strigolactone receptor D14, as Nakamura et al. (2013) observed that, in a SL-dependent manner, D14 of rice is able to interact with the DELLA protein and, in this way, negatively control the mycorrhization (Yu et al. 2014; Jin et al. 2016; Floss et al. 2013). We wonder if the protein encoded by the *SlDLK2* is involved in the mycorrhizal development and functioning through binding DELLA and activating GA signalling. To elucidate this question, experiments are being carried out in order to analyze GA-related gene expression and GA hormone content also in *SlDLK2* overexpressing AM roots. In addition, the interaction between SlDLK2 protein and DELLA is currently being evaluated using a co-immunoprecipitation (Co-IP) strategy.

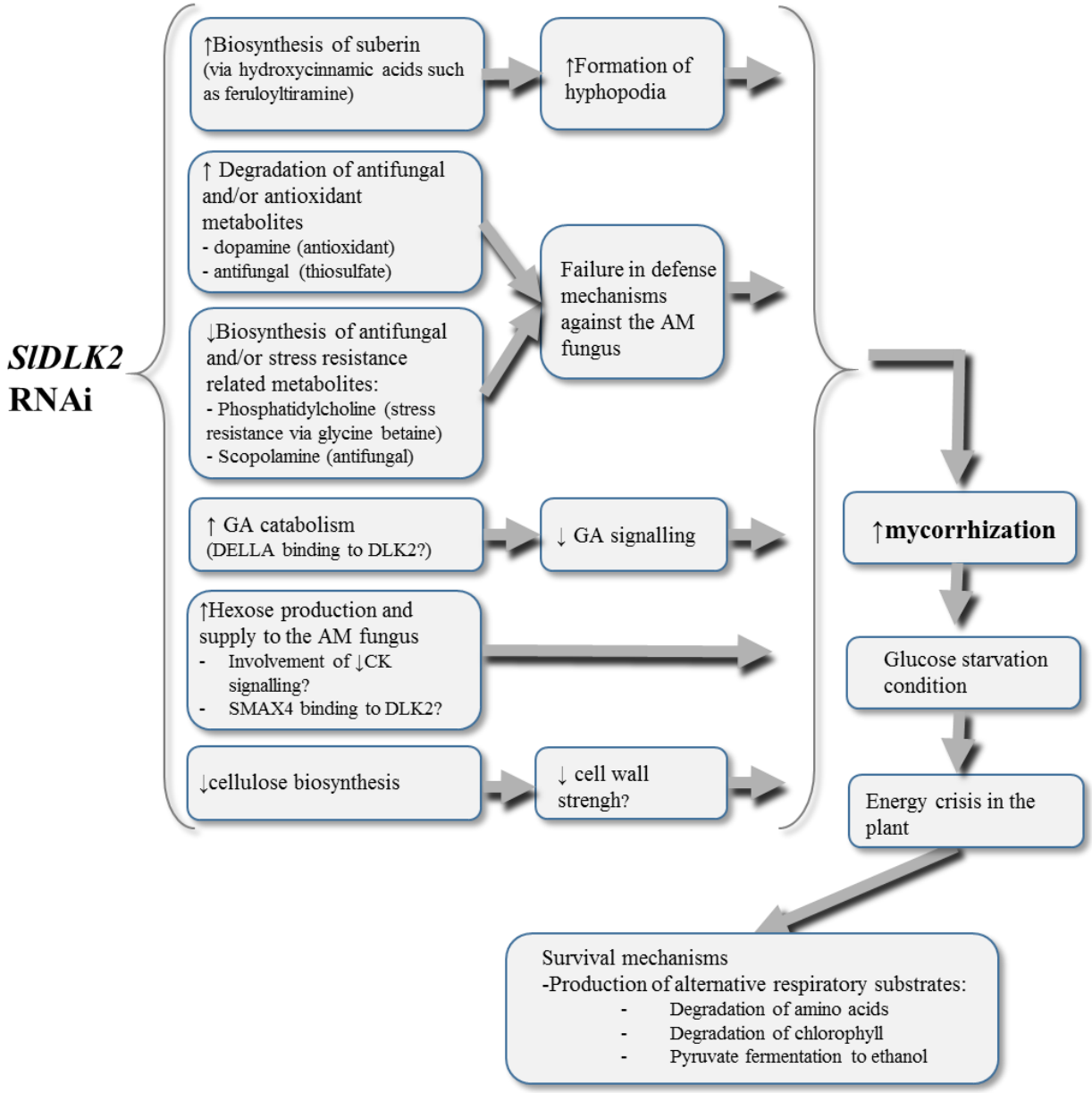

Figure 18. Hypothetical model of plant responses upon *SlDLK2* silencing in mycorrhizal roots. The diagram summarizes the proposed effects of *SlDLK2* silencing on mycorrhizal tomato roots after analyzing the RNA-seq data. Transcriptomic changes observed in these roots are associated to an expected increase of suberin biosynthesis, a failure in defense mechanisms, a repression on GA signaling, an induced hexose production and supply to the AM fungus, and a decreased cellulose biosynthesis. Altogether may contribute to the higher mycorrhizal development and functionality in the *SlDLK2* RNAi roots, which is suggested to trigger a glucose starvation situation and the initiation of mechanisms to overcome the energy crisis condition in the plant.

Future perspectives

Next-generation sequencing techniques and the resulting datasets have provided us with many pieces of a complex puzzle, that is, identification of tomato metabolic processes related to Arbuscular Mycorrhiza formation and have revealed important changes to these pathways associated with *SlDLK2* RNA interference. Efforts are currently being done in order to perform complementary RNA-seq analyses on *SlDLK2* overexpressing plants which have important alterations in arbuscule morphology. As well the public access to the genomic sequences and expressed sequence tag resources of *R. irregularis* DAOM197198 (http://genome.jgi-psf.org/Rhiir2_1) offers the possibility to make a comparative study of differential expressed fungal genes under mycorrhizal wild type and *SlDKL2* transgenic hairy roots.

SlDLK2 protein is involved in signaling inhibition of arbuscule branching in tomato and then might function as a negative regulator of the mycorrhization process. Further research is required to confirm the direct relationships between the metabolic pathways alterations observed in our results and SlDLK2 protein activity. In this line of research, it would be interesting to analyze the interaction of SlDLK2 with DELLA protein or others regulator such as SMXL4, and to measure hexoses and cellulose contents on *SlDLK2* OE and RNAi mycorrhizal roots to confirm our speculations concerning a role of *SlDLK2* in inhibiting hexose production and inducing cellulose biosynthesis.

Bibliography

Abdel-Motaal FF, El-Zayat SA, Kosaka Y, El-Sayed MA, Kashima R, Maeda Y, Nassar MS, Ito S-i (2010) Antifungal activities of hyoscyamine and scopolamine against two major rice pathogens: *Magnaporthe oryzae* and *Rhizoctonia solani*. Journal of general plant pathology 76 (2):102-111

Allen MF, Moore Jr TS, Christensen M (1980) Phytohormone changes in *Bouteloua gracilis* infected by vesicular–arbuscular mycorrhizae: I. Cytokinin increases in the host plant. Can J Bot 58 (3):371-374

Anders S, Huber W (2010) Differential expression analysis for sequence count data. Genome Biol 11 (10):R106

Anders S, Pyl PT, Huber W (2015) HTSeq—a Python framework to work with high-throughput sequencing data. Bioinformatics 31 (2):166-169

Araújo WL, Tohge T, Ishizaki K, Leaver CJ, Fernie AR (2011) Protein degradation–an alternative respiratory substrate for stressed plants. Trends Plant Sci 16 (9):489-498

Arimura G-i, Ozawa R, Shimoda T, Nishioka T (2000) Herbivory-induced volatiles elicit defence genes in lima bean leaves. Nature 406 (6795):512

Aroca R, Ruiz-Lozano JM, Zamarreño ÁM, Paz JA, García-Mina JM, Pozo MJ, López-Ráez JA (2013) Arbuscular mycorrhizal symbiosis influences strigolactone production under salinity and alleviates salt stress in lettuce plants. J Plant Physiol 170 (1):47-55

Balestrini R, Gómez-Ariza J, Lanfranco L, Bonfante P (2007) Laser microdissection reveals that transcripts for five plant and one fungal phosphate transporter genes are contemporaneously present in arbusculated cells. Mol Plant-Microbe Interact 20 (9):1055-1062

Barker SJ, Tagu D (2000) The roles of auxins and cytokinins in mycorrhizal symbioses. J Plant Growth Regul 19 (2):144-154

Beisson F, Li Y, Bonaventure G, Pollard M, Ohlrogge JB (2007) The acyltransferase GPAT5 is required for the synthesis of suberin in seed coat and root of Arabidopsis. Plant Cell 19 (1):351-368

Boldt K, Pörs Y, Haupt B, Bitterlich M, Kühn C, Grimm B, Franken P (2011) Photochemical processes, carbon assimilation and RNA accumulation of sucrose transporter genes in tomato arbuscular mycorrhiza. J Plant Physiol 168 (11):1256-1263

Bonfante-Fasolo P (1984) Anatomy and morphology of VA mycorrhizae.

Breuillin-Sessoms F, Floss DS, Gomez SK, Pumplin N, Ding Y, Levesque-Tremblay V, Noar RD, Daniels DA, Bravo A, Eaglesham JB (2015) Suppression of arbuscule degeneration in *Medicago truncatula* phosphate transporter4 mutants is dependent on the ammonium transporter 2 family protein *AMT2;3*. Plant Cell 27 (4):1352-1366

Breuillin F, Schramm J, Hajirezaei M, Ahkami A, Favre P, Druege U, Hause B, Bucher M, Kretzschmar T, Bossolini E, Kuhlemeier C, Martinoia E, Franken P, Scholz U, Reinhardt D (2010) Phosphate systemically inhibits development of arbuscular mycorrhiza in *Petunia hybrida* and represses genes involved in mycorrhizal functioning. Plant J 64 (6):1002-1017. doi:10.1111/j.1365-313X.2010.04385.x

Carver T, Zeyen R, Bushnell W, Robbins M (1994) Inhibition of phenylalanine ammonia lyase and cinnamyl alcohol dehydrogenase increases quantitative susceptibility of barley to powdery mildew (Erysiphe graminis DC). Physiol Mol Plant Pathol 44 (4):261-272

Cipollone R, Ascenzi P, Visca P (2007) Common themes and variations in the rhodanese superfamily. IUBMB life 59 (2):51-59

Cosme M, Ramireddy E, Franken P, Schmülling T, Wurst S (2016) Shoot-and root-borne cytokinin influences arbuscular mycorrhizal symbiosis. Mycorrhiza 26 (7):709-720

Cosme M, Wurst S (2013) Interactions between arbuscular mycorrhizal fungi, rhizobacteria, soil phosphorus and plant cytokinin deficiency change the root morphology, yield and quality of tobacco. Soil Biol Biochem 57:436-443

Chabaud M, Boisson-Dernier A, Zhang J, Taylor CG, Yu O, Barker DG (2006) *Agrobacterium rhizogenes*-mediated root transformation. The *Medicago truncatula* handbook, version November

Chabot S, Bécard G, Piché Y (1992) Life cycle of *Glomus intraradix* in root organ culture. Mycologia:315-321

Chalker-Scott L (1999) Environmental significance of anthocyanins in plant stress responses. Photochem Photobiol 70 (1):1-9

Chen A, Gu M, Sun S, Zhu L, Hong S, Xu G (2011) Identification of two conserved cis-acting elements, MYCS and P1BS, involved in the regulation of mycorrhiza-activated phosphate transporters in eudicot species. New Phytol 189 (4):1157-1169

Chen F, Ro D-K, Petri J, Gershenzon J, Bohlmann J, Pichersky E, Tholl D (2004) Characterization of a root-specific Arabidopsis terpene synthase responsible for the formation of the volatile monoterpene 1, 8-cineole. Plant Physiol 135 (4):1956-1966

Dangles O, Fargeix G, Dufour C (2000) Antioxidant properties of anthocyanins and tannins: a mechanistic investigation with catechin and the 3′, 4′, 7-trihydroxyflavylium ion. Journal of the Chemical Society, Perkin Transactions 2 (8):1653-1663

Datta SK, Muthukrishnan S (1999) Pathogenesis-related proteins in plants. CRC press,

Delaux PM, Bécard G, Combier JP (2013) NSP1 is a component of the Myc signaling pathway. New Phytol 199 (1):59-65

Demchenko K, Winzer T, Stougaard J, Parniske M, Pawlowski K (2004) Distinct roles of *Lotus japonicus SYMRK* and *SYM15* in root colonization and arbuscule formation. New Phytol 163 (2):381-392

Farré-Armengol G, Filella I, Llusià J, Peñuelas J (2017) β-Ocimene, a Key Floral and Foliar Volatile Involved in Multiple Interactions between Plants and Other Organisms. Molecules 22 (7):1148

Fiorilli V, Catoni M, Miozzi L, Novero M, Accotto GP, Lanfranco L (2009) Global and cell-type gene expression profiles in tomato plants colonized by an arbuscular mycorrhizal fungus. New Phytol 184 (4):975-987

Floss DS, Levy JG, Lévesque-Tremblay V, Pumplin N, Harrison MJ (2013) DELLA proteins regulate arbuscule formation in arbuscular mycorrhizal symbiosis. Proc Natl Acad Sci 110 (51):E5025-E5034

Fontana A, Reichelt M, Hempel S, Gershenzon J, Unsicker SB (2009) The effects of arbuscular mycorrhizal fungi on direct and indirect defense metabolites of Plantago lanceolata L. J Chem Ecol 35 (7):833-843

Foo E, Ross JJ, Jones WT, Reid JB (2013) Plant hormones in arbuscular mycorrhizal symbioses: an emerging role for gibberellins. Ann Bot 111 (5):769-779

Franke R, Schreiber L (2007) Suberin—a biopolyester forming apoplastic plant interfaces. Curr Opin Plant Biol 10 (3):252-259

Fusconi A (2013) Regulation of root morphogenesis in arbuscular mycorrhizae: what role do fungal exudates, phosphate, sugars and hormones play in lateral root formation? Ann Bot 113 (1):19-33

Gange A, West H (1994) Interactions between arbuscular mycorrhizal fungi and foliar-feeding insects in Plantago lanceolata L. New Phytol 128 (1):79-87

García-Garrido JM, Ocampo JA (2002) Regulation of the plant defence response in arbuscular mycorrhizal symbiosis. J Exp Bot 53 (373):1377-1386

García-Olmedo F, Molina A, Alamillo JM, Rodríguez-Palenzuéla P (1998) Plant defense peptides. Peptide Science 47 (6):479-491

García Garrido JM, León Morcillo RJ, Martín Rodríguez JA, Ocampo Bote JA (2010) Variations in the mycorrhization characteristics in roots of wild-type and ABA-deficient tomato are accompanied by specific transcriptomic alterations. Mol Plant-Microbe Interact 23 (5):651-664. doi:10.1094/MPMI-23-5-0651

Genre A, Bonfante P (1998) Actin versus tubulin configuration in arbuscule-containing cells from mycorrhizal tobacco roots. New Phytol 140 (4):745-752

Genre A, Chabaud M, Timmers T, Bonfante P, Barker DG (2005) Arbuscular mycorrhizal fungi elicit a novel intracellular apparatus in *Medicago truncatula* root epidermal cells before infection. Plant Cell 17 (12):3489-3499. doi:10.1105/tpc.105.035410

Genre A, Ivanov S, Fendrych M, Faccio A, Žárský V, Bisseling T, Bonfante P (2011) Multiple exocytotic markers accumulate at the sites of perifungal membrane biogenesis in arbuscular mycorrhizas. Plant Cell Physiol 53 (1):244-255

Ghorbanpour M, Ghafarzadegan R, Khavazi K, Hatami M (2013) Two main tropane alkaloids variations of black henbane (Hyoscyamus niger) under PGPRs inoculation and water deficit stress induction at flowering stage. Journal of Medicinal Plants 1 (45):29-42

Gianinazzi-Pearson V, Dumas-Gaudot E, Gollotte A, Alaoui AT, Gianinazzi S (1996) Cellular and molecular defence-related root responses to invasion by arbuscular mycorrhizal fungi. New Phytol 133 (1):45-57

Gobbato E, Marsh JF, Vernié T, Wang E, Maillet F, Kim J, Miller JB, Sun J, Bano SA, Ratet P (2012) A GRAS-type transcription factor with a specific function in mycorrhizal signaling. Curr Biol 22 (23):2236-2241

Guether M, Balestrini R, Hannah M, He J, Udvardi MK, Bonfante P (2009) Genome-wide reprogramming of regulatory networks, transport, cell wall and membrane biogenesis during arbuscular mycorrhizal symbiosis in Lotus japonicus. New Phytol 182 (1):200-212

Güimil S, Chang H-S, Zhu T, Sesma A, Osbourn A, Roux C, Ioannidis V, Oakeley EJ, Docquier M, Descombes P (2005) Comparative transcriptomics of rice reveals an ancient pattern of response to microbial colonization. Proc Natl Acad Sci 102 (22):8066-8070

Gutjahr C, Parniske M (2013) Cell and developmental biology of arbuscular mycorrhiza symbiosis. Annu Rev Cell Dev Biol 29

Gutjahr C, Paszkowski U (2009) Weights in the balance: jasmonic acid and salicylic acid signaling in root-biotroph interactions. Mol Plant-Microbe Interact 22 (7):763-772

Heck C, Kuhn H, Heidt S, Walter S, Rieger N, Requena N (2016) Symbiotic fungi control plant root cortex development through the novel GRAS transcription factor MIG1. Curr Biol 26 (20):2770-2778

Hildebrandt TM, Nesi AN, Araújo WL, Braun H-P (2015) Amino acid catabolism in plants. Mol plant 8 (11):1563-1579

Hirano K, Ueguchi-Tanaka M, Matsuoka M (2008) GID1-mediated gibberellin signaling in plants. Trends Plant Sci 13 (4):192-199

Hodge A, Campbell CD, Fitter AH (2001) An arbuscular mycorrhizal fungus accelerates decomposition and acquires nitrogen directly from organic material. Nature 413 (6853):297-299

Hohnjec N, Czaja-Hasse LF, Hogekamp C, Küster H (2015) Pre-announcement of symbiotic guests: transcriptional reprogramming by mycorrhizal lipochitooligosaccharides shows a strict co-dependency on the GRAS transcription factors NSP1 and RAM1. BMC Genomics 16 (1):994

Hohnjec N, Vieweg MF, Pühler A, Becker A, Küster H (2005) Overlaps in the transcriptional profiles of *Medicago truncatula* roots inoculated with two different *Glomus* fungi provide insights into the genetic program activated during arbuscular mycorrhiza. Plant Physiol 137 (4):1283-1301

Honggang WGW (1989) Effects of VA mycorrhizal fungi on growth, nutrient uptake and effective compounds in Chinese medicinal herb *Datura stramonium* L. Scientia Agricultura Sinica 5:008

Huang W, Xian Z, Kang X, Tang N, Li Z (2015) Genome-wide identification, phylogeny and expression analysis of GRAS gene family in tomato. BMC Plant Biol 15 (1):209

Ismond KP, Dolferus R, De Pauw M, Dennis ES, Good AG (2003) Enhanced low oxygen survival in *Arabidopsis* through increased metabolic flux in the fermentative pathway. Plant Physiol 132 (3):1292-1302

Jahromi F, Aroca R, Porcel R, Ruiz-Lozano JM (2008) Influence of salinity on the in vitro development of *Glomus intraradices* and on the in vivo physiological and molecular responses of mycorrhizal lettuce plants. Microb Ecol 55 (1):45

Jin Y, Liu H, Luo D, Yu N, Dong W, Wang C, Zhang X, Dai H, Yang J, Wang E (2016) DELLA proteins are common components of symbiotic rhizobial and mycorrhizal signalling pathways. Nat Commun 7

Jones JM, Clairmont L, Macdonald ES, Weiner CA, Emery RN, Guinel FC (2015) *E151* (*sym15*), a pleiotropic mutant of pea (*Pisum sativum* L.), displays low nodule number, enhanced mycorrhizae, delayed lateral root emergence, and high root cytokinin levels. J Exp Bot 66 (13):4047-4059

Joung JG, Corbett AM, Fellman SM, Tieman DM, Klee HJ, Giovannoni JJ, Fei Z (2009) Plant MetGenMAP: an integrative analysis system for plant systems biology. Plant Physiol 151 (4):1758-1768. doi:10.1104/pp.109.145169

Kapoor R, Singh N (2017) Arbuscular Mycorrhiza and Reactive Oxygen Species. In: Arbuscular Mycorrhizas and Stress Tolerance of Plants. Springer, pp 225-243

Keeling CI, Bohlmann J (2006) Genes, enzymes and chemicals of terpenoid diversity in the constitutive and induced defence of conifers against insects and pathogens. New Phytol 170 (4):657-675

Laffont C, Rey T, André O, Novero M, Kazmierczak T, Debellé F, Bonfante P, Jacquet C, Frugier F (2015) The CRE1 cytokinin pathway is differentially recruited depending on *Medicago truncatula* root environments and negatively regulates resistance to a pathogen. PloS one 10 (1):e0116819

Lévy J, Bres C, Geurts R, Chalhoub B, Kulikova O, Duc G, Journet E-P, Ané J-M, Lauber E, Bisseling T (2004) A putative Ca2+ and calmodulin-dependent protein kinase required for bacterial and fungal symbioses. Science 303 (5662):1361-1364

Liang B, Li C, Ma C, Wei Z, Wang Q, Huang D, Chen Q, Li C, Ma F (2017) Dopamine alleviates nutrient deficiency-induced stress in Malus hupehensis. Plant Physiol Biochem 119:346-359

Liu J, Blaylock LA, Endre G, Cho J, Town CD, VandenBosch KA, Harrison MJ (2003) Transcript profiling coupled with spatial expression analyses reveals genes involved in distinct developmental stages of an arbuscular mycorrhizal symbiosis. Plant Cell 15 (9):2106-2123

López-Ráez JA, Verhage A, Fernandez I, Garcia JM, Azcón-Aguilar C, Flors V, Pozo MJ (2010) Hormonal and transcriptional profiles highlight common and differential host responses to arbuscular mycorrhizal fungi and the regulation of the oxylipin pathway. J Exp Bot 61 (10):2589-2601. doi:10.1093/jxb/erq089

Maillet F, Poinsot V, André O, Puech-Pagès V, Haouy A, Gueunier M, Cromer L, Giraudet D, Formey D, Niebel A (2011) Fungal lipochitooligosaccharide symbiotic signals in arbuscular mycorrhiza. Nature 469 (7328):58

Manthey K, Krajinski F, Hohnjec N, Firnhaber C, Pühler A, Perlick AM, Küster H (2004) Transcriptome profiling in root nodules and arbuscular mycorrhiza identifies a collection of novel genes induced during *Medicago truncatula* root endosymbioses. Mol Plant-Microbe Interact 17 (10):1063-1077

Martin-Rodriguez JA, Huertas R, Ho-Plagaro T, Ocampo JA, Tureckova V, Tarkowska D, Ludwig-Muller J, Garcia-Garrido JM (2016) Gibberellin-Abscisic Acid Balances during Arbuscular Mycorrhiza Formation in Tomato. Frontiers in plant science 7:1273. doi:10.3389/fpls.2016.01273

Martín-Rodríguez JÁ, Ocampo JA, Molinero-Rosales N, Tarkowská D, Ruíz-Rivero O, García-Garrido JM (2015) Role of gibberellins during arbuscular mycorrhizal formation in tomato: new insights revealed by endogenous quantification and genetic analysis of their metabolism in mycorrhizal roots. Physiol Plant 154 (1):66-81

Mazzeo MF, Cacace G, Ferriello F, Puopolo G, Zoina A, Ercolano MR, Siciliano RA (2014) Proteomic investigation of response to forl infection in tomato roots. Plant Physiol Biochem 74:42-49

Medina JH, Gagnon H, Piché Y, Ocampo JA, Garcí JM, Vierheilig H (2003) Root colonization by arbuscular mycorrhizal fungi is affected by the salicylic acid content of the plant. Plant Sci 164 (6):993-998

Mithran M, Paparelli E, Novi G, Perata P, Loreti E (2014) Analysis of the role of the pyruvate decarboxylase gene family in Arabidopsis thaliana under low-oxygen conditions. Plant Biol 16 (1):28-34

Mittler R, Vanderauwera S, Gollery M, Van Breusegem F (2004) Reactive oxygen gene network of plants. Trends Plant Sci 9 (10):490-498

Nakamura H, Xue Y-L, Miyakawa T, Hou F, Qin H-M, Fukui K, Shi X, Ito E, Ito S, Park S-H (2013) Molecular mechanism of strigolactone perception by DWARF14. Nat Commun 4:2613

Niu Y, Zhao T, Xu X, Li J (2017) Genome-wide identification and characterization of GRAS transcription factors in tomato (*Solanum lycopersicum*). PeerJ 5:e3955. doi:10.7717/peerj.3955

Oldroyd GE (2013) Speak, friend, and enter: signalling systems that promote beneficial symbiotic associations in plants. Nat Rev Microbiol 11 (4):252-263

Ophir R, Pang X, Halaly T, Venkateswari J, Lavee S, Galbraith D, Or E (2009) Gene-expression profiling of grape bud response to two alternative dormancy-release stimuli expose possible links between impaired mitochondrial activity, hypoxia, ethylene-ABA interplay and cell enlargement. Plant Mol Biol 71 (4-5):403

Park H-J, Floss DS, Levesque-Tremblay V, Bravo A, Harrison MJ (2015) Hyphal branching during arbuscule development requires *RAM1*. Plant Physiol:pp. 01155.02015

Pedone-Bonfim MVL, da Silva FSB, Maia LC (2015) Production of secondary metabolites by mycorrhizal plants with medicinal or nutritional potential. Acta Physiol Plant 37 (2):27. doi:10.1007/s11738-015-1781-3

Phillips JM, Hayman D (1970) Improved procedures for clearing roots and staining parasitic and vesicular-arbuscular mycorrhizal fungi for rapid assessment of infection. Trans Br Mycol Soc 55 (1):158IN116-161IN118

Pumplin N, Harrison MJ (2009) Live-cell imaging reveals periarbuscular membrane domains and organelle location in Medicago truncatula roots during arbuscular mycorrhizal symbiosis. Plant Physiol 151 (2):809-819. doi:10.1104/pp.109.141879

Pumplin N, Mondo SJ, Topp S, Starker CG, Gantt JS, Harrison MJ (2010) *Medicago truncatula* Vapyrin is a novel protein required for arbuscular mycorrhizal symbiosis. Plant J 61 (3):482-494. doi:10.1111/j.1365-313X.2009.04072.x

Ranocha P, Dima O, Nagy R, Felten J, Corratgé-Faillie C, Novák O, Morreel K, Lacombe B, Martinez Y, Pfrunder S (2013) Arabidopsis WAT1 is a vacuolar auxin transport facilitator required for auxin homoeostasis. Nat Commun 4:2625

Ravnskov S, Wu Y, Graham JH (2003) Arbuscular mycorrhizal fungi differentially affect expression of genes coding for sucrose synthases in maize roots. New Phytol 157 (3):539-545

Rich MK, Courty PE, Roux C, Reinhardt D (2017) Role of the GRAS transcription factor *ATA/RAM1* in the transcriptional reprogramming of arbuscular mycorrhiza in *Petunia hybrida*. BMC Genomics 18 (1):589. doi:10.1186/s12864-017-3988-8

Rich MK, Schorderet M, Bapaume L, Falquet L, Morel P, Vandenbussche M, Reinhardt D (2015) The petunia GRAS transcription factor *ATA/RAM1* regulates symbiotic gene expression and fungal morphogenesis in arbuscular mycorrhiza. Plant Physiol 168 (3):788-797

Rittenberg D, Foster G (1940) A new procedure for quantitative analysis by isotope dilution, with application to the determination of amino acids and fatty acids. J Biol Chem 133:737-744

Rivero J, Gamir J, Aroca R, Pozo MJ, Flors V (2015) Metabolic transition in mycorrhizal tomato roots. Front Microbiol 6

Rouhier N, Gelhaye E, Jacquot J-P (2004) Plant glutaredoxins: still mysterious reducing systems. Cell Mol Life Sci 61 (11):1266-1277

Ruzicka DR, Hausmann NT, Barrios-Masias FH, Jackson LE, Schachtman DP (2012) Transcriptomic and metabolic responses of mycorrhizal roots to nitrogen patches under field conditions. Plant Soil 350 (1-2):145-162

Sakamoto A, Murata N (2002) The role of glycine betaine in the protection of plants from stress: clues from transgenic plants. Plant, Cell Environ 25 (2):163-171

Sauer N (2007) Molecular physiology of higher plant sucrose transporters. FEBS Lett 581 (12):2309-2317

Schaarschmidt S, González M-C, Roitsch T, Strack D, Sonnewald U, Hause B (2007) Regulation of arbuscular mycorrhization by carbon. The symbiotic interaction cannot be improved by increased carbon availability accomplished by root-specifically enhanced invertase activity. Plant Physiol 143 (4):1827-1840

Schliemann W, Ammer C, Strack D (2008) Metabolite profiling of mycorrhizal roots of *Medicago truncatula*. Phytochemistry 69 (1):112-146

Schreiber L (2010) Transport barriers made of cutin, suberin and associated waxes. Trends Plant Sci 15 (10):546-553

Schubert A, Allara P, Morte A (2004) Cleavage of sucrose in roots of soybean (Glycine max) colonized by an arbuscular mycorrhizal fungus. New Phytol 161 (2):495-501

Shachar-Hill Y, Pfeffer PE, Douds D, Osman SF, Doner LW, Ratcliffe RG (1995) Partitioning of intermediary carbon metabolism in vesicular-arbuscular mycorrhizal leek. Plant Physiol 108 (1):7-15

Shaul-Keinan O, Gadkar V, Ginzberg I, Grünzweig JM, Chet I, Elad Y, Wininger S, Belausov E, Eshed Y, Atzmon N (2002) Hormone concentrations in tobacco roots change during arbuscular mycorrhizal colonization with *Glomus intraradices*. New Phytol 154 (2):501-507

Shtark OY, Sulima AS, Zhernakov AI, Kliukova MS, Fedorina JV, Pinaev AG, Kryukov AA, Akhtemova GA, Tikhonovich IA, Zhukov VA (2016) Arbuscular mycorrhiza development in pea (*Pisum sativum* L.) mutants impaired in five early nodulation genes including putative orthologs of *NSP1* and *NSP2*. Symbiosis 68 (1-3):129-144

Shu B, Li W, Liu L, Wei Y, Shi S (2016) Transcriptomes of arbuscular mycorrhizal fungi and litchi host interaction after tree girdling. Front Microbiol 7

Siciliano V, Genre A, Balestrini R, Cappellazzo G, Pierre J, Bonfante P (2007) Transcriptome analysis of arbuscular mycorrhizal roots during development of the prepenetration apparatus. Plant Physiol 144 (3):1455-1466

Solaiman MZ, Saito M (1997) Use of sugars by intraradical hyphae of arbuscular mycorrhizal fungi revealed by radiorespirometry. New Phytol 136 (3):533-538

Soundappan I, Bennett T, Morffy N, Liang Y, Stanga JP, Abbas A, Leyser O, Nelson DC (2015) SMAX1-LIKE/D53 family members enable distinct MAX2-dependent responses to strigolactones and karrikins in Arabidopsis. Plant Cell 27 (11):3143-3159

Sperling P, Franke S, Lüthje S, Heinz E (2005) Are glucocerebrosides the predominant sphingolipids in plant plasma membranes? Plant Physiol Biochem 43 (12):1031-1038

Stanga JP, Morffy N, Nelson DC (2016) Functional redundancy in the control of seedling growth by the karrikin signaling pathway. Planta 243 (6):1397-1406

Stanga JP, Smith SM, Briggs WR, Nelson DC (2013) SUPPRESSOR OF MORE AXILLARY GROWTH2 1 controls seed germination and seedling development in *Arabidopsis*. Plant Physiol 163 (1):318-330

Szakiel A, Pączkowski C, Henry M (2011) Influence of environmental biotic factors on the content of saponins in plants. Phytochem Rev 10 (4):493-502

Taira J, Tsuchida E, Katoh MC, Uehara M, Ogi T (2015) Antioxidant capacity of betacyanins as radical scavengers for peroxyl radical and nitric oxide. Food Chem 166:531-536

Takeda N, Handa Y, Tsuzuki S, Kojima M, Sakakibara H, Kawaguchi M (2015) Gibberellins interfere with symbiosis signaling and gene expression and alter colonization by arbuscular mycorrhizal fungi in Lotus japonicus. Plant Physiol 167 (2):545-557

Takeda N, Sato S, Asamizu E, Tabata S, Parniske M (2009) Apoplastic plant subtilases support arbuscular mycorrhiza development in *Lotus japonicus*. Plant J 58 (5):766-777. doi:10.1111/j.1365-313X.2009.03824.x

Takeda N, Tsuzuki S, Suzaki T, Parniske M, Kawaguchi M (2013) CERBERUS and NSP1 of Lotus japonicus are common symbiosis genes that modulate arbuscular mycorrhiza development. Plant Cell Physiol 54 (10):1711-1723

Tanaka R, Tanaka A (2007) Tetrapyrrole biosynthesis in higher plants. Annu Rev Plant Biol 58:321-346

Tian C, Wan P, Sun S, Li J, Chen M (2004) Genome-wide analysis of the GRAS gene family in rice and *Arabidopsis*. Plant Mol Biol 54 (4):519-532. doi:10.1023/b:plan.0000038256.89809.57

Trapnell C, Pachter L, Salzberg SL (2009) TopHat: discovering splice junctions with RNA-Seq. Bioinformatics 25 (9):1105-1111

Trapnell C, Williams BA, Pertea G, Mortazavi A, Kwan G, Van Baren MJ, Salzberg SL, Wold BJ, Pachter L (2010) Transcript assembly and quantification by RNA-Seq reveals unannotated transcripts and isoform switching during cell differentiation. Nat Biotechnol 28 (5):511-515

Turrini A, Sbrana C, Pitto L, Ruffini Castiglione M, Giorgetti L, Briganti R, Bracci T, Evangelista M, Nuti M, Giovannetti M (2004) The antifungal Dm-AMP1 protein from *Dahlia merckii* expressed in *Solanum melongena* is released in root exudates and differentially affects pathogenic fungi and mycorrhizal symbiosis. New Phytol 163 (2):393-403

Urbanová T, Tarkowská D, Novák O, Hedden P, Strnad M (2013) Analysis of gibberellins as free acids by ultra performance liquid chromatography–tandem mass spectrometry. Talanta 112:85-94

Ussuf K, Laxmi N, Mitra R (2001) Proteinase inhibitors: plant-derived genes of insecticidal protein for developing insect-resistant transgenic plants. Curr Sci:847-853

Végh A, Incze N, Fábián A, Huo H, Bradford KJ, Balázs E, Soós V (2017) Comprehensive Analysis of DWARF14-LIKE2 (DLK2) Reveals Its Functional Divergence from Strigolactone-Related Paralogs. Front Plant Sci 8:1641

Wallner E-S, López-Salmerón V, Belevich I, Poschet G, Jung I, Grünwald K, Sevilem I, Jokitalo E, Hell R, Helariutta Y (2017) Strigolactone-and Karrikin-Independent SMXL Proteins Are Central Regulators of Phloem Formation. Curr Biol 27 (8):1241-1247

Wang E, Schornack S, Marsh JF, Gobbato E, Schwessinger B, Eastmond P, Schultze M, Kamoun S, Oldroyd GE (2012) A common signaling process that promotes mycorrhizal and oomycete colonization of plants. Curr Biol 22 (23):2242-2246

Wang L, Wang B, Jiang L, Liu X, Li X, Lu Z, Meng X, Wang Y, Smith SM, Li J (2015) Strigolactone Signaling in Arabidopsis Regulates Shoot Development by Targeting D53-Like SMXL Repressor Proteins for Ubiquitination and Degradation. Plant Cell 27 (11):3128-3142. doi:10.1105/tpc.15.00605

Wróbel-Kwiatkowska M, Starzycki M, Zebrowski J, Oszmiański J, Szopa J (2007) Lignin deficiency in transgenic flax resulted in plants with improved mechanical properties. J Biotechnol 128 (4):919-934

Wu YY, Hou BH, Lee WC, Lu SH, Yang CJ, Vaucheret H, Chen HM (2017) DCL2-and RDR6-dependent transitive silencing of SMXL4 and SMXL5 in Arabidopsis dcl4 mutants causes defective phloem transport and carbohydrate over-accumulation. Plant J

Wurst S, Dugassa-Gobena D, Langel R, Bonkowski M, Scheu S (2004) Combined effects of earthworms and vesicular–arbuscular mycorrhizas on plant and aphid performance. New Phytol 163 (1):169-176

Xue L, Cui H, Buer B, Vijayakumar V, Delaux P-M, Junkermann S, Bucher M (2015) Network of GRAS transcription factors involved in the control of arbuscule development in Lotus japonicus. Plant Physiol 167 (3):854-871

Yano K, Yoshida S, Müller J, Singh S, Banba M, Vickers K, Markmann K, White C, Schuller B, Sato S (2008) CYCLOPS, a mediator of symbiotic intracellular accommodation. Proc Natl Acad Sci 105 (51):20540-20545

Yao R, Ming Z, Yan L, Li S, Wang F, Ma S, Yu C, Yang M, Chen L, Chen L (2016) DWARF14 is a non-canonical hormone receptor for strigolactone. Nature 536 (7617):469-473

Yoshitomi K, Taniguchi S, Tanaka K, Uji Y, Akimitsu K, Gomi K (2016) Rice terpene synthase 24 (*OsTPS24*) encodes a jasmonate-responsive monoterpene synthase that produces an antibacterial γ-terpinene against rice pathogen. J Plant Physiol 191:120-126

Yu N, Luo D, Zhang X, Liu J, Wang W, Jin Y, Dong W, Liu J, Liu H, Yang W (2014) A DELLA protein complex controls the arbuscular mycorrhizal symbiosis in plants. Cell Res 24 (1):130

Yurkov A, Veselova S, Jacobi L, Stepanova G, Yemelyanov V, Kudoyarova G, Shishova M (2017) The effect of inoculation with arbuscular mycorrhizal fungus *Rhizophagus irregularis* on cytokinin content in a highly mycotrophic *Medicago lupulina* line under low phosphorus level in the soil. Plant Soil Environ 63 (11):519-524

Zhang L, Yang T, Li X, Hao H, Xu S, Cheng W, Sun Y, Wang C (2014) Cloning and characterization of a novel Athspr promoter specifically active in vascular tissue. Plant Physiol Biochem 78:88-96

Zhang Q, Blaylock LA, Harrison MJ (2010) Two *Medicago truncatula* half-ABC transporters are essential for arbuscule development in arbuscular mycorrhizal symbiosis. Plant Cell 22 (5):1483-1497

Zhang W, Yang L, Li M, Ma B, Yan C, Chen J (2015a) Omics-based comparative transcriptional profiling of two contrasting rice genotypes during early infestation by small brown planthopper. International journal of molecular sciences 16 (12):28746-28764

Zhang X, Pumplin N, Ivanov S, Harrison MJ (2015b) EXO70I Is Required for Development of a Sub-domain of the Periarbuscular Membrane during Arbuscular Mycorrhizal Symbiosis. Curr Biol 25 (16):2189-2195. doi:10.1016/j.cub.2015.06.075

Zhao LH, Zhou XE, Yi W, Wu Z, Liu Y, Kang Y, Hou L, de Waal PW, Li S, Jiang Y, Scaffidi A, Flematti GR, Smith SM, Lam VQ, Griffin PR, Wang Y, Li J, Melcher K, Xu HE (2015) Destabilization of strigolactone receptor DWARF14 by binding of ligand and E3-ligase signaling effector DWARF3. Cell Res 25 (11):1219-1236. doi:10.1038/cr.2015.122

Zhou F, Lin Q, Zhu L, Ren Y, Zhou K, Shabek N, Wu F, Mao H, Dong W, Gan L, Ma W, Gao H, Chen J, Yang C, Wang D, Tan J, Zhang X, Guo X, Wang J, Jiang L, Liu X, Chen W, Chu J, Yan C, Ueno K, Ito S, Asami T, Cheng Z, Wang J, Lei C, Zhai H, Wu C, Wang H, Zheng N, Wan J (2013) D14-SCF(D3)-dependent degradation of D53 regulates strigolactone signalling. Nature 504 (7480):406-410. doi:10.1038/nature12878

Zubek S, Rola K, Szewczyk A, Majewska ML, Turnau K (2015) Enhanced concentrations of elements and secondary metabolites in Viola tricolor L. induced by arbuscular mycorrhizal fungi. Plant Soil 390 (1):129-142. doi:10.1007/s11104-015-2388-6

General Discussion

The formation of AM in plant roots is a complex and tightly regulated process. Establishment of the association requires a signal exchange, in which plant-derived strigolactones are perceived by the AM fungi (Akiyama et al. 2005b), which in turn produce a mixture of chitooligosaccharides and lipochitooligosaccharides that appear to function as fungal signalling molecules that activate the symbiosis signalling pathway, a plant signalling process necessary for establishment of the AM symbiosis (Maillet et al. 2011; Genre et al. 2013; Sun et al. 2015).

To accommodate the fungal structures, the host cell undergoes drastic subcellular changes. Molecular and genetic tools for the study of AM fungi are very limited and as such very little is known about the fungal molecular mechanisms that control the development of mycorrhizal infection structures inside plant roots. Interestingly, recent research on genome assembly and gene annotation of different isolates of the model strain *R. irregularis* has showed remarkable genome variations that affects all gene ontology terms and Pfam protein domains, as well as putative mycorrhiza-induced small secreted effector-like proteins (SPs) and other symbiosis differentially expressed genes (Chen et al. 2018). Additionally, recent data indicate that although most expressed SPs of *R. irregularis* show equal expression levels in the interaction with all host plants assayed, a subset shows significant differential expression depending on the host plant. Furthermore, SPs expression is controlled locally in the hyphal network in response to host dependent cues (Zeng et al. 2018). The next and exciting challenges will be to functionally study the role of such candidate effector proteins in symbiosis.

On the side of the plant, much greater progress has been made in understanding how the plant orchestrates the symbiosis process. Cellular reprograming and transcriptional regulation mechanisms have been described to accommodate plant roots to arbuscular mycorrhizal symbiosis, particularly in those root cells that harbour the arbuscules, the site of nutrient transfer between the plant and the fungus that are therefore of crucial importance for the AM symbiosis (Harrison 2012; Pimprikar and Gutjahr 2018).

The different chapters of this Thesis have dealt exhaustively different aspects on regulation of arbuscule development and function in tomato plants. Instead, in this section we show an integrative brief discussion of the current knowledge and the contribution of this work in the processes that lead to AM fungal colonization, focusing on arbuscule development and regulation.

Cytological rearrangements during arbuscule development

Two main events take place during early stages of fungal entry into the epidermis, the formation by the host cell of the pre-penetration apparatus (PPA) that is accompanied by nuclear movement, and the occurrence of low frequency nuclear calcium spiking in outer cortical cells (Genre et al. 2005; Sieberer et al. 2012). Once the fungus enters the PPA, the frequency of calcium spiking increases. PPA formation is not exclusive for epidermal cells, since it is also observed during arbuscule development in cortical cells (Genre et al. 2008).

The development of arbuscule-containing cells is accompanied by the fragmentation of the large central vacuole into a tubular network, nuclear movement, vesicle trafficking and membrane protein localization (Pumplin and Harrison 2009; Harrison 2012). Plastids and mitochondria increase in number and assemble around the arbuscule (Fester et al. 2001; Lohse et al. 2005; Hans et al. 2004) which could be a reflection of the increment of metabolic activity in these organelles during arbuscule formation and function. The plant cell nucleus increases in size, as a sign of the massive transcriptional reprogramming, which is observed prior to and during arbuscule formation (Pimprikar and Gutjahr 2018). Accompanying these cytological changes, the cytoskeleton reorganizes extensively in arbuscule-containing cells (Genre and Bonfante 1998; Blancaflor et al. 2001; Genre et al. 2008). Different types of microtubule and actin filament patterns were observed in arbuscule-containing cells (Timonen and Peterson 2002) and both actin filaments and microtubules form a dense array around the arbuscule branches (Carling and Brown 1982; Blancaflor et al. 2001) Balestrini et al. 1992. But also, the microtubules in cells adjacent to arbuscules or in contact with intercellular hyphae are also

reorganised suggesting an active role of the plant cytoskeleton in mycorrhization rather than passive reaction to the physical pressure created by the fungus invaginating the plant plasma membrane (Blancaflor et al. 2001).

The developing arbuscules are continuously surrounded by a plant-derived membrane, called the peri-arbuscular membrane (PAM) (Gutjahr and Parniske 2013), which separates the fungal hyphae from the host cytoplasm and serves as the interface for nutrient exchange between the symbionts (Luginbuehl et al. 2017; MacLean et al. 2017). Two different periarbuscular membrane domains has been defined, the truck domain that forms the base of the arbuscule and contains proteins that are also present in the plasma membrane, and the branch domain that envelops the fine hyphal branches of the arbuscule and harbours an exclusive and specialized set of proteins which are mainly involved in nutrient exchange between the plant and the fungus (Pumplin and Harrison 2009). The accumulation of the ER, Golgi stacks and the trans-Golgi network around the arbuscule branches during arbuscule formation and other evidences (Genre et al. 2011; Ivanov et al. 2012; Zhang et al. 2015b; Pan et al. 2016) indicate a predominant role for exocytosis in the construction of the PAM and delivery of PAM resident proteins (reviewed in Harrison and Ivanov (2017) and supported by several studies . Some components of the secretion pathway were shown to be required for periarbuscular membrane formation, including SNARE proteins and the EXO70I subunit of the exocyst coplex. EXO70I has been shown to be required for the efficient incorporation of two ABC transporter subfamily G (ABCG) proteins, STR and STR2, into the periarbuscular membrane (Zhang et al. 2015b; Zhang et al. 2010; Gutjahr et al. 2012), and EXO70I partially co-localizes, and physically interacts, with a plant-specific protein called VAPYRIN (Zhang et al. 2015b). The localization and domain structure of VAPYRIN suggest that it might have a structural role in the rearrangement of cell cytoplasm and/or the formation of the periarbuscular membrane during hyphal colonization (Feddermann et al. 2010; Pumplin et al. 2010; Feddermann and Reinhardt 2011). It seems that the deposition of periarbuscular membrane-localised proteins depends on their time of expression as well as the redirection of the secretion pathway to the periarbuscular membrane.

Then, presumable, the function of cytoskeleton during arbuscule formation is related to this exocytosis activity due that cytoskeleton participates in vesicle trafficking in plant cells of cell wall material (Zhu et al. 2015; Oda et al. 2014; Kong et al. 2015) and membranous cargoes (Yamada et al. 2017). Arbuscule development has been reported to be accompanied by specific vesicle trafficking (Zhang et al. 2015b; Gavrin et al. 2016; Huisman et al. 2016; Harrison and Ivanov 2017) but, to date, it is not clear whether the strong cytoskeletal modifications observed in mycorrhizal root cells are related to high intracellular trafficking levels and to membrane and cell wall polarization in these AM colonized roots.

In this work we have identified the mycorrhizal-responsive *tsb* gene among a *Solanaceae* family-specific group of Microtubule Associated Protein (MAPs) encoding genes which play an essential role in pollen development and have the capacity to restructure the microtubule cytoskeleton (Liu et al. 2009; Liu et al. 2013). We show that the tomato *tsb* gene is expressed in arbuscule-containing cells, which means that microtubule cytoskeleton remodelling may play a role during mycorrhization. *Tsb* gene overexpression clearly induces arbuscule activity rather than AM development, resulting in a significant enhancement of arbuscule-specific gene expression, including *RAM1, PT4, STR, AMT2.2* and *EXO84*, probably due to a greater arbuscule stability and/or lifespan associated to cytoskeleton alterations in the OE plants. Interestingly, our results provide initial proof of a relationship between cytoskeleton remodelling and periarbuscular membrane functionality in arbuscule-containing cells. It is also important to note that this study also provides an insight into the existence of specific biological machinery commonly shared by arbuscule-containing cells and the pollen tube, two cell types undergoing strong membrane polarization, as previously suggested by other authors (Nguema-Ona et al. 2012; Nouri and Reinhardt 2015).

Different levels of regulation of Arbuscule branching

The arbuscule is the symbiotic structure of nutrient exchange in MA association. It is an ephemeral structure (2-3 days), subjected to the succession of mechanisms of

formation and degeneration (Kobae and Hata 2010). All the processes that affect its formation and functionality are especially relevant for the efficiency of the symbiosis, measured in terms of benefit for the plant.

Fungal signals (chitooligosaccharides and lipochitooligosaccharides) and hormonal signals (through gibberellic-acid signalling) are thought to regulate transcription factors that control gene expression during arbuscule development. Extensive transcriptional changes are induced during the formation of arbuscules, and many genes involved in nutrient transport, primary and specialised metabolism, cell wall modification, the secretion pathway and signal transduction were found to be upregulated in arbuscule-containing cells (Gomez et al. 2009; Hohnjec et al. 2005; Gaude et al. 2012; Handa et al. 2015; Hogekamp and Küster 2013). A precise temporal and spatial regulation of gene expression is a key to proper arbuscule development. SYMBIOSIS RECEPTOR KINASE (SYMRK) (Endre et al. 2002; Stracke et al. 2002) is thought to act as a co-receptor in the recognition of fungal signals; the potassium channel DOESN'T MAKE INFECTIONS 1 (DMI1) and the calcium channel CNGC15 are located on the nuclear membrane and coordinate the induction of perinuclear calcium oscillations (Hogekamp and Küster 2013; Genre et al. 2008). CCaMK is activated by calcium oscillations and phosphorylates the transcription factor CYCLOPS. In a complex with DELLA proteins, CYCLOPS regulates the expression of RAM1, a GRAS domain transcription factor that is able to interact with several other GRAS-domain proteins, such as RAD1, and regulates the expression of genes involved in arbuscule development and nutrient exchange between the plant and the fungus, including several lipid-biosynthesis and export related genes such as *FatM*, *RAM2*, and STR (Luginbuehl et al. 2017; Gobbato et al. 2012; Park et al. 2015).

The closest homolog of RAM1 is RAD1. RAD1 also interacts with RAM1 in heterologous systems (Park et al. 2015; Xue et al. 2015). The phenotype of *L. japonicus rad1* mutants is similar to that of *ram1* (Xue et al. 2015). However, in *Medicago*, *rad1* mutants display a somewhat weaker phenotype that *ram1* (Park et al. 2015). It appears that the relative importance of RAM1 and RAD1 in supporting arbuscule development differs between *Lotus* and *Medicago* and this fact provides an evidence for a diversification in the regulatory networks between species.

Additionally, rice and *Medicago* RAM1 interact with DELLA INTERACTING PROTEIN1 (DIP1), and DIP1 also interacts with DELLA (Yu et al. 2014). The significance of these interactions in AM development is still unclear.

In the RNA-seq analysis performed here, we found that the tomato *SlGRAS27* gene was significantly induced upon AM inoculation in tomato. This is the putative homolog of *MtRAM1* and *PhATA/RAM* from *Medicago* and *Petunia*, respectively, where it is required for the morphogenesis of arbuscules (Rich et al. 2015), and to support arbuscule branching (Park et al. 2015). We identified also that tomato *SlGRAS28* is the homolog gene to *LjRAD1* from *Lotus*, whose mutation triggers an accelerated degeneration and a strongly reduced number of arbuscules (Xue et al. 2015). *SlGRAS28* is a closet homologous to *SlGRAS27*, and it was observed also to increase its gene expression under mycorrhizal conditions. In the HAM subfamily, we found that *SlGRAS47* is the homolog to *DIP1* genes from rice, *Medicago* and *Lotus*. Ours results suggest that also in tomato the mechanism of arbuscule branching is regulated by a number of common GRAS transcription factors. Now, mutual interactions and the importance and the individual role of each of them should be studied.

It is broadly known that the formation of AM is inhibited when there is high availability of Pi in the soil. This phenomenon has been widely studied, although the primary causes of this inhibition are not known (Balzergue et al. 2013). A recent study with mycorrhized rice plants, subjected to different doses of Pi and analysed after a short period of exposure to this nutrient, has shown that Pi treatment strongly inhibits the formation of new arbuscules, but does not affect the maintenance or function of the existing ones, which directs the action of Pi on the mechanism of generation of arbuscules (Kobae et al. 2016). It has been also proved that mycorrhization stimulates the metileritrol phosphate (MEP) pathway and consequently the metabolism of apocarotenoids in the root, and that at least a group of them, derived from cyclohexanones (CH), can have a regulatory role in the life cycle of arbuscules. Thus, it has been proposed that these compounds accelerate the senescence of mature arbuscules and make possible the replacement of old arbuscules by young and functional arbuscules, maintaining a high population of active arbuscules (Walter 2013). Nothing is known about whether CH-derivatives

production is induced by a still unknown signal generated in the mature arbuscules (e.g. lowering of the level of P exchanged), or whether this mechanism is nonspecific and inherent in the development of the arbuscule, . If it is true, however, that phosphorus deficiency stimulates the expression of apocarotenoid metabolism genes which code for carotenoid cleavage enzymes (carotenoid cleavage dioxygenases-CCDs) responsible for generation of these compounds.

In this context, we have identified here an□□□□□hydrolase protein, encoded by the *SlDKL2* gene induced in cells with arbuscules, and we have analysed the structural properties of this protein, as well as quantified its ability to bind to synthetic SLs. This protein is not a canonical receptor of SLs or Karrikins, although it has structural characteristics conducive to acting as a receptor for apocarotenoid compounds. Our results raised the idea of C13 α-ionol derivatives as potential candidates to bind SlDLK2, linking the production of ionone-related compounds with the regulation of the arbuscule formation. It is tenting to speculate that this signalling might be accomplished through binding of the SlDLK2 receptor, as supported by our thermal shift assays with the SlDLK2 protein and the α- and β-ionone compounds.

Functional analysis and molecular studies of RNAi and OE hairy roots performed here point out to a negative role of the AM inducible gene *SlDLK2* during mycorrhization, likely focused on inhibiting arbuscule hyphal branching. *SlDKL2* overexpression leads to the impossibility of arbuscules to branch. In agreement, comparative qPCR analysis reveals that this specific gene overexpression led to a down regulation in the expression of arbuscule-related genes encoding for periarbuscular membrane transporters or proteins involved in membrane trafficking, what might be related to the loss of periarbuscular membrane surrounding arbuscule fines branches.

Interesting, the expression of fungal ammonium transporters (AMT1; AMT2) appear not to be highly affected in an negative way, as happened with the plant transporters located at the periarbuscular membrane of *SlDLK2* OE plants, suggesting that ammonium uptake takes place not only in arbuscule branches. Similarly, the expression pattern of MST2 (mycorrhizal-induced high-affinity monosaccharide transporter from the AM fungus *R. irregularis*) indicates that sugar uptake takes

place also in intraradical hyphae (Helber et al. 2011). These results may indicate the less dependence of the arbuscule on the part of the AM fungus, which have the capacity to capture nutrients at different levels of its intraradical mycelium.

Several interesting aspects emerge from our study. Firstly, it would be of great interest to elucidate the chemical structure of the biological ligand of the SlDLK2 receptor and to establish its production dynamics during mycorrhization, as well as discover its direct role on the branching of the fungus. Secondly, and knowing that arbuscule branching is regulated by a number of GRAS transcription factors, it is very intriguing to know if there is a functional relationship between the regulatory system mediated by GRAS transcription factors and the regulation mediated by the production and action of specific apocarotenoids.

GRAS transcription factors: emerging actors in AM regulation

Genetic evidences show that nodulation in legumes and mycorrhization in most plant species share a common signalling pathway (Common Symbiosis Signaling Pathway-CSSP), where GRAS transcription factors (GRAS TFs), among other actors, have a relevant role. GRAS TFs play an important role as regulators of plant development, GA signalling, the response to stresses and, as we have mentioned, the regulation of symbiotic processes (Tian et al. 2004). In symbiosis, the first GRAS transcription factor characterized was NSP2 (Nodulation Signaling Pathway 2) that forms a DNA binding complex together with another GRAS factor, NSP1, activating the expression of early nodulation genes (Hirsch et al. 2009). NSP2 and NSP1 genes are also expressed during mycorrhization (Liu et al. 2011), and the interaction of NSP2 with RAM1 has been demonstrated (Gobbato et al. 2012). NSP1 and NSP2 regulate the expression of genes related to the biosynthesis of SLs and therefore can affect the stimulation of mycorrhization mediated by this hormone or other derived compounds, such as certain apocarotenoids. In fact, double *nsp1 / nsp2* mutants have low levels of strigolactones and low mycorrhization (Liu et al. 2011).

In recent years, the search for new inducible GRAS TFs during mycorrhization has been intensified (Heck et al. 2016; Xue et al. 2015), and the symbiotic role of some

of them has been demonstrated. Thus, the previously mentioned RAM1 is necessary for the branching of the arbuscule (Park et al. 2015); RAD1 (Required for Arbuscule Development 1) is essential for the maintenance and functionality of the arbuscules (Park et al. 2015); DIP1 (DELLA Interacting Protein 1) interacts with RAM1 and DELLA in rice for the control of the formation of arbuscules (Yu et al. 2014), and MIG1 (Mycorrhiza-Induced GRAS 1) is necessary for the remodelling in size and shape of the cortex cells, necessary for the accommodation of fungal arbuscule (Heck et al. 2016). MIG1 is able to interact with DELLA1, and it has been proposed that a MIG1–DELLA1 complex regulates root development to accommodate fungal infection structures during the AM symbiosis. MIG1 belongs to a novel clade of GRAS-domain proteins that is absent in the non-host *A. thaliana*, and several members of this clade are transcriptionally upregulated during mycorrhizal colonization, suggesting that additional GRAS-domain proteins could play a role in regulating AM development (Heck et al. 2016).

As mentioned above, DELLA proteins, which constitute a subfamily of GRAS transcription factors, are necessary for the regulation of the development of the arbuscule at different levels. Paradoxically, DELLA protein is also involved in the degeneration of arbuscules. It has been described the existence of a transcription regulatory complex formed by DELLA and NSP1 which, together with the transcription factor MYB1 (MYB-like family), form a regulatory module for the transcription of genes encoding proteins with hydrolytic activity (proteases, chitinases, etc.,) associated with the process of arbuscular degeneration (Floss et al. 2017). Therefore, the DELLA protein is involved both in the formation and the degeneration of arbuscules, which suggests that the same factors may participate in the formation of different transcription regulatory complexes (understood as the association of transcription factors) that modulate formation and degeneration of arbuscules and hence the importance of regulatory mechanisms for the formation of these regulatory complexes.

In the RNA-seq analysis performed here, we found an overall alteration in the expression of genes encoding for GRAS transcription factors, suggesting that the GRAS network have an essential role in the transcriptional reprogramming occurring in the tomato host cell during mycorrhization, as reported for other

species (Xue et al. 2015; Gobbato et al. 2012; Rich et al. 2015). We have identified here the symbiotic *RAM1, NSP1, NSP2, RAD1, MGI1,* and *DIP1* GRAS genes and their expression patterns corroborate their AM inducibility. Additionality, we have identified others GRAS factors, especially those of the SCR (SCARECROW), SCL3 (SCARECROW-LIKE3), or SHR (SHORT-ROOT) subfamilies, which increase their expression during mycorrhization, but have not yet been studied in terms of their possible role in the symbiotic process. Members of the SCR, SCL3 and SHR families form a regulating module in certain root development processes, and recently this module has been shown to interact with the GA-DELLA signalling (Zhang et al. 2011; Heo et al. 2011). Given the relevant role of GAs and DELLAs in AM formation and functioning, it is tenting to speculate that these new GRAS TFs may also take part of the complex system of regulation of the development of AM arbuscules on the roots.

Life cycle of Arbuscules: a working model

A regulation model of arbuscule formation/degradation we propose it is shown in Figure 1. After the initial signal exchange, fungal hyphae differentiate to form hyphopodia to enter host epidermal cell by the formation by the host cell of the pre-penetration apparatus and the occurrence of a low frequency nuclear calcium spiking in outer cortical cell. Intraradical fungal hyphae traverse epidermal cells and outer cortical cell layers to reach the inner cortex where arbuscules were formed.

The DELLA/GAs complex is a regulatory module for the formation/degradation of arbuscules on AM, and this complex is balanced according to the availability of Pi and the concentration of GAs, which directs the degradation of DELLA. In favourable situations of low availability of Pi and low levels of GAs, the integrated and coordinated action of symbiotic genes activated by calcium oscillations (CYCLOPS, CCaMK), DELLA and other possible GRAS transcription factors, including NSP1/2, activate the process of arbuscular formation, directed between others by RAM1. RAM1 itself is a transcriptional regulator and it is specifically involved in arbuscule development. In parallel, MIG1–DELLA complex regulates root development to accommodate fungal infection structures in host cells during the AM symbiosis.

The own development and functionality of the arbuscule propitiates an increase of Pi at the cellular level, and the activation of the synthesis of compounds derived from the MEP metabolism, including GAs and specific apocarotenoids, as well as its possible α,β-hydrolase protein receptors that could regulate the degree of arbuscule branching. The cell autonomous wave of GA accumulation triggers DELLA degradation and therefore arbuscule maintenance at the maturity state. However, high level of GAs promotes its own degradation mediated by the catabolism action of GA_2 oxidases that leads to a new accumulation of DELLA protein which now directs arbuscule degradation via specific hydrolases activated by the regulatory module DELLA-NSP1-MYB1. Therefore, a low gibberellin level would promote DELLA stability and consequently arbuscule formation (in non-colonized cells) or degradation (in cells with mature arbuscules), while a high gibberellin level would trigger DELLA degradation and therefore arbuscule maintenance at maturity. These events could be modulated by the relationship between DELLA and other possible GRAS factors (SCL3, SCR or SHR) that interact with the GA-DELLA signalling.

The degradation of the arbuscule implies the decrease of cellular Pi levels, the decrease of GA levels and the change in the relation of DELLA with other transcription factors, which altogether constitutes a propitious situation for the generation of a new arbuscular cycle. In short, the proposed hypothesis suggests that the formation/degeneration cycle of the arbuscules is directed by the integration and interaction of different regulatory elements, such as the dual role of DELLA modulated by GA homeostasis, the activity of multiple GRAS TFs, the cellular availability of Pi, and the generation of regulatory signals derived from the metabolism of apocarotenoids as well as their specific receptors (α,β-hydrolase-type receptors).

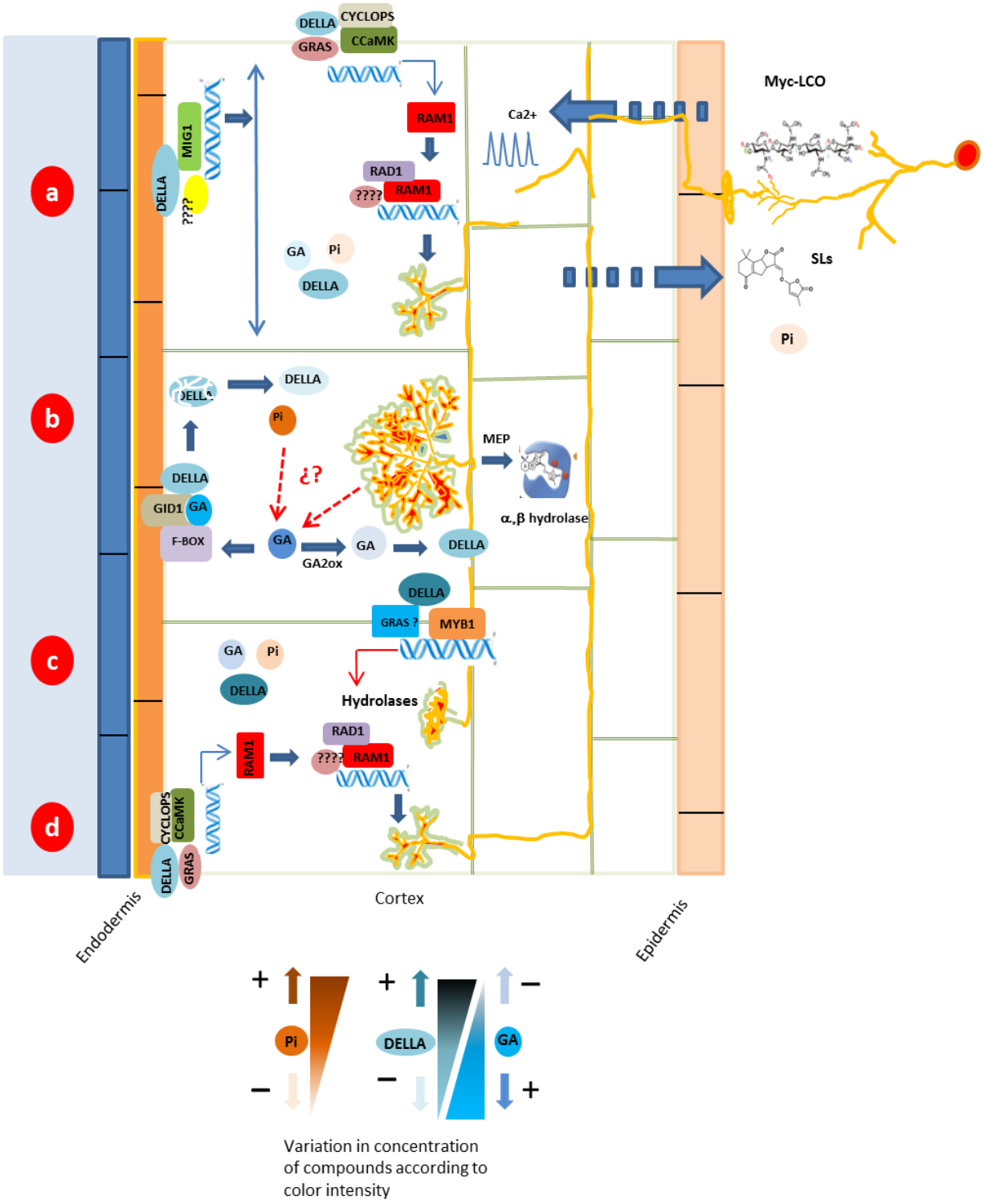

Figure 1. Regulation of arbuscule formation. (a) After perception of the AM fungal LCOs and COs, the CSSP is activated, which includes the phosphorylation of CYCLOPs by CCaMK, and the formation of a complex together with DELLA, that activates the expression of symbiotic genes such as *RAM1* involved in the formation of the arbuscule. Particularly RAM1, through the interaction with other GRAS TFs such as RAD1 is required for arbuscule morphogenesis and arbuscule branching. In this initiation of arbuscule formation Pi concentration is low, and then gibberellins (GAs) are also low, and available DELLA increases which, in a complex with MIG1, induces cell expansion for arbuscule formation (a). By contrast, in mature arbuscules, as nutritional exchange occurs, Pi concentration

increases and, consequently, GA levels are also higher. By one side, GA is perceived by the GID1 receptor, and DELLA degradation by an F-box protein is activated. However, by the other side GA activates the catabolism of GAs by a negative feedback mechanism, so DELLA level is counterbalanced. In addition, in mature arbuscules, the MEP pathway for the biosynthesis of apocarotenoids is activated, and the ligand of the DLK2 receptor might be synthesized in order to restrict arbuscule branching (b). Finally, when arbuscules became inactive, Pi supply and Pi levels decrease in the arbuscule containing cell, and then also GAs decrease and available DELLA increases. DELLA, in a complex with MYB1 and probably other TFs, is able to activate the expression of several hydrolases and other genes involved in arbuscule degeneration (c). When the arbuscule is completely degraded, the same cell is ready to host the initiation of a new arbuscule cycle (d). Pi, DELLA and GA contents in each stage are indicate following the color legend.

Conclusions/Conclusiones

Conclusions

1. *tsb* belongs to a Solanaceae-specific group of pollen-specific expressed genes encoding MAPs with an essential function in pollen development. *Tsb* gene is also specifically expressed in the arbuscule containing cells and has the ability to rearrange the MT cytoskeleton of the root cortical cells, pointing to the existence of a specific biological machinery commonly shared between two types of cells undergoing a strong membrane polarization, the arbuscule-containing cells and the pollen tube.
2. *tsb* has an essential role in arbuscule functionality, what provides the first hint of the role of the microtubule cytoskeleton rearrangements during mycorrhization.
3. *SlDLK2* is induced in arbuscular mycorrhizal roots and it is specifically expressed in arbuscule containing cells. It encodes for α,β-hydrolase protein closely related to the canonical receptors of strigolactones and karrikins (D14 and KAI2 receptors), and SlDLK2 conserves the catalytic triad and the associated hydrolytic activity, suggesting a role as signaling receptor. Although it cannot be ruled that the specific biological ligand of SlDLK2 might be a molecule with a butenolide ring, such as SLs or karrikins, our results raised the idea of C13 α-ionol derivatives as potential candidates to bind SlDLK2.
4. SlDLK2 acts as a negative regulator during mycorrhization, likely focused on inhibiting arbuscule hyphal branching, and then controlling mycorrhizal colonization at late stages of the symbiosis. Additionally, our results suggest that SlDLK2 might be also important to activate GA signaling, restrict hexose production and supply to the AM fungus, and induce a number of resistance mechanisms, in order to control AM fungal development.

Conclusiones

1. *El tsb* pertenece a un grupo de genes que se expresan específicamente en el polen y que codifican para MAPs con una función esencial en el desarrollo del polen
2. El *tsb* tiene un papel esencial en la funcionalidad del arbúsculo, lo que supone la primera prueba de la posible función que tienen las reorganizaciones del citosqueleto durante la micorrización.
3. SlDLK2 se induce en las raíces micorrizadas y se expresa específicamente en las células que contienen arbúsculos. Este gen codifica para una proteína α,β-hidrolasa muy cercanan filogenéticamente a los receptores canónicos de estrigolactonas y karrikinas (receptores D14 y KAI2), y SlDLK2 conserva la tríada catalítica y la actividad hidrolítica asociada, lo que sugiere que SlDLK2 podría desempeñar una función como receptor de señales. Aunque no se puede descartar que el ligando biológico específico de SlDLK2 sea una molécula con un anillo butenolide, tal y como las SLs y las karrikinas, nuestros resultados apuntan a los derivados C13 α-ionoles como candidatos potenciales a unir SlDLK2.
4. SlDLK2 actúa como un regulador negativo durante la micorrización, probablememte a través de la inhibición de la ramificación de los arbúsculos, y controla la colonización micorrícica en las etapas tardías de la simbiosis. Además, nuestros resultados sugieren que SlDLK2 podría ser también importante en la activación de la señalización por GAs, en la restricción de la producción y aporte de hexosas al hongo MA, y en la inducción de una serie de mecanismos de defensa, con el objetivo de controlar el desarrollo fúngico.

General Bibliography

Achard P, Cheng H, De Grauwe L, Decat J, Schoutteten H, Moritz T, Van Der Straeten D, Peng J, Harberd NP (2006) Integration of plant responses to environmentally activated phytohormonal signals. Science 311 (5757):91-94

Achard P, Liao L, Jiang C, Desnos T, Bartlett J, Fu X, Harberd NP (2007) DELLAs contribute to plant photomorphogenesis. Plant Physiol 143 (3):1163-1172

Achard P, Renou J-P, Berthomé R, Harberd NP, Genschik P (2008) Plant DELLAs restrain growth and promote survival of adversity by reducing the levels of reactive oxygen species. Curr Biol 18 (9):656-660

Aggarwal A, Kadian N, Tanwar A, Yadav A, Gupta K (2011) Role of arbuscular mycorrhizal fungi (AMF) in global sustainable development. Journal of Applied and Natural Science 3 (2):340-351

Akiyama K, Hayashi H (2006) Strigolactones: chemical signals for fungal symbionts and parasitic weeds in plant roots. Ann Bot 97 (6):925-931

Akiyama K, Matsuzaki K-i, Hayashi H (2005a) Plant sesquiterpenes induce hyphal branching in arbuscular mycorrhizal fungi. Nature 435 (7043):824-827

Akiyama K, Matsuzaki K, Hayashi H (2005b) Plant sesquiterpenes induce hyphal branching in arbuscular mycorrhizal fungi. Nature 435 (7043):824-827. doi:10.1038/nature03608

Al-Karaki GN, Hammad R, Rusan M (2001) Response of two tomato cultivars differing in salt tolerance to inoculation with mycorrhizal fungi under salt stress. Mycorrhiza 11 (1):43-47

Alexander T, Toth R, Meier R, Weber HC (1989) Dynamics of arbuscule development and degeneration in onion, bean, and tomato with reference to vesicular–arbuscular mycorrhizae in grasses. Can J Bot 67 (8):2505-2513

Amor BB, Shaw SL, Oldroyd GE, Maillet F, Penmetsa RV, Cook D, Long SR, Dénarié J, Gough C (2003) The NFP locus of Medicago truncatula controls an early step of Nod factor signal transduction upstream of a rapid calcium flux and root hair deformation. Plant J 34 (4):495-506

Amora-Lazcano E, Vazquez M, Azcon R (1998) Response of nitrogen-transforming microorganisms to arbuscular mycorrhizal fungi. Biol Fertility Soils 27 (1):65-70

Angle J, Heckman J (1986) Effect of soil pH and sewage sludge on VA mycorrhizal infection of soybeans. Plant Soil 93 (3):437-441

Aroca R, Ruiz-Lozano JM, Zamarreño ÁM, Paz JA, García-Mina JM, Pozo MJ, López-Ráez JA (2013) Arbuscular mycorrhizal symbiosis influences strigolactone production under salinity and alleviates salt stress in lettuce plants. J Plant Physiol 170 (1):47-55

Azcón-Aguilar C, Barea J (1997) Applying mycorrhiza biotechnology to horticulture: significance and potentials. Scientia Horticulturae 68 (1-4):1-24

Bago B, Pfeffer PE, Abubaker J, Jun J, Allen JW, Brouillette J, Douds DD, Lammers PJ, Shachar-Hill Y (2003) Carbon export from arbuscular mycorrhizal roots involves the translocation of carbohydrate as well as lipid. Plant Physiol 131 (3):1496-1507

Bago B, Pfeffer PE, Shachar-Hill Y (2000) Carbon metabolism and transport in arbuscular mycorrhizas. Plant Physiol 124 (3):949-958

Balemi T, Negisho K (2012) Management of soil phosphorus and plant adaptation mechanisms to phosphorus stress for sustainable crop production: a review. Journal of soil science and plant nutrition 12 (3):547-562

Balestrini R, Gómez-Ariza J, Lanfranco L, Bonfante P (2007) Laser microdissection reveals that transcripts for five plant and one fungal phosphate transporter genes are contemporaneously present in arbusculated cells. Mol Plant-Microbe Interact 20 (9):1055-1062

Baltruschat H (1987) Evaluation of the suitability of expanded clay as carrier material for VA mycorrhiza spores in field inoculation of maize. Angew Bot

Balzergue C, Chabaud M, Barker DG, Bécard G, Rochange SF (2013) High phosphate reduces host ability to develop arbuscular mycorrhizal symbiosis without affecting root calcium spiking responses to the fungus. Front Plant Sci 4:426

Baylis G (1975) The magnolioid mycorrhiza and mycotrophy in root systems derived from it. Pages 373–389in FE Sanders, B. Mosse, & PB Tinker (eds.), Endomycorrhizas. Academic Press, London. Google Scholar,

Bécard G, Doner L, Rolin D, Douds D, Pfeffer P (1991) Identification and quantification of trehalose in vesicular-arbuscular mycorrhizal fungi by in vivo13C NMR and HPLC analyses. New Phytol 118 (4):547-552

Bécard G, Fortin J (1988) Early events of vesicular–arbuscular mycorrhiza formation on Ri T-DNA transformed roots. New Phytol 108 (2):211-218

Beilby JP (1983) Effects of inhibitors on early protein, RNA, and lipid synthesis in germinating vesicular–arbuscular mycorrhizal fungal spores of Glomus caledonium. Canadian journal of microbiology 29 (5):596-601

Beilby JP, Kidby DK (1980) Biochemistry of ungerminated and germinated spores of the vesicular-arbuscular mycorrhizal fungus, *Glomus caledonius*: changes in neutral and polar lipids. J Lipid Res 21 (6):739-750

Benabdellah K, Merlos MA, Azcon-Aguilar C, Ferrol N (2009) GintGRX1, the first characterized glomeromycotan glutaredoxin, is a multifunctional enzyme that responds to oxidative stress. Fungal Genet Biol 46 (1):94-103. doi:10.1016/j.fgb.2008.09.013

Benhamou N, Fortin JA, Hamel C, St-Arnaud M, Shatilla A (1994) Resistance responses of mycorrhizal Ri T-DNA-transformed carrot roots to infection by Fusarium oxysporum f. sp. chrysanthemi. Phytopathology 84 (9):958-968

Besserer A, Bécard G, Jauneau A, Roux C, Séjalon-Delmas N (2008) GR24, a synthetic analog of strigolactones, stimulates the mitosis and growth of the arbuscular mycorrhizal fungus Gigaspora rosea by boosting its energy metabolism. Plant Physiol 148 (1):402-413

Besserer A, Puech-Pages V, Kiefer P, Gomez-Roldan V, Jauneau A, Roy S, Portais JC, Roux C, Becard G, Sejalon-Delmas N (2006) Strigolactones stimulate arbuscular mycorrhizal fungi by activating mitochondria. PLoS Biol 4 (7):e226. doi:10.1371/journal.pbio.0040226

Bitterlich M, Krügel U, Boldt-Burisch K, Franken P, Kühn C (2014a) Interaction of brassinosteroid functions and sucrose transporter SlSUT2 regulate the formation of arbuscular mycorrhiza. Plant Signal Behav 9 (10):e970426

Bitterlich M, Krügel U, Boldt-Burisch K, Franken P, Kühn C (2014b) The sucrose transporter SlSUT2 from tomato interacts with brassinosteroid functioning and affects arbuscular mycorrhiza formation. Plant J 78 (5):877-889

Blancaflor EB, Zhao L, Harrison MJ (2001) Microtubule organization in root cells of *Medicago truncatula* during development of an arbuscular mycorrhizal symbiosis with *Glomus versiforme*. Protoplasma 217 (4):154-165

Blanke V, Renker C, Wagner M, Füllner K, Held M, Kuhn AJ, Buscot F (2005) Nitrogen supply affects arbuscular mycorrhizal colonization of Artemisia vulgaris in a phosphate-polluted field site. New Phytol 166 (3):981-992

Boldt K, Pörs Y, Haupt B, Bitterlich M, Kühn C, Grimm B, Franken P (2011) Photochemical processes, carbon assimilation and RNA accumulation of sucrose transporter genes in tomato arbuscular mycorrhiza. J Plant Physiol 168 (11):1256-1263

Bonfante P, Requena N (2011) Dating in the dark: how roots respond to fungal signals to establish arbuscular mycorrhizal symbiosis. Curr Opin Plant Biol 14 (4):451-457

Bowen G (1980) Mycorrhizal roles in tropical plants and ecosystems. Mycorrhizal roles in tropical plants and ecosystems:165-190

Bravo A, Brands M, Wewer V, Dörmann P, Harrison MJ (2017) Arbuscular mycorrhiza-specific enzymes FatM and RAM2 fine-tune lipid biosynthesis to promote development of arbuscular mycorrhiza. New Phytol 214 (4):1631-1645

Bravo A, York T, Pumplin N, Mueller LA, Harrison MJ (2016) Genes conserved for arbuscular mycorrhizal symbiosis identified through phylogenomics. Nat Plants 2 (2):15208

Breuillin F, Schramm J, Hajirezaei M, Ahkami A, Favre P, Druege U, Hause B, Bucher M, Kretzschmar T, Bossolini E, Kuhlemeier C, Martinoia E, Franken P, Scholz U, Reinhardt D (2010) Phosphate systemically inhibits development of arbuscular mycorrhiza in *Petunia hybrida* and represses genes involved in mycorrhizal functioning. Plant J 64 (6):1002-1017. doi:10.1111/j.1365-313X.2010.04385.x

Bronick CJ, Lal R (2005) Soil structure and management: a review. Geoderma 124 (1-2):3-22

Brown M, King E (1982) Morphology and histology of vesicular-arbuscular mycorrhizae. A. Anatomy and cytology. Methods and principles of mycorrhizal research Amer Phytopath Soc: St Paul:15-21

Brundrett M, Bougher N, Dell B, Grove T (1996) Working Ylith Mycorrhizas in Forestry and Agriculture.

Brundrett MC (2002) Coevolution of roots and mycorrhizas of land plants. New Phytol 154 (2):275-304

Brundrett MC, Tedersoo L (2018) Evolutionary history of mycorrhizal symbioses and global host plant diversity. New Phytol

Buee M, Rossignol M, Jauneau A, Ranjeva R, Bécard G (2000) The pre-symbiotic growth of arbuscular mycorrhizal fungi is induced by a branching factor partially purified from plant root exudates. Mol Plant-Microbe Interact 13 (6):693-698

Buendia L, Wang T, Girardin A, Lefebvre B (2016) The LysM receptor-like kinase SlLYK10 regulates the arbuscular mycorrhizal symbiosis in tomato. New Phytol 210 (1):184-195

Calvet C, Pera J, Barea J (1993) Growth response of marigold *(Tagetes erecta* L.) to inoculation with *Glomus mosseae*, Trichoderma aureoviride and *Pythium ultimum* in a peat-perlite mixture. Plant Soil 148 (1):1-6

Campos-Soriano L, García-Martínez J, Segundo BS (2012) The arbuscular mycorrhizal symbiosis promotes the systemic induction of regulatory defence-related genes in rice leaves and confers resistance to pathogen infection. Mol Plant Pathol 13 (6):579-592

Camps C, Jardinaud MF, Rengel D, Carrère S, Hervé C, Debellé F, Gamas P, Bensmihen S, Gough C (2015) Combined genetic and transcriptomic analysis reveals three major signalling pathways activated by Myc-LCOs in Medicago truncatula. New Phytol 208 (1):224-240

Carling D, Brown M (1982) Anatomy and physiology of vesicular-arbuscular and nonmycorrhizal roots. Phytopathology 72 (8):1

Carotenuto G, Chabaud M, Miyata K, Capozzi M, Takeda N, Kaku H, Shibuya N, Nakagawa T, Barker DG, Genre A (2017) The rice LysM receptor-like kinase OsCERK1 is required for the perception of short-chain chitin oligomers in arbuscular mycorrhizal signaling. New Phytol 214 (4):1440-1446

Clark R (1997) Arbuscular mycorrhizal adaptation, spore germination, root colonization, and host plant growth and mineral acquisition at low pH. Plant Soil 192 (1):15-22

Conn CE, Nelson DC (2016) Evidence that KARRIKIN-INSENSITIVE2 (KAI2) receptors may perceive an unknown signal that is not karrikin or strigolactone. Front Plant Sci 6:1219

Cordier C, Pozo MJ, Barea J-M, Gianinazzi S, Gianinazzi-Pearson V (1998) Cell defense responses associated with localized and systemic resistance to *Phytophthora parasitica* induced in tomato by an arbuscular mycorrhizal fungus. Mol Plant-Microbe Interact 11 (10):1017-1028

Cosme M, Fernández I, Van der Heijden MG, Pieterse CM (2018) Non-mycorrhizal Plants: The Exceptions that Prove the Rule. Trends Plant Sci

Cosme M, Wurst S (2013) Interactions between arbuscular mycorrhizal fungi, rhizobacteria, soil phosphorus and plant cytokinin deficiency change the root morphology, yield and quality of tobacco. Soil Biol Biochem 57:436-443

Coughlan AP, Dalpé Y, Lapointe L, Piché Y (2000) Soil pH-induced changes in root colonization, diversity, and reproduction of symbiotic arbuscular mycorrhizal fungi from healthy and declining maple forests. Canadian Journal of Forest Research 30 (10):1543-1554

Couzigou J-M, Lauressergues D, André O, Gutjahr C, Guillotin B, Bécard G, Combier J-P (2017) Positive gene regulation by a natural protective miRNA enables arbuscular mycorrhizal symbiosis. Cell host & microbe 21 (1):106-112

Czaja LF, Hogekamp C, Lamm P, Maillet F, Martinez EA, Samain E, Dénarié J, Küster H, Hohnjec N (2012) Transcriptional responses toward diffusible signals from symbiotic microbes reveal MtNFP-and MtDMI3-dependent reprogramming of host gene expression by arbuscular mycorrhizal fungal lipochitooligosaccharides. Plant Physiol 159 (4):1671-1685

Chabaud M, Genre A, Sieberer BJ, Faccio A, Fournier J, Novero M, Barker DG, Bonfante P (2011) Arbuscular mycorrhizal hyphopodia and germinated spore exudates trigger Ca2+ spiking in the legume and nonlegume root epidermis. New Phytol 189 (1):347-355

Chabot S, Bécard G, Piché Y (1992) Life cycle of *Glomus intraradix* in root organ culture. Mycologia:315-321

Chen A, Gu M, Sun S, Zhu L, Hong S, Xu G (2011) Identification of two conserved cis-acting elements, MYCS and P1BS, involved in the regulation of mycorrhiza-activated phosphate transporters in eudicot species. New Phytol 189 (4):1157-1169

Chen EC, Morin E, Beaudet D, Noel J, Yildirir G, Ndikumana S, Charron P, St-Onge C, Giorgi J, Krüger M (2018) High intraspecific genome diversity in the model arbuscular mycorrhizal symbiont *Rhizophagus irregularis*. New Phytol

Chen S, Jin W, Liu A, Zhang S, Liu D, Wang F, Lin X, He C (2013) Arbuscular mycorrhizal fungi (AMF) increase growth and secondary metabolism in cucumber subjected to low temperature stress. Scientia Horticulturae 160:222-229

Dangeard P (1896) Une maladie du peuplier dans l'ouest de la France. Botaniste 58:38-43

Daniels B, Trappe JM (1980) Factors affecting spore germination of the vesicular-arbuscular mycorrhizal fungus, Glomus epigaeus. Mycologia:457-471

Davière J-M, Achard P (2013) Gibberellin signaling in plants. Development 140 (6):1147-1151

Davière J-M, Achard P (2016) A pivotal role of DELLAs in regulating multiple hormone signals. Mol plant 9 (1):10-20

Davison J, Moora M, Öpik M, Adholeya A, Ainsaar L, Bâ A, Burla S, Diedhiou A, Hiiesalu I, Jairus T (2015) Global assessment of arbuscular mycorrhizal fungus diversity reveals very low endemism. Science 349 (6251):970-973

De Mita S, Streng A, Bisseling T, Geurts R (2014) Evolution of a symbiotic receptor through gene duplications in the legume–rhizobium mutualism. New Phytol 201 (3):961-972

de Oliveira V, Garbaye J (1989) Microorganisms stimulating the establishment of mycorrhizal symbiosis. a review. Eur J For Pathol

Delaux P-M, Radhakrishnan GV, Jayaraman D, Cheema J, Malbreil M, Volkening JD, Sekimoto H, Nishiyama T, Melkonian M, Pokorny L (2015) Algal ancestor of land plants was preadapted for symbiosis. Proc Natl Acad Sci 112 (43):13390-13395

Delaux PM, Bécard G, Combier JP (2013) NSP1 is a component of the Myc signaling pathway. New Phytol 199 (1):59-65

Den Camp RO, Streng A, De Mita S, Cao Q, Polone E, Liu W, Ammiraju JS, Kudrna D, Wing R, Untergasser A (2011) LysM-type mycorrhizal receptor recruited for rhizobium symbiosis in nonlegume *Parasponia*. Science 331 (6019):909-912

Dermatsev V, WEINGARTEN-BAROR C, Resnick N, Gadkar V, Wininger S, Kolotilin I, MAYZLISH-GATI E, Zilberstein A, Koltai H, Kapulnik Y (2010) Microarray analysis and functional tests suggest the involvement of expansins in the early stages of symbiosis of the arbuscular mycorrhizal fungus Glomus intraradices on tomato (Solanum lycopersicum). Mol Plant Pathol 11 (1):121-135

Devers EA, Teply J, Reinert A, Gaude N, Krajinski F (2013) An endogenous artificial microRNA system for unraveling the function of root endosymbioses related genes in Medicago truncatula. BMC Plant Biol 13 (1):82

Dickie IA, Bolstridge N, Cooper JA, Peltzer DA (2010) Co-invasion by Pinus and its mycorrhizal fungi. New Phytol 187 (2):475-484

Dickson S (2004) The Arum–Paris continuum of mycorrhizal symbioses. New Phytol 163 (1):187-200

Doidy J, Grace E, Kühn C, Simon-Plas F, Casieri L, Wipf D (2012) Sugar transporters in plants and in their interactions with fungi. Trends Plant Sci 17 (7):413-422

Douds DD, Pfeffer PE, Shachar-Hill Y (2000) Carbon partitioning, cost, and metabolism of arbuscular mycorrhizas. In: Arbuscular mycorrhizas: physiology and function. Springer, pp 107-129

El Ghachtouli N, Martin-Tanguy J, Paynot M, Gianinazzi S (1996) First-report of the inhibition of arbuscular mycorrhizal infection of Pisum sativum by specific and irreversible inhibition of polyamine biosynthesis or by gibberellic acid treatment. FEBS Lett 385 (3):189-192

Endre G, Kereszt A, Kevei Z, Mihacea S, Kaló P, Kiss GB (2002) A receptor kinase gene regulating symbiotic nodule development. Nature 417 (6892):962

Etemadi M, Gutjahr C, Couzigou J-M, Zouine M, Lauressergues D, Timmers A, Audran C, Bouzayen M, Bécard G, Combier J-P (2014) Auxin perception is required for arbuscule development in arbuscular mycorrhizal symbiosis. Plant Physiol 166 (1):281-292

Ezawa T, Smith SE, Smith FA (2002) P metabolism and transport in AM fungi. Plant Soil 244 (1-2):221-230

Favre P, Bapaume L, Bossolini E, Delorenzi M, Falquet L, Reinhardt D (2014) A novel bioinformatics pipeline to discover genes related to arbuscular mycorrhizal symbiosis based on their evolutionary conservation pattern among higher plants. BMC Plant Biol 14 (1):333

Feddermann N, Muni D, Reddy R, Zeier T, Stuurman J, Ercolin F, Schorderet M, Reinhardt D (2010) The PAM1 gene of petunia, required for intracellular accommodation and morphogenesis of arbuscular mycorrhizal fungi, encodes a homologue of VAPYRIN. Plant J 64 (3):470-481

Feddermann N, Reinhardt D (2011) Conserved residues in the ankyrin domain of VAPYRIN indicate potential protein-protein interaction surfaces. Plant Signal Behav 6 (5):680-684

Fellbaum CR, Gachomo EW, Beesetty Y, Choudhari S, Strahan GD, Pfeffer PE, Kiers ET, Bücking H (2012) Carbon availability triggers fungal nitrogen uptake and transport in arbuscular mycorrhizal symbiosis. Proc Natl Acad Sci 109 (7):2666-2671

Feng S, Martinez C, Gusmaroli G, Wang Y, Zhou J, Wang F, Chen L, Yu L, Iglesias-Pedraz JM, Kircher S (2008) Coordinated regulation of *Arabidopsis thaliana* development by light and gibberellins. Nature 451 (7177):475

Fernández I, Merlos M, López-Ráez J, Martínez-Medina A, Ferrol N, Azcón C, Bonfante P, Flors V, Pozo M (2014) Defense related phytohormones regulation in arbuscular mycorrhizal symbioses depends on the partner genotypes. J Chem Ecol 40 (7):791-803

Fester T (2008) Plastid reorganization in arbuscular mycorrhizal roots. Plant Cell Compartments—Selected Topics Kerala, India: Research Signpost:335-354

Fester T, Strack D, Hause B (2001) Reorganization of tobacco root plastids during arbuscule development. Planta 213 (6):864-868

Field KJ, Cameron DD, Leake JR, Tille S, Bidartondo MI, Beerling DJ (2012) Contrasting arbuscular mycorrhizal responses of vascular and non-vascular plants to a simulated Palaeozoic CO 2 decline. Nat Commun 3:835

Filion M, St-Arnaud M, Jabaji-Hare S (2003) Quantification of Fusarium solani f. sp. phaseoli in mycorrhizal bean plants and surrounding mycorrhizosphere soil using real-time polymerase chain reaction and direct isolations on selective media. Phytopathology 93 (2):229-235

Fiorilli V, Catoni M, Miozzi L, Novero M, Accotto GP, Lanfranco L (2009) Global and cell-type gene expression profiles in tomato plants colonized by an arbuscular mycorrhizal fungus. New Phytol 184 (4):975-987

Fitter A (1977) Influence of mycorrhizal infection on competition for phosphorus and potassium by two grasses. New Phytol 79 (1):119-125

Fitter A (2006) What is the link between carbon and phosphorus fluxes in arbuscular mycorrhizas? A null hypothesis for symbiotic function. New Phytol 172 (1):3-6

Fitter A, Garbaye J (1994) Interactions between mycorrhizal fungi and other soil organisms. Plant Soil 159 (1):123-132

Flematti GR, Dixon KW, Smith SM (2015) What are karrikins and how were they 'discovered'by plants? BMC Biol 13 (1):108

Floss DS, Gomez SK, Park H-J, MacLean AM, Müller LM, Bhattarai KK, Lévesque-Tremblay V, Maldonado-Mendoza IE, Harrison MJ (2017) A transcriptional program for arbuscule degeneration during AM symbiosis is regulated by MYB1. Curr Biol 27 (8):1206-1212

Floss DS, Lévesque-Tremblay V, Park H-J, Harrison MJ (2016) DELLA proteins regulate expression of a subset of AM symbiosis-induced genes in Medicago truncatula. Plant Signal Behav 11 (4):e1162369

Floss DS, Levy JG, Lévesque-Tremblay V, Pumplin N, Harrison MJ (2013) DELLA proteins regulate arbuscule formation in arbuscular mycorrhizal symbiosis. Proc Natl Acad Sci 110 (51):E5025-E5034

Floss DS, Schliemann W, Schmidt J, Strack D, Walter MH (2008) RNA interference-mediated repression of MtCCD1 in mycorrhizal roots of Medicago truncatula causes accumulation of C27 apocarotenoids, shedding light on the functional role of CCD1. Plant Physiol 148 (3):1267-1282

Fonouni-Farde C, Tan S, Baudin M, Brault M, Wen J, Mysore KS, Niebel A, Frugier F, Diet A (2016) DELLA-mediated gibberellin signalling regulates Nod factor signalling and rhizobial infection. Nat Commun 7:12636

Foo E, Ross JJ, Jones WT, Reid JB (2013) Plant hormones in arbuscular mycorrhizal symbioses: an emerging role for gibberellins. Ann Bot 111 (5):769-779

Fukazawa J, Mori M, Watanabe S, Miyamoto C, Ito T, Takahashi Y (2017) DELLA-GAF1 Complex is a Main Component in Gibberellin Feedback Regulation of GA20ox2 in *Arabidopsis*. Plant Physiol:pp. 00282.02017

Fukazawa J, Teramura H, Murakoshi S, Nasuno K, Nishida N, Ito T, Yoshida M, Kamiya Y, Yamaguchi S, Takahashi Y (2014) DELLAs function as coactivators of GAI-ASSOCIATED FACTOR1 in regulation of gibberellin homeostasis and signaling in Arabidopsis. Plant Cell 26 (7):2920-2938

Furlan V, Fortin JA (1977) Effects of light intensity on the formation of vesicular-arbuscular endomycorrhizas on *Allium cepa* by *Gigaspora calospora*. New Phytol 79 (2):335-340

Fusconi A (2013) Regulation of root morphogenesis in arbuscular mycorrhizae: what role do fungal exudates, phosphate, sugars and hormones play in lateral root formation? Ann Bot 113 (1):19-33

Gabriel-Neumann E, Neumann G, Leggewie G, George E (2011) Constitutive overexpression of the sucrose transporter SoSUT1 in potato plants increases arbuscular mycorrhiza fungal root colonization under high, but not under low, soil phosphorus availability. J Plant Physiol 168 (9):911-919

Galbraith M, Horn D (1972) Structures of the natural products blumenols A, B, and C. Journal of the Chemical Society, Chemical Communications (3):113-114

Gallou A, Declerck S, Cranenbrouck S (2012) Transcriptional regulation of defence genes and involvement of the WRKY transcription factor in arbuscular mycorrhizal potato root colonization. Funct Integr Genomics 12 (1):183-198. doi:10.1007/s10142-011-0241-4

García Garrido JM, León Morcillo RJ, Martín Rodríguez JA, Ocampo Bote JA (2010) Variations in the mycorrhization characteristics in roots of wild-type and ABA-deficient tomato are accompanied by specific transcriptomic alterations. Mol Plant-Microbe Interact 23 (5):651-664. doi:10.1094/MPMI-23-5-0651

Gaude N, Bortfeld S, Duensing N, Lohse M, Krajinski F (2012) Arbuscule-containing and non-colonized cortical cells of mycorrhizal roots undergo extensive and specific reprogramming during arbuscular mycorrhizal development. Plant J 69 (3):510-528. doi:10.1111/j.1365-313X.2011.04810.x

Gavito ME, Olsson PA, Rouhier H, Medina-Peñafiel A, Jakobsen I, Bago A, Azcón-Aguilar C (2005) Temperature constraints on the growth and functioning of root organ cultures with arbuscular mycorrhizal fungi. New Phytol 168 (1):179-188

Gavrin A, Chiasson D, Ovchinnikova E, Kaiser BN, Bisseling T, Fedorova EE (2016) VAMP721a and VAMP721d are important for pectin dynamics and release of bacteria in soybean nodules. New Phytol 210 (3):1011-1021. doi:10.1111/nph.13837

Genre A, Bonfante P (1997) A mycorrhizal fungus changes microtubule orientation in tobacco root cells. Protoplasma 199 (1):30-38

Genre A, Bonfante P (1998) Actin versus tubulin configuration in arbuscule-containing cells from mycorrhizal tobacco roots. New Phytol 140 (4):745-752

Genre A, Bonfante P (1999) Cytoskeleton-related proteins in tobacco mycorrhizal cells: gamma-tubulin and clathrin localisation. Eur J Histochem 43:105-111

Genre A, Chabaud M, Balzergue C, Puech-Pagès V, Novero M, Rey T, Fournier J, Rochange S, Bécard G, Bonfante P (2013) Short-chain chitin oligomers from arbuscular mycorrhizal fungi trigger nuclear Ca2+ spiking in *Medicago truncatula* roots and their production is enhanced by strigolactone. New Phytol 198 (1):190-202

Genre A, Chabaud M, Faccio A, Barker DG, Bonfante P (2008) Prepenetration apparatus assembly precedes and predicts the colonization patterns of arbuscular mycorrhizal fungi within the root cortex of both Medicago truncatula and Daucus carota. Plant Cell 20 (5):1407-1420

Genre A, Chabaud M, Timmers T, Bonfante P, Barker DG (2005) Arbuscular mycorrhizal fungi elicit a novel intracellular apparatus in *Medicago truncatula* root epidermal cells before infection. Plant Cell 17 (12):3489-3499. doi:10.1105/tpc.105.035410

Genre A, Ivanov S, Fendrych M, Faccio A, Žárský V, Bisseling T, Bonfante P (2011) Multiple exocytotic markers accumulate at the sites of perifungal membrane biogenesis in arbuscular mycorrhizas. Plant Cell Physiol 53 (1):244-255

Genre A, Ortu G, Bertoldo C, Martino E, Bonfante P (2009) Biotic and abiotic stimulation of root epidermal cells reveals common and specific responses to arbuscular mycorrhizal fungi. Plant Physiol 149 (3):1424-1434. doi:10.1104/pp.108.132225

Giaquinta RT (1983) Phloem loading of sucrose. Annual Review of Plant Physiology 34 (1):347-387

Giovannetti M, Mosse B (1980) An evaluation of techniques for measuring vesicular arbuscular mycorrhizal infection in roots. New Phytol 84 (3):489-500

Gobbato E, Marsh JF, Vernié T, Wang E, Maillet F, Kim J, Miller JB, Sun J, Bano SA, Ratet P (2012) A GRAS-type transcription factor with a specific function in mycorrhizal signaling. Curr Biol 22 (23):2236-2241

Gobbato E, Wang E, Higgins G, Bano SA, Henry C, Schultze M, Oldroyd GE (2013) RAM1 and RAM2 function and expression during arbuscular mycorrhizal symbiosis and Aphanomyces euteiches colonization. Plant Signal Behav 8 (10):e26049

Gomez-Roldan V, Fermas S, Brewer PB, Puech-Pagès V, Dun EA, Pillot J-P, Letisse F, Matusova R, Danoun S, Portais J-C (2008) Strigolactone inhibition of shoot branching. Nature 455 (7210):189

Gomez SK, Javot H, Deewatthanawong P, Torres-Jerez I, Tang Y, Blancaflor EB, Udvardi MK, Harrison MJ (2009) *Medicago truncatula* and *Glomus intraradices* gene expression in cortical cells harboring arbuscules in the arbuscular mycorrhizal symbiosis. BMC Plant Biol 9:10. doi:10.1186/1471-2229-9-10

Gomi K, Sasaki A, Itoh H, Ueguchi-Tanaka M, Ashikari M, Kitano H, Matsuoka M (2004) GID2, an F-box subunit of the SCF E3 complex, specifically interacts with phosphorylated SLR1 protein and regulates the gibberellin-dependent degradation of SLR1 in rice. Plant J 37 (4):626-634

Gonzalez-Chavez M, Carrillo-Gonzalez R, Wright S, Nichols K (2004) The role of glomalin, a protein produced by arbuscular mycorrhizal fungi, in sequestering potentially toxic elements. Environ Pollut 130 (3):317-323

Govindarajulu M, Pfeffer PE, Jin H, Abubaker J, Douds DD, Allen JW, Bücking H, Lammers PJ, Shachar-Hill Y (2005) Nitrogen transfer in the arbuscular mycorrhizal symbiosis. Nature 435 (7043):819-823

Graham J (2000) Assessing costs of arbuscular mycorrhizal symbiosis in agroecosystems. Current advances in mycorrhizae research:127-140

Grant C, Bittman S, Montreal M, Plenchette C, Morel C (2005) Soil and fertilizer phosphorus: Effects on plant P supply and mycorrhizal development. Canadian Journal of Plant Science 85 (1):3-14

Griffiths J, Murase K, Rieu I, Zentella R, Zhang Z-L, Powers SJ, Gong F, Phillips AL, Hedden P, Sun T-p (2006) Genetic characterization and functional analysis of the GID1 gibberellin receptors in Arabidopsis. Plant Cell 18 (12):3399-3414

Grime J, Mackey J, Hillier S, Read D (1987) Floristic diversity in a model system using experimental microcosms. Nature 328 (6129):420

Groth M, Kosuta S, Gutjahr C, Haage K, Hardel SL, Schaub M, Brachmann A, Sato S, Tabata S, Findlay K (2013) Two Lotus japonicus symbiosis mutants impaired at distinct steps of arbuscule development. Plant J 75 (1):117-129

Guether M, Balestrini R, Hannah M, He J, Udvardi MK, Bonfante P (2009) Genome-wide reprogramming of regulatory networks, transport, cell wall and membrane biogenesis during arbuscular mycorrhizal symbiosis in Lotus japonicus. New Phytol 182 (1):200-212

Guillotin B, Etemadi M, Audran C, Bouzayen M, Bécard G, Combier JP (2017) Sl-IAA27 regulates strigolactone biosynthesis and mycorrhization in tomato (var. MicroTom). New Phytol 213 (3):1124-1132

Güimil S, Chang H-S, Zhu T, Sesma A, Osbourn A, Roux C, Ioannidis V, Oakeley EJ, Docquier M, Descombes P (2005) Comparative transcriptomics of rice reveals an ancient pattern of response to microbial colonization. Proc Natl Acad Sci 102 (22):8066-8070

Gutjahr C (2014) Phytohormone signaling in arbuscular mycorhiza development. Curr Opin Plant Biol 20:26-34

Gutjahr C, Gobbato E, Choi J, Riemann M, Johnston MG, Summers W, Carbonnel S, Mansfield C, Yang SY, Nadal M, Acosta I, Takano M, Jiao WB, Schneeberger K, Kelly KA, Paszkowski U (2015) Rice perception of symbiotic arbuscular mycorrhizal fungi requires the karrikin receptor complex. Science 350 (6267):1521-1524. doi:10.1126/science.aac9715

Gutjahr C, Novero M, Guether M, Montanari O, Udvardi M, Bonfante P (2009) Presymbiotic factors released by the arbuscular mycorrhizal fungus Gigaspora margarita induce starch accumulation in Lotus japonicus roots. New Phytol 183 (1):53-61

Gutjahr C, Novero M, Welham T, Wang T, Bonfante P (2011) Root starch accumulation in response to arbuscular mycorrhizal colonization differs among Lotus japonicus starch mutants. Planta 234 (3):639

Gutjahr C, Parniske M (2013) Cell and developmental biology of arbuscular mycorrhiza symbiosis. Annu Rev Cell Dev Biol 29

Gutjahr C, Parniske M (2017) Cell Biology: Control of Partner Lifetime in a Plant–Fungus Relationship. Curr Biol 27 (11):R420-R423

Gutjahr C, Radovanovic D, Geoffroy J, Zhang Q, Siegler H, Chiapello M, Casieri L, An K, An G, Guiderdoni E (2012) The half-size ABC transporters STR1 and STR2 are indispensable for mycorrhizal arbuscule formation in rice. Plant J 69 (5):906-920

Hall I (1978) Effect of vesicular-arbuscular mycorrhizas on two varieties of maize and one of sweetcorn. N Z J Agric Res 21 (3):517-519

Hammer EC, Pallon J, Wallander H, Olsson PA (2011) Tit for tat? A mycorrhizal fungus accumulates phosphorus under low plant carbon availability. FEMS Microbiol Ecol 76 (2):236-244

Handa Y, Nishide H, Takeda N, Suzuki Y, Kawaguchi M, Saito K (2015) RNA-seq transcriptional profiling of an arbuscular mycorrhiza provides insights into regulated and coordinated gene expression in Lotus japonicus and Rhizophagus irregularis. Plant Cell Physiol 56 (8):1490-1511

Hans J, Hause B, Strack D, Walter MH (2004) Cloning, characterization, and immunolocalization of a mycorrhiza-inducible 1-deoxy-d-xylulose 5-phosphate reductoisomerase in arbuscule-containing cells of maize. Plant Physiol 134 (2):614-624. doi:10.1104/pp.103.032342

Hao Z, Fayolle L, van Tuinen D, Chatagnier O, Li X, Gianinazzi S, Gianinazzi-Pearson V (2012) Local and systemic mycorrhiza-induced protection against the ectoparasitic nematode *Xiphinema index* involves priming of defence gene responses in grapevine. J Exp Bot 63 (10):3657-3672

Harberd NP, King KE, Carol P, Cowling RJ, Peng J, Richards DE (1998) Gibberellin: inhibitor of an inhibitor of...? Bioessays 20 (12):1001-1008

Hardham AR, Takemoto D, White RG (2008) Rapid and dynamic subcellular reorganization following mechanical stimulation of Arabidopsis epidermal cells mimics responses to fungal and oomycete attack. BMC Plant Biol 8 (1):63

Harrier LA, Millam S (2001) Biolistic transformation of arbuscular mycorrhizal fungi. Mol Biotechnol 18 (1):25-33

Harrison MJ (1999) Molecular and cellular aspects of the arbuscular mycorrhizal symbiosis. Annu Rev Plant Biol 50 (1):361-389

Harrison MJ (2012) Cellular programs for arbuscular mycorrhizal symbiosis. Curr Opin Plant Biol 15 (6):691-698. doi:10.1016/j.pbi.2012.08.010

Harrison MJ, Dewbre GR, Liu J (2002) A phosphate transporter from *Medicago truncatula* involved in the acquisition of phosphate released by arbuscular mycorrhizal fungi. Plant Cell 14 (10):2413-2429

Harrison MJ, Ivanov S (2017) Exocytosis for endosymbiosis: membrane trafficking pathways for development of symbiotic membrane compartments. Curr Opin Plant Biol 38:101-108

Hartnett DC, Wilson GW (1999) Mycorrhizae influence plant community structure and diversity in tallgrass prairie. Ecology 80 (4):1187-1195

Hayashi T, Banba M, Shimoda Y, Kouchi H, Hayashi M, Imaizumi-Anraku H (2010) A dominant function of CCaMK in intracellular accommodation of bacterial and fungal endosymbionts. Plant J 63 (1):141-154

Hayman D, Mosse B (1971) PLANT GROWTH RESPONSES TO VESICULAR-ARBUSCULAR MYCORRHIZA. New Phytol 70 (1):19-27

Heck C, Kuhn H, Heidt S, Walter S, Rieger N, Requena N (2016) Symbiotic fungi control plant root cortex development through the novel GRAS transcription factor MIG1. Curr Biol 26 (20):2770-2778

Heijden MG, Martin FM, Selosse MA, Sanders IR (2015) Mycorrhizal ecology and evolution: the past, the present, and the future. New Phytol 205 (4):1406-1423

Helber N, Requena N (2008) Expression of the fluorescence markers DsRed and GFP fused to a nuclear localization signal in the arbuscular mycorrhizal fungus Glomus intraradices. New Phytol 177 (2):537-548

Helber N, Wippel K, Sauer N, Schaarschmidt S, Hause B, Requena N (2011) A versatile monosaccharide transporter that operates in the arbuscular mycorrhizal fungus Glomus sp is crucial for the symbiotic relationship with plants. Plant Cell 23 (10):3812-3823

Helgason T, Merryweather JW, Young JPW, Fitter AH (2007) Specificity and resilience in the arbuscular mycorrhizal fungi of a natural woodland community. J Ecol 95 (4):623-630

Heo JO, Chang KS, Kim IA, Lee MH, Lee SA, Song SK, Lee MM, Lim J (2011) Funneling of gibberellin signaling by the GRAS transcription regulator scarecrow-like 3 in the Arabidopsis root. Proceedings of the National Academy of Sciences of the United States of America 108 (5):2166-2171. doi:10.1073/pnas.1012215108

Herbers K, Meuwly P, Frommer WB, Métraux J-P, Sonnewald U (1996) Systemic acquired resistance mediated by the ectopic expression of invertase: possible hexose sensing in the secretory pathway. Plant Cell 8 (5):793-803

Hewitt EJ (1966) Sand and water culture methods used in the study of plant nutrition. Commenwealth Agricultural Bureaux,

Hijikata N, Murase M, Tani C, Ohtomo R, Osaki M, Ezawa T (2010) Polyphosphate has a central role in the rapid and massive accumulation of phosphorus in extraradical mycelium of an arbuscular mycorrhizal fungus. New Phytol 186 (2):285-289

Hirano Y, Nakagawa M, Suyama T, Murase K, Shirakawa M, Takayama S, Sun T-p, Hakoshima T (2017) Structure of the SHR–SCR heterodimer bound to the BIRD/IDD transcriptional factor JKD. Nat Plants 3 (3):17010

Hirsch S, Kim J, Munoz A, Heckmann AB, Downie JA, Oldroyd GE (2009) GRAS proteins form a DNA binding complex to induce gene expression during nodulation signaling in Medicago truncatula. Plant Cell 21 (2):545-557. doi:10.1105/tpc.108.064501

Ho-Plágaro T, Huertas R, Tamayo-Navarrete MI, Ocampo JA, García-Garrido JM (2018) An improved method for Agrobacterium rhizogenes-mediated transformation of tomato suitable for the study of arbuscular mycorrhizal symbiosis. Plant Methods 14 (1):34. doi:10.1186/s13007-018-0304-9

Ho I, Trappe J (1973) Translocation of 14 C from Festuca plants to their endomycorrhizal fungi. Nature New Biology 244 (131):30

Hoeksema JD, Chaudhary VB, Gehring CA, Johnson NC, Karst J, Koide RT, Pringle A, Zabinski C, Bever JD, Moore JC (2010) A meta-analysis of context-dependency in plant response to inoculation with mycorrhizal fungi. Ecol Lett 13 (3):394-407

Hofferek V, Mendrinna A, Gaude N, Krajinski F, Devers EA (2014) MiR171h restricts root symbioses and shows like its target NSP2 a complex transcriptional regulation in Medicago truncatula. BMC Plant Biol 14 (1):199

Hogekamp C, Küster H (2013) A roadmap of cell-type specific gene expression during sequential stages of the arbuscular mycorrhiza symbiosis. BMC Genomics 14 (1):306

Hohnjec N, Czaja-Hasse LF, Hogekamp C, Küster H (2015) Pre-announcement of symbiotic guests: transcriptional reprogramming by mycorrhizal lipochitooligosaccharides shows a strict co-dependency on the GRAS transcription factors NSP1 and RAM1. BMC Genomics 16 (1):994

Hohnjec N, Vieweg MF, Pühler A, Becker A, Küster H (2005) Overlaps in the transcriptional profiles of *Medicago truncatula* roots inoculated with two different *Glomus* fungi provide insights into the genetic program activated during arbuscular mycorrhiza. Plant Physiol 137 (4):1283-1301

Huang S, Jin L, Du J, Li H, Zhao Q, Ou G, Ao G, Yuan M (2007) SB401, a pollen-specific protein from *Solanum berthaultii*, binds to and bundles microtubules and F-actin. Plant J 51 (3):406-418. doi:10.1111/j.1365-313X.2007.03153.x

Huisman R, Hontelez J, Mysore KS, Wen J, Bisseling T, Limpens E (2016) A symbiosis-dedicated SYNTAXIN OF PLANTS 13II isoform controls the formation of a stable host-microbe interface in symbiosis. New Phytol 211 (4):1338-1351. doi:10.1111/nph.13973

Ivanov S, Fedorova EE, Limpens E, De Mita S, Genre A, Bonfante P, Bisseling T (2012) Rhizobium-legume symbiosis shares an exocytotic pathway required for arbuscule formation. Proceedings of the National Academy of Sciences of the United States of America 109 (21):8316-8321. doi:10.1073/pnas.1200407109

Ivanov S, Harrison MJ (2014) A set of fluorescent protein-based markers expressed from constitutive and arbuscular mycorrhiza-inducible promoters to label organelles, membranes and cytoskeletal elements in *Medicago truncatula*. Plant J 80 (6):1151-1163. doi:10.1111/tpj.12706

Jabaji-Hare S (1988) Lipid and fatty acid profiles of some vesicular-arbuscular mycorrhizal fungi: contribution to taxonomy. Mycologia:622-629

Jaiti F, Meddich A, El Hadrami I (2007) Effectiveness of arbuscular mycorrhizal fungi in the protection of date palm (*Phoenix dactylifera* L.) against bayoud disease. Physiol Mol Plant Pathol 71 (4-6):166-173

Janos D (1975) Effects of vesicular-arbuscular mycorrhizae on lowland tropical rainforest trees.

Javot H, Penmetsa RV, Terzaghi N, Cook DR, Harrison MJ (2007a) A Medicago truncatula phosphate transporter indispensable for the arbuscular mycorrhizal symbiosis. Proc Natl Acad Sci 104 (5):1720-1725

Javot H, Pumplin N, Harrison MJ (2007b) Phosphate in the arbuscular mycorrhizal symbiosis: transport properties and regulatory roles. Plant, Cell Environ 30 (3):310-322

Jayaraman D, Gilroy S, Ane J-M (2014) Staying in touch: mechanical signals in plant–microbe interactions. Curr Opin Plant Biol 20:104-109

Jefferson R (1989) The GUS reporter gene system. Nature 342 (6251):837

Jefferson RA, Burgess SM, Hirsh D (1986) beta-Glucuronidase from Escherichia coli as a gene-fusion marker. Proc Natl Acad Sci 83 (22):8447-8451

Ji K, Kai W, Zhao B, Sun Y, Yuan B, Dai S, Li Q, Chen P, Wang Y, Pei Y (2014) SlNCED1 and SlCYP707A2: key genes involved in ABA metabolism during tomato fruit ripening. J Exp Bot 65 (18):5243-5255

Jiang C, Gao X, Liao L, Harberd NP, Fu X (2007) Phosphate starvation root architecture and anthocyanin accumulation responses are modulated by the gibberellin-DELLA signaling pathway in Arabidopsis. Plant Physiol 145 (4):1460-1470

Jiang Y, Wang W, Xie Q, Liu N, Liu L, Wang D, Zhang X, Yang C, Chen X, Tang D (2017) Plants transfer lipids to sustain colonization by mutualistic mycorrhizal and parasitic fungi. Science:eaam9970

Jin Y, Liu H, Luo D, Yu N, Dong W, Wang C, Zhang X, Dai H, Yang J, Wang E (2016) DELLA proteins are common components of symbiotic rhizobial and mycorrhizal signalling pathways. Nat Commun 7

Jung SC, Martinez-Medina A, Lopez-Raez JA, Pozo MJ (2012) Mycorrhiza-induced resistance and priming of plant defenses. J Chem Ecol 38 (6):651-664

Kamel L, Keller-Pearson M, Roux C, Ané JM (2017a) Biology and evolution of arbuscular mycorrhizal symbiosis in the light of genomics. New Phytol 213 (2):531-536

Kamel L, Tang N, Malbreil M, San Clemente H, Le Marquer M, Roux C, Frei dit Frey N (2017b) The comparison of expressed candidate secreted proteins from two arbuscular mycorrhizal fungi unravels common and specific molecular tools to invade different host plants. Front Plant Sci 8:124

Karimi M, Inze D, Depicker A (2002) GATEWAY vectors for *Agrobacterium*-mediated plant transformation. Trends Plant Sci 7 (5):193-195

Keymer A, Pimprikar P, Wewer V, Huber C, Brands M, Bucerius SL, Delaux P-M, Klingl V, von Roepenack-Lahaye E, Wang TL (2017) Lipid transfer from plants to arbuscular mycorrhiza fungi. Elife 6

Kiers ET, Duhamel M, Beesetty Y, Mensah JA, Franken O, Verbruggen E, Fellbaum CR, Kowalchuk GA, Hart MM, Bago A (2011) Reciprocal rewards stabilize cooperation in the mycorrhizal symbiosis. Science 333 (6044):880-882

Kinden DA, Brown MF (1975) Electron microscopy of vesicular-arbuscular mycorrhizae of yellow poplar. II. Intracellular hyphae and vesicles. Canadian Journal of Microbiology 21 (11):1768-1780

Klingner A, Bothe H, Wray V, Marner F-J (1995) Identification of a yellow pigment formed in maize roots upon mycorrhizal colonization. Phytochemistry 38 (1):53-55

Klironomos JN, McCune J, Hart M, Neville J (2000) The influence of arbuscular mycorrhizae on the relationship between plant diversity and productivity. Ecol Lett 3 (2):137-141

Kloppholz S, Kuhn H, Requena N (2011) A secreted fungal effector of Glomus intraradices promotes symbiotic biotrophy. Curr Biol 21 (14):1204-1209

Kobae Y, Fujiwara T (2014) Earliest colonization events of Rhizophagus irregularis in rice roots occur preferentially in previously uncolonized cells. Plant Cell Physiol 55 (8):1497-1510

Kobae Y, Gutjahr C, Paszkowski U, Kojima T, Fujiwara T, Hata S (2014) Lipid droplets of arbuscular mycorrhizal fungi emerge in concert with arbuscule collapse. Plant Cell Physiol 55 (11):1945-1953

Kobae Y, Hata S (2010) Dynamics of periarbuscular membranes visualized with a fluorescent phosphate transporter in arbuscular mycorrhizal roots of rice. Plant Cell Physiol 51 (3):341-353. doi:10.1093/pcp/pcq013

Kobae Y, Kameoka H, Sugimura Y, Saito K, Ohtomo R, Fujiwara T, Kyozuka J (2018) Strigolactone biosynthesis genes of rice is required for the punctual entry of arbuscular mycorrhizal fungi into the roots. Plant Cell Physiol

Kobae Y, Ohmori Y, Saito C, Yano K, Ohtomo R, Fujiwara T (2016) Phosphate treatment strongly inhibits new arbuscule development but not the maintenance of arbuscule in mycorrhizal rice roots. Plant Physiol:pp. 00127.02016

Koide RT, Schreiner RP (1992) Regulation of the vesicular-arbuscular mycorrhizal symbiosis. Annu Rev Plant Biol 43 (1):557-581

Koltai H, LekKala SP, Bhattacharya C, Mayzlish-Gati E, Resnick N, Wininger S, Dor E, Yoneyama K, Yoneyama K, Hershenhorn J (2010) A tomato strigolactone-impaired mutant displays aberrant shoot morphology and plant interactions. J Exp Bot 61 (6):1739-1749

Kong Z, Ioki M, Braybrook S, Li S, Ye Z-H, Lee Y-RJ, Hotta T, Chang A, Tian J, Wang G (2015) Kinesin-4 functions in vesicular transport on cortical microtubules and regulates cell wall mechanics during cell elongation in plants. Mol plant 8 (7):1011-1023

Krajinski F, Courty P-E, Sieh D, Franken P, Zhang H, Bucher M, Gerlach N, Kryvoruchko I, Zoeller D, Udvardi M (2014) The H+-ATPase HA1 of Medicago truncatula is essential for phosphate transport and plant growth during arbuscular mycorrhizal symbiosis. Plant Cell 26 (4):1808-1817

Kretzschmar T, Kohlen W, Sasse J, Borghi L, Schlegel M, Bachelier JB, Reinhardt D, Bours R, Bouwmeester HJ, Martinoia E (2012) A petunia ABC protein controls strigolactone-dependent symbiotic signalling and branching. Nature 483 (7389):341

Krings M, Taylor TN, Hass H, Kerp H, Dotzler N, Hermsen EJ (2007) Fungal endophytes in a 400-million-yr-old land plant: infection pathways, spatial distribution, and host responses. New Phytol 174 (3):648-657

Krüger M, Krüger C, Walker C, Stockinger H, Schüßler A (2012) Phylogenetic reference data for systematics and phylotaxonomy of arbuscular mycorrhizal fungi from phylum to species level. New Phytol 193 (4):970-984

Kryvoruchko IS, Sinharoy S, Torres-Jerez I, Sosso D, Pislariu CI, Guan D, Murray J, Benedito VA, Frommer WB, Udvardi MK (2016) *MtSWEET11*, a Nodule-Specific Sucrose Transporter of *Medicago truncatula*. Plant Physiol 171 (1):554-565. doi:10.1104/pp.15.01910

Kubota M, McGonigle TP, Hyakumachi M (2005) Co-occurrence of Arum-and Paris-type morphologies of arbuscular mycorrhizae in cucumber and tomato. Mycorrhiza 15 (2):73-77

Kuhn H, Küster H, Requena N (2010) Membrane steroid-binding protein 1 induced by a diffusible fungal signal is critical for mycorrhization in Medicago truncatula. New Phytol 185 (3):716-733

Lahmidi NA, Courty P-E, Brulé D, Chatagnier O, Arnould C, Doidy J, Berta G, Lingua G, Wipf D, Bonneau L (2016) Sugar exchanges in arbuscular mycorrhiza: RiMST5 and RiMST6, two novel Rhizophagus irregularis monosaccharide transporters, are involved in both sugar uptake from the soil and from the plant partner. Plant Physiol Biochem 107:354-363

Lambert D, Cole H, Baker D (1980) Variation in the Response of Alfalfa Clones and Cultivars to Mycorrhizae and Phosphorus 1. Crop Sci 20 (5):615-618

Latef AAHA, Hashem A, Rasool S, Abd_Allah EF, Alqarawi A, Egamberdieva D, Jan S, Anjum NA, Ahmad P (2016) Arbuscular mycorrhizal symbiosis and abiotic stress in plants: A review. Journal of plant biology 59 (5):407-426

Lauressergues D, Delaux PM, Formey D, Lelandais-Brière C, Fort S, Cottaz S, Bécard G, Niebel A, Roux C, Combier JP (2012) The microRNA miR171h modulates arbuscular mycorrhizal colonization of *Medicago truncatula* by targeting NSP2. Plant J 72 (3):512-522

Lemonnier P, Gaillard C, Veillet F, Verbeke J, Lemoine R, Coutos-Thévenot P, La Camera S (2014) Expression of Arabidopsis sugar transport protein STP13 differentially affects glucose transport activity and basal resistance to Botrytis cinerea. Plant Mol Biol 85 (4-5):473-484

Lewis D, Harley J (1965) Carbohydrate physiology of mycorrhizal roots of beech. New Phytol 64 (2):224-237

Lin K, Limpens E, Zhang Z, Ivanov S, Saunders DG, Mu D, Pang E, Cao H, Cha H, Lin T (2014) Single nucleus genome sequencing reveals high similarity among nuclei of an endomycorrhizal fungus. PLoS Genet 10 (1):e1004078

Liu BQ, Jin L, Zhu L, Li J, Huang S, Yuan M (2009) Phosphorylation of microtubule-associated protein SB401 from *Solanum berthaultii* regulates its effect on microtubules. J Integr Plant Biol 51 (3):235-242. doi:10.1111/j.1744-7909.2008.00797.x

Liu C, Li S, Yue J, Xiao W, Zhao Q, Zhu D, Yu J (2015) Microtubule-Associated Protein SBgLR Facilitates Storage Protein Deposition and Its Expression Leads to Lysine Content Increase in Transgenic Maize Endosperm. International journal of molecular sciences 16 (12):29772-29786. doi:10.3390/ijms161226199

Liu C, Qi X, Zhao Q, Yu J (2013) Characterization and functional analysis of the potato pollen-specific microtubule-associated protein SBgLR in tobacco. PloS one 8 (3):e60543. doi:10.1371/journal.pone.0060543

Liu J, Maldonado-Mendoza I, Lopez-Meyer M, Cheung F, Town CD, Harrison MJ (2007) Arbuscular mycorrhizal symbiosis is accompanied by local and systemic alterations in gene expression and an increase in disease resistance in the shoots. Plant J 50 (3):529-544

Liu W, Kohlen W, Lillo A, Op den Camp R, Ivanov S, Hartog M, Limpens E, Jamil M, Smaczniak C, Kaufmann K, Yang WC, Hooiveld GJ, Charnikhova T, Bouwmeester HJ, Bisseling T, Geurts R (2011) Strigolactone biosynthesis in *Medicago truncatula* and rice requires the symbiotic GRAS-type transcription factors *NSP1* and *NSP2*. Plant Cell 23 (10):3853-3865. doi:10.1105/tpc.111.089771

Lohse S, Schliemann W, Ammer C, Kopka J, Strack D, Fester T (2005) Organization and metabolism of plastids and mitochondria in arbuscular mycorrhizal roots of Medicago truncatula. Plant Physiol 139 (1):329-340

Lopez-Obando M, Ligerot Y, Bonhomme S, Boyer F-D, Rameau C (2015) Strigolactone biosynthesis and signaling in plant development. Development 142 (21):3615-3619

López-Pedrosa A, González-Guerrero M, Valderas A, Azcón-Aguilar C, Ferrol N (2006) *GintAMT1* encodes a functional high-affinity ammonium transporter that is expressed in the extraradical mycelium of *Glomus intraradices*. Fungal Genet Biol 43 (2):102-110

López-Ráez JA, Fernández I, García JM, Berrio E, Bonfante P, Walter MH, Pozo MJ (2015) Differential spatio-temporal expression of carotenoid cleavage dioxygenases regulates apocarotenoid fluxes during AM symbiosis. Plant Sci 230:59-69

López-Ráez JA, Verhage A, Fernandez I, Garcia JM, Azcón-Aguilar C, Flors V, Pozo MJ (2010) Hormonal and transcriptional profiles highlight common and differential host responses to arbuscular mycorrhizal fungi and the regulation of the oxylipin pathway. J Exp Bot 61 (10):2589-2601. doi:10.1093/jxb/erq089

López-Ráez JA, Kohlen W, Charnikhova T, Mulder P, Undas AK, Sergeant MJ, Verstappen F, Bugg TD, Thompson AJ, Ruyter-Spira C (2010) Does abscisic acid affect strigolactone biosynthesis? New Phytol 187 (2):343-354

Luginbuehl LH, Menard GN, Kurup S, Van Erp H, Radhakrishnan GV, Breakspear A, Oldroyd GE, Eastmond PJ (2017) Fatty acids in arbuscular mycorrhizal fungi are synthesized by the host plant. Science:eaan0081

MacLean AM, Bravo A, Harrison MJ (2017) Plant signaling and metabolic pathways enabling arbuscular mycorrhizal symbiosis. Plant Cell 29 (10):2319-2335

Madsen LH, Tirichine L, Jurkiewicz A, Sullivan JT, Heckmann AB, Bek AS, Ronson CW, James EK, Stougaard J (2010) The molecular network governing nodule organogenesis and infection in the model legume Lotus japonicus. Nat Commun 1:10

Maekawa T, Kusakabe M, Shimoda Y, Sato S, Tabata S, Murooka Y, Hayashi M (2008) Polyubiquitin promoter-based binary vectors for overexpression and gene silencing in Lotus japonicus. Mol Plant-Microbe Interact 21 (4):375-382

Maier W, Peipp H, Schmidt J, Wray V, Strack D (1995) Levels of a terpenoid glycoside (blumenin) and cell wall-bound phenolics in some cereal mycorrhizas. Plant Physiol 109 (2):465-470

Maillet F, Poinsot V, André O, Puech-Pagès V, Haouy A, Gueunier M, Cromer L, Giraudet D, Formey D, Niebel A (2011) Fungal lipochitooligosaccharide symbiotic signals in arbuscular mycorrhiza. Nature 469 (7328):58

Malbreil M, Tisserant E, Martin F, Roux C (2014) Genomics of arbuscular mycorrhizal fungi: Out of the shadows. In: Advances in Botanical Research, vol 70. Elsevier, pp 259-290

Maldonado-Mendoza IE, Harrison MJ (2017) RiArsB and RiMT-11: Two novel genes induced by arsenate in arbuscular mycorrhiza. Fungal Biology

Manck-Götzenberger J, Requena N (2016) Arbuscular mycorrhiza symbiosis induces a major transcriptional reprogramming of the potato SWEET sugar transporter family. Front Plant Sci 7:487

Martin-Rodriguez JA, Huertas R, Ho-Plagaro T, Ocampo JA, Tureckova V, Tarkowska D, Ludwig-Muller J, Garcia-Garrido JM (2016) Gibberellin-Abscisic Acid Balances during Arbuscular Mycorrhiza Formation in Tomato. Frontiers in plant science 7:1273. doi:10.3389/fpls.2016.01273

Martín-Rodríguez JÁ, León-Morcillo R, Vierheilig H, Ocampo JA, Ludwig-Müller J, García-Garrido JM (2011) Ethylene-dependent/ethylene-independent ABA regulation of tomato plants colonized by arbuscular mycorrhiza fungi. New Phytol 190 (1):193-205

Martin FM, Uroz S, Barker DG (2017) Ancestral alliances: plant mutualistic symbioses with fungi and bacteria. Science 356 (6340):eaad4501

McGinnis KM, Thomas SG, Soule JD, Strader LC, Zale JM, Sun T-p, Steber CM (2003) The Arabidopsis SLEEPY1 gene encodes a putative F-box subunit of an SCF E3 ubiquitin ligase. Plant Cell 15 (5):1120-1130

Meixner C, Ludwig-Müller J, Miersch O, Gresshoff P, Staehelin C, Vierheilig H (2005) Lack of mycorrhizal autoregulation and phytohormonal changes in the supernodulating soybean mutant nts1007. Planta 222 (4):709-715

Menge J, Munnecke D, Johnson E, Carnes D (1978) Dosage response of the vesicular-arbuscular mycorrhizal fungi Glomus fasciculatus and G. constrictus to methyl bromide. Phytopathology 68 (9):1368

Meyer JR, Linderman R (1986) Response of subterranean clover to dual inoculation with vesicular-arbuscular mycorrhizal fungi and a plant growth-promoting bacterium, Pseudomonas putida. Soil Biol Biochem 18 (2):185-190

Miller R, Jastrow J (2000) Mycorrhizal fungi influence soil structure. In: Arbuscular mycorrhizas: physiology and function. Springer, pp 3-18

Miyata K, Kozaki T, Kouzai Y, Ozawa K, Ishii K, Asamizu E, Okabe Y, Umehara Y, Miyamoto A, Kobae Y (2014) The bifunctional plant receptor, OsCERK1, regulates both chitin-triggered immunity and arbuscular mycorrhizal symbiosis in rice. Plant Cell Physiol 55 (11):1864-1872

Mohammadi K, Khalesro S, Sohrabi Y, Heidari G (2011) A review: beneficial effects of the mycorrhizal fungi for plant growth. J Appl Environ Biol Sci 1 (9):310-319

Nadal M, Sawers R, Naseem S, Bassin B, Kulicke C, Sharman A, An G, An K, Ahern KR, Romag A (2017) An N-acetylglucosamine transporter required for arbuscular mycorrhizal symbioses in rice and maize. Nat Plants 3 (6):17073

Nadimi M, Beaudet D, Forget L, Hijri M, Lang BF (2012) Group I intron–mediated trans-splicing in mitochondria of gigaspora rosea and a robust phylogenetic affiliation of arbuscular mycorrhizal fungi with mortierellales. Mol Biol Evol 29 (9):2199-2210

Nagahashi G, Douds DD (2000) Partial separation of root exudate components and their effects upon the growth of germinated spores of AM fungi. Mycol Res 104 (12):1453-1464

Nagata M, Yamamoto N, Shigeyama T, Terasawa Y, Anai T, Sakai T, Inada S, Arima S, Hashiguchi M, Akashi R (2015) Red/far red light controls arbuscular mycorrhizal colonization via jasmonic acid and strigolactone signaling. Plant Cell Physiol 56 (11):2100-2109

Nelson DC, Scaffidi A, Dun EA, Waters MT, Flematti GR, Dixon KW, Beveridge CA, Ghisalberti EL, Smith SM (2011) F-box protein MAX2 has dual roles in karrikin and strigolactone signaling in Arabidopsis thaliana. Proc Natl Acad Sci 108 (21):8897-8902

Nguema-Ona E, Coimbra S, Vicré-Gibouin M, Mollet J-C, Driouich A (2012) Arabinogalactan proteins in root and pollen-tube cells: distribution and functional aspects. Ann Bot 110 (2):383-404

Nouri E, Breuillin-Sessoms F, Feller U, Reinhardt D (2014) Phosphorus and nitrogen regulate arbuscular mycorrhizal symbiosis in Petunia hybrida. PloS one 9 (3):e90841

Nouri E, Reinhardt D (2015) Flowers and mycorrhizal roots–closer than we think? Trends Plant Sci 20 (6):344-350

Nuñez MA, Horton TR, Simberloff D (2009) Lack of belowground mutualisms hinders Pinaceae invasions. Ecology 90 (9):2352-2359

O'Connor PJ, Smith SE, Smith FA (2002) Arbuscular mycorrhizas influence plant diversity and community structure in a semiarid herbland. New Phytol 154 (1):209-218

Oda Y, Iida Y, Nagashima Y, Sugiyama Y, Fukuda H (2014) Novel coiled-coil proteins regulate exocyst association with cortical microtubules in xylem cells via the conserved oligomeric golgi-complex 2 protein. Plant Cell Physiol 56 (2):277-286

Oláh B, Brière C, Bécard G, Dénarié J, Gough C (2005) Nod factors and a diffusible factor from arbuscular mycorrhizal fungi stimulate lateral root formation in Medicago truncatula via the DMI1/DMI2 signalling pathway. Plant J 44 (2):195-207

Oldroyd GE (2013) Speak, friend, and enter: signalling systems that promote beneficial symbiotic associations in plants. Nat Rev Microbiol 11 (4):252-263

Pan H, Oztas O, Zhang X, Wu X, Stonoha C, Wang E, Wang B, Wang D (2016) A symbiotic SNARE protein generated by alternative termination of transcription. Nat Plants 2 (2):15197

Park H-J, Floss DS, Levesque-Tremblay V, Bravo A, Harrison MJ (2015) Hyphal branching during arbuscule development requires *RAM1*. Plant Physiol:pp. 01155.02015

Park S, Takano Y, Matsuura H, Yoshihara T (2004) Antifungal compounds from the root and root exudate of *Zea mays*. Biosci, Biotechnol, Biochem 68 (6):1366-1368

Parniske M (2008) Arbuscular mycorrhiza: the mother of plant root endosymbioses. Nat Rev Microbiol 6 (10):763-775

Pérez-Tienda J, Testillano PS, Balestrini R, Fiorilli V, Azcón-Aguilar C, Ferrol N (2011) *GintAMT2*, a new member of the ammonium transporter family in the arbuscular mycorrhizal fungus *Glomus intraradices*. Fungal Genet Biol 48 (11):1044-1055

Peters W, Latka I (1986) Electron microscopic localization of chitin using colloidal gold labelled with wheat germ agglutinin. Histochem Cell Biol 84 (2):155-160

Pfeffer PE, Douds DD, Bécard G, Shachar-Hill Y (1999) Carbon uptake and the metabolism and transport of lipids in an arbuscular mycorrhiza. Plant Physiol 120 (2):587-598

Phillips JM, Hayman D (1970) Improved procedures for clearing roots and staining parasitic and vesicular-arbuscular mycorrhizal fungi for rapid assessment of infection. Trans Br Mycol Soc 55 (1):158IN116-161IN118

Pimprikar P, Carbonnel S, Paries M, Katzer K, Klingl V, Bohmer MJ, Karl L, Floss DS, Harrison MJ, Parniske M (2016) A CCaMK-CYCLOPS-DELLA complex activates transcription of *RAM1* to regulate arbuscule branching. Curr Biol 26 (8):987-998

Pimprikar P, Gutjahr C (2018) Transcriptional regulation of arbuscular mycorrhiza development. Plant Cell Physiol 59 (4):673-690

Piotrowski JS, Lekberg Y, Harner MJ, Ramsey PW, Rillig MC (2008) Dynamics of mycorrhizae during development of riparian forests along an unregulated river. Ecography 31 (2):245-253

Pirozynski K, Malloch D (1975) The origin of land plants: a matter of mycotrophism. BioSyst 6 (3):153-164

Plett JM, Daguerre Y, Wittulsky S, Vayssières A, Deveau A, Melton SJ, Kohler A, Morrell-Falvey JL, Brun A, Veneault-Fourrey C (2014) Effector MiSSP7 of the mutualistic fungus Laccaria bicolor stabilizes the Populus JAZ6 protein and represses jasmonic acid (JA) responsive genes. Proc Natl Acad Sci 111 (22):8299-8304

Postma JW, Olsson PA, Falkengren-Grerup U (2007) Root colonisation by arbuscular mycorrhizal, fine endophytic and dark septate fungi across a pH gradient in acid beech forests. Soil Biol Biochem 39 (2):400-408

Pozo MJ, Azcón-Aguilar C (2007) Unraveling mycorrhiza-induced resistance. Curr Opin Plant Biol 10 (4):393-398

Pozo MJ, Azcón-Aguilar C, Dumas-Gaudot E, Barea JM (1999) β-1, 3-glucanase activities in tomato roots inoculated with arbuscular mycorrhizal fungi and/or *Phytophthora parasitica* and their possible involvement in bioprotection. Plant Sci 141 (2):149-157

Pozo MJ, Jung SC, López-Ráez JA, Azcón-Aguilar C (2010) Impact of arbuscular mycorrhizal symbiosis on plant response to biotic stress: the role of plant defence mechanisms. In: Arbuscular mycorrhizas: physiology and function. Springer, pp 193-207

Pozo MJ, Van Der Ent S, Van Loon L, Pieterse CM (2008) Transcription factor MYC2 is involved in priming for enhanced defense during rhizobacteria-induced systemic resistance in Arabidopsis thaliana. New Phytol 180 (2):511-523

Puga MI, Mateos I, Charukesi R, Wang Z, Franco-Zorrilla JM, de Lorenzo L, Irigoyen ML, Masiero S, Bustos R, Rodríguez J (2014) SPX1 is a phosphate-dependent inhibitor of Phosphate Starvation Response 1 in Arabidopsis. Proc Natl Acad Sci 111 (41):14947-14952

Pumplin N, Harrison MJ (2009) Live-cell imaging reveals periarbuscular membrane domains and organelle location in *Medicago truncatula* roots during arbuscular mycorrhizal symbiosis. Plant Physiol 151 (2):809-819. doi:10.1104/pp.109.141879

Pumplin N, Mondo SJ, Topp S, Starker CG, Gantt JS, Harrison MJ (2010) *Medicago truncatula* Vapyrin is a novel protein required for arbuscular mycorrhizal symbiosis. Plant J 61 (3):482-494. doi:10.1111/j.1365-313X.2009.04072.x

Redecker D, Kodner R, Graham LE (2000) Glomalean fungi from the Ordovician. Science 289 (5486):1920-1921

Reinhardt D (2007) Programming good relations—development of the arbuscular mycorrhizal symbiosis. Curr Opin Plant Biol 10 (1):98-105

Rich MK, Courty PE, Roux C, Reinhardt D (2017) Role of the GRAS transcription factor *ATA/RAM1* in the transcriptional reprogramming of arbuscular mycorrhiza in *Petunia hybrida*. BMC Genomics 18 (1):589. doi:10.1186/s12864-017-3988-8

Rich MK, Schorderet M, Bapaume L, Falquet L, Morel P, Vandenbussche M, Reinhardt D (2015) The petunia GRAS transcription factor *ATA/RAM1* regulates symbiotic gene expression and fungal morphogenesis in arbuscular mycorrhiza. Plant Physiol 168 (3):788-797

Rich MK, Schorderet M, Reinhardt D (2014) The role of the cell wall compartment in mutualistic symbioses of plants. Front Plant Sci 5:238

Rillig MC (2004) Arbuscular mycorrhizae and terrestrial ecosystem processes. Ecol Lett 7 (8):740-754

Rillig MC, Mummey DL (2006) Mycorrhizas and soil structure. New Phytol 171 (1):41-53

Roitsch T, Balibrea M, Hofmann M, Proels R, Sinha A (2003) Extracellular invertase: key metabolic enzyme and PR protein. J Exp Bot 54 (382):513-524

Rose S, Youngberg C (1981) Tripartite associations in snowbrush (Ceanothus velutinus): effect of vesicular–arbuscular mycorrhizae on growth, nodulation, and nitrogen fixation. Can J Bot 59 (1):34-39

Ruan Y-L (2014) Sucrose metabolism: gateway to diverse carbon use and sugar signaling. Annu Rev Plant Biol 65:33-67

Rubio V, Linhares F, Solano R, Martín AC, Iglesias J, Leyva A, Paz-Ares J (2001) A conserved MYB transcription factor involved in phosphate starvation signaling both in vascular plants and in unicellular algae. Genes Dev 15 (16):2122-2133

Ruiz-Lozano JM, Porcel R, Azcón C, Aroca R (2012) Regulation by arbuscular mycorrhizae of the integrated physiological response to salinity in plants: new challenges in physiological and molecular studies. J Exp Bot 63 (11):4033-4044

Ruiz-Lozano J, Azcon R, Gomez M (1996) Alleviation of salt stress by arbuscular-mycorrhizal *Glomus* species in *Lactuca sativa* plants. Physiol Plant 98 (4):767-772

Ruiz-Lozano JM, Aroca R, Zamarreño ÁM, Molina S, Andreo-Jiménez B, Porcel R, García-Mina JM, Ruyter-Spira C, López-Ráez JA (2016) Arbuscular mycorrhizal symbiosis induces strigolactone biosynthesis under drought and improves drought tolerance in lettuce and tomato. Plant, Cell Environ 39 (2):441-452

Russo G, Spinella S, Sciacca E, Bonfante P, Genre A (2013) Automated analysis of calcium spiking profiles with CaSA software: two case studies from root-microbe symbioses. BMC Plant Biol 13 (1):224

Ruyter-Spira C, Al-Babili S, Van Der Krol S, Bouwmeester H (2013) The biology of strigolactones. Trends Plant Sci 18 (2):72-83

Ruzicka DR, Hausmann NT, Barrios-Masias FH, Jackson LE, Schachtman DP (2012) Transcriptomic and metabolic responses of mycorrhizal roots to nitrogen patches under field conditions. Plant Soil 350 (1-2):145-162

Salzer P, Hager A (1991) Sucrose Utilization of the Ectomycorrhizal Fungi *Amanita muscaria* and *Hebeloma crustuliniforme* Depends on the Cell Wall-bound Invertase Activity of their Host *Picea abies*. Plant Biol 104 (6):439-445

Sanders F, Sheikh N (1983) The development of vesicular-arbuscular mycorrhizal infection in plant root systems. In: Tree Root Systems and Their Mycorrhizas. Springer, pp 223-246

Schaarschmidt S, González M-C, Roitsch T, Strack D, Sonnewald U, Hause B (2007) Regulation of arbuscular mycorrhization by carbon. The symbiotic interaction cannot be improved by increased carbon availability accomplished by root-specifically enhanced invertase activity. Plant Physiol 143 (4):1827-1840

Schaarschmidt S, Gresshoff PM, Hause B (2013) Analyzing the soybean transcriptome during autoregulation of mycorrhization identifies the transcription factors GmNF-YA1a/b as positive regulators of arbuscular mycorrhization. Genome Biol 14 (6):R62

Schaarschmidt S, Roitsch T, Hause B (2006) Arbuscular mycorrhiza induces gene expression of the apoplastic invertase LIN6 in tomato (*Lycopersicon esculentum*) roots. J Exp Bot 57 (15):4015-4023

Schenck N, Graham S, Green N (1975) Temperature and light effect on contamination and spore germination of vesicular-arbuscular mycorrhizal fungi. Mycologia 67 (6):1189-1192

Schubert A, Allara P, Morte A (2004) Cleavage of sucrose in roots of soybean (*Glycine max*) colonized by an arbuscular mycorrhizal fungus. New Phytol 161 (2):495-501

Schüßler A, Martin H, Cohen D, Fitz M, Wipf D (2006) Characterization of a carbohydrate transporter from symbiotic glomeromycotan fungi. Nature 444 (7121):933

Schüßler A, Walker C (2010) The Glomeromycota: a species list with new families and new genera. The Royal Botanic Garden Kew, Botanische Staatssammlung Munich, and Oregon State University

Schutzendubel A, Polle A (2002) Plant responses to abiotic stresses: heavy metal-induced oxidative stress and protection by mycorrhization. J Exp Bot 53 (372):1351-1365

Schüβler A, Schwarzott D, Walker C (2001) A new fungal phylum, the Glomeromycota: phylogeny and evolution. Mycol Res 105 (12):1413-1421. doi:https://doi.org/10.1017/S0953756201005196

Selosse M-A, Bessis A, Pozo MJ (2014) Microbial priming of plant and animal immunity: symbionts as developmental signals. Trends Microbiol 22 (11):607-613

Serrani JC, Sanjuán R, Ruiz-Rivero O, Fos M, García-Martínez JL (2007) Gibberellin regulation of fruit set and growth in tomato. Plant Physiol 145 (1):246-257

Shachar-Hill Y, Pfeffer PE, Douds D, Osman SF, Doner LW, Ratcliffe RG (1995) Partitioning of intermediary carbon metabolism in vesicular-arbuscular mycorrhizal leek. Plant Physiol 108 (1):7-15

Shtark OY, Sulima AS, Zhernakov AI, Kliukova MS, Fedorina JV, Pinaev AG, Kryukov AA, Akhtemova GA, Tikhonovich IA, Zhukov VA (2016) Arbuscular mycorrhiza development in pea (*Pisum sativum* L.) mutants impaired in five early nodulation genes including putative orthologs of *NSP1* and *NSP2*. Symbiosis 68 (1-3):129-144

Sieberer BJ, Chabaud M, Fournier J, Timmers AC, Barker DG (2012) A switch in Ca2+ spiking signature is concomitant with endosymbiotic microbe entry into cortical root cells of Medicago truncatula. Plant J 69 (5):822-830

Siebers M, Brands M, Wewer V, Duan Y, Hölzl G, Dörmann P (2016) Lipids in plant–microbe interactions. Biochimica et Biophysica Acta (BBA)-Molecular and Cell Biology of Lipids 1861 (9):1379-1395

Sieverding E, da Silva GA, Berndt R, Oehl F (2015) *Rhizoglomus*, a new genus of the Glomeraceae. Mycotaxon 129 (2):373-386

Singh R, Choudhary A, Gulati A, Dahiya H, Jaiwal P, Sengar R (1997) Response of plants to salinity in interaction with other abiotic and biotic factors.

Singh S, Katzer K, Lambert J, Cerri M, Parniske M (2014) CYCLOPS, a DNA-binding transcriptional activator, orchestrates symbiotic root nodule development. Cell host & microbe 15 (2):139-152

Singh S, Parniske M (2012) Activation of calcium-and calmodulin-dependent protein kinase (CCaMK), the central regulator of plant root endosymbiosis. Curr Opin Plant Biol 15 (4):444-453

SMITH D, MUSCATINE L, LEWIS D (1969) Carbohydrate movement from autotrophs to heterotrophs in parasitic and mutualistic symbiosis. Biological Reviews 44 (1):17-85

Smith S, Gianinazzi-Pearson V (1988) Physiological interactions between symbionts in vesicular-arbuscular mycorrhizal plants. Annu Rev Plant Physiol Plant Mol Biol 39 (1):221-244

Smith S, Read D (2008) Mycorrhizal Symbiosis. 3 th. Academic Press. London.,

Sokolski S, Dalpé Y, Seguin S, Khasa D, Levesque CA, Piché Y (2010) Conspecificity of DAOM 197198, the model arbuscular mycorrhizal fungus, with *Glomus irregulare*: molecular evidence with three protein-encoding genes. Botany 88 (9):829-838

Solaiman MZ, Saito M (1997) Use of sugars by intraradical hyphae of arbuscular mycorrhizal fungi revealed by radiorespirometry. New Phytol 136 (3):533-538

Song Y, Chen D, Lu K, Sun Z, Zeng R (2015) Enhanced tomato disease resistance primed by arbuscular mycorrhizal fungus. Front Plant Sci 6:786

Song YY, Ye M, Li C, He X, Zhu-Salzman K, Wang RL, Su YJ, Luo SM, Zeng RS (2014) Hijacking common mycorrhizal networks for herbivore-induced defence signal transfer between tomato plants. Scientific reports 4:3915

Souza T (2015) Glomeromycota classification. In: Handbook of Arbuscular Mycorrhizal Fungi. Springer, pp 87-128

Sparks E, Wachsman G, Benfey PN (2013) Spatiotemporal signalling in plant development. Nature Reviews Genetics 14 (9):631

St Arnaud M, Elsen A (2005) Interaction of arbuscular mycorrhizal fungi with soil-borne pathogens and non-pathogenic rhizosphere micro-organisms. In: In vitro culture of mycorrhizas. Springer, pp 217-231

Stinson KA, Campbell SA, Powell JR, Wolfe BE, Callaway RM, Thelen GC, Hallett SG, Prati D, Klironomos JN (2006) Invasive plant suppresses the growth of native tree seedlings by disrupting belowground mutualisms. PLoS Biol 4 (5):e140

Stockinger H, Walker C, Schüßler A (2009) '*Glomus intraradices* DAOM197198', a model fungus in arbuscular mycorrhiza research, is not *Glomus intraradices*. New Phytol 183 (4):1176-1187

Strack D, Fester T (2006) Isoprenoid metabolism and plastid reorganization in arbuscular mycorrhizal roots. New Phytol 172 (1):22-34

Stracke S, Kistner C, Yoshida S, Mulder L, Sato S, Kaneko T, Tabata S, Sandal N, Stougaard J, Szczyglowski K (2002) A plant receptor-like kinase required for both bacterial and fungal symbiosis. Nature 417 (6892):959

Sun J, Miller JB, Granqvist E, Wiley-Kalil A, Gobbato E, Maillet F, Cottaz S, Samain E, Venkateshwaran M, Fort S (2015) Activation of symbiosis signaling by arbuscular mycorrhizal fungi in legumes and rice. Plant Cell 27 (3):823-838

Takeda N, Handa Y, Tsuzuki S, Kojima M, Sakakibara H, Kawaguchi M (2015) Gibberellins interfere with symbiosis signaling and gene expression and alter colonization by arbuscular mycorrhizal fungi in Lotus japonicus. Plant Physiol 167 (2):545-557

Takeda N, Tsuzuki S, Suzaki T, Parniske M, Kawaguchi M (2013) CERBERUS and NSP1 of Lotus japonicus are common symbiosis genes that modulate arbuscular mycorrhiza development. Plant Cell Physiol 54 (10):1711-1723

Tani C, Ohtomo R, Osaki M, Kuga Y, Ezawa T (2009) ATP-dependent but proton gradient-independent polyphosphate-synthesizing activity in extraradical hyphae of an arbuscular mycorrhizal fungus. Appl Environ Microbiol 75 (22):7044-7050

Taylor TN, Osborn JM (1996) The importance of fungi in shaping the paleoecosystem. Rev Palaeobot Palynol 90 (3-4):249-262

Tian C, Wan P, Sun S, Li J, Chen M (2004) Genome-wide analysis of the GRAS gene family in rice and *Arabidopsis*. Plant Mol Biol 54 (4):519-532. doi:10.1023/b:plan.0000038256.89809.57

Timonen S, Peterson RL (2002) Cytoskeleton in mycorrhizal symbiosis. Plant Soil 244 (1):199-210

Tisserant E, Malbreil M, Kuo A, Kohler A, Symeonidi A, Balestrini R, Charron P, Duensing N, dit Frey NF, Gianinazzi-Pearson V (2013) Genome of an arbuscular mycorrhizal fungus provides insight into the oldest plant symbiosis. Proc Natl Acad Sci 110 (50):20117-20122

To A, Joubès J, Barthole G, Lécureuil A, Scagnelli A, Jasinski S, Lepiniec L, Baud S (2012) WRINKLED transcription factors orchestrate tissue-specific regulation of fatty acid biosynthesis in Arabidopsis. Plant Cell 24 (12):5007-5023

Tommerup I (1985) Inhibition of spore germination of vesicular-arbuscular mycorrhizal fungi in soil. Trans Br Mycol Soc 85 (2):267-278

Toro KS, Brachmann A (2016) The effector candidate repertoire of the arbuscular mycorrhizal fungus Rhizophagus clarus. BMC Genomics 17 (1):101

Toro M, Azcón R, Barea J (1998) The use of isotopic dilution techniques to evaluate the interactive effects of Rhizobium genotype, mycorrhizal fungi, phosphate-solubilizing rhizobacteria and rock phosphate on nitrogen and phosphorus acquisition by Medicago sativa. New Phytol 138 (2):265-273

Torres-Vera R, García JM, Pozo MJ, López-Ráez JA (2016) Expression of molecular markers associated to defense signaling pathways and strigolactone biosynthesis during the early interaction tomato-Phelipanche ramosa. Physiol Mol Plant Pathol 94:100-107

Trouvelot A (1986) Mesure du taux de mycorhization VA d'un systeme radiculaire. Recherche de methodes d'estimation ayant une significantion fonctionnelle. Mycorrhizae: physiology and genetics:217-221

Tsuzuki S, Handa Y, Takeda N, Kawaguchi M (2016) Strigolactone-induced putative secreted protein 1 is required for the establishment of symbiosis by the arbuscular mycorrhizal fungus Rhizophagus irregularis. Mol Plant-Microbe Interact 29 (4):277-286

Udvardi MK, Scheible W-R (2005) GRAS genes and the symbiotic green revolution. Science 308 (5729):1749-1750

Upadhyaya H, Panda SK, Bhattacharjee MK, Dutta S (2010) Role of arbuscular mycorrhiza in heavy metal tolerance in plants: prospects for phytoremidiation. Journal of Phytology 2 (7)

Van Der Heijden MG, Bardgett RD, Van Straalen NM (2008) The unseen majority: soil microbes as drivers of plant diversity and productivity in terrestrial ecosystems. Ecol Lett 11 (3):296-310

Van der Heijden MG, Klironomos JN, Ursic M, Moutoglis P, Streitwolf-Engel R, Boller T, Wiemken A, Sanders IR (1998) Mycorrhizal fungal diversity determines plant biodiversity, ecosystem variability and productivity. Nature 396 (6706):69

Vogelsang KM, Bever JD (2009) Mycorrhizal densities decline in association with nonnative plants and contribute to plant invasion. Ecology 90 (2):399-407

Vogelsang KM, Reynolds HL, Bever JD (2006) Mycorrhizal fungal identity and richness determine the diversity and productivity of a tallgrass prairie system. New Phytol 172 (3):554-562

Vos C, Claerhout S, Mkandawire R, Panis B, De Waele D, Elsen A (2012) Arbuscular mycorrhizal fungi reduce root-knot nematode penetration through altered root exudation of their host. Plant Soil 354 (1-2):335-345

Wagg C, Jansa J, Stadler M, Schmid B, Van Der Heijden MG (2011) Mycorrhizal fungal identity and diversity relaxes plant–plant competition. Ecology 92 (6):1303-1313

Walter MH (2013) Role of carotenoid metabolism in the arbuscular mycorrhizal symbiosis. Molecular Microbial Ecology of the Rhizosphere: Volume 1 & 2:513-524

Walter MH, Stauder R, Tissier A (2015) Evolution of root-specific carotenoid precursor pathways for apocarotenoid signal biogenesis. Plant Sci 233:1-10

Wang E, Schornack S, Marsh JF, Gobbato E, Schwessinger B, Eastmond P, Schultze M, Kamoun S, Oldroyd GE (2012) A common signaling process that promotes mycorrhizal and oomycete colonization of plants. Curr Biol 22 (23):2242-2246

Wang P, Hawkins TJ, Richardson C, Cummins I, Deeks MJ, Sparkes I, Hawes C, Hussey PJ (2014a) The plant cytoskeleton, NET3C, and VAP27 mediate the link between the plasma membrane and endoplasmic reticulum. Curr Biol 24 (12):1397-1405. doi:10.1016/j.cub.2014.05.003

Wang P, Hussey PJ (2015) Interactions between plant endomembrane systems and the actin cytoskeleton. Front Plant Sci 6

Wang W, Shi J, Xie Q, Jiang Y, Yu N, Wang E (2017) Nutrient exchange and regulation in arbuscular mycorrhizal symbiosis. Mol plant

Wang Z, Ruan W, Shi J, Zhang L, Xiang D, Yang C, Li C, Wu Z, Liu Y, Yu Y (2014b) Rice SPX1 and SPX2 inhibit phosphate starvation responses through interacting with PHR2 in a phosphate-dependent manner. Proc Natl Acad Sci 111 (41):14953-14958

Wasternack C, Hause B (2013) Jasmonates: biosynthesis, perception, signal transduction and action in plant stress response, growth and development. An update to the 2007 review in Annals of Botany. Ann Bot 111 (6):1021-1058

Waters MT, Gutjahr C, Bennett T, Nelson DC (2017) Strigolactone Signaling and Evolution. Annu Rev Plant Biol 68:291-322. doi:10.1146/annurev-arplant-042916-040925

Waters MT, Nelson DC, Scaffidi A, Flematti GR, Sun YK, Dixon KW, Smith SM (2012) Specialisation within the DWARF14 protein family confers distinct responses to karrikins and strigolactones in Arabidopsis. Development 139 (7):1285-1295. doi:10.1242/dev.074567

Waters MT, Scaffidi A, Flematti G, Smith SM (2015) Substrate-induced degradation of the α/β-fold hydrolase KARRIKIN INSENSITIVE2 requires a functional catalytic triad but is independent of MAX2. Mol plant 8 (5):814-817

Waters MT, Scaffidi A, Sun YK, Flematti GR, Smith SM (2014) The karrikin response system of Arabidopsis. Plant J 79 (4):623-631

Wellman CH, Osterloff PL, Mohiuddin U (2003) Fragments of the earliest land plants. Nature 425 (6955):282

Wewer V, Brands M, Dörmann P (2014) Fatty acid synthesis and lipid metabolism in the obligate biotrophic fungus Rhizophagus irregularis during mycorrhization of Lotus japonicus. Plant J 79 (3):398-412

Wild R, Gerasimaite R, Jung J-Y, Truffault V, Pavlovic I, Schmidt A, Saiardi A, Jessen HJ, Poirier Y, Hothorn M (2016) Control of eukaryotic phosphate homeostasis by inositol polyphosphate sensor domains. Science:aad9858

Willige BC, Ghosh S, Nill C, Zourelidou M, Dohmann EM, Maier A, Schwechheimer C (2007) The DELLA domain of GA INSENSITIVE mediates the interaction with the GA INSENSITIVE DWARF1A gibberellin receptor of Arabidopsis. Plant Cell 19 (4):1209-1220

Wu P, Shou H, Xu G, Lian X (2013) Improvement of phosphorus efficiency in rice on the basis of understanding phosphate signaling and homeostasis. Curr Opin Plant Biol 16 (2):205-212

Wu Q-S, Xia R-X, Zou Y-N (2008) Improved soil structure and citrus growth after inoculation with three arbuscular mycorrhizal fungi under drought stress. European journal of soil biology 44 (1):122-128

Xue L, Cui H, Buer B, Vijayakumar V, Delaux P-M, Junkermann S, Bucher M (2015) Network of GRAS transcription factors involved in the control of arbuscule development in *Lotus japonicus*. Plant Physiol 167 (3):854-871

Yamada K, Saijo Y, Nakagami H, Takano Y (2016) Regulation of sugar transporter activity for antibacterial defense in Arabidopsis. Science 354 (6318):1427-1430

Yamada M, Tanaka-Takiguchi Y, Hayashi M, Nishina M, Goshima G (2017) Multiple kinesin-14 family members drive microtubule minus end–directed transport in plant cells. J Cell Biol 216 (6):1705-1714

Yang G, Liu N, Lu W, Wang S, Kan H, Zhang Y, Xu L, Chen Y (2014) The interaction between arbuscular mycorrhizal fungi and soil phosphorus availability influences plant community productivity and ecosystem stability. J Ecol 102 (4):1072-1082

Yang S-Y, Grønlund M, Jakobsen I, Grotemeyer MS, Rentsch D, Miyao A, Hirochika H, Kumar CS, Sundaresan V, Salamin N (2012) Nonredundant regulation of rice arbuscular mycorrhizal symbiosis by two members of the PHOSPHATE TRANSPORTER1 gene family. Plant Cell 24 (10):4236-4251

Yano K, Yoshida S, Müller J, Singh S, Banba M, Vickers K, Markmann K, White C, Schuller B, Sato S (2008) CYCLOPS, a mediator of symbiotic intracellular accommodation. Proc Natl Acad Sci 105 (51):20540-20545

Yao M, Desilets H, Charles M, Boulanger R, Tweddell R (2003) Effect of mycorrhization on the accumulation of rishitin and solavetivone in potato plantlets challenged with Rhizoctonia solani. Mycorrhiza 13 (6):333-336

Yoneyama K, Xie X, Kim HI, Kisugi T, Nomura T, Sekimoto H, Yokota T, Yoneyama K (2012) How do nitrogen and phosphorus deficiencies affect strigolactone production and exudation? Planta 235 (6):1197-1207

Yoneyama K, Yoneyama K, Takeuchi Y, Sekimoto H (2007) Phosphorus deficiency in red clover promotes exudation of orobanchol, the signal for mycorrhizal symbionts and germination stimulant for root parasites. Planta 225 (4):1031-1038

Yoshida H, Hirano K, Sato T, Mitsuda N, Nomoto M, Maeo K, Koketsu E, Mitani R, Kawamura M, Ishiguro S (2014) DELLA protein functions as a transcriptional activator through the DNA binding of the indeterminate domain family proteins. Proc Natl Acad Sci 111 (21):7861-7866

Yoshida S, Kameoka H, Tempo M, Akiyama K, Umehara M, Yamaguchi S, Hayashi H, Kyozuka J, Shirasu K (2012) The D3 F-box protein is a key component in host strigolactone responses essential for arbuscular mycorrhizal symbiosis. New Phytol 196 (4):1208-1216

Young JPW (2015) Genome diversity in arbuscular mycorrhizal fungi. Curr Opin Plant Biol 26:113-119

Yu N, Luo D, Zhang X, Liu J, Wang W, Jin Y, Dong W, Liu J, Liu H, Yang W (2014) A DELLA protein complex controls the arbuscular mycorrhizal symbiosis in plants. Cell Res 24 (1):130

Zangaro W, Ansanelo AP, Lescano LEAM, de Almeida Alves R, Rondina ABL, Nogueira MA (2012) Infection intensity, spore density and inoculum potential of arbuscular mycorrhizal fungi decrease during secondary succession in tropical Brazilian ecosystems. J Trop Ecol 28 (5):453-462

Zeng T, Holmer R, Hontelez J, Te Lintel-Hekkert B, Marufu L, de Zeeuw T, Wu F, Schijlen E, Bisseling T, Limpens E (2018) Host- and stage-dependent secretome of the arbuscular mycorrhizal fungus Rhizophagus irregularis. Plant J 94 (3):411-425. doi:10.1111/tpj.13908

Zhang Q, Blaylock LA, Harrison MJ (2010) Two *Medicago truncatula* half-ABC transporters are essential for arbuscule development in arbuscular mycorrhizal symbiosis. Plant Cell 22 (5):1483-1497

Zhang X, Dong W, Sun J, Feng F, Deng Y, He Z, Oldroyd GE, Wang E (2015a) The receptor kinase CERK1 has dual functions in symbiosis and immunity signalling. Plant J 81 (2):258-267

Zhang X, Pumplin N, Ivanov S, Harrison MJ (2015b) EXO70I Is Required for Development of a Sub-domain of the Periarbuscular Membrane during Arbuscular Mycorrhizal Symbiosis. Curr Biol 25 (16):2189-2195. doi:10.1016/j.cub.2015.06.075

Zhang ZL, Ogawa M, Fleet CM, Zentella R, Hu J, Heo JO, Lim J, Kamiya Y, Yamaguchi S, Sun TP (2011) Scarecrow-like 3 promotes gibberellin signaling by antagonizing master growth repressor DELLA in Arabidopsis. Proceedings of the National Academy of Sciences of the United States of America 108 (5):2160-2165. doi:10.1073/pnas.1012232108

Zhao Y, Zhao Q, Ao G, Yu J (2006) Characterization and functional analysis of a pollen-specific gene st901 in *Solanum tuberosum*. Planta 224 (2):405-412. doi:10.1007/s00425-006-0226-z

Zhou J, Jiao F, Wu Z, Li Y, Wang X, He X, Zhong W, Wu P (2008) OsPHR2 is involved in phosphate-starvation signaling and excessive phosphate accumulation in shoots of plants. Plant Physiol 146 (4):1673-1686

Zhu C, Ganguly A, Baskin TI, McClosky DD, Anderson CT, Foster C, Meunier KA, Okamoto R, Berg H, Dixit R (2015) The fragile Fiber1 kinesin contributes to cortical microtubule-mediated trafficking of cell wall components. Plant Physiol 167 (3):780-792

Zhu X, Song F, Liu S, Liu T, Zhou X (2012) Arbuscular mycorrhizae improves photosynthesis and water status of *Zea mays* L. under drought stress. Plant Soil Environ 58 (4):186-191

Supplementary information

Supplementary Table S1. RNA-seq data: wt-I *vs* NI.

Up- and down- regulated genes in AM-roots vs uninoculated roots by >10 fold change

ID (SolDB accesión)	**Fold Change**	**P value**	**Description**
Solyc08g065690.1.1	273.80	1.04E-65	Vacuolar-processing enzyme
Solyc08g079780.2.1	266.00	1.73E-79	Blue copper protein, putative
Solyc03g117450.2.1	220.97	1.33E-50	Major allergen Pru ar 1
TCONS_00030605	204.20	1.57E-62	
Solyc04g072480.3.1	194.00	6.37E-60	phosphopantothenate-cysteine ligase-like protein
Solyc01g005940.3.1	175.70	5.06E-57	Phytoene synthase
Solyc12g056000.2.1	161.40	7.08E-88	Cysteine protease, putative
Solyc02g081240.1.1	155.03		Glutathione s-transferase, putative
Solyc01g010260.3.1	154.91	4.25E-52	Cytochrome P450
Solyc12g056020.1.1	151.06	6.14E-60	Cysteine protease, putative
Solyc04g071920.2.1	141.72	5.02E-57	Protein kinase-like protein
Solyc07g014680.3.1	140.05	1.53E-50	sodium transporter HKT1,2
Solyc01g095260.1.1	139.18	1.85E-73	Acidic endochitinase
Solyc11g007970.2.1	131.50	1.82E-42	4-coumarate--CoA ligase like
Solyc11g068590.2.1	130.81	6.15E-46	Germin-like protein 1
Solyc05g055490.2.1	130.14	3.50E-55	Monocopper oxidase-like protein SKU5
Solyc12g056500.1.1	119.74	1.97E-40	Blue copper protein, putative
TCONS_00033759	118.42	2.12E-42	
Solyc11g072750.2.1	117.13	1.33E-42	Chitinase
Solyc07g042880.1.1	111.77	3.94E-40	Cytochrome P450
Solyc09g072700.3.1	107.50	6.07E-67	Peroxidase
Solyc04g080400.2.1	100.74	4.02E-37	FAD-binding Berberine family protein
Solyc03g098090.2.1	92.18	6.08E-48	CASP-like protein
Solyc04g015790.1.1	80.49	2.40E-33	LOW QUALITY:guanosine nucleotide diphosphate dissociation inhibitor 1
Solyc06g034010.1.1	80.48	2.74E-32	LOW QUALITY:Protein kinase superfamily protein
Solyc06g066830.3.1	77.80	3.35E-38	2-oxoglutarate-dependent dioxygenase-related family protein
Solyc11g012010.2.1	70.75	2.66E-35	RPM1 interacting protein 4, putative
Solyc05g013890.2.1	67.28	6.59E-33	ABC transporter B family protein
Solyc07g052070.2.1	66.35	3.64E-33	Cytochrome P450
Solyc09g072780.2.1	63.85	6.88E-34	Peptide transporter
Solyc12g096780.2.1	59.41	1.24E-31	Zinc binding dehydrogenase, putative
Solyc07g064450.3.1	59.03	7.91E-40	Cytochrome P450
Solyc05g009960.3.1	58.07	7.25E-38	Clavaminate synthase-like protein family
Solyc12g057050.2.1	56.68	1.73E-27	NOD26-like intrinsic protein 3.2
Solyc06g072950.2.1	54.83	1.94E-99	ABC transporter B family protein
Solyc12g049190.2.1	54.31	1.54E-28	Leucine-rich repeat receptor-like protein kinase family protein
Solyc10g078840.2.1	54.17	2.93E-29	Germin-like protein 1
Solyc10g079540.1.1	50.82	6.37E-22	O-methyltransferase
Solyc04g080480.1.1	50.57	9.89E-42	4-coumarate--CoA ligase-like 4
Solyc02g072370.2.1	50.42		Subtilisin-like protease

Solyc08g067080.2.1	49.92	3.52E-25	Ammonium transporter
Solyc09g066450.2.1	49.09	2.15E-37	GRAS family transcription factor
Solyc01g005090.3.1	48.66	3.05E-34	Type I inositol-1,4,5-trisphosphate 5-phosphatase CVP2
Solyc01g095250.1.1	48.01	3.67E-52	Acidic endochitinase
Solyc11g065480.2.1	47.62	4.22E-23	transferring glycosyl group transferase (DUF604)
TCONS_00053706	46.98	5.04E-21	
Solyc08g007050.2.1	46.75	2.02E-23	Cytochrome P450
Solyc11g065910.1.1	46.36	2.63E-37	Aspartic protease inhibitor 9
Solyc08g062200.2.1	45.96	3.63E-32	Plant regulator RWP-RK family protein
Solyc01g091760.2.1	45.85	2.61E-30	Ethylene-responsive transcription factor
Solyc08g069170.2.1	45.57	1.10E-22	Receptor protein kinase, putative
Solyc11g007250.2.1	44.93	2.65E-23	Protein kinase like protein
Solyc07g005080.1.1	44.69	6.51E-25	LOW QUALITY:Chitinase, putative
TCONS_00001533	43.85		
Solyc06g007860.1.1	43.38	9.08E-31	LOW QUALITY:S-norcoclaurine synthase
Solyc07g009235.1.1	42.94	8.33E-26	Defensin-like protein
Solyc07g006610.3.1	42.78	3.18E-38	Tyrosine kinase family protein
Solyc04g015770.1.1	41.94	3.73E-19	LOW QUALITY:Phosphatidylinositol N-acetyglucosaminlytransferase subunit P-like protein
Solyc02g077870.1.1	41.54	2.67E-22	LOW QUALITY:membrane-associated kinase regulator
Solyc11g072760.1.1	41.45	4.99E-33	Chitinase
Solyc01g088110.1.1	40.24	1.33E-22	LOW QUALITY:metacaspase 5
Solyc01g106160.2.1	39.48	2.35E-21	Clade XVIII lectin receptor kinase
Solyc12g010490.2.1	39.19	9.37E-21	AP2-like ethylene-responsive transcription factor family
Solyc06g083933.1.1	39.01	1.49E-20	Zinc finger, C2H2
Solyc05g005870.3.1	37.77	2.03E-22	nodulin-related MtN21 family protein
Solyc00g108555.1.1	37.76	3.63E-24	Chaperone protein DNAj, putative
Solyc01g094430.1.1	37.27	1.17E-30	Ripening related protein family
Solyc00g170200.1.1	37.00	9.07E-42	LOW QUALITY:Sigma factor sigB regulation protein rsbQ
Solyc03g110950.1.1	35.72		LOW QUALITY:GRAS family transcription factor
Solyc01g011497.1.1	35.60	1.36E-23	defensin-like protein
Solyc10g007960.1.1	35.50	1.25E-20	Allene oxide synthase
Solyc08g074715.1.1	34.07	5.08E-31	Ripening related protein family
Solyc05g005660.1.1	32.20	6.85E-20	LOW QUALITY:Serine-threonine protein kinase, putative
Solyc12g009950.1.1	31.43	3.24E-16	Peroxidase
Solyc03g118760.3.1	30.95	4.77E-18	Tubulin beta chain
Solyc10g011840.2.1	30.63	8.07E-22	phosphopantothenate-cysteine ligase-like protein
Solyc04g079330.2.1	30.50	4.12E-31	Carboxypeptidase
Solyc01g102360.2.1	30.47	6.45E-16	Nitrate transporter protein 1.2-like protein
Solyc07g064120.2.1	30.15	2.02E-26	ABC transporter B family protein
Solyc02g069543.1.1	29.78	2.46E-25	LOW QUALITY:Protein prune-like protein
Solyc02g083160.2.1	28.40	3.74E-17	GDSL esterase/lipase
Solyc01g111960.3.1	28.32	3.98E-16	GDSL esterase/lipase family
Solyc05g043360.2.1	28.27	6.07E-18	Laccase
Solyc01g081080.2.1	27.67	2.96E-18	Replication factor C subunit, putative
Solyc04g077760.1.1	27.50	9.76E-21	LOW QUALITY:Exocyst complex component 7
Solyc09g011130.2.1	27.35	3.93E-24	NAD(P)-binding Rossmann-fold superfamily protein
Solyc08g014360.2.1	27.35	2.04E-16	Cinnamyl alcohol dehydrogenase
Solyc09g072720.2.1	27.18	6.85E-18	Exocyst complex component 8

Solyc01g006640.1.1	27.17	2.45E-22	LOW QUALITY:AMP-dependent synthetase and ligase family protein
Solyc02g084930.3.1	27.10	7.71E-48	Cytochrome P450 family protein
Solyc08g062140.1.1	26.70	2.72E-16	LOW QUALITY:MAP kinase kinase kinase 62
Solyc01g090660.3.1	26.50	2.79E-16	carotenoid cleavage dioxygenase7
Solyc07g005685.1.1	26.13	1.29E-37	Carboxypeptidase
Solyc02g085060.2.1	25.99	7.25E-16	Replication factor C subunit 3
Solyc03g013340.3.1	25.68	2.23E-18	NOD26-like intrinsic protein 2.1
Solyc04g050940.2.1	24.91	7.78E-15	Tyrosine kinase family protein
Solyc08g065710.2.1	24.45	2.34E-14	Vacuolar-processing enzyme
Solyc05g006360.1.1	24.21	2.89E-16	Metalloendoproteinase 1, putative
Solyc02g038720.2.1	24.17	6.22E-15	LOW QUALITY:Acyl carrier protein
Solyc07g052960.2.1	24.06	1.28E-15	GRAS family TF
Solyc03g098710.1.1	24.06	1.09E-13	Kunitz trypsin inhibitor
Solyc06g065600.1.1	24.05	9.30E-15	Non-specific lipid-transfer protein
Solyc01g067370.3.1	23.85	1.40E-15	TSB
Solyc04g005000.1.1	23.78	1.63E-18	LOW QUALITY:TRICHOME BIREFRINGENCE-LIKE 20
Solyc07g006630.3.1	23.75	5.53E-19	CONSTANS-like protein
Solyc11g008840.2.1	23.46	5.41E-15	ATP-binding protein, putative
Solyc01g006840.3.1	23.44	6.16E-22	Calcium-dependent protein kinase, putative
Solyc01g009400.3.1	22.71	4.72E-23	Peroxidase
Solyc07g054390.1.1	22.55	1.10E-14	LOW QUALITY:QWRF motif protein (DUF566)
Solyc07g005630.3.1	22.38	2.41E-19	LOW QUALITY:Defensin
Solyc10g009150.3.1	22.09	1.11E-50	Organ-specific protein S2
Solyc11g018535.1.1	22.07	9.93E-16	Metal transporter, putative
Solyc07g005680.3.1	21.85	5.28E-17	Carboxypeptidase
Solyc02g086460.3.1	21.75	1.17E-43	A-kinase anchor-like protein
Solyc12g007220.2.1	21.45	4.12E-14	Major facilitator superfamily protein
Solyc11g010850.2.1	20.86	8.30E-34	1-deoxy-D-xylulose 5-phosphate synthase
Solyc01g080790.3.1	20.45	2.22E-14	Plant basic secretory family protein
Solyc11g071880.2.1	20.43	1.53E-12	receptor-like kinase2
Solyc02g078710.1.1	20.34	1.99E-13	F-box/kelch-repeat protein
Solyc02g087500.2.1	20.07		Glycerol-3-phosphate acyltransferase
Solyc10g086450.1.1	19.33	1.55E-13	LOW QUALITY:cyclin-dependent protein kinase inhibitor
Solyc04g040120.1.1	19.31	5.06E-23	Fatty acid desaturase
Solyc10g009310.3.1	19.08	2.37E-18	Cytochrome P450
Solyc01g095550.2.1	19.00	3.69E-18	LOW QUALITY:Protein kinase family protein
Solyc11g067320.1.1	18.83	1.07E-18	Sulfotransferase
Solyc04g078710.2.1	18.72	7.15E-12	Subtilisin-like protease
Solyc04g051460.3.1	18.47	2.22E-12	Protein kinase family protein
Solyc08g077000.1.1	18.35	2.02E-12	LOW QUALITY:Zinc finger, C2H2
Solyc01g008415.1.1	18.28		Defensin
Solyc06g005910.3.1	18.18	2.24E-20	Tubulin beta chain
Solyc11g018530.2.1	18.17	1.86E-23	root-specific metal transporter
Solyc10g007620.2.1	18.13	2.25E-11	Glutathione S-transferase
Solyc04g071780.3.1	18.09	1.16E-13	Cytochrome P450
Solyc12g096380.1.1	17.91	4.69E-12	Cationic amino acid transporter
Solyc04g005720.3.1	17.81	1.10E-13	Caleosin-related family protein
Solyc02g083700.3.1	17.80	1.12E-37	Alpha-mannosidase

Solyc05g014330.1.1	17.74	1.75E-12	LOW QUALITY:HXXXD-type acyl-transferase family protein
Solyc03g097860.1.1	17.66	3.84E-12	Potassium transporter
Solyc07g055440.2.1	17.66	1.41E-15	Cytochrome P450
Solyc01g081610.3.1	17.61	7.54E-44	Beta-hexosaminidase
Solyc11g018495.1.1	17.43	7.83E-14	Beta-galactosidase
Solyc08g074480.1.1	17.40	6.85E-27	14 kDa proline-rich protein DC2.15
TCONS_00021063	17.40	5.65E-11	
Solyc12g096620.1.1	17.29	3.20E-19	GDSL esterase
Solyc09g089490.3.1	17.29	7.23E-12	Proteinase inhibitor I
Solyc09g008360.2.1	17.15	7.18E-11	LOW QUALITY:Heparan-alpha-glucosaminide N-acetyltransferase
Solyc03g078500.3.1	17.12	1.04E-12	UDP-glucuronosyltransferase
Solyc08g079300.3.1	17.12	2.20E-28	Cytochrome P450 family protein
Solyc11g021060.2.1	17.10	1.14E-55	TOMARPIX proteinase inhibitor
Solyc07g020870.2.1	17.09	3.66E-22	Transducin/WD40 repeat-like superfamily protein
Solyc10g018320.1.1	17.08	1.43E-12	Plant invertase/pectin methylesterase inhibitor
Solyc08g008087.1.1	17.07	6.92E-25	1-aminocyclopropane-1-carboxylate synthase
Solyc09g091700.3.1	16.91	7.60E-35	NADP-dependent alkenal double bond reductase
Solyc00g136565.1.1	16.88	7.61E-15	2-oxoglutarate-dependent dioxygenase-related family protein
Solyc05g044490.2.1	16.84	7.51E-19	NBS-LRR resistance protein-like protein
Solyc03g020080.3.1	16.83	5.75E-23	Pin-II type proteinase inhibitor 69
Solyc10g085500.2.1	16.73	4.00E-11	Cytochrome P450, putative
Solyc03g115750.1.1	16.73	2.01E-15	Xyloglucan galactosyltransferase KATAMARI1
Solyc07g051820.3.1	16.72	2.09E-11	Cellulose synthase family protein
Solyc04g081860.3.1	16.71	3.60E-14	Peroxidase
Solyc12g006570.2.1	16.63	3.42E-11	Sesquiterpene synthase
Solyc04g064900.2.1	16.53	4.72E-13	Endoglucanase
Solyc07g008230.1.1	16.53	3.39E-19	Glycosyltransferase
Solyc07g005070.1.1	16.49	1.20E-12	Molecular chaperone Hsp40/DnaJ family protein
Solyc12g096770.1.1	16.45	2.24E-39	LOW QUALITY:HXXXD-type acyl-transferase family protein, putative
Solyc11g007480.1.1	16.40	2.14E-11	Glycosyltransferase
Solyc00g071180.3.1	16.15	5.31E-12	multicystatin
Solyc06g083910.3.1	16.08	2.30E-27	2-oxoglutarate (2OG) and Fe(II)-dependent oxygenase superfamily protein
Solyc04g064630.3.1	16.05	8.84E-13	Bidirectional sugar transporter SWEET
Solyc07g006940.2.1	16.02	2.20E-16	Receptor-like kinase
Solyc02g062190.2.1	15.98	1.87E-11	tryptophan aminotransferase related 2
Solyc04g063370.2.1	15.90	9.88E-61	Receptor-like kinase
Solyc09g090360.3.1	15.88	3.73E-17	Phosphate transporter PHO1-like protein
Solyc10g080650.2.1	15.82	1.20E-11	Ethylene-responsive transcription factor
Solyc08g007960.1.1	15.72	8.23E-11	LOW QUALITY:Nuclear transcription factor Y protein
Solyc03g113820.2.1	15.71	7.92E-29	Alpha-n-acetylglucosaminidase, putative
Solyc01g059900.3.1	15.54	1.07E-10	Dirigent protein
Solyc06g068570.3.1	15.33	2.68E-17	AP2-like ethylene-responsive transcription factor
TCONS_00047230	15.24	9.74E-11	
Solyc09g014530.3.1	15.10	4.07E-30	MLP
Solyc07g043700.2.1	15.05	1.26E-15	Acylsugar acyltransferase 3
Solyc11g007300.2.1	14.91	7.33E-10	Pleiotropic drug resistance ABC transporter
Solyc04g005170.1.1	14.76	6.92E-12	BZip transcription factor
Solyc12g042980.2.1	14.62	4.06E-11	2-oxoglutarate-dependent dioxygenase

Solyc06g009610.1.1	14.59	8.72E-14	LOW QUALITY:GRAS family transcription factor, putative
Solyc07g018130.2.1	14.47	1.26E-11	ABC transporter B family protein
Solyc06g062390.3.1	14.43	6.50E-29	Acid phosphatase-like protein 1
Solyc11g068600.1.1	14.35	1.17E-09	Germin-like protein 1
Solyc08g066650.3.1	14.16	1.77E-38	Carotenoid Cleavage Dioxygenase 8
Solyc11g007980.2.1	14.15	7.91E-31	Cytochrome P450
Solyc12g088710.2.1	14.13	3.42E-10	Glycosyltransferase
Solyc05g008910.3.1	14.11	2.38E-13	Class I glutamine amidotransferase-like superfamily protein
Solyc07g043640.3.1	14.10	1.18E-19	AMP-dependent synthetase and ligase family protein
Solyc06g035980.3.1	14.00	1.26E-15	alpha/beta-Hydrolases superfamily protein
Solyc09g011700.1.1	13.99	4.24E-11	Copper transporter, putative
Solyc00g030000.1.1	13.94	1.31E-09	LOW QUALITY:Cellulose synthase
Solyc10g078610.1.1	13.93	1.47E-15	Ethylene-responsive transcription factor
Solyc03g115620.2.1	13.78	1.86E-10	weak chloroplast movement under blue light protein (DUF827)
Solyc01g094460.3.1	13.76	4.16E-52	AT hook motif DNA-binding family protein
Solyc07g008380.2.1	13.71	5.89E-15	HXXXD-type acyl-transferase family protein, putative
Solyc03g090990.1.1	13.68	3.89E-13	SlCortical cell-delineating protein
Solyc09g074780.3.1	13.68	4.72E-28	Zinc finger protein
Solyc10g081500.1.1	13.67	7.98E-22	LOW QUALITY:Ankyrin repeat-containing protein
Solyc02g066960.3.1	13.66	9.49E-13	Glycosyltransferase
Solyc03g020060.3.1	13.45	5.59E-12	Pin-II type proteinase inhibitor 69
Solyc08g076040.2.1	13.43	1.72E-11	5'-AMP-activated protein kinase subunit gamma-3, putative
Solyc12g088280.2.1	13.42	1.38E-13	Serine carboxypeptidase, putative
Solyc09g008910.2.1	13.37	1.88E-36	Cytochrome P450
Solyc01g065700.3.1	13.21	6.91E-14	Protein phosphatase 2C family protein
Solyc02g078570.3.1	13.05	5.56E-38	Epoxide hydrolase
Solyc04g015800.1.1	13.02		LOW QUALITY:TCP transcription factor
Solyc10g005030.3.1	12.74	7.81E-66	Pseudo-response regulator 9
Solyc10g011900.3.1	12.72	1.21E-11	Late embryogenesis abundant protein
Solyc06g084240.2.1	12.66	1.24E-17	copalyl diphosphate synthase
Solyc02g094340.1.1	12.52	6.97E-20	GRAS family transcription factor
Solyc03g083320.3.1	12.50	8.76E-33	calcium sensor calcineurin B
Solyc02g080450.1.1	12.36	7.46E-20	LOW QUALITY:CELLULOSE SYNTHASE INTERACTIVE 3
Solyc12g009270.1.1	12.30	1.07E-11	Plant invertase/pectin methylesterase inhibitor superfamily protein
Solyc02g065280.3.1	12.29	1.71E-28	Methyl esterase
Solyc10g085830.2.1	12.25	1.60E-18	Caffeic acid O-methyltransferase
Solyc09g084465.1.1	12.20	2.52E-10	Wound-induced proteinase inhibitor 1
Solyc08g078910.2.1	12.10	2.33E-13	Bifunctional inhibitor/lipid-transfer protein/seed storage 2S albumin superfamily protein
Solyc11g010400.2.1	12.08	4.84E-19	2-oxoglutarate (2OG) and Fe(II)-dependent oxygenase superfamily protein
Solyc05g047580.3.1	12.04	4.93E-17	Terpene cyclase/mutase family member
Solyc04g040160.3.1	12.01	3.11E-14	Pheophorbide A oxygenase, putative
Solyc05g006730.3.1	12.01	4.80E-31	Glutathione S-transferase family protein
Solyc09g084460.3.1	11.99	6.75E-09	Proteinase inhibitor I
Solyc03g005950.2.1	11.98	1.70E-08	Major facilitator superfamily protein
Solyc03g122070.2.1	11.98	3.33E-20	ABC transporter B family-like protein
Solyc11g069630.1.1	11.88	9.86E-10	LOW QUALITY:LysM type receptor kinase
Solyc01g094380.2.1	11.87	6.56E-09	LOW QUALITY:Protein O-glucosyltransferase 1
Solyc08g077870.3.1	11.82	8.68E-14	Pentatricopeptide repeat (PPR) superfamily protein

Solyc10g080270.1.1	11.82	6.21E-13	LOW QUALITY:SPOC domain / Transcription elongation factor S-II protein
Solyc12g010980.2.1	11.80	3.54E-39	HXXXD-type acyl-transferase family protein
Solyc07g062810.3.1	11.76	2.14E-38	Branched-chain-amino-acid aminotransferase-like protein
Solyc08g014240.3.1	11.69	2.32E-12	Isopropylmalate synthase
Solyc03g006173.1.1	11.66	1.30E-24	LOW QUALITY:DUF538 family protein (Protein of unknown function, DUF538)
Solyc08g080950.1.1	11.64	6.92E-09	Ripening related protein family
Solyc10g076500.2.1	11.59	5.49E-24	Leucine-rich-repeat receptor-like protein
Solyc08g079230.1.1	11.58	1.56E-08	Bifunctional inhibitor/lipid-transfer protein/seed storage 2S albumin superfamily protein
Solyc11g068580.1.1	11.56	1.92E-11	Germin-like protein 1
Solyc09g010480.1.1	11.52	3.07E-09	LOW QUALITY:forkhead box protein G1
Solyc12g019627.1.1	11.48	1.74E-09	Cytochrome P450
Solyc06g031697.1.1	11.45	1.48E-08	WAT1-related protein
Solyc05g053750.2.1	11.44	3.53E-08	Lipase
Solyc06g050900.3.1	11.41	3.57E-11	Major facilitator superfamily protein
Solyc09g008913.1.1	11.41	2.62E-17	Cytochrome P450
Solyc05g048790.1.1	11.34	4.39E-09	Ripening related protein family
Solyc12g006280.2.1	11.28	9.25E-12	Homeodomain-like superfamily protein
Solyc02g076980.3.1	11.20	2.13E-50	cysteine protease
Solyc01g097430.3.1	11.18	3.94E-08	ABC transporter
Solyc07g043670.1.1	11.14	8.54E-14	LOW QUALITY:HXXXD-type acyl-transferase family protein
Solyc04g015820.1.1	11.13	4.11E-09	LOW QUALITY:ferrochelatase 1
Solyc11g005610.1.1	11.12	1.59E-09	LOW QUALITY:GRAS family transcription factor
Solyc09g089505.1.1	11.08	1.45E-08	Proteinase inhibitor I
Solyc12g096240.2.1	10.99	6.70E-10	Tyrosine aminotransferase
Solyc11g005890.2.1	10.99	1.15E-08	Chitinase 1, putative
Solyc01g008620.3.1	10.98	2.78E-17	Beta-1,3-glucanase
Solyc00g322635.1.1	10.98	1.06E-11	MLP-like protein 28
Solyc03g112120.2.1	10.89	7.85E-22	Protein prune
Solyc06g008930.3.1	10.85	1.17E-11	MLP-like protein 31
Solyc03g091010.1.1	10.79	5.41E-09	Sl Cortical cell-delineating protein
Solyc12g096840.2.1	10.67	3.19E-11	Tyramine N-feruloyltransferase 4/11, putative
Solyc04g057940.3.1	10.66	1.67E-11	Transducin/WD40 repeat-like superfamily protein
Solyc02g090080.1.1	10.66	2.27E-11	LOW QUALITY:double-stranded-RNA-binding protein 4
Solyc09g014820.3.1	10.66	2.64E-13	LURP-one-like protein
Solyc11g018490.2.1	10.63	5.52E-08	Beta-galactosidase
Solyc11g071580.2.1	10.63	7.52E-09	aldehyde oxidase 5pseudogene
Solyc12g098560.2.1	10.61	5.50E-66	Glucan endo-1,3-beta-glucosidase-like protein
Solyc10g079340.2.1	10.61	6.73E-09	Glycosyltransferase
Solyc12g005790.2.1	10.61	2.40E-09	Peroxidase 27
Solyc06g066860.2.1	10.56		2-oxoglutarate-dependent dioxygenase-related family protein
Solyc12g019140.2.1	10.50	3.43E-08	Pectin lyase-like superfamily protein
Solyc12g006460.2.1	10.47	5.48E-32	Cytochrome P450
Solyc03g098760.2.1	10.45		Kunitz-type protease inhibitor-like protein
Solyc01g007895.1.1	10.43	2.17E-18	basic helix-loop-helix (bHLH) DNA-binding superfamily protein
Solyc08g066710.2.1	10.39	7.95E-08	Carotenoid 9,10(9',10')-cleavage dioxygenase 1, putative isoform 1
Solyc05g055150.1.1	10.36	6.93E-08	LOW QUALITY:CASP-like protein
Solyc08g007130.3.1	10.31	5.45E-11	Beta-amylase

Solyc11g068970.1.1	10.26	1.86E-09	aluminum activated malate transporter family protein
Solyc04g082350.1.1	10.25	5.02E-08	LOW QUALITY:HXXXD-type acyl-transferase family protein, putative
Solyc10g083400.1.1	10.25	6.51E-19	Cytochrome P450, putative
Solyc08g067170.2.1	10.23	7.65E-13	Retrovirus-related Pol polyprotein from transposon TNT 1-94
Solyc02g092820.3.1	10.22	6.90E-151	IAA-amido synthetase 3-4
Solyc07g054700.3.1	10.20	1.66E-07	LOW QUALITY:Peptidoglycan-binding lysin domain-containing protein
Solyc05g008570.2.1	10.18	1.03E-07	Acyl-[acyl-carrier-protein] hydrolase
Solyc08g066720.2.1	10.16	8.32E-08	Carotenoid cleavage dioxygenase
Solyc04g079505.1.1	10.10	1.87E-08	Serpin-like protein
Solyc07g052457.1.1	10.06	9.48E-08	LOW QUALITY:Late embryogenesis abundant hydroxyproline-rich glycoprotein family, putative
Solyc04g074340.3.1	10.00	3.28E-13	Glycosyltransferase

ID (SolDB accesión)	**Fold Change**	**P value**	**Description**
mRNA:Solyc04g007470.3.1	-29.81	8.68E-42	Drought responsive Zinc finger protein
mRNA:Solyc01g066040.2.1	-21.41	2.92E-29	LOW QUALITY:WD40 domain-containing protein
mRNA:Solyc12g013830.2.1	-17.95	1.76E-13	Metallothionein
mRNA:Solyc09g090800.2.1	-17.89	1.67E-12	AWPM-19-like membrane family protein
mRNA:Solyc06g068160.3.1	-16.89	1.32E-24	SNF4
mRNA:Solyc03g006360.3.1	-16.83	8.27E-33	Auxin-repressed protein
mRNA:Solyc12g010820.2.1	-16.61	2.01E-28	Late embryogenesis abundant protein-like
mRNA:Solyc06g060970.2.1	-13.16	2.90E-09	Expansin-like protein
mRNA:Solyc01g009660.2.1	-11.81	2.47E-09	Low-temperature-induced 65 kDa-like protein
mRNA:Solyc04g051280.3.1	-11.55	3.95E-14	Transmembrane protein, putative
mRNA:Solyc03g112590.3.1	-11.17	1.61E-41	cell division cycle 48
mRNA:Solyc06g075990.3.1	-11.10	6.64E-12	dessication-induced 1VOC superfamily protein
mRNA:Solyc11g067250.2.1	-11.05	7.18E-09	Poly [ADP-ribose] polymerase
mRNA:Solyc08g044265.1.1	-10.98	1.90E-12	Fatty acid hydroxylase superfamily
mRNA:Solyc08g075150.3.1	-10.40	3.72E-09	Coiled-coil domain-containing 73
mRNA:Solyc05g024360.1.1	-10.27	2.27E-12	Disease resistance protein (TIR-NBS-LRR class)

Supplementary Table S2. RNA-seq data: i*DLK2*-I *vs* NI.

Up- and down- regulated genes in Sl*DLK2* RNAi AM-roots vs uninoculated roots by >10 fold change

ID (SolDB accesión)	Fold Change	P value	Description
Solyc08g079780.2.1	768.10	4.25E-102	Blue copper protein, putative (AHRD V3.3 *** B9RBW4_RICCO)
Solyc03g117450.2.1	668.82	1.21E-53	Major allergen Pru ar 1 (AHRD V3.3 *** A0A0B2QY84_GLYSO)
Solyc07g054710.1.1	591.38	4.15E-54	LOW QUALITY:Peptidoglycan-binding lysin domain-containing protein (AHRD V3.3 *** A0A103XTI0_CYNCS)
Solyc04g072480.3.1	502.92	3.75E-58	phosphopantothenate-cysteine ligase-like protein (AHRD V3.3 *** AT5G02080.5)
TCONS_00030605	497.44	2.74E-69	
Solyc02g081240.1.1	375.05	2.08E-46	Glutathione s-transferase, putative (AHRD V3.3 *** B9SKR6_RICCO)
Solyc12g056500.1.1	352.19	9.14E-37	Blue copper protein, putative (AHRD V3.3 *** B9RBW4_RICCO)
Solyc05g055490.2.1	324.70	5.57E-59	Monocopper oxidase-like protein SKU5 (AHRD V3.3 *** A0A199UQM4_ANACO)
Solyc10g079540.1.1	312.60	3.24E-35	O-methyltransferase (AHRD V3.3 *** A0A1B4Z3W3_9ROSA)
Solyc11g007970.2.1	306.86	8.46E-35	4-coumarate--CoA ligase like (AHRD V3.3 *** A0A0K9P263_ZOSMR)
Solyc07g054700.3.1	279.98	2.30E-33	LOW QUALITY:Peptidoglycan-binding lysin domain-containing protein (AHRD V3.3 *** A0A103XTI0_CYNCS)
TCONS_00021063	251.40	1.74E-31	
Solyc08g069170.2.1	250.62	1.85E-32	Receptor protein kinase, putative (AHRD V3.3 *** B9RHT1_RICCO)
Solyc12g056020.1.1	229.40	5.74E-40	Cysteine protease, putative (AHRD V3.3 *** B9SBS9_RICCO)
Solyc04g071920.2.1	224.21	5.18E-56	Protein kinase-like protein (AHRD V3.3 *** A0A087GP50_ARAAL)
Solyc07g042880.1.1	222.47	7.03E-36	Cytochrome P450 (AHRD V3.3 *** A0A161ABB0_OCIBA)
Solyc11g072750.2.1	221.91	9.34E-45	Chitinase (AHRD V3.3 *** G7KL79_MEDTR)
Solyc10g078840.2.1	221.67	2.49E-115	Germin-like protein 1 (AHRD V3.3 *** B9N5Q7_POPTR)
Solyc12g009950.1.1	219.37	4.07E-30	Peroxidase (AHRD V3.3 *** K4DC83_SOLLC)
Solyc01g010260.3.1	219.19	3.97E-40	Cytochrome P450 (AHRD V3.3 *** A0A103XPY7_CYNCS)
Solyc03g098710.1.1	210.29	2.56E-40	Kunitz trypsin inhibitor (AHRD V3.3 *** B8Y888_TOBAC)
Solyc12g056000.2.1	209.71	1.73E-84	Cysteine protease, putative (AHRD V3.3 *** B9SBS8_RICCO)
Solyc04g080400.2.1	186.68	1.15E-27	FAD-binding Berberine family protein (AHRD V3.3 *** S1SMZ8_THECC)
Solyc09g008360.2.1	185.67	1.81E-27	LOW QUALITY:Heparan-alpha-glucosaminide N-acetyltransferase (AHRD V3.3 *** A0A0B2STS8_GLYSO)
Solyc01g005940.3.1	181.40	2.12E-32	Phytoene synthase (AHRD V3.3 *** A0A0K1L5A0_MALDO)
Solyc12g049190.2.1	179.09	1.01E-41	Leucine-rich repeat receptor-like protein kinase family protein (AHRD V3.3 *-* AT4G08850.1)
Solyc11g071880.2.1	176.20	2.28E-41	receptor-like kinase2
TCONS_00053706	168.52	9.95E-22	
Solyc11g012010.2.1	167.42	2.22E-36	RPM1 interacting protein 4, putative (AHRD V3.3 *** A0A061GGZ7_THECC)
Solyc10g007620.2.1	157.12	8.00E-26	Glutathione S-transferase (AHRD V3.3 *** A0A184WEV6_SIRGR)
Solyc01g095260.1.1	156.84	1.13E-33	Acidic endochitinase (AHRD V3.3 *** W9R015_9ROSA)
Solyc11g007300.2.1	148.60	6.94E-23	Pleiotropic drug resistance ABC transporter (AHRD V3.3 *-* W0TUG3_ACAMN)
Solyc03g098090.2.1	143.42	5.15E-45	CASP-like protein (AHRD V3.3 *** K4BJM4_SOLLC)
Solyc06g069610.1.1	139.95	2.86E-24	LOW QUALITY:LysM type receptor kinase (AHRD V3.3 *** G7JZ13_MEDTR)
Solyc09g072780.2.1	129.37	7.85E-31	Peptide transporter (AHRD V3.3 *** W9QSK6_9ROSA)
Solyc06g083933.1.1	129.35	2.09E-23	Zinc finger, C2H2 (AHRD V3.3 *-* A0A124SIE2_CYNCS)
Solyc04g080480.1.1	128.20	8.84E-101	4-coumarate--CoA ligase-like 4 (AHRD V3.3 *** 4CLL4_ARATH)
Solyc08g007050.2.1	125.34	1.08E-22	Cytochrome P450 (AHRD V3.3 *** A0A0B0PH67_GOSAR)

Solyc06g034010.1.1	118.31	4.98E-18	LOW QUALITY:Protein kinase superfamily protein (AHRD V3.3 --* AT4G01330.3)
TCONS_00033759	117.00	1.86E-17	
Solyc05g008910.3.1	115.06	8.59E-44	Class I glutamine amidotransferase-like superfamily protein (AHRD V3.3 *-* AT5G38200.1)
Solyc10g007960.1.1	115.03	2.34E-131	Allene oxide synthase (AHRD V3.3 *** Q5NDE2_SOLTU)
Solyc00g030000.1.1	114.72	1.61E-28	LOW QUALITY:Cellulose synthase (AHRD V3.3 *** A0A118J5T2_CYNCS)
Solyc10g085500.2.1	110.72	1.44E-38	Cytochrome P450, putative (AHRD V3.3 *** B9SRM6_RICCO)
Solyc07g052070.2.1	106.23	2.57E-27	Cytochrome P450 (AHRD V3.3 *** A0A118JYC4_CYNCS)
Solyc02g085060.2.1	105.00	2.60E-20	Replication factor C subunit 3 (AHRD V3.3 *** A0A151TIB1_CAJCA)
Solyc03g005950.2.1	104.79	1.38E-23	Major facilitator superfamily protein (AHRD V3.3 *** A0A061GLA6_THECC)
Solyc11g065480.2.1	103.35	1.59E-20	transferring glycosyl group transferase (DUF604) (AHRD V3.3 *** AT5G41460.1)
Solyc12g057050.2.1	103.24	3.89E-20	NOD26-like intrinsic protein 3.2
Solyc07g054725.1.1	100.57	1.45E-16	LOW QUALITY:Peptidoglycan-binding lysin domain-containing protein (AHRD V3.3 *** A0A103XTI0_CYNCS)
Solyc07g062670.1.1	94.91	2.85E-19	LOW QUALITY:Clavata3/ESR (CLE) gene family member (AHRD V3.3 --* A0A072TRR8_MEDTR)
Solyc01g081080.2.1	93.57	3.59E-26	Replication factor C subunit, putative (AHRD V3.3 *-* B9T608_RICCO)
Solyc11g007250.2.1	86.92	1.77E-18	Protein kinase like protein (AHRD V3.3 *** Q0WN21_ARATH)
Solyc02g077870.1.1	86.49	1.37E-18	LOW QUALITY:membrane-associated kinase regulator (AHRD V3.3 --* AT5G26230.1)
Solyc05g013890.2.1	85.77	9.65E-25	ABC transporter B family protein (AHRD V3.3 *** G7JF16_MEDTR)
Solyc05g005660.1.1	85.09	3.06E-22	LOW QUALITY:Serine-threonine protein kinase, putative (AHRD V3.3 *** A0A061E7N5_THECC)
Solyc02g065190.3.1	84.77	1.54E-74	Cytochrome P450 (AHRD V3.3 *** Q8H0I6_PETHY)
Solyc09g072700.3.1	83.19	7.96E-58	Peroxidase (AHRD V3.3 *** K4CUU6_SOLLC)
Solyc05g048780.1.1	82.55	6.69E-18	Ripening related protein family (AHRD V3.3 *** A0A072TZD6_MEDTR)
Solyc03g118760.3.1	82.25	2.58E-38	Tubulin beta chain (AHRD V3.3 *** TBB_HORVU)
Solyc03g098760.2.1	80.29	4.11E-24	Kunitz-type protease inhibitor-like protein (AHRD V3.3 *** Q2XPY0_SOLTU)
Solyc07g009235.1.1	77.93	3.28E-34	Defensin-like protein (AHRD V3.3 -** H6SWQ0_DATGL)
Solyc05g043360.2.1	77.08	2.10E-17	Laccase (AHRD V3.3 *** A0A067JKU4_JATCU)
Solyc07g006610.3.1	76.51	3.67E-95	Tyrosine kinase family protein (AHRD V3.3 *** G7JD53_MEDTR)
Solyc12g010490.2.1	74.67	3.62E-17	AP2-like ethylene-responsive transcription factor family (AHRD V3.3 *** A0A151UF47_CAJCA)
Solyc09g072720.2.1	73.01	2.43E-21	Exocyst complex component 8 (AHRD V3.3 *** A0A0B0PVF9_GOSAR)
Solyc02g069543.1.1	70.81	7.19E-37	LOW QUALITY:Protein prune-like protein (AHRD V3.3 *-* W9RW59_9ROSA)
Solyc12g089230.2.1	70.77	3.24E-16	Peptide transporter (AHRD V3.3 *** A0A072V2Y9_MEDTR)
Solyc07g005080.1.1	70.35	6.71E-19	LOW QUALITY:Chitinase, putative (AHRD V3.3 *** B9SC02_RICCO)
Solyc03g044960.2.1	69.30	1.84E-16	Calcium uniporter protein, mitochondrial (AHRD V3.3 *** A0A0B2SA24_GLYSO)
Solyc07g005110.3.1	69.00	8.00E-32	Receptor-like kinase CHRK1 (AHRD V3.3 *** Q9SWX8_TOBAC)
Solyc01g088110.1.1	68.94	2.68E-16	LOW QUALITY:metacaspase 5 (AHRD V3.3 --* AT1G79330.1)
Solyc04g078710.2.1	67.79	1.66E-19	Subtilisin-like protease (AHRD V3.3 *** A0A151U5K8_CAJCA)
Solyc06g008930.3.1	67.70	9.44E-46	MLP-like protein 31 (AHRD V3.3 -** A0A151QPB6_CAJCA)
Solyc08g079230.1.1	67.00	3.28E-55	Bifunctional inhibitor/lipid-transfer protein/seed storage 2S albumin superfamily protein (AHRD V3.3 *** A0A061DW53_THECC)
Solyc07g014680.3.1	65.81	2.57E-14	sodium transporter HKT1,2
Solyc03g006650.2.1	65.36	1.50E-32	Sugar transporter protein 10
Solyc08g014360.2.1	65.30	2.65E-15	Cinnamyl alcohol dehydrogenase (AHRD V3.3 *** A0A1B0YY99_DAUCA)

Solyc08g062200.2.1	64.54	7.73E-32	Plant regulator RWP-RK family protein (AHRD V3.3 *-* AT1G64530.1)
Solyc04g015820.1.1	64.52	2.63E-27	LOW QUALITY:ferrochelatase 1 (AHRD V3.3 --* AT5G26030.2)
Solyc01g095250.1.1	63.18	8.24E-47	Acidic endochitinase (AHRD V3.3 *** W9R015_9ROSA)
Solyc08g074715.1.1	63.18	6.04E-25	Ripening related protein family (AHRD V3.3 *** A0A072TPZ5_MEDTR)
Solyc01g111960.3.1	63.03	5.58E-15	GDSL esterase/lipase family (AHRD V3.3 *** A0A151QLH4_CAJCA)
Solyc00g141360.1.1	62.81	1.35E-15	LOW QUALITY:Disease resistance protein (AHRD V3.3 *-* Q9SBC3_SOLLC)
Solyc04g055130.1.1	62.76	1.22E-15	LOW QUALITY:C2 domain protein (AHRD V3.3 *** A0A072UZT9_MEDTR)
Solyc04g072800.3.1	62.49	1.02E-27	phosphoglycerate/bisphosphoglycerate mutase (AHRD V3.3 *** AT1G78050.1)
Solyc04g071690.3.1	62.39	2.64E-31	Alba DNA/RNA-binding protein (AHRD V3.3 *-* AT1G76010.2)
Solyc03g034110.3.1	62.02	4.56E-98	Homeobox-leucine zipper family protein (AHRD V3.3 *** B9MXR7_POPTR)
Solyc01g090660.3.1	61.56	2.70E-42	carotenoid cleavage dioxygenase7
Solyc01g094430.1.1	61.53	8.15E-26	Ripening related protein family (AHRD V3.3 *** G7L3M5_MEDTR)
Solyc06g066830.3.1	61.00	1.14E-29	2-oxoglutarate-dependent dioxygenase-related family protein (AHRD V3.3 *** B9GL08_POPTR)
Solyc00g108555.1.1	60.65	1.93E-21	Chaperone protein DNAj, putative (AHRD V3.3 *** B9SSK0_RICCO)
Solyc05g053750.2.1	60.45	1.99E-12	Lipase (AHRD V3.3 *** K4C255_SOLLC)
Solyc01g011497.1.1	59.88	8.48E-15	defensin-like protein (AHRD V3.3 *** AT1G19610.1)
Solyc09g066450.2.1	59.81	1.26E-40	GRAS family transcription factor (AHRD V3.3 *** A0A061DWK6_THECC)
Solyc02g078710.1.1	59.77	5.04E-15	F-box/kelch-repeat protein (AHRD V3.3 *** W9SF98_9ROSA)
Solyc01g097430.3.1	58.99	1.89E-17	ABC transporter (AHRD V3.3 *** A0A0M3R8G1_9SOLA)
Solyc07g054390.1.1	58.33	8.20E-15	LOW QUALITY:QWRF motif protein (DUF566) (AHRD V3.3 *** AT2G20815.1)
Solyc05g044490.2.1	58.25	4.98E-48	NBS-LRR resistance protein-like protein (AHRD V3.3 *** A1Y9R1_SOLLC)
Solyc01g106160.2.1	58.01	1.00E-14	Clade XVIII lectin receptor kinase (AHRD V3.3 *** K4B2I4_SOLLC)
Solyc05g007770.3.1	57.54	1.65E-22	NAC domain TF
Solyc08g077000.1.1	57.30	1.30E-14	LOW QUALITY:Zinc finger, C2H2 (AHRD V3.3 *** A0A103XFH7_CYNCS)
Solyc06g007860.1.1	57.02	2.57E-32	LOW QUALITY:S-norcoclaurine synthase (AHRD V3.3 *** A0A0B2SNQ7_GLYSO)
Solyc06g072950.2.1	56.02	6.37E-107	ABC transporter B family protein (AHRD V3.3 *** G7J9Q4_MEDTR)
Solyc11g065910.1.1	54.94	9.68E-47	Aspartic protease inhibitor 9 (AHRD V3.3 --* API9_SOLTU)
Solyc07g064450.3.1	53.88	1.53E-41	Cytochrome P450 (AHRD V3.3 *** A0A061FD55_THECC)
Solyc01g109090.2.1	53.50	4.09E-26	LOW QUALITY:mRNA, clone: RTFL01-34-C05 (AHRD V3.3 -** E4MXL5_EUTHA)
Solyc08g062140.1.1	53.23	1.10E-13	LOW QUALITY:MAP kinase kinase kinase 62
Solyc01g091760.2.1	52.67	7.85E-33	Ethylene-responsive transcription factor (AHRD V3.3 *** W9R099_9ROSA)
Solyc04g005000.1.1	52.45	7.89E-17	LOW QUALITY:TRICHOME BIREFRINGENCE-LIKE 20 (AHRD V3.3 --* AT3G02440.2)
Solyc07g006630.3.1	51.59	4.63E-28	CONSTANS-like protein (AHRD V3.3 *** B2MW87_SOLLC)
Solyc12g007220.2.1	50.75	3.57E-16	Major facilitator superfamily protein (AHRD V3.3 *** AT1G52190.1)
Solyc01g067370.3.1	50.66	1.99E-18	TSB
Solyc03g006410.3.1	49.33	1.28E-13	DUF506 family protein (AHRD V3.3 *** G7IPT8_MEDTR)
Solyc10g079780.1.1	48.07	1.76E-16	Dolichyl-diphosphooligosaccharide--protein glycosyltransferase subunit DAD1 (AHRD V3.3 -** DAD1_ORYSI)
Solyc11g008840.2.1	47.95	2.90E-13	ATP-binding protein, putative (AHRD V3.3 *-* A0A072V076_MEDTR)
Solyc07g055700.3.1	47.88	4.27E-20	Unknown protein (AHRD V3.3)
Solyc11g007480.1.1	47.02	3.20E-13	Glycosyltransferase (AHRD V3.3 *** K4D509_SOLLC)
Solyc10g086450.1.1	46.84	4.23E-13	LOW QUALITY:cyclin-dependent protein kinase inhibitor (AHRD V3.3 --* AT5G04470.1)

Solyc10g011840.2.1	46.65	5.83E-18	phosphopantothenate-cysteine ligase-like protein (AHRD V3.3 *** AT5G02080.7)
Solyc04g051460.3.1	46.46	5.85E-13	Protein kinase family protein (AHRD V3.3 *-* Q9LQ29_ARATH)
Solyc04g079330.2.1	46.12	2.71E-68	Carboxypeptidase (AHRD V3.3 *** K4BV17_SOLLC)
Solyc12g096840.2.1	45.96	6.90E-26	Tyramine N-feruloyltransferase 4/11, putative (AHRD V3.3 *** B9T0B8_RICCO)
Solyc11g005890.2.1	45.90	2.04E-15	Chitinase 1, putative (AHRD V3.3 *** B9RU38_RICCO)
Solyc01g006840.3.1	45.67	1.23E-25	Calcium-dependent protein kinase, putative (AHRD V3.3 *** B9RL17_RICCO)
Solyc12g096780.2.1	45.40	2.20E-11	Zinc binding dehydrogenase, putative (AHRD V3.3 *** B9SW66_RICCO)
Solyc01g005090.3.1	44.50	4.75E-25	Type I inositol-1,4,5-trisphosphate 5-phosphatase CVP2 (AHRD V3.3 *** A0A0B2RAB0_GLYSO)
Solyc02g062190.2.1	43.84	1.94E-12	tryptophan aminotransferase related 2 (AHRD V3.3 *** AT4G24670.2)
Solyc10g080270.1.1	43.11	9.01E-30	LOW QUALITY:SPOC domain / Transcription elongation factor S-II protein (AHRD V3.3 --* AT5G11430.6)
Solyc02g080120.2.1	42.92	2.15E-29	Gibberellin 2-beta- dioxygenase 7
Solyc01g059900.3.1	42.45	1.99E-36	Dirigent protein (AHRD V3.3 *** K4AW97_SOLLC)
Solyc07g051820.3.1	42.38	5.62E-12	Cellulose synthase family protein (AHRD V3.3 *** B9GTW0_POPTR)
Solyc07g061730.3.1	42.28	3.22E-60	gibberellin 2-oxidase 5
Solyc11g017100.1.1	42.12	4.23E-14	LOW QUALITY:GRAS family transcription factor
Solyc10g011900.3.1	42.09	4.15E-18	Late embryogenesis abundant protein (AHRD V3.3 *** B5TV69_CAMSI)
Solyc11g018490.2.1	42.02	4.23E-12	Beta-galactosidase (AHRD V3.3 *-* K4D6Q4_SOLLC)
Solyc08g068850.3.1	41.60	2.67E-43	Proton pump interactor 1 (AHRD V3.3 *-* D5L6G0_SOLTU)
Solyc05g006360.1.1	40.86	2.55E-14	Metalloendoproteinase 1, putative (AHRD V3.3 *** B9S2J2_RICCO)
Solyc03g078500.3.1	40.81	5.68E-17	UDP-glucuronosyltransferase
Solyc11g018495.1.1	40.16	7.85E-16	Beta-galactosidase (AHRD V3.3 *-* K4D6Q3_SOLLC)
Solyc06g068570.3.1	39.95	1.51E-30	AP2-like ethylene-responsive transcription factor
Solyc08g014240.3.1	39.62	8.92E-38	Isopropylmalate synthase (AHRD V3.3 *** A0A0G2T9V8_SOLPN)
Solyc11g005430.2.1	39.34	4.18E-16	WAT1-related protein (AHRD V3.3 *** K4D4F6_SOLLC)
Solyc01g006640.1.1	39.26	1.90E-27	LOW QUALITY:AMP-dependent synthetase and ligase family protein (AHRD V3.3 *** A0A061GTM3_THECC)
Solyc10g086570.3.1	39.23	8.90E-43	Chaperone DnaJ (AHRD V3.3 *** A0A0B0NPS3_GOSAR)
Solyc04g077760.1.1	39.18	1.17E-19	LOW QUALITY:Exocyst complex component 7 (AHRD V3.3 *** W9RYK4_9ROSA)
Solyc04g015810.1.1	39.06	4.74E-11	LOW QUALITY:Heat stress transcription factor B-1 (AHRD V3.3 --* HSFB1_ARATH)
Solyc12g088280.2.1	38.72	3.29E-24	Serine carboxypeptidase, putative (AHRD V3.3 *-* Q9FX26_ARATH)
Solyc08g029000.3.1	38.48	2.76E-17	Lipoxygenase (AHRD V3.3 *** Q43800_TOBAC)
Solyc03g013340.3.1	38.10	1.13E-13	NOD26-like intrinsic protein 2.1
Solyc07g005070.1.1	37.92	6.56E-16	Molecular chaperone Hsp40/DnaJ family protein (AHRD V3.3 --* AT1G80030.4)
Solyc11g071580.2.1	37.90	9.02E-21	aldehyde oxidase 5pseudogene
Solyc06g065600.1.1	37.70	5.72E-11	Non-specific lipid-transfer protein (AHRD V3.3 *** K4C7I9_SOLLC)
TCONS_00047230	37.64	2.57E-11	
Solyc02g087500.2.1	37.44	3.79E-17	Glycerol-3-phosphate acyltransferase (AHRD V3.3 *** A0A0M4FCN7_9SOLA)
Solyc07g052960.2.1	37.23	2.36E-11	GRAS family TF
Solyc07g064120.2.1	37.04	8.90E-29	ABC transporter B family protein (AHRD V3.3 *** G7JF16_MEDTR)
Solyc01g005680.3.1	36.84	1.03E-30	Cytokinin riboside 5'-monophosphate phosphoribohydrolase (AHRD V3.3 *** K4ASD4_SOLLC)
Solyc08g080950.1.1	36.58	4.95E-11	Ripening related protein family (AHRD V3.3 *** G7L3L3_MEDTR)
Solyc03g097860.1.1	36.57	7.14E-11	Potassium transporter (AHRD V3.3 *** M1BRC1_SOLTU)
Solyc01g068410.3.1	36.05	1.01E-17	SlPIN5

Solyc11g066140.2.1	36.00	3.62E-34	P-hydroxybenzoic acid efflux pump subunit aaeB (AHRD V3.3 *** A0A061GW63_THECC)
Solyc02g077575.1.1	35.79	3.17E-13	MLO-like protein (AHRD V3.3 *** G9BBX3_CAPAN)
Solyc01g104900.3.1	35.62	4.75E-62	NAC domain protein, (AHRD V3.3 *** A0A061E1M1_THECC)
TCONS_00000297	35.44	1.46E-10	
Solyc08g007960.1.1	34.91	1.20E-10	LOW QUALITY:Nuclear transcription factor Y protein (AHRD V3.3 *** G7ITK9_MEDTR)
Solyc09g089600.1.1	34.55	8.58E-11	LOW QUALITY:Zinc finger, C2H2 (AHRD V3.3 *** A0A103XID6_CYNCS)
Solyc02g062890.2.1	34.50	7.41E-20	polyol monosaccharide transporter 5
Solyc06g073165.1.1	34.32	1.20E-20	LOW QUALITY:BURP domain-containing protein (AHRD V3.3 *-* AT1G23760.1)
Solyc12g096240.2.1	33.18	1.23E-15	Tyrosine aminotransferase (AHRD V3.3 *** E2JFA7_PERFR)
Solyc07g055440.2.1	33.14	2.81E-23	Cytochrome P450 (AHRD V3.3 *-* A0A103YA09_CYNCS)
Solyc07g056100.1.1	33.09	2.92E-18	LOW QUALITY:ArgH (DUF639) (AHRD V3.3 --* AT2G21720.2)
Solyc01g087010.3.1	32.93	3.63E-19	Carbohydrate esterase plant-like protein (AHRD V3.3 *** G7I2A7_MEDTR)
Solyc05g005870.3.1	32.92	1.35E-12	nodulin-related MtN21 family protein
Solyc07g005680.3.1	32.87	1.39E-21	Carboxypeptidase (AHRD V3.3 *-* K4CB39_SOLLC)
Solyc07g061720.3.1	32.33	2.59E-18	gibberellin 2-oxidase 4
Solyc06g066420.3.1	32.11	6.68E-25	Oxidative stress 3, putative isoform 1 (AHRD V3.3 *** A0A061GC09_THECC)
Solyc07g005630.3.1	32.05	6.46E-10	LOW QUALITY:Defensin (AHRD V3.3 -** W8S9R7_ECLPR)
Solyc03g032210.3.1	31.83	9.53E-110	AMP-dependent synthetase and ligase family protein (AHRD V3.3 *** AT2G17650.1)
Solyc10g018320.1.1	31.77	2.95E-14	Plant invertase/pectin methylesterase inhibitor (AHRD V3.3 *** G7KG88_MEDTR)
Solyc12g096380.1.1	31.74	1.07E-09	Cationic amino acid transporter (AHRD V3.3 *** S8D7Y4_9LAMI)
Solyc01g080790.3.1	30.96	1.42E-33	Plant basic secretory family protein (AHRD V3.3 *** B9GHT3_POPTR)
Solyc01g095550.2.1	30.93	1.03E-24	LOW QUALITY:Protein kinase family protein (AHRD V3.3 *** AT5G41730.2)
Solyc03g082790.3.1	30.63	1.20E-09	LOW QUALITY:extensin-like 54
Solyc11g067320.1.1	30.54	7.80E-20	Sulfotransferase (AHRD V3.3 *** K4D9Y9_SOLLC)
Solyc01g087810.2.1	30.42	1.10E-18	subtilisin-like serine protease family protein
Solyc01g102675.1.1	30.19	2.35E-50	Leucine-rich repeat receptor-like protein kinase (AHRD V3.3 *-* Q8GY50_ARATH)
Solyc01g096175.1.1	30.07	1.54E-11	Protein yippee-like (AHRD V3.3 *** A0A0J8FX54_BETVU)
TCONS_00009236	29.77	8.98E-10	
Solyc01g015080.3.1	29.64	5.37E-12	Peroxidase (AHRD V3.3 *** K4AUE2_SOLLC)
Solyc02g081800.1.1	29.57	4.03E-11	LOW QUALITY:HXXXD-type acyl-transferase family protein (AHRD V3.3 *** AT3G26040.1)
Solyc10g083400.1.1	29.45	6.43E-37	Cytochrome P450, putative (AHRD V3.3 *** B9T5M5_RICCO)
Solyc08g066720.2.1	29.05	7.86E-33	Carotenoid cleavage dioxygenase (AHRD V3.3 *** B6UEM5_MAIZE)
Solyc02g087070.3.1	29.05	8.91E-18	alpha-DOX1
Solyc11g018535.1.1	28.91	2.51E-16	Metal transporter, putative (AHRD V3.3 *-* B9S2W4_RICCO)
Solyc01g009400.3.1	28.76	6.30E-18	Peroxidase (AHRD V3.3 *** K4ATD6_SOLLC)
Solyc07g020870.2.1	28.58	2.98E-43	Transducin/WD40 repeat-like superfamily protein (AHRD V3.3 *** A0A061GNL9_THECC)
Solyc04g055140.1.1	28.52	1.36E-42	LOW QUALITY:Nitric oxide synthase-interacting protein, putative (AHRD V3.3 *** A0A061DQB5_THECC)
Solyc06g072320.3.1	28.45	6.99E-13	Serine palmitoyltransferase (AHRD V3.3 *** B3Y000_NICBE)
Solyc09g025230.3.1	28.41	7.35E-13	Phosphatidylinositol transfer protein (AHRD V3.3 *** A0A0K9NNU5_ZOSMR)
Solyc11g072760.1.1	28.17	1.18E-24	Chitinase (AHRD V3.3 *** G7KL79_MEDTR)
Solyc11g069030.2.1	28.06	2.78E-23	blind

Solyc10g080920.2.1	27.97	2.33E-15	Myb family transcription factor family protein (AHRD V3.3 *** B9GRM8_POPTR)
Solyc05g014330.1.1	27.93	2.28E-09	LOW QUALITY:HXXXD-type acyl-transferase family protein (AHRD V3.3 *** AT1G24430.1)
Solyc11g007880.1.1	27.75	2.57E-09	LOW QUALITY:cyclin-dependent kinase inhibitor (AHRD V3.3 --* AT1G10690.1)
Solyc08g007090.2.1	27.71	7.66E-15	Expansin-like protein (AHRD V3.3 *** W9SU42_9ROSA)
Solyc09g008560.3.1	27.69	1.95E-10	2-oxoglutarate (2OG) and Fe(II)-dependent oxygenase superfamily protein (AHRD V3.3 *** AT2G36690.2)
Solyc03g020015.1.1	27.52	9.96E-49	Respiratory burst oxidase homolog protein C (AHRD V3.3 --* RBOHC_ARATH)
Solyc07g008230.1.1	27.50	3.61E-32	Glycosyltransferase (AHRD V3.3 *** K4CBU2_SOLLC)
Solyc07g052457.1.1	27.45	3.12E-09	LOW QUALITY:Late embryogenesis abundant hydroxyproline-rich glycoprotein family, putative (AHRD V3.3 *** A0A061E901_THECC)
Solyc06g033850.3.1	27.38	2.25E-17	Dehydration responsive element-binding factor protein (AHRD V3.3 --* A0A0K0K9Y3_ELECO)
Solyc05g048790.1.1	27.22	3.97E-10	Ripening related protein family (AHRD V3.3 *** G7L460_MEDTR)
Solyc11g069680.1.1	27.17	3.67E-10	LOW QUALITY:HXXXD-type acyl-transferase family protein (AHRD V3.3 *** AT3G26040.1)
Solyc09g009420.1.1	27.17	2.08E-10	LOW QUALITY:AMP-dependent synthetase and ligase family protein (AHRD V3.3 --* AT2G47240.4)
Solyc02g069547.1.1	26.78	3.71E-09	Protein prune like (AHRD V3.3 *-* A0A0B2RGS0_GLYSO)
Solyc07g007290.1.1	26.68	1.50E-13	LOW QUALITY:Flavin-containing monooxygenase (AHRD V3.3 *** A0A022R7T6_ERYGU)
Solyc10g081780.2.1	26.51	4.40E-19	RING/U-box superfamily protein (AHRD V3.3 *** AT2G35910.1)
Solyc03g115750.1.1	26.09	4.70E-17	Xyloglucan galactosyltransferase KATAMARI1 (AHRD V3.3 *** W9RU56_9ROSA)
Solyc09g065750.3.1	25.93	9.71E-82	Beta-carotene isomerase D27 (AHRD V3.3 *** R4HZ96_MEDTR)
Solyc09g011130.2.1	25.84	2.11E-20	NAD(P)-binding Rossmann-fold superfamily protein (AHRD V3.3 *** AT5G06060.1)
Solyc12g006280.2.1	25.77	2.26E-19	Homeodomain-like superfamily protein (AHRD V3.3 *-* AT2G40260.1)
Solyc05g055150.1.1	25.72	1.06E-08	LOW QUALITY:CASP-like protein (AHRD V3.3 *** K4C2J2_SOLLC)
Solyc07g018130.2.1	25.72	3.43E-18	ABC transporter B family protein (AHRD V3.3 *** G7JF16_MEDTR)
Solyc05g007870.2.1	25.57	4.76E-30	R2R3MYB transcription factor 117
Solyc02g082450.3.1	25.47	1.31E-62	Auxin efflux carrier family protein (AHRD V3.3 *** AT2G17500.4)
Solyc07g043200.2.1	25.14	1.15E-08	Zinc transporter protein (AHRD V3.3 *** D5LMF9_9FABA)
Solyc01g109100.2.1	24.93	6.12E-10	LOW QUALITY:phytochrome interacting factor 3-like 5 (AHRD V3.3 --* AT2G20180.6)
Solyc07g053900.2.1	24.88	1.63E-08	DUF506 family protein (AHRD V3.3 *** G7JTT3_MEDTR)
Solyc00g100880.3.1	24.88	1.51E-60	LURP-one-like protein (AHRD V3.3 *** AT1G53875.1)
Solyc05g015658.1.1	24.79	1.27E-08	Serine/threonine protein phosphatase 7 long form isogeny (AHRD V3.3 *** A0A151SGZ7_CAJCA)
Solyc12g013700.2.1	24.78	1.54E-59	Stem-specific protein tsjt1, putative (AHRD V3.3 *** D6BRF0_JATCU)
Solyc12g096620.1.1	24.75	2.57E-22	GDSL esterase
Solyc10g079810.1.1	24.61	4.52E-14	LOW QUALITY:mediator of RNA polymerase II transcription subunit (AHRD V3.3 --* AT2G10440.2)
Solyc04g064900.2.1	24.55	3.17E-10	Endoglucanase (AHRD V3.3 *** A0A022PNY7_ERYGU)
Solyc01g102680.3.1	24.52	2.54E-77	Leucine-rich repeat receptor-like protein kinase (AHRD V3.3 *-* Q8GY50_ARATH)
Solyc08g069220.2.1	24.40	2.33E-08	LOW QUALITY:U-box domain-containing protein 13 (AHRD V3.3 *-* W9SD18_9ROSA)
Solyc04g071780.3.1	24.25	1.70E-12	Cytochrome P450 (AHRD V3.3 *** A0A103XLI8_CYNCS)
Solyc04g076150.3.1	24.25	5.61E-11	LOW QUALITY:Peptide upstream ORF protein (AHRD V3.3 *** G7J561_MEDTR)
Solyc03g006490.3.1	24.04	5.39E-27	glutaminase domain-containing protein
Solyc08g068450.1.1	24.03	1.71E-08	LOW QUALITY:Serine/threonine-protein phosphatase 2A regulatory subunit delta isoform (AHRD V3.3 --* A0A1D1YJ73_9ARAE)
Solyc04g055150.1.1	23.89	1.99E-34	LOW QUALITY:C2 domain protein (AHRD V3.3 *** A0A072UZT9_MEDTR)

Solyc08g066710.2.1	23.67	1.98E-08	Carotenoid 9,10(9',10')-cleavage dioxygenase 1, putative isoform 1 (AHRD V3.3 *-* A0A061GK16_THECC)
Solyc12g006570.2.1	23.67	3.47E-08	Sesquiterpene synthase (AHRD V3.3 *** G5CV52_SOLLC)
Solyc02g077790.1.1	23.67	9.10E-09	LOW QUALITY:Ethylene-responsive transcription factor (AHRD V3.3 --* A0A087HKS2_ARAAL)
Solyc07g006940.2.1	23.59	1.02E-16	Receptor-like kinase (AHRD V3.3 *** G7JT83_MEDTR)
Solyc00g071180.3.1	23.46	3.17E-14	multicystatin
Solyc10g080650.2.1	23.35	1.56E-09	Ethylene-responsive transcription factor (AHRD V3.3 *-* W9RCL9_9ROSA)
Solyc04g005170.1.1	23.22	3.42E-12	BZip transcription factor (AHRD V3.3 *** Q9AT29_PHAVU)
Solyc01g099870.2.1	23.22	1.60E-11	Bidirectional sugar transporter SWEET (AHRD V3.3 *-* M1CB29_SOLTU)
Solyc06g005910.3.1	23.22	1.04E-18	Tubulin beta chain (AHRD V3.3 *** M1BVE7_SOLTU)
Solyc01g100095.1.1	23.18	4.99E-23	RING/U-box superfamily protein, putative (AHRD V3.3 *** A0A061E1W0_THECC)
Solyc03g112540.3.1	23.13	6.20E-94	NAD(P)-binding Rossmann-fold superfamily protein (AHRD V3.3 *** AT5G50130.1)
Solyc06g068830.2.1	23.07	5.07E-25	Ethylene-responsive transcription factor (AHRD V3.3 *-* W9S0J2_9ROSA)
Solyc09g084460.3.1	23.05	6.16E-10	Proteinase inhibitor I (AHRD V3.3 *** Q43648_SOLTU)
Solyc09g005365.1.1	23.03	2.65E-14	Myb-like transcription factor family protein (AHRD V3.3 *-* A0A072U1W8_MEDTR)
Solyc02g078500.2.1	22.73	2.15E-10	Stem-specific protein TSJT1, putative (AHRD V3.3 *** B9RZ68_RICCO)
Solyc08g008060.1.1	22.73	3.74E-08	NAD(P)-binding Rossmann-fold superfamily protein (AHRD V3.3 *** AT4G23420.2)
Solyc04g040160.3.1	22.73	9.97E-19	Pheophorbide A oxygenase, putative (AHRD V3.3 *** B9T573_RICCO)
Solyc04g063370.2.1	22.67	4.52E-109	Receptor-like kinase (AHRD V3.3 *** A0A072V0S7_MEDTR)
Solyc02g085800.1.1	22.48	6.06E-09	Alpha/beta-Hydrolases superfamily protein (AHRD V3.3 *** A0A061EB00_THECC)
Solyc09g074580.2.1	22.47	8.61E-39	Glutaredoxin (AHRD V3.3 *** A0A103XPG8_CYNCS)
Solyc01g087980.3.1	22.38	1.99E-21	LOW QUALITY:BPS1, putative (AHRD V3.3 *** A0A072TVX0_MEDTR)
Solyc12g099730.2.1	22.34	1.31E-20	transferring glycosyl group transferase (DUF604) (AHRD V3.3 *** AT1G01570.2)
Solyc12g088710.2.1	22.25	4.94E-08	Glycosyltransferase (AHRD V3.3 *** K4DGU2_SOLLC)
Solyc03g005537.1.1	22.25	2.91E-21	Phosphate transporter (AHRD V3.3 *** Q9AYT2_TOBAC)
Solyc01g094460.3.1	22.21	2.42E-82	AT hook motif DNA-binding family protein (AHRD V3.3 *** A0A072TNY7_MEDTR)
Solyc03g122050.1.1	22.15	3.70E-37	ABC transporter B family-like protein (AHRD V3.3 *-* G7L8C5_MEDTR)
Solyc11g069020.2.1	22.09	5.98E-15	Disease resistance protein (AHRD V3.3 *** A0A118JXS4_CYNCS)
Solyc01g090150.1.1	21.97	5.71E-08	Unknown protein (AHRD V3.3)
Solyc02g077800.1.1	21.92	1.82E-09	LOW QUALITY:Serine/arginine-rich splicing factor RSZ23 (AHRD V3.3 --* RZP23_ORYSJ)
Solyc07g008380.2.1	21.66	2.79E-25	HXXXD-type acyl-transferase family protein, putative (AHRD V3.3 *** A0A061E8Z9_THECC)
Solyc10g084070.1.1	21.49	2.85E-56	LOW QUALITY:Endoglucanase (AHRD V3.3 --* A0A022RID5_ERYGU)
Solyc09g010480.1.1	21.48	6.48E-11	LOW QUALITY:forkhead box protein G1 (AHRD V3.3 *** AT2G37530.1)
Solyc12g070080.2.1	21.48	2.58E-45	Fatty acid amide hydrolase (AHRD V3.3 *** A0A172CJD2_POPTO)
Solyc05g039950.2.1	21.46	1.49E-24	HXXXD-type acyl-transferase family protein (AHRD V3.3 *** AT3G26040.1)
Solyc03g122070.2.1	21.42	4.48E-68	ABC transporter B family-like protein (AHRD V3.3 *** G7L8C5_MEDTR)
Solyc07g005685.1.1	21.37	3.18E-27	Carboxypeptidase (AHRD V3.3 *-* M1ARY0_SOLTU)
Solyc04g026140.1.1	21.32	5.22E-07	LOW QUALITY:Cysteine-rich receptor-kinase-like protein (AHRD V3.3 --* A0A072U9Q5_MEDTR)
Solyc10g050990.1.1	21.16	1.16E-24	Pyruvate kinase (AHRD V3.3 --* A9TZX1_PHYPA)
Solyc09g091550.3.1	21.16	5.24E-09	SAM dependent carboxyl methyltransferase (AHRD V3.3 *** A0A103XKM2_CYNCS)
Solyc05g015850.3.1	21.15	3.16E-81	WRKY transcription factor 75
Solyc07g054750.1.1	21.07	1.40E-16	LOW QUALITY:Wound-responsive family protein (AHRD V3.3 *** A0A061E3U8_THECC)
Solyc07g009080.3.1	21.00	3.53E-10	AMP-dependent synthetase and ligase family protein (AHRD V3.3 --* AT1G21530.1)
Solyc03g098720.3.1	20.96	5.83E-08	Kunitz trypsin inhibitor (AHRD V3.3 *** Q4W188_POPTN)

Solyc10g009310.3.1	20.95	7.14E-15	Cytochrome P450 (AHRD V3.3 *** F4YF83_9APIA)
Solyc11g008820.2.1	20.89	5.00E-35	Endoglucanase (AHRD V3.3 *** A0A0V0II53_SOLCH)
Solyc11g066420.1.1	20.87	1.88E-17	LOW QUALITY:Protein SENSITIVE TO PROTON RHIZOTOXICITY 1 (AHRD V3.3 *** A0A151SAJ5_CAJCA)
Solyc01g008620.3.1	20.83	1.70E-13	Beta-1,3-glucanase (AHRD V3.3 *** Q9SYX6_TOBAC)
Solyc10g006150.3.1	20.83	6.00E-39	DUF4408 domain protein (AHRD V3.3 *** G7K8L0_MEDTR)
Solyc01g081610.3.1	20.82	3.35E-92	Beta-hexosaminidase (AHRD V3.3 *** D3TI69_SOLLC)
Solyc07g056670.3.1	20.82	6.65E-22	gibberellin 2-oxidase 2
Solyc04g040180.3.1	20.81	2.99E-82	S-adenosylmethionine-dependent methyltransferase, putative (AHRD V3.3 *** B9SZS6_RICCO)
Solyc12g019627.1.1	20.77	5.09E-11	Cytochrome P450 (AHRD V3.3 *-* A0A103XIA9_CYNCS)
Solyc09g011700.1.1	20.67	1.16E-08	Copper transporter, putative (AHRD V3.3 *** A0A061ERR1_THECC)
Solyc03g115620.2.1	20.52	1.39E-08	weak chloroplast movement under blue light protein (DUF827) (AHRD V3.3 *-* AT1G12150.2)
Solyc10g050980.1.1	20.35	1.67E-53	PAB-dependent poly(A)-specific ribonuclease subunit PAN2 (AHRD V3.3 -** A0A1D1XPR6_9ARAE)
Solyc05g046290.3.1	20.31	3.46E-111	Xyloglucan endotransglucosylase/hydrolase (AHRD V3.3 *** K4C0W2_SOLLC)
Solyc07g052370.3.1	20.23	1.49E-09	Cytochrome P450 (AHRD V3.3 *** Q9M7M3_CAPAN)
Solyc04g057940.3.1	19.81	8.36E-55	Transducin/WD40 repeat-like superfamily protein (AHRD V3.3 *** A0A061EZ85_THECC)
Solyc10g078610.1.1	19.78	2.03E-23	Ethylene-responsive transcription factor (AHRD V3.3 *** W9RCL9_9ROSA)
Solyc06g060450.3.1	19.71	9.19E-15	Transmembrane emp24 domain-containing protein 10, putative (AHRD V3.3 *** B9RJ70_RICCO)
Solyc05g054380.2.1	19.67	3.52E-08	Major allergen d 1 (AHRD V3.3 *** Q8L6K9_MALDO)
Solyc05g055270.1.1	19.65	7.60E-11	Galactose oxidase/kelch repeat superfamily protein (AHRD V3.3 --* AT5G60570.3)
Solyc08g077870.3.1	19.62	4.94E-21	Pentatricopeptide repeat (PPR) superfamily protein (AHRD V3.3 --* AT3G22670.1)
Solyc08g008087.1.1	19.58	2.00E-49	1-aminocyclopropane-1-carboxylate synthase (AHRD V3.3 *** P93235_SOLLC)
Solyc01g109180.3.1	19.57	2.57E-19	Long-Chain Acyl-CoA Synthetase (AHRD V3.3 *** A0A0G2SJ83_SALMI)
Solyc10g011920.2.1	19.49	6.24E-13	Phenylalanine ammonia-lyase (AHRD V3.3 *** A0A124SBF6_CYNCS)
Solyc10g086630.1.1	19.48	1.28E-17	LOW QUALITY:Legume-specific protein (AHRD V3.3 *** S5VRI2_9FABA)
Solyc02g038720.2.1	19.34	1.44E-06	LOW QUALITY:Acyl carrier protein (AHRD V3.3 *** K4B5W6_SOLLC)
Solyc00g170200.1.1	19.29	2.07E-35	LOW QUALITY:Sigma factor sigB regulation protein rsbQ (AHRD V3.3 *** A0A0B2Q4V2_GLYSO)
Solyc08g076040.2.1	19.20	7.55E-09	5'-AMP-activated protein kinase subunit gamma-3, putative (AHRD V3.3 *** A0A061GE25_THECC)
Solyc09g014820.3.1	19.19	1.71E-16	LURP-one-like protein (AHRD V3.3 *** G7KW19_MEDTR)
Solyc07g054570.1.1	19.13	5.14E-07	LOW QUALITY:Galactose oxidase/kelch repeat superfamily protein, putative (AHRD V3.3 *** A0A061GGR0_THECC)
Solyc08g077330.3.1	19.12	1.37E-31	Expansin-like protein (AHRD V3.3 *** W9SU42_9ROSA)
Solyc04g011490.3.1	19.06	4.76E-10	CASP-like protein (AHRD V3.3 *** K4BPK2_SOLLC)
Solyc05g046000.3.1	19.00	5.36E-09	Peroxidase (AHRD V3.3 *** K4C0T3_SOLLC)
Solyc03g115365.1.1	18.96	8.01E-12	Protein TIC 214 (AHRD V3.3 --* TI214_NICTO)
Solyc01g106170.3.1	18.94	4.19E-141	AGAMOUS-like MADS-box transcription factor (AHRD V3.3 *-* Q84LE8_GINBI)
Solyc04g026053.1.1	18.78	4.03E-07	LOW QUALITY:Cysteine-rich receptor-kinase-like protein (AHRD V3.3 --* A0A072UBL3_MEDTR)
Solyc03g006710.1.1	18.77	8.74E-11	Calcium-binding family protein (AHRD V3.3 *** B9I910_POPTR)
Solyc01g087090.3.1	18.77	8.65E-10	beta glucosidase 8 (AHRD V3.3 --* AT3G62750.1)
Solyc06g066820.3.1	18.72	7.21E-20	Le3OH-13b-hydroxylase
Solyc07g043700.2.1	18.71	3.04E-11	Acylsugar acyltransferase 3 (AHRD V3.3 *** ASAT3_SOLLC)
Solyc11g066800.2.1	18.68	1.38E-34	Amino acid transporter, putative (AHRD V3.3 *** B9SN74_RICCO)
Solyc10g008530.1.1	18.66	6.38E-07	LOW QUALITY:F-box/kelch-repeat protein (AHRD V3.3 *** W9SF98_9ROSA)
Solyc07g063410.3.1	18.59	5.47E-57	JA2-like
Solyc07g042630.3.1	18.52	1.33E-72	Terpene cyclase/mutase family member (AHRD V3.3 *** V9LYF2_9SOLA)

Solyc00g272810.1.1	18.51	3.29E-12	Tyramine N-feruloyltransferase 4/11, putative (AHRD V3.3 *** B9T0B8_RICCO)
Solyc08g067170.2.1	18.50	2.02E-26	Retrovirus-related Pol polyprotein from transposon TNT 1-94 (AHRD V3.3 *-* A0A151TCY2_CAJCA)
Solyc03g020050.3.1	18.47	2.83E-08	VIROID-INDUCIBLE PROTEINASE INHIBITOR II
Solyc04g078660.1.1	18.40	4.82E-15	LOW QUALITY:HXXXD-type acyl-transferase family protein (AHRD V3.3 *** AT5G42830.1)
Solyc09g084465.1.1	18.34	3.56E-08	Wound-induced proteinase inhibitor 1 (AHRD V3.3 *-* ICI1_SOLLC)
Solyc05g056500.1.1	18.33	2.09E-18	U-box domain-containing protein 25 (AHRD V3.3 *** W9QUC2_9ROSA)
Solyc05g054655.1.1	18.31	2.56E-11	Zinc finger family protein (AHRD V3.3 *-* B9HM54_POPTR)
Solyc04g011470.2.1	18.25	5.68E-07	CASP-like protein (AHRD V3.3 *** K4BPK0_SOLLC)
Solyc03g121090.3.1	18.20	4.40E-08	Oxidative stress 3, putative isoform 2 (AHRD V3.3 *** A0A061GIQ6_THECC)
Solyc11g066270.2.1	18.16	3.13E-10	xyloglucan endotransglucosylase-hydrolase 6
Solyc08g006730.1.1	18.16	1.01E-24	Tyramine N-feruloyltransferase 4/11 (AHRD V3.3 *** THT11_TOBAC)
Solyc12g089325.1.1	18.00	2.00E-08	Casparian strip membrane protein 2 (AHRD V3.3 --* CASP2_SORBI)
Solyc09g082530.2.1	17.98	1.60E-08	Leucine-rich repeat receptor-like protein kinase family (AHRD V3.3 *** A0A0K9PTR8_ZOSMR)
Solyc04g076440.1.1	17.97	1.60E-15	LOW QUALITY:Tetratricopeptide repeat-like superfamily protein (AHRD V3.3 *-* A0A061FLU3_THECC)
Solyc12g096960.2.1	17.96	9.25E-11	Major allergen d 1 (AHRD V3.3 *** Q8L6K9_MALDO)
Solyc07g054940.2.1	17.94	7.36E-07	2-oxoglutarate (2OG) and Fe(II)-dependent oxygenase superfamily protein (AHRD V3.3 *-* AT2G44800.1)
Solyc01g094380.2.1	17.84	8.82E-07	LOW QUALITY:Protein O-glucosyltransferase 1 (AHRD V3.3 *** A0A0B2PAD6_GLYSO)
Solyc12g013850.2.1	17.78	8.82E-14	Core-2/I-branching beta-1,6-N-acetylglucosaminyltransferase family protein (AHRD V3.3 *** F4JIW2_ARATH)
Solyc07g054745.1.1	17.76	2.68E-09	LOW QUALITY:Wound-responsive family protein (AHRD V3.3 *** A0A061E3U8_THECC)
Solyc02g083700.3.1	17.71	1.87E-44	Alpha-mannosidase (AHRD V3.3 *** K4BAN8_SOLLC)
Solyc02g084930.3.1	17.70	1.05E-51	Cytochrome P450 family protein (AHRD V3.3 *** G7LDW2_MEDTR)
Solyc01g107950.2.1	17.70	1.56E-11	bHLH transcription factor 008
Solyc09g007790.1.1	17.68	2.77E-15	LOW QUALITY:Senescence regulator (AHRD V3.3 *** G7IRS7_MEDTR)
Solyc08g007480.2.1	17.63	8.35E-11	DUF1442 family protein (AHRD V3.3 *** G7KG69_MEDTR)
TCONS_00017471	17.40	8.47E-15	
Solyc08g074255.1.1	17.38	3.28E-12	LOW QUALITY:NBS/LRR resistance protein-like protein (AHRD V3.3 *** Q8LKJ0_CAPAN)
Solyc07g063420.3.1	17.22	1.34E-63	NAC domain transcription factor
Solyc05g006790.2.1	17.16	7.56E-15	Actin cross-linking protein, putative (AHRD V3.3 *** A0A061E7B5_THECC)
Solyc08g062220.3.1	17.09	2.26E-49	Glycosyltransferase (AHRD V3.3 *** K4CL11_SOLLC)
Solyc07g009030.3.1	17.08	1.19E-06	defensin-like protein (AHRD V3.3 *** AT1G19610.1)
Solyc12g099870.2.1	17.04	1.18E-06	Leucine-rich repeat receptor-like protein kinase family protein (AHRD V3.3 *** AT4G08850.1)
Solyc04g008140.2.1	16.96	4.92E-09	NBS-LRR resistance protein-like protein (AHRD V3.3 *** A1Y9R1_SOLLC)
Solyc02g094340.1.1	16.96	7.91E-29	GRAS family transcription factor (AHRD V3.3 *** A0A061ECZ9_THECC)
Solyc01g108910.3.1	16.90	4.17E-56	Maternal effect embryo arrest protein, putative (AHRD V3.3 *** G7JNK2_MEDTR)
Solyc01g091100.2.1	16.87	3.01E-62	LOW QUALITY:Plant invertase/pectin methylesterase inhibitor (AHRD V3.3 *** G7KG88_MEDTR)
Solyc02g078510.3.1	16.84	2.46E-13	Acylsugar acyltransferase 3 (AHRD V3.3 *-* A0A0B5JC18_SOLHA)
Solyc00g052940.3.1	16.83	3.39E-49	WAT1-related protein (AHRD V3.3 *** A0A068UX44_COFCA)
Solyc12g007040.2.1	16.83	6.14E-09	LOW QUALITY:FKBP-like peptidyl-prolyl cis-trans isomerase family protein (AHRD V3.3 --* AT4G26555.2)
Solyc12g005440.1.1	16.74	1.87E-33	LOW QUALITY:HXXXD-type acyl-transferase family protein, putative (AHRD V3.3 *** A0A061E8Z9_THECC)
Solyc12g006560.2.1	16.73	2.03E-15	Early nodulin-93 (AHRD V3.3 *** A0A061GV12_THECC)
Solyc09g066400.2.1	16.71	4.61E-07	Cytochrome P450 (AHRD V3.3 *** Q9AVQ2_SOLTU)
Solyc08g078460.3.1	16.70	2.85E-91	Oxidoreductase family protein (AHRD V3.3 *** AT4G17370.1)
Solyc08g079300.3.1	16.69	3.98E-38	Cytochrome P450 family protein (AHRD V3.3 *** U5GNW2_POPTR)

Solyc11g010850.2.1	16.66	9.20E-58	1-deoxy-D-xylulose 5-phosphate synthase (AHRD V3.3 *** B6E973_STERE)
Solyc04g080540.2.1	16.49	1.24E-16	DNA polymerase epsilon catalytic subunit A, putative (AHRD V3.3 *** A0A061FCM9_THECC)
Solyc12g100170.1.1	16.47	1.87E-10	LOW QUALITY:2-oxoglutarate-dependent dioxygenase-related family protein (AHRD V3.3 *** B9GL08_POPTR)
Solyc03g006890.2.1	16.42	6.47E-10	Kinase superfamily protein (AHRD V3.3 *** A0A061G0U3_THECC)
Solyc04g054260.3.1	16.41	5.58E-53	Cytochrome P450 family protein (AHRD V3.3 *** B9HFW5_POPTR)
TCONS_00051882	16.40	1.74E-19	
Solyc10g008120.3.1	16.29	4.14E-13	O-methyltransferase (AHRD V3.3 *** A0A1B4Z3W3_9ROSA)
Solyc09g015430.3.1	16.25	1.96E-06	Negative regulator of sporulation MDS3 (AHRD V3.3 --* A0A0B0N6H6_GOSAR)
Solyc03g112120.2.1	16.23	1.81E-56	Protein prune (AHRD V3.3 *** A0A1D1YXQ3_9ARAE)
Solyc04g005720.3.1	16.15	1.48E-07	Caleosin-related family protein (AHRD V3.3 *** AT1G70680.1)
Solyc11g011240.1.1	16.14	9.24E-09	geranylgeranyl pyrophosphate synthase 1
Solyc05g052880.3.1	16.11	2.20E-06	Plant/T7H20-70 protein (AHRD V3.3 *** A0A072U1L2_MEDTR)
Solyc04g081860.3.1	16.08	1.50E-07	Peroxidase (AHRD V3.3 *** K4BVR5_SOLLC)
Solyc04g040120.1.1	16.00	2.18E-15	Fatty acid desaturase (AHRD V3.3 *** I3RV99_9ERIC)
Solyc12g088330.1.1	15.97	1.64E-18	LOW QUALITY:ZCF37, putative (AHRD V3.3 *** A0A061F7D6_THECC)
TCONS_00032385	15.86	2.62E-06	
Solyc11g027840.2.1	15.84	4.08E-53	1,4-beta-D-glucanase (AHRD V3.3 *** B4FHX7_MAIZE)
Solyc08g078180.1.1	15.81	9.63E-42	Ethylene Response Factor A.1
Solyc03g020060.3.1	15.61	1.84E-55	Pin-II type proteinase inhibitor 69 (AHRD V3.3 *** A0A097J9C9_CAPAN)
Solyc05g010000.1.1	15.61	1.46E-20	LOW QUALITY:Protein IDA (AHRD V3.3 *** A0A0B2RXU6_GLYSO)
Solyc09g091700.3.1	15.60	2.99E-31	NADP-dependent alkenal double bond reductase (AHRD V3.3 *** I3SE71_MEDTR)
Solyc11g018530.2.1	15.57	3.45E-26	root-specific metal transporter
Solyc02g090080.1.1	15.56	3.77E-09	LOW QUALITY:double-stranded-RNA-binding protein 4 (AHRD V3.3 --* AT3G62800.3)
Solyc00g136565.1.1	15.56	5.44E-11	2-oxoglutarate-dependent dioxygenase-related family protein (AHRD V3.3 *** B9GL08_POPTR)
Solyc07g006560.3.1	15.54	8.22E-09	Hypersensitive response assisting protein (AHRD V3.3 *** Q9SWC6_CAPAN)
Solyc10g086200.1.1	15.48	2.30E-07	SAUR-like auxin-responsive protein family (AHRD V3.3 *** AT2G37030.1)
Solyc04g009780.1.1	15.43	1.74E-15	RING/U-box superfamily protein (AHRD V3.3 *** A0A061FQW5_THECC)
Solyc02g087920.3.1	15.42	1.42E-30	NAC domain protein, (AHRD V3.3 *** A0A061EFK4_THECC)
Solyc09g008090.3.1	15.36	7.00E-08	Glycosyltransferase (AHRD V3.3 *** A0A0D5ZDE5_PANGI)
Solyc12g088870.1.1	15.30	3.23E-09	PHD finger transcription factor (AHRD V3.3 --* AT5G58610.9)
Solyc09g074600.1.1	15.28	2.75E-19	Glutaredoxin (AHRD V3.3 *** A0A103Y7J3_CYNCS)
Solyc02g086110.3.1	15.25	1.02E-27	peptidase M50B-like protein (AHRD V3.3 *** AT1G67060.1),Pfam:PF13398
Solyc12g005720.1.1	15.21	1.52E-69	Cysteine-rich RLK (Receptor-like kinase) protein (AHRD V3.3 *** G7IKM1_MEDTR)
Solyc07g062790.1.1	15.18	3.98E-06	Homeobox-leucine zipper protein family (AHRD V3.3 *-* AT1G69780.1)
Solyc07g008520.3.1	15.13	2.66E-62	Peptide transporter (AHRD V3.3 *** W9RPK3_9ROSA)
Solyc05g053060.1.1	15.13	2.22E-06	LOW QUALITY:ATP synthase subunit beta, chloroplastic (AHRD V3.3 --* ATPB_SOYBN)
Solyc01g065700.3.1	15.11	1.57E-13	Protein phosphatase 2C family protein (AHRD V3.3 *** AT5G27930.2)
Solyc01g066190.1.1	15.08	1.88E-14	LOW QUALITY:Splicing factor 3B subunit 3 (AHRD V3.3 --* A0A0B2RZM2_GLYSO)
Solyc02g080580.1.1	15.07	7.05E-27	LOW QUALITY:senescence regulator (Protein of unknown function, DUF584) (AHRD V3.3 *** AT4G04630.1)
Solyc03g033290.1.1	15.05	4.23E-06	LOW QUALITY:tracheary element differentiation-related 6 (AHRD V3.3 *** AT1G43790.1)
Solyc03g059050.2.1	15.04	3.59E-08	LOW QUALITY:NADH-ubiquinone oxidoreductase chain 3 (AHRD V3.3 --* NU3M_PINSY)
Solyc07g007280.3.1	15.01	4.07E-06	chlororespiratory reduction 6 (AHRD V3.3 *** AT2G47910.2)
Solyc09g090835.1.1	14.99	5.35E-23	GRAS family transcription factor, putative (AHRD V3.3 *-* A0A061DR51_THECC)

Solyc06g034000.2.1	14.99	4.24E-08	R2R3MYB transcription factor 95
Solyc05g052890.3.1	14.97	1.55E-20	Cytochrome f (AHRD V3.3 --* CYF_PINTH)
Solyc07g008550.3.1	14.88	2.35E-07	Purple acid phosphatase (AHRD V3.3 *** K4CBX4_SOLLC)
Solyc04g054890.3.1	14.87	1.73E-94	Acyl-coenzyme A oxidase (AHRD V3.3 *** K4BSN7_SOLLC)
Solyc12g013710.2.1	14.84	6.97E-10	light dependent NADH:protochlorophyllide oxidoreductase 1
Solyc06g065060.2.1	14.80	1.38E-11	FAD-binding Berberine family protein (AHRD V3.3 *** A0A061GF79_THECC)
Solyc10g081390.1.1	14.78	3.10E-06	LOW QUALITY:transmembrane protein (AHRD V3.3 -** AT3G47510.1)
Solyc00g048510.3.1	14.77	1.36E-66	Phloem protein 2 (AHRD V3.3 *** D0R6I7_MALDO)
Solyc01g086670.3.1	14.68	2.65E-58	LOW QUALITY:Expressed protein-RZ53 (AHRD V3.3 --* E0CW61_9ORYZ)
Solyc03g123970.1.1	14.67	5.06E-06	LOW QUALITY:Lipid-binding serum glycoprotein family protein isoform 2 (AHRD V3.3 *-* A0A061GA66_THECC)
Solyc03g020080.3.1	14.59	1.72E-30	Pin-II type proteinase inhibitor 69 (AHRD V3.3 *** A0A097J9C9_CAPAN)
Solyc04g081960.1.1	14.58	1.09E-17	LOW QUALITY:Syringolide-induced protein 14-1-1 (AHRD V3.3 *** G7I8D2_MEDTR)
Solyc03g090990.1.1	14.57	3.05E-09	SlCortical cell-delineating protein
Solyc02g067750.3.1	14.56	5.17E-11	Carbonic anhydrase (AHRD V3.3 *** B1VK36_SOLLC)
Solyc02g080450.1.1	14.54	1.05E-31	LOW QUALITY:CELLULOSE SYNTHASE INTERACTIVE 3 (AHRD V3.3 --* AT1G77460.4)
Solyc07g007930.3.1	14.50	2.18E-35	Alkaline alpha-galactosidase seed imbibition protein (AHRD V3.3 *** Q8H6N3_SOLLC)
Solyc09g089490.3.1	14.38	7.03E-06	Proteinase inhibitor I (AHRD V3.3 *** Q3S492_SOLTU)
Solyc01g106173.1.1	14.36	3.07E-09	PDI-like 2-3 (AHRD V3.3 --* AT2G32920.1)
TCONS_00014695	14.34	7.67E-06	
Solyc06g060070.3.1	14.34	2.37E-36	1-aminocyclopropane-1-carboxylate oxidase (AHRD V3.3 *** A0A0G3FFL2_FICCA)
Solyc10g081500.1.1	14.27	2.82E-35	LOW QUALITY:Ankyrin repeat-containing protein (AHRD V3.3 *** A0A103YI11_CYNCS)
Solyc12g096770.1.1	14.25	3.42E-40	LOW QUALITY:HXXXD-type acyl-transferase family protein, putative (AHRD V3.3 *** A0A061E8Z9_THECC)
Solyc08g074250.2.1	14.20	1.44E-08	Disease resistance protein (CC-NBS-LRR class) family (AHRD V3.3 *** AT5G35450.2)
Solyc01g010490.3.1	14.19	7.80E-06	Cytochrome P450 (AHRD V3.3 *** A0A061FSW2_THECC)
Solyc01g107060.2.1	14.15	2.01E-16	LOW QUALITY:3beta-hydroxysteroid-dehydrogenase/decarboxylase isoform 2 (AHRD V3.3 --* HSDD2_ARATH)
Solyc11g065470.2.1	14.09	8.00E-09	transferring glycosyl group transferase (DUF604) (AHRD V3.3 *** AT5G41460.1)
Solyc11g007980.2.1	14.08	2.42E-26	Cytochrome P450 (AHRD V3.3 *** Q9AVQ2_SOLTU)
TCONS_00012240	14.03	1.01E-05	
Solyc05g055320.3.1	14.03	8.05E-07	Peroxidase (AHRD V3.3 *** K4C2K8_SOLLC)
Solyc04g051270.2.1	14.02	3.88E-09	CASP-like protein (AHRD V3.3 *** K4BS87_SOLLC)
Solyc01g108680.3.1	14.02	2.59E-13	Methyl esterase (AHRD V3.3 *** A0A072UEL6_MEDTR)
Solyc03g005530.1.1	14.01	1.04E-12	Phosphate transporter (AHRD V3.3 *** Q9AYT2_TOBAC)
Solyc10g055473.1.1	13.98	9.54E-06	LOW QUALITY:Retrovirus-related Pol polyprotein from transposon TNT 1-94 (AHRD V3.3 *** A0A151RVI7_CAJCA)
Solyc05g009210.1.1	13.97	1.48E-09	LOW QUALITY:membrane-associated kinase regulator (AHRD V3.3 *** AT1G68330.1)
Solyc09g074810.3.1	13.95	1.90E-19	basic helix-loop-helix (bHLH) DNA-binding superfamily protein (AHRD V3.3 *** AT5G51790.2)
TCONS_00013718	13.93	4.58E-20	
Solyc03g120690.3.1	13.85	1.06E-31	Dynein light chain family protein (AHRD V3.3 *** B9GXB1_POPTR)
Solyc09g066310.3.1	13.84	2.09E-18	2-oxoglutarate (2OG) and Fe(II)-dependent oxygenase superfamily protein (AHRD V3.3 *** AT5G24530.1)
Solyc02g079240.1.1	13.83	2.26E-10	LOW QUALITY:Wound-responsive family protein (AHRD V3.3 --* AT4G10265.1)
Solyc10g008620.3.1	13.73	1.27E-05	LOW QUALITY:Unknown protein (AHRD V3.3)
Solyc02g077225.1.1	13.70	1.17E-05	Outer arm dynein light chain 1 protein (AHRD V3.3 --* AT2G34680.2)
Solyc11g005610.1.1	13.65	1.60E-08	LOW QUALITY:GRAS family transcription factor (AHRD V3.3 *** G7LD66_MEDTR)

Solyc04g054376.1.1	13.61	1.08E-05	Retrovirus-related Pol polyprotein from transposon TNT 1-94 (AHRD V3.3 *-* POLX_TOBAC)
Solyc02g062230.1.1	13.61	1.31E-07	Small auxin up-regulated RNA32
Solyc09g083310.2.1	13.59	1.12E-05	E3 ubiquitin ligase DRIP2-like protein (AHRD V3.3 *-* A0A0B0N1B0_GOSAR)
Solyc01g109320.3.1	13.56	1.51E-29	Protein DETOXIFICATION (AHRD V3.3 *** K4B3E5_SOLLC)
Solyc02g086460.3.1	13.55	7.15E-25	A-kinase anchor-like protein (AHRD V3.3 --* AT5G40450.2)
Solyc09g015380.1.1	13.54	7.78E-12	Abscisic acid receptor (AHRD V3.3 *** G7KT83_MEDTR)
Solyc02g088180.3.1	13.50	6.71E-11	NAC domain-containing protein (AHRD V3.3 *** A0A060A652_BOENI)
Solyc12g010940.1.1	13.50	4.68E-16	LOW QUALITY:DUF1685 family protein (AHRD V3.3 *** A0A072V475_MEDTR)
Solyc09g089505.1.1	13.48	4.33E-07	Proteinase inhibitor I (AHRD V3.3 *** K7WNW8_SOLTU)
Solyc02g037495.1.1	13.48	6.42E-135	AMP-dependent synthetase and ligase family protein (AHRD V3.3 *** AT5G16340.1)
Solyc01g102875.1.1	13.48	4.20E-19	Germin family protein (AHRD V3.3 *** G7I5N4_MEDTR)
Solyc02g071875.1.1	13.44	1.09E-24	Leucine-rich repeat receptor-like protein kinase (AHRD V3.3 *** C0LGF2_ARATH)
Solyc06g073585.1.1	13.44	3.23E-12	Rhodanese/Cell cycle control phosphatase superfamily protein (AHRD V3.3 *-* AT2G21045.1)
Solyc09g066150.1.1	13.41	1.64E-06	Cytochrome P450, putative (AHRD V3.3 *** B9S4U5_RICCO)
Solyc08g074495.1.1	13.38	1.58E-07	Glycosyltransferase (AHRD V3.3 *** A0A022RAZ3_ERYGU)
Solyc05g047530.3.1	13.31	1.94E-12	trans-cinnamate 4-monooxygenase
TCONS_00028278	13.31	1.64E-09	
Solyc10g018150.2.1	13.30	1.05E-06	SlCytochromeP450
Solyc05g050890.2.1	13.29	5.59E-11	Peroxidase (AHRD V3.3 *** K4C1C1_SOLLC)
Solyc01g110830.3.1	13.28	2.10E-06	Small auxin up-regulated RNA20
Solyc09g009810.1.1	13.25	1.62E-41	LOW QUALITY:TSA: Wollemia nobilis Ref_Wollemi_Transcript_15479_650 transcribed RNA sequence (AHRD V3.3 *** A0A0C9RS79_9SPER)
Solyc07g065500.2.1	13.24	2.38E-45	CCAAT-binding transcription factor
Solyc10g047170.2.1	13.21	2.26E-05	sulfate transporter 1
TCONS_00042433	13.19	1.85E-05	
Solyc05g014590.3.1	13.19	3.26E-26	basic helix-loop-helix (bHLH) DNA-binding superfamily protein (AHRD V3.3 *** AT5G57150.1)
Solyc01g073780.2.1	13.15	2.60E-10	LOW QUALITY:Cysteine/Histidine-rich C1 domain family protein (AHRD V3.3 *-* AT2G44380.1)
Solyc01g073860.3.1	13.14	7.23E-39	Cysteine/Histidine-rich C1 domain family protein (AHRD V3.3 *** AT2G44380.1)
Solyc02g076980.3.1	13.13	1.47E-29	cysteine protease
Solyc02g071970.1.1	13.11	9.23E-15	LOW QUALITY:F-box and Leucine Rich Repeat domains containing protein (AHRD V3.3 --* AT1G80960.6)
Solyc07g044710.2.1	13.10	3.36E-07	3-hydroxyisobutyryl-CoA hydrolase-like protein (AHRD V3.3 *** A0A072V5U1_MEDTR)
Solyc06g061215.1.1	13.08	1.86E-07	Proteinase inhibitor II (AHRD V3.3 *-* B3F0C1_TOBAC)
Solyc02g070450.2.1	13.06	9.11E-34	Glucan endo-1,3-beta-glucosidase, putative (AHRD V3.3 *** B9S109_RICCO)
Solyc06g065550.2.1	13.05	7.48E-19	Cysteine/Histidine-rich C1 domain family protein (AHRD V3.3 --* AT5G40590.1)
Solyc07g043640.3.1	13.02	2.21E-11	AMP-dependent synthetase and ligase family protein (AHRD V3.3 *** AT2G17650.1)
Solyc03g096540.3.1	13.00	6.11E-12	PLAT domain-containing protein 1 (AHRD V3.3 *** PLAT1_ARATH)
Solyc02g077810.1.1	12.99	6.39E-06	LOW QUALITY:Ethylene-responsive transcription factor (AHRD V3.3 *-* A0A087HKS2_ARAAL)
Solyc05g025890.2.1	12.98	1.34E-17	Acyl-CoA N-acyltransferases (NAT) superfamily protein (AHRD V3.3 *** AT2G06025.6)
Solyc01g006050.2.1	12.94	1.14E-24	LOW QUALITY:Transmembrane protein 45B (AHRD V3.3 *** A0A151U0K4_CAJCA)
Solyc11g068580.1.1	12.90	1.86E-09	Germin-like protein 1 (AHRD V3.3 *** B9MYQ6_POPTR)
Solyc06g070950.2.1	12.86	1.05E-33	ABC transporter A family protein (AHRD V3.3 *** A0A072UUA7_MEDTR)
TCONS_00052436	12.85	3.18E-06	
Solyc05g050870.3.1	12.83	2.23E-10	Peroxidase (AHRD V3.3 *** K4C1C0_SOLLC)
TCONS_00041358	12.75	1.41E-08	

Solyc04g071080.1.1	12.74	1.29E-19	Extensin (AHRD V3.3 *** Q06446_SOLTU)
Solyc02g092820.3.1	12.73	7.59E-78	IAA-amido synthetase 3-4
Solyc12g042840.2.1	12.70	1.19E-08	Lactoylglutathione lyase / glyoxalase I family protein (AHRD V3.3 *** AT1G80160.3)
Solyc11g069630.1.1	12.68	4.15E-07	LOW QUALITY:LysM type receptor kinase (AHRD V3.3 *** D3KU02_LOTJA)
Solyc08g007130.3.1	12.66	6.59E-17	Beta-amylase (AHRD V3.3 *** K4CIK0_SOLLC)
Solyc08g079990.2.1	12.65	2.15E-05	Subtilisin-like protease (AHRD V3.3 *** A0A151SNY0_CAJCA)
Solyc03g044830.3.1	12.64	3.73E-28	Transducin/WD40 repeat-like superfamily protein (AHRD V3.3 *** AT3G18950.1)
Solyc09g089865.1.1	12.62	1.80E-11	DZC (Disease resistance/zinc finger/chromosome condensation-like region) domain containing protein (AHRD V3.3 --* AT1G31880.2)
Solyc02g065090.3.1	12.61	3.64E-18	Patatin (AHRD V3.3 *** A0A0E0J487_ORYNI)
Solyc10g085285.1.1	12.49	7.89E-06	Chalcone and stilbene synthase family protein (AHRD V3.3 --* AT4G00040.1)
Solyc10g009150.3.1	12.48	7.90E-19	Organ-specific protein S2 (AHRD V3.3 *** F2VPS2_SOLNI)
Solyc08g006740.3.1	12.47	5.50E-57	aromatic amino acid decarboxylase 2
Solyc07g026650.3.1	12.46	2.08E-07	1-aminocyclopropane-1-carboxylate oxidase 5
Solyc11g072830.1.1	12.46	6.80E-39	Chitinase (AHRD V3.3 *** G7KL79_MEDTR)
Solyc02g063250.3.1	12.45	1.94E-15	Peptide methionine sulfoxide reductase MsrA (AHRD V3.3 *** W9S0U3_9ROSA)
Solyc05g054650.1.1	12.43	1.74E-15	Zinc finger family protein (AHRD V3.3 *** B9HM54_POPTR)
Solyc08g005120.3.1	12.42	7.37E-17	Cinnamoyl-CoA reductase-like protein (AHRD V3.3 *** G7KDR3_MEDTR)
Solyc05g053860.3.1	12.40	1.02E-05	Organic cation/carnitine transporter (AHRD V3.3 *** A0A072TPM4_MEDTR)
Solyc01g008650.3.1	12.38	9.39E-33	Cytochrome P450 (AHRD V3.3 *** Q9AVQ2_SOLTU)
Solyc01g059965.1.1	12.37	1.40E-16	Beta-1,3-glucanase (AHRD V3.3 *** G9G7S0_HEVBR)
Solyc02g068470.1.1	12.36	3.39E-75	LOW QUALITY:VQ motif-containing protein, putative (AHRD V3.3 *-* A0A061DVP3_THECC)
Solyc03g098770.1.1	12.36	2.73E-05	LOW QUALITY:COP1 (AHRD V3.3 --* Q9MAZ5_ORYSJ)
Solyc09g009610.2.1	12.34	1.30E-20	Purple acid phosphatase (AHRD V3.3 *** K4CQZ0_SOLLC)
Solyc05g051583.1.1	12.32	3.37E-22	F-box family protein, putative (AHRD V3.3 *** A0A061FZW6_THECC)
Solyc09g074780.3.1	12.27	6.13E-31	Zinc finger protein (AHRD V3.3 *** E9NZV2_PHAVU)
Solyc04g076730.1.1	12.25	7.18E-34	LOW QUALITY:Transmembrane protein, putative (AHRD V3.3 *** G7JEX2_MEDTR)
Solyc06g009610.1.1	12.22	1.63E-09	LOW QUALITY:GRAS family transcription factor, putative (AHRD V3.3 *** A0A061EWU1_THECC)
Solyc02g089580.3.1	12.22	5.50E-07	Late embryogenesis abundant protein family protein (AHRD V3.3 *** A0A061EH65_THECC)
Solyc02g083730.3.1	12.20	1.33E-39	Rhodanese-related sulfurtransferase (AHRD V3.3 *** G7JXI1_MEDTR)
Solyc06g069640.3.1	12.18	3.09E-05	dCTP pyrophosphatase 1 (AHRD V3.3 *** A0A151SL49_CAJCA)
Solyc03g005630.3.1	12.17	5.82E-10	Mammalian uncoordinated homology 13, domain 2 (AHRD V3.3 *** A0A103Y0Q9_CYNCS)
Solyc03g019830.3.1	12.16	4.58E-12	Receptor kinase (AHRD V3.3 *** B6SWV2_MAIZE)
Solyc01g094160.1.1	12.13	8.28E-09	Regulator of chromosome condensation (RCC1) family with FYVE zinc finger domain-containing protein (AHRD V3.3 --* AT1G65920.2)
Solyc06g061210.3.1	12.13	4.99E-12	Galactoside 2-alpha-L-fucosyltransferase (AHRD V3.3 *** FUT1_PEA)
Solyc01g099340.3.1	12.12	7.01E-38	Zinc finger protein (AHRD V3.3 *** E9NZV2_PHAVU)
Solyc01g005230.3.1	12.12	3.08E-11	S-adenosyl-L-methionine-dependent methyltransferase superfamily protein (AHRD V3.3 *** AT5G37990.1)
Solyc03g044560.1.1	12.11	2.46E-06	LOW QUALITY:NAC domain containing protein 35 (AHRD V3.3 --* AT2G02450.2)
Solyc08g006020.3.1	12.09	3.65E-05	NAC domain protein, (AHRD V3.3 *-* A0A061F8R9_THECC)
Solyc11g069750.2.1	12.09	2.13E-05	High-affinity nitrate transporter (AHRD V3.3 *** Q76IJ7_PRUPE)
Solyc07g008240.3.1	12.06	9.32E-86	Non-symbiotic hemoglobin 1 (AHRD V3.3 *** HBL1_GOSHI)
Solyc03g078620.1.1	12.05	1.26E-15	LOW QUALITY:Nitric oxide synthase-interacting protein, putative (AHRD V3.3 *** A0A061DQB5_THECC)
Solyc06g009425.1.1	11.97	4.03E-08	GDSL-like Lipase/Acylhydrolase superfamily protein (AHRD V3.3 --* AT1G75920.4)
Solyc12g056710.2.1	11.97	2.86E-08	NAD(P)-binding Rossmann-fold superfamily protein (AHRD V3.3 *** AT1G52340.1),Pfam:PF13561

Solyc01g086660.2.1	11.86	1.53E-66	LOW QUALITY:agenet domain protein (DOMAIN OF UNKNOWN FUNCTION 724 2) (AHRD V3.3 --* AT1G11420.1)
Solyc01g087800.2.1	11.85	1.01E-09	LOW QUALITY:Subtilisin-like protease (AHRD V3.3 *** O82777_SOLLC)
Solyc01g097570.2.1	11.79	2.49E-15	LOW QUALITY:kinase-like protein (AHRD V3.3 --* AT1G66940.4)
Solyc07g052480.3.1	11.74	2.82E-46	isocitrate lyase LEU18678
Solyc10g005030.3.1	11.73	3.24E-60	Pseudo-response regulator 9 (AHRD V3.3 *** D0PPG9_CASSA)
Solyc04g064630.3.1	11.70	7.15E-18	Bidirectional sugar transporter SWEET (AHRD V3.3 *** K4BT54_SOLLC)
TCONS_00021313	11.67	4.40E-05	
Solyc08g079850.2.1	11.67	1.53E-06	Subtilisin-like protease (AHRD V3.3 *** A0A151TJQ6_CAJCA)
Solyc01g079940.3.1	11.67	7.88E-44	Eukaryotic aspartyl protease family protein (AHRD V3.3 *** AT1G03220.1)
Solyc11g068970.1.1	11.65	5.27E-08	aluminum activated malate transporter family protein (AHRD V3.3 *** AT1G08440.1)
Solyc03g115870.3.1	11.63	4.08E-121	Thioredoxin (AHRD V3.3 *** A0A072UTZ5_MEDTR)
Solyc02g078150.3.1	11.59	3.44E-38	DUF506 family protein (AHRD V3.3 *** G7IPT8_MEDTR)
Solyc06g031697.1.1	11.58	8.43E-16	WAT1-related protein (AHRD V3.3 *** K4C4J4_SOLLC)
Solyc08g076380.2.1	11.57	5.97E-05	AP2-like ethylene-responsive transcription factor (AHRD V3.3 *** A0A072TQP3_MEDTR)
Solyc06g084240.2.1	11.56	5.02E-29	copalyl diphosphate synthase
Solyc04g054340.1.1	11.55	3.33E-15	LOW QUALITY:transmembrane protein (AHRD V3.3 --* AT5G65440.9)
Solyc01g080020.2.1	11.50	3.14E-11	Eukaryotic aspartyl protease family protein, putative (AHRD V3.3 *** A0A061ELJ0_THECC)
Solyc02g085070.1.1	11.49	1.03E-08	LOW QUALITY:alpha/beta-Hydrolases superfamily protein (AHRD V3.3 *** AT4G36530.2)
Solyc12g057040.2.1	11.47	1.17E-22	cryptochrome 1b
Solyc09g074490.3.1	11.46	5.14E-06	Unknown protein (AHRD V3.3)
Solyc09g074430.3.1	11.43	5.22E-15	Sl Monooxygenase
Solyc08g080630.3.1	11.41	4.90E-40	Ethylene-responsive proteinase inhibitor 1 (AHRD V3.3 *** IER1_SOLLC)
Solyc03g033750.1.1	11.40	5.53E-05	P-loop containing nucleoside triphosphate hydrolases superfamily protein (AHRD V3.3 *-* AT3G50940.1)
Solyc03g094020.3.1	11.40	7.19E-11	Alpha-glucosidase-like (AHRD V3.3 *** Q5NBJ1_ORYSJ)
Solyc12g056310.2.1	11.37	6.81E-05	LURP-one-like protein (AHRD V3.3 *** AT1G53875.1)
Solyc02g092400.1.1	11.34	5.20E-08	Late embryogenesis abundant hydroxyproline-rich glycoprotein family, putative (AHRD V3.3 *** A0A061GGT6_THECC)
Solyc01g006580.3.1	11.30	8.49E-17	2-oxoglutarate-dependent dioxygenase-related family protein (AHRD V3.3 *** B9GL08_POPTR)
Solyc09g009130.3.1	11.24	8.71E-08	Phytosulfokine 3, putative (AHRD V3.3 *** A0A061ESV9_THECC)
Solyc06g062560.2.1	11.23	3.30E-48	phosphatase 14B
Solyc03g121420.3.1	11.18	5.06E-12	Inorganic pyrophosphatase 2 (AHRD V3.3 *** A0A0B2S4R2_GLYSO)
Solyc10g075170.2.1	11.14	9.14E-20	Aspartate aminotransferase (AHRD V3.3 *-* A0A067JJ16_JATCU)
TCONS_00044869	11.08	5.58E-25	
Solyc03g098700.1.1	11.07	7.37E-05	Kunitz-type protease inhibitor D (AHRD V3.3 *** M1LA62_SOLTU)
Solyc03g112320.3.1	11.06	1.29E-37	Ferric reduction oxidase 8 (AHRD V3.3 *** W9RI94_9ROSA)
Solyc09g075410.3.1	11.05	3.37E-06	Pollen Ole e 1 allergen and extensin family protein (AHRD V3.3 *** B9GSD1_POPTR)
Solyc01g087040.2.1	11.03	2.04E-30	PsbP-like (AHRD V3.3 *** A0A0U9HL69_KLEFL)
Solyc12g013610.2.1	11.03	3.09E-50	LOW QUALITY:calmodulin-binding protein (DUF1645) (AHRD V3.3 *** AT2G15760.1)
Solyc11g011030.2.1	11.03	1.79E-15	Pto-responsive gene 1
TCONS_00038381	10.98	1.84E-05	
Solyc05g008220.3.1	10.96	5.23E-36	Plastid movement impaired protein (AHRD V3.3 *** A0A072VEV4_MEDTR)
Solyc07g007240.3.1	10.93	5.19E-15	Metallocarboxypeptidase inhibitor (AHRD V3.3 *** A0A0A0VBW2_SOLTU)
Solyc06g070960.2.1	10.89	2.21E-07	ABC transporter family protein (AHRD V3.3 *** A0A097P9Q6_HEVBR)
Solyc08g080310.1.1	10.86	1.66E-10	Protein DETOXIFICATION (AHRD V3.3 *** K4CP31_SOLLC)
Solyc11g067330.1.1	10.86	1.91E-06	Acylsugar acyltransferase 3 (AHRD V3.3 *** ASAT3_SOLLC)

Solyc02g088307.1.1	10.85	1.51E-09	Serine/threonine protein phosphatase 2A 57 kDa regulatory subunit B' beta isoform (AHRD V3.3 --* 2A5B_ARATH)
Solyc06g064760.1.1	10.81	5.77E-11	NBS-LRR resistance protein-like protein (AHRD V3.3 *** A1Y9R1_SOLLC)
Solyc08g079235.1.1	10.81	4.49E-12	Plant invertase/pectin methylesterase inhibitor (AHRD V3.3 *** G7KG88_MEDTR)
Solyc10g080620.1.1	10.78	3.15E-05	LOW QUALITY:NAD(P)H-quinone oxidoreductase subunit 2 A, chloroplastic (AHRD V3.3 --* NU2C1_HORVU)
Solyc01g006910.3.1	10.77	8.22E-07	RING/U-box superfamily protein (AHRD V3.3 *** AT5G06490.1)
Solyc06g009490.3.1	10.76	6.92E-07	Pentatricopeptide repeat-containing protein (AHRD V3.3 *-* A0A0B2SEE4_GLYSO)
Solyc12g099345.1.1	10.73	2.10E-18	calmodulin-binding transcription activator (AHRD V3.3 *-* AT3G16940.2)
Solyc07g009020.2.1	10.73	1.82E-05	defensin-like protein (AHRD V3.3 *** AT1G19610.1)
Solyc05g007950.3.1	10.71	1.84E-11	LERNALE L.esculentum ribonuclease le
Solyc04g082120.3.1	10.69	2.54E-60	Prolyl oligopeptidase family protein (AHRD V3.3 *** AT1G76140.1)
Solyc04g083140.2.1	10.68	1.13E-09	Cytochrome P450 (AHRD V3.3 *** Q9AVQ2_SOLTU)
Solyc12g017340.1.1	10.62	4.09E-06	LOW QUALITY:Cation efflux family protein (AHRD V3.3 --* A0A061FA80_THECC)
Solyc04g064690.3.1	10.62	3.65E-06	Peroxidase (AHRD V3.3 *** K4BT60_SOLLC)
Solyc04g040090.3.1	10.62	4.11E-07	Strictosidine synthase-like protein (AHRD V3.3 *** A7WPL3_TOBAC)
Solyc10g086460.2.1	10.60	1.47E-09	Actin (AHRD V3.3 *** ACT1_TOBAC)
Solyc10g079340.2.1	10.57	6.71E-06	Glycosyltransferase (AHRD V3.3 *** K4D2H5_SOLLC)
Solyc09g008910.2.1	10.56	2.91E-29	Cytochrome P450 (AHRD V3.3 *** A0A061ETV7_THECC)
Solyc01g105940.3.1	10.55	3.12E-16	Cineol synthase (AHRD V3.3 *** G1JUH5_SOLLC)
Solyc09g030370.3.1	10.54	4.28E-15	GDSL esterase/lipase (AHRD V3.3 *** A0A0B2SPC5_GLYSO)
Solyc11g008200.1.1	10.52	1.04E-09	LOW QUALITY:Major facilitator superfamily protein (AHRD V3.3 *** AT2G39210.1)
Solyc12g017350.2.1	10.52	6.21E-06	Cation diffusion facilitator 9
TCONS_00007876	10.51	1.09E-04	
Solyc10g012095.1.1	10.49	4.18E-10	LOW QUALITY:Retrovirus-related Pol polyprotein from transposon TNT 1-94 (AHRD V3.3 *-* POLX_TOBAC)
Solyc01g105060.3.1	10.48	1.28E-41	Beta-hydroxyacyl-ACP dehydratase (AHRD V3.3 *** F2VYC9_HELAN)
Solyc02g005340.3.1	10.47	1.19E-04	Oligopeptide transporter, putative (AHRD V3.3 *** B9T1I2_RICCO)
Solyc08g074400.2.1	10.46	6.23E-09	keratin-associated protein (DUF1218) (AHRD V3.3 *** AT4G31130.1)
Solyc00g322635.1.1	10.46	2.14E-13	MLP-like protein 28 (AHRD V3.3 *** AT1G70830.2)
Solyc01g105600.3.1	10.46	1.99E-17	Phage capsid scaffolding protein (GPO) serine peptidase (AHRD V3.3 --* G7KAI6_MEDTR)
Solyc01g020170.1.1	10.46	1.17E-04	LOW QUALITY:bHLH transcription factor 074
Solyc10g080510.1.1	10.45	5.75E-09	clade XII lectin receptor kinase
Solyc12g062940.2.1	10.44	2.40E-05	Exostosin-like (AHRD V3.3 *** Q2HVN7_MEDTR)
Solyc01g087280.1.1	10.43	1.51E-07	Pectin lyase-like superfamily protein (AHRD V3.3 *** AT3G07970.1)
Solyc10g078495.1.1	10.40	1.37E-37	Aquaporin SIP1-1 (AHRD V3.3 *-* W9R1G9_9ROSA)
Solyc12g019140.2.1	10.40	1.25E-04	Pectin lyase-like superfamily protein (AHRD V3.3 *** AT2G43880.1)
Solyc11g043140.2.1	10.39	2.37E-05	HAUS augmin-like complex subunit 6 (AHRD V3.3 --* A0A1D1Y0Z2_9ARAE)
Solyc06g083850.3.1	10.36	5.71E-08	NAC domain protein, (AHRD V3.3 *** A0A061DNM9_THECC)
Solyc03g043710.1.1	10.35	1.74E-11	Clade IX lectin receptor kinase (AHRD V3.3 *** K4BFZ2_SOLLC)
Solyc07g044970.1.1	10.34	5.18E-17	LOW QUALITY:P-loop containing nucleoside triphosphate hydrolases superfamily protein (AHRD V3.3 --* AT2G16790.5),Pfam:PF13671
Solyc07g052580.1.1	10.33	2.10E-08	LOW QUALITY:F-box protein, putative (AHRD V3.3 *** Q6L3P8_SOLDE)
Solyc01g005850.2.1	10.33	4.98E-08	LOW QUALITY:Extensin-like protein Dif54 (AHRD V3.3 *** Q43505_SOLLC)
Solyc06g082020.3.1	10.25	1.30E-12	Alternative NAD(P)H dehydrogenase 1 (AHRD V3.3 --* A0A061GX18_THECC)
Solyc04g082350.1.1	10.25	1.38E-04	LOW QUALITY:HXXXD-type acyl-transferase family protein, putative (AHRD V3.3 *** A0A061FL86_THECC)
Solyc02g071820.3.1	10.23	2.86E-11	Receptor-like protein kinase (AHRD V3.3 *** B9I1R1_POPTR)
Solyc03g007275.1.1	10.23	5.40E-10	Unknown protein (AHRD V3.3)

Solyc01g091700.3.1	10.19	4.40E-30	F-box family protein (AHRD V3.3 *** B9IC61_POPTR)
Solyc05g051200.1.1	10.17	2.06E-11	ethylene-responsive factor 1
Solyc12g021175.1.1	10.17	6.35E-05	Retrovirus-related Pol polyprotein from transposon TNT 1-94 (AHRD V3.3 *-* A0A151SVD8_CAJCA)
Solyc03g080030.3.1	10.15	4.48E-14	PGPS/D3 (AHRD V3.3 *** Q9ZTN4_PETHY)
Solyc06g083500.3.1	10.15	4.38E-40	Kinase family protein (AHRD V3.3 *** D7L628_ARALL)
Solyc02g021350.3.1	10.14	4.68E-14	Nucleosome assembly protein family (AHRD V3.3 *** A9RDJ7_PHYPA)
Solyc07g006170.3.1	10.14	1.88E-21	Exostosin family protein (AHRD V3.3 *** A0A061F0X5_THECC)
Solyc06g060960.2.1	10.13	1.63E-06	Histone-lysine N-methyltransferase, H3 lysine-9 specific SUVH6 (AHRD V3.3 *-* W9S0E6_9ROSA)
Solyc01g080800.3.1	10.13	8.80E-09	Plant basic secretory family protein (AHRD V3.3 *** B9GHT3_POPTR)
Solyc05g012180.3.1	10.13	2.45E-60	methyl esterase 13 (AHRD V3.3 *** AT1G26360.1)
Solyc10g008350.3.1	10.12	5.48E-16	50S ribosomal protein L20, chloroplastic (AHRD V3.3 --* RK20_PHAAO)
Solyc03g031630.3.1	10.11	3.56E-08	Calcium-binding EF-hand family protein (AHRD V3.3 *** A0A061DTS7_THECC)
Solyc02g065000.1.1	10.07	2.50E-27	Calcium-binding EF-hand (AHRD V3.3 *** A0A103YH91_CYNCS)
Solyc12g014355.1.1	10.07	1.04E-11	Leucine-rich repeat transmembrane protein kinase (AHRD V3.3 *-* AT1G53430.1)
Solyc01g005630.2.1	10.02	3.35E-05	Ethylene-responsive transcription factor (AHRD V3.3 *** W9SBA4_9ROSA)
Solyc01g009935.1.1	10.02	3.35E-05	SAUR-like auxin-responsive family protein (AHRD V3.3 *** I3T7S1_MEDTR)
Solyc06g009125.1.1	10.01	3.79E-05	with no lysine (K) kinase 1 (AHRD V3.3 --* AT3G04910.3)
Solyc12g009270.1.1	10.01	2.13E-06	Plant invertase/pectin methylesterase inhibitor superfamily protein (AHRD V3.3 *** A0A061GSW0_THECC)
Solyc11g005320.1.1	10.01	1.24E-06	RING/U-box superfamily protein (AHRD V3.3 *** AT1G49230.1)
Solyc06g082030.3.1	10.00	7.88E-63	2-oxoglutarate (2OG) and Fe(II)-dependent oxygenase superfamily protein (AHRD V3.3 *** AT5G58660.1)
Solyc01g096880.3.1	-10.13	2.58E-09	Major facilitator superfamily protein (AHRD V3.3 *** AT2G26690.1)
Solyc06g066700.1.1	-10.15	3.55E-05	serine-rich protein-like protein (AHRD V3.3 --* AT3G13227.1)
Solyc06g006080.3.1	-10.25	2.55E-16	thiamine biosynthesis protein ThiC
Solyc02g080465.1.1	-10.28	5.83E-05	Protein kinase family protein (AHRD V3.3 --* Q9LQ29_ARATH)
Solyc02g068410.2.1	-10.28	1.18E-05	Polygalacturonase QRT3-like protein (AHRD V3.3 *** A0A0B0NBR9_GOSAR)
Solyc06g008570.1.1	-10.37	1.08E-04	transcription initiation factor IIF subunit alpha RAP74 (AHRD V3.3 --* AT4G12610.1)
Solyc08g076025.1.1	-10.40	2.89E-17	Tudor/PWWP/MBT superfamily protein (AHRD V3.3 *** G7K6J4_MEDTR)
Solyc10g054550.2.1	-10.42	1.33E-04	FAD-binding Berberine family protein (AHRD V3.3 *** AT5G44400.1)
Solyc12g056970.1.1	-10.50	2.50E-09	Eukaryotic translation initiation factor 2B (eIF-2B) family protein (AHRD V3.3 --* AT1G53900.3)
Solyc06g051320.3.1	-10.60	7.30E-06	HXXXD-type acyl-transferase family protein, putative (AHRD V3.3 *** A0A061EWX8_THECC)
Solyc01g105770.2.1	-10.83	4.38E-09	LOW QUALITY:Leguminosin group485 secreted peptide (AHRD V3.3 *** A0A072UVS4_MEDTR)
Solyc01g057175.1.1	-11.03	6.66E-05	Potassium channel (AHRD V3.3 --* A0A059Q2G9_9POAL)
Solyc02g070060.2.1	-11.05	4.78E-14	FAD-binding Berberine family protein (AHRD V3.3 *** AT2G34790.1)
Solyc03g093800.1.1	-11.14	1.58E-100	glycine-rich protein (AHRD V3.3 *-* AT5G61660.1)
Solyc07g062980.3.1	-11.20	1.05E-19	Squamosa promoter-binding protein, putative (AHRD V3.3 *** B9T4B7_RICCO)
Solyc02g071020.3.1	-11.30	6.27E-07	centrosomal protein (AHRD V3.3 --* AT1G79390.1)
Solyc06g009010.1.1	-11.33	3.04E-14	Nuclear transcription factor Y protein (AHRD V3.3 *** I3TAW4_MEDTR)
Solyc08g079160.3.1	-11.44	6.09E-18	Vacuolar-processing enzyme (AHRD V3.3 *** VPE_SOYBN)
Solyc02g081330.3.1	-11.50	1.43E-14	phytoene synthase 2
Solyc10g078770.2.1	-11.63	2.03E-08	Seed maturation protein (AHRD V3.3 *** Q9LKC5_GLYTO)
Solyc12g088190.2.1	-11.65	2.15E-60	Amino acid permease (AHRD V3.3 *** A0A0K9P9F3_ZOSMR)
Solyc09g005610.3.1	-11.69	8.07E-13	transcription factor-like protein (AHRD V3.3 *** AT1G58330.1)
Solyc09g010510.3.1	-11.70	2.24E-12	NAD(P)-binding Rossmann-fold superfamily protein (AHRD V3.3 *-* AT2G37540.2)
Solyc08g044260.3.1	-11.91	3.02E-08	Fatty acid hydroxylase superfamily (AHRD V3.3 *** AT1G02205.2)

Solyc11g069110.2.1	-11.96	3.26E-05	vesicle-associated membrane protein 726 (AHRD V3.3 --* AT1G04760.2)
Solyc03g065250.3.1	-11.98	5.48E-59	Fatty acid hydroxylase superfamily protein (AHRD V3.3 *** A0A072TKE8_MEDTR)
Solyc10g055210.2.1	-12.02	7.43E-07	Dirigent protein (AHRD V3.3 *** K4D1B4_SOLLC)
Solyc10g080060.1.1	-12.09	1.03E-29	MIZU-KUSSEI-like protein (Protein of unknown function, DUF617) (AHRD V3.3 *-* AT2G41660.1)
Solyc03g117230.1.1	-12.11	3.63E-15	Ethylene-responsive transcription factor (AHRD V3.3 *** W9RS64_9ROSA)
Solyc12g042550.2.1	-12.25	1.47E-09	Importin subunit alpha (AHRD V3.3 --* IMA_SOLLC)
Solyc07g053810.3.1	-12.27	8.48E-09	Squamosa promoter binding protein 4
Solyc03g058330.3.1	-12.49	9.28E-08	Seed maturation protein LEA 4 (AHRD V3.3 *** Q9FNW3_GLYTO)
Solyc07g045140.3.1	-12.52	4.01E-14	transmembrane protein (AHRD V3.3 *** AT4G12680.1)
Solyc02g063350.1.1	-12.53	3.69E-87	Calcium binding protein (AHRD V3.3 *** Q93YA8_SESRO)
Solyc07g021340.3.1	-12.57	5.73E-45	Transmembrane protein, putative (AHRD V3.3 *** A0A072UUM3_MEDTR)
Solyc05g044630.3.1	-12.63	6.74E-16	NifU-like protein 3 (AHRD V3.3 *-* W9RHZ6_9ROSA)
Solyc10g075110.2.1	-12.84	2.07E-13	Non-specific lipid-transfer protein (AHRD V3.3 *** M1AVB9_SOLTU)
Solyc02g093590.3.1	-12.85	6.18E-23	Zinc finger CONSTANS-LIKE 7-like protein (AHRD V3.3 *** A0A0B0PB06_GOSAR)
TCONS_00038322	-13.01	2.01E-06	
Solyc09g061793.1.1	-13.07	3.16E-07	Cytochrome P450 (AHRD V3.3 *-* A0A103Y530_CYNCS)
Solyc11g021360.2.1	-13.12	3.52E-07	Protease Do-like 7 (AHRD V3.3 --* DEGP7_ARATH)
Solyc06g009190.3.1	-13.20	6.24E-24	Pectinesterase (AHRD V3.3 *** K4C3U9_SOLLC)
Solyc10g049560.2.1	-13.47	1.24E-09	ARM repeat superfamily protein (AHRD V3.3 --* AT1G60190.1)
Solyc03g034030.3.1	-13.53	2.06E-09	Late embryogenesis abundant (LEA) protein (AHRD V3.3 -** AT4G36600.2)
Solyc09g075210.3.1	-13.62	3.54E-89	Late embryogenesis abundant protein Lea5 (AHRD V3.3 *** F2VPP8_SOLNI)
Solyc02g093890.1.1	-13.63	7.97E-39	Emb|CAB62340.1 (AHRD V3.3 *** Q9FKS6_ARATH)
Solyc01g100090.1.1	-13.71	1.18E-05	LOW QUALITY:Wall-associated receptor kinase-like 20 (AHRD V3.3 *** A0A061F2M9_THECC)
Solyc12g089350.2.1	-13.73	4.06E-19	GDSL esterase/lipase (AHRD V3.3 *** A0A0B2SN40_GLYSO)
Solyc04g081900.3.1	-14.12	1.07E-55	Cysteine/Histidine-rich C1 domain family protein (AHRD V3.3 --* AT2G44380.1)
Solyc09g090790.3.1	-14.16	9.94E-55	R2R3MYB transcription factor 79
Solyc05g024160.3.1	-14.32	6.45E-19	Pyruvate dehydrogenase E1 component subunit beta (AHRD V3.3 *** B6T6H3_MAIZE)
Solyc02g061800.2.1	-14.61	6.60E-19	Peptidyl-prolyl cis-trans isomerase (AHRD V3.3 *** K4B670_SOLLC)
Solyc03g080060.1.1	-14.63	9.00E-12	LOW QUALITY:Clade XV lectin receptor kinase (AHRD V3.3 *** A0A0K1U1X9_SOLLC)
Solyc02g077980.2.1	-14.79	1.62E-08	Late embryogenesis abundant protein (LEA) family protein (AHRD V3.3 --* AT4G13230.1)
Solyc02g077970.3.1	-14.85	1.43E-05	Late embryogenesis abundant, putative (AHRD V3.3 *** B9RBC1_RICCO)
Solyc04g072740.3.1	-14.88	3.10E-11	Sulfate transporter, putative (AHRD V3.3 *** B9RJF7_RICCO)
Solyc01g009660.2.1	-14.95	1.06E-07	Low-temperature-induced 65 kDa-like protein (AHRD V3.3 *-* A0A0B0MRR8_GOSAR)
Solyc09g082550.3.1	-15.22	1.39E-74	Sulfate transporter (AHRD V3.3 *** D7LTZ8_ARALL)
Solyc01g049880.3.1	-15.78	8.99E-24	DegP protease 7 (AHRD V3.3 --* AT3G03380.2)
Solyc01g108830.2.1	-16.03	4.70E-11	Methyl esterase (AHRD V3.3 *-* A0A072UEL6_MEDTR)
Solyc03g112590.3.1	-16.06	3.59E-46	cell division cycle 48 (AHRD V3.3 *** AT3G09840.1)
Solyc12g008430.2.1	-16.13	6.68E-19	Malic enzyme (AHRD V3.3 *** M0ZHN3_SOLTU)
Solyc06g067980.3.1	-16.62	1.54E-09	Late embryogenesis abundant protein (AHRD V3.3 --* Q2QKE8_CATRO)
Solyc05g015490.3.1	-16.64	2.10E-56	Lipid transfer protein (AHRD V3.3 *** A0A0M3SGG1_GOSAR)
Solyc03g005840.2.1	-16.73	3.63E-10	Outward rectifying potassium channel protein (AHRD V3.3 *** A0A072UNK3_MEDTR)
Solyc06g007460.3.1	-16.77	1.29E-09	Epidermal patterning factor-like protein (AHRD V3.3 *** G7K0R6_MEDTR)
Solyc09g015070.3.1	-17.03	4.11E-24	Aldo/keto reductase (AHRD V3.3 *** A0A103XQA6_CYNCS)
Solyc03g117800.3.1	-17.08	6.81E-63	Fatty acid hydroxylase superfamily (AHRD V3.3 *** AT5G57800.1)

Solyc01g100760.2.1	-17.22	3.27E-23	plant/protein (Protein of unknown function, DUF538) (AHRD V3.3 *** AT1G56580.1)
Solyc10g078780.2.1	-17.43	1.77E-08	Seed maturation protein LEA 4 (AHRD V3.3 *** Q9FNX1_GLYCA)
Solyc02g089190.2.1	-17.92	4.33E-13	R2R3MYB transcription factor 29
Solyc06g068160.3.1	-18.12	1.16E-33	SNF4
Solyc11g008260.2.1	-18.35	9.88E-37	Papain family cysteine protease (AHRD V3.3 *** AT3G54940.2)
Solyc05g024260.3.1	-18.95	1.21E-10	Bidirectional sugar transporter SWEET (AHRD V3.3 *** K4BZR4_SOLLC)
Solyc03g025810.3.1	-19.03	4.91E-07	Low-temperature-induced 65 kDa-like protein (AHRD V3.3 *-* A0A0B0MRR8_GOSAR)
Solyc01g100770.2.1	-19.74	7.91E-37	LOW QUALITY:plant/protein (Protein of unknown function, DUF538) (AHRD V3.3 *** AT1G56580.1)
Solyc04g051280.3.1	-20.06	4.89E-15	Transmembrane protein, putative (AHRD V3.3 *-* A0A072VMC3_MEDTR)
Solyc12g010545.1.1	-20.57	6.21E-60	LOW QUALITY:NAC domain-containing protein 78 (AHRD V3.3 --* M7YSE5_TRIUA)
Solyc01g104710.3.1	-20.86	5.84E-47	thionin-like protein (AHRD V3.3 -** AT1G25275.2)
Solyc08g077410.3.1	-21.90	3.67E-19	Cytochrome c oxidase subunit 6B (AHRD V3.3 *** A0A151TJ10_CAJCA)
Solyc05g024373.1.1	-22.05	1.97E-09	Disease resistance protein (TIR-NBS-LRR class) family (AHRD V3.3 --* AT5G46450.3)
Solyc07g064860.2.1	-22.14	4.61E-10	pumilio 13 (AHRD V3.3 --* AT5G43090.1)
Solyc11g020990.2.1	-22.15	3.40E-14	Proteinase inhibitor II (AHRD V3.3 *** B3F0C1_TOBAC)
Solyc06g054060.1.1	-22.57	2.75E-32	LOW QUALITY:Lipid transfer protein (AHRD V3.3 *** Q5MJA5_CAPAN)
Solyc06g061100.3.1	-23.65	1.07E-14	aluminum activated malate transporter family protein (AHRD V3.3 *** AT5G46610.1)
Solyc03g097440.3.1	-24.19	8.79E-57	Dehydrogenase/reductase SDR family protein 7-like protein (AHRD V3.3 *** A0A0B0P5K8_GOSAR)
Solyc08g016415.1.1	-25.82	1.50E-10	kinesin-like calmodulin-binding protein (ZWICHEL) (AHRD V3.3 --* AT5G65930.2)
Solyc12g010820.2.1	-26.15	1.55E-19	Late embryogenesis abundant protein-like (AHRD V3.3 *-* Q9LF88_ARATH)
Solyc01g099880.3.1	-26.87	2.98E-15	Bidirectional sugar transporter SWEET (AHRD V3.3 *** K4B122_SOLLC)
Solyc01g006720.3.1	-27.24	7.37E-16	ABC transporter family protein (AHRD V3.3 *** B9IIG9_POPTR)
Solyc01g105750.1.1	-27.44	2.15E-09	LOW QUALITY:Leguminosin group485 secreted peptide (AHRD V3.3 *** A0A072UVS4_MEDTR)
Solyc12g013830.2.1	-27.71	4.72E-11	Metallothionein (AHRD V3.3 -** B8YM44_SOLNI)
Solyc06g069070.1.1	-27.95	1.62E-68	Lipid transfer protein (AHRD V3.3 *** S4TID2_GOSHI)
Solyc01g020378.1.1	-28.38	2.91E-49	LOW QUALITY:Calcium-binding EF-hand family protein, putative (AHRD V3.3 *** A0A061FAV4_THECC)
Solyc03g116390.3.1	-28.63	2.24E-11	Late embryogenesis abundant protein (AHRD V3.3 *** E1AZA3_SOLLC)
TCONS_00020994	-29.38	1.62E-17	
Solyc01g014270.3.1	-29.39	1.56E-29	LETM1-like protein (AHRD V3.3 --* AT3G11560.4)
Solyc09g065410.3.1	-29.67	1.01E-22	Lipid transfer protein (AHRD V3.3 *** B7FGM2_MEDTR)
Solyc05g024370.1.1	-30.08	3.91E-17	disease resistance protein (TIR-NBS-LRR class) (AHRD V3.3 *-* AT5G17680.2)
Solyc02g064720.3.1	-30.44	2.84E-21	phototropic-responsive NPH3 family protein
Solyc05g024360.1.1	-32.16	2.57E-12	Disease resistance protein (TIR-NBS-LRR class) (AHRD V3.3 *-* A0A072U6R9_MEDTR)
Solyc10g081840.2.1	-33.61	6.59E-51	Nuclear transcription factor Y subunit (AHRD V3.3 *-* A0A0K9P8V1_ZOSMR)
Solyc07g062530.3.1	-33.79	1.15E-98	phosphoenolpyruvate carboxylase 2
Solyc08g067500.2.1	-33.88	1.60E-19	Non-specific lipid-transfer protein (AHRD V3.3 *** K4CLX6_SOLLC)
Solyc01g087180.3.1	-34.38	1.49E-41	Microspore-specific promoter 2, putative (AHRD V3.3 --* A0A061G480_THECC)
Solyc03g006360.3.1	-34.92	1.43E-57	Auxin-repressed protein (AHRD V3.3 *** K7VPG9_SOLTU)
TCONS_00004971	-35.44	1.47E-24	
Solyc07g045145.1.1	-35.86	4.35E-45	transmembrane protein (AHRD V3.3 *-* AT4G12680.1)
Solyc01g112230.3.1	-36.25	3.12E-53	Metallothionein-like protein (AHRD V3.3 *** Q9FUJ8_SESIN)
Solyc12g098900.2.1	-37.54	8.32E-21	Late embryogenesis abundant protein (AHRD V3.3 *** J7F2C7_CAMSI)
Solyc11g056650.2.1	-38.28	9.61E-83	bHLH transcription factor 096
Solyc11g012590.2.1	-38.46	6.86E-17	CASP-like protein (AHRD V3.3 *** M1B0Y6_SOLTU)

Solyc08g044265.1.1	-41.75	1.85E-18	Fatty acid hydroxylase superfamily (AHRD V3.3 *** AT1G02205.5)
Solyc01g057170.3.1	-43.67	1.37E-12	DEAD-box ATP-dependent RNA helicase 48 (AHRD V3.3 --* RH48_ORYSJ)
Solyc04g005380.3.1	-43.76	1.32E-82	Ninja-family protein AFP1-like protein (AHRD V3.3 *** V5KZR9_SOLNI)
Solyc01g066040.2.1	-46.33	4.49E-27	LOW QUALITY:WD40 domain-containing protein (AHRD V3.3 --* AT2G47410.6)
Solyc04g007470.3.1	-46.55	9.15E-55	Drought responsive Zinc finger protein
Solyc05g041140.3.1	-50.81	3.37E-13	Protease inhibitor/seed storage/lipid transfer family protein (AHRD V3.3 *** B9HHI8_POPTR)
Solyc02g084850.3.1	-53.28	8.99E-79	Abscisic acid and environmental stress-inducible protein TAS14 (AHRD V3.3 *** TAS14_SOLLC)
Solyc04g072250.3.1	-53.60	6.32E-16	Heat-shock protein, putative (AHRD V3.3 *** B9SMA2_RICCO)
Solyc03g034380.1.1	-55.76	1.95E-14	Lipid transfer protein (AHRD V3.3 *** S4TID2_GOSHI)
Solyc03g026050.3.1	-59.80	1.13E-35	Terminal flower 1 (AHRD V3.3 *** G7ZV36_MEDTR)
Solyc03g079880.3.1	-62.52	4.58E-112	Protease inhibitor/seed storage/lipid transfer family protein (AHRD V3.3 *** B9HHI8_POPTR)
Solyc01g014100.3.1	-84.19	1.59E-28	CLE protein 1
Solyc08g075150.3.1	-89.59	1.58E-51	Coiled-coil domain-containing 73 (AHRD V3.3 *** A0A0B0NIE5_GOSAR)
Solyc06g061110.2.1	-90.16	2.84E-26	Seed maturation protein (AHRD V3.3 *** Q2XSJ3_GLYTO)
Solyc06g075990.3.1	-90.95	1.89E-22	dessication-induced 1VOC superfamily protein (AHRD V3.3 *** AT1G07645.1)
Solyc07g063905.1.1	-92.13	4.62E-28	RING/U-box superfamily protein (AHRD V3.3 --* AT3G13430.4)
Solyc05g053160.3.1	-111.44	8.85E-25	AWPM-19-like membrane family protein (AHRD V3.3 *** B9HSV5_POPTR)
Solyc09g090800.2.1	-116.92	2.06E-75	AWPM-19-like membrane family protein (AHRD V3.3 *** B9HSV5_POPTR)
Solyc06g060970.2.1	-443.74	1.81E-144	Expansin-like protein (AHRD V3.3 *** Q0WRS3_ARATH)

Supplementary Table S3. RNA-seq data: i*DLK2*-I *vs* wt-I.

Up- and down- regulated genes in Sl*DLK2* RNAi AM-roots vs control AM-roots by >10 fold change

ID (SolDB accesión)	Fold Change	P value	Description
Solyc09g082600.2.1	16.16	3.78E-17	Chlorophyllase (AHRD V3.3 *** F1BPW6_SOLPN)
Solyc08g077330.3.1	16.15	8.73E-30	Expansin-like protein (AHRD V3.3 *** W9SU42_9ROSA)
Solyc07g056670.3.1	14.59	5.98E-23	gibberellin 2-oxidase 2
Solyc06g033850.3.1	12.57	3.76E-15	Dehydration responsive element-binding factor protein (AHRD V3.3 --* A0A0K0K9Y3_ELECO)
Solyc06g072210.1.1	12.43	8.87E-21	Kunitz trypsin inhibitor (AHRD V3.3 *** B8Y888_TOBAC)
Solyc01g049820.2.1	11.28	8.84E-13	LOW QUALITY:P-loop containing nucleoside triphosphate hydrolases superfamily protein, putative isoform 1 (AHRD V3.3 *** A0A061GRZ3_THECC)
Solyc11g027840.2.1	11.22	8.72E-23	1,4-beta-D-glucanase (AHRD V3.3 *** B4FHX7_MAIZE)
Solyc08g076730.3.1	10.83	1.10E-70	Tetratricopeptide repeat (TPR)-like superfamily protein (AHRD V3.3 *** AT4G17940.1)
Solyc02g077800.1.1	10.77	1.70E-11	LOW QUALITY:Serine/arginine-rich splicing factor RSZ23 (AHRD V3.3 --* RZP23_ORYSJ)
Solyc09g008560.3.1	10.33	5.47E-21	2-oxoglutarate (2OG) and Fe(II)-dependent oxygenase superfamily protein (AHRD V3.3 *** AT2G36690.2)
Solyc12g006560.2.1	10.28	2.82E-14	Early nodulin-93 (AHRD V3.3 *** A0A061GV12_THECC)
Solyc10g075175.1.1	9.88	2.63E-22	Aspartate aminotransferase (AHRD V3.3 *** B9HDA1_POPTR)
Solyc09g074600.1.1	9.31	1.24E-13	Glutaredoxin (AHRD V3.3 *** A0A103Y7J3_CYNCS)
Solyc04g080540.2.1	9.20	9.22E-25	DNA polymerase epsilon catalytic subunit A, putative (AHRD V3.3 *** A0A061FCM9_THECC)
Solyc01g087090.3.1	9.16	6.87E-11	beta glucosidase 8 (AHRD V3.3 --* AT3G62750.1)
Solyc07g062670.1.1	9.12	4.68E-14	LOW QUALITY:Clavata3/ESR (CLE) gene family member (AHRD V3.3 --* A0A072TRR8_MEDTR)
Solyc10g075170.2.1	8.76	1.98E-23	Aspartate aminotransferase (AHRD V3.3 *-* A0A067JJ16_JATCU)
Solyc10g086630.1.1	8.44	8.41E-32	LOW QUALITY:Legume-specific protein (AHRD V3.3 *** S5VRI2_9FABA)
Solyc09g065390.1.1	8.31	6.14E-14	LOW QUALITY:Pre-mRNA cleavage complex 2 protein Pcf11, putative isoform 2 (AHRD V3.3 *-* A0A061GBF7_THECC)
Solyc10g012095.1.1	8.29	7.42E-11	LOW QUALITY:Retrovirus-related Pol polyprotein from transposon TNT 1-94 (AHRD V3.3 *-* POLX_TOBAC)
Solyc01g106105.1.1	8.02	3.43E-11	LOW QUALITY:F-box family protein with a domain of Uncharacterized protein function, putative (AHRD V3.3 *-* A0A061E0S9_THECC)
Solyc06g035940.3.1	8.02	6.30E-10	Homeobox leucine zipper protein (AHRD V3.3 *** A0A072TNH2_MEDTR)
Solyc01g100460.3.1	7.83	2.14E-40	BZIP transcription factor family protein (AHRD V3.3 *** B9GSS6_POPTR)
Solyc08g065645.1.1	7.65	1.02E-10	LOW QUALITY:Retrovirus-related Pol polyprotein from transposon TNT 1-94 (AHRD V3.3 *-* POLX_TOBAC)
Solyc08g066100.3.1	7.53	4.82E-15	ATP-dependent 6-phosphofructokinase (AHRD V3.3 *** A0A0V0IM90_SOLCH)
TCONS_00020233	7.44	7.37E-13	
Solyc09g011390.3.1	7.44	6.69E-21	Major facilitator superfamily protein (AHRD V3.3 *** AT3G53960.1)
TCONS_00000297	7.42	4.45E-08	
Solyc01g087010.3.1	7.32	2.09E-12	Carbohydrate esterase plant-like protein (AHRD V3.3 *** G7I2A7_MEDTR)
Solyc01g106510.2.1	7.21	3.55E-27	LOW QUALITY:F-box protein (AHRD V3.3 *** A0A1D1YUP5_9ARAE)
Solyc07g054760.1.1	7.17	1.00E-10	LOW QUALITY:Wound-responsive family protein (AHRD V3.3 *** AT4G10265.1)

Solyc10g085190.2.1	7.15	1.82E-10	2-oxoglutarate (2OG) and Fe(II)-dependent oxygenase superfamily protein (AHRD V3.3 *** AT3G11180.1)
Solyc09g059335.1.1	6.89	1.09E-08	Retrovirus-related Pol polyprotein from transposon TNT 1-94 (AHRD V3.3 *-* POLX_TOBAC)
Solyc05g014300.1.1	6.89	4.00E-13	LOW QUALITY:NAC domain containing protein 5 (AHRD V3.3 --* AT1G02250.1)
Solyc07g054810.1.1	6.84	8.81E-31	LOW QUALITY:glutamate-1-semialdehyde 2,1-aminomutase 2 (AHRD V3.3 --* AT3G48730.1)
Solyc06g050870.3.1	6.82	1.32E-07	Hypoxia-responsive family protein (AHRD V3.3 *** A0A061FYY0_THECC)
Solyc01g066200.1.1	6.68	4.40E-19	LOW QUALITY:Glucan endo-1,3-beta-glucosidase 8 (AHRD V3.3 --* W9S9M9_9ROSA)
Solyc05g047530.3.1	6.63	1.75E-07	trans-cinnamate 4-monooxygenase
Solyc01g104750.3.1	6.58	1.01E-08	WAT1-related protein (AHRD V3.3 *** K4B247_SOLLC)
Solyc02g089140.2.1	6.57	5.66E-09	LOW QUALITY:SIN3-like 1 (AHRD V3.3 --* AT3G01320.2)
Solyc03g044460.1.1	6.52	4.11E-16	LOW QUALITY:basic helix-loop-helix (bHLH) DNA-binding superfamily protein (AHRD V3.3 *-* AT3G50330.1)
Solyc09g082480.2.1	6.49	2.04E-10	RNA-directed DNA methylation protein (AHRD V3.3 *** G7K3Q7_MEDTR)
Solyc04g017740.1.1	6.48	3.68E-16	LOW QUALITY:pyridoxal-phosphate-dependent serine hydroxymethyltransferase, putative (DUF632) (AHRD V3.3 --* AT3G51290.3)
TCONS_00006004	6.47	3.19E-07	
Solyc05g039950.2.1	6.42	1.87E-11	HXXXD-type acyl-transferase family protein (AHRD V3.3 *** AT3G26040.1)
Solyc07g008240.3.1	6.34	3.23E-07	Non-symbiotic hemoglobin 1 (AHRD V3.3 *** HBL1_GOSHI)
Solyc03g123770.1.1	6.28	4.88E-12	LOW QUALITY:Disease resistance protein (AHRD V3.3 --* Q19HX1_ARATH)
Solyc12g056710.2.1	6.26	6.95E-08	NAD(P)-binding Rossmann-fold superfamily protein (AHRD V3.3 *** AT1G52340.1),Pfam:PF13561
Solyc07g054745.1.1	6.20	6.44E-08	LOW QUALITY:Wound-responsive family protein (AHRD V3.3 *** A0A061E3U8_THECC)
Solyc08g074720.2.1	6.20	5.20E-07	LOW QUALITY:Late embryogenesis abundant protein (AHRD V3.3 *** A0A075C704_9CARY)
Solyc03g121090.3.1	6.16	2.33E-07	Oxidative stress 3, putative isoform 2 (AHRD V3.3 *** A0A061GIQ6_THECC)
Solyc10g011730.3.1	6.10	1.40E-07	Arabinogalactan peptide 20 (AHRD V3.3 *** AGP20_ARATH)
Solyc06g066430.3.1	6.08	1.97E-19	SUN-like protein 18
Solyc02g083730.3.1	6.04	3.32E-30	Rhodanese-related sulfurtransferase (AHRD V3.3 *** G7JXI1_MEDTR)
Solyc01g087810.2.1	6.03	4.47E-08	subtilisin-like serine protease family protein
Solyc01g094160.1.1	5.93	1.79E-09	Regulator of chromosome condensation (RCC1) family with FYVE zinc finger domain-containing protein (AHRD V3.3 --* AT1G65920.2)
Solyc08g068450.1.1	5.91	8.40E-07	LOW QUALITY:Serine/threonine-protein phosphatase 2A regulatory subunit delta isoform (AHRD V3.3 --* A0A1D1YJ73_9ARAE)
Solyc01g099620.3.1	5.90	7.05E-11	Respiratory burst oxidase, putative (AHRD V3.3 *** B9RFA3_RICCO)
Solyc02g071970.1.1	5.86	1.69E-08	LOW QUALITY:F-box and Leucine Rich Repeat domains containing protein (AHRD V3.3 --* AT1G80960.6)
Solyc00g080750.3.1	5.83	9.21E-12	Plastid movement impaired protein (AHRD V3.3 *** A0A072VEV4_MEDTR)
Solyc10g076400.2.1	5.82	4.23E-08	Trichome birefringence-like protein (AHRD V3.3 *** G7JKP3_MEDTR)
Solyc06g008750.1.1	5.76	3.00E-06	Glutaredoxin (AHRD V3.3 *** E9NZT9_PHAVU)
Solyc09g009420.1.1	5.66	3.78E-07	LOW QUALITY:AMP-dependent synthetase and ligase family protein (AHRD V3.3 --* AT2G47240.4)
Solyc10g076510.2.1	5.65	3.86E-10	Pyruvate decarboxylase (AHRD V3.3 *** Q8H9C6_SOLTU)
Solyc08g074255.1.1	5.64	3.44E-07	LOW QUALITY:NBS/LRR resistance protein-like protein (AHRD V3.3 *** Q8LKJ0_CAPAN)
Solyc03g031880.3.1	5.57	1.17E-09	Amine oxidase family protein (AHRD V3.3 *** B9H3J5_POPTR)

Solyc08g062220.3.1	5.56	2.43E-18	Glycosyltransferase (AHRD V3.3 *** K4CL11_SOLLC)
Solyc04g016430.3.1	5.53	2.01E-10	Cytokinin oxidase/dehydrogenase-like (AHRD V3.3 *** I0IUQ8_SOLLC)
Solyc08g068850.3.1	5.50	3.74E-14	Proton pump interactor 1 (AHRD V3.3 *-* D5L6G0_SOLTU)
Solyc09g092130.3.1	5.48	1.96E-10	Sucrose-phosphate synthase (AHRD V3.3 *** A0A0U1ZVB4_LYCBA)
Solyc00g141360.1.1	5.47	1.96E-09	LOW QUALITY:Disease resistance protein (AHRD V3.3 *-* Q9SBC3_SOLLC)
Solyc02g076830.1.1	5.46	3.62E-39	Serine/threonine-protein kinase (AHRD V3.3 *-* A0A199VI10_ANACO)
Solyc12g013690.2.1	5.46	1.90E-15	FAD/NAD(P)-binding oxidoreductase family protein (AHRD V3.3 *** AT5G05320.1)
Solyc11g011880.2.1	5.45	1.81E-13	Protein kinase (AHRD V3.3 *** A9CM11_IPONI)
Solyc12g009880.1.1	5.42	9.00E-13	LOW QUALITY:Serine-rich protein-related (AHRD V3.3 *** A0A061GN42_THECC)
Solyc02g092290.3.1	5.40	8.01E-15	F-box family protein (AHRD V3.3 *** B9GFH4_POPTR)
Solyc12g099870.2.1	5.34	5.47E-06	Leucine-rich repeat receptor-like protein kinase family protein (AHRD V3.3 *** AT4G08850.1)
Solyc01g066290.2.1	5.33	1.41E-40	LOW QUALITY:Xaa-Pro aminopeptidase 1 (AHRD V3.3 --* A0A199W6F4_ANACO)
Solyc09g074580.2.1	5.31	6.61E-09	Glutaredoxin (AHRD V3.3 *** A0A103XPG8_CYNCS)
Solyc12g007040.2.1	5.31	1.77E-06	LOW QUALITY:FKBP-like peptidyl-prolyl cis-trans isomerase family protein (AHRD V3.3 --* AT4G26555.2)
Solyc03g115600.3.1	5.30	3.90E-12	Zinc finger protein (AHRD V3.3 *-* A0A0B0MNI3_GOSAR)
TCONS_00009236	5.29	6.54E-07	
Solyc00g247300.3.1	5.23	1.12E-32	Cytochrome P450 family protein (AHRD V3.3 *** B9HFW6_POPTR)
Solyc12g015920.2.1	5.21	1.38E-19	Heavy metal transport/detoxification superfamily protein (AHRD V3.3 *-* AT5G48290.1)
Solyc04g040180.3.1	5.19	1.78E-10	S-adenosylmethionine-dependent methyltransferase, putative (AHRD V3.3 *** B9SZS6_RICCO)
Solyc10g081390.1.1	5.16	2.11E-18	LOW QUALITY:transmembrane protein (AHRD V3.3 -** AT3G47510.1)
Solyc01g107950.2.1	5.13	2.99E-06	bHLH transcription factor 008
Solyc06g072430.2.1	5.11	1.59E-05	BAG family molecular chaperone regulator 5 (AHRD V3.3 *-* W9QTU5_9ROSA)
Solyc08g005525.1.1	5.08	3.86E-06	Plant invertase/pectin methylesterase inhibitor superfamily protein (AHRD V3.3 --* AT4G00080.1)
Solyc01g110847.1.1	5.08	1.64E-11	SAUR-like auxin-responsive protein family (AHRD V3.3 *** A0A061DYL9_THECC)
Solyc02g062310.1.1	5.06	3.65E-06	BURP domain protein RD22 (AHRD V3.3 *-* RD22_ARATH)
Solyc08g007090.2.1	5.02	4.70E-06	Expansin-like protein (AHRD V3.3 *** W9SU42_9ROSA)
Solyc02g077240.3.1	5.00	7.94E-08	Pyruvate decarboxylase (AHRD V3.3 *** Q1I1D9_CITSI)
TCONS_00038641	4.99	1.14E-05	
Solyc04g054376.1.1	4.93	2.06E-05	Retrovirus-related Pol polyprotein from transposon TNT 1-94 (AHRD V3.3 *-* POLX_TOBAC)
Solyc09g082220.1.1	4.92	4.81E-13	LOW QUALITY:Acetyltransferase (GNAT) domain protein (AHRD V3.3 *** A0A072U473_MEDTR)
Solyc10g050990.1.1	4.87	2.11E-05	Pyruvate kinase (AHRD V3.3 --* A9TZX1_PHYPA)
Solyc11g008820.2.1	4.83	1.46E-10	Endoglucanase (AHRD V3.3 *** A0A0V0II53_SOLCH)
Solyc07g054770.1.1	4.81	4.65E-06	Wound-responsive family protein (AHRD V3.3 *** A0A061E3U8_THECC)
Solyc08g077380.3.1	4.80	1.58E-14	Purine permease (AHRD V3.3 *** A0A072UNZ2_MEDTR)
Solyc04g054340.1.1	4.80	1.14E-05	LOW QUALITY:transmembrane protein (AHRD V3.3 --* AT5G65440.9)

Solyc06g074170.3.1	4.79	5.05E-29	NAC domain protein, (AHRD V3.3 *** A0A061GVZ7_THECC)
Solyc12g099345.1.1	4.79	3.24E-09	calmodulin-binding transcription activator (AHRD V3.3 *-* AT3G16940.2)
Solyc09g091770.1.1	4.77	2.23E-05	LOW QUALITY:Protein NRT1/ PTR FAMILY 1.2 (AHRD V3.3 --* PTR6_ARATH)
Solyc01g005680.3.1	4.77	1.49E-12	Cytokinin riboside 5'-monophosphate phosphoribohydrolase (AHRD V3.3 *** K4ASD4_SOLLC)
Solyc07g065970.2.1	4.74	6.75E-11	Chaperone protein DNAj, putative (AHRD V3.3 *-* B9SXA3_RICCO)
Solyc01g109320.3.1	4.70	9.01E-10	Protein DETOXIFICATION (AHRD V3.3 *** K4B3E5_SOLLC)
TCONS_00050863	4.68	4.50E-08	
Solyc02g078380.3.1	4.67	1.53E-24	Stem-specific protein TSJT1 (AHRD V3.3 *** A0A151T7D1_CAJCA)
Solyc06g054620.3.1	4.65	2.00E-10	Zinc finger transcription factor 43
Solyc07g007930.3.1	4.62	1.12E-12	Alkaline alpha-galactosidase seed imbibition protein (AHRD V3.3 *** Q8H6N3_SOLLC)
Solyc02g021350.3.1	4.62	1.12E-08	Nucleosome assembly protein family (AHRD V3.3 *** A9RDJ7_PHYPA)
Solyc07g054790.1.1	4.61	1.20E-05	Wound-responsive family protein (AHRD V3.3 *** A0A061E3U8_THECC)
Solyc08g078180.1.1	4.59	3.77E-12	Ethylene Response Factor A.1
Solyc12g057073.1.1	4.58	1.04E-05	Pyrophosphate-energized vacuolar membrane proton pump (AHRD V3.3 --* AVP_VIGRR)
TCONS_00027595	4.57	1.50E-06	
Solyc06g065530.3.1	4.55	4.44E-16	GDSL-like lipase/acylhydrolase superfamily protein
Solyc08g005540.2.1	4.54	4.81E-14	Amino acid permease family protein (AHRD V3.3 *** AT1G31830.1)
Solyc01g109800.2.1	4.54	2.34E-06	LOW QUALITY:Transmembrane protein, putative (AHRD V3.3 *-* G7J762_MEDTR)
Solyc03g043700.3.1	4.51	8.73E-43	U-box domain-containing protein (AHRD V3.3 *** A0A0K9PMJ3_ZOSMR)
Solyc12g008660.1.1	4.51	1.03E-12	Zinc finger transcription factor 73
Solyc10g080670.2.1	4.48	2.08E-12	Transmembrane protein, putative (AHRD V3.3 *** A2Q5V9_MEDTR)
Solyc02g078460.3.1	4.46	1.19E-14	abscisic acid-insensitive RING protein 4-like
Solyc05g015850.3.1	4.43	9.46E-16	WRKY transcription factor 75
Solyc12g017700.2.1	4.43	6.49E-09	ATP-dependent RNA helicase (AHRD V3.3 *** A0A0K9PGQ5_ZOSMR)
Solyc10g006150.3.1	4.39	1.04E-10	DUF4408 domain protein (AHRD V3.3 *** G7K8L0_MEDTR)
Solyc03g044960.2.1	4.38	1.67E-05	Calcium uniporter protein, mitochondrial (AHRD V3.3 *** A0A0B2SA24_GLYSO)
Solyc03g006410.3.1	4.38	4.87E-07	DUF506 family protein (AHRD V3.3 *** G7IPT8_MEDTR)
Solyc03g007890.3.1	4.37	3.43E-05	class 2 small heat shock protein Le-HSP17.6
Solyc08g006470.3.1	4.36	1.04E-13	Zinc finger protein (AHRD V3.3 *** A0A0B2RI16_GLYSO)
Solyc11g072630.2.1	4.35	2.32E-11	mitogen-activated protein kinase 4
Solyc04g081460.2.1	4.31	1.40E-25	calcineurin B-like protein 10 (AHRD V3.3 --* AT4G33000.6)
Solyc05g053000.1.1	4.30	2.70E-12	AT hook motif DNA-binding family protein (AHRD V3.3 *** A0A072V017_MEDTR)
Solyc02g083280.3.1	4.30	1.05E-10	Rhodanese-related sulfurtransferase (AHRD V3.3 *** B7FGV4_MEDTR)
Solyc01g090150.1.1	4.30	8.11E-05	Unknown protein (AHRD V3.3)
Solyc03g123970.1.1	4.30	6.63E-05	LOW QUALITY:Lipid-binding serum glycoprotein family protein isoform 2 (AHRD V3.3 *-* A0A061GA66_THECC)

Solyc06g050520.2.1	4.30	2.23E-08	dehydration responsive element binding protein 1
Solyc08g005120.3.1	4.29	7.05E-08	Cinnamoyl-CoA reductase-like protein (AHRD V3.3 *** G7KDR3_MEDTR)
Solyc02g071875.1.1	4.29	1.17E-08	Leucine-rich repeat receptor-like protein kinase (AHRD V3.3 *** C0LGF2_ARATH)
Solyc11g069750.2.1	4.29	4.54E-10	High-affinity nitrate transporter (AHRD V3.3 *** Q76IJ7_PRUPE)
Solyc04g055130.1.1	4.29	1.04E-06	LOW QUALITY:C2 domain protein (AHRD V3.3 *** A0A072UZT9_MEDTR)
Solyc06g073990.2.1	4.29	6.63E-07	Gb:AAF02129.1, putative (AHRD V3.3 *** A0A061GVZ4_THECC)
Solyc06g070960.2.1	4.27	3.00E-10	ABC transporter family protein (AHRD V3.3 *** A0A097P9Q6_HEVBR)
Solyc09g066400.2.1	4.27	1.19E-04	Cytochrome P450 (AHRD V3.3 *** Q9AVQ2_SOLTU)
Solyc11g045690.2.1	4.26	1.33E-04	Ethylene-responsive transcription factor, putative (AHRD V3.3 *** B9RGV0_RICCO)
Solyc10g047170.2.1	4.25	7.37E-11	sulfate transporter 1
Solyc04g071340.3.1	4.25	7.28E-11	Fructose-1,6-bisphosphatase (AHRD V3.3 *** A0A068JD95_TOBAC)
Solyc10g083900.2.1	4.24	1.49E-07	R2R3MYB transcription factor 27
Solyc04g076440.1.1	4.23	4.79E-07	LOW QUALITY:Tetratricopeptide repeat-like superfamily protein (AHRD V3.3 *-* A0A061FLU3_THECC)
Solyc01g100095.1.1	4.20	9.89E-06	RING/U-box superfamily protein, putative (AHRD V3.3 *** A0A061E1W0_THECC)
Solyc06g074995.1.1	4.19	3.88E-07	High affinity nitrate transporter protein (AHRD V3.3 *-* Q84MZ9_TOBAC)
Solyc02g090120.1.1	4.19	8.49E-05	LOW QUALITY:Inositol 1,4,5-trisphosphate receptor-interacting protein-like 2 (AHRD V3.3 -** A0A1D1XL30_9ARAE)
Solyc05g006790.2.1	4.16	2.46E-07	Actin cross-linking protein, putative (AHRD V3.3 *** A0A061E7B5_THECC)
Solyc04g071690.3.1	4.15	4.02E-06	Alba DNA/RNA-binding protein (AHRD V3.3 *-* AT1G76010.2)
Solyc12g057070.2.1	4.14	3.38E-08	Glycosyltransferase (AHRD V3.3 *** Q589Y2_TOBAC)
Solyc06g068450.2.1	4.12	2.69E-11	Non-specific serine/threonine protein kinase (AHRD V3.3 *** K4C820_SOLLC)
Solyc03g059050.2.1	4.11	2.14E-05	LOW QUALITY:NADH-ubiquinone oxidoreductase chain 3 (AHRD V3.3 --* NU3M_PINSY)
Solyc08g067410.2.1	4.10	4.01E-11	3-ketoacyl-CoA synthase (AHRD V3.3 *** A0A023PMK5_TOBAC)
Solyc09g075610.3.1	4.09	1.39E-11	GATA transcription factor, putative (AHRD V3.3 *** B9RNI7_RICCO)
Solyc09g098160.3.1	4.09	5.14E-13	pirin
Solyc08g077480.3.1	4.09	3.14E-16	senescence-associated family protein (DUF581) (AHRD V3.3 *** AT4G17670.1)
Solyc05g052880.3.1	4.09	1.25E-04	Plant/T7H20-70 protein (AHRD V3.3 *** A0A072U1L2_MEDTR)
Solyc02g093910.3.1	4.07	1.55E-05	Kelch repeat-containing protein family (AHRD V3.3 *** A0A151RD96_CAJCA)
Solyc10g017960.2.1	4.07	3.52E-07	F-box protein PP2-A13 (AHRD V3.3 *** P2A13_ARATH)
Solyc05g025890.2.1	4.06	3.03E-06	Acyl-CoA N-acyltransferases (NAT) superfamily protein (AHRD V3.3 *** AT2G06025.6)
Solyc05g055270.1.1	4.05	2.69E-09	Galactose oxidase/kelch repeat superfamily protein (AHRD V3.3 --* AT5G60570.3)
Solyc03g005520.1.1	4.03	4.08E-05	Ethylene-responsive transcription factor (AHRD V3.3 *** F2Y9E9_COFAR)
Solyc11g005430.2.1	4.00	7.58E-08	WAT1-related protein (AHRD V3.3 *** K4D4F6_SOLLC)
Solyc07g007325.1.1	4.00	2.74E-21	Serine-rich protein-related (AHRD V3.3 *-* A0A061GN42_THECC)
Solyc09g065350.1.1	4.00	5.28E-05	LOW QUALITY:ovate family protein 18
Solyc11g069700.2.1	3.99	2.16E-10	Elongation factor 1-alpha (AHRD V3.3 *** EF1A_SOLLC)

TCONS_00041358	3.98	1.30E-05	
Solyc06g054625.1.1	3.97	6.93E-12	Zinc finger CCCH domain-containing protein 32 (AHRD V3.3 *-* A0A151STD4_CAJCA)
Solyc07g026650.3.1	3.96	2.77E-04	1-aminocyclopropane-1-carboxylate oxidase 5
Solyc05g046290.3.1	3.96	2.41E-15	Xyloglucan endotransglucosylase/hydrolase (AHRD V3.3 *** K4C0W2_SOLLC)
Solyc06g071620.3.1	3.96	2.27E-10	U5 small nuclear ribonucleoprotein helicase (AHRD V3.3 *** AT1G20960.2)
Solyc03g044560.1.1	3.96	2.04E-04	LOW QUALITY:NAC domain containing protein 35 (AHRD V3.3 --* AT2G02450.2)
Solyc07g065340.1.1	3.94	1.40E-16	Serine acetyltransferase (AHRD V3.3 *** Q6STL5_NICPL)
Solyc12g010920.2.1	3.94	1.54E-05	Oleosin (AHRD V3.3 *** K4DCH8_SOLLC)
Solyc10g081790.1.1	3.93	3.56E-08	RING/U-box superfamily protein (AHRD V3.3 *** AT5G06490.1)
Solyc07g054550.1.1	3.92	2.06E-06	LOW QUALITY:3-ketoacyl-CoA synthase 10 (AHRD V3.3 --* AT2G26250.1)
Solyc01g073860.3.1	3.92	1.62E-04	Cysteine/Histidine-rich C1 domain family protein (AHRD V3.3 *** AT2G44380.1)
Solyc04g016420.3.1	3.91	1.84E-10	Mediator of RNA polymerase II transcription subunit 23 (AHRD V3.3 *-* A0A061EVL7_THECC)
Solyc03g005500.1.1	3.91	8.33E-05	Ethylene-responsive transcription factor (AHRD V3.3 *** W9R427_9ROSA)
Solyc03g095310.3.1	3.90	1.63E-11	Cytochrome P450 protein (AHRD V3.3 *** A0A0B0P3Q6_GOSAR)
Solyc02g065000.1.1	3.90	2.36E-09	Calcium-binding EF-hand (AHRD V3.3 *** A0A103YH91_CYNCS)
Solyc12g009300.2.1	3.90	3.57E-15	fruit sucrose synthase
Solyc05g007950.3.1	3.90	1.05E-07	LERNALE L.esculentum ribonuclease le
Solyc10g078205.1.1	3.89	2.99E-04	Cytochrome P450 (AHRD V3.3 *-* A9ZT63_COPJA)
Solyc01g079940.3.1	3.88	1.31E-07	Eukaryotic aspartyl protease family protein (AHRD V3.3 *** AT1G03220.1)
Solyc09g059460.3.1	3.87	1.26E-15	Vacuolar iron transporter (VIT) family protein (AHRD V3.3 *-* A0A061G9Q5_THECC)
Solyc12g006680.2.1	3.86	1.60E-07	Early nodulin 93 protein (AHRD V3.3 *** A3FGC9_9ROSI)
Solyc11g069680.1.1	3.86	3.23E-04	LOW QUALITY:HXXXD-type acyl-transferase family protein (AHRD V3.3 *** AT3G26040.1)
Solyc10g050980.1.1	3.86	3.62E-04	PAB-dependent poly(A)-specific ribonuclease subunit PAN2 (AHRD V3.3 -** A0A1D1XPR6_9ARAE)
Solyc11g070070.2.1	3.86	4.03E-13	Zinc finger transcription factor 70
Solyc01g091030.3.1	3.85	2.02E-09	Small auxin up-regulated RNA1
Solyc08g068710.1.1	3.84	1.40E-10	Tyramine n-hydroxycinnamoyl transferase (AHRD V3.3 *** Q5D8C0_CAPAN)
Solyc07g061720.3.1	3.83	3.49E-04	gibberellin 2-oxidase 4
Solyc10g012090.1.1	3.83	5.43E-07	LOW QUALITY:Ferredoxin-thioredoxin reductase catalytic chain, chloroplastic (AHRD V3.3 --* FTRC_MAIZE)
Solyc02g080120.2.1	3.83	7.54E-06	Gibberellin 2-beta- dioxygenase 7
Solyc06g053715.1.1	3.83	1.53E-07	S-locus lectin protein kinase family protein (AHRD V3.3 --* AT1G61390.2)
Solyc12g008477.1.1	3.82	3.99E-04	RING/U-box superfamily protein (AHRD V3.3 *-* AT3G19950.3)
Solyc12g096950.2.1	3.81	2.41E-07	TLD-domain containing nucleolar protein, putative isoform 1 (AHRD V3.3 *** A0A061ENH1_THECC)
Solyc11g011980.2.1	3.79	7.70E-12	Transducin/WD40 repeat-like superfamily protein (AHRD V3.3 *** AT2G32950.1)
Solyc04g072343.1.1	3.79	3.44E-07	Glycosyltransferase (AHRD V3.3 --* I1GLZ7_BRADI)
Solyc04g074380.3.1	3.78	4.17E-07	Glycosyltransferase (AHRD V3.3 *-* M1D1E1_SOLTU)

Solyc06g065550.2.1	3.78	1.77E-07	Cysteine/Histidine-rich C1 domain family protein (AHRD V3.3 --* AT5G40590.1)
Solyc01g087040.2.1	3.77	4.11E-08	PsbP-like (AHRD V3.3 *** A0A0U9HL69_KLEFL)
Solyc05g016690.3.1	3.77	2.41E-11	Nudix hydrolase (AHRD V3.3 *** A0A061GGI6_THECC)
Solyc10g005460.3.1	3.75	7.78E-14	MYB transcription factor (AHRD V3.3 *** A0A0U3IU11_MESCR)
Solyc05g007900.2.1	3.75	4.42E-04	LOW QUALITY:RING/U-box superfamily protein, putative (AHRD V3.3 *** A0A061EHX5_THECC)
Solyc09g008840.3.1	3.75	1.12E-10	Pyruvate kinase family protein (AHRD V3.3 *** AT3G52990.1)
Solyc03g044830.3.1	3.74	1.00E-06	Transducin/WD40 repeat-like superfamily protein (AHRD V3.3 *** AT3G18950.1)
Solyc11g051145.1.1	3.74	2.90E-04	Retrovirus-related Pol polyprotein from transposon TNT 1-94 (AHRD V3.3 *-* POLX_TOBAC)
Solyc06g066360.2.1	3.73	2.38E-10	RING/FYVE/PHD zinc finger protein, putative (AHRD V3.3 *-* G7IWF3_MEDTR)
Solyc09g008780.3.1	3.72	5.21E-14	Sulfite exporter TauE/SafE family protein (AHRD V3.3 *** AT2G36630.1)
Solyc01g096175.1.1	3.72	3.56E-04	Protein yippee-like (AHRD V3.3 *** A0A0J8FX54_BETVU)
TCONS_00023676	3.72	2.16E-06	
Solyc07g005110.3.1	3.71	1.08E-05	Receptor-like kinase CHRK1 (AHRD V3.3 *** Q9SWX8_TOBAC)
Solyc01g068410.3.1	3.71	6.01E-05	SlPIN5
Solyc09g082530.2.1	3.71	6.45E-09	Leucine-rich repeat receptor-like protein kinase family (AHRD V3.3 *** A0A0K9PTR8_ZOSMR)
Solyc10g084170.1.1	3.71	3.83E-04	BAG family molecular chaperone regulator 5 (AHRD V3.3 *-* W9QTU5_9ROSA)
Solyc10g081780.2.1	3.70	2.81E-05	RING/U-box superfamily protein (AHRD V3.3 *** AT2G35910.1)
Solyc01g108190.3.1	3.69	3.67E-13	Calcium-binding EF-hand (AHRD V3.3 *** A0A118JV88_CYNCS)
Solyc12g042480.2.1	3.69	1.32E-07	Cytochrome P450 family protein (AHRD V3.3 *** B9HFW5_POPTR)
Solyc07g064720.3.1	3.69	3.24E-08	GDSL esterase/lipase (AHRD V3.3 *** W9RB61_9ROSA)
Solyc05g025953.1.1	3.68	1.19E-05	En/Spm transposon protein-like (AHRD V3.3 --* Q9LH00_ARATH)
Solyc02g078370.1.1	3.67	5.06E-04	Anther-specific protein TA-29 (AHRD V3.3 *** TA29_TOBAC)
Solyc01g079930.2.1	3.67	3.08E-05	Xyloglucan-specific endoglucanase inhibitor 9 (AHRD V3.3 *** G8GYH9_SOLTU)
Solyc12g049550.2.1	3.67	1.29E-04	GDSL esterase/lipase 5 (AHRD V3.3 *** GLIP5_ARATH)
Solyc03g113130.3.1	3.65	1.24E-11	2-aminoethanethiol dioxygenase (AHRD V3.3 *** A0A0B0PVN9_GOSAR)
Solyc02g079150.2.1	3.65	2.42E-07	F-box family protein (AHRD V3.3 *** B9H220_POPTR)
TCONS_00034365	3.65	2.34E-04	
Solyc08g079480.3.1	3.64	4.06E-12	DUF1442 family protein (AHRD V3.3 *** G7KG71_MEDTR)
Solyc03g082420.3.1	3.63	2.14E-04	Heat shock protein (AHRD V3.3 *** A9QVH3_9FABA)
Solyc12g010570.1.1	3.63	1.18E-08	Tetraspanin family protein (AHRD V3.3 *** A0A072V357_MEDTR)
Solyc07g056390.3.1	3.62	2.36E-21	Endoplasmic oxidoreductin-1, putative (AHRD V3.3 *** B9T812_RICCO)
Solyc02g065090.3.1	3.62	1.25E-07	Patatin (AHRD V3.3 *** A0A0E0J487_ORYNI)
Solyc03g112320.3.1	3.61	5.29E-11	Ferric reduction oxidase 8 (AHRD V3.3 *** W9RI94_9ROSA)
Solyc06g008930.3.1	3.61	9.03E-07	MLP-like protein 31 (AHRD V3.3 -** A0A151QPB6_CAJCA)
TCONS_00026190	3.60	8.00E-05	

Solyc08g006410.3.1	3.58	2.11E-05	Glycosyltransferase (AHRD V3.3 *** K4CIC9_SOLLC)
Solyc02g085260.1.1	3.58	8.34E-06	LOW QUALITY:Peptidase M20/M25/M40 family protein (AHRD V3.3 --* AT1G44180.3)
Solyc07g026675.1.1	3.57	7.92E-10	myb-like transcription factor family protein (AHRD V3.3 *-* AT5G56840.1)
Solyc04g080705.1.1	3.56	2.55E-15	Bifunctional nuclease 1 (AHRD V3.3 *** BBD1_ARATH)
Solyc07g054430.3.1	3.56	4.09E-05	Glutamate formiminotransferase 1 (AHRD V3.3 *** B4F7V5_MAIZE)
Solyc06g072940.2.1	3.55	1.48E-05	auxin canalization protein (DUF828) (AHRD V3.3 *-* AT5G57770.1)
Solyc04g016230.3.1	3.55	9.25E-11	Glycosyltransferase (AHRD V3.3 *** M1DUF2_SOLTU)
Solyc09g030370.3.1	3.55	2.48E-04	GDSL esterase/lipase (AHRD V3.3 *** A0A0B2SPC5_GLYSO)
Solyc07g053300.1.1	3.54	2.04E-04	ABC transporter family protein (AHRD V3.3 *** B9I1V7_POPTR)
Solyc06g054570.1.1	3.53	2.84E-05	Glutaredoxin family protein (AHRD V3.3 *** D7LYE9_ARALL)
Solyc01g106520.1.1	3.53	4.13E-08	LOW QUALITY:F-box protein SKIP23 (AHRD V3.3 *-* A0A151TCP0_CAJCA)
Solyc02g080220.3.1	3.52	1.72E-11	Pectinesterase (AHRD V3.3 *** K4B9P3_SOLLC)
Solyc06g059740.3.1	3.52	2.94E-04	Alcohol dehydrogenase (AHRD V3.3 *** ADH_MALDO)
Solyc01g086660.2.1	3.51	2.15E-08	LOW QUALITY:agenet domain protein (DOMAIN OF UNKNOWN FUNCTION 724 2) (AHRD V3.3 --* AT1G11420.1)
Solyc07g064070.2.1	3.51	1.15E-04	U4/U6 small nuclear ribonucleoprotein Prp31 (AHRD V3.3 *** A0A0B0PVX3_GOSAR)
Solyc03g124050.3.1	3.50	6.69E-08	Receptor protein kinase, putative (AHRD V3.3 *** B9RHT1_RICCO)
Solyc01g100390.3.1	3.49	5.31E-05	Pyrophosphate-energized vacuolar membrane proton pump (AHRD V3.3 *** AVP_VIGRR)
Solyc11g066250.2.1	3.48	6.45E-20	Carboxypeptidase (AHRD V3.3 *** K4D9N3_SOLLC)
Solyc12g008485.1.1	3.48	8.83E-04	RING/U-box superfamily protein (AHRD V3.3 *-* AT1G80400.1)
Solyc08g074250.2.1	3.48	6.20E-04	Disease resistance protein (CC-NBS-LRR class) family (AHRD V3.3 *** AT5G35450.2)
Solyc08g006730.1.1	3.47	6.05E-05	Tyramine N-feruloyltransferase 4/11 (AHRD V3.3 *** THT11_TOBAC)
TCONS_00038639	3.47	9.75E-04	
Solyc02g077770.3.1	3.46	5.72E-14	bidirectional amino acid transporter 1 (AHRD V3.3 --* AT2G01170.2)
Solyc12g099340.2.1	3.46	1.10E-08	calmodulin-binding transcription activator (AHRD V3.3 *** AT3G16940.3)
Solyc01g108910.3.1	3.45	8.42E-04	Maternal effect embryo arrest protein, putative (AHRD V3.3 *** G7JNK2_MEDTR)
Solyc07g062825.1.1	3.45	9.89E-04	F-box/RNI-like superfamily protein (AHRD V3.3 --* AT3G58930.5)
Solyc06g054640.2.1	3.43	3.48E-08	DUF506 family protein (AHRD V3.3 *** G7LD84_MEDTR)
Solyc02g091100.3.1	3.43	6.84E-09	Thiamine pyrophosphate dependent pyruvate decarboxylase family protein (AHRD V3.3 *** AT5G17380.1)
Solyc03g032210.3.1	3.43	2.40E-04	AMP-dependent synthetase and ligase family protein (AHRD V3.3 *** AT2G17650.1)
Solyc05g008110.3.1	3.43	1.15E-09	hydroxyproline-rich glycoprotein family protein (AHRD V3.3 --* AT1G23040.3)
Solyc06g082020.3.1	3.42	4.63E-09	Alternative NAD(P)H dehydrogenase 1 (AHRD V3.3 --* A0A061GX18_THECC)
Solyc04g082050.3.1	3.41	1.11E-09	Ganglioside-induced differentiation-associated protein 2 (AHRD V3.3 *** A0A199VGA4_ANACO)
Solyc12g087860.2.1	3.41	4.75E-05	RING/U-box superfamily protein, putative (AHRD V3.3 *** A0A061FLH6_THECC)
Solyc12g008550.2.1	3.41	9.97E-16	Peptidase M28 family protein (AHRD V3.3 *-* AT5G19740.1)
Solyc08g068790.2.1	3.41	1.15E-10	Tyramine n-hydroxycinnamoyl transferase (AHRD V3.3 *** Q5D8C0_CAPAN)

Solyc01g090980.1.1	3.40	6.62E-07	LOW QUALITY:cyclic nucleotide-gated channel 6 (AHRD V3.3 --* AT2G23980.9)
Solyc09g075040.3.1	3.40	1.09E-06	E3 ubiquitin-protein ligase (AHRD V3.3 *** K4CV81_SOLLC)
Solyc09g008830.3.1	3.40	9.02E-04	Transcription factor, putative (AHRD V3.3 *** B9RIA5_RICCO)
Solyc07g063930.3.1	3.40	2.95E-12	Organic cation transporter, putative (AHRD V3.3 *** B9SY49_RICCO)
Solyc09g007790.1.1	3.40	7.45E-04	LOW QUALITY:Senescence regulator (AHRD V3.3 *** G7IRS7_MEDTR)
Solyc05g051900.3.1	3.39	7.47E-10	Major facilitator superfamily transporter (AHRD V3.3 *** A0A0K0KFR2_CARHR)
Solyc02g080580.1.1	3.39	4.94E-07	LOW QUALITY:senescence regulator (Protein of unknown function, DUF584) (AHRD V3.3 *** AT4G04630.1)
Solyc02g065430.1.1	3.39	1.47E-07	LOW QUALITY:DUF4228 domain protein (AHRD V3.3 *** G7K9H8_MEDTR)
Solyc09g008200.3.1	3.39	1.75E-28	Heavy metal transport/detoxification superfamily protein (AHRD V3.3 *** AT5G03380.1)
Solyc09g007130.3.1	3.39	8.11E-10	3-methyl-2-oxobutanoate hydroxymethyltransferase (AHRD V3.3 *** K4CQA3_SOLLC)
Solyc04g040090.3.1	3.38	7.96E-06	Strictosidine synthase-like protein (AHRD V3.3 *** A7WPL3_TOBAC)
Solyc07g065980.3.1	3.38	1.53E-42	alkaline alpha-galactosidase seed imbibition protein
Solyc01g091490.3.1	3.37	1.05E-05	Class III homeobox-leucine zipper protein (AHRD V3.3 --* I0IUI3_9ASPA)
Solyc01g111570.3.1	3.37	8.34E-15	Kinase family protein (AHRD V3.3 *** B9H1A0_POPTR)
Solyc04g055140.1.1	3.36	7.99E-10	LOW QUALITY:Nitric oxide synthase-interacting protein, putative (AHRD V3.3 *** A0A061DQB5_THECC)
Solyc02g082450.3.1	3.36	7.47E-04	Auxin efflux carrier family protein (AHRD V3.3 *** AT2G17500.4)
Solyc04g011490.3.1	3.36	5.87E-04	CASP-like protein (AHRD V3.3 *** K4BPK2_SOLLC)
Solyc06g068500.3.1	3.35	3.89E-11	Chaperone DnaJ domain protein (AHRD V3.3 *** B7FGF7_MEDTR)
Solyc02g071815.1.1	3.35	1.05E-03	Leucine-rich repeat receptor-like protein kinase (AHRD V3.3 *-* C0LGF2_ARATH)
Solyc08g007930.2.1	3.34	9.20E-05	SUN-like protein 20
Solyc01g100370.3.1	3.34	4.22E-13	Adenine nucleotide alpha hydrolases-like superfamily protein (AHRD V3.3 *** AT3G62550.1)
Solyc08g007230.2.1	3.33	3.13E-14	Ethylene-responsive transcription factor (AHRD V3.3 *** A0A024CAT9_BRAJU)
Solyc09g089930.2.1	3.33	8.09E-10	ethylene responsive factor E.2
Solyc03g096550.3.1	3.32	4.81E-04	PLAT domain-containing protein 1 (AHRD V3.3 *** PLAT1_ARATH)
Solyc04g077810.1.1	3.32	6.60E-08	LOW QUALITY:ZCF37, putative (AHRD V3.3 *** A0A061F7D6_THECC)
Solyc12g043030.2.1	3.32	7.02E-19	Sulfate transporter, putative (AHRD V3.3 *** B9SQC2_RICCO)
Solyc09g074350.1.1	3.31	9.43E-18	LOW QUALITY:chromatin remodeling factor17 (AHRD V3.3 --* AT5G18620.2)
Solyc06g035970.3.1	3.31	1.93E-04	Tubulin beta chain (AHRD V3.3 *** TBB_HORVU)
Solyc05g046270.3.1	3.30	6.65E-07	Protein Ycf2 (AHRD V3.3 --* YCF2_OENGL)
Solyc11g071830.2.1	3.30	6.93E-05	DnaJ protein homolog (AHRD V3.3 *** DNJH_CUCSA)
Solyc06g053710.3.1	3.30	4.41E-07	ethylene receptor homolog (ETR4)
Solyc12g096030.1.1	3.30	4.56E-04	LOW QUALITY:Mitochondrial carrier protein (AHRD V3.3 *** F8WLA3_CITUN)
Solyc01g104725.1.1	3.29	1.52E-05	organic solute transporter ostalpha protein (DUF300) (AHRD V3.3 --* AT4G21570.2)
Solyc03g121420.3.1	3.29	1.10E-06	Inorganic pyrophosphatase 2 (AHRD V3.3 *** A0A0B2S4R2_GLYSO)
Solyc06g069150.1.1	3.29	5.64E-09	LOW QUALITY:Zinc finger BED domain-containing protein DAYSLEEPER (AHRD V3.3 --* DSLE_ARATH)

Solyc05g008910.3.1	3.29	7.37E-04	Class I glutamine amidotransferase-like superfamily protein (AHRD V3.3 *-* AT5G38200.1)
Solyc08g069060.3.1	3.28	6.50E-12	Hexosyltransferase (AHRD V3.3 *-* K4CMC6_SOLLC)
Solyc01g091100.2.1	3.28	1.55E-10	LOW QUALITY:Plant invertase/pectin methylesterase inhibitor (AHRD V3.3 *** G7KG88_MEDTR)
Solyc08g014010.3.1	3.28	5.34E-07	Transmembrane protein, putative (AHRD V3.3 *** A0A072VMY8_MEDTR)
Solyc02g082060.2.1	3.28	2.49E-10	LOW QUALITY:PPPDE putative thiol peptidase family protein (AHRD V3.3 *** AT4G25680.1)
Solyc08g068730.1.1	3.28	5.16E-09	Tyramine n-hydroxycinnamoyl transferase (AHRD V3.3 *** Q5D8C0_CAPAN)
Solyc05g052680.1.1	3.27	1.19E-06	LOW QUALITY:HXXXD-type acyl-transferase family protein (AHRD V3.3 *** AT2G39980.1)
Solyc07g008250.3.1	3.27	4.43E-07	EIN3-binding F-box-like protein (AHRD V3.3 *** G7I706_MEDTR)
Solyc02g086110.3.1	3.27	1.13E-06	peptidase M50B-like protein (AHRD V3.3 *** AT1G67060.1),Pfam:PF13398
Solyc06g068830.2.1	3.27	2.34E-06	Ethylene-responsive transcription factor (AHRD V3.3 *-* W9S0J2_9ROSA)
Solyc12g096570.1.1	3.26	6.21E-04	ARGOS (AHRD V3.3 *** C7SFP7_SOLLC)
Solyc12g096840.2.1	3.26	4.21E-13	Tyramine N-feruloyltransferase 4/11, putative (AHRD V3.3 *** B9T0B8_RICCO)
Solyc08g079700.2.1	3.26	2.00E-21	Zinc finger A20 and AN1 domain-containing stress-associated protein (AHRD V3.3 *** V5PZR5_9CARY)
Solyc12g010430.1.1	3.26	7.42E-09	LOW QUALITY:NHL domain protein (AHRD V3.3 --* AT3G01430.1)
Solyc02g071870.3.1	3.25	1.08E-06	Receptor protein kinase, putative (AHRD V3.3 *** Q9C6G5_ARATH)
Solyc02g092120.3.1	3.24	3.21E-10	Phytosulfokines 3 family protein (AHRD V3.3 *** B9IBM1_POPTR)
Solyc07g005300.1.1	3.24	9.94E-07	LOW QUALITY:RING-finger, DEAD-like helicase, PHD and SNF2 domain-containing protein (AHRD V3.3 --* AT2G40770.3)
Solyc02g081830.3.1	3.23	9.71E-09	Haloacid dehalogenase-like hydrolase domain-containing protein 3 (AHRD V3.3 *** W9RRW5_9ROSA),Pfam:PF00702
Solyc01g060240.3.1	3.23	4.95E-10	cAMP-regulated phosphoprotein 19-related protein (AHRD V3.3 --* AT4G16146.1)
Solyc02g087070.3.1	3.23	6.68E-04	alpha-DOX1
Solyc01g006050.2.1	3.22	8.72E-04	LOW QUALITY:Transmembrane protein 45B (AHRD V3.3 *** A0A151U0K4_CAJCA)
Solyc05g056500.1.1	3.22	7.86E-05	U-box domain-containing protein 25 (AHRD V3.3 *** W9QUC2_9ROSA)
Solyc06g066420.3.1	3.22	2.06E-03	Oxidative stress 3, putative isoform 1 (AHRD V3.3 *** A0A061GC09_THECC)
Solyc04g078690.3.1	3.22	1.40E-04	bHLH transcription factor 035
Solyc09g007520.3.1	3.21	3.51E-06	Peroxidase (AHRD V3.3 *** K4CQE1_SOLLC)
Solyc11g005290.2.1	3.21	1.79E-15	RING/U-box superfamily protein (AHRD V3.3 *-* AT1G49230.1)
Solyc03g005330.1.1	3.21	4.52E-04	Non-specific serine/threonine protein kinase (AHRD V3.3 *** K4BDV7_SOLLC)
Solyc10g080920.2.1	3.21	7.22E-05	Myb family transcription factor family protein (AHRD V3.3 *** B9GRM8_POPTR)
Solyc07g008810.1.1	3.20	3.59E-04	LOW QUALITY:Monovalent Cation:Proton antiporter-2 family (AHRD V3.3 --* C1EH01_MICCC)
Solyc09g010250.1.1	3.19	1.92E-03	importin alpha isoform 4 (AHRD V3.3 --* AT1G09270.3)
TCONS_00050415	3.18	2.27E-03	
Solyc06g074990.2.1	3.18	6.96E-07	putative high affinity nitrate transporter 2
Solyc07g056340.3.1	3.18	2.13E-14	RNA-binding protein, putative (AHRD V3.3 *** B9T754_RICCO)
Solyc07g054780.1.1	3.18	1.33E-03	LOW QUALITY:Wound-responsive family protein (AHRD V3.3 *** AT4G10265.1)
Solyc04g072000.3.1	3.17	5.21E-09	Chitinase (AHRD V3.3 *** A0A1B1HY32_9APIA)

Solyc10g007880.3.1	3.17	1.39E-06	Cytochrome P450 (AHRD V3.3 *-* A0A103YA09_CYNCS)
Solyc09g098190.3.1	3.17	1.25E-07	Signal peptide peptidase-like protein (AHRD V3.3 *-* A0A072TX77_MEDTR)
Solyc09g065770.1.1	3.17	2.49E-15	LOW QUALITY:Ubiquitin-conjugating enzyme/RWD-like protein, putative (AHRD V3.3 *** A0A061DQB8_THECC)
Solyc09g089870.3.1	3.17	2.44E-14	bHLH transcription factor 061
Solyc01g066190.1.1	3.16	2.41E-03	LOW QUALITY:Splicing factor 3B subunit 3 (AHRD V3.3 --* A0A0B2RZM2_GLYSO)
TCONS_00049710	3.16	1.91E-15	
Solyc05g008120.3.1	3.16	9.24E-07	Chaperone DnaJ (AHRD V3.3 *** A0A0B0MDP3_GOSAR)
Solyc09g007730.3.1	3.16	8.33E-06	Kinase family protein (AHRD V3.3 *** B9NAB5_POPTR)
Solyc11g010210.1.1	3.15	3.25E-06	WEB family protein, chloroplastic (AHRD V3.3 *-* A0A199V6Z9_ANACO)
Solyc10g086200.1.1	3.15	6.57E-04	SAUR-like auxin-responsive protein family (AHRD V3.3 *** AT2G37030.1)
Solyc08g065940.3.1	3.15	3.68E-10	Zinc finger CCCH domain-containing protein (AHRD V3.3 *** R4QQJ8_CUCME)
Solyc06g005520.3.1	3.15	4.15E-09	Protein kinase (AHRD V3.3 *** C6ZRV6_SOYBN)
Solyc08g068700.1.1	3.14	4.76E-09	Tyramine n-hydroxycinnamoyl transferase (AHRD V3.3 *** Q5D8C0_CAPAN)
Solyc09g072880.3.1	3.14	2.16E-08	Fluorescent in blue light, chloroplastic-like protein (AHRD V3.3 *** A0A0B0PKQ3_GOSAR)
Solyc03g031920.3.1	3.14	9.71E-07	Oligopeptide transporter, putative (AHRD V3.3 *** B9SIR4_RICCO)
Solyc01g106500.3.1	3.14	5.24E-08	Leucine-rich receptor-like protein kinase family protein (AHRD V3.3 *** AT1G09970.1)
Solyc05g014230.3.1	3.14	8.09E-07	RING finger protein (AHRD V3.3 *** A0A0B0MVX3_GOSAR)
Solyc05g007580.1.1	3.13	8.72E-06	ZF-HD homeobox domain-containing protein (AHRD V3.3 *** A4UV09_SOLTU)
Solyc10g061960.2.1	3.13	1.60E-15	Phosphatidylinositol-4-phosphate 5-kinase 5-like protein (AHRD V3.3 *** A0A0B0PLQ6_GOSAR)
Solyc05g052670.1.1	3.13	1.48E-04	LOW QUALITY:HXXXD-type acyl-transferase family protein (AHRD V3.3 *** AT2G39980.1)
TCONS_00033772	3.12	1.02E-05	
Solyc06g066770.1.1	3.12	2.54E-09	Kelch repeat-containing F-box family protein (AHRD V3.3 *** B9GEJ8_POPTR)
Solyc04g080700.3.1	3.11	6.42E-16	Bifunctional nuclease 1 (AHRD V3.3 *-* BBD1_ARATH)
Solyc02g063320.3.1	3.11	3.13E-05	U-box domain-containing protein (AHRD V3.3 *** A0A0K9PMJ3_ZOSMR)
Solyc02g078250.3.1	3.11	1.25E-03	CASP-like protein (AHRD V3.3 *** K4B950_SOLLC)
Solyc03g122320.1.1	3.10	2.65E-05	LOW QUALITY:P-loop nucleoside triphosphate hydrolase superfamily protein (AHRD V3.3 --* G7I3Y4_MEDTR)
Solyc10g049427.1.1	3.10	1.84E-03	LOW QUALITY:Retrovirus-related Pol polyprotein from transposon TNT 1-94 (AHRD V3.3 *-* A0A151S124_CAJCA)
Solyc01g006910.3.1	3.10	9.85E-04	RING/U-box superfamily protein (AHRD V3.3 *** AT5G06490.1)
Solyc10g078920.2.1	3.10	6.45E-04	Thioredoxin (AHRD V3.3 *** G7KVF9_MEDTR)
Solyc01g102410.3.1	3.10	1.69E-12	Glutamyl-tRNA synthetase (AHRD V3.3 *** G7IAE3_MEDTR)
Solyc01g096670.3.1	3.10	4.04E-06	Cytochrome P450, putative (AHRD V3.3 *** B9SJN4_RICCO)
Solyc04g025373.1.1	3.10	2.88E-03	Retrovirus-related Pol polyprotein from transposon TNT 1-94 (AHRD V3.3 *-* POLX_TOBAC)
Solyc12g099790.2.1	3.09	4.79E-05	Calcium-dependent protein kinase, putative (AHRD V3.3 *** B9SJ93_RICCO)
Solyc03g112090.3.1	3.09	3.50E-06	high-affinity nitrate transporter-like protein (AHRD V3.3 *-* AT4G24715.1)
Solyc09g011330.2.1	3.08	3.25E-07	Serine/threonine-protein kinase (AHRD V3.3 *** M1C8X1_SOLTU)

Solyc07g008620.1.1	3.08	8.11E-09	EIX receptor 1
Solyc12g042600.2.1	3.08	1.84E-03	Glycosyltransferase (AHRD V3.3 *** K4DF51_SOLLC)
Solyc12g010670.1.1	3.07	2.25E-08	RING/U-box superfamily protein (AHRD V3.3 *-* AT1G74990.1)
Solyc10g018340.1.1	3.07	7.47E-07	Small auxin up-regulated RNA71
Solyc03g111310.3.1	3.07	1.87E-22	SNF1-related protein kinase regulatory subunit gamma 1 (AHRD V3.3 *** A0A061G5Z8_THECC)
Solyc10g077120.2.1	3.06	7.34E-11	Photosystem II core complex proteins psbY (AHRD V3.3 *** A0A061EES6_THECC)
Solyc11g008680.2.1	3.06	1.11E-03	Acyl-[acyl-carrier-protein] desaturase (AHRD V3.3 *** A0A060IKL1_NICBE)
Solyc01g106170.3.1	3.06	2.01E-17	AGAMOUS-like MADS-box transcription factor (AHRD V3.3 *-* Q84LE8_GINBI)
Solyc02g079530.3.1	3.06	5.81E-05	GTPase Der (DUF707) (AHRD V3.3 --* AT4G12840.3)
Solyc01g059965.1.1	3.06	1.19E-06	Beta-1,3-glucanase (AHRD V3.3 *** G9G7S0_HEVBR)
Solyc11g011340.2.1	3.06	1.09E-13	cultivar Rio Grande ELI3
Solyc09g014720.2.1	3.05	1.52E-03	Kinase, putative (AHRD V3.3 *** B9RE26_RICCO)
Solyc05g006660.3.1	3.05	1.20E-07	CW14 protein (DUF1336) (AHRD V3.3 *** AT1G59650.1)
Solyc07g056080.1.1	3.05	3.05E-07	LOW QUALITY:Acidic endochitinase SE2 (AHRD V3.3 --* CHIE_BETVU)
Solyc04g009780.1.1	3.05	6.78E-04	RING/U-box superfamily protein (AHRD V3.3 *** A0A061FQW5_THECC)
Solyc08g076170.1.1	3.05	2.24E-07	LOW QUALITY:50S ribosomal protein L22, chloroplastic (AHRD V3.3 -** RK22_CHLAT)
Solyc06g054610.2.1	3.05	3.13E-09	NAD(P)H-quinone oxidoreductase subunit K, chloroplastic (AHRD V3.3 --* NDHK_HELAN)
Solyc04g011470.2.1	3.05	2.84E-03	CASP-like protein (AHRD V3.3 *** K4BPK0_SOLLC)
Solyc12g005850.2.1	3.05	5.04E-16	Protein DETOXIFICATION (AHRD V3.3 *** K4DBC3_SOLLC)
Solyc02g069045.1.1	3.05	5.77E-05	Phloem protein 2 (AHRD V3.3 *** D0R6I7_MALDO)
Solyc03g096430.1.1	3.05	4.19E-05	LOW QUALITY:CLIP-associating protein 1 (AHRD V3.3 --* A0A0B2NZ56_GLYSO)
Solyc12g014355.1.1	3.04	5.53E-04	Leucine-rich repeat transmembrane protein kinase (AHRD V3.3 *-* AT1G53430.1)
Solyc09g009130.3.1	3.04	2.94E-03	Phytosulfokine 3, putative (AHRD V3.3 *** A0A061ESV9_THECC)
Solyc05g055370.1.1	3.03	8.70E-07	LOW QUALITY:Transmembrane 9 superfamily member (AHRD V3.3 --* A0A199W436_ANACO)
Solyc03g111530.3.1	3.03	2.98E-03	cysteine-rich RECEPTOR-like kinase (AHRD V3.3 *-* AT4G23230.1)
Solyc11g006740.2.1	3.03	1.82E-05	F-box protein PP2 (AHRD V3.3 *** A0A059PC27_CICAR)
Solyc11g011400.2.1	3.03	1.02E-06	Linoleate 9S-lipoxygenase (AHRD V3.3 --* LOXB_PHAVU)
Solyc03g005537.1.1	3.03	2.50E-05	Phosphate transporter (AHRD V3.3 *** Q9AYT2_TOBAC)
Solyc03g121430.2.1	3.02	5.20E-04	Inorganic pyrophosphatase 2 (AHRD V3.3 *-* PPSP2_ARATH)
Solyc05g014280.3.1	3.02	1.85E-03	small heat shock protein 1
Solyc02g037495.1.1	3.02	4.59E-08	AMP-dependent synthetase and ligase family protein (AHRD V3.3 *** AT5G16340.1)
Solyc06g075020.3.1	3.02	2.31E-03	ABC transporter G family-like protein (AHRD V3.3 *** A0A072UJT7_MEDTR)
Solyc05g008820.3.1	3.02	3.44E-07	Lipid phosphate phosphatase-like protein (AHRD V3.3 *** A0A072U232_MEDTR)
Solyc05g054655.1.1	3.02	8.37E-04	Zinc finger family protein (AHRD V3.3 *-* B9HM54_POPTR)
Solyc11g066880.2.1	3.02	3.68E-04	Phytosulfokine 3, putative (AHRD V3.3 *** A0A061ESV9_THECC)

Solyc09g005110.3.1	3.02	9.79E-09	Pyruvate decarboxylase (AHRD V3.3 *** Q8H9C6_SOLTU)
Solyc02g088205.1.1	3.01	1.91E-07	Activating signal cointegrator 1 complex subunit 1 (AHRD V3.3 --* A0A1D1XDP2_9ARAE)
Solyc05g018230.3.1	3.01	3.60E-07	Sugar transporter protein 12
Solyc12g014590.2.1	3.00	6.61E-07	Pirin-like protein family (AHRD V3.3 *** A0A151SXI4_CAJCA)
Solyc09g008380.3.1	-3.01	7.31E-07	Pectate lyase (AHRD V3.3 *** K4CQM6_SOLLC)
TCONS_00025980	-3.01	8.01E-04	
Solyc03g120870.3.1	-3.01	3.14E-05	CASP-like protein (AHRD V3.3 *** K4BMN6_SOLLC)
Solyc03g117260.2.1	-3.01	3.11E-04	transmembrane protein, putative (DUF247) (AHRD V3.3 *** AT3G02645.1)
Solyc07g055810.3.1	-3.02	8.68E-19	Receptor-like protein kinase (AHRD V3.3 *** B9I1R1_POPTR)
Solyc08g066635.1.1	-3.02	1.24E-03	LOW QUALITY:BED zinc finger,hAT family dimerization domain, putative (AHRD V3.3 *-* A0A061FD65_THECC)
Solyc10g009550.3.1	-3.02	1.92E-09	LOW QUALITY:WRKY transcription factor 42
Solyc01g090800.3.1	-3.02	4.17E-04	cyclinU2_1
Solyc05g024370.1.1	-3.03	3.16E-03	disease resistance protein (TIR-NBS-LRR class) (AHRD V3.3 *-* AT5G17680.2)
Solyc02g090580.3.1	-3.03	3.89E-09	ternary complex factor MIP1 leucine-zipper protein (Protein of unknown function, DUF547) (AHRD V3.3 *** AT4G37080.3)
Solyc01g095530.2.1	-3.04		LOW QUALITY:cytoplasmic tRNA 2-thiolation protein (AHRD V3.3 *** AT3G55570.1)
Solyc01g005990.3.1	-3.04	1.05E-06	Lipid transfer protein (AHRD V3.3 *** A0A072TPI6_MEDTR)
Solyc02g083640.3.1	-3.04	1.09E-06	Tetratricopeptide repeat (TPR)-like superfamily protein (AHRD V3.3 *** AT3G51280.1)
TCONS_00022031	-3.04	9.21E-04	
Solyc01g095390.3.1	-3.04	7.71E-05	Intracellular protein transporter USO1-like protein (AHRD V3.3 *** G7KAQ1_MEDTR)
Solyc02g092490.3.1	-3.05	4.99E-09	Acyl-CoA N-acyltransferases (NAT) superfamily protein (AHRD V3.3 *** AT2G23060.1)
Solyc02g069490.3.1	-3.05	1.06E-10	Sterol reductase (AHRD V3.3 *** E1VD17_SOLTU)
Solyc08g008610.3.1	-3.05	1.12E-05	Alpha/beta-Hydrolases superfamily protein (AHRD V3.3 *** A0A061G3V4_THECC)
Solyc04g056380.3.1	-3.06	2.30E-05	Seipin (AHRD V3.3 *** A0A0B0N0V2_GOSAR)
Solyc03g006260.3.1	-3.07	1.68E-03	Calcium-binding EF-hand (AHRD V3.3 *-* A0A103XMB0_CYNCS)
Solyc02g055370.3.1	-3.07	5.37E-04	Transcriptional factor B3 family protein (AHRD V3.3 *-* AT4G31650.2)
Solyc02g084680.2.1	-3.07	2.83E-07	Lateral root primordium protein-related, putative (AHRD V3.3 *** A0A061DFV6_THECC)
Solyc11g061720.1.1	-3.07	4.26E-09	Kinase family protein (AHRD V3.3 *** D7KZX1_ARALL)
Solyc02g086760.1.1	-3.08	4.76E-04	LOW QUALITY:transmembrane protein (AHRD V3.3 *** AT3G01516.2)
Solyc10g078370.2.1	-3.09	1.67E-13	Auxin Efflux Facilitator 9
Solyc03g058910.3.1	-3.10	2.26E-03	Pectate lyase (AHRD V3.3 *** M1A3P9_SOLTU)
Solyc01g097770.3.1	-3.10	6.98E-04	phototropin 2
Solyc05g051940.3.1	-3.10	8.71E-04	Major facilitator superfamily transporter (AHRD V3.3 *** A0A0K0KFR2_CARHR)
Solyc01g104030.3.1	-3.10	4.82E-06	Potassium channel (AHRD V3.3 *** Q9SSV3_NICPA)
Solyc06g074110.3.1	-3.11	3.25E-07	BHLH transcription factor-like protein (AHRD V3.3 *-* A0A072UK41_MEDTR)
Solyc02g083070.2.1	-3.12	1.25E-03	LOW QUALITY:DUF241 domain protein (AHRD V3.3 *** G7LA86_MEDTR)

Solyc01g009190.2.1	-3.12	2.35E-03	Double-stranded RNA-binding protein 1 (AHRD V3.3 *** W9RGH4_9ROSA)
Solyc08g065140.1.1	-3.12	2.29E-12	Late embryogenesis abundant (LEA) hydroxyproline-rich glycoprotein family (AHRD V3.3 *** AT1G17620.1)
Solyc06g054310.1.1	-3.13	3.37E-13	LOW QUALITY:Fantastic four-like protein (AHRD V3.3 *** G7IE53_MEDTR)
Solyc12g011300.2.1	-3.13	2.13E-03	Glutathione s-transferase, putative (AHRD V3.3 *** B9T3K4_RICCO)
Solyc03g097170.3.1	-3.13	4.70E-06	Cinnamoyl-CoA reductase, putative (AHRD V3.3 *** B9S247_RICCO)
Solyc04g005810.3.1	-3.15	4.18E-04	Thioredoxin family protein (AHRD V3.3 *** B9IJS4_POPTR)
Solyc04g077490.3.1	-3.15	1.18E-07	AP2-like ethylene-responsive transcription factor (AHRD V3.3 *** A0A072VCJ1_MEDTR)
Solyc12g008350.2.1	-3.15	1.33E-08	dehydration responsive element binding protein 2
Solyc09g059560.2.1	-3.16	6.02E-06	BED zinc finger,hAT family dimerization domain, putative (AHRD V3.3 *** A0A061FD65_THECC)
Solyc08g080400.1.1	-3.16	9.17E-17	GRAS family transcription factor (AHRD V3.3 *** A0A061G628_THECC)
Solyc02g091050.3.1	-3.16	2.45E-15	Protein DETOXIFICATION (AHRD V3.3 *** K4BCQ4_SOLLC)
Solyc09g065070.2.1	-3.17	2.89E-04	Aluminum activated malate transporter family protein, putative (AHRD V3.3 *** A0A061DXR0_THECC)
Solyc01g100770.2.1	-3.17	2.00E-04	LOW QUALITY:plant/protein (Protein of unknown function, DUF538) (AHRD V3.3 *** AT1G56580.1)
Solyc01g067540.1.1	-3.17	2.00E-04	Ethylene-responsive transcription factor (AHRD V3.3 *** W9R6V3_9ROSA)
Solyc03g111550.3.1	-3.18	5.15E-04	GDSL esterase/lipase (AHRD V3.3 *** A0A0B2PXL8_GLYSO)
Solyc03g025710.3.1	-3.18	1.01E-03	Acyl-CoA N-acyltransferases-like protein (AHRD V3.3 *** Q9C7G6_ARATH)
Solyc02g089640.3.1	-3.20	7.70E-07	cellulose-synthase-like
Solyc10g080340.2.1	-3.20	1.45E-13	Protein DETOXIFICATION (AHRD V3.3 *** K4D2S4_SOLLC)
Solyc02g069560.3.1	-3.20	6.69E-11	Protein CHUP1, chloroplastic-like protein (AHRD V3.3 *** A0A0B0NZW9_GOSAR)
Solyc01g100760.2.1	-3.21	1.59E-03	plant/protein (Protein of unknown function, DUF538) (AHRD V3.3 *** AT1G56580.1)
Solyc07g054950.2.1	-3.21	7.52E-05	cyclinD6_1
Solyc04g078310.3.1	-3.21	7.02E-08	cyclin A3_1
Solyc07g053020.2.1	-3.21	2.39E-05	NBS-LRR type disease resistance protein (AHRD V3.3 *** Q19PJ0_POPTR)
Solyc07g008420.3.1	-3.22	3.84E-05	Blue copper (AHRD V3.3 *** A0A0B0N2W0_GOSAR)
Solyc01g100900.3.1	-3.22		WAT1-related protein (AHRD V3.3 *** K4B1C1_SOLLC)
Solyc11g040140.2.1	-3.22	6.90E-07	Xyloglucan endotransglucosylase/hydrolase (AHRD V3.3 *** K4D7Y8_SOLLC)
Solyc01g096940.3.1	-3.23	2.71E-06	Receptor-like kinase 17 (AHRD V3.3 *** A5A0Y6_SOLCH)
Solyc11g065600.2.1	-3.24	1.08E-03	xyloglucan endotransglucosylase-hydrolase 4
Solyc02g090220.3.1	-3.24	1.07E-06	Zinc finger, Dof-type (AHRD V3.3 *** A0A124SC40_CYNCS)
Solyc03g005960.3.1	-3.25	1.90E-05	protein kinase LESK1
Solyc08g077170.3.1	-3.26		Peptide transporter, putative (AHRD V3.3 *** B9S1I2_RICCO)
Solyc12g006640.2.1	-3.26	2.21E-04	Lactoylglutathione lyase / glyoxalase I family protein (AHRD V3.3 *** AT1G80160.3)
Solyc01g100920.3.1	-3.26		WAT1-related protein (AHRD V3.3 *** K4B1C3_SOLLC)
Solyc12g040450.2.1	-3.27	2.98E-05	Ubiquitin-protein ligase, putative (AHRD V3.3 --* G7JLF9_MEDTR)
Solyc01g103630.3.1	-3.27	8.00E-10	Lactoylglutathione lyase / glyoxalase I family protein (AHRD V3.3 *** A0A061DWL3_THECC)

Solyc06g007790.1.1	-3.27	8.95E-04	LOW QUALITY:Transmembrane protein, putative (AHRD V3.3 *-* G7L045_MEDTR)
Solyc07g043460.3.1	-3.29	9.36E-23	Cytochrome P450, putative (AHRD V3.3 *** A0A061E4E7_THECC)
Solyc08g068160.2.1	-3.29	1.07E-04	Flavin-containing monooxygenase (AHRD V3.3 *** K4CM40_SOLLC)
Solyc07g053600.3.1	-3.30	1.64E-13	Receptor-like protein kinase HSL1 (AHRD V3.3 *** HSL1_ARATH)
Solyc08g013740.3.1	-3.30	1.17E-03	S-adenosyl-L-methionine-dependent methyltransferases superfamily protein (AHRD V3.3 *** AT4G10440.1)
Solyc06g083080.3.1	-3.31	7.49E-05	Pathogenic type III effector avirulence factor Avr cleavage site-containing protein (AHRD V3.3 *** A0A118JW76_CYNCS)
Solyc12g009770.1.1	-3.31	1.31E-03	LOW QUALITY:Leucine-rich-repeat receptor-like protein (AHRD V3.3 *** A0A097BR55_GOSBA)
Solyc05g052245.1.1	-3.31	6.04E-04	Expansin (AHRD V3.3 *** G4XZW3_9GENT)
Solyc11g065720.2.1	-3.33	5.08E-06	ABC transporter-like family-protein (AHRD V3.3 *** A0A072VNR4_MEDTR)
Solyc08g067500.2.1	-3.34	1.34E-03	Non-specific lipid-transfer protein (AHRD V3.3 *** K4CLX6_SOLLC)
Solyc02g077250.2.1	-3.34	4.54E-05	LOW QUALITY:TCP transcription factor 1
Solyc08g078080.3.1	-3.35	2.71E-18	Pentatricopeptide repeat-containing protein (AHRD V3.3 *** A0A103XFF0_CYNCS)
Solyc05g053120.1.1	-3.35	1.20E-06	Glycosyltransferase (AHRD V3.3 *** A0A0A1WC49_NICAT)
Solyc02g084440.3.1	-3.36	7.22E-05	Fructose-bisphosphate aldolase
Solyc10g079320.2.1	-3.36	2.76E-07	Glycosyltransferase (AHRD V3.3 *** K4D2H3_SOLLC)
Solyc01g109790.3.1	-3.37	6.90E-11	ADP-glucose pyrophosphorylase large subunit 1
Solyc01g098060.1.1	-3.37	5.73E-04	MADS-box transcription factor family protein (AHRD V3.3 *-* AT1G72350.1)
Solyc10g048180.1.1	-3.37	1.18E-03	Amino acid transporter, putative (AHRD V3.3 *** B9SMC5_RICCO)
Solyc03g093330.3.1	-3.37	7.21E-06	Non-specific serine/threonine protein kinase (AHRD V3.3 *** K4C1J5_SOLLC)
Solyc12g040860.2.1	-3.38	1.61E-04	Glucan endo-1,3-beta-glucosidase, putative (AHRD V3.3 *** A0A061FDC8_THECC)
Solyc08g062490.3.1	-3.40	1.52E-04	WRKY transcription factor 50
Solyc05g046010.3.1	-3.42	1.43E-15	Peroxidase (AHRD V3.3 *** K4C0T4_SOLLC)
Solyc12g087940.2.1	-3.43	3.55E-06	Eukaryotic aspartyl protease family protein (AHRD V3.3 *** A0A061FET5_THECC)
Solyc09g061890.3.1	-3.43	1.12E-25	Pectate lyase (AHRD V3.3 *** M1BAL5_SOLTU)
Solyc01g108000.3.1	-3.47	3.39E-09	Kinase family protein (AHRD V3.3 *** D7L9X7_ARALL)
Solyc02g082820.3.1	-3.48	1.32E-09	cyclin B2
Solyc07g041640.3.1	-3.50	3.92E-05	Growth-regulating factor-like protein (AHRD V3.3 *** A0A072US13_MEDTR)
Solyc08g083190.3.1	-3.51	6.22E-05	Alpha/beta-Hydrolases superfamily protein (AHRD V3.3 *** A0A061G3V4_THECC)
Solyc04g054445.1.1	-3.54	1.00E-04	LOW QUALITY:Leucine-rich repeat receptor-like protein kinase family protein (AHRD V3.3 *** AT4G08850.1)
Solyc07g043500.1.1	-3.55	2.45E-18	Glycosyltransferase (AHRD V3.3 *** K4CEK8_SOLLC)
Solyc07g007750.3.1	-3.56	6.20E-06	Defensin protein (AHRD V3.3 *** B1N678_SOLLC)
Solyc02g069910.2.1	-3.56	1.73E-10	LOW QUALITY:BnaC07g36860D protein (AHRD V3.3 -** A0A078DYT9_BRANA)
Solyc03g120380.3.1	-3.57	2.30E-05	auxin-regulated IAA19
Solyc05g051400.3.1	-3.57	1.66E-16	Mitochondrial carrier protein (AHRD V3.3 *** A0A0K9PSM6_ZOSMR)
Solyc06g050560.3.1	-3.58	6.81E-09	Receptor-like kinase (AHRD V3.3 *** C4TP22_SOYBN)

Solyc04g016200.1.1	-3.58	2.92E-09	Glycosyltransferase (AHRD V3.3 *** Q8RXA4_SOLLC)
Solyc12g044630.2.1	-3.59	3.14E-04	Profilin (AHRD V3.3 *** M1CJS2_SOLTU)
Solyc07g062530.3.1	-3.60	1.22E-04	phosphoenolpyruvate carboxylase 2
Solyc01g073640.3.1	-3.62	1.75E-13	alcohol dehydrogenase-3,Pfam:PF13561
Solyc03g097050.3.1	-3.63	3.41E-11	Cellulose synthase-like protein (AHRD V3.3 *** L0ATQ4_POPTO)
Solyc07g005390.3.1	-3.63	9.59E-08	aldehyde dehydrogenase 11A3 (AHRD V3.3 *** AT2G24270.3)
Solyc10g080880.2.1	-3.64	4.30E-06	SlPIN7
Solyc12g040790.2.1	-3.67	5.18E-26	Phosphoethanolamine N-methyltransferase (AHRD V3.3 *** A0A075BJJ7_LYCBA)
Solyc08g006790.3.1	-3.70	2.13E-16	Early nodulin-like protein (AHRD V3.3 *** G7J9U0_MEDTR)
Solyc10g085080.2.1	-3.75	1.24E-04	8-amino-7-oxononanoate synthase (AHRD V3.3 *** AT3G09050.1)
Solyc11g042560.1.1	-3.79	3.52E-09	Ethylene-responsive transcription factor ERF021 family (AHRD V3.3 *** A0A151SD08_CAJCA)
Solyc06g070900.3.1	-3.82	6.13E-06	TCP transcription factor 17
Solyc02g083090.1.1	-3.83	1.02E-05	LOW QUALITY:DUF241 domain protein (AHRD V3.3 *** G7LA83_MEDTR)
Solyc04g074000.3.1	-3.84	1.51E-08	Receptor protein kinase, putative (AHRD V3.3 *-* A0A061FG24_THECC)
Solyc06g008580.3.1	-3.87	1.05E-04	auxin-regulated IAA22
Solyc05g051640.3.1	-3.87	1.73E-05	Non-specific serine/threonine protein kinase (AHRD V3.3 *** K4C1J5_SOLLC)
Solyc10g054840.2.1	-3.89	8.23E-05	X-intrinsic protein 1.1
Solyc10g076280.2.1	-3.91	9.13E-06	Solute carrier family 40 member 1 (AHRD V3.3 *** A0A151RSH4_CAJCA)
Solyc02g087440.3.1	-3.92	3.41E-05	DUF248-1 (AHRD V3.3 --* A0A161CGG5_POPTO)
Solyc02g032550.2.1	-3.96	6.07E-08	Apyrase (AHRD V3.3 *** APY_SOLTU)
Solyc03g031660.1.1	-3.97	1.37E-05	LOW QUALITY:Homer protein isoform 2 (AHRD V3.3 *-* A0A061GHT7_THECC)
Solyc03g114850.3.1	-3.99	2.02E-12	Squamosa promoter binding protein 6a
Solyc05g009490.2.1	-4.01	1.23E-05	DNA polymerase epsilon catalytic subunit (AHRD V3.3 --* AT2G27120.3)
Solyc04g008500.3.1	-4.03	8.48E-08	Zinc finger protein, putative (AHRD V3.3 *** B9S7A8_RICCO)
Solyc06g009190.3.1	-4.03	1.87E-05	Pectinesterase (AHRD V3.3 *** K4C3U9_SOLLC)
Solyc08g068150.3.1	-4.15	2.00E-10	BURP domain-containing protein (AHRD V3.3 *** B2ZPK7_SOLLC)
Solyc08g074480.1.1	-4.17	6.80E-09	14 kDa proline-rich protein DC2.15 (AHRD V3.3 *** A0A0B2P545_GLYSO)
Solyc04g009030.3.1	-4.21	4.74E-05	Glyceraldehyde-3-phosphate dehydrogenase (AHRD V3.3 *** K4BP59_SOLLC)
Solyc07g043490.1.1	-4.22	6.24E-25	UDP-Gal:Tomatidine Galactosyltransferase
Solyc03g114230.2.1	-4.25	2.48E-12	bHLH transcription factor 082
Solyc06g035700.1.1	-4.29	1.72E-11	Dehydration responsive element binding transcription factor (AHRD V3.3 *** W6FIY4_9ROSA)
Solyc04g072740.3.1	-4.29	5.75E-05	Sulfate transporter, putative (AHRD V3.3 *** B9RJF7_RICCO)
Solyc08g067340.3.1	-4.31	7.10E-25	WRKY transcription factor 46
Solyc11g068620.2.1	-4.32	7.03E-13	NAC-domain protein
Solyc05g009180.1.1	-4.34	1.86E-12	LOW QUALITY:Zinc finger family protein (AHRD V3.3 *** B9HWF8_POPTR)

Solyc10g018780.2.1	-4.37	4.20E-09	Squamosa promoter binding protein 8a
Solyc07g065110.1.1	-4.47	4.76E-22	Lipid transfer protein (AHRD V3.3 *** G7J041_MEDTR)
Solyc10g006920.3.1	-4.63	3.73E-11	CBS domain-containing protein (AHRD V3.3 *** A0A061GEK1_THECC)
Solyc05g053400.2.1	-4.78	1.99E-08	Glycosyltransferase (AHRD V3.3 *** A0A0A1WC49_NICAT)
Solyc07g017600.3.1	-4.92	2.57E-31	Pectinesterase (AHRD V3.3 *** K4CCH4_SOLLC)
Solyc10g083510.2.1	-5.17	1.84E-13	Growth-regulating factor (AHRD V3.3 *** A0A072U430_MEDTR)
Solyc08g083170.1.1	-5.32	5.03E-09	LOW QUALITY:bHLH transcription factor 056
Solyc03g120290.3.1	-5.58	4.26E-11	thionin-like protein (AHRD V3.3 *** AT1G12663.1)
Solyc08g007820.1.1	-6.10	8.25E-17	C-repeat binding factor (AHRD V3.3 *** A0A0B5KMN4_ACTCH)
Solyc08g007805.1.1	-6.43	1.10E-17	NADH dehydrogenase 1 alpha subcomplex subunit 8 (AHRD V3.3 *-* A0A0K9PKB1_ZOSMR)